National Research Council Canada

Conseil national de recherches Canada

NRC · CNRC

Canadian Journal of Fisheries and Aquatic Sciences

Journal canadien des sciences halieutiques et aquatiques

http://www.nrc.ca/cisti/journals

ISSN 0706-652X / CJFSDX 56(8) 1329–1519 (1999)

The *Canadian Journal of Fisheries and Aquatic Sciences*, previously published as *Contributions to Canadian Biology* 1901–1925, *Contributions to Canadian Biology and Fisheries* 1926–1934, *Journal of the Biological Board of Canada* 1934–1937, and *Journal of the Fisheries Research Board of Canada* 1938–1979, is issued monthly to form annual volumes of 12 numbers plus supplements.

Editorial policy: The Journal publishes original research articles, perspectives (syntheses, critiques, re-evaluations), discussions (comment and reply), and rapid communications. Manuscripts may concern cells, organisms, populations, communities, ecosystems, or processes that affect aquatic systems. They may cover a range of disciplines including biology and ecology of marine and freshwater organisms, limnology, oceanography, physiology, toxicology, genetics, economics, disease, and management. Preference will be given to manuscripts that emphasize understanding of observed phenomena and interpretation of experimental results. The Journal encourages papers that lead from clearly stated purpose or rationale and from testable hypotheses, concepts, or questions to identifiable conclusions or syntheses. Such papers may amplify, modify, question, or redirect accumulated knowledge embodied in contemporary perceptions of a particular state of aquatic sciences. The Journal discourages papers that are essentially descriptive, except in emerging disciplines; have only site-specific or local applications (a certain year, place, taxon, chemical compound, etc.); only confirm previously established principles; or apply standard techniques without breaking new methodological ground.

Manuscripts for publication should be submitted to the Editors, Canadian Journal of Fisheries and Aquatic Sciences, Department of Zoology, University of Guelph, Guelph, ON N1G 2W1, Canada (519-824-4120 ext. 2646; fax: 519-767-9798; e-mail: cjfas@uoguelph.ca).

Submissions in either English or French are acceptable. The information must be original, that is, not copyrighted, published, or submitted elsewhere except in abstract form or unless by written consent of the Editor. NRC accepts no responsibility for statements or opinions expressed by a contributor. Acceptance of an advertisement, announcement, or other material does not imply endorsement by either the *Journal*'s Editors or NRC. The use of proprietary names does not imply endorsement of the product or company.

Correspondence concerning accepted manuscripts and corrected proofs should be sent to NRC Research Press, National Research Council of Canada, Ottawa, ON K1A 0R6, Canada.

Instructions to Authors are published once a year in the first issue of each volume. Copies are available from NRC Research Press or from our Web site. The **Publication Policy** of NRC Research Press is also available at our Web site:
http://www.nrc.ca/cisti/journals/rj.html

Microfilm: Issues from 1934 through the current volume can be purchased on 16- or 35-mm microfilm. Photocopies of individual articles or issues can be purchased from University Microfilms International, 330 North Zeeb Road, Ann Arbor, MI 48106, U.S.A.

U.S. periodical postage paid at Champlain, N.Y., and at additional mailing offices. Attention U.S. POSTMASTER: Send address changes to **Canadian Journal of Fisheries and Aquatic Sciences**, c/o USACAN Media Distribution Center, P.O. Box 2888, Plattsburg, NY 12901, U.S.A.

Publié sans interruption depuis 1901, le *Journal canadien des sciences halieutiques et aquatiques* a paru sous plusieurs titres : *Contributions to Canadian Biology* 1901–1925, *Contributions to Canadian Biology and Fisheries* 1926–1934, *Journal of the Biological Board of Canada* 1934–1937, et *Journal of the Fisheries Research Board of Canada* 1938–1979. Le *Journal* paraît tous les mois, formant ainsi un volume de 12 numéros, et offre en plus jusqu'à deux suppléments par année.

Politique éditoriale : On publie, dans le Journal, des articles rendant compte de recherche originale, des perspectives (synthèses, critiques et réévaluations), des discussions (commentaires et réponses) et des communications rapides. Les documents peuvent porter sur les cellules, organismes, populations, communautés, écosystèmes ou processus qui affectent les systèmes aquatiques. Ils peuvent relever de divers domaines y compris la biologie et l'écologie des organismes marins et d'eau douce, la limnologie, l'océanographie, la physiologie, la toxicologie, la génétique, l'économie, la pathologie et la gestion. On accorde la préséance aux articles qui contribuent à la compréhension de phénomènes observés et à l'interprétation de résultats expérimentaux. On invite les auteurs à soumettre des articles ayant des objectifs précis ou relevant d'hypothèses, de concepts ou de questions vérifiables et se terminant par de solides conclusions ou d'utiles synthèses. Ces articles enrichissent, changent, mettent en question ou réorientent les connaissances acquises sur divers aspects des sciences aquatiques. On décourage toutefois la soumission d'articles simplement descriptifs (à moins qu'il ne s'agisse de nouvelles disciplines), d'application très limitée (applicables à une seule année, une seule région ou un seul taxon, portant sur un unique composé chimique, etc.); d'articles qui ne font que reprendre les principes énoncés dans des articles précédents; et d'articles rendant compte de l'application de normes sans gain de méthodologie.

Les auteurs voudront adresser leurs **manuscrits** aux directeurs scientifiques, Journal canadien des sciences halieutiques et aquatiques, Département de Zoologie, University of Guelph, Guelph, ON N1G 2W1, Canada (519-824-4120 poste. 2646; télécopieur : 519-767-9798; adresse électronique : cjfas@uoguelph.ca).

Les contributions peuvent être en anglais ou en français. Elles doivent être originales, c.-à.-d. qu'elles ne doivent pas avoir fait l'objet d'un copyright, avoir été publiées ou soumises ailleurs, sauf sous forme abrégée ou avec le consentement du rédacteur. Le CNRC ne se tient en aucune façon responsable des opinions exprimées par un collaborateur ou des déclarations qui pourrait faire ce dernier. La publication d'annonces publicitaires, d'avis et autres n'implique pas l'endossement de leur contenu par les directeurs du *Journal* ou du CNRC. L'utilisation des noms de marques de commerce ne signifie aucunement une sanction du produit en question ou de la compagnie qui le fabrique.

La correspondance ayant trait aux manuscrits acceptés et les **épreuves corrigés** doivent être envoyées aux Presses scientifiques du CNRC, Conseil national de recherches du Canada, Ottawa, ON K1A 0R6, Canada.

Recommandations aux auteurs sont publiés une fois par année dans le premier numéro de chaque volume. Des copies, ainsi que la **Politique de publication**, sont disponibles auprès des Presses scientifiques du CNRC ou au site Web :
http://www.nrc.ca/cisti/journals/rj.html

Microfilms : On peut acheter sur microfilms de 16 ou 35 mm tous les numéros depuis 1934. Des photocopies d'articles ou de numéros individuels sont aussi en vente auprès de University Microfilms International, 330 North Zeeb Road, Ann Arbor, MI 48106, É.-U.

This journal is indexed or abstracted in / Ce journal est signalé ou résumé dans
Aquatic Sciences and Fisheries Abstracts, Biological & Agricultural Index, CAB Abstracts (Centre for Agriculture and Biosciences), Chemical Abstracts, Current Awareness in Biological Sciences, Current Contents, FAO Freshwater and Aquaculture Contents Tables, FAO Marine Science Contents Tables, GEOBASE – Geo Abstracts, Meteorological and Geoastrophysical Abstracts, Oceanic Abstracts, Science Citation Index, Biological Abstracts, Environment Abstracts, Environmental Periodicals Bibliography, GEOREF, Life Sciences Collection, ABSEARCH, and PASCAL Database

Volume 56, Number 8, August 1999

Canadian Journal of Fisheries and Aquatic Sciences

Published by the National Research Council of Canada

Volume 56, numéro 8, août 1999

Journal canadien des sciences halieutiques et aquatiques

Publié par le Conseil national de recherches du Canada

Editors / directeurs scientifiques John C. Roff and Moira M. Ferguson

Assistant to the Editors / adjointe aux directeurs scientifiques **Holly Foster**

Associate Editors / directeurs scientifique associés

D. Boisclair, *Université de Montréal*
U. Borgmann, *Environment Canada, Burlington*
S.E. Campana, *DFO/MPO, Dartmouth*
D.G. Dixon, *University of Waterloo*
A.E. Dizon, *National Marine Fisheries Service, La Jolla, Calif.*
J.J. Dodson, *Université Laval*
J.A. Downing, *Iowa State University*
K.T. Frank, *DFO/MPO, Dartmouth*
D.F. Houlihan, *University of Aberdeen, Aberdeen, Scotland*
F.A. Huntingford, *University of Glasgow*
J.A. Hutchings, *Dalhousie University*
G.S. Jamieson, *DFO/MPO, Nanaimo*
B. Jonsson, *Norwegian Institute for Nature Research, Oslo, Norway*
L. Legendre, *Université Laval*
D.M. Mason, *Purdue University, West Lafayette, Ind.*
A. Mazumder, *University of Victoria*
D.L. Parrish, *Vermont Cooperative Fish and Wildlife Research Unit (USGS/BRD), University of Vermont*
P. Pepin, *DFO/MPO, St. John's*
R.M. Peterman, *Simon Fraser University*
E.E. Prepas, *University of Alberta*
T.M. Powell, *University of California, Berkeley, Calif.*
T.J. Quinn II, *University of Alaska–Fairbanks, Juneau, Alaska*
T.P. Quinn, *University of Washington*
R.D. Robarts, *Environment Canada, Saskatoon*
B. Sainte-Marie, *DFO/MPO, Mont-Joli*
P.F. Sale, *University of Windsor*
D.W. Schindler, *University of Alberta*
S.J. Smith, *DFO/MPO, Dartmouth*
W.G. Sprules, *University of Toronto*
R.J. Thompson, *Memorial University of Newfoundland*
C.J. Walters, *University of British Columbia*
R.D. Ward, *CSIRO Division of Fisheries, Australia*
C.M. Wood, *McMaster University*
B. de Young, *Memorial University of Newfoundland*

NRC Research Press / Presses scientifiques du CNRC

Editor-in-chief / directeur général **Bruce P. Dancik**

Assistant Editor-in-chief / directeur général adjoint **Iain E.P. Taylor**

Journals Program / Programme des revues

(Fax / télécopieur : 613-952-7656; e-mail / adresse électronique : research.journals@nrc.ca;
URL: http://www.nrc.ca/cisti/journals/)

Director / directrice **Aldyth Holmes**

Business Manager / gestionnaire des affaires **Paul McClymont**

Managing Editor / rédactrice administrative **Cecily M. Pearson (613-993-9099)**

Publication Officer / agente de publication **Jennifer McColl**

Advertising / annonces publicitaires **Judy Heyman (613-993-0151)**

Reprints / tirés à part **Roxanne Landriault (613-990-2254)**

Subscriptions / abonnements **Helen Goulet (613-993-9084)**

© National Research Council of Canada 1999. World rights reserved.
No part of this publication may be reproduced, stored, or transmitted in any form or by any means, without the written permission of the publisher, except as stated below.

The National Research Council of Canada grants **permission*** to individuals to make single copies of articles for personal use. Any person may reproduce short excerpts from articles in the journal for any purpose that respects the moral rights of authors, provided that the source is fully acknowledged. As a courtesy, the consent of authors of such material should be obtained directly from the author.

Authorization to reproduce items for other than personal use, as stated above, is granted by the National Research Council of Canada provided that the copyright fee of $7.00 per copy is paid directly to CANCOPY, One Yonge Street, Suite 1900, Toronto, ON M5E 1E5, Canada.

*The above permission does not extend to other kinds of copying, such as copying for general distribution, for advertising, or promotional purposes, for creating new collective works, or for resale. For such copying, arrangements must be made with the publisher, National Research Council of Canada, Ottawa, ON K1A 0R6, Canada.

© Conseil national de recherches du Canada 1999. Tous droits réservés.
Il est interdit de reproduire, de sauvegarder ou de transmettre quelque partie de la présente publication dans quelque format ou de quelque façon sans le consentement écrit de l'éditeur, à l'exception des conditions suivantes.

Le Conseil national de recherches du Canada accorde aux particuliers le droit de faire des copies individuelles pour leur usage personnel. Toute personne peut reproduire de courts extraits des articles de la Revue pour autant que les droits moraux de l'auteur soient respectés et que la mention de provenance soit clairement indiquée. Il est de convenance de demander le consentement de l'auteur avant de faire mention de son travail.

On obtiendra l'autorisation de reproduire des articles à d'autres fins que l'usage personnel (tel qu'on l'a décrit ci-dessus) auprès du Conseil national de recherches du Canada pour autant que des redevances de droits d'auteurs de 7,00 $/copie soient versées au CANCOPY, One Yonge Street, Suite 1900, Toronto, ON M5E 1E5, Canada.

*La permission ci-dessus ne s'applique pas à la reproduction à grande échelle, telle que la reproduction aux fins de distribution générale, publicitaire ou promotionnelle, de compilation de nouveaux ouvrages collectifs ou de revente. Dans de tels cas, il faudra ratifier une entente particulière avec l'éditeur, le Conseil national de recherches du Canada, Ottawa, ON K1A 0R6, Canada.

Subscription information

The *Canadian Journal of Fisheries and Aquatic Sciences* (ISSN 0706-652X) is published monthly by the National Research Council of Canada. 1999 annual subscription rates (second class postage) for Canada are $578CAN institutional and $182CAN personal, for US & foreign $578US institutional and $182US personal. For air mail add $150US to foreign rate. Canadian customers please include 7% GST (business no. 12149 1807 RT 0275). Subscriptions are entered for the calendar year. Remittances should be made payable to the Receiver General for Canada credit NRC. Price for regular single issues: institutional, $75.00; personal, $25.00. Supplements will be priced separately. Special rates apply to members of Canadian scientific and engineering societies if they subscribe through their respective societies.

There are no refunds on cancelled subscriptions once delivery has begun. Claims for missing issues should be made within four months (N. America) or six months (outside N. America) following the date of publication. The publisher expects to supply missing issues only when losses have occurred in transit and when the reserve stock will permit. For change of address and subscription enquiries: Subscription Office, NRC Research Press, National Research Council of Canada, Ottawa, ON K1A 0R6, Canada; tel: 613-993-9084; fax: 613-952-7656; e-mail: research.journals@nrc.ca.

Microform backfiles are available from UMI, P.O. Box 1346, Ann Arbor, MI 48106-1346, U.S.A., and Micromedia Ltd., 20 Victoria St., Toronto, ON M5C 2N8, Canada.

The 1999 issues of the *Canadian Journal of Fisheries and Aquatic Sciences* are available on the Web. Pricing information can be found at

http://www.nrc.ca/cisti/journals/

Renseignements sur l'abonnement

Journal canadien des sciences halieutiques et aquatiques (ISSN 0706-652X) est une publication mensuelle du Conseil national de recherches du Canada. Le prix de l'abonnement annuel au Canada (courrier de deuxième classe) est de 578 $CAN pour les organismes et de 182 $CAN pour les particuliers. À l'étranger (y compris les É.-U.), le prix de l'abonnement est de 578 $US pour les organismes et de 182 $US pour les particuliers. L'expédition par avion exige des frais de 150 $US en sus du prix d'abonnement à l'étranger. Les clients du Canada doivent ajouter la TPS de 7% (numéro d'entreprise 12149 1807 RT 0275). Les abonnements sont pour l'année civile. Tout paiement doit être adressé au Receveur général du Canada, crédit du CNRC. Le prix par numéro est de 75 $ pour les organismes et de 25 $ pour les particuliers. Le prix des hors-série varie. Les membres des sociétés canadiennes de sciences et de génie bénéficient de taux préférentiels en s'abonnant via leurs sociétés respectives.

Aucun remboursement ne sera accordé ni aucune annulation acceptée une fois que les livraisons auront commencé. Les réclamations de numéros manquants devront être soumises dans les quatre mois (Amérique du Nord) ou dans les six mois (à l'extérieur de l'Amérique du Nord) suivant la date de publication. L'éditeur ne fournira de numéros manquants que si le document a été perdu pendant l'expédition et que si le stock le permet. Adressez tout changement d'adresse ou toute question quant à l'abonnement au : Bureau des abonnements, Presses scientifiques du CNRC, Conseil national de recherches Canada, Ottawa, ON K1A 0R6, Canada; téléphone : 613-993-9084; télécopieur : 613-952-7656; adresse électronique : research.journals@nrc.ca.

On peut obtenir les fichiers rétrospectifs sur **microforme** auprès de UMI, P.O. Box 1346, Ann Arbor, MI 48106-1346, É.-U., et auprès de Micromedia Ltée, 20 rue Victoria, Toronto, ON M5C 2N8, Canada.

Les numéros de 1999 de *Journal canadien des sciences halieutiques et aquatiques* sont accessibles sur le Web. On trouvera des renseignements sur les tarifs à

http://www.nrc.ca/cisti/journals/rjfr.html

Application of an ion-exchange separation technique and thermal ionization mass spectrometry to ^{226}Ra determination in otoliths for radiometric age determination of long-lived fishes

Allen H. Andrews, Kenneth H. Coale, Jocelyn L. Nowicki, Craig Lundstrom, Zenon Palacz, Erica J. Burton, and Gregor M. Cailliet

Abstract: To improve the accuracy and precision of radiometric age determination using ^{210}Pb: ^{226}Ra disequilibria in otoliths of fishes, a technique was developed incorporating an ion-exchange procedure followed by isotope-dilution thermal ionization mass spectrometry (TIMS) to determine ^{226}Ra. This technique counts ionized radium atoms directly; therefore, the uncertainty of the technique is superior to conventional radio-decay dependent techniques. Calcium and barium are major components of the otolith matrix that can interfere with TIMS analysis of radium. To remove these interferants, an ion-exchange separation procedure was developed. This procedure was tested by applying it to otolith samples from three fish species in three separate radiometric ageing studies. The resultant separations and TIMS determinations indicate that the procedure efficiently separates radium from calcium and barium. Measured ^{226}Ra activities for each species were similar to previous radiometric ageing studies, with the exception of one sample. When results were compared with traditional ^{226}Ra determination techniques, radon emanation and α-spectrometry, the separation procedure with isotope-dilution TIMS had significant advantages. Samples over three times smaller than attempted in other studies were processed with decreased uncertainty and processing time.

Résumé : Pour accroître l'exactitude et la précision de la détermination radiométrique de l'âge par le déséquilibre du ratio ^{210}Pb:^{226}Ra dans les otolithes des poissons, on a mis au point une technique utilisant une procédure d'échange d'ions suivie d'une analyse au moyen de la spectrométrie de masse à thermo-ionisation avec dilution des isotopes pour déterminer le ^{226}Ra. Cette technique compte directement les atomes de radium ionisés, de sorte que l'efficacité de cette technique est supérieure aux techniques classiques qui dépendent de la décroissance de la radioactivité. Le calcium et le baryum sont des composantes de la matrice des otolithes qui peuvent interférer avec l'analyse du radium par spectrométrie de masse à thermo-ionisation. Pour éliminer ces interférences, on a mis au point une technique de séparation par échange d'ions. On a testé cette technique en l'appliquant aux échantillons d'otolithes de trois espèces de poissons dans trois études distinctes de détermination radiométrique de l'âge. Les séparations résultantes et les déterminations par spectrométrie de masse à thermo-ionisation indiquent que cette technique sépare efficacement le radium du calcium et du baryum. Les activités du ^{226}Ra mesurées chez chaque espèce étaient semblables à celles obtenues dans d'autres études de détermination radiométrique de l'âge, à l'exception d'un échantillon. La comparaison de nos résultats avec ceux des techniques classiques de détermination du ^{226}Ra, de la technique utilisant l'émanation du radon et de l'α-spectrométrie a montré que notre technique de séparation suivie de l'analyse par spectrométrie de masse à thermo-ionisation avec dilution des isotopes comporte des avantages importants. On a pu traiter plus rapidement et avec un plus faible degré d'incertitude des échantillons plus de trois fois plus petits que ceux utilisés dans d'autres études.

[Traduit par la Rédaction]

Received June 12, 1998. Accepted February 23, 1999.
J14649

A.H. Andrews,[1] K.H. Coale, J.L. Nowicki, E.J. Burton, and G.M. Cailliet. Moss Landing Marine Laboratories, P.O. Box 450, Moss Landing, CA 95039-0450, U.S.A.
C. Lundstrom[2] and Z. Palacz.[3] University of California, Santa Cruz, Department of Earth Sciences, Santa Cruz, CA 95064, U.S.A.

[1]Author to whom all correspondence should be addressed. e-mail: andrews@mlml.calstate.edu
[2]Present address: Brown University, Geological Sciences, Providence, RI 02912, U.S.A.
[3]Present address: Micromass UK Ltd., Floats Rd., Wythenshawe, Manchester M23 9LZ, United Kingdom.

© 1999 NRC Canada

Introduction

Fisheries management strategies rely heavily on accurate age determinations. Age is typically determined in fishes by performing one of several techniques. The most common technique is counting growth increments in calcified structures (i.e., otoliths; Beamish and McFarlane 1987). The annual periodicity of growth increments in these structures is often assumed and, until recently, this assumption was rarely validated (Beamish and McFarlane 1983). The problem with typical age validation techniques is that they have limited applicability to deepwater or long-lived fishes because of slow growth, fine growth-increment structure, and barotrauma upon capture (Mace et al. 1990; McFarlane and Beamish 1995). One technique that can be used to validate age estimates for these fishes is a radiometric approach that exploits the disequilibria of ^{210}Pb and ^{226}Ra in otoliths as a natural chronometer (Smith et al. 1991; Bergstad 1995).

An essential requirement for utilizing ^{210}Pb:^{226}Ra disequilibria for age determination is the capability of measuring the activity of these radioisotopes with high precision and accuracy at very low levels, from femtograms (10^{-15} g) for ^{226}Ra to attograms (10^{-18} g) for ^{210}Pb. Detection of ^{210}Pb is typically accomplished through the autodeposition and α-spectrometric determination of its daughter, ^{210}Po (Flynn 1968). Because ^{210}Pb is the result of ingrowth from ^{226}Ra, low ^{210}Pb:^{226}Ra atom ratios exist in otolith material. Direct mass determination methods, therefore, are not feasible for ^{210}Pb at this time. Two techniques traditionally used to determine ^{226}Ra are scintillation counting of its daughter ^{222}Rn via radon emanation and direct α-spectrometry of ^{226}Ra in a filtered precipitate.

The radon emanation technique has been applied to otoliths, as part of the radiometric ageing technique, of six fish species: *Sebastes diploproa* (Bennett et al. 1982); *Sebastes mentella* (Campana et al. 1990); *Anoplopoma fimbria* (Kastelle et al. 1994); *Sebastes rufus* (Watters 1995); and *Sebastolobus altivelis* and *S. alascanus* (Kline 1996). This technique uses the α-decay of ^{222}Rn as a proxy for ^{226}Ra determination. The first ichthyological application of this radiometric ageing technique used whole otoliths for both ^{210}Pb and ^{226}Ra determination (Bennett et al. 1982). Use of whole otoliths, however, can be imprecise and requires application of mass-growth models that are not always robust (Francis 1995). To circumvent the need for mass-growth models, a method was developed to extract the oldest part of the otolith, the core, which represents the first few years of growth (Campana et al. 1990). Because otolith cores can be small (i.e., 0.01 to 0.05 g), cores from similar age/size-classes must be pooled to attain measurable activity. A sample size of approximately 1 g, however, can produce a large error for the radon emanation technique (Bennett et al. 1982). Therefore, ^{226}Ra determination is usually performed on pooled whole otoliths with the necessary assumption that ^{226}Ra uptake is in constant proportion to the otolith mass growth rate.

To determine ^{226}Ra, direct α-spectrometry has also been used as part of the radiometric ageing technique for six fish species: *Hoplostethus atlanticus* (Fenton et al. 1991; Smith et al. 1995); *Allocyttus verrucosus* (Stewart et al. 1995); three species of the family Lutjanidae (Milton et al. 1995); and *Macruronus novaezelandiea* (Fenton and Short 1995). In this technique, ^{226}Ra is isolated by co-precipitation with barium, using a ^{133}Ba yield tracer followed by α-spectrometric determination of the ^{226}Ra on calibrated detectors (Fenton et al. 1990). Because this technique has a lower background and, therefore, a lower detection limit, a smaller sample size can be used (~1 g). This technique has been applied to otolith core samples and whole otolith samples where cores were too small to be efficiently extracted.

Determining ^{226}Ra in otoliths using the radon emanation and direct α-spectrometry has worked well for radiometric ageing, but aspects of the technique made improvement desirable. Difficulties in developing relevant and verifiable mass growth-rate models and the uncertainty of the constant ^{226}Ra uptake assumption make the use of otolith cores preferable when possible. The large sample size typically required for a low uncertainty using radon emanation, however, make the use of cores problematic because the pooling of cores from hundreds to thousands of similarly aged fish would be necessary (e.g., >10 g; Campana et al. 1990; Watters 1995; Kline 1996). For the small sample sizes typically associated with the use of otolith cores, the determination of ^{226}Ra via direct α-spectrometry has produced the lowest uncertainty for samples with low mass and ^{226}Ra activity (Fenton et al. 1991). Both techniques (radon emanation and α-spectrometry), however, are time-consuming (3–5 weeks) and can lead to large analytical uncertainties (e.g., range of ~4–150%; Bennett et al. 1982; Campana et al. 1990; Fenton et al. 1991; Kastelle et al. 1994; Fenton and Short 1995; Milton et al. 1995; Smith et al. 1995; Stewart et al. 1995; Watters 1995; Kline 1996).

Because some fish species have a longevity that may exceed 100 years (4 to 5 half-lives of ^{210}Pb), the utility of the radiometric ageing technique becomes increasingly dependent on the analytical uncertainty of the technique. As the activity of ^{210}Pb asymptotically approaches the activity of ^{226}Ra, the analytical uncertainty becomes a larger proportion of the age estimate (Fig. 1). For example, a 10% error for a radiometric age of 60 years would be +25.5 to –14 years. A hypothetical reduction of this error to 1% significantly reduces the uncertainty to +1.7 to –1.3 years. Additionally, a reduction in error increases the applicable age range. A 10% error for a radiometric age of 120 years becomes undefined at the upper limit (the ^{210}Pb:^{226}Ra ratio can not exceed 1.0) and –52.3 years at the lower limit. A reduction of the error to 1% reduces the age uncertainty where the upper limit becomes defined (+26.9 and –11 years). A reduction of the error inherent in the technique would increase the applicability of the radiometric ageing technique to fish approaching 150 years and would reduce the age estimate uncertainty. As an example, reduced error in accelerator mass spectrometry was highly significant where age estimate uncertainty was reduced and the applicable age range was increased (Vogel et al. 1995).

In recent studies, thermal ionization mass spectrometry (TIMS) has been used to measure very small quantities of ^{238}U and ^{232}Th series isotopes, including radium, in volcanic rocks. High precision and accuracy and low detection limits have been reported for this technique (Cohen and O'Nions 1991). By using isotope-dilution TIMS, radium is measured directly by counting the ionized atoms with low detection

© 1999 NRC Canada

Fig. 1. Conceptual view of the effect of error in the measurement of ^{210}Pb and ^{226}Ra on the age estimate uncertainty. Given are two hypothetical scenarios where the ^{210}Pb:^{226}Ra activity ratio yields a 10% error and a reduced error of 1%. Note that a reduction from 10% to 1% reduces the age uncertainty considerably and increases the utility of the technique to fish that approach 150 years. Examples of fish species that show how longevity can vary among fishes are listed along the age axis. The Atlantic bluefin tuna (*Thunnus thynnus*) is an example of a fish that has relatively fast growth and an estimated longevity of 20 to greater than 30 years (Prince and Pulos 1983). The longevity of the Pacific grenadier (*Coryphaenoides acrolepis*) has been validated to at least 46 years and may approach 70 years, and the orange roughy (*Hoplostethus atlanticus*) has been validated to approximately 100 to 120 years (Smith et al. 1995; Andrews et al. 1999). Candidates for the greatest longevity in fishes are members of the sturgeon family at over 150 years (Anonymous 1954).

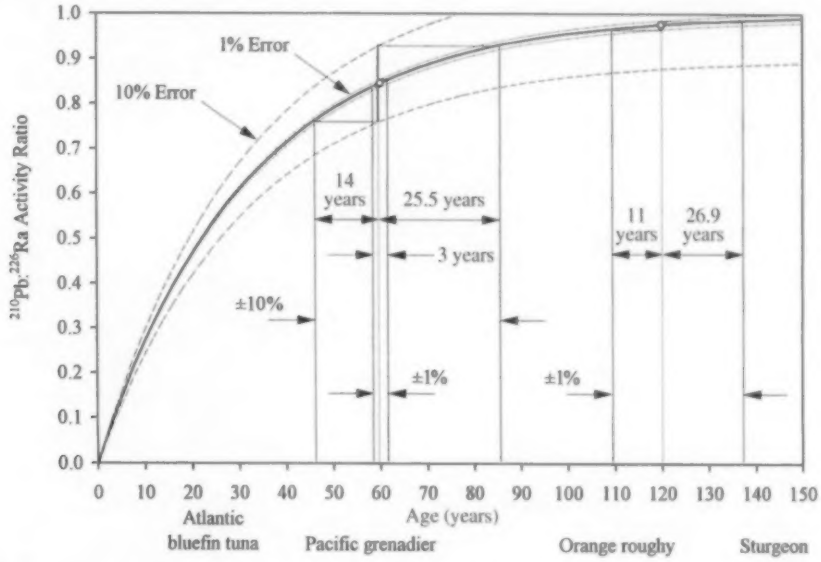

limits and high analytical precision (Volpe et al. 1991). The elemental composition of otoliths, however, is very different from that of volcanic rocks. Of concern are high concentrations of calcium and barium and an organic component called otolin. Each of these constituents must be reduced to very low levels, while conserving radium, to prevent ionization suppression of the radium signal and elevated background levels during TIMS analysis (Cohen and O'Nions 1991).

This paper describes a technique to determine ^{226}Ra directly in otoliths using an adapted ion-exchange procedure (Chabaux et al. 1994) and isotope-dilution TIMS. To test the application of this technique, ^{226}Ra activity was determined in otoliths of three fish species using isotope-dilution TIMS. In some otolith samples, ^{210}Pb was also measured for the purpose of radiometric age determination, the results of which will be discussed in future publications. The focus of this paper is the determination of ^{226}Ra activity in otoliths using the new technique and a comparison with the traditional techniques, where the benefits of TIMS are discussed.

Materials and methods

Determination of ^{226}Ra activity was performed on sagittal otoliths from three fish species. The species analyzed were shortspine thornyhead (*Sebastolobus alascanus*) collected off California in Monterey Bay and in the Gulf of the Farallones, Atlantic tarpon (*Megalops atlanticus*) from inshore waters of Florida, and yelloweye rockfish (*Sebastes ruberrimus*) from off southeastern Alaska. Whole adult *S. alascanus* otoliths were selected and pooled to attain samples of approximately 1 g. The purpose of these samples was for comparison with similar whole otolith samples processed using radon emanation (Kline 1996) and direct α-spectrometry (John Butler, NOAA, Southwest Fisheries Science Center, P.O. Box 271, La Jolla, CA 92038-0271, personal communication). Whole young-of-the-year *M. atlanticus* otoliths were pooled based on collection site (Collier-Seminole and Jack Island State Parks in southern Florida) and date to determine if exogenous ^{210}Pb would present a problem in ageing adults. Because traditional age is more reliable for young-of-the-year, radiometric age can be used to determine if exogenous ^{210}Pb is incorporated. Otolith cores (first 4 years of growth) of *S. ruberrimus* were extracted using procedures given elsewhere (Andrews et al. 1999) and were pooled into age-groups. A sample weight of 0.5 to 1.0 g was targeted in this study. In addition, one whole otolith sample was processed for a comparison of whole versus core ^{226}Ra activities.

Because of the extremely low levels of ^{226}Ra and ^{210}Pb, trace-metal precautions were exercised during sample processing (Watters 1995). All acids used were double distilled (GFS Chemicals®) and dilutions were made using Millipore®-filtered Milli-Q (MQ) water (18 MΩ·cm^{-1}). Because the technique used for ^{210}Pb determination had only a minor modification and was performed before ^{226}Ra analysis, the details of the procedure were described elsewhere (Andrews et al. 1999).

Otolith cleaning and dissolution

Otolith samples were cleaned, dried, and weighed before dissolution in the following manner. Rough cleaning began with hydrating the otoliths in de-ionized water for at least 5 min. Samples were agitated and rinsed three times with each of the following:

© 1999 NRC Canada

Table 1. Overview of column separation procedures.

	Calcium removal			Barium removal	
		Volume (mL)			
	Reagent	First pass	Second pass	Reagent	Volume (μL)
Ion-exchange resin	AG® 50W-X8 (Bio-Rad)	13[a]	13[a]	Sr® resin (EiChroM Ind.)	150[a]
Clean and	MQ water	100	100	MQ water	1000
condition	2.5–6.0 N HCl	50	50	1.1 N HNO_3	800
Introduction	Sample[b]	5	1	Sample[d]	50
Beaker rinse	6.0 N HCl	5	1	1.1 N HNO_3	50
Wash	6.0 N HCl	30	38	1.1 N HNO_3	150
Elution	6.0 N HCl	80[c]	80[c]	1.1 N HNO_3	450[c]

[a]Rinsed resin added in MQ water.
[b]Sample dissolved in 6.0 N HCl.
[c]Radium and barium fraction.
[d]Sample dissolved in 1.1 N HNO_3.
[e]Radium fraction.

(*i*) a mixture of de-ionized water and Micro® laboratory cleaner, (*ii*) de-ionized water, and (*iii*) MQ water. Fine cleaning was performed by sequentially stepping between agitation in four cleaning solutions with a Branson 2200 sonicator and a triple rinse with MQ water. The four cleaning solutions with agitation times were (*i*) MQ water (10 min), (*ii*) 0.15 N HNO_3 (1 min), (*iii*) basic 1:1 mixture of 30% H_2O_2:0.4 N NaOH (10 min), (*iv*) MQ water (10 min), and (*iv*) 0.001 N HNO_3 (3 times at 1 min). After the final rinse, samples were dried to constant weight (at least 24 h) in an oven at 80°C, cooled in a desiccator, and weighed to ±0.0001 g.

Dried and weighed samples were placed in acid-cleaned 100 mL Teflon® PFA griffin beakers. While on a hot plate at 80°C, 8.0 N HNO_3 was added to the otoliths in 1 mL aliquots until dissolved. The dissolved sample was dried, redissolved with 1 mL of 8.0 N HNO_3, and dried again. This was repeated 5 times. Before drying the fifth dissolution completely, 1 mL of 6.0 N HCl was added to form an aqua regia solution. This solution was dried, redissolved with 1 mL 6.0 N HCl, and dried again. Dissolution in 1 mL of 6.0 N HCl was repeated 5 times, which left the final sample in the desired chloride form. The repeated drying and dissolution enhanced the oxidation of otolin, a potential interferant.

Determination of ^{210}Pb activity

To determine ^{210}Pb activity in some of the otolith samples (*M. atlanticus* and *S. ruberrimus*) as part of independent radiometric ageing studies, α-spectrometry was performed on plated ^{210}Po samples spiked with ^{208}Po as a yield tracer (Andrews et al.1999). In previous studies, ascorbic acid was added to inhibit autodeposition of divalent iron (Kline 1996). Because ascorbic acid is an organic that can raise the background count levels in the TIMS analysis and because iron content in otoliths is low (Dannevig 1956), it was not used in this study. Radium blanks included the polonium plating steps to account for any potential radium contamination. The solution remaining after polonium autodeposition was recovered for ^{226}Ra analysis.

Radium separation

The separation of radium from calcium and barium is essential for obtaining good radium ionization efficiency during TIMS. This was achieved by applying a three column, ion-exchange separation procedure. Elution characteristics for each column separation were determined using otolith samples and calcium and barium standards, where the collection intervals were optimized using flame atomic absorption spectrophotometry (AA). Solid/solute distribution coefficients provided by the manufacturer were used to estimate the acid strength necessary to achieve the greatest separation between radium, barium, and any remaining calcium in the third cation exchange column. Based on these findings, an optimized ion-exchange separation procedure was developed (Table 1).

To determine ^{226}Ra using isotope-dilution TIMS, the dissolved otolith sample was spiked gravimetrically with a ^{228}Ra yield tracer. The ^{228}Ra solution was prepared by separating ^{228}Ra from its parent ^{232}Th. The atomic ratio of ^{232}Th to ^{230}Th in the solution was greater than 1.6 million, producing a ^{228}Ra to ^{226}Ra ratio in the yield tracer of 0.2855 ± 0.0057 as of June 1, 1995. The ^{228}Ra spike solution was calibrated against NBS and geological standards. The spike was added to the sample after polonium plating, which avoided autodeposition of ^{228}Th (daughter of ^{228}Ra) and subsequent contamination of the α-detector from ^{228}Th recoil (Sill and Olson 1970). The amount of ^{228}Ra added to each sample was estimated to attain a ^{226}Ra:^{228}Ra atom ratio close to one. The spiked sample was dried and examined to determine the next step in the separation procedure. If the residue was not white, the sample was redissolved with 1 mL of 8.0 N HNO_3 and dried. This was repeated until a white residue was obtained. Before the final drying was complete, an aqua regia transition to 6.0 N HCl was created by adding 1 mL of 6.0 N HCl. This solution was dried. Dissolution with 6.0 N HCl and drying was repeated three times. All of these steps were repeated until the residue was as white as possible.

Calcium removal: two column separation

The first column type was a 10 mL chromatography column with a 20 mL reservoir (Bio-Rad Laboratories, Econo-Pac 10 Column). A rinsed slurry of Bio-Rad AG® 50W-X8 cation exchange resin and MQ water was added into the acid-cleaned column to achieve 13 mL of settled resin. The settled resin was cleaned and conditioned by passing 100 mL of MQ water followed by 5 mL 2.5 N HCl, 5 mL 4.0 N HCl, and 40 mL 6.0 N HCl through the column. Conditioning the column shrinks the resin volume to 10 mL with a length:width aspect ratio of 3.9.

The sample was redissolved in 5 mL of 6.0 N HCl over mild heat (50–60°C) covered with a watch glass. The 5 mL sample was cooled, loaded onto the column, allowed to settle into the resin, and the beaker was rinsed with an additional 5 mL of 6.0 N HCl. Using the sample pipette tip, the acid rinse was introduced by allowing 1 mL to settle into the resin before adding the remaining 4 mL. Once the acid rinse settled into the resin, two 1 mL aliquots of 6.0 N HCl were added to begin washing the column. Each of these aliquots were allowed to settle into the resin prior to adding 28 mL of 6.0 N HCl column wash. The column wash was allowed to settle into the resin and the collected eluant containing the bulk of the calcium was discarded (40 mL). An acid-cleaned 100 mL Teflon® PFA griffin beaker was placed under the column to collect the radium fraction. The radium fraction was collected in the next

© 1999 NRC Canada

80 mL of 6.0 N HCl added to the column in portions that kept the reservoir full to maximize the flow rate (~1.5 mL·min^{-1}). Once the 80 mL sample fraction was collected, the beaker was placed on a hot plate at 90–100°C and taken to dryness. The sample was never boiled and the heat was reduced when a crystalline residue began to form. While samples were drying, the same columns were cleaned and conditioned for a second pass, as in the first preparation, and the separation procedure was repeated from the beginning of this paragraph.

Barium removal: third column separation

The second column type was a custom 150 µL microcolumn made of TFE heat-shrink tubing (6.35 mm ID) shrunk over a hand-machined stainless steel die. Die dimensions were 6.35 mm (0.25 in.) in diameter by 57 mm (2.25 in.) in length for the reservoir which tapers down to 2.38 mm (0.094 in.) in diameter by 35 mm (1.38 in.) in length for the column volume. Enough tubing was used to create an 800 µL reservoir and a constricted tip with minimal dead volume. A frit made of porous polyethylene (2 mm thickness with 10 µm pore size) was cut and squeezed tightly down the column and into the tip. The acid-cleaned microcolumn was prepared for sample processing by adding a slurry of MQ water and 50–100 µm Sr® resin (EiChroM Industries, Darien, Ill.). For best results, the column was filled with MQ water first and then the resin was added to the water and allowed to settle into the column to just below the taper of the reservoir. Cleaning and conditioning were performed by passing 1000 µL of MQ water followed by 800 µL of 1.1 N HNO_3 through the column. The conditioned microcolumn contained 150 mL of Sr® resin and had a length:width aspect ratio of 13.1.

To prepare a sample for introduction to the third column, the sample was dissolved with 100 µL of 8.0 N HNO_3. Droplets were swirled in the beaker bottom, gathered together, and dried at 90–100°C. If the dried sample spot was not white, the sample was treated with an aqua regia solution of 10–30 µL of 8.0 N HNO_3 and 10–30 µL of 6.0 N HCl, dried at 90–100°C, and redissolved in 10–30 µL of 8.0 N HNO_3. The last two steps were repeated until the sample was as white as possible.

The sample spot was redissolved with 50 µL of 1.1 N HNO_3 over mild heat (60–70°C), cooled, and added to the microcolumn with a 100 µL pipette. The sample was allowed to settle into the resin and then a beaker rinse of 50 µL 1.1 N HNO_3 was added to the column. A column wash of 150 µL of 1.1 N HNO_3 was added and allowed to settle into the resin. The eluant (250 µL of 1.1 N HNO_3) was discarded. Radium elution was performed by adding 450 µL of 1.1 N HNO_3 to the column, while the barium remained on the column, and the sample fraction was collected in an acid-cleaned 3 mL Teflon® PFA sample vial. The collected sample was then placed on a hot plate at 90–100°C and dried. If the spot was not clear and very small (0.5 mm), an aqua regia solution of 1 drop of 8.0 N HNO_3 and 1 drop of 6.0 N HCl was added and dried at 90–100°C. These steps were repeated until the sample would not lighten or shrink any further. The sample spot was then redissolved two times in 1 drop of 6.0 N HCl and dried into the chloride form. Microcolumns were cleaned by passing 2000 µL of MQ water and were stored upright in a vial of MQ water.

Thermal ionization mass spectrometry

To use TIMS, the final sample from the separation procedure must be loaded onto a metallic filament. The design was a 1-cm-long single-filament assembly made of 4 pass zone-refined 99.999% rhenium (0.020 in. wide and 0.001 in. thick; H. Cross Co., Weehawken, N.J.). Before loading the sample, the filament was out-gassed in a diffusion pump vacuum chamber at 3.5 amps for 30 min (~1700°C) once the vacuum was less than 10^{-6} torr. Filaments were allowed to cool in the pumped-down chamber before removal. To minimize organic interference during analysis, sample loading began immediately after out-gassing. Tantalum activator solution (2 µL of 1% Ta solution, Birck 1986) were evaporated onto the filament to enhance ionization (Cohen and O'Nions 1991). Samples in the teflon vials were transferred to the filament in two successive 1 µL additions of 1 N HCl. The tantalum activator and the samples were dried as they were loaded by passing 0.8 amps through the filament. Once loaded, an additional 20 s period of increased amperage (1.5 amps) was applied to further secure the sample to the filament and drive off any remaining acid.

Radium analysis was performed on a Vacuum Generators 54-30 Thermal Ionization Mass Spectrometer, equipped with an energy filter and an ion-counting daly-detector. The dark current on the detector was 20 counts per minute (cpm) and dead time was 22 ns. The accuracy and linearity of this detector at signals up to 1 million counts per second (cps) has been verified by repeated measurements of NBS standard U-010. The following TIMS radium analysis procedure is similar to the procedure outlined in Cohen and O'Nions (1991). Prepared filament samples were placed in the TIMS sample turret, pumped down overnight, and analyzed the following day. First a programmed warm-up sequence raised the filament to 2.4 amps (1150°C) over 15 min. After raising the filament manually to approximate operating temperatures (1197 to 1220°C), the residual ^{138}Ba signal was used to focus the beam for counting the much weaker ^{226}Ra and ^{228}Ra signals. The ^{138}Ba signal typically varied between 20 000 and 3 million cps at this point. Once focused, unspiked samples (samples containing no added ^{228}Ra) were scanned to determine if measurable natural ^{228}Ra existed in the otoliths. In all samples analyzed, no natural ^{228}Ra was recovered and, therefore, no adjustment to the ^{226}Ra determination was required.

Spiked samples and blanks were analyzed with a programmed sequence of readings at atomic mass unit (amu) 226 and 228 with background readings at amu 225.5. First the scanning of the amu range 224.5 to 228.5 was performed to ensure that organic interference had been minimized. When the background from amu 224.5 to 228.5 appeared uniform and the ^{226}Ra signal was as high as could be attained by focusing procedures (30 to >100 cps), analysis began. On spiked samples, where ^{226}Ra:^{228}Ra was near unity, analysis was performed by peak-hopping between amu 226 and amu 228 after taking a 20 s baseline measurement at amu 225.5 (background compensation). A measurement cycle consisted of a 5 s integration on amu 228, a 10 s integration on amu 226, and a 5 s integration on amu 228. Twenty ratios were taken per block and an analysis generally consisted of 5 blocks (or until the desired precision was attained). Data were obtained in the filament temperature range of 1180–1300°C. At higher temperatures, residual calcium ionization interfered with the radium ionization. The ^{226}Ra:^{228}Ra atom ratio was calculated as the mean (±SE) of all the readings taken in the analysis with outlying values statistically eliminated by the analysis routine.

Because the TIMS detected atomic ^{226}Ra:^{228}Ra ratio was equal to the unknown atomic ratio of the sample, the known number of atoms in the ^{228}Ra spike can be used to determine the unknown number of ^{226}Ra atoms. Hence, ^{226}Ra activity was determined, after correcting for ^{226}Ra contributed by the spike, by multiplying the number of ^{226}Ra atoms by the ^{226}Ra decay constant.

Results

Radium separation

Based on AA determinations, the separation of calcium and barium (used as a proxy for radium) for the first pass on the AG® 50W-X8 ion-exchange column was good, but the elements co-eluted to a small extent (Fig. 2). To conserve any sample in the co-elution, the selected sample collection interval began in the tail of the calcium elution at 40 mL and

© 1999 NRC Canada

Fig. 2. Elution characteristics of the first pass using 6.0 N HCl on the AG® 50-X8 cation exchange column for calcium (○) and barium (■). In these experiments, barium was used as a stable proxy for radium. Calcium eluted strongly in the first 40 mL and then tailed to approach zero at 60 mL. The beginning of the barium elution was within the calcium tail and, therefore, the collection interval for the radium and barium fraction was from 40 to 120 mL.

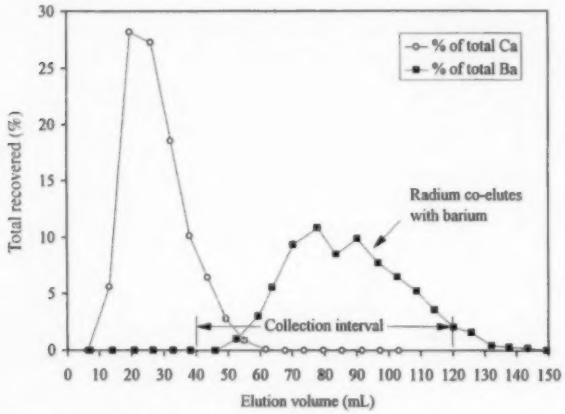

Fig. 3. Elution characteristics of the second pass using 6.0 N HCl on the AG® 50-X8 cation exchange column for calcium (○) and barium (■). To more clearly evaluate the separation, calcium and barium elutions were performed separately but were plotted together. The collection interval for the radium and barium fraction was from 40 to 120 mL

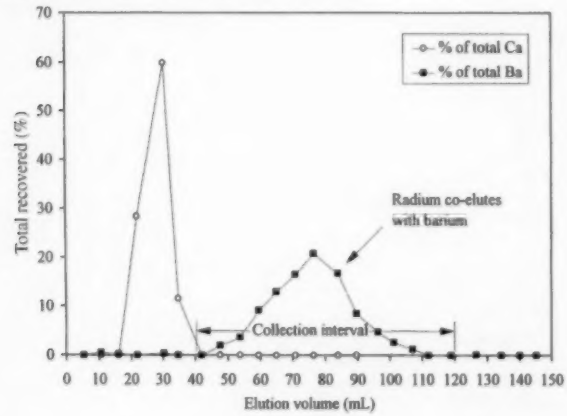

ended at 120 mL. Less than 10% of the total calcium was found in the selected collection interval.

The second pass on the AG® 50W-X8 ion-exchange column better separated the calcium and barium (radium) fractions, which did not co-elute to a measurable extent (Fig. 3). The selected sample collection interval was the same as in the first column pass. A calculated 1% of the total calcium may have remained in the sample fraction. Recovery of barium, and presumably radium, through the first two ion-exchange columns was greater than 90%.

Fig. 4. Elution characteristics of the third column pass using 1.1 N HNO_3 on the Sr® resin microcolumn for calcium (○) and barium (■). Based on the distribution coefficients provided by EiChroM Industries, Darien, Ill., radium eluted between calcium and barium. The optimal collection interval which minimizes calcium and barium was determined to be 250–700 µL using TIMS.

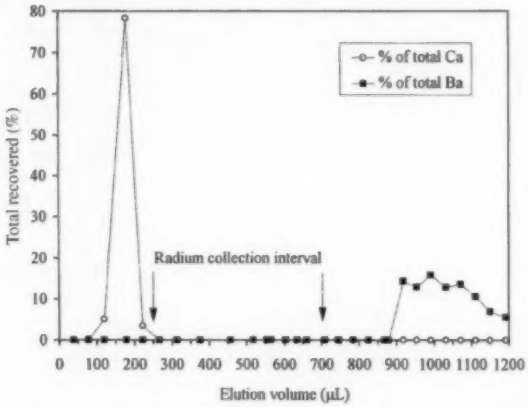

An acid strength of 1.1 N HNO_3 achieved the greatest separation between calcium, barium, and radium on the Sr® resin microcolumn. Based on the distribution coefficients of the Sr® resin, a radium sample collection interval of 250 to 700 µL was selected between the calcium and barium elution intervals (Fig. 4). A small sample spot (<0.5 mm) remained after drying and was used for radium determination on the TIMS.

Thermal ionization mass spectrometry

Seventeen samples consisting of 15 otolith samples from three fish species and two spiked ^{228}Ra yield-tracer blanks were processed for radium determination using isotope-dilution TIMS. Three of the 15 otolith samples, one from each species, were not spiked with ^{228}Ra to verify that natural quantities of ^{228}Ra were insignificant relative to potential spike quantities. Results indicate that naturally occurring ^{228}Ra for each species is at or below TIMS background. Spiked blanks indicated the ion-exchange separation procedures do not contribute measurable ^{226}Ra to samples. The twelve spiked samples produced ^{226}Ra activities ranging from 0.0255 ± 0.0004 dpm·g^{-1} to 1.65 ± 0.03 dpm·g^{-1} (Table 2).

During sample analysis, the signal strength of calcium, barium, and radium were observed qualitatively. The ^{226}Ra signal was usually strong (as high as 500 cps) and had low or no background interference from organics (usually <1 cps). The residual calcium and barium signals were much stronger than the radium signals (approximately 20 000 and 3 million cps, respectively). Samples with the highest analytical uncertainties typically had the highest residual calcium and barium signals.

Technique comparison

Determination of ^{226}Ra using the ion-exchange separation procedure and isotope-dilution TIMS in otoliths from three fish species revealed a wide range of activity levels (Ta-

© 1999 NRC Canada

Table 2. Summary of sample types for each species.

Species	Sample type (whole or core)	Number of otoliths	Sample weight (g)	^{226}Ra (dpm·g^{-1})	^{226}Ra % error
Sebastolobus alascanus	Whole	7	1.0150	0.0306	1.44
	Whole	8	1.2607	0.0323	2.29
Megalops atlanticus	Whole[a]	35	0.5068	0.201	1.38
	Whole[a,b]	26	0.525	0.306	1.05
	Whole[a]	28	0.564	1.65	1.60
Sebastes ruberrimus	Core	10	0.303	0.0305	2.49
	Core	10	0.319	0.0255	1.75
	Core	14	0.471	0.0298	1.91
	Core	19	0.561	0.0331	3.66
	Core	23	0.587	0.0296	2.26
	Core	20[c]	0.592	0.0283	4.88
	Whole	1	0.8819	0.0263	6.70

Note: Number of otoliths used corresponds to the number of fish in each sample because one otolith of each pair was sectioned for traditional ageing.

[a]Young-of-the-year.

[b] ^{210}Pb data taken to estimate age and assess exogenous ^{210}Pb in the otolith material.

[c]Approximate number.

ble 2). Whole and cored otolith samples from *S. alascanus* and *S. ruberrimus* contained the lowest ^{226}Ra activities and have similar levels. The whole young-of-the-year otoliths from *M. atlanticus* contained ^{226}Ra activities that ranged from approximately 10 to 100 times the activity of the two deepwater species. The ^{210}Pb activity for the juvenile *M. atlanticus* sample to be aged was 0.00243 ± 0.00017 dpm. Calculated age based on the ratio of ^{210}Pb:^{226}Ra activities was 0.51 ± 0.04 years.

To allow direct comparison of these results with existing studies, some reported ^{226}Ra uncertainties were recalculated as a percentage of the reported ^{226}Ra activity. These comparisons are reported here with other features that are an improvement relative to existing techniques. The ^{226}Ra activities for *S. alascanus* are unique because they were compared with ^{226}Ra results from radon emanation and direct α-spectrometry for the same species. The TIMS ^{226}Ra activities for this species are the lowest, with radon emanation and direct α-spectrometry ranging higher (Table 3). Each determination was performed on similar but independent whole otolith samples. Because the *S. ruberrimus* samples are otolith-core samples, the sample size and ^{226}Ra measurements were compared with results from two recent radiometric ageing studies on two different fish species (*Anoplopoma fimbria* and *Macruronus novaezelandiae*) where otolith cores were used (Table 4). Sample size, analytical uncertainty, and processing time were significantly reduced relative to these studies.

Discussion

The primary objective of this study was to separate radium from calcium and barium in otoliths and to determine ^{226}Ra using isotope-dilution TIMS. The initial approach was to use a technique developed for volcanic rocks where barium is the primary suppressant to the detection of radium using TIMS (Volpe et al. 1991). Attempts to use this technique resulted in samples too high in calcium and barium to measure radium. Because otoliths are high in calcium (38% by weight; Dannevig 1956), in addition to barium (~5–10 ppm; Edmonds et al. 1991), a recently developed ion-exchange separation technique was applied (Chabaux et al. 1994). With modifications, calcium and barium were successfully reduced and measurable radium was recovered.

There were problems with organic contamination in the developmental stages of the ion-exchange separation procedure. Samples analyzed using TIMS had an elevated and noisy background (high counts at amu 225.5) which was attributed to organic interference from otolin (0.2–10% in otoliths by weight; Degens et al. 1969). This observation led to the rigorous sample dissolution and oxidation procedures reported here. As a result of this procedure, the observed organic interference on the thermal ionization mass spectrometer was reduced to very low levels (<1 cps).

The samples used in this analysis were very diverse in composition and resultant ^{226}Ra activity (Table 2). Whole otoliths from adult *S. alascanus*, whole young-of-the-year

Table 3. Comparison of results for *S. alascanus* otoliths using each technique.

	Technique	Sample size range (g)	^{226}Ra activity range (dpm·g^{-1})	Analytical uncertainty (%)
This study	TIMS	1.0150–1.2607	0.0306–0.0323	1.44–2.29
Kline (1996)	Radon emanation	15.631–16.588	0.0387–0.0504	3.4–5.2
Butler[a] (unpublished data)	α-spectrometry	1.23–1.65[b]	0.0495–0.0697	5.8–6.6

Note: Otolith samples were similar but from different fish samples.

[a]John Butler, Southwest Fisheries Science Center, P.O. Box 271, La Jolla, CA 92038-0271, personal communication.

[b]Before cleaning.

© 1999 NRC Canada

Table 4. A comparison of results for *S. ruberrimus* cores with two studies using otolith cores and one of the other two ^{226}Ra assessment techniques.

	Technique	Sample size range (g)	^{226}Ra activity range (dpm·g^{-1})	Analytical uncertainty (%)	Processing time
This study *S. ruberrimus*	TIMS	0.303–0.592	0.0255–0.0331	1.75–4.88	7–10 days
Kastelle et al. (1994) *A. fimbria*	Radon emanation	0.9227–1.3748	0.288–0.517	~4	5–6 weeks[a]
Fenton and Short (1995) *M. novaevelandiae*	α-spectrometry	~1[b]	0.0179–0.0290	~12–21	3.5–4 weeks[c]

Note: Kastelle et al. (1994) used radon emanation on sablefish (*Anoplopoma fimbria*) and Fenton and Short (1995) used direct α-spectrometry on hoki (*Macruronus novazelandiae*).

[a]Craig Kastelle, Alaska Fisheries Science Center, National Marine Fisheries Service, NOAA, 7600 Sand Point Way NE, Seattle, WA 90915-0070, personal communication.

[b]Specific sample weights not reported.

[c]Gwen Fenton, Department of Zoology, University of Tasmania Hobart, Tasmania, 700.0, Australia, personal communication.

otoliths from *M. atlanticus*, and cored otoliths from *S. ruberrimus* ranged from greater than a gram to less than half of a gram with ^{226}Ra activities covering almost 2 orders of magnitude. The error for these samples varies from optimal (~1–2.5%) to greater than 3%. The high error for some of the *S. ruberrimus* samples (3.66 to 6.70%) was attributed to high calcium and low radium counts. The ^{226}Ra activity results were used as part of separate radiometric ageing studies for each fish species, which are in progress or in preparation for publication.

Differences in the ^{226}Ra levels determined for whole otoliths of *S. alascanus* using radon emanation and direct α-spectrometry prompted a follow-up ^{226}Ra determination using the new TIMS technique (Table 3). The ^{226}Ra activities determined using TIMS are lower than the results for the other two techniques, but more similar to Kline (1996). Kline (1996) pooled many otoliths to attain a very large sample size that provided for a low error but may have obscured individual differences. The α-spectrometry on similar-sized samples had higher error than the TIMS results. TIMS results are similar to Kline (1996) and differences between direct α-spectrometry and TIMS may indicate varying ^{226}Ra activities between fish from different locations. This seems possible because some of the samples used in this study were taken from a location off the Farallon Islands, California, north of Monterey Bay, California, where Kline (1996) collected. Geographical variation of radium in the natural environment is supported by the findings in otoliths of juvenile *M. atlanticus* and Pacific grenadier, *Coryphaenoides acrolepis* (Andrews et al. 1999).

Determination of ^{226}Ra and ^{210}Pb for young-of-the-year *M. atlanticus* samples was part of a feasibility study to determine if radiometric age determination would be applicable to adult otolith cores. To determine if exogenous ^{210}Pb would be a factor in radiometric age determination of adult *M. atlanticus*, age was calculated for a young-of-the-year sample using the measured ^{210}Pb and ^{226}Ra activities. If exogenous ^{210}Pb was accumulated in significant quantities, then the calculated radiometric age would be greater than the known age of these juveniles (<1 year). Measurements of ^{210}Pb in this sample resulted in a radiometric age that agreed with the expected average age of about 6 months (0.51 ± 0.04 years). The conclusion was that exogenous ^{210}Pb was not incorporated into juvenile otoliths of *M. atlanticus*.

The range of ^{226}Ra activity among the *M. atlanticus* samples can be attributed to the variable water chemistry of inshore waters where the juveniles were collected (Fanning et al. 1982; Crabtree et al. 1995; Moore 1996). The sample with the highest activity (1.65 ± 0.03) was collected in Collier-Seminole State Park, Florida, whereas the two more similar samples (0.201 ± 0.003 and 0.306 ± 0.003) were collected in Jack Island State Park, Florida. This variability, however, was not a detrimental factor for this technique because ^{226}Ra and ^{210}Pb were determined from the same sample. A follow-up study to validate the estimated longevity of *M. atlanticus* using the new ion-exchange separation technique and isotope-dilution TIMS was successful (Andrews et al. 1997).

Some of the advantages of the new technique can be demonstrated by comparing the results from otolith cores of *S. ruberrimus* with two recent radiometric ageing studies (Table 4). By comparing the TIMS results with the radon emanation results for *Anoplopoma fimbria* (Kastelle et al. 1994), the new technique measured ^{226}Ra activity that was about ten times lower in samples more than three times smaller with lower analytical uncertainty. A comparison with the α-spectrometry results for *Macruronus novaezelandiae* (Fenton and Short 1995) indicate ^{226}Ra activities were similar, but sample size was about three times smaller with greatly reduced analytical uncertainty. Processing time (from cleaning cores to radium results) for this technique was significantly reduced from 3.5–6 weeks, for the other two techniques, to 7–10 days.

Because ^{226}Ra activities observed for *S. alascanus* and *M. atlanticus* varied considerably among the samples (Tables 2 and 3), the potential for variation of ^{226}Ra uptake among the individuals in a sample must be considered in future radiometric ageing studies. To increase the accuracy of radiometric age determination using otolith cores and to avoid the assumption of constant ^{226}Ra uptake, ^{210}Pb and ^{226}Ra activities should be measured in each sample. Variation of ^{226}Ra activity within the pooled sample has no effect on age determination because average ^{210}Pb:^{226}Ra disequilibria yields average age. Because of the analytical advantages inherent in the TIMS technique, the assumption of constant uptake becomes unnecessary and radiometric age determination be-

© 1999 NRC Canada

comes more accurate. In a companion study, this technique was successfully applied to the radiometric age determination of the Pacific grenadier (Andrews et al. 1999).

Because this technique has improved the accuracy and processing time of ^{226}Ra determination, the most significant source of error and analytical processing time in radiometric age determination is now associated with the ^{210}Pb analysis via α-spectrometry. For the radiometric age determined for the juvenile *M. atlanticus* sample, approximately 87% of the error contribution came from the ^{210}Pb analysis.

The ^{226}Ra activities determined for the otoliths of the three species studied are generally in the range of values reported by all of the previously cited fish ageing studies (0.004 ± 0.006 to 0.517 ± 0.021 dpm·g^{-1}), with the exception of one *M. atlanticus* sample (1.65 ± 0.03 dpm·g^{-1}). This is the highest ^{226}Ra activity yet reported in the otoliths of fish by more than a factor of three. Preliminary radiometric age determinations made for *S. ruberrimus* and the successful application of the new technique to the Pacific grenadier (Andrews et al. 1999) and Atlantic tarpon (Andrews et al. 1997), indicate the new ion-exchange separation procedure coupled with isotope-dilution TIMS is an effective technique for determining ^{226}Ra in otoliths for the purpose of radiometric age determination.

Acknowledgments

We wish to thank Roy Crabtree and the Florida Department of Environmental Protection for samples and financial support in the Atlantic tarpon portion of this project; Victoria O'Connell and the Alaska Department of Fish and Game for samples and financial support in the yelloweye rockfish portion of this project; Mike Gordon and Steve Fitzwater for assistance with the atomic absorption spectrophotometry; Craig Kastelle and Dan Kimura for assistance with error analysis. The Atlantic tarpon portion of this project was supported in part under funding from the department of the Interior, U.S. Fish and Wildlife Service, Federal Aid for Sportfish Restoration, Project Number F-59. A majority of the research was funded by a grant from the National Sea Grant College Program, National Oceanic and Atmospheric Administration, U.S. Department of Commerce, under grant number NA36RG0537, project number R/F-148, through the California State Resources Agency. The views expressed herein are those of the authors and do not necessarily reflect the views of NOAA or any of its sub-agencies. The U.S. government is authorized to reproduce and distribute for governmental purposes.

References

Andrews, A.H., Burton, E.J., Coale, K.H., and Cailliet, G.M. 1997. Final report: application of radiometric age determination to the Atlantic tarpon, *Megalops atlanticus*. Florida Department of Environmental Protection Contract No. MR113, St. Petersburg, Fla.

Andrews, A.H., Cailliet, G.M., Coale, K.H. 1999. Age and growth of the Pacific grenadier (Family Macrouridae, *Coryphaenoides acrolepis*) with age estimate validation using an improved radiometric ageing technique. Can. J. Fish. Aquat. Sci. **56**: 1339–1350.

Anonymous. 1954. 152-year-old lake sturgeon caught in Ontario. Comm. Fish. Rev. **16**(9): 28.

Beamish, R.J., and McFarlane, G.A. 1983. The forgotten requirement for age validation in fisheries biology. Trans. Am. Fish. Soc. **112**: 735–743.

Beamish, R.J., and McFarlane, G.A. 1987. Current trends in age determination methodology. *In* The age and growth of fish. *Edited by* R.C. Summerfelt and G.E. Hall. The Iowa State University Press, Ames, Iowa. pp. 15–42.

Bennett, J.T., Boehlert, G.W., and Turekian, K.K. 1982. Confirmation of longevity in *Sebastes diploproa* (Pisces: Scorpaenidae) from ^{210}Pb/^{226}Ra measurements in otoliths. Mar. Biol. **71**: 209–215.

Bergstad, O.A. 1995. Age determination of deep-water fishes: experiences, status and challenges for the future. *In* Deep-water fisheries of the north Atlantic oceanic slope. NATO ASI Series. Ser. E. Applied Sciences. Vol. 296. *Edited by* Alan G. Hopper. Kluwer Academic Press, Dordrecht, Netherlands. pp. 267–283.

Birck, J.L. 1986. Precision K–Rb–Sr isotopic analysis: application to Rb–Sr chronology. Chem. Geol. **56**: 73–83.

Campana, S.E., Zwanenburg, K.C.T., and Smith, J.N. 1990. ^{210}Pb/^{226}Ra determination of longevity in redfish. Can. J. Fish. Aquat. Sci. **47**: 163–165.

Chabaux, F., Othman, D.B., and Birck, J.L. 1994. A new Ra–Ba chromatographic separation and its application to Ra mass-spectrometric measurement in volcanic rocks. Chem. Geol. **119**: 191–197.

Cohen, A.S., and O'Nions, R.K. 1991. Precise determination of femtogram quantities of radium by thermal ionization mass spectrometry. Anal. Chem. **63**: 2705–2708.

Crabtree, R.E., Cyr, E.C., and Dean, J.M. 1995. Age and growth of tarpon, *Megalops atlanticus*, from South Florida waters. Fish. Bull. **93**: 619–628.

Dannevig, E.H. 1956. Chemical composition of the zones in cod otoliths. J. Cons. Int. Explor. Mer, **21**(2): 156–159.

Degens, E.T., Deuser, W.G., and Haedrich, R.L. 1969. Molecular structure and composition of otoliths. Mar. Biol. **2**: 105–113.

Edmonds, J.S., Caputi, N., and Morita, M. 1991. Stock discrimination by trace-element analysis of otoliths of orange roughy (*Hoplostethus atlanticus*), a deep-water marine teleost. Aust. J. Mar. Freshwater Res. **42**: 383–389.

Fanning, K.A., Breland, J.A., and Byrne, R.H. 1982. Radium-226 and radon-222 in the coastal waters of west Florida: high concentrations and atmospheric degassing. Science (Wash.), **215**: 667–670.

Fenton, G.E., and Short, S.A. 1995. Radiometric analysis of blue grenadier, *Macruronus novaezelandiae*, otolith cores. Fish. Bull. **93**: 391–396.

Fenton, G.E., Ritz, D.A., and Short, S.A. 1990. ^{210}Pb/^{226}Ra disequilibria in otoliths of blue grenadier, *Macruronus novaezelandiae*: problems associated with radiometric ageing. Aust. J. Freshwater Res. **41**: 467–473.

Fenton, G.E., Short, S.A., and Ritz, D.A. 1991. Age determination of orange roughy, *Hoplostethus atlanticus* (Pisces: Trachichthyidae) using ^{210}Pb:^{226}Ra disequilibria. Mar. Biol. **109**: 197–202.

Flynn, W.W. 1968. The determination of low levels of polonium-210 in environmental materials. Anal. Chim. Acta, **43**: 221–227.

Francis, R.I.C.C. 1995. The problem of specifying otolith-mass growth parameters in the radiometric estimation of fish age using whole otoliths. Mar. Biol. **124**: 169–176.

Kastelle, C.R., Kimura, D.K., Nevissi, A.E., and Gunderson, D.R. 1994. Using Pb-210/Ra-226 disequilibria for sablefish, *Anoplopoma fimbria*, age validation. Fish. Bull. **92**: 292–301.

© 1999 NRC Canada

Kline, D.E. 1996. Radiochemical age verification for two deep-sea rockfishes (*Sebastolobus altivelis* and *S. alascanus*). M.S. thesis, California State University, San Jose, Calif.

Mace, P.M., Fenaughty, J.M., Coburn, R.P., and Doonan, I.J. 1990. Growth and productivity of orange roughy (*Hoplostethus atlanticus*) on the north Chatham Rise. N.Z. J. Mar. Freshwater Res. **24**: 105–109.

McFarlane, G.A., and Beamish, R.J. 1995. Validation of the otolith cross-section method of age determination for sablefish (*Anoplopoma fimbria*) using oxytetracycline. *In* Recent developments in fish otolith research. *Edited by* D.H. Secor, J.M. Dean, and S.E. Campana. The Belle W. Baruch Library in Marine Science, No. 19. University of South Carolina Press, Columbia, South Carolina. pp. 319–329.

Milton, D.A., Short, S.A., O'Neill, M.F., and Blaber, S.J.M. 1995. Ageing of three species of tropical snapper (Lutjanidae) from the Gulf of Carpentaria, Australia, using radiometry and otolith ring counts. Fish. Bull. **93**: 103–115.

Moore, W.S. 1996. Large groundwater inputs to coastal waters revealed by ^{226}Ra enrichments. Nature (London), **380**: 612–614.

Prince, E.D., and Pulos, L.M. (*Editors*). 1983. Proceedings of the international workshop on age determination of oceanic pelagic fishes: tunas, billfishes, and sharks. National Oceanic and Atmospheric Adminstration (NOAA) Technical Report NMFS 8, Washington, D.C.

Sill, C.W., and Olson, D.G. 1970. Sources and prevention of recoil contamination of solid-state alpha detectors. Anal. Chem. **42**(13): 1596–1607.

Smith, D.C., Fenton, G.E., Robertson, S.G., and Short, S.A. 1995. Age determination and growth of orange roughy (*Hoplostethus atlanticus*): a comparison of annulus counts with radiometric ageing. Can. J. Fish. Aquat. Sci. **52**: 391–401.

Smith, J.N., Nelson, R., and Campana, S.E. 1991. The use of Pb-210/Ra-226 and Th-228/Ra-228 dis-equilibria in the ageing of otoliths of marine fish. *In* Radionuclides in the study of marine processes. *Edited by* P.J. Kershaw and D. Woodhead. Elsevier Science, New York. pp.350–359.

Stewart, B.D., Fenton, G.E., Smith, D.C., and Short, S.A. 1995. Validation of otolith-increment age estimates for a deepwater fish species, the warty oreo, *Allocyttus verrucosus*, by radiometric analysis. Mar. Biol. **123**: 29–38.

Vogel, J.S., Turteltaub, K.W., Finkel, R., and Nelson, D.E. 1995. Accelerator mass spectrometry: isotope quantification at attomole sensitivity. Anal. Chem. **67**(11): 353A–359A.

Volpe, A.M., Olivares, J.A., and Murrell, M.T. 1991. Determination of radium isotope ratios and abundances in geologic samples by thermal ionization mass spectrometry. Anal. Chem. **63**: 913–916.

Watters, D.L. 1995. Age determination and confirmation from otoliths of the bank rockfish, *Sebastes rufus* (Scorpaenidae). M.S. thesis, California State University, San Jose, Calif.

© 1999 NRC Canada

Age and growth of the Pacific grenadier (*Coryphaenoides acrolepis*) with age estimate validation using an improved radiometric ageing technique

Allen H. Andrews, Gregor M. Cailliet, and Kenneth H. Coale

Abstract: Current and historic longevity estimates for the Pacific grenadier (*Coryphaenoides acrolepis*) range from 6 to greater than 60 years. Age estimates in this study using growth increment counts in thin otolith sections indicate the Pacific grenadier is a long-lived fish. To validate this growth information, age was determined using the radioactive disequilibria of ^{210}Pb and ^{226}Ra in otolith cores from adult Pacific grenadier. Radiometric ages closely agreed with age estimates from counting growth increments, which confirms their annual periodicity. Radiometric results indicate the Pacific grenadier can live at least 55.8 years (–7.4, +10.1 years). Growth increment counts from large fish indicate longevity may approach 73 years. Because the Pacific grenadier is long-lived and matures late in life, it may be vulnerable to heavy fishing pressure. Therefore, conservation measures need to be taken to sustain this rapidly developing fishery.

Résumé : Selon les estimations actuelles et passées, la longévité du grenadier à écailles rudes (*Coryphaenoides acrolepis*) serait de 6 ans à plus de 60 ans. Les estimations de l'âge de la présente étude, dans laquelle on a dénombré les incréments de croissance sur des coupes fines d'otolithes, indiquent que ce poisson vit longtemps. Pour valider cette information issue des incréments de croissance, on a déterminé l'âge au moyen du déséquilibre radioactif du ^{210}Pb et du ^{226}Ra dans des coupes d'otolithes de grenadier à écailles rudes adultes. Les âges obtenus par mesures radiométriques coïncidaient étroitement avec les estimations de l'âge par dénombrement des incréments de croissance, ce qui confirme la périodicité annuelle de ces derniers. Les résultats des mesures radiométriques indiquent que ce poisson peut vivre au moins 55,8 ans (–7,4, +10,1 ans). Les dénombrements des incréments de croissance chez de gros poissons indiquent que la longévité de l'espèce peut approcher 73 ans. Comme le grenadier à écailles rudes vit longtemps et atteint la maturité à un âge avancé, il peut être vulnérable aux fortes pressions de pêche. C'est pourquoi on doit prendre des mesures de conservation pour assurer la durabilité de cette pêche en pleine croissance.

[Traduit par la Rédaction]

Introduction

The Pacific grenadier, *Coryphaenoides acrolepis* (family Macrouridae), is a benthopelagic, deepwater fish species that inhabits the continental slopes of the northern Pacific Ocean. Its range is circum-north Pacific from Baja California, Mexico, to northern Japan and into the Bering Sea (Iwamoto and Stein 1974; Cohen et al. 1990). Its typical depth range is from 600 to 2500 m (Iwamoto and Stein 1974) with a population density maximum near 1500 m (Stein and Pearcy 1982; Matsui et al. 1990).

Until recently, fishermen regarded the Pacific grenadier as a trash fish because the fillets were small (~25% of the total fish weight) and had low market value (US$0.08 to US$0.16 per pound ex-vessel). In recent years, the Pacific grenadier has been discovered to have desirable culinary attributes (Matsui et al. 1990) and has become a large commercial fishery in California and Oregon (Fig. 1). Landings for California until 1992 were primarily from Eureka, California. After 1992, landings from Monterey Bay, California, increased substantially to nearly 900 t (~2 million pounds) in 1996 (Leos 1996 and 1997). Before 1995, greater than 95% of the landings were from trawlers. For 1995 and 1996, greater than 90% of the landings were from set lines targeting the Pacific grenadier (Leos 1997). Because of these landings, the Pacific grenadier is no longer in the "other" category and has become the fifth largest fishery in Monterey Bay, California, and thirteenth in the state of California at 1130 t (~2.5 million pounds) for 1996 (Leos 1996 and 1997).

To properly manage this rapidly developing fishery, the age structure and growth characteristics of the Pacific grenadier must be known along with other life history characteristics. Some life history aspects are known (Stein and Pearcy 1982; Matsui et al. 1990), but longevity estimates have been variable. Recent and historic age and longevity estimates range from 6 to greater than 60 years (Kulikova 1957; Brothers et al. 1976; Mulcahey et al. 1979; Wilson 1982; Matsui et al. 1990).

Fisheries management strategies rely heavily on accurate

Received June 12, 1998. Accepted February 23, 1999.
J14650

A.H. Andrews,[1] G.M. Cailliet, and K.H. Coale. Moss Landing Marine Laboratories, P.O. Box 450, Moss Landing, CA 95039-0450, U.S.A.

[1]Author to whom all correspondence should be addressed.
e-mail: andrews@mlml.calstate.edu

© 1999 NRC Canada

Fig. 1. Landings of Pacific grenadier for California and Oregon from 1980 to 1996 given in metric tons (t). Landings for Washington, Canada, and Alaska have been 0 or negligible.

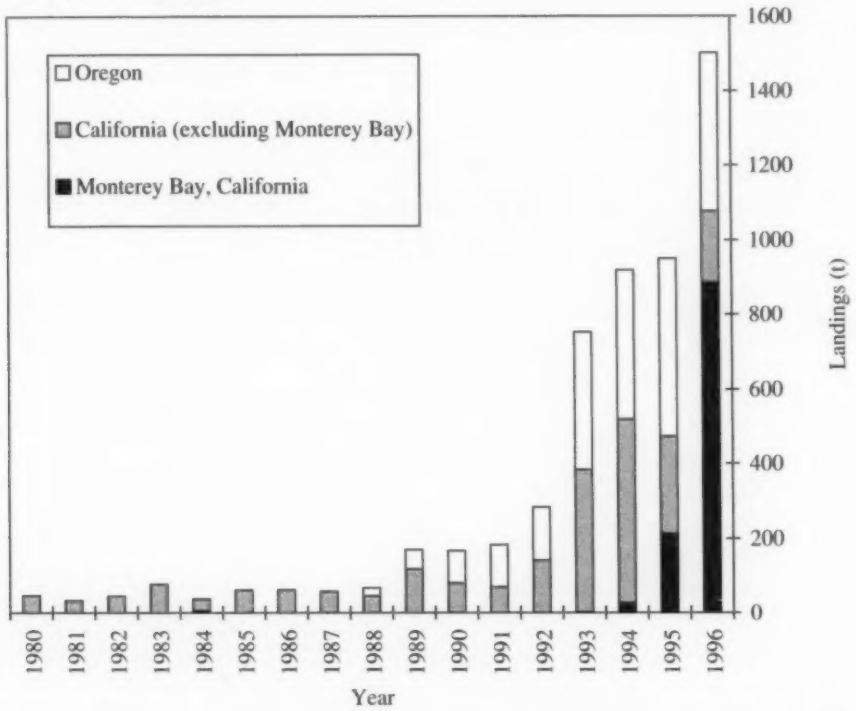

age determinations. Age of fishes is typically determined by using one of several techniques, with growth increment counts in calcified structures being most common (Beamish and McFarlane 1987). The annual periodicity of growth increments in these structures is often assumed. Until recently this assumption was rarely validated (Beamish and McFarlane 1983). As a consequence, underestimation of longevity and overfishing may have led to the decline of the Pacific Ocean perch (*Sebastes alutus*) of the northeastern Pacific Ocean and the orange roughy (*Hoplostethus atlanticus*) off New Zealand (Beamish 1979; Smith et al. 1995).

The problem with typical growth increment age validation techniques is that they have limited applicability to deep-water or long-lived fishes (Mace et al. 1990; McFarlane and Beamish 1995). One technique that can be used to validate age estimates for these fishes is the radiometric ageing technique, which uses the disequilibria of ^{210}Pb and ^{226}Ra in otoliths as a natural chronometer (Smith et al. 1991; Bergstad 1995). This technique has been successfully applied to 12 fish species (Bennett et al. 1982; Campana et al. 1990; Fenton et al. 1991; Kastelle et al. 1994; Fenton and Short 1995; Milton et al. 1995; Smith et al. 1995; Stewart et al. 1995; Watters 1995; Kline 1996).

In this study, the age and growth of the Pacific grenadier was estimated using a traditional ageing technique, validated using an improved radiometric ageing technique, and compared with other age and growth studies of the Pacific grenadier. Improvements made to the radiometric ageing technique in a concurrent study have been used here (Andrews et al. 1999). Ageing results were discussed in the context of known life history information and management recommendations were made.

Materials and methods

Pacific grenadier were collected east of Santa Cruz, California, in November 1992 and off of Oregon and Washington in October 1992 and December 1993. As sagittal otoliths were extracted, fish total length (TL), pre-anal fin length (PAF), snout to dorsal fin (SD), and head length (HL) were recorded to the nearest millimetre. PAF was defined as snout to the base of the first anal fin ray. SD was defined as snout to the base of the first dorsal fin ray. HL was defined as snout to the posterior-most tip of the operculum. A partial length analysis was conducted on fish with intact tails. Otolith weight was measured to the nearest milligram, and length, width, and height were measured to the nearest 0.1 mm. Extracted otoliths were temporarily stored in de-ionized water and ethanol (50%) buffered with marble chips. Cleaned otoliths were stored dry in glass vials.

Traditional otolith ageing

Transverse otolith sections mounted to slides and viewed under a dissecting microscope with transmitted light were used to estimate age. The ageing criteria was based on several very well-defined sections (Fig. 2). The sulcal region was usually used, but the distal margin was also used for some samples. Otolith sections that did not have quantifiable increments were removed from the analysis. Readable otoliths were aged independently by two readers three times each. Average percent error (APE) and index of precision (D) were used to test the reproducibility of ageing between readers (Beamish and Fournier 1981; Chang 1982). Consul-

© 1999 NRC Canada

Fig. 2. Three views of a transverse otolith section with increasing magnification centered on the sulcal region. The full section view is at a magnification of 10× and shows some of the growth increments visible toward the distal margin (top of section). The two are successive views are at magnifications of 32× and 50×. Markers indicate quantified growth increments, which rapidly become compressed toward the margin. This growth pattern was used as a search image in ageing other otolith sections. This section was aged at 41 years.

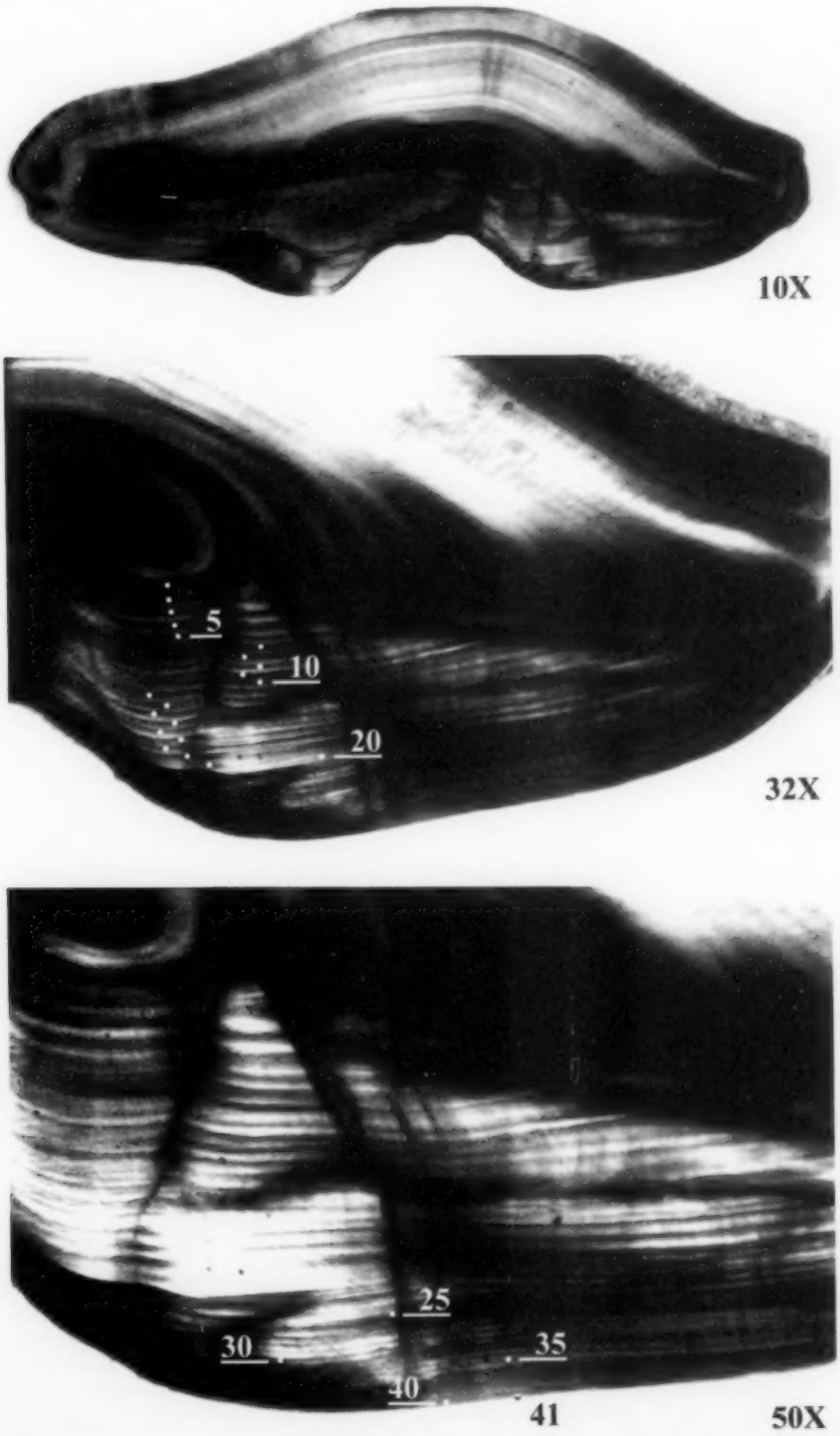

© 1999 NRC Canada

tation between readers on ageing criteria was used to resolve differences and final age estimates were assigned by the first reader. A von Bertalanffy growth function was fitted, using FISHPARM software (Saila et al. 1988), to the final age estimates to describe growth parameters.

Age-group determination and core extraction

Before otoliths were selected for ageing using growth increment counts, sample weight requirements were considered for age-groups consisting of pooled otolith cores. Dimensions and weight of otoliths from juvenile fish (estimated age 5 years) were used to determine core size and weight. The number of otoliths needed to perform the analysis was determined and a subsample of otoliths were held aside for radiometric analysis.

Because otoliths were difficult to age and the amount of otolith material must be maximized for radiometric analysis, age was determined using a simple linear regression of otolith weight to section age. Sexes were separated and age groups were formed using both otoliths from each fish. To discriminate dissimilar fish from potential age-group members, a multiple linear regression, incorporating fish length (PAF), otolith weight, and an interaction term (otolith length multiplied by PAF), was used to determine age. Agreement of ages determined for each fish by each regression was used to determine group membership. Fish with regression ages that differed by greater than an arbitrary 10% were not included in the age-group. The age of the age-group members was determined from the simple linear regression. The age range for each age-group was kept as narrow as was permitted by the amount of otolith mass needed. The average age of the age-group was an age-weighted average based on the estimated age of each core in the sample. An age-group weight of 1 g was targeted, but lower amounts were used where sufficient sample was unavailable.

The otoliths selected for each age-group were cored to the size of a 5-year-old otolith. Average dimensions determined from three juvenile otoliths were 5.0 mm long, 3.0 mm wide, and 1.0 mm thick. Each core was extracted by cutting a 6 mm transverse section and hand grinding to the core dimensions. A weight of approximately 0.02 g per otolith core was targeted based on an average of the three juvenile otoliths.

Radiometric analysis

To address some of the assumptions of this technique, whole juvenile and adult otoliths were analyzed. To determine if exogenous ^{210}Pb was incorporated during otolith formation, a sample of whole otoliths from juvenile fish was included as an age-group. For comparative purposes, an adult whole-otolith pair was analyzed for ^{226}Ra to assess if an ontogenetic difference occurs in ^{226}Ra uptake.

Each pooled otolith core sample was analyzed for ^{210}Pb and ^{226}Ra. To determine ^{210}Pb, α-spectrometry of ^{210}Po, its daughter product, was performed. Determination of ^{226}Ra was performed using a new technique that uses isotope-dilution thermal ionization mass spectrometry (TIMS; Andrews et al. 1999). The details of ^{210}Pb determination are described here, but only the details of ^{226}Ra determination that vary from Andrews et al. (1999) are stated here.

Because of the extremely low levels of ^{210}Pb and ^{226}Ra, trace-metal precautions were exercised during sample cleaning and processing (Watters 1995). All acids used were double distilled (GFS Chemicals®) and dilutions were made using Millipore® filtered Milli-Q water (18 MΩ·cm^{-1}). Thorough cleaning and repeated dissolution of the core samples was performed prior to radiometric analysis (Andrews et al. 1999).

To determine ^{210}Pb activity in samples where it is very low, ^{210}Pb activity was determined by proxy using the autodeposition and α-spectrometric determination of its daughter, ^{210}Po (Flynn 1968). To ensure that all of the ^{210}Po was due to ingrowth from ^{210}Pb and that ^{210}Po:^{210}Pb was in secular equilibrium, all samples were at least 2 years old (from date of capture). Samples prepared for ^{210}Po analysis were spiked with a yield tracer, ^{208}Po, calibrated against NBS and geological standards. The amount added was estimated to be 5 times the activity of ^{210}Po in the otolith sample to reduce counting error in the determination of ^{210}Pb activity.

To isolate the polonium isotopes for the purpose of α-spectrometry, the isotopes were autodeposited onto a silver planchet. Spiked samples were redissolved in approximately 50 mL of 0.5 N HCl on a hot plate covered with a watch-glass. Samples were completely dissolved and the temperature was elevated to ~90°C before plating. The ^{210}Po and ^{208}Po-tracer were autodeposited at this temperature onto a purified silver planchet (99.999%, A.F. Murphy Die and Machine Co., North Quincy, Mass.) held in a rotating teflon holder over a 4-h period (Flynn 1968). Planchets were counted using both silicon surface barrier detectors and ion implant detectors in 8 Tennelec TC256 α-spectrometers interfaced with a multichannel analyzer and an 8-channel digital multiplexer. Counts were collected with Nucleus® software on an IBM-PC. Radium blanks were included in these steps to account for any potential radium contamination. The sample remaining after polonium autodeposition was recovered for ^{226}Ra analysis.

The activity of ^{210}Po was calculated using the α-spectrometry counts for ^{210}Po and ^{208}Po. These counts were corrected for background counts (reagent counts not above background) by subtracting the amount of counts calculated to occur for the counting period. Adjusted sample counts for ^{208}Po and ^{210}Po were corrected for decay during the counting period and the activity of ^{210}Po was calculated based on the known ^{208}Po activity (Andrews 1997). Because the activity of ^{210}Po was in secular equilibrium with ^{210}Pb, the activity of ^{210}Po was equal to the ^{210}Pb activity. This activity was corrected for ^{210}Pb ingrowth from ^{226}Ra to the time of capture (Andrews 1997).

Determination of ^{226}Ra was performed using an elemental separation procedure and isotope-dilution TIMS, described elsewhere (Andrews et al. 1999). The only exception to the procedure used for these samples was the collection intervals used for each column separation. In the first two column passes, where calcium removal occurs, the collection interval was from 35 to 120 mL, instead of 40 to 120 mL. For the third column pass, where radium is isolated, the collection interval was from 300 to 700 μL, instead of 250 to 700 μL. These intervals were changed as a result of this study to improve radium separation and recovery and to further reduce calcium.

Radiometric age determination

Age determination was performed using the measured ^{210}Pb and ^{226}Ra activities in the following equations. Because the activities were measured using the same sample, the calculation was independent of sample mass. For adult samples, where estimated age was greater than the 5-year core, radiometric age was calculated as follows using an equation derived from Smith et al. (1991) to compensate for the ingrowth gradient of ^{210}Pb:^{226}Ra in the otolith core,

$$t_{age} = \frac{\ln\left(\dfrac{1 - A^{210}\mathrm{Pb}_{tc}}{A^{226}\mathrm{Ra}_{TIMS}\left(1 - R_0\left(\dfrac{1 - e^{-\lambda T}}{-\lambda T}\right)\right)}\right)}{-\lambda} + T,$$

where t_{age} is the radiometric age at the time of capture, $A^{210}\mathrm{Pb}_{tc}$ is the ^{210}Pb activity corrected to time of capture, $A^{226}\mathrm{Ra}_{TIMS}$ is the ^{226}Ra activity measured using TIMS, R_0 is the ratio of ^{210}Pb:^{226}Ra initially incorporated, λ is the decay constant for ^{210}Pb (ln(2)/22.26 years), and T is the core age (5 years). The radiometric age calcula-

© 1999 NRC Canada

Fig. 3. Von Bertalanffy growth functions were fitted to estimated ages from growth zone counts and pre-anal fin lengths (PAF) for females (χ), males (○), and immature (●). Immature fish were used in each growth function. Total length (TL), shown on the right vertical axis, was calculated based on PAF.

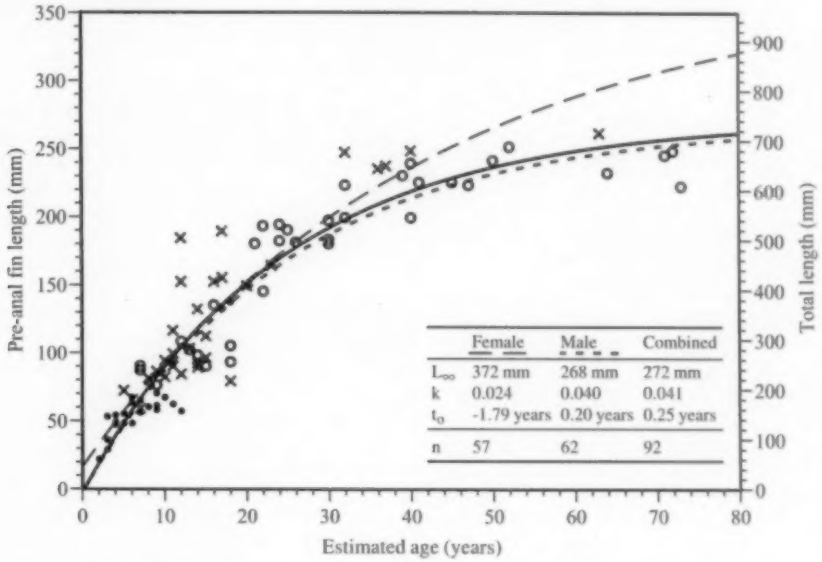

tion for the juvenile age-group was determined by iteration of an equation derived from Smith et al. (1991):

$$\frac{A^{210}\mathrm{Pb}_{\mathrm{tc}}}{A^{226}\mathrm{Ra}_{\mathrm{TIMS}}} = 1-(1-R_0)\left(\frac{1-e^{-\lambda t_{age}}}{\lambda t_{age}}\right),$$

where all equation components were as defined above.

Age estimate accuracy

A comparison of estimated age versus radiometric age was performed in two plots and one statistical analysis. First, the estimated age of the age-groups and measured ^{210}Pb:^{226}Ra activity ratios were plotted with expected ^{210}Pb:^{226}Ra ingrowth curves. Concordance of these data with the expected ingrowth curves were used as an indicator of age estimate accuracy. A direct comparison of estimated age was also performed by plotting the radiometric age opposite estimated age. A linear regression was applied to these data and plotted with a line of agreement. A paired two-sample *t*-test was used to determine if a significant difference existed between the age estimates.

Results

A total of 747 Pacific grenadier was collected from waters off California, Oregon, and Washington. Of these fish, 128 with intact tails were used in the partial length analysis. All three partial lengths (PAF, SD, and HL) had linear relationships which predicted total length well with coefficients of determination close to 1. Head length had an r^2 = 0.988 (TL = 4.69(HL) + 20.2), snout to dorsal length had an r^2 = 0.987 (TL = 4.31(SD) + 21.2), and preanal fin length had an r^2 = 0.985 (TL = 2.53(PAF) + 73.0). Fish used in this analysis ranged in size from 124 mm to 688 mm TL. Because PAF had the largest proportion of the total length, it was chosen as the length used in growth analyses and was used to determine total length.

Traditional ageing

Fish chosen for traditional age determination numbered 178 and ranged in size from 22 mm to 272 mm PAF. Transverse sections were very difficult to age. APE was comparable between readers at about 6%, but *D* indicated precision was better for the first reader (6 and 10%, respectively). Forty-three percent of the readings between readers were within 1 year, 55% within 2 years, 80% within 5 years, and 95% within 10 years. Most of the differences between readers resulted from lower age estimates made by the second reader on old otolith sections (69%). Precision estimates were 6.3% (APE) between readers. Consultation between readers usually resolved differences greater than 10%. Age estimates were ultimately finalized by the first reader. For 32 of the specimens, the second otolith of the pair was sectioned for another attempt at ageing. Twenty could not be aged after examining both sections. Ninety-two of the otoliths selected could be aged (52%).

Three von Bertalanffy growth functions were fitted to the PAF lengths and estimated ages from growth zone counts to describe growth characteristics for females, males, and combined sexes; juveniles were factored into each determination (Fig. 3). The growth curves for males and combined sexes have similar growth curves, but females appear to have slower growth and a greater maximum length.

Age-group determination and core extraction

Otolith weight predicted section age for each sex well with coefficients of determination close to 1. Female regression age had an r^2 = 0.863 (regression age = 88.6(otolith weight) + 4.8) and male regression age had an r^2 = 0.927 (regression age = 91.3(otolith weight) + 4.6).

Six adult age-groups (3 female, 3 male), as determined by the age regressions, and one juvenile age-group were selected for radiometric analysis (Table 1). Age-groups ranged

© 1999 NRC Canada

Table 1. Composition of age-groups used for radiometric age determination. Mean length (PAF, mm) is given for comparison.

Age-group (years)	Sex	Number of fish	Number of otoliths	Sample size (g)	Mean length ± SD (PAF, mm)
1–3	Juvenile	46	92	0.9147	44 ± 2
14–20	Female	19	35	1.2279	143 ± 14
30–41	Female	15	29	0.9823	224 ± 19
43–54	Female	10	19	0.6242	245 ± 13
34–38	Male	21	39	0.5315	196 ± 12
40–45	Male	21	41	0.7458	207 ± 16
46–56	Male	12	23	0.4717	216 ± 19

from as low as 1 year for the juvenile sample to a maximum of 56 years for the oldest age-group. Dissimilar fish eliminated from the age-groups by comparing age regressions resulted in the removal of 9–33% of the potential group members. The number of fish in the adult age-groups ranged from 10 to 21, but the juvenile age-group numbered higher at 46 because the otoliths were smaller than the cores. Both otoliths were used from each fish, except where otoliths were lost in the coring process. Target sample size was 1 g. Some samples were closer to 0.5 g because sufficient sample was unavailable. Average core weight for the female samples, processed first, were slightly higher (0.03 g) than the targeted core weight (0.02 g). Male samples were cored a little smaller and more closely approached the target core weight. Total sample weight for each age-group ranged from 0.4717 g to 1.2279 g. Mean length was also calculated for each age-group (± SD).

Radiometric analysis

The results of the radiometric determinations are given in the form of activity (dpm·g^{-1}, disintegrations per minute per gram) and a ratio of activities (Table 2). The activity of ^{210}Pb increased, as expected, 25 times from 0.0022 dpm·g^{-1} in the juvenile samples to 0.0568 dpm·g^{-1} in the oldest adult sample. Standard error for this determination ranged from 4.4 to 7.8%. The activity of ^{226}Ra ranged from 0.0419 to 0.1245 dpm·g^{-1}, where the highest activity was from the juvenile sample. This was 2.2 times higher than the mean adult sample activity (0.0568 ± 0.01 dpm·g^{-1}) and nearly 3 times the lowest activity measured. The activity of the adult whole-otolith pair was similar to the lowest adult sample. Error for ^{226}Ra was very low and ranged from 1.07 to 4.35% (1 SE). The activity ratio of ^{210}Pb:^{226}Ra increased, as predicted by estimated age, from a low of 0.018 for the juvenile age-group to 0.798 for the oldest adult age-group.

Radiometric age determination

Radiometric age determined using the activity ratio was in close agreement with the average estimated age of the age-groups (Table 3). Each age-group range overlapped the radiometric age range. The low radiometric age for the 1–3 age-group indicated that uptake of exogenous ^{210}Pb (R_0, Campana et al. 1990) by juveniles was insignificant. Therefore, radiometric age was determined based on the measured activity ratios and no adjustment was necessary.

Age estimate accuracy

A graphical comparison of the age-groups versus the measured ^{210}Pb:^{226}Ra activity ratio plotted with the expected ingrowth curves indicated that age estimate accuracy was good (Fig. 4). The 1–3 age-group was closely associated with the ingrowth curve for an R_0 of 0.0. This indicated uptake of exogenous ^{210}Pb was insignificant and that it was the most accurate model for what to expect in adult otolith cores. The horizontal bar for each data point was the range of otolith weight derived age estimates. The 95% confidence interval from the otolith weight regression broadened the age group ranges by 3 to 7 years. This is a liberal estimate of this variation because outlying otoliths were eliminated with the multiple linear regression comparison (age estimates that differed between the two regressions by more than an arbitrary 10% were removed). The strong concordance of the data points with the expected ingrowth curve indicated the otolith weight regression was a good predictor of age and that growth zone age estimates were accurate.

A direct comparison of estimated age with radiometric age indicated ages were statistically in agreement (Fig. 5). Data points were all in close proximity to the line of agreement. A regression of these data showed a high correlation and a slope very close to 1 with an intercept near the origin. A paired two-sample t-test comparison indicated that there was no significant difference between estimated age and radiometric age (t = 0.427, P = 0.684).

Discussion

Partial length defined

Partial lengths have been used to indicate total length of grenadier from the north Atlantic (Atkinson 1991). The Pacific grenadier often has a tail that is apparently intact, but a few centimetres can be missing with little evidence. Most broken tails occurred during capture by trawling. In some cases, tails were lost during life and regenerated, where regenerated means growth of fin rays from the severed edge. For a few fish, approximately 10 to 20% of the total length was lost during life. In this study, approximately 80% of the fish collected had damaged, broken, or regenerated tails. For fish greater than 500 mm TL, calculated tail loss from trawling was as high as 18% of the total length.

Use of a standardized partial length is needed for consistency in grenadier fishery data collection. Many different partial lengths have been used and some are poorly defined and ambiguous (Atkinson 1991; Wilson 1982; Bergstad 1990; Matsui et al. 1990; Kelly et al. 1997). Because the anus is often distorted by barotrauma, the distance from the first anal fin ray to the snout is the most easily measured. This distance is best defined as pre-anal fin length and should be given the unambiguous acronym PAF. For these reasons, PAF was chosen as the partial length for the Pacific grenadier in this study. It is further proposed that the partial length measurement for grenadier be standardized in these terms and that use of HL or SD be used where the anal fin is missing or badly damaged.

Traditional age estimation

A graphical comparison of growth curves from this study and other studies revealed differences and similarities

© 1999 NRC Canada

Table 2. Results of radiometric analysis for ^{210}Pb and ^{226}Ra activity determinations for each age-group. A single whole otolith pair from one fish is also listed for comparison with core results.

Age-group (years)	Sample size (g)	^{210}Pb activity (dpm·g^{-1})[a]	^{210}Pb % error (SE)	^{226}Ra activity (dpm·g^{-1})	^{226}Ra % error (SE)	^{210}Pb:^{226}Ra activity ratio
1–3	0.9147	0.0022	7.8	0.1245	1.94	0.018
14–20	1.2279	0.0124	5.9	0.0419	1.38	0.295
30–41	0.9823	0.0320	4.4	0.0546	1.26	0.587
43–54	0.6242	0.0385	5.1	0.0510	1.37	0.755
34–38	0.5315	0.0391	5.4	0.0583	1.07	0.670
40–45	0.7458	0.0415	5.5	0.0639	4.35	0.649
46–56	0.4717	0.0568	4.8	0.0711	2.45	0.798
Otolith pair[b]	1.2826	NM	NA	0.0419	2.88	NA

Note: NM, not measured; NA, not applicable.
[a]Corrected to time of capture.
[b]Whole otolith pair from an individual adult fish.

Table 3. Comparison of estimated and radiometric ages for each age-group.

Age-group (years)	Average estimated age (years)	Radiometric age (years)	Radiometric age range (years)
1–3	2	1.2	1.1–1.3
14–20	17	14.0	13.1–14.9
30–41	36	31.9	29.6–34.4
34–38	36	39.2	35.5–43.3
40–45	43	37.5	32.6–43.7
43–54	48	49.2	43.7–55.9
46–56	51	55.8	48.4–65.9

Fig. 4. Observed ^{210}Pb:^{226}Ra activity ratios for age-groups plotted with expected activity ratio ingrowth curves. Horizontal bars represent age range of the otolith cores in the age-group (with 95% confidence interval). Vertical bars indicate analytical uncertainty in the determination of ^{210}Pb and ^{226}Ra activities. Expected activity ratio ingrowth curves also incorporate possible initial uptake ratios (R_0) of ^{210}Pb:^{226}Ra.

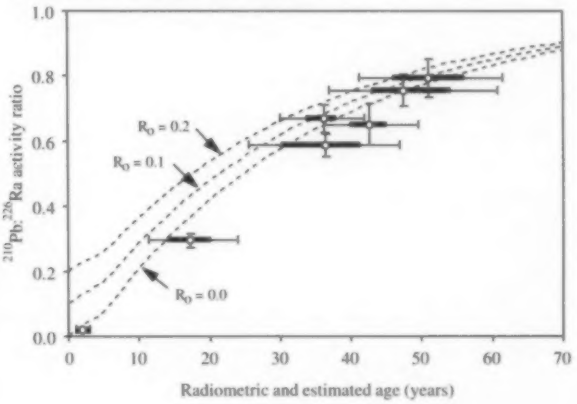

(Fig. 6). Kulikova (1957) did not calculate growth parameters, but for comparative purposes, growth parameters were calculated using the average length given for each estimated age. In that case, the growth constant was very high (k = 0.435) and longevity was very low (~6 years) relative to validated estimates in this study (Fig. 3). This growth constant was unrealistically greater than many fast-growing fishes (i.e., tuna and billfishes; Prince and Pulos 1983). The growth curve fitted to age estimates determined by Matsui et al. (1990) was very similar to the male and combined sexes growth curves in this study. It must be noted that Matsui et al. (1990) used snout to anus length (less than PAF by approximately 1%). The upper end of the female growth curve in this study is largely unsupported by data, but it is important to mention that some otoliths from females greater than 300 mm PAF were aged greater than 90 years. These otoliths were not included in this study because growth increments were very fine and confusing toward the margin and were also aged as low as 65 years. The difficulty of ageing otolith sections for this species was similar to recent findings for the roundnose grenadier (Kelly et al. 1997). The asymptotic length of the female growth curve more closely approximates the maximum size reported (~900 mm TL, Cohen et al. 1990). Therefore, it is possible that females get larger than males with increasing age, as may also be indicated by Matsui et al. (1990).

A comparison of historic and recent age estimates indicates the age and growth of the Pacific grenadier was variable and age was usually underestimated (Table 4). The first Pacific grenadier age estimates were for specimens collected in the Bering and Okhotsk seas and the Kuril-Kamchatka trench, where scales were used to estimate a longevity of 6 years (Kulikova 1957). Scales can be unreliable, however, as a conserved record of age (Simkiss 1974; Yoklavich and Boehlert 1987). This result is an underestimate by a factor of 10 or more. Brothers et al. (1976) used extrapolation of daily increments to estimate the age of one fish. A Pacific grenadier with similar length would actually be about 3 times older. The first attempt at quantification of annual growth increments in transverse otolith sections used 15 fish collected off San Diego, California (Mulcahey et al. 1979). They found otoliths difficult to age and cautiously estimated age at 15 to 25 years for the size range of fish used. In this study, similarly sized fish would be 2 to 3 times older. A detailed examination of scales, vertebrae, and otoliths from 130 fish collected off southern California resulted in an estimated longevity of approximately 20 years (Wilson 1982). Otolith sections were determined, however, to be too ambiguous for age estimation. This was true for about half of the otoliths used in this study, but Wilson's (1982) longevity es-

© 1999 NRC Canada

Fig. 5. Comparison of estimated age versus radiometric age. The solid line represents agreement between age estimates (slope of 1). The broken line was a regression of the compared ages. Bars for estimated ages represent the age range of each age-group (with 95% confidence interval). Bars for the radiometric ages represent the range between high and low age based on analytical uncertainties.

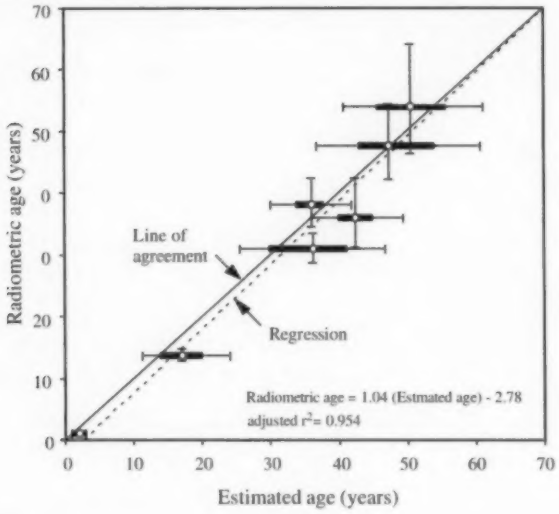

timate was low by a factor of 3 to 4. Most recently, otolith break-and-burn was used on 60 fish collected off northern Baja California, Mexico, to central California (Matsui et al. 1990). Longevity was estimated to be greater than 60 years, which is very similar to the result of this study.

Radiometric analysis

Use of otolith cores for radiometric age determination was typically limited to a minimum of approximately 1 g of material because of instrument detection limits (Kastelle et al. 1994; Fenton and Short 1995). Because of cleaner procedures and the application of isotope-dilution TIMS, sample size can be lower than 0.5 g (Table 2). Reduced error associated with ^{226}Ra determination make the analytical uncertainty of ^{210}Pb determination the limiting factor in radiometric ageing. In this study, uncertainty in ^{210}Pb activity contributes 7.8% of the error where activity was very low (juvenile sample) and decreases to approximately 5% as age and activity increase (Table 2). Typically, the error for ^{226}Ra determination was lower than 2%. In this study, reported error greater than 2% was attributed to high calcium in the sample. An alteration of the technique remedied this problem (Andrews et al. 1999).

In some radiometric ageing studies, ^{226}Ra activity was inferred from other samples, rather than measured directly, because of the detection limits of ^{222}Rn emanation (Bennett et al. 1982; Campana et al. 1990; Watters 1995; Kline 1996). Results from this study indicate ^{226}Ra activity can vary among samples and presumably among individuals (Table 2). The ^{226}Ra activity for the juvenile sample was the highest activity measured in this study. Some juvenile specimens were collected from upper slope areas near the Columbia River mouth. Because freshwater is a source of ^{226}Ra, elevated environmental levels of ^{226}Ra may explain the higher activity (Osterberg et al. 1963; Moore 1996). Use of an average ^{226}Ra activity in this study causes significant changes to radiometric age. This emphasizes the necessity of measuring ^{210}Pb and ^{226}Ra for each sample in future studies.

Assumption clarification

The radiometric ageing technique requires several assumptions depending on the analytical circumstances. The typical assumptions are as follows. (*i*) The otolith is a closed system with no loss or migration of post-formational radionuclides in the ^{226}Ra decay series through to ^{210}Po; this is necessary because loss of nuclides would result in lower ^{210}Pb activity and subsequently underestimated age. (*ii*) Uptake of exogenous nuclides in the ^{226}Ra decay series is negligible relative to ingrowth from ^{226}Ra; this is necessary to attribute ^{210}Pb activity in the otolith to ingrowth from ^{226}Ra. (*iii*) Uptake of ^{226}Ra is in constant proportion to the otolith mass growth rate; this assumption is necessary when whole otoliths are used and is largely circumvented when otolith cores are used (Kimura and Kastelle 1995).

The assumption that an otolith is a closed system is well supported by studies of coraline carbonate properties and of otolith structure and formation. A proposed violation of this assumption is the loss of ^{222}Rn, the daughter of ^{226}Ra, from the otolith via diffusion as a noble gas (West and Gauldie 1994). Although loss of ^{222}Rn seems possible because it is a non-reactive gas that can enter the interstitial lamellar spaces via α-recoil (Fleischer et al. 1975) and diffuse out of the otolith, there is strong evidence that indicates this does not occur in the in vivo otolith. Any ^{222}Rn that enters the lamellar spaces is entering a matrix of water and otolin, a secreted neuroprotein (Pannella 1980). A recent study of the sorption characteristics of ^{222}Rn in the presence of organic matter indicated that the ^{222}Rn would tend to remain in the sorbent otolin (Morawska and Phillips 1993).

The lack of Ostwald ripening and cementation in otoliths support the assumption that there is no post-formational migration of nuclides. Ostwald ripening, a process in which small crystals (more soluble than larger ones) dissolve and reprecipitate onto larger crystals, has been demonstrated not to occur in otoliths. Studies using ^{45}Ca indicate that once calcium is incorporated it remains immobilized in otoliths (Simkiss 1974; Campana 1983; Yoklavich and Boehlert 1987). This suggests that the crystalline structure of the otolith is conserved and well regulated during and after growth. This is supported by the existence of polyanions in the organic matrix, called nucleation barriers, which confine crystalline growth to one direction (Wheeler and Sikes 1984).

The only exogenous nuclide in the ^{226}Ra decay series that is an uptake concern for samples that are greater than 2 years old (from date of collection) is ^{210}Pb. Any exogenous ^{210}Po would have decayed away and all nuclides from ^{226}Ra through to ^{210}Pb are very short lived (seconds to minutes). Because ^{210}Pb exists in the natural environment, it must be assessed as a potential contaminant. Measuring ^{210}Pb in juvenile otoliths is currently the most applicable technique for assessing the possibility of direct incorporation of ^{210}Pb.

The assumption that ^{226}Ra uptake is in constant proportion to mass growth-rate is only necessary when whole otoliths

© 1999 NRC Canada

Fig. 6. Comparison of von Bertalanffy growth functions from two other studies with the results of this study. The growth function for Kulikova (1957) was calculated using the published average length-at-age where total lengths were converted to PAF.

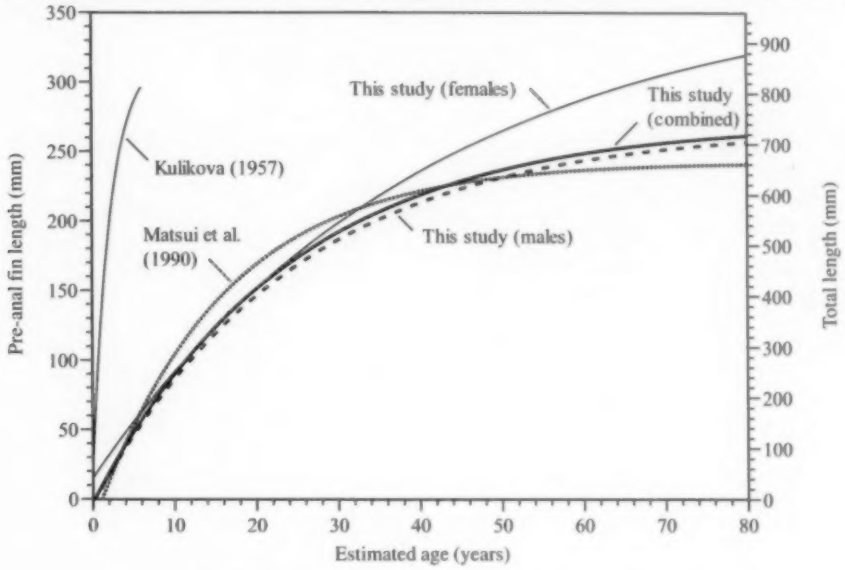

Table 4. Comparison of age and longevity estimates for the Pacific grenadier. Age estimates for fish of the given length(s) are listed with the ageing technique and number of fish.

Author	Technique	Number of fish	Length (TL, mm)	Age at length (years)
Kulikova (1957)	Scales	92	820 (max.)	6+
Brothers et al. (1976)	Daily increment extrapolation	1	580	10–11
Mulcahey et al. (1979)	Sagittal otolith sections	15	640–840	15–25
Wilson, R.R., Jr. (1982)	Scales and vertebrae	130	820 (max.)	18–20
Matsui et al. (1990)	Sagittal otolith break and burn	60	600–700	>60

and an otolith mass growth model are used (Bennett et al. 1982). A violation of this assumption was documented for the blue grenadier (Gadidae: *Macruronus novaezelandiae*; Fenton et al. 1990). The radiometric ageing technique could not be used on whole otoliths because the activity of ^{226}Ra decreased in otoliths from juveniles to adults. This was attributed to an ontogenetic movement from estuarine and inshore waters, where environmental ^{226}Ra can be significantly higher (Moore 1996), to deeper, offshore waters. A radiometric analysis of otolith cores from this species, however, was successful (Fenton and Short 1995).

The two most important assumptions in this study were: (*i*) the otolith was a closed system and (*ii*) the incorporation of exogenous ^{210}Pb was negligible. These assumptions can be more closely scrutinized with the increased accuracy of the radiometric ageing technique using cleaner techniques and isotope-dilution TIMS (Andrews et al. 1999). If ^{222}Rn loss was a problem, the radiometric disequilibria of ^{210}Pb:^{226}Ra would consistently underestimate fish age. In this study, it is very unlikely that the traditional age estimates of each age-group were underestimated by the precise amount necessary to compensate for ^{222}Rn loss. Because the use of TIMS has increased the accuracy of the radiometric ageing technique, tolerance for such an error was very low. Exogenous ^{210}Pb was eliminated as a possible factor by ageing the juvenile age-group (1–3 years). It was highly unlikely that uptake of ^{210}Pb in adults would be different from juveniles.

Age estimate accuracy

The strong concordance of measured ^{210}Pb:^{226}Ra with the expected ingrowth curves validated age estimation using growth increments in the Pacific grenadier (Fig. 4). Because the 1–3 age-group showed extremely low ^{210}Pb activity, the most applicable ingrowth model was for an R_0 of 0.0. Variation of the data points around the ingrowth curve could be explained by the analytical uncertainty associated with the technique and the age-group age range. Although variation of otolith weight derived age could have been as high as ±10 years for the oldest fish, use of the multiple linear regression as a tool to discriminate dissimilarities reduced this variability to 10% of the regression age estimate. Because this variation could not be accurately assessed, the 95% confidence interval for the otolith weight regressions was used to estimate the contribution of this error to the age range.

Statistical agreement between estimated age and radiometric age further supports validation of the age estimates (Fig. 5). Radiometric age determinations confirm a longevity of at least 55.8 years (–7.4, +10.1 years) and validate the annual periodicity of the growth increments used to estimate

© 1999 NRC Canada

age. Based on similar growth increment interpretations, the longevity of the Pacific grenadier may be at least 73 years.

Life histories

Longevity estimates for two similar grenadier species of the North Atlantic differ considerably. The roundnose grenadier has longevity estimates that range from 50 to 72 years, which were similar to the Pacific grenadier (Bergstad 1990; Kelly et al. 1997). Age validation of these estimates was limited to young fish using marginal increment analysis (Gordon and Swan 1996). This species can attain a greater length (1.5 to 2 m TL) and appears to have a higher growth rate than the Pacific grenadier. In contrast, the roughhead grenadier has a relatively low estimated longevity of 13 years for males and 22 years for females (Savvatimsky 1994). Age estimates, however, were based largely on scales and validation has not been performed. Grenadier from other parts of the world are also thought to have a relatively low longevity (Rannou 1976; Middleton and Musick 1986; Morales-Nin 1990; Specchi et al. 1995). It is possible that the grenadier family consists of a series of species complexes that differ in growth characteristics, as is thought to be the case for the eastern Pacific Ocean rockfishes (*Sebastes* spp.; Mary Yoklavich, National Marine Fisheries, Pacific Fisheries Environmental Laboratory, Pacific Grove, CA 93950, personal communication), but age validation is necessary for most members of both families.

Maturity at length from several studies can be used to estimate age at maturity for the Pacific grenadier. Length at maturity is estimated to occur at approximately 500 mm TL (ca. 170 mm PAF) for males and from 460 to 650 mm TL (ca. 153 to 230 mm PAF) for females (Stein and Pearcy 1982; Matsui et al. 1990). Based on the growth functions calculated for each sex, maturity may occur between 20 and 40 years for females and at 20 years for males. This is much later in life than the typically larger and faster-growing roundnose grenadier, where 50% maturity occurs at 8 to 11 years (Kelly et al. 1997).

It is important to consider the potential age of Pacific grenadier being landed in Oregon and Monterey Bay, California, because landings have increased substantially (Fig 1). Landings for Oregon have been about 91% male, where most range in size from about 450 to 650 mm TL (Mike Hosie, Oregon Department of Fish and Wildlife, PO Box 5430, Charleston, OR 97420, personal communication). The small percentage of females landed were typically larger (550 to 650 mm TL). Based on the calculated growth functions, fish being landed may range in age from 20 to 50 years for males and 30 to 40 years for females. Landings for Monterey Bay, California, consist of fish ranging in size from 550 to 650 mm TL (~95%) with some small individuals at approximately 300 mm TL (~5%). Sex composition was not known. Based on both growth functions, age of the large fish may be from 30 to 50 years and the small fish may be approximately 10 years old. Because maturity occurs late in life, some of the smaller fish being landed may be sexually immature.

Much remains unknown about the Pacific grenadier that would be necessary to develop a sustainable fishery. Population size and distribution and the movement of individuals in the population are probably the most important aspects of this fishery that need research. Catch per unit effort information needs to be compiled and analyzed for abundance estimates in areas already being fished. Other studies including break-away tag and recapture coupled with deep trawling and submersible transects could be used to estimate population characteristics at depths greater than current commercial fishing depths. Until this information is gathered, the Pacific grenadier fishery should be managed cautiously by setting strict and small quotas.

Acknowledgments

We would like to thank George Boehlert and Mary Yoklavich of Pacific Fisheries Environmental Laboratory, Dave Woodbury of NMFS at Tiburon, Calif., Erica Burton of MLML, and Jodi Thomas. We have procured fish specimens and, in some cases, valuable ship-time from the following organizations: (*i*) NOAA, Southwest Fisheries Science Center, the National Marine Fisheries Service, special thanks to John Butler; (*ii*) NOAA, Alaska Fisheries Science Center, National Marine Fisheries Service, special thanks to Bob Lauth, Jerry Hoff, Craig Kastelle, and Dan Kimura; (*iii*) Oregon Department of Fish and Wildlife, special thanks to Mike Hosie; (*iv*) California Department of Fish and Game, special thanks to Bob Lea and Bob Leos; (*v*) University of California, San Diego/Scripps Institute of Oceanography; (*vi*) Pacific Biological Station, Nanaimo, British Columbia, special thanks to Bill Andrews and Kathy Rutherford. Measurement of radium samples using TIMS was performed by colleagues in the Department of Earth Sciences at the University of California, Santa Cruz. Special thanks to Craig Lundstrom, Zenon Palacz, Pete Holden, and the University of California, Santa Cruz. Special thanks to Brown Lines Trucking Company for donating shipping supplies and costs for delivery of 1 ton of fish collected by Alaska Fisheries Science Center. This research was funded by a grant from the National Sea Grant College Program, National Oceanic and Atmospheric Administration, U.S. Department of Commerce, under grant number NA36RG0537, project number R/F-148 through the California State Resources Agency. The views expressed herein are those of the authors and do not necessarily reflect the views of NOAA or any of its sub-agencies. The U.S. government is authorized to reproduce and distribute for government purposes.

References

Andrews, A.H. 1997. Age and growth of the Pacific grenadier (family Macrouridae, *Coryphaenoides acrolepis*) with age estimate validation using an improved radiometric ageing technique. M.S. thesis, California State University, San Jose, Calif.

Andrews, A.H., Coale, K.H., Nowicki, J., Lundstrom, C., Palacz, Z., and Cailliet, G.M. 1999. Application of a new ion-exchange separation technique and isotope-dilution thermal ionization mass spectrometry to ^{226}Ra determination in otoliths for radiometric age determination of long-lived fishes. Can. J. Fish. Aquat. Sci. **56**: 1329–1338.

Atkinson, D.B. 1991. Relationships between pre-anal fin length and total length of roughhead grenadier (*Macrourus berglax* Lacépède) in the north-west Atlantic. J. Northwest Atl. Fish. Sci. **11**: 7–9.

© 1999 NRC Canada

Beamish, R.J. 1979. New information on the longevity of Pacific ocean perch (*Sebastes alutus*). J. Fish. Res. Board Can. **36**: 1395–1400.

Beamish, R.J., and Fournier, D.A. 1981. A method of comparing the precision of a set of age determinations. Can. J. Fish. Aquat. Sci. **38**: 982–983.

Beamish, R.J., and McFarlane, G.A. 1983. The forgotten requirement for age validation in fisheries biology. Trans. Am. Fish. Soc. **112**: 735–743.

Beamish, R.J., and McFarlane, G.A. 1987. Current trends in age determination methodology. *In* The age and growth of fish. *Edited by* R.C. Summerfelt and G.E. Hall. The Iowa State University Press, Ames, Iowa. pp. 15–42.

Bennett, J.T., Boehlert, G.W., and Turekian, K.K. 1982. Confirmation of longevity in *Sebastes diploproa* (Pisces: Scorpaenidae) from $^{210}Pb/^{226}Ra$ measurements in otoliths. Mar. Biol. **71**: 209–215.

Bergstad, O.A. 1990. Distribution, population structure, growth and reproduction of the roundnose grenadier *Coryphaenoides rupestris* (Pisces: Macrouridae) in the deep waters of the Skagerrak. Mar Biol. **107**: 25–39.

Bergstad, O.A. 1995. Age determination of deep-water fishes: experiences, status and challenges for the future. *In* Deep-water fisheries of the north Atlantic oceanic slope. NATO ASI Series. Series E: Applied Sciences. Vol. 296. *Edited by* Alan G. Hopper. Kluwer Academic Press, Dordrecht, Netherlands. pp. 267–283.

Brothers, E.B., Mathews, C.P., Lasker, R. 1976. Daily growth increments in otoliths from larval and adult fishes. Fish. Bull. **74**(1): 1–8.

Campana, S.E. 1983. Calcium deposition and otolith check formation during periods of stress in coho salmon, *Oncorhynchus kisutch*. Comp. Biochem. Physiol. A, **75**: 215–220.

Campana, S.E., Zwanenburg, K.C., and Smith, J.N. 1990. $^{210}Pb/^{226}Ra$ determination of longevity in redfish. Can. J. Fish. Aquat. Sci. **47**: 163–165.

Chang, W.Y.B. 1982. A statistical method for evaluating the reproducibility of age determination. Can. J. Fish. Aquat. Sci. **39**: 1208–1210.

Cohen, D.M., Inada, T., Iwamoto, T., and Scialabba, N. 1990. FAO species catalogue. Vol. 10. Gadiform fishes of the world (Order Gadiformes). An annotated and illustrated catalogue of cods, hakes, grenadiers and other gadiform fishes known to date. FAO Fisheries Synopsis No. 125, Vol. 10. Rome, FAO.

Fenton, G.E., and, Short, S.A. 1995. Radiometric analysis of blue grenadier, *Macruronus novaezelandiae*, otolith cores. Fish. Bull. **93**: 391–396.

Fenton, G.E., Ritz, D.A., and Short, S.A. 1990. $^{210}Pb/^{226}Ra$ disequilibria in otoliths of blue grenadier, *Macruronus novaezelandiae*; problems associated with radiometric ageing. Aust. J. Mar. Freshwater Res. **41**: 467–473.

Fenton, G.E., Short, S.A., and Ritz, D.A. 1991. Age determination of orange roughy, *Hoplostethus atlanticus* (Pisces: Trachichthyidae) using ^{210}Pb:^{226}Ra disequilibria. Mar. Biol. **109**: 197–202.

Fleischer, R.L., Price, P.B., and Walker, R.M. 1975. Nuclear tracks in solids. University of California Press, Berkeley, Calif.

Flynn, W.W. 1968. The determination of low levels of polonium-210 in environmental materials. Anal. Chim. Acta, **43**: 221–227.

Gordon, J.D.M., and Swan, S.C. 1996. Validation of age readings from otoliths of juvenile roundnose grenadier, *Coryphaenoides rupestris*, a deep-water macrourid fish. J. Fish Biol. **49**(A): 289–297.

Iwamoto, T., and Stein, D.L. 1974. A systematic review of the rattail fishes (Macrouridae: Gadiformes) from Oregon and adjacent waters. Calif. Acad. Sci., Occas. Pap. 111. pp. 1–79.

Kastelle, C.R., Kimura, D.K., Nevissi, A.E., and Gunderson, D.R. 1994. Using Pb-210/Ra-226 disequilibria for sablefish, *Anoplopoma fimbria*, age validation. Fish. Bull. **92**: 292–301.

Kelly, C.J., Connolly, P.L., and Braken, J.J. 1997. Age estimation, growth, maturity and distribution of the roundnose grenadier from the Rockall trough. J. Fish Biol. **50**: 1–17.

Kimura, D.K., and Kastelle, C.R. 1995. Perspectives on the relationship between otolith growth and the conversion of isotope activity ratios to fish ages. Can. J. Fish. Aquat. Sci. **52**: 2296–2303.

Kline, D.E. 1996. Radiochemical age verification for two deep-sea rockfishes (*Sebastolobus altivelis* and *S. alascanus*). M.S. thesis, California State University, San Jose, Calif.

Kulikova, E.B. 1957. Growth and age of deep-water fishes. Tr. Inst. Okeanol. Akad. Nauk. SSSR, **20**: 347–355. (Translated from Russian by Am. Inst. Biol. Soc. pp. 284–290. 1959.)

Leos, B. (*Editor*). 1996. Monterey Bay commercial fisheries report: an annual newsletter to the commercial fishing industry. Cal. Dep. Fish Game No. 7, Monterey, Calif.

Leos, B. (*Editor*). 1997. Monterey Bay commercial fisheries report: an annual newsletter to the commercial fishing industry. Cal. Dep. Fish Game No. 8, Monterey, Calif.

Mace, P.M., Fenaughty, J.M., Coburn, R.P., and Doonan, I.J. 1990. Growth and productivity of orange roughy (*Hoplostethus atlanticus*) on the north Chatham Rise. N.Z. J. Mar. Freshwater Res. **24**: 105–109.

Matsui, T., Kato, S., and Smith, S.E. 1990. Biology and potential use of Pacific grenadier, *Coryphaenoides acrolepis*, off California. Mar. Fish. Rev. **52**(3): 1–17.

McFarlane, G.A., and Beamish, R.J. 1995. Validation of the otolith cross-section method of age determination for sablefish (*Anoplopoma fimbria*) using oxytetracycline. *In* Recent developments in fish otolith research. *Edited by* D.H. Secor, J.M. Dean, and S.E. Campana. The Belle W. Baruch Library in Marine Science, No. 19. University of South Carolina Press, Columbia, South Carolina. pp. 319–329.

Middleton, R.W., and Musick, J.A. 1986. Abundance and distribution of the family Macrouridae (Pisces: Gadiformes) in the Norfolk Canyon area. Fish. Bull. **84**(1): 35–62.

Milton, D.A., Short, S.A., O'Neill, M.F., and Blaber, S.J.M. 1995. Ageing of three species of tropical snapper (Lutjanidae) from the Gulf of Carpentaria, Australia, using radiometry and otolith ring counts. Fish. Bull. **93**: 103–115.

Moore, W.S. 1996. Large groundwater inputs to coastal waters revealed by ^{226}Ra enrichments. Nature (London), **380**: 612–614.

Morales-Nin, B. 1990. A first attempt determining growth patterns of some Mediterranean deep-sea fishes. Sci. Mar. **54**: 241–248.

Morawska, L., and Phillips, C.R. 1993. Dependence of the radon emanation coefficient on radium distribution and internal structure of the material. Geochim. Cosmochim. Acta, **57**: 1783–1797.

Mulcahey, S.A., Killingley, J.S., Phleger, C.F., and Berger, W.H. 1979. Isotopic composition of otoliths from a benthopelagic fish *Coryphaenoides acrolepis*, Macrouridae: Gadiformes. Oceanol. Acta, **2**: 423–427.

Osterberg, C., Carey, A.G., and Curl, H. 1963. Acceleration of sinking rates of radionuclides in the ocean. Nature (London), **200**: 1276–1277.

Pannella, G. 1980. Growth patterns in fish sagittae. *In* Skeletal growth of aquatic organisms. *Edited by* D.C. Rhoades and R.A. Lutz. Plenum Publishing Corp., New York. pp. 519–560.

Prince, E.D., and Pulos, L.M. (*Editors*). 1983. Proceedings of the

© 1999 NRC Canada

international workshop on age determination of oceanic pelagic fishes: tunas, billfishes, and sharks. NOAA Technical Report NMFS 8.

Rannou, M. 1976. Age and growth of a bathyal fish: *Nezumia sclerorhynchus* (Macrouridae, Gadiform) in Alboran Sea. Cah. Biol. Mar. **XVII**: 413–421.

Saila, S.B., Recksiek, C.W., and Prager, M.H. 1988. Basic fisheries science programs: a compendium of microcomputer programs and manual of operation. *In* Developments in aquaculture and fisheries science. Vol. 18. Elsevier Science Publishers, Amsterdam.

Savvatimsky, P.I. 1994. Age structure of roughhead grenadier (*Macrourus berglax*) in the Northwest Atlantic, 1985. NAFO Sci. Coun. Stud. **20**: 53–64.

Simkiss, K. 1974. Calcium metabolism of fish in relation to ageing. *In* The proceedings of an international symposium on ageing of fish. *Edited by* T.B. Bagenal. Unwin Brothers Limited, The Gresham Press, Old Woking, Surrey, England. pp. 1–12.

Smith, D.C., Fenton, G.E., Robertson, S.G., and Short, S.A. 1995. Age determination and growth of orange roughy (*Hoplostethus atlanticus*): a comparison of annulus counts with radiometric ageing. Can. J. Fish. Aquat. Sci. **52**: 391–401.

Smith, J.N., Nelson, R., and Campana, S.E. 1991. The use of Pb-210/Ra-226 and Th-228/Ra-228 disequilibria in the ageing of otoliths of marine fish. *In* Radionuclides in the study of marine processes. *Edited by* P.J. Kershaw and D.S. Woodhead. Elsevier Applied Science, New York. pp. 350–359.

Specchi, M., Valli, G., Pizzul, E., Salpietro, L., and Cassetti, P. 1995. Osservazioni preliminari sulla struttura di popolazione di alcune specie batiali catturate nel basso tirreno. Biol. Mar. Medit. **2**(2): 519–521.

Stein, D.L., and Pearcy, W.G. 1982. Aspects of reproduction, early life history, and biology of macrourid fishes of Oregon, U.S.A. Deep-Sea Res. **29**(11A): 1373–1379.

Stewart, B.D., Fenton, G.E., Smith, D.C., and Short, S.A. 1995. Validation of otolith-increment age estimates for a deepwater fish species, the warty oreo *Allocyttus verrucosus*, by radiometric analysis. Mar. Biol. **123**: 29–38.

Watters, D.L. 1995. Age determination and confirmation from otoliths of the bank rockfish, *Sebastes rufus* (Scorpaenidae). M.S. thesis, California State University, San Jose, Calif.

West, I.F., and Gauldie, R.W. 1994. Perspectives: determination of fish age using ^{210}Pb:^{226}Ra disequilibrium methods. Can. J. Fish. Aquat. Sci. **51**: 2333–2340.

Wheeler, A.P., and Sikes, C.S. 1984. Regulation of carbonate calcification by organic matrix. Am. Zool. **24**: 933–944.

Wilson, R.R., Jr. 1982. A comparison of ages estimated by the polarized light method with ages estimated by vertebrae in females of *Coryphaenoides acrolepis* (Pisces: Macrouridae). Deep-Sea Res. **29**(11A): 1373–1379.

Yoklavich, M.M., and Boehlert, G.W. 1987. Daily growth increments in otoliths of juvenile black rockfish, *Sebastes melanops*: an evaluation of autoradiography as a new method of validation. Fish. Bull. **85**: 826–832.

© 1999 NRC Canada

Attenuation of ultraviolet radiation in a large lake with low dissolved organic matter concentrations

R.E.H. Smith, J.A. Furgal, M.N. Charlton, B.M. Greenberg, V. Hiriart, and C. Marwood

Abstract: Solar radiation spectra were measured in mesotrophic Lake Erie in 1997 to determine the principal factors influencing ultraviolet radiation (UVR) attenuation. Water clarity ranged widely, with the diffuse vertical attenuation coefficient for photosynthetically active radiation (K_{dl}PAR) varying from 0.26 to 17.2 m^{-1}, and UVR attenuation varied positively and significantly with K_{dl}PAR. Particle concentration (total suspended solids, TSS) was the single most useful water quality characteristic for predicting broadband UVB (305–320 nm) and UVA (320–400 nm) attenuation. Dissolved organic carbon concentration (DOC) and fluorescence were much less important than TSS in predicting UVR attenuation over the typical range of water clarity (K_{dl}PAR < 2 m^{-1}). The predominant role of TSS in UVR attenuation could not be explained by phytoplankton or other absorbing organic matter in the particulate phase, suggesting instead an important role for scattering. Attenuation spectra through the UV region were not monotonic at the higher particle concentrations and could not be modelled solely as a function of DOC as previously reported for other lakes. Attenuation at 310 and 320 nm confirmed the conclusion from spectrally integrated measurements that particles are the dominant agents of variable UVR attenuation in Lake Erie.

Résumé : On a mesuré en 1997 le spectre du rayonnement solaire dans le lac Érié, un lac mésotrophe, pour déterminer les principaux facteurs responsables de l'atténuation du rayonnement ultraviolet (UV). La clarté de l'eau variait beaucoup, le coefficient d'atténuation verticale diffuse du rayonnement photosynthétiquement utilisable (K_{dl}RPU) variant de 0,26 à 17,2 m^{-1}, tandis que l'atténuation des UV variait significativement en raison directe de K_{dl}RPU. La concentration des particules (solides totaux en suspension, STS) était la seule caractéristique de l'eau utile pour prévoir l'atténuation des UVB (305–320 nm) et des UVA (320–400 nm). La fluorescence et la concentration du carbone organique dissous (COD) étaient beaucoup moins importantes que les STS pour prévoir l'atténuation des UV dans les conditions habituelles de clarté de l'eau (K_{dl}RPU < 2 m^{-1}). Le rôle prédominant des STS dans l'atténuation des UV ne pouvait être expliqué par la présence de phytoplancton ou d'autres matières organiques absorbantes dans la phase particulaire, ce qui laisse penser que la dispersion jouait un rôle important. Les spectres d'atténuation des UV n'étaient pas monotones aux plus fortes concentrations de particules et ne pouvaient être mis en relation uniquement avec le COD, comme on l'a déjà fait pour d'autres lacs. L'atténuation à 310 et 320 nm a confirmé l'idée que, d'après les mesures spectrales, les particules sont les principales responsables de l'atténuation variable des UV dans le lac Érié.

[Traduit par la Rédaction]

Introduction

The ecology of ultraviolet radiation (UVR) in freshwaters has received renewed attention in recent years and there is growing evidence that UVR can be a stressful and selective factor for a variety of freshwater organisms (e.g., Vincent and Roy 1993; Bothwell et al. 1994; Leavitt et al. 1997). Freshwater ecosystems, like other parts of the biosphere, are subject to increasing incident fluxes of ultraviolet-B radiation (UVB, 290–320 nm) consequent to diminished concentrations of ozone in the stratosphere (e.g., Kerr and McElroy 1993). There is also evidence for systematic changes in penetration of UVR, including ultraviolet-A radiation (UVA, 320–400 nm), as a consequence of anthropogenic influences on hydrology and geochemistry (Schindler et al.1996; Yan et al. 1996). The latter influences may actually be more important for freshwater ecosystems than the global changes in stratospheric ozone (Morris et al. 1995; Williamson et al. 1996), but their assessment depends on a good understanding of the factors controlling UVR attenuation in natural waters.

As for other solar radiation wavebands, the attenuation of UVR in natural waters is in principle due to both scattering and absorption processes (Kirk 1983, 1994). Although scattering does not in itself extinguish radiation, it effectively increases the pathlength that the average photon must travel. Apparent optical properties such as the vertical attenuation coefficient therefore increase with the strength of scattering, while the depth of penetration of the radiation decreases. The vertical attenuation in the water column can be approxi-

Received August 6, 1998. Accepted February 26, 1999.
J14732

R.E.H. Smith,[1] J.A. Furgal, B.M. Greenberg, V. Hiriart, and C. Marwood. Biology Department, University of Waterloo, Waterloo, ON N2L 3G1, Canada.
M.N. Charlton. Environment Canada, National Water Research Institute, Burlington, ON L7R 4A6, Canada.

[1]Author to whom all correspondence should be addressed.
e-mail: rsmith@sciborg.uwaterloo.ca

© 1999 NRC Canada

mately modelled by Beer's Law, treating the diffuse vertical attenuation coefficient as the sum of contributions from water itself, dissolved organic matter (DOM), and particles; the particles can be further resolved into organic (often pigment-containing particles) and inorganic classes (Kirk 1983). It has long been recognized that DOM is a powerful absorber of UVR, and recent work has indicated that DOM is the dominant agent of variable UVR attenuation among lakes (Scully and Lean 1994; Morris et al. 1995; Morris and Hargreaves 1997). Systematic changes in hydrology (e.g., hotter, drier climate) or geochemistry (e.g., increased atmospheric deposition of strong acids) can cause diminished DOM concentrations in affected surface waters and thus an increased exposure of aquatic organisms to both UVA and UVB (Schindler et al. 1996; Yan et al. 1996; Morris and Hargreaves 1997). The dominance of DOM-mediated absorption in variable UVR attenuation is not universal among natural waters, however. In the oceans, where DOM concentrations are characteristically lower than in freshwaters, pigmented particles (phytoplankton) are also important determinants of UVR attenuation (e.g., Baker and Smith 1982). Nonetheless, DOM is increasingly viewed as the critical quantity regulating UVR attenuation even in lakes of low DOM concentration (e.g., Williamson et al. 1996). If generally true, this has the fortuitous advantage that useful apparent optical properties such as the diffuse vertical attenuation coefficient are more easily modelled and applied in systems where absorption dominates attenuation (Kirk 1983, 1994).

Kirk (1994) noted that direct measurements of UVR attenuation in inland waters were comparatively scarce. Two recent studies have done much to remedy this lack (Scully and Lean 1994; Morris et al.1995) and to make the case for the importance of UVR absorption by DOM. Both studies concerned mainly oligotrophic lakes with widely variable DOM contents. There are many inland surface waters that, by comparison with those surveyed, are rather low and consistent in their DOM contents but more variable in particle contents (e.g., Mortimer 1987; Effler et al. 1991). Lake Erie is such a lake and has undergone a systematic clarification in at least certain areas over the past 15 years as nutrient loading controls and filtering by exotic freshwater mussels of the genus *Dreissena* have diminished particle, especially phytoplankton, concentrations (e.g., Leach 1993). Similar events have more recently unfolded in other areas of the Laurentian Great Lakes, such as Saginaw Bay of Lake Huron (Fahnenstiel et al. 1995). The generality and future direction of such trends are not at present obvious, but *Dreissena* continues to thrive and spread and nutrient inputs continue to be held at relatively low levels (e.g., Klerks et al. 1996; Dermott and Kerec 1997). We are currently unable to answer the question of how the UVR exposure of aquatic organisms in these large lake ecosystems is altered as water clarity changes.

In this study, we attempted to determine how changes in clarity (as evidenced in the visible wavebands) and relevant water quality characteristics (particlate and DOM concentrations) influence UVR attenuation in Lake Erie. We were particularly concerned with assessing the ability of DOM concentrations to predict UVR attenuation in a system that is characterized by relatively high, but variable, particle loads.

Materials and methods

Sampling and radiometry

All radiometric measurements were performed under natural solar radiation while aboard the CCGS *Limnos* (Canada Centre for Inland Waters, Burlington, Ont.) between May 6 and August 28, 1997. The stations were distributed widely about the lake but with higher emphasis on the west basin than on the east and central basins (Fig. 1; Table 1). The west basin is relatively shallow (mean depth 7.4 m) and receives most of the sediment and nutrient loading to the lake, while the central and east basins are deeper (18.3 and 25 m mean depth, respectively) and characteristically lower in nutrients, suspended particles, and phytoplankton (Mortimer 1987; Dahl et al. 1995). It was not our purpose to characterize and compare the differing properties of the basins, but the disposition of sites among basins and over time did allow us to sample a wide range of water column conditions to help elucidate the factors responsible for variable UVR penetration.

An Oriel Instaspec diode array spectroradiometer (Oriel Corp. Stratford, Conn.) was equipped with a waterproofed collecting sphere with true cosine reponse to permit underwater measurements. The radiometer was calibrated with a lamp traceable to National Bureau of Standards specifications. Comparisons against a calibrated Optronics radiometer and measurements under well-defined artificial spectra in the laboratory have confirmed that the Oriel under our setup is capable of accurate measurements of UVR down to approximately 270 nm (Marwood and Greenberg 1996; Nilawati et al. 1997). It was not possible to deploy the instrument in the water column itself, so we instead used high-capacity pumps to fill a large white polyethylene tub (75 × 115 cm area, 75 cm depth) with surface water (1 m depth) from each station studied. Spectral radiation measurements were then made without delay in the tub, with stirring to keep particles suspended. This arrangement was workable because we needed to lower the collecting sphere only 20 cm to obtain sufficient attenuation for calculation of attenuation coefficients in the UV. Light scattered directly from the walls would not enter the collecting sphere appreciably at such depths. We also restricted our work to within 1.5 h of solar noon on clear days to ensure a relatively high solar angle and a high proportion of direct light. Vertical attenuation coefficients for photosynthetically active radiation (K_{dl}PAR) measured in the tub did not differ systematically from those determined by measurements in the water column (using a LI-COR cosine collector quantum probe) at corresponding stations (R.E.H. Smith, unpublished data), confirming that the influence of the tub walls was minimal for PAR and, probably, for UVR as well. Scully and Lean (1994) followed a similar procedure in their work on Lake Ontario.

Wavelength calibration was always performed, just before measurements were taken, by reference to known absorption lines in the incident solar spectrum. Radiation was measured and recorded at intervals of 0.5 nm from 300 to 750 nm. There was, however, very little radiation recorded below 305 nm. UVB was therefore characterized in this study by the radiation recorded in the interval 305–320 nm, which was measured with good reproducibility.

Diffuse vertical attenuation coefficients (K_d) were quantified by regression analysis of the usual Beer's Law formulation for diffuse attenuation:

$$(1) \qquad \ln[E(z)] = a - K_d \cdot Z$$

where $E(z)$ is irradiance at depth z. Following Scully and Lean (1994), we examined two ways of averaging the attenuation over the UVB and UVA wavebands. In the first, spectral irradiance at depth is integrated across the waveband of interest and then regression analysis is performed to define what Scully and Lean 1994) termed the integrated attenuation coefficient, K_{dl}. This was done for both UVB and UVA (320–400 nm) wavebands. The second ap-

© 1999 NRC Canada

Fig. 1. Chart of Lake Erie showing positions of stations sampled for the present study in 1997 (numbered circles) plus others in the Lake Erie surveillance program (unnumbered circles). Latitude and longitude in °N and °W, respectively.

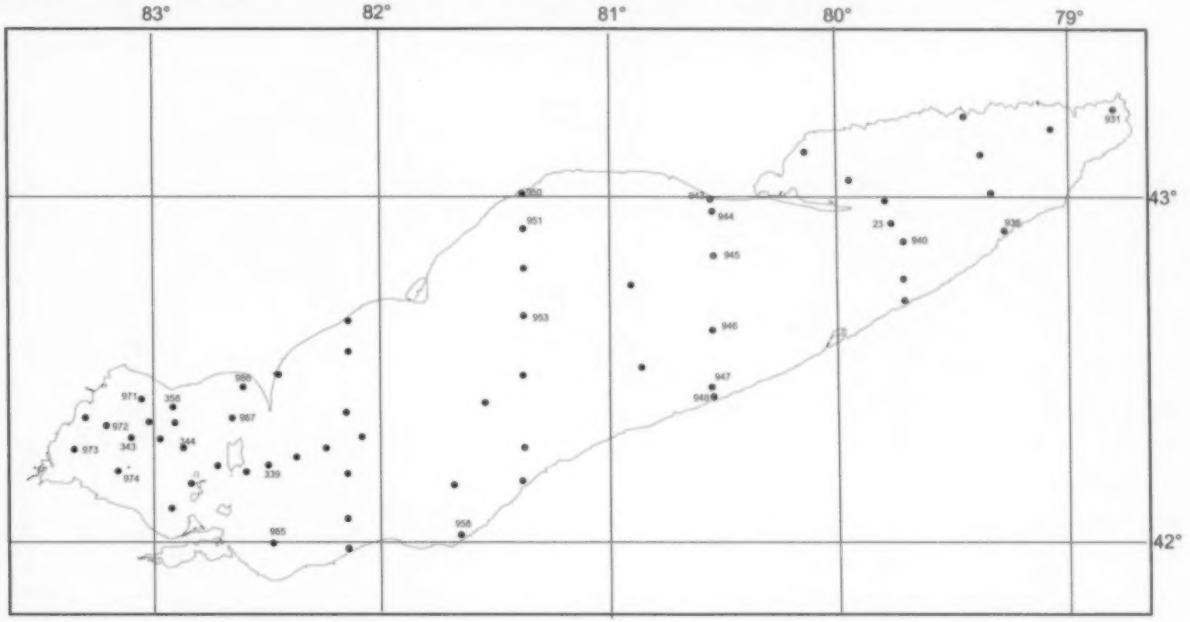

proach to averaging entailed application of eq. 1 to spectral radiation data to define K_d at intervals of 0.5 nm, after which the K_d values were averaged across the waveband of interest to provide what Scully and Lean (1994) termed energy-weighted values, K_{dew}.

Water column characteristics

Samples of the well-mixed water in the deck tub were taken to determine attributes of potential significance to radiation attenuation. Aliquots of 100 mL were filtered through glass fiber filters (GF/F, nominal pore size 0.8 μm) and chlorophyll *a* (Chl *a*) subsequently determined on 90% acetone extracts by fluorometry (Strickland and Parsons 1972; Furgal and Smith 1997). Total suspended solids (TSS) were estimated by filtering 500–1000 mL of water through a precombusted, preweighed filter (GF/F), drying to constant weight, and then reweighing.

DOM was assessed both as dissolved organic carbon (DOC) concentration and as fluorescence (DOC_f). DOC was determined on the filtrate of the TSS samples, acidifying the samples to pH 2 with HCl pending analysis some 3–4 months later. All samples were analyzed by a UV oxidation method (Environment Canada 1994) that has been shown to give similar results to a high-temperature oxidation method in comparable waters (Scully and Lean 1994). Field blanks were obtained by filtering high-quality, charcoal-treated distilled water through virgin filters.

DOC_f was measured with a Turner model 111 fluorometer with filters and standardization as specified in Scully and Lean (1994). The excitation and emission peaks were at 365 and 437 nm, respectively. Fluorescence values were standardized and expressed as milligrams of quinine sulfate per litre. DOC_f was measured both on filtrate of the TSS samples and on whole water.

Statistical analyses

We used correlation analysis, scatterplots, and regression analysis to test for interrelationships among predictor variables, assess homogeneity of variance, and quantify the power of various combinations of variables to predict UVR attenuation (Draper and Smith 1966; Wilkinson 1992). We used an alpha of 0.05 throughout in assessing significance. Plots of residuals indicated acceptable homogeneity of variance, and the best regression models were free of significant outliers or points of leverage (Wilkinson 1992) without any data transformations. The data did suffer from a very unequal distribution between high and low values of UVR attenuation and associated variables and from a high incidence of significant linear correlations among potential predictor variables in the total data set. The implications of the distributional problem were assessed by analyzing both the total data set and a subset over which the data distribution was acceptably uniform as judged by scatterplots and correlation analysis (see further explanation in the Results section). We emphasized linear models and saw little justification in the scatterplots for exploration of nonlinear models. However, we did test nonlinear power functions of a type used by other investigators, using both derivative-based and derivative-free iterative least squares methods to fit the models (Wilkinson 1992). We restricted our exploration of multiple linear regression models to only two predictor variables because our data set was of modest size, and intercorrelations among predictor variables became more problematic in more complicated models.

Results

UVR was rapidly attenuated with depth, even at the clearer stations encountered (e.g., Fig. 2). This was particularly true of UVB, yet we were able to measure it at three or four depths below surface in all cases. Spectra recorded at different depths were quite coherent and supported calculation of vertical attenuation coefficients in nearly all cases. Figure 3 illustrates the fit of the data to the regression model used to estimate diffuse vertical attenuation coefficients for integrated UVB ($K_{dl}B$) and UVA ($K_{dl}A$) radiation for a station that returned among the weaker regressions; most regressions were much stronger.

© 1999 NRC Canada

Table 1. Water quality variables and diffuse vertical attenuation coefficients (m^{-1}) for integrated PAR (K_{dI}PAR), UVA (K_{dI}A), and UVB (K_{dI}B) and for monochromatic radiation at 310 nm (K_{dI}310) and 320 nm (K_{dI}320) in Lake Erie, 1997.

Date	Stn. No.	Basin	DOC	DOC_f	Chl *a*	TSS	K_{dI}PAR	K_{dI}A	K_{dI}B	K_{dI}310	K_{dI}320
May 8	945	Central	nd	3.48	nd	2.3	2.1	2.76	3.64	3.98	3.5
May 8	943	Central	nd	4.24	nd	109	8.68	18.23	25.35	24.8	25.5
May 8	950	Central	nd	4.7	nd	40.5	4.66	9.6	11.12	9.47	12.2
June 4	973	West	4.6	50.29	1.49	124	17.17	49.48	50.49	41.8	60.4
June 4	972	West	2.8	9.86	0.93	30.4	2.13	5.93	11.17	7.56	9.1
June 4	971	West	2.3	3.64	2.04	9.8	0.71	2.51	4.41	7.31	2.1
June 4	343	West	3.3	14.57	6.39	34	4.2	11.3	12.17	10.7	12.6
June 5	951	Central	2.6	2.62	0.54	2.8	0.26	0.97	1.94	2.13	1.8
June 5	950	Central	2.9	6.25	1.29	19.4	2.7	5.9	6.27	9.57	8.6
June 30	931	East	3.1	3.97	0.55	1.2	1	1.34	2.31	2.52	2
June 30	936	East	2.9	3.97	0.81	1.7	1.9	1.82	3.04	2.36	3.1
July 1	944	Central	2.6	2.33	0.35	0.8	0.96	1.67	2.55	2.95	2.3
July 1	943	Central	2.5	1.92	0.29	1	0.57	0.93	1.56	1.74	1.4
July 2	967	West	2.7	4.63	1.28	7	1.29	2.31	4.05	4.33	3.7
July 2	966	West	2.6	4.63	1.77	1.4	0.27	1.08	2.73	3.55	2.7
July 2	358	West	2.5	4.02	1.89	2.1	0.83	1.46	2.68	2.67	2.4
July 2	344	West	2.4	3.66	3.07	2.8	0.79	1.58	2.72	3.21	2.7
July 29	23	East	2.8	3.33	2.34	0.7	0.92	1.39	2.36	2.67	2
July 29	940	East	2.6	2.58	1.65	0.7	1.63	1.9	2.87	3.35	2.5
July 30	953	Central	2.5	4.33	1.43	0.8	0.68	1.36	2.25	2.25	2
July 31	958	Central	2.5	4.36	2.34	1.1	0.55	1.81	3.14	3.39	2.9
July 31	965	Central	6.3	5.4	3.31	1.8	0.33	0.91	2.43	2.93	2
July 31	339	West	2.5	4.6	2.56	1.3	0.52	1.18	2.78	3.4	2.4
August 26	946	Central	2.5	3.29	1.31	1.4	0.26	0.84	2.94	7.23	1.8
August 26	947	Central	2.6	3.55	0.83	1.6	1.56	2.33	3.49	3.58	3.2
August 26	948	Central	2.3	4.08	1.49	3.1	1.99	2.82	4.12	4.72	4.3
August 27	974	West	5.2	5	2.96	5.5	1.04	2.68	3.48	2.73	3.3
August 27	972	West	2.3	4.52	2.43	7.5	1.7	3.2	4.7	4.5	4.5
Mean			2.7	6.1	1.86	14.6	2.14	4.97	6.53	6.32	6.52
Median			2.6	4.08	1.57	2.3	1	1.86	3.09	3.4	2.7

Note: DOC, dissolved organic carbon (mg $C \cdot L^{-1}$); DOC_f, DOC fluorescence (mg quinine sulfate $\cdot L^{-1}$); Chl *a*, chlorophyll *a* ($\mu g \cdot L^{-1}$); TSS, total suspended solids ($mg \cdot L^{-1}$); nd, no data.

The K_{dI}B and K_{dI}A did not differ systematically from coefficients calculated by averaging the wavelength-specific attenuation coefficient throughout each waveband (K_{dew}B and K_{dew}A; data not shown). Linear regression analysis showed that the two types of broadband attenuation coefficients were highly and linearly correlated for both UVA and UVB, with intercepts not significantly different from zero and slopes not significantly different from unity at $p = 0.05$. This was true whether the analysis used the total data set or only the stations with K_{dI}PAR < 2 m^{-1}. Since the mode of averaging did not seem to influence the estimated values for broadband UVB or UVA attenuation, only the coefficients based on integrated radiation (K_{dI}B and K_{dI}A) will be considered further.

The distribution of K_{dI} in the total data set for each of the three wavebands (UVB, UVA, and PAR) was strongly skewed towards the lower values, as reflected in the large difference between mean and median values (Table 1). The maximum observed K_{dI}B was 50 m^{-1}, but nearly 80% of the values were ≤5 m^{-1} (Table 1). The maximum value observed for K_{dI}PAR was >16 m^{-1}, but 75% of the values were ≤2 m^{-1}. The relatively infrequent incidents of high attenuation coefficients corresponded to stations at which the water column was obviously very turbid, and the distribution of TSS values confirms that the stations concerned had relatively high particle loads in the water column (Table 1).

Over the entire data set, there were some significant linear correlations among potential predictor variables for UVR attenuation (Table 2). TSS, DOC_f, and K_{dI}PAR in particular were highly and positively intercorrelated. Thus, water transparency in the visible (K_{dI}PAR) was closely related to the hypothetically more fundamental characteristics of particle and DOM concentrations, as measured by TSS and DOC_f. Correlations involving Chl *a* or DOC were weaker and had probability levels >0.3, except for the correlation between Chl *a* and DOC_f. When analysis was restricted to the modal range of K_{dI}PAR (<2 m^{-1}), no significant correlations were found among any of the potential predictor variables. Over this more typical range of water transparency, K_{dI}PAR was therefore more independent of water quality characteristics.

Over the entire observed range of K_{dI}B (i.e., the full data set), a number of relatively strong linear relationships were found between K_{dI}B and potential predictor variables (Table 3). The best single predictor was K_{dI}PAR, closely followed by TSS. Measures of DOM were less closely related to K_{dI}B, and Chl *a* had no significant relationship with K_{dI}B. All possible pairs of predictor variables (DOC, Chl *a*, DOC_f,

© 1999 NRC Canada

Fig. 2. Spectral irradiance for the UVB and UVA wavebands at three depths in water from a midlake station (station 23) on July 30, 1997.

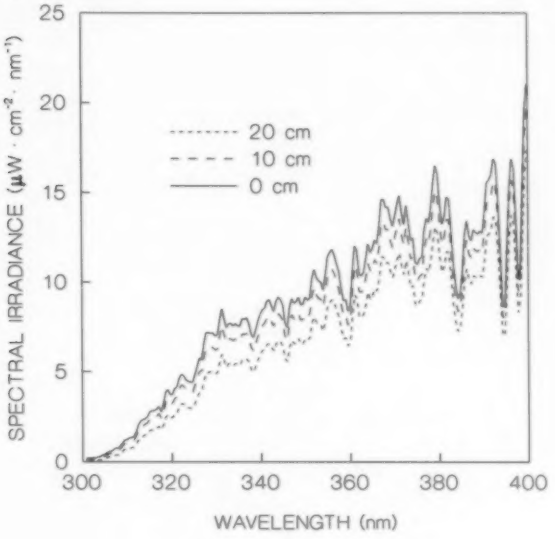

Fig. 3. Spectrally integrated UVB (circles, 305–320 nm) and UVA (triangles, 320–400 nm) versus depth for water from midlake station 23, July 30, 1997. The lines were fitted by linear regression to estimate the diffuse vertical attenuation coefficient for each waveband (Table 1), with percent explained variation (R^2) of 84% ($p < 0.01$) for UVB and 72% ($p < 0.03$) for UVA.

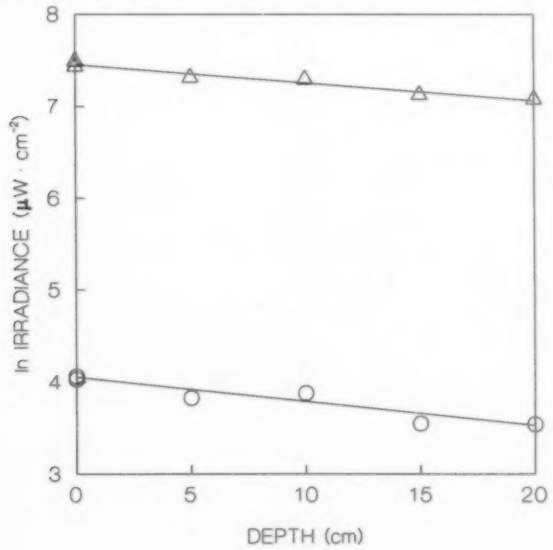

TSS, and K_{dl}PAR) were explored in multiple regression models. The model with the highest R^2 (model 6) (Table 3; Fig. 4) used both TSS and DOC_f as predictors and explained 99% of the variation in K_{dl}B. The F statistics indicated that TSS accounted for nearly 70% of the variation, while DOC_f accounted for approximately 30%. A model with K_{dl}PAR and TSS as predictors (not shown) was nearly as good (R^2 = 97%), and K_{dl}PAR accounted for nearly 90% of the explained variation. These relationships were obviously dictated largely by the infrequent high values for K_{dl}B. Although very similar results were obtained when the station with the very highest K_{dl}B was dropped from the analysis, the applicability of such relationships to the majority of stations, among which K_{dl}B varied relatively little, is certainly questionable. Furthermore, the multiple regression models were only slightly more successful than the best simple regression models and were confounded by significant linear correlations among DOC_f, TSS, and K_{dl}PAR. Examination of the data did not suggest any transformations or alternative models that might disentangle the simultaneous influence of these three variables.

Table 2. Pearson correlation coefficients among potential predictor variables (definitions and units as in Table 1) for UVR attenuation, with values for entire data set followed in parentheses by those for the typical range of water clarity (K_{dl}PAR < 2 m^{-1}) only.

	DOC	Chl *a*	DOC_f	TSS
Chl *a*	0.2 (–0.4)			
DOC_f	0.5 (–0.3)	0.6* (0.4)		
TSS	0.5 (–0.3)	0.4 (0.7)	0.9* (0.4)	
K_{dl}PAR	0.6 (0.0)	0.4 (–0.2)	0.8* (0.1)	0.8* (0.1)

Note: Asterisks denote significance at $p = 0.05$.

The modal range for K_{dl}PAR was <2 m^{-1}, and regression analysis was again used to explore predictive relationships for K_{dl}B among the corresponding subset of stations. Measures of DOM proved of little value in predicting K_{dl}B in the subset, and Chl *a* continued to show no significant correlation with K_{dl}B (Table 3). Although barely significant, model 7 indicated a surprising negative relationship between K_{dl}B and DOC. Both TSS and K_{dl}PAR were significantly correlated with K_{dl}B, but TSS was by far the best single predictor. By pairwise exploration of multiple regression models, the best predictive relationship (model 12) (Table 3; Fig. 5) was found to use TSS and K_{dl}PAR, with TSS accounting for 73% of the explained variation. The relationship was highly significant, but the proportion of explained variation was still lower (R^2 = 74%) than for the best model of the entire data set. DOC_f, which was a useful predictor in the total data set, did not explain any significant additional variation when paired with any of the other variables. There were no significant linear correlations among the predictor variables in this more restricted portion of the data set.

The nature of the best predictive model for K_{dl}B thus varied between the full data set and the subset (model 6 versus model 12, Table 3), but the two models did not actually differ very strongly in their predictions. Model 12, for low-attenuation stations, tended to underestimate the strength of attenuation at the most turbid stations, but its divergence from model 6 became serious only at the very highest attenuations (Fig. 4). Model 6, derived from the whole data set, actually made rather similar predictions to model 12 among the low-attenuation stations (Fig. 5), even though DOC_f did not explain any significant share of the variance. This points to the dominant, and relatively consistent, influence of TSS

© 1999 NRC Canada

Table 3. Linear regression models for predicting the integrated UVB attenuation coefficient ($K_{dI}B$, m^{-1}) in Lake Erie using all data (models 1–6) or only stations with a diffuse vertical attenuation coefficient ($K_{dI}PAR$) of <2 m^{-1} for PAR (models 7–12).

Model No.	Model description	Sample size	R^2	p
1	$K_{dI}B$ = –43.381 + 18.127 (±2.034)·DOC	25	0.77	<0.001
2	$K_{dI}B$ = 4.694 + 0.558 (±1.573)·Chl *a*	25	0	0.726
3	$K_{dI}B$ = 0.392 + 0.988 (±0.096)·DOC_f	28	0.79	<0.001
4	$K_{dI}B$ = 1.953 + 0.308 (±0.019)·TSS	28	0.91	<0.001
5	$K_{dI}B$ = 0.266 + 2.855 (±0.095)·$K_{dI}PAR$	28	0.97	<0.001
6	$K_{dI}B$ = 0.547 + 0.208 (±0.007)·TSS + 0.465 (±0.024)·DOC_f	28	0.99	<0.001
7	$K_{dI}B$ = 7.313 – 1.686 (±0.810)·DOC	21	0.14	0.051
8	$K_{dI}B$ = 2.560 + 0.249 (±0.195)·Chl *a*	21	0.03	0.218
9	$K_{dI}B$ = 1.584 + 0.364 (±0.188)·DOC_f	21	0.12	0.068
10	$K_{dI}B$ = 2.322 + 0.246 (±0.046)·TSS	21	0.58	<0.001
11	$K_{dI}B$ = 2.204 + 0.823 (±0.284)·$K_{dI}PAR$	21	0.27	0.01
12	$K_{dI}B$ = 1.818 + 0.219 (±0.037)·TSS + 0.611 (±0.175)·$K_{dI}PAR$	21	0.74	<0.001

Note: See Table 1 for definitions and units of other variables.

Fig. 4. Relationship between $K_{dI}B$ predicted by model 6 (Table 3) and the observed values for the total data set (n = 28). The symbols represent the observations and the solid line is the fit of model 6. The dashed line shows the fit of model 12 (Table 3) extrapolated to the entire data set.

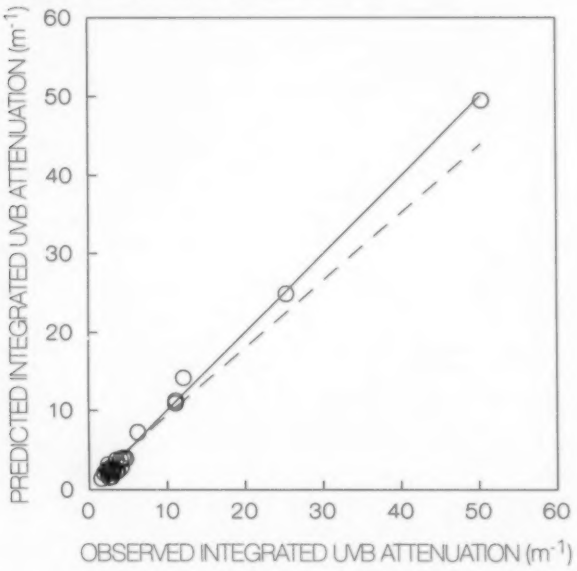

Fig. 5. Relationship between $K_{dI}B$ predicted by model 12 (Table 3) and the observed values for stations with $K_{dI}PAR$ < 2 m^{-1} (n = 22). The symbols represent the observations and the solid line is the fit of model 12. The dashed line shows the fit of model 6 (Table 3) as derived from the entire data set (including $K_{dI}PAR$ > 2 m^{-1}).

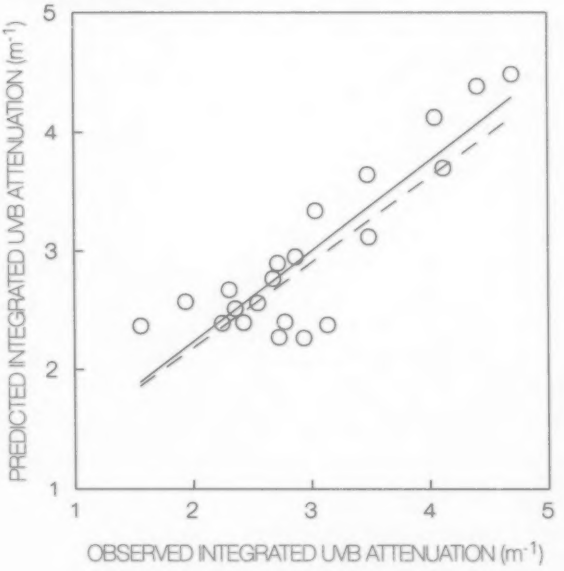

and additional unidentified factors that determine $K_{dI}PAR$ across the entire range of turbidity encountered here.

The quality of the suspended particulates was not directly determined but could conceivably include a significant proportion of light-absorbing organic material. Fluorescence of whole water, including particulates, was highly correlated with soluble fluorescence (Fig. 6). The relationship had an intercept not significantly different from zero and a slope significantly, but only modestly, larger than unity (1.22 ± 0.077 SE, n = 28), indicating that fluorescing organic matter in the particulate phase accounted for only 18% of total fluorescence on average. Regression analyses of $K_{dI}B$ on whole-water fluorescence, alone or in combination with other variables, always gave the same or poorer results than those using soluble fluorescence. Thus, there was no evidence that the important influence of suspended solids on $K_{dI}B$ was due to organic matter in the particulate phase. An obvious test of this conclusion would be to determine the predictive ability of the organic versus inorganic fractions of the particulate matter, but the samples were lost before they could be combusted to enable this test.

Predictive relationships for $K_{dI}A$ were also explored using regression analysis on the whole data set and the subset of more typical clarity ($K_{dI}PAR$ < 2 m^{-1}). The results for $K_{dI}A$ (Table 4) were quite similar to those for $K_{dI}B$. The major

© 1999 NRC Canada

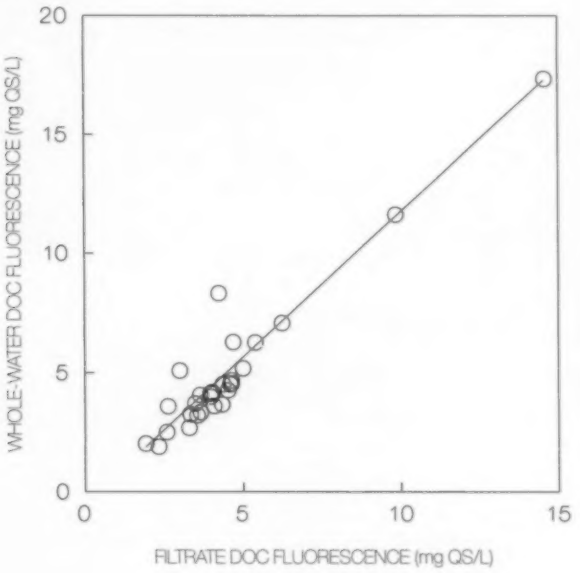

Fig. 6. Relationship between whole-water fluorescence (DOC_{fw}) and the fluorescence of filtered water (DOC_f) together with the fitted linear model $DOC_{fw} = -0.446$ (±0.393 SE) + 1.219 (±0.077 SE)·DOC_f, $R^2 = 0.90$, $p < 0.001$. One point at very high DOC_f (50.2 mg quinine sulfate·L^{-1}) was excluded to resolve the remaining points better; the relationship is little altered by its inclusion.

difference was a greater importance of K_{dl}PAR. The best model for the whole data set (model 6, Table 4) used K_{dl}PAR and DOC_f instead of TSS and DOC_f but was little different from the model using the latter two variables (R^2 = 0.986). As for the K_{dl}B regressions, intercorrelations among the predictor variables in the total data set confounded interpretation of the multiple regression models. For the subset of data corresponding to more typical water clarity, the best model (model 12, Table 4) used K_{dl}PAR and TSS and performed much better than any model with only one predictor variable. Measures of DOM (DOC, DOC_f) were of little value in predicting K_{dl}A and added no significant increase in explained variation when paired with TSS or K_{dl}PAR.

Similar analyses were done to determine the best correlations and predictive relationships for spectral attenuation coefficients at two different wavelengths, 310 nm (K_{310}) and 320 nm (K_{320}). As for the broadband attenuation coefficients, the spectral attenuation coefficients were highly and positively correlated with both TSS and K_{dl}PAR in the whole data set ($R^2 > 0.91$). The best multiple regression models represented slight improvements ($R^2 > 0.96$ for the multiple models) and used the different predictor combinations of TSS, K_{dl}PAR, and DOC_f with almost equal success. In the data subset representing more typical water clarity (K_{dl}PAR < 2 m^{-1}), only TSS was significantly correlated with K_{310}, and no other variable improved the predictive power of TSS alone. The proportion of explained variation was, however, lower than with the best models for K_{dl}B (R^2 = 0.55), probably reflecting the greater measurement error in K_{310}. In the subset, K_{320} was best predicted by a multiple regression on TSS and K_{dl}PAR, just as for K_{dl}A and with a similar R^2 of 0.74. TSS and K_{dl}PAR each accounted for about half of the explained variation. DOC_f, which was uncorrelated with K_{310}, was significantly correlated with K_{320} but explained much less variation than did TSS or K_{dl}PAR.

The spectral distribution of attenuation coefficients varied strongly among stations (e.g., Fig. 7), and a fully satisfactory model for spectral attenuation coefficients has not yet been found for our data set. For stations in the typical clarity range (K_{dl}PAR < 2 m^{-1}, e.g., station 23), the attenuation spectra were monotonic and had the general shape of a negative exponential function. At the more turbid stations the spectra were not monotonic but instead had a peak in the long-UVB to short-UVA portion of the spectrum (Fig. 7). The peak appeared to move to longer wavelengths as TSS increased among stations. The appearance of the peak was not simply a problem of difficulties in measuring the rapidly attenuated short wavelengths at such turbid stations. For example, station 972 showed a clear peak in attenuation near 320 nm, even though the UVR (320 nm) penetrating to 10 cm depth was greater than 30% of incident, well within the sensitivity of our radiometer. For the monotonic spectra observed at the stations of typical water clarity (K_{dl}PAR < 2 m^{-1}), we tested the power model of Morris et al. (1995):

$$(2) \qquad \ln[K_d(\lambda)] = -a\cdot\lambda + b\cdot DOC^c$$

where $K_d(\lambda)$ is the spectral attenuation coefficient. The model was significant ($p < 0.001$) but had an R^2 of only 54%. The parameter estimates were 0.0113, 4.26, and 0.062 for a, b, and c, respectively, and were significantly lower than reported in Morris et al. (1995). For the same stations, a simpler model of the form

$$(3) \qquad \ln[K_d(\lambda)] = a - b\cdot\lambda$$

performed equally well (R^2 = 53%, a = 92.4, b = 0.0113), indicating that variations in DOC do not help explain any significant portion of the variation in spectral attenuation over the typical clarity range. The best model for spectral attenuation for the relatively clear-water stations was

$$(4) \qquad \ln[K_{norm}] = a - b\cdot\lambda$$

where K_{norm} is $K_d(\lambda)$ normalized to the value at 320 nm. The model based on eq. 4 yielded an R^2 of 80%, with values of 3.29 and 0.011 for a and b, respectively, indicating that better predictions are possible when the variation of attenuation at 320 nm is accounted for. The relatively good performance of eq. 4 was not true for the entire data set, however. No model that we tested could manage an R^2 greater than 20% when the high-turbidity stations were included.

Discussion

Our results for Lake Erie are in contrast with two recent studies which showed that DOM is the dominant agent of variable UVR attenuation among lakes (Scully and Lean 1994; Morris et al. 1995) and that particles are unimportant. The predictive relationships for UVR attenuation presented from the interlake studies, which were based on measures of DOM, were tested against our Lake Erie data, failed to make

© 1999 NRC Canada

Table 4. Linear regression models for predicting the integrated UVA attenuation coefficient ($K_{dl}A$, m^{-1}) in Lake Erie using all data (models 1–6) or only stations with a diffuse vertical attenuation coefficient ($K_{dl}PAR$) of <2 m^{-1} for PAR (models 7–12).

Model No.	Model description	Sample size	R^2	p
1	$K_{dl}A = -45.039 + 18.238\ (\pm 1.986)\cdot DOC$	25	0.78	<0.001
2	$K_{dl}A = 3.209 + 0.628\ (\pm 1.571)\cdot Chl\ a$	25	0	0.693
3	$K_{dl}A = -1.183 + 0.992\ (\pm 0.075)\cdot DOC_f$,	28	0.87	<0.001
4	$K_{dl}A = 0.747 + 0.285\ (\pm 0.024)\cdot TSS$	28	0.83	<0.001
5	$K_{dl}A = -1.059 + 2.752\ (\pm 0.090)\cdot K_{dl}PAR$	28	0.97	<0.001
6	$K_{dl}A = -1.441 + 0.322\ (\pm 0.032)\cdot DOC_f + 2.013\ (\pm 0.083)\cdot K_{dl}PAR$	28	0.99	<0.001
7	$K_{dl}A = 5.255 - 1.375\ (\pm 0.647)\cdot DOC$	22	0.14	0.046
8	$K_{dl}A = 1.545 + 0.090\ (\pm 0.159)\cdot Chl\ a$	22	0	0.577
9	$K_{dl}A = 0.958 + 0.196\ (\pm 0.162)\cdot DOC_f$	22	0.02	0.239
10	$K_{dl}A = 1.302 + 0.137\ (\pm 0.045)\cdot TSS$	22	0.28	0.01
11	$K_{dl}A = 0.820 + 0.950\ (\pm 0.186)\cdot K_{dl}PAR$	22	0.54	<0.001
12	$K_{dl}A = 0.565 + 0.113\ (\pm 0.027)\cdot TSS + 0.867\ (\pm 0.139)\cdot K_{dl}PAR$	22	0.75	<0.001

Note: See Table 1 for definitions and units of other variables.

Fig. 7. Diffuse vertical attenuation coefficient spectra for three stations chosen to illustrate the results for water with suspended particles at relatively low (station 23, TSS = 0.7 $mg\cdot L^{-1}$, dashed line), relatively high (station 972, TSS = 30.4 $mg\cdot L^{-1}$, dotted line), and very high (station 973, TSS = 124.0 $mg\cdot L^{-1}$, solid line) concentrations. The attenuation coefficients have been normalized to unity at 320 nm.

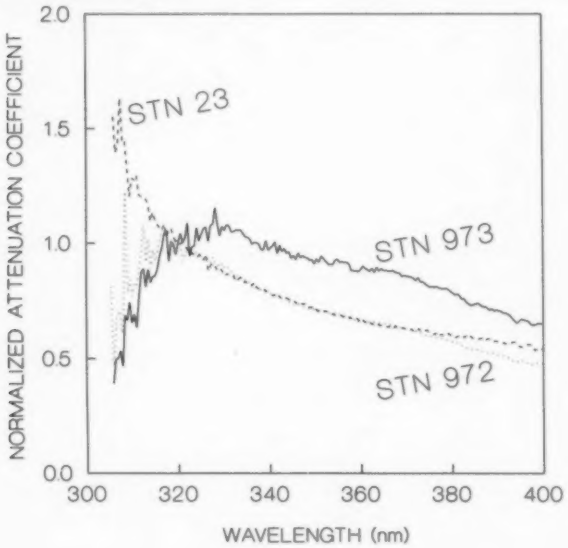

statistically significant predictions over the typical range of water clarity ($K_{dl}PAR < 2\ m^{-1}$), and were inferior (in terms of R^2) over the total data set. Scully and Lean (1994) and Morris et al. (1995) both found that power functions of DOC best described the relationship between UVR attenuation and DOC, but we found no improvement in predictive power or distribution of residuals when comparing such models with the linear functions presented here. On the other hand, we confirmed for ourselves, using the data published by Morris et al. (1995), that TSS was indeed a very inferior, and usually statistically insignificant, predictor of UVR attenuation among their lakes. This was true even when we constrained their data set to lakes with DOC concentrations within the range that we observed in Lake Erie. Scully and Lean (1994) also reported that particles, as measured by Chl *a* or particulate organic carbon concentrations, failed to make useful predictions of UVR attenuation among their lakes. Scully and Lean (1994) measured particles only as Chl *a* or particulate organic carbon and may therefore not have detected the influence of resuspended material with low organic content. Morris et al. (1995), however, did measure TSS (PM in their terminology) and yet failed to detect much influence of particulate matter.

The simplest explanation of this apparent contradiction would seem to be the relative variability of DOC and particles in Lake Erie compared with the interlake data sets. In Lake Erie, the most sediment influenced of the Laurentian Great Lakes (Mortimer 1987), the range of TSS concentrations was approximately 20 times that of DOC. By contrast, the range of DOC among the lakes studied by Morris et al. (1995) was approximately equal to that of TSS, or approximately half as large if DOC was constrained to the 2–6 $mg\cdot L^{-1}$ interval (comparable with Lake Erie). Compared with the systems in the interlake studies, Lake Erie had much greater variability in particles than in DOC, and the absolute concentrations of particles in Lake Erie were also systematically larger than in the interlake systems. Despite the abundance of particles in Lake Erie's water column, the median values for $K_{dl}B$ and $K_{dl}A$ were comparable with those for lakes of low to moderate DOC (i.e., 2–4 mg $C\cdot L^{-1}$) studied by Scully and Lean (1994) and Morris et al. (1995). Only at the very highest particle concentrations (TSS > 100 $mg\cdot L^{-1}$) did the UVR attenuation coefficients approach or surpass those observed in lakes of high DOC (>10 m^{-1}). Organisms in Lake Erie may therefore be exposed to considerable amounts of UVR, by freshwater standards, even though the lake is relatively turbid to PAR.

An additional, or alternative, explanation of the relatively poor relationship between DOC and UVR attenuation in Lake Erie might relate to DOC quality or the accuracy of our DOC measurements. There is substantial variation in spectral absorption properties of natural DOC (Morris et al. 1995; Vodacek et al. 1997) and of narrower classes such as humic and fulvic acids (Lawrence 1980; McKnight et al.

© 1999 NRC Canada

1994). Environmental variables such as pH can also alter absorption properties of DOC. For our low-turbidity stations in Lake Erie, we were able to model the normalized UVR spectral attenuation as a function of wavelength (eq. 4), obtaining an exponent of 0.011 nm^{-1} (95% CI = 0.010–0.012) that was similar to some values previously reported for freshwaters (Morris et al. 1995) and for freshwater-influenced marine systems (Vodacek et al. 1997). For the lower turbidity stations, among which the predictive ability of DOC measurements was poorest, there was therefore little evidence that the optical properties of the DOC in Lake Erie were unusual or highly variable.

At the higher particle concentrations, the UVR attenuation spectra revealed a nonmonotonic shape that has not, to our knowledge, been reported elsewhere and is not interpretable in terms of any published spectra for UVR absorption by natural DOC. The only likely explanation is that the scattering agents at turbid stations in Lake Erie are maximally effective at wavelengths in the long UVB – short UVA region, thus increasing the effective pathlength for such photons. Modelling of nonmolecular scattering is computationally intensive and requires information about the size distribution and refractive index of the scattering agents, as well as the angular distribution of the light field (Kirk 1994), and cannot be undertaken with the data available here. Given that the scattering agents at turbid stations are probably clay particles with dimensions on the order of 1 µm, however, a peak scattering efficiency in the 310–340 nm range is not unlikely (Kirk 1994).

DOC measurements, which have been controversial of late, are prone to numerous errors and inaccuracies (Wangersky 1993) and it is possible that our sampling and analytical methods were not sufficiently well controlled to quantify DOC variation over the limited range observable in Lake Erie. We did take the usual precautions in sampling, including the running of field blanks, and the method used to determine DOC here (UV oxidation, Environment Canada 1994) has been shown to give similar results to high-temperature oxidation in samples from lakes in our study area (Scully and Lean 1994). Perhaps the best evidence that errors in DOC measurement were not responsible for our results comes from the measurements of DOC_f. Conducted and standardized aboard ship, on fresh samples, the fluorescence measurements should be reliable. They also help to address the DOC quality issue, since fluorescence is a relatively direct measure of photochemically active DOC, the fraction that should be most responsible for UVR absorption (Scully and Lean 1994). Even though DOC_f corresponded very well to UVR attenuation in Scully and Lean's (1994) lakes, it was no more helpful than DOC in predicting UVR attenuation in Lake Erie.

In some lakes with high particulate turbidity (e.g., Burley Griffin, Australia), the absorption spectra of the particulate matter resemble those of the DOM, suggesting that organic matter adsorbed to particles is an important optical component in total attenuation (Kirk 1983, 1994). In Lake Erie, the DOC_f measurements suggested that the light-absorbing organic content of particles in Lake Erie was generally low, contributing <20% of the photoactive organic pool in the water. Phytoplankton can also be important particulate agents of UVR attenuation in the ocean (e.g., Baker and Smith 1982), but in Lake Erie, as in other lakes reported on recently (Scully and Lean 1994; Morris et al. 1995), the Chl *a* data gave no evidence that phytoplankton have any significant effect on UVR penetration. The important influence of particles, as estimated by TSS, on UVR attenuation in Lake Erie would instead appear to reflect a major influence of scattering exerted by particles of relatively low organic content, presumably resuspended or riverine sediments. This important particle influence was not restricted to times of unusually high particle loads but also existed among the relatively low-turbidity stations.

In fact, the relatively small influence of DOC and more dominant influence of particles was most evident in Lake Erie when we restricted our analysis to the less turbid stations, among which $K_{dl}B$ varied only from 1.6 to 4.7 m^{-1}. This is a small range compared with that observed in the interlake studies of Scully and Lean (1994) and Morris et al. (1995). To some extent, our different results may reflect the fact that we are pushing the limits of what simple empirical models of apparent optical properties can hope to accomplish (Kirk 1983), although the recorded variation of UVR attenuation among our low-turbidity stations was certainly not negligible. The corresponding range in the 1% depth for integrated UVB was approximately from 1 to 3 m, a considerable range in the volume of lake exposed to potential UVB effects. The "best" models for UVR attenuation derived in the present study, unlike those in recent interlake studies (Scully and Lean 1994; Morris et al. 1995), are not immediately interpretable in terms of the fundamental factors (water, DOM, organic particles, and inorganic particles) influencing light absorption in natural waters (Kirk 1983) because they typically require measurements of $K_{dl}PAR$. Predictions made with multiple regression models in which the predictor variables are intercorrelated, as for the total Lake Erie data set, should be viewed cautiously in any case, particularly if extrapolating outside the range of the data set analyzed. The models are therefore more important for demonstrating the importance of particles than for predicting UVR attenuation generally. Significant advance in modelling and forecasting of the UVR environment in the lake, based on water column characteristics, will require an approach that deals more in the intrinsic optical properties and treats scattering explicitly (e.g., Jerome et al. 1987; Effler et al. 1991), and this in turn will require much more knowledge of particle characteristics in the lake.

Of late, much emphasis has been placed on the key role of DOC in determining UVR (and PAR) penetration in lakes and the consequences for UVR exposure that result from changes (often anthropogenic) in DOC concentration (Schindler et al. 1996; Williamson et al. 1996; Yan et al. 1996). In Lake Erie and certain other parts of the Laurentian Great Lakes, recent increases in water transparency, as measured variously by Secchi depth, transmissometry, and estimates of $K_{dl}PAR$, have been pronounced (e.g., Leach 1993; Fahnenstiel et al. 1995) but have not been linked to changes in DOC. Instead, the increased transparency has been coincident with diminished concentrations of phytoplankton, which in turn are thought to be caused by diminished nutrient loading and, most recently and more importantly, filtering activity by invading mussels of the genus *Dreissena* (e.g., Leach 1993; Nicholls and Hopkins 1993; Fahnenstiel

© 1999 NRC Canada

et al. 1995). The proximate mechanisms by which nutrients and mussels may control water clarity in the affected systems have not, however, been explicitly defined. Our results suggest that the direct effects of mussels and nutrient controls on phytoplankton are not the principal mechanism underlying the increased water clarity and will not have any significant bearing on UVR exposure of organisms in the lake. Not only is Chl *a* unrelated to UVR attenuation in our data set, it is also unrelated to K_{dl}PAR as measured by us in 1997 or by Dahl et al. (1995) in 1993. Jerome et al. (1987) estimated a Chl *a* specific attenuation cross section of approximately 0.0215 $m^2 \cdot mg\ Chl\ a^{-1}$ in Lake Ontario and suggested that a similar value should apply to Lake Erie. If true, then the variations in Chl *a* observed in Lake Erie could account for only a small fraction of the variation in K_{dl}PAR. For the relatively clear stations, for example (K_{dl}PAR < 2 m^{-1}), the variation in Chl *a* was about 3 $mg \cdot m^{-3}$. This corresponds to an expected variation of about 0.067 m^{-1} in K_{dl}PAR compared with an observed range of >1.5 m^{-1}. Working in Lake Champlain, a system with many similarities to Lake Erie, Effler et al. (1991) found that phytoplankton were only minor determinants of variable PAR attenuation. Effler et al. (1991) showed that both scattering and absorption effects were important to PAR attenuation in Lake Champlain and that particles other than phytoplankton were important in both regards. This contrasts with the situation in many oceanic areas and some lakes, where scattering is less important and phytoplankton are significant determinants of water transparency and K_{dl}PAR (Kirk 1983).

The influence of nutrient controls and filtering activities of mussels on water transparancy and UVR penetration therefore appears likely to be mediated largely by changes in nonphytoplankton particle concentrations in lakes such as Erie and Champlain. It is not immediately apparent how inorganic nutrient loading per se could have much influence on the prevalence of particles of terriginous and (or) sediment origin in the water column outside the immediate area of effluent plumes, although measures to control diffuse loading (e.g., agricultural runoff) may also help to limit sediment inputs. *Dreissena* does appear, however, to be competent in removing nonphytoplankton particles from the water column and in depositing them, largely in consolidated form, on the bottom (e.g., Klerks et al. 1996). The efficiency and regulation of such removal, and the subsequent fate of the deposited material, would appear to be important areas for research in systems subject to *Dreissena*'s influence.

Acknowledgments

We thank the officers and crew of the CCGS *Limnos* and the Technical Operations Branch of the Canada Centre for Inland Waters for their help. Financial support was from Natural Sciences and Engineering Research Council of Canada grants to R.E.H.S. and B.M.G. and an Environment Canada Science Horizons Internship to J.A.F.

References

Baker, K.S., and Smith, R.C. 1982. Spectral irradiance penetration in natural waters. *In* Role of solar ultraviolet radiation in marine ecosystems. *Edited by* J. Calkins. Plenum Press, New York. pp. 233–246.

Bothwell, M.L., Sherbot, D.M., and Pollack, C.M. 1994. Ecosystem response to solar ultraviolet-B radiation: influence of trophic level interactions. Science (Washington, D.C.), **265**: 97–100.

Dahl, J.A., Graham, D.M., Dermott, R., Johannsson, O.E., Millard, E.S., and Myles, D.D. 1995. Lake Erie 1993, western, west central and eastern basins: change in trophic status, and assessment of the abundance, biomass and production of the lower trophic levels. Can. Tech. Rep. Fish. Aquat. Sci. No. 2070.

Dermott, R., and Kerec, D. 1997. Changes to the deepwater benthos of eastern Lake Erie since the invasion of *Dreissena*. Can. J. Fish. Aquat. Sci. **54**: 922–930.

Draper, N., and Smith, H. 1966. Applied regression analysis. John Wiley & Sons, New York.

Effler, S.W., Perkins, M., and Johnson, D.L. 1991. Optical heterogeneity in Lake Champlain. J. Gt. Lakes Res. **17**: 322–332.

Environment Canada. 1994. Analytical methods manual. 1. Inland Water Directorate, Water Quality Branch, Ottawa, Ont.

Fahnenstiel, G.L., Lang, G.A., Nalepa, T.F., and Johengen, T.H. 1995. Effects of zebra mussel (*Dreissena polymorpha*) colonization on water quality parameters in Saginaw Bay, Lake Huron. J. Gt. Lakes Res. **21**: 435–448.

Furgal, J.A., and Smith, R.E.H. 1997. Ultraviolet radiation and photosynthesis by Georgian Bay phytoplankton of varying nutrient and photoadaptive status. Can. J. Fish. Aquat. Sci. **54**: 1659–1667.

Jerome, J.H., Bukata, R.P., and Bruton, J.E. 1987. Existing and anticipated irradiation in the hypolimnetic waters of central Lake Erie. J. Gt. Lakes Res. **13**: 568–577.

Kerr, J.B., and McElroy, C.T. 1993. Evidence for large upward trends of ultraviolet-B radiation linked to ozone depletion. Science (Washington, D.C.), **262**: 1032–1034.

Kirk, J.T.O. 1983. Light and photosynthesis in aquatic ecosystems. Cambridge University Press, Cambridge, U.K.

Kirk, J.T.O. 1994. Optics of UV-B radiation in natural waters. Arch. Hydrobiol. Beih. Ergebn. Limnol. **43**: 1–16.

Klerks, P.L., Fraleigh, P.C., and Lawniczak, J.E. 1996. Effects of zebra mussels (*Dreissena polymorpha*) on seston levels and sediment deposition in western Lake Erie. Can. J. Fish. Aquat. Sci. **53**: 2284–2291.

Lawrence, J. 1980. Semi-quantitative determination of fulvic acid, tannin and lignin in natural waters. Water Res. **14**: 373–377.

Leach, J.H. 1993. Impacts of the zebra mussel (*Dreissena polymorpha*) on water quality and fish spawning reefs in western Lake Erie. *In* Zebra mussels. Biology, impacts and control. *Edited by* T.F. Nalepa and D.W. Schloesser. Lewis Publishers, Boca Raton, Fla. pp. 381–397.

Leavitt, P.R., Vinebrooke, R.D., Donald, D.B., Smol, J.P., and Schindler, D.W. 1997. Past ultraviolet radiation environments in lakes derived from fossil pigments. Nature (Lond.), **388**: 457–459.

Marwood, C.A., and Greenberg, B.M. 1996. Effect of supplementary UV-B radiation on chlorophyll synthesis and accumulation of photosystems during chloroplast development in *Spriodela oligorrhiza*. Photochem. Photobiol. **64**: 664–670.

McKnight, D.M., Andrews, E.D., and Spaulding, S.A. 1994. Aquatic fulvic acids in algal-rich antarctic ponds. Limnol. Oceanogr. **39**: 1972–1979.

Morris, D.P., and Hargreaves, B.R. 1997. The role of photochemical degradation of dissolved organic carbon in regulating the UV transparency of three lakes on the Pocono Plateau. Limnol. Oceanogr. **42**: 239–249.

© 1999 NRC Canada

Morris, D.P., Zagarese, H., Williamson, C.E., Balseiro, E.G., Hargreaves, B.R., Modenutti, B., Moeller, R., and Queimalinos, C. 1995. The attenuation of solar UV radiation in lakes and the role of dissolved organic matter. Limnol. Oceanogr. **40**: 1381–1391.

Mortimer, C.H. 1987. Fifty years of physical investigations and related limnological studies on Lake Erie, 1928–1977. J. Gt. Lakes Res. **13**: 407–435.

Nicholls, K.H., and Hopkins, G.J. 1993. Recent changes in Lake Erie (north shore) phytoplankton: cumulative impacts of phosphorus leading reductions and the zebra mussel introduction. J. Gt. Lakes Res. **19**: 637–647.

Nilawati, J., Greenberg, B.M., and Smith, R.E.H. 1997. Influence of ultraviolet radiation on growth and photosynthesis of two cold ocean diatoms. J. Phycol. **33**: 215–224.

Schindler, D.W., Curtis, P.J., Parker, B.R., and Stainton, M.P. 1996. Consequences of climate warming and lake acidification for UV-B penetration in North American boreal lakes. Nature (Lond.), **379**: 705–707.

Scully, N.M., and Lean, D.R.S. 1994. The attenuation of ultraviolet radiation in temperate lakes. Arch. Hydrobiol. Beih. Ergebn. Limnol. **43**: 135–144.

Strickland, J.D., and Parsons, T.R. 1972. A practical manual of seawater analysis. Bull. Fish. Res. Board Can. No. 167.

Vincent, W.F., and Roy, S. 1993. Solar ultraviolet radiation and aquatic primary production: damage, protection and recovery. Environ. Rev. **1**: 1–12.

Vodacek, A., Blough, N.V., DeGrandpre, M.D., Peltzer, E.T., and Nelson, R.K. 1997. Seasonal variation of CDOM and DOC in the Middle Atlantic Bight: terrestrial inputs and photooxidation. Limnol. Oceanogr. **42**: 674–686.

Wangersky, P.J. 1993. Dissolved organic carbon methods: a critical review. Mar. Chem. **41**: 61–74.

Wilkinson, L. 1992. Systat for Windows, version 5. Systat Inc., Evanston, Ill.

Williamson, C.E., Stemberger, R.S., Morris, D.P., Frost, T.M., and Paulsen, S.G. 1996. Ultraviolet radiation in North American lakes: attenuation estimates from DOC measurements and implications for plankton communities. Limnol. Oceanogr. **41**: 1024–1034.

Yan, N.D., Keller, W., Scully, N.M., Lean, D.R.S., and Dillon, P.J. 1996. Increased UV-B penetration in a lake owing to drought-induced acidification. Nature (Lond.), **381**: 141–143.

© 1999 NRC Canada

Influence of turbidity on piscivory in largemouth bass (*Micropterus salmoides*)

Scott M. Reid, Michael G. Fox, and Thomas H. Whillans

Abstract: In situ and laboratory feeding trials coupled with stomach content analysis of largemouth bass (*Micropterus salmoides*) were performed to examine how turbidity influences the size selectivity and capture rates of prey. No significant differences in the capture success of adult largemouth bass preying on northern redbelly dace (*Phoxinus eos*) were observed during in situ feeding trials in two Lake Ontario coastal wetlands differing in turbidity level (2.3 and 20 nephlometric turbity units (NTU)). During 1-h laboratory feeding trials, the overall number of fathead minnows (*Pimephales promelas*) captured was not significantly different among 1-, 18-, and 37-NTU treatments. However, at 70 NTU, the number of fathead minnows captured was significantly lower than that at the lowest turbidity treatment. Selection by juvenile largemouth bass of the smallest size-class of fathead minnow decreased as turbidity increased. No significant differences in piscivory were apparent between juvenile largemouth bass collected from turbid and clear habitats. Stomach content comparisons of juvenile largemouth bass seined from six clear and turbid habitats suggest that piscivory is primarily regulated by the availability of vulnerable size-classes of prey fish, as opposed to water clarity.

Résumé : On a réalisé in situ et en laboratoire des essais d'alimentation, accompagnés d'analyses du contenu stomacal, sur l'achigan à grande bouche (*Micropterus salmoides*) pour examiner comment la turbidité influe sur la taille et les taux de capture des proies. On n'a observé aucune différence significative dans les taux de capture réalisés par des achigans à grande bouche adultes se nourrissant de ventres rouges du nord (*Phoxinus eos*) durant des essais d'alimentation in situ dans deux milieux humides des rives du lac Ontario dont les turbidités différaient (2,3 et 20 unités mephlometric de turbidité (NTU)). Dans les essais d'alimentation en laboratoire d'une durée de 1 h, le nombre total de têtes-de-boules (*Pimephales promelas*) capturés n'était pas significativement différent selon la turbidité (1,18 et 37 NTU). Cependant, à 70 NTU, le nombre de têtes-de-boules capturés était significativement inférieur à celui observé à la plus faible turbidité. Avec l'accroissement de la turbidité, les achigans à grande bouche juvéniles capturaient moins les plus petites têtes-de-boules. On n'a observé aucune différence significative dans les habitudes piscivores des achigans à grande bouche juvéniles provenant d'eaux turbides et d'eaux claires. Les comparaisons des contenus stomacaux d'achigans à grande bouche juvéniles capturés à la senne dans six habitats clairs et turbides laissent penser que les habitudes piscivores sont principalement régulées par la disponibilité des proies vulnérables en vertu de leur taille, et non pas par la clarté de l'eau.

[Traduit par la Rédaction]

Introduction

The influence of turbidity on planktivory has been explored both experimentally (Miner and Stein 1993) and theoretically (Aksnes and Giske 1993). However, comparatively few experimental studies have focused on the effect of turbidity on piscivory (Gregory and Levings 1996). Understanding the influence of turbid conditions is important, given the value of naturally turbid systems (e.g., Fraser River Estuary), widespread sediment pollution impacting waterbodies in North America, and current efforts to rehabilitate systems degraded by turbidity.

The ability of visually feeding fish species to forage is generally accepted to be impaired by turbidity (Bruton 1985; Hecht and van der Lingen 1992). However, in the case of piscivorous fish, the negative effect of turbidity on the ability to detect prey may be offset by compensatory changes in prey searching behaviour (Vollestad et al. 1986; Miner and Stein 1996), the reduced ability of prey fish to detect predators in turbid water (Gregory 1993), and the potential for learning (Ware 1971) and developmental and evolutionary responses (Rahmann et al. 1978; Gregory 1994) in piscivores to offset the negative effects of turbid conditions.

The vulnerability of individual prey to capture, once encountered, may increase under turbid conditions as the ability to detect and escape predators decreases. Miner and Stein (1996) observed an exponential decline in the distance at which bluegill (*Lepomis macrochirus*) were able to detect a potential predator as turbidity increased. Turbidity may also diminish the advantage of schooling behaviour in predator avoidance. Fish school cohesiveness and coordination have been shown to weaken under poor light conditions

Received May 14, 1998. Accepted February 16, 1999.
J14589

S.M. Reid. Golder Associates Ltd., 940 6th Ave. SW, Calgary, AB T2P 3T1, Canada.
M.G. Fox.[1] Environmental and Resource Studies Program and Department of Biology, Trent University, Peterborough, ON K9J 7B8, Canada.
T.H.Whillans. Environmental and Resource Studies Program, Trent University, Peterborough, ON K9J 7B8, Canada.

[1]Author to whom all correspondence should be addressed.
e-mail: mfox@trentu.ca

© 1999 NRC Canada

(Vandenbyllaardt et al. 1991). Startle responses have also been shown to weaken with increased turbidity (Gregory 1993).

The vulnerability of prey fish to capture has been demonstrated to relate to their size difference relative to that of predators (Hambright 1991; Johnson and Post 1996). However, the pattern of size selection normally exhibited by piscivores on their piscine prey may be altered by turbidity. Crowl (1989) found that the reactive distance of largemouth bass (*Micropterus salmoides*) to crayfish prey was size dependent in clear water but independent of size in turbid water. Since the distance at which prey are detected is an important component of predation success, the loss of size selectivity in prey detection in turbid water could ultimately alter the size, and energy value, of prey consumed.

Differences in the effect of turbidity on predator populations based on the turbidity of the water that they inhabit could occur as a result of experience, developmental responses to turbid conditions early in life, or evolutionary adaptation to turbid environments. Previous experience in turbid conditions can increase the threshold turbidity level required to elicit behavioural changes (Bisson and Bilby 1982). Alternatively, a poor light environment can impair the development of visual structures, as shown by the study of Rahmann et al. (1978) on rainbow trout (*Oncorhynchus mykiss*). On an evolutionary level, two closely related minnow species (*Pseudobarbus afer* and *Psedobarbus asper*) that inhabit waters differing in turbidity contain significantly different neural structures, with the clear stream congenor (*P. afer*) possessing larger neural structures related to vision. No compensatory development in other neural structures has been found in *P. asper* (Cambray 1994).

In this study, we examined the effect of turbidity on prey consumption and prey size selectivity in piscivorous largemouth bass with a combination of in situ and laboratory feeding trials and field data. We tested the following hypotheses on the effects of turbidity on piscivorous feeding: (*i*) turbid water conditions negatively affect the ability of largemouth bass to capture piscine prey, (*ii*) the body size of piscine prey captured by largemouth bass will differ in clear and turbid water, and (*iii*) the effect of turbidity on the quantity of piscine prey consumed and on prey selectivity will be of lesser magnitude in largemouth bass from turbid waterbodies than in those from clear waterbodies.

Methods

In situ feeding trials

In situ feeding trials were conducted along the north shore of Lake Ontario in two coastal wetlands with contrasting turbidities to test whether turbidity negatively affects the capture rates of adult largemouth bass preying on a schooling prey species, northern redbelly dace (*Phoxinus eos*). The clear site, Wesleyville Marsh (43°57′N, 77°22′W), is a 3-ha wetland bordered by emergent vegetation and with moderate amounts of submersed vegetation throughout the open-water zone. The turbid site, Oshawa Second Marsh (43°52′N, 78°49′W), is a 123-ha shallow wetland bordered by emergent vegetation. Oshawa Second Marsh is virtually devoid of submersed vegetation. The high turbidity level in this marsh (mean = 17.8 nephlometric turbity units (NTU) in June 1993) has been attributed to the resuspension of bottom sediments by wind-generated wave action and carp (*Cyprinus carpio*), suspended sediment from two creeks that drain surrounding agricultural urban land, and high algal standing biomass (Symington-Sager 1995).

Predators and prey used in the in situ feeding trials were collected from low-turbidity waterbodies near Trent University (Peterborough, Ont.). Largemouth bass were collected with overnight sets of 1.2-m trap nets from East Twin Lake (44°27′N, 77°54′W) in July and August, 1995. Northern redbelly dace were collected from a small, clear wetland adjacent to Coon Lake (44°32′N, 78°12′W) with minnow traps and a 15-m bag seine (6-mm mesh size). All fish were transported back to Trent University and held in 1425-L round fibreglass holding tanks. Before the feeding trials, individual largemouth bass were fed northern redbelly dace for a minimum of 1 week.

Forty-eight-hour feeding trials were conducted during August 8–17, 1995, at Wesleyville Marsh and during August 24–30, 1995, at Oshawa Second Marsh within enclosures composed of a 2.5 × 5 × 1 m bag of knotless netting (3.2-mm ace-style mesh), open at the top, and suspended from enclosure walls. Detailed descriptions of materials and the construction of enclosure walls can be found in Symington-Sager (1995). Enclosure bags extended at least 0.3 m above the water surface to prevent fish from escaping, and lengths of rope were strung across the top at 0.5-m intervals to deter avian predation. Mean water depths during the trials were 66.3 and 63.7 cm for Wesleyville Marsh and Oshawa Second Marsh, respectively. No vegetation was present within the enclosures.

Nine 48-h trials were conducted in each marsh, with each trial consisting of an enclosure holding one adult largemouth bass and 40 northern redbelly dace prey. Northern redbelly dace were added to the enclosures 24 h before the onset of the trials. Largemouth bass were later added at the beginning of the trial after being held for 24 h in a separate enclosure. The nine largemouth bass used in these experiments ranged in size from 192 to 245 mm forklength (FL). Individual largemouth bass grew no more than 2 mm in length during the time between the Wesleyville Marsh and Oshawa Second Marsh trials. The mean lengths of northern redbelly dace used in Wesleyville Marsh and Oshawa Second Marsh trials were 49.1 and 47.5 mm FL, respectively. Temperature and turbidity measurements were taken daily between 11:00 and 12:30. Turbidity (NTU) was measured from water samples taken from the midwater column using an HF Scientific DRT-15B turbidity meter. At the end of each Wesleyville Marsh trial, individual largemouth bass were removed from their enclosure, transported back to their holding tanks at Trent University, and maintained on a diet of northern redbelly dace until they were used again at Oshawa Second Marsh. Northern redbelly dace remaining at the end of trials in both marshes were sacrificed, counted, and measured (forklength).

As individual bass were used once in both marshes, the number of northern redbelly dace consumed was compared using a paired *t* test (Zar 1984). In order to identify whether temperature differences between the two marshes could influence hunger and therefore capture rates, the mean water temperatures taken at each site were compared using the Mann–Whitney *U* test (Zar 1984).

Laboratory feeding trials

Laboratory feeding trials were conducted to examine the effects of turbidity on prey consumption rate and prey size selection and to determine whether these effects differed in largemouth bass populations subjected to different turbidity levels in their native waterbodies. Juvenile largemouth bass (83–130 mm FL) were collected along the shorelines of Cootes Paradise (43°16′N, 79°54′W) (September 6–8, 1995) and Rice Lake (44°12′N,79°53′W) (September 10, 1995) with a 15-m bag seine (6-mm mesh). The turbid collection site, Cootes Paradise, is a 250-ha marsh located at the west end of Hamilton Harbour. It is predominantly open water with isolated patches of emergent vegetation along the shoreline. Poor underwater light conditions have been related to high suspended sediment concentrations and, to a lesser degree, phytoplankton

© 1999 NRC Canada

(Symington-Sager 1995). Largemouth bass were also seined from the north shore of Rice Lake at Serpent Mounds Provincial Park. Rice Lake is characterized by a high submerged macrophyte biomass and clear underwater light conditions. Fathead minnows (*Pimephales promelas*) were collected from a clear, shallow pond within the Trent University campus with minnow and plexiglass traps. No piscivorous fish species occur within the pond, so the fathead minnows were considered naive to this predator type. Fathead minnows were used as a prey species because turbidity has been observed to weaken their ability to school and therefore avoid predation (Vandenbyllaardt et al. 1991).

Captured largemouth bass and fathead minnows were held indoors in 1425-L round fibreglass tanks at Trent University. Largemouth bass were fed fathead minnows every 2 or 3 days for 2 weeks before feeding trials commenced. Largemouth bass from both sites took to feeding on fathead minnows upon first presentation. Largemouth bass were starved for 24 h prior to their use in a feeding trial.

Eight feeding trials were conducted at each of four turbidity levels (1, 18, 37, and 70 NTU). The lower three turbidity levels used in these trials are representative of the range of non-storm levels found to occur in previously studied Lake Ontario wetlands (Symington-Sager 1995), whereas the highest turbidity treatment was selected to represent the extreme highs that might occur during storms or freshets. These turbidities were generated by mixing a predetermined mass of bentonite clay (0, 100, 165, and 375 g, respectively) in the tanks until the suspension appeared homogeneous. The suspension was allowed to settle for 1 h before adding the fish. Pretrial measurements demonstrated that turbidity levels remained constant for 2–3 h after the initial 1-h settling period.

The 1-h feeding trials were conducted in indoor 1425-L round fibreglass tanks during the period from September 23 to October 6. Light intensities from overhead fluorescent lighting, measured at the water surface with a General Electric type 214 light meter, ranged from 430 to 538 lx. In each trial, a pair of juvenile largemouth bass from the same population were presented with 24 fathead minnows, six from each of four size-classes (26–30, 31–35, 36–40, and 41–45 mm FL). Before feeding trials, largemouth bass were acclimated in the tanks for 1 h. Fathead minnows were concurrently acclimated to the same turbidity in a 10-L bucket and were then added to the tanks. After 1 h, largemouth bass were dipnetted from the tanks, and fathead minnows were collected, measured, and counted after the tanks were partly drained.

As there were multiple dependent variables during each feeding trial (four prey size-classes), a two-way MANOVA was used to test for turbidity and population effects on the number of fathead minnows consumed per trial (Tabachnick and Fidell 1996). One-way MANOVA's with the appropriate Bonferonni adjustment were used for pairwise comparisons to identify significant differences among turbidity treatments.

Comparison of piscivory in clear and turbid habitats

Stomach contents and piscine prey availability of juvenile largemouth bass were examined from three clear and three turbid sites to assess the influence of turbidity on piscivory under natural conditions. Five of the six sites are situated along the north shore of Lake Ontario. The sixth site was located on Rice Lake, about 20 km north of Lake Ontario. The three turbid sites are degraded coastal wetlands characterized by a lack of submersed aquatic vegetation and high levels of suspended sediment.

Juvenile largemouth bass (<132 mm FL) and fish of other species small enough to be potential prey of these largemouth bass were collected with a 15-m bag seine (6-mm mesh) during September 6–18, 1996. Captured largemouth bass were sacrificed in an ice-water slurry and frozen until stomach contents were examined. Potential prey species captured during seining were enumerated, identified to species, and measured for forklength.

The level of turbidity and the biomass of submersed aquatic macrophytes were measured at each site on the same day that the fish were collected. Water samples taken from the middle of the water column were used to assess turbidity. Submersed aquatic macrophyte biomass was estimated by harvesting all plant material from within ten 0.25-m^2 quadrats laid along a randomly selected 10-m transect at a water depth of 1 m parallel to the shoreline. Collected plant material was bagged and frozen. Mass was measured after plant material was dried in a drying oven for 48 h at 80°C.

Stomach contents were removed from thawed largemouth bass and stored in 70% ethanol until identification. Invertebrate prey species were classified as either zooplankton or macroinvertebrates and enumerated. Fish found in the stomachs were identified to species (Auer 1982) where possible, and their length was estimated by direct measurement with a dissecting microscope using an ocular micrometer at 0.8 magnification. If the tail was damaged, length was estimated by comparing measurements of body width with measurements of individuals from the same species caught during seining at the sampling site.

In order to compare the frequency of piscivory among sites, the number of fish found in the stomach of each largemouth bass was compared using one-way ANOVA and Tukey HSD multiple comparisons (Wilkinson et al. 1992). The number of prey within individual stomachs was $\log_{10}(x + 1)$ transformed to meet ANOVA assumptions. Statistical differences in the length of juvenile largemouth bass among collection sites were also tested with one-way ANOVA and Tukey HSD multiple comparisons.

The availability of vulnerable prey size-classes at each site was assessed by calculating the mean percentage of fish caught in seine hauls vulnerable to capture by individual juvenile largemouth bass. This approach has been applied to explain patterns in piscivory in juvenile largemouth bass by Olson (1996). Most of the piscine prey found in largemouth bass stomachs and caught in seine hauls were sunfish (*Lepomis* spp.); those with fork lengths less than 40% of individual largemouth bass were assumed to be vulnerable to predation (Olson 1996). The significance of this relationship was examined using least-squares regression, after raw data were arcsine transformed to meet least-squares regression assumptions (Zar 1984).

Results

In situ feeding trials

The mean number of northern redbelly dace eaten per trial by largemouth bass in the in situ enclosures was 21.6 (±2.3 SE) and 20.6 (±3.1) in Wesleyville Marsh (mean NTU = 2.3) and Oshawa Second Marsh (mean NTU = 20), respectively. There was no significant difference between sites in the number of northern redbelly dace consumed ($t = 0.39$, df = 8, $P = 0.71$). The mean water temperature in Wesleyville Marsh (27.3°C) was 4° higher than that of Oshawa Second Marsh (23.3°C) during the trials, and this difference was statistically significant (Mann–Whitney U test, $P < 0.001$). At these temperatures, estimates of mean daily maximum consumption derived from the Hewitt and Johnson (1992) bioenergetics model and the individual masses of largemouth bass used in the feeding trials differed by less than 1%. This suggests that the difference between sites in water temperature had little effect on the number of northern redbelly dace consumed. Similarly, the small increase in body size between the times that these trials were conducted in Wesleyville Marsh and Oshawa Second Marsh (≤2 mm per individual largemouth bass) would have had a negligible effect on prey consumption differences between the two sites.

© 1999 NRC Canada

Fig. 1. Comparison of the mean number of fathead minnows eaten by Cootes Paradise (shaded bars) and Rice Lake (open bars) juvenile largemouth bass during 1-h feeding trials across four levels of turbidity. Vertical bars represent ±1 SE.

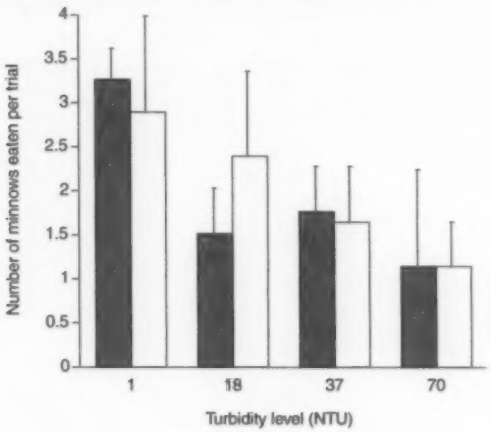

Table 1. Summary of MANOVA pairwise comparisons of turbidity level effect on the number of fathead minnows eaten from four prey size-classes during laboratory trials.

Turbidity (NTU) comparison	Wilk's lambda	Probability
1 vs. 18	0.669	0.024
1 vs. 37	0.753	0.094
1 vs. 70	0.575	0.004*
18 vs. 37	0.998	1.000
18 vs. 70	0.905	0.592
37 vs. 70	0.933	0.745

Note: A Bonferonni-adjusted type I error rate of 0.0083 was used to denote statistical significance (asterisk).

Laboratory feeding trials

The trend during 1-h feeding trials was a decrease in the mean number of fathead minnows captured by juvenile largemouth bass as turbidity increased (Fig. 1). Turbidity was the only significant treatment effect on the number of fathead minnows consumed (MANOVA, Wilk's lambda, $P < 0.05$). As turbidity increased from 1 to 70 NTU, the number of fathead minnows captured by Cootes Paradise and Rice Lake largemouth bass decreased by 35 and 39%, respectively. However, the number of fathead minnows captured from the four available size-classes was only significantly lower at 70 NTU (Table 1). The selection of different size-classes of fathead minnows by juvenile largemouth bass shifted as turbidity increased. At 1 NTU, the smallest size-classes of fathead minnows tended to be most vulnerable to capture by juvenile largemouth bass (Fig. 2). As turbidity increased, the capture rates of small fathead minnows decreased markedly, whereas there was little change in the rate of capture of large fathead minnows. At 37 and 70 NTU, there was little or no difference between the rates of capture of small and large fathead minnows.

Fig. 2. Comparison of the mean number of fathead minnows eaten of four size-classes across four turbidity levels by juvenile largemouth bass (Cootes Paradise and Rice Lake largemouth bass combined) during 1-h feeding trials. Vertical bars represent ±1 SE.

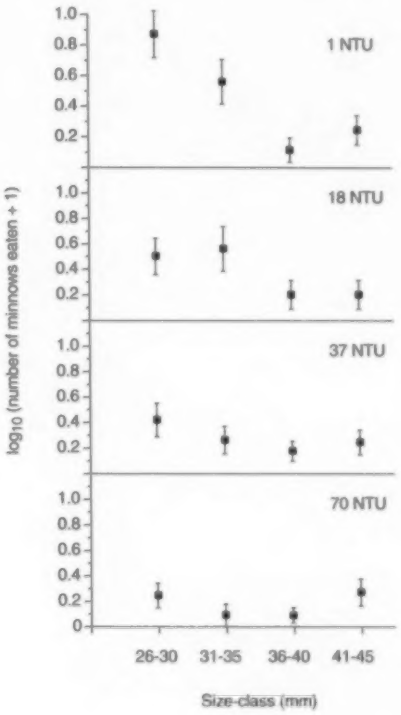

Piscivory in clear and turbid habitats

A total of 180 juvenile largemouth bass ranging in size from 43 to 132 mm FL were collected from the six comparison sites. Catches from seine hauls from four of the six sites were numerically dominated by sunfish (pumpkinseed (*Lepomis gibbosus*) and a lesser number of bluegill), with these species making up 42–93% of the total number of fish seined. Alewife (*Alosa pseudoharengus*) and several species of shiner (*Notemigonus* and *Notropis* spp.) comprised 76% of the catch in Rouge River marshes (a turbid site), and the blackchin shiner (*Notropis heterodon*) comprised 72% of the fish captured at Black River (a clear site).

There was a significant difference among sites in the mean number of fish found in juvenile largemouth bass stomachs ($F_{5,174} = 4.7$, $P = 0.005$). Post hoc comparisons among sites showed that significantly higher numbers of prey fish were found in the stomachs of juvenile largemouth bass collected from the Humber River marshes (a turbid site) than in those from either Black River (a clear site) or Frenchman's Bay (a turbid site) (Fig. 3) (Tukey HSD, $P < 0.001$ for both comparisons). Additionally, the highest percentage of largemouth bass containing fish in their stomachs were captured from Humber River marshes (61%) and the lowest percentages from Black River (5%) and Frenchman's Bay (4%) (Table 2). These differences in piscivory were more clearly related to the body size of juveniles in the

© 1999 NRC Canada

Fig. 3. Comparison of the mean number of fish found in the stomachs of juvenile largemouth bass collected from six comparison sites. Clear and turbid sites are differentiated by open and shaded bars, respectively. HR, Humber River marshes; HH, Hamilton Harbour; RL, Rice Lake; RR, Rouge River marshes; BR, Black River; FB, Frenchman's Bay. Vertical bars represent ±1 SE.

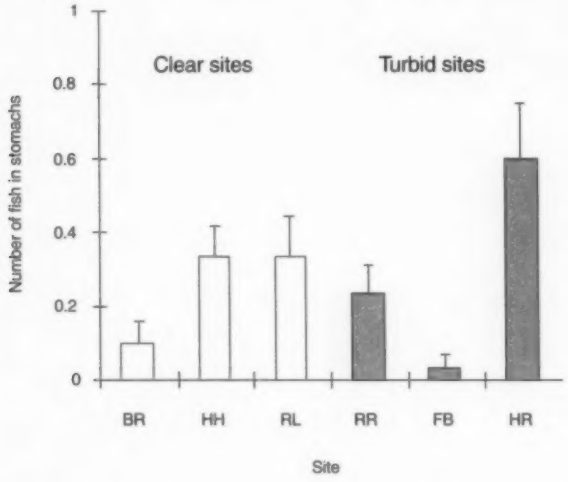

study sites than the turbidity of the water, in that sites that were significantly different in piscine prey consumption were also significantly different in mean body length (Tukey HSD, $P = 0.003$ and $P < 0.001$ for comparisons of Humber River marshes with Black River and Frenchman's Bay, respectively).

Most of the identifiable fish found in the stomachs of juveniles were sunfish except for Black River, where the three fish found in largemouth bass stomachs were all blackchin shiners. Measurable prey fish in the stomachs of all juveniles examined were less than 40% of the forklength of the largemouth bass. When 40% of the predator's forklength was used as a threshold for vulnerability to capture (Olson 1996), there was a significant linear relationship between the frequency of piscivory at each site and the percentage of sunfish vulnerable to capture (Fig. 4).

Discussion

Influence of turbidity on the quantity of piscine prey consumed by piscivores

The results of our study suggest that turbidities as high as 38 NTU do not decrease the ability of largemouth bass to capture piscine prey. The lack of a turbidity effect on piscine prey consumption under all but extreme (70 NTU) conditions was demonstrated in in situ enclosures with adult largemouth bass and in 1-h feeding trials with juvenile largemouth bass. The lack of an effect in lower turbidities was further evidenced by the absence of differences in piscivory between juvenile largemouth bass sampled in clear and turbid habitats. Although turbidity has been shown to decrease the ability of piscivores to visually identify prey (Foster 1979; Crowl 1989), previous studies on the effect of turbidity on the capture rates of piscivores have resulted in inconsistent findings. This inconsistency may be the result of three factors: changes in predator behaviour, changes in prey fish behaviour, and experimental design.

Laboratory feeding trials with juvenile largemouth bass, juvenile walleye (*Stizostedion vitreum*) (Vandenbyllaardt et al. 1991), and adult rainbow trout (Ginetz and Larkin 1976) have demonstrated a negative turbidity effect on piscivory. Conversely, neither Mauck and Coble (1971) nor Gregory and Levings (1996) were able to identify any turbidity effect on the number of prey fish captured by adult northern pike (*Esox lucius*) and cutthroat trout (*Oncorhynchus clarki*). Field studies have also not observed consistent turbidity effects. Foster (1979) reported a reduction in the number of fish and a greater frequency of macroinvertebrates within the stomachs of largemouth bass and grass pickerel (*Esox americanus vermiculatus*) under turbid conditions. Lower consumption of prey fish by northern pike in turbid lakes has also been noted in Canadian and Norwegian Lakes (Vollestad et al. 1986; Craig and Babulak 1989). However, neither our study nor the study of Bolton (1985) was able to demonstrate a relationship between water clarity and piscivory in populations of juvenile largemouth bass.

Gregory and Levings (1996) suggested that reduced prey encounters in turbid water could be compensated for by prey fish exhibiting riskier behaviour such as increased feeding activity. Increased predator activity (Vollestad et al. 1986; Miner and Stein 1996) in turbid waters may also weaken the negative effect caused by reductions in predator search volumes. Also, prey vulnerability to capture once located by a predator is likely greater under turbid or low-light conditions (Howick and O'Brien 1983). Escape responses of juvenile fish to predators have been observed to be weaker in turbid waters (Gregory 1993). The cohesion and coordination of schools of fathead minnows were qualitatively observed during our study and by Vandebyllaardt et al. (1991) to weaken at high levels of turbidity. Individual schooling fish may therefore become more vulnerable to prey capture as turbidity increases.

Differences among study conclusions may simply result from the levels of turbidity, species, and life stages examined. Reductions in capture rates by juvenile largemouth bass (this study) and juvenile walleye (Vandenbyllaardt et al. 1991) preying on fathead minnows occurred only at relatively high turbidities (70 and 100 NTU, respectively). Turbidities assessed in field comparisons that identified turbidity effects (Foster 1979; Hecht and van der Lingen 1992) were two to three times higher than those at the turbid sites sampled in our study (>80 and 68–91 NTU, respectively). Comparisons in in situ feeding trials (our study) and in Gregory and Levings (1996) were all below 50 NTU.

Encounter rates during some studies or turbidity treatments may also not be sufficiently limiting to cause a reduction in capture rates due to small experimental container size or long trial lengths (Gregory and Levings 1996). Extending feeding trials from 1 to 4 h removed a negative turbidity effect on juvenile walleye capture rates at high turbidities (Vandenbyllaardt et al. 1991). It is possible that the duration of in situ feeding trials (48 h) with adult largemouth bass may have compensated for any reductions in foraging ability

© 1999 NRC Canada

Table 2. Turbidity levels, submersed macrophyte biomass, and numerical occurrence of general diet categories in the stomachs of juvenile largemouth bass seined from clear (c) and turbid (t) sites.

Site	Turbidity (NTU)	Submersed macrophyte biomass (g dry mass·m^{-3})	Zooplankton (%)	Macro-invertebrates (%)	Fish (%)	Other (%)	Number of empty stomachs
Black River (c)	1.7	58.0	14	79	5	2	5
Hamilton Harbour (c)	1.4	41.4	0.4	70	21	86	1
Rice Lake (c)	4.1	25.6	7	59	31	3	3
Rouge River marshes (t)	24.1	0	33	43	2	4	5
Frenchman's Bay (t)	28	0	27	58	4	11	7
Humber River marshes (t)	38.2	0	0	38	61	1	5

Fig. 4. Relationship between the percentage of piscivorous juvenile largemouth bass found at each of the comparison sites and the percentage of sunfish collected within size-classes vulnerable to capture. HR, Humber River marshes; HH, Hamilton Harbour; RL, Rice Lake; RR, Rouge River marshes; BR, Black River; FB, Frenchman's Bay. Vertical bars represent ±1 SE.

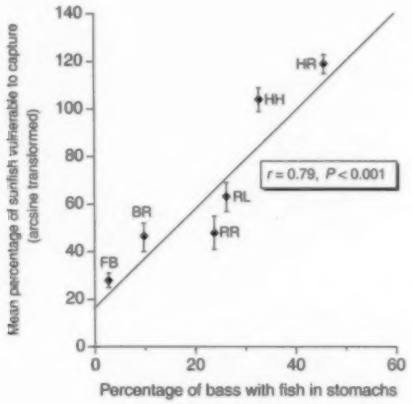

due to increased turbidity. However, the absence of a turbidity effect on juvenile largemouth bass was consistent at turbidity levels less than 70 NTU across different foraging time frames and experimental designs (1-h feeding trials and field collections).

A confounding effect in the field component of our study is the influence of macrophyte beds on piscivory at clear sites. Reduced prey capture ability of largemouth bass at high stem densities or submersed macrophyte biomass has been demonstrated experimentally, and it has also been observed in natural populations (Bettoli et al. 1992; Gregory and Levings 1996). Clear sites visited both in our study and at the Oklahoma reservoir studied by Bolton (1985) were characterized by a high biomass of submersed macrophytes. The absence of an observed turbidity effect could be interpreted as the result of both clear, densely vegetated habitats and turbid structureless ones representing difficult foraging habitats for juvenile largemouth bass.

Gregory and Levings (1996) found that a high artificial macrophyte density (1000 stems·m^{-2}) in clear conditions caused a stronger (and statistically significant) reduction on the mean predation rate by cutthroat trout on juvenile salmonids than turbidity (13–49 NTU).

Influence of turbidity on size-selective predation

Despite size dependence in the reactive distance to zooplankton as turbidity increases, the size selectivity of planktivorous fish is generally unaffected by turbid water conditions (Hecht and van der Langen 1992). The greater selection of smaller size-classes of fathead minnows by juvenile largemouth bass in our laboratory feeding trials diminished as turbidity increased, and no positive selection for smaller prey was evident at turbidities of 37 NTU and above (Fig. 2). Reductions in prey selectivity as turbidity increases have also been reported for adult largemouth bass and grass pickerel (Foster 1979) and skipjack (Hecht and van der Lingen 1992).

The loss of the influence of prey size and movement on reactive distance observed in largemouth bass under low-light and turbid conditions suggests a reduced ability to discriminate between different prey types (Howick and O'Brien 1983; Crowl 1989). Crowl (1989), who observed largemouth bass attacking stones under turbid conditions, argued that largemouth bass switch their foraging strategy to attacking any potential prey to compensate for reduced encounter opportunities. The reduction in size selectivity observed in this study likely reflects a reduction in the ability of largemouth bass to discriminate between prey types and a shift in foraging strategy to compensate for reduced prey encounter rates. It is interesting to note that a shift in size-selective prey capture was not observed during feeding trials with juvenile walleye (Vandenbyllaardt et al. 1991). These researchers hypothesized that the possession of a tapetum lucidum enhances the ability of walleye to discriminate the contrast of the prey image from the turbid background.

The influence of turbidity on perceived predation risk in juvenile chinook salmon (*Oncorhynchus tshawytscha*) (as suggested by changes in feeding rate) is size dependent (Gregory 1994). Howick and O'Brien (1983) also observed poor light conditions to impair the ability of all size-classes of bluegill except the smallest to detect predators. Turbidity may therefore change the vulnerability of different size-classes of prey unequally and therefore patterns of selection, or capture.

Population differences

While population differences have been identified for the preference of spawning habitat, water temperature, and depth for some species (Savino et al. 1993), few studies have tested for differences in feeding ability among wild fish populations ("stock effect"). Savino et al. (1993) failed to

© 1999 NRC Canada

identify any population ("strain") level differences in lake trout (*Salvelinus namaycush*) fry feeding on daphnids, despite differences in habitat preference. In contrast, Weis and Khan (1991) found mummichogs (*Fundulus heteroclitus*) from a pollution-stressed population to be inefficient predators on guppies (*Poecilia reticulata*) as compared with an unstressed control population. However, the latter study was unable to differentiate whether pollution stress or a lack of prior experience with live prey at the polluted site caused the poor foraging ability.

Differences in piscivory between populations of juvenile largemouth bass were dependent on the availability of vulnerable size-classes of sunfish. Examination of the stomach contents from field collections and of capture rates during laboratory feeding trials of juvenile largemouth bass from Rice Lake and Cootes Paradise suggests that individuals from both populations function equally as piscivores. It is not known if light conditions at the turbid comparison sites were sufficiently poor to impair the development of visual ability and (or) structures (Rahmann et al. 1978) or to motivate largemouth bass to learn alternative foraging strategies. Additionally, dense beds of macrophytes at the clear sites that provide visual cover for prey fish could also provide a similar learning environment for piscivores, one characterized by few short-range encounters with prey.

In summary, results from this and other studies indicate that there is no significant reduction in the frequency of piscivory at intermediate levels of turbidity (18–50 NTU), although changes in the size selectivity of prey capture did occur. Piscivory in juvenile largemouth bass populations at these turbidities is instead predicted by the availability of vulnerable size classes of prey fish. The mechanisms identified in this discussion to offset the substantial reductions in the search volumes of piscivores are still largely hypothetical. Unfortunately, the turbid conditions of interest severely limit the ability of researchers to document concurrent changes in the behaviour of piscivores and their piscine prey (especially under quasi-natural conditions). Alternative behavioural study designs that do not require visual observation need to be applied in order to answer these questions. In addition, future studies designed to separate the effects of turbidity from those of submersed vegetation on piscivory and that focus on prey-specific traits that affect their vulnerability under turbid conditions would increase our understanding of the effects of turbidity on piscivory in natural systems.

Acknowledgements

We would like to thank Sandra Dickman and Martha Allen for assisting with data collection in the field and Leon Carl, John Casselman, and two anonymous reviewers for comments on an earlier version of this manuscript. We would also like to thank Keith Somers for providing statistical advice on the study. This study was supported by a Tri-Council Grant through McMaster University. The manuscript is based on a thesis submitted by S.M. Reid in partial fulfillment of the requirements for the degree of Master of Science from Trent University.

References

Aksnes, D.L., and Giske, J. 1993. A theoretical model of aquatic visual feeding. Ecol. Model. **67**: 233–250.

Auer, N.A. 1982. Identification of larval fishes of the Great Lakes Basin with emphasis on the Lake Michigan drainage. Spec. Publ. 82-3. Great Lakes Fishery Commission, Ann Arbor, Mich.

Bettoli, P.W., Maceina, M.J., Noble, R.L., and Betsill, R.K. 1992. Piscivory in largemouth bass as function of aquatic vegetation abundance. Trans. Am. Fish. Soc. **12**: 509–516.

Bisson, P.A., and Bilby, R.E. 1982. Avoidance of suspended sediment by juvenile coho salmon. N. Am. J. Fish. Manage. **4**: 371–374.

Bolton, B.D. 1985. A comparison of stomach contents of largemouth bass and white crappie from turbid and clear portions of Thunderbird Reservoir, Oklahoma. M.Sc. thesis, University of Oklahoma, Norman, Okla.

Bruton, M.N. 1985. Effects of suspensoids on fish. Hydrobiologia, **125**: 221–241.

Cambray, J.A. 1994. Effects of turbidity on the neural structures of two closely related redfin minnows, *Pseudobarbus afer* and *P. asper*, in the Gamtoos River system, South Africa. S. Afr. J. Zool. **29**: 126–131.

Craig, J.F., and Babaluk, J.A. 1989. Relationship of condition of walleye (*Stizostedion vitreum*) and northern pike(*Esox lucius*) to water clarity, with special reference to Dauphin Lake, Manitoba. Can. J. Fish. Aquat. Sci. **46**: 1581–1586.

Crowl, T.A. 1989. Effects of crayfish size, orientation, and movement on the reactive distance of largemouth bass foraging in clear and turbid water. Hydrobiologia, **183**: 133–140.

Foster, J.R. 1979. Factors influencing the predator–prey relations of a small esocid, the grass pickerel (*Esox americanus vermiculatus*). Ph.D. thesis, University of Toronto, Toronto, Ont.

Ginetz, R.M., and Larkin, P.A. 1976. Factors affecting rainbow trout (*Salmo gairdneri*) predation on migrant fry of sockeye salmon (*Oncorhynchus nerka*). J. Fish. Res. Board Can. **33**: 19–24.

Gregory, R.S. 1993. The effect of turbidity on the predator avoidance behaviour of juvenile chinook salmon (*Oncorhynchus tshawytscha*). Can. J. Fish. Aquat. Sci. **50**: 241–246.

Gregory, R.S. 1994. The influence of ontogeny, perceived risk of predation and visual ability on the foraging behaviour of juvenile chinook salmon. *In* Theory and application in fish feeding ecology. *Edited by* D.J. Stouder, K.L. Fresh, and R.J. Feller. Belle W. Baruch Libr. Mar. Sci. No. 18. University of South Carolina Press, Columbia, S.C. pp. 271–284.

Gregory, R.S., and Levings, C.D. 1996. The effects of turbidity and vegetation on the risk of juvenile salmonids, *Oncoryhnchus* spp., to predation by adult cutthroat trout, *O. clarkii*. Environ. Biol. Fishes, **47**: 279–288.

Hambright, K.D. 1991. Experimental analysis of prey selection by largemouth bass: role of predator mouth width and prey body depth. Trans. Am. Fish. Soc. **120**: 500–508.

Hecht, T., and van der Lingen, C.D. 1992. Turbidity induced changes in the foraging strategies in estuaries. S. Afr. J. Zool. **27**: 95–107.

Hewitt, S.W., and Johnson, B.L. 1992. Fish bioenergetics model 2; an upgrade of a generalized bioenergetics model of fish growth for microcomputers. University of Wisconsin Sea Grant Institute WIS-SG-92-250, Madison, Wis.

Howick, G.L., and O'Brien, W.J. 1983. Piscivorous feeding behaviour of largemouth bass: an experimental approach. Trans. Am. Fish. Soc. **112**: 508–516.

© 1999 NRC Canada

Johnson, J.M., and Post, D.M. 1996. Morphological constraints on intracohort cannibalism in age-0 largemouth bass. Trans. Am. Fish. Soc. **125**: 809–812.

Mauck, W.L., and Coble, D.W. 1971. Vulnerability of some fishes to northern pike (*Esox lucius*) predation. J. Fish. Res. Board Can. **28**: 957–969.

Miner, J.G., and Stein, R.A. 1993. Interactive influence of turbidity and light on larval bluegill (*Lepomis macrochirus*) foraging. Can. J. Fish. Aquat. Sci. **50**: 781–788.

Miner, J.G., and Stein, R.A. 1996. Detection of predators and habitat choice by small bluegills: effects of turbidity and alternative prey. Trans. Am. Fish. Soc. **125**: 97–103.

Olson, M.H. 1996. Ontogenetic niche shifts in largemouth bass: variability and consequences for first year growth. Ecology, **77**: 179–190.

Rahmann, H., Jeserich, G., and Zeutzius, I. 1978. Ontogeny of visual acuity of rainbow trout under normal and light deprivation. Behaviour, **68**: 315–321.

Savino, J.F., Henry, M.G., and Kincaid, H.L. 1993. Factors affecting feeding behavior and survival of juvenile lake trout in Great Lakes. Trans. Am. Fish. Soc. **122**: 366–377.

Symington-Sager, E. 1995. Factors influencing the recovery of submersed vegetation in four Lake Ontario coastal marshes. M.Sc. thesis, Trent University, Peterborough, Ont.

Tabachnick, B.G., and Fidell, L.S. 1996. Using multivariate statistics. 3rd ed. Harper Collins College Publishers, New York.

Vandenbyllaardt, L., Ward, F.J., Braekevelt, C.R., and McIntyre, D.B. 1991. Relationships between turbidity, piscivory and development of the retina in juvenile walleyes. Trans. Am. Fish. Soc. **120**: 382–390.

Vollestad, L.A., Skurdal, J., and Qvenild, T. 1986. Habitat use, growth, and feeding of pike (*Esox lucius* L.) in four Norwegian lakes. Arch. Hydrobiol. **108**: 107–117.

Ware, D.M. 1971. Predation by rainbow trout (*Salmo gairdneri*): the effect of experience. J. Fish. Res. Board Can. **28**: 1847–1852.

Weis, J.S., and Khan, A.A. 1991. Reduction in prey capture ability and condition of mummichogs from a polluted habitat. Trans. Am. Fish. Soc. **120**: 127–129.

Wilkinson, L., Hill, M., and Varg, E. 1992. SYSTAT: statistics, version 5.2. SYSTAT, Inc., Evanston, Ill.

Zar, J.H. 1984. Biostatistical analysis. 2nd ed. Prentice-Hall, Englewood Cliffs, N.J.

© 1999 NRC Canada

Effect of temperature on the P4501A response in winter- and summer-acclimated Arctic char (*Salvelinus alpinus*) after oral benzo[*a*]pyrene exposure

Even H. Jørgensen and Johannes Wolkers

Abstract: In this study, the time-dependent P450 response to oral benzo[*a*]pyrene exposure at 1 and 10°C was investigated in winter- and summer-acclimated Arctic char (*Salvelinus alpinus*). In both seasons, a strong induction of CYP1A activities and protein levels (measured only in the winter experiment) were seen at both 1 and 10°C. At 1°C, the responses were delayed and more long-lasting than at 10°C. No within-season difference between 1 and 10°C in the magnitude of the induction response was found, but due to elevated baseline CYP1A activities, the induction response was seven times lower in winter- as compared with the response in summer-acclimated Arctic char. The results show that the CYP1A enzymes of the Arctic char respond to temperature changes in a compensatory way, and they are promising with respect to the applicability of the P450 enzyme system of the Arctic char as a biomarker for monitoring polycyclic aromatic hydrocarbon contamination in high-latitude environments. More studies are needed, however, to reveal seasonal differences in the biomarker response to pollutants.

Résumé : Dans cette étude, on a étudié chez des ombles chevaliers (*Salvelinus alpinus*) acclimatés à l'hiver et à l'été la réponse dans le temps du cytochrome P450 après exposition, par voie orale, des poissons au benzo[*a*]pyrène à 1 et à 10°C. Dans les deux saisons, on a observé une forte augmentation des activités des enzymes CYP1A et des niveaux de protéines (mesurés seulement dans l'expérience hivernale) tant à 1°C qu'à 10°C. À 1°C, les réponses étaient retardées, et s'étendaient sur une plus longue période qu'à 10°C. On n'a observé aucune différence intra-saisonnière entre 1 et 10°C dans le degré d'induction, mais en raison des activités de base élevées des enzymes CYP1A, l'induction a été sept fois plus faible chez les ombles chevaliers acclimatés à l'hiver que chez les ombles chevaliers acclimatés à l'été. Les résultats montrent que les enzymes CYP1A de l'omble chevalier répondent aux changements de température de façon compensatoire et offrent un potentiel intéressant en ce qui a trait à l'utilisation du cytochrome P450 de l'omble chevalier comme biomarqueur pour la surveillance de la contamination par les hydrocarbures aromatiques polycycliques sous les hautes latitudes. On devra cependant effectuer d'autres études pour établir les différences saisonnières dans la réponse du biomarqueur aux polluants.

[Traduit par la Rédaction]

Introduction

Aquatic pollution is an increasing problem worldwide, and even in remote arctic areas, high concentrations of several pollutants have been detected (e.g., Muir et al. 1992). The polycyclic aromatic hydrocarbons (PAHs) are of major concern because of their carcinogenic and mutagenic potential (Selkirk 1977). These pollutants originate primarily from combustion processes as well as exploitation and transport of oil and gas resources in the Arctic and elsewhere. Since the Arctic may contain some of the world's largest petroleum reserves, future exploitation and production activities may result in increasing levels of petroleum hydrocarbons in these areas. As environmental monitoring becomes increasingly important, attention has been directed towards the search for sensitive and reliable biomarkers that can be used to assess the exposure to, and effects of, xenobiotics (e.g., Bucheli and Fent 1995; Goksøyr 1995; Holdway et al. 1995).

The cytochrome P4501A (CYP1A) enzymes of fish are known to be highly inducible by a wide range of pollutants, including PAHs (Goksøyr and Förlin 1992). There is also strong evidence that the induction of CYP1A in fish is related to the levels of PAHs in the animal in a dose-dependent manner (Stegeman and Hahn 1994). This characteristic has resulted in considerable attention being paid to the potential of the CYP1A system as a biomarker of organic pollutants. Validation through field studies of this system as a biomarker of both chronic contamination and acute pollution has confirmed this potential (Bucheli and Fent 1995; Goksøyr 1995).

Previous investigations have shown that fish may respond with elevated hepatic P450-dependent activity to decreasing temperatures (temperature compensation) but also that at low temperatures, the activity may be reduced or absent

Received November 3, 1998. Accepted March 17, 1999. J14876

E.H. Jørgensen.[1] Norwegian Institute for Nature Research, N-9296, Polar Environmental Centre, Tromsø, Norway.
J. Wolkers. Akvaplan-NIVA AS, N-9296, Polar Environmental Centre, Tromsø, Norway.

[1]Author to whom all correspondence should be addressed. e-mail: even.jorgensen@ninatos.ninaniku.no

© 1999 NRC Canada

(Andersson and Förlin 1992; Stegeman and Hahn 1994). In some cases, a stronger influence of temperature than of the contaminant on the CYP1A system has been found (Sleiderink et al. 1995). Only limited effort has been made to develop and validate the P450 enzyme system as a biomarker of pollutant contamination in high-latitude aquatic environments. So far, induction at temperatures close to 0°C has been reported in only one high-latitude fish species, Arctic cod (*Boreogadus saida*) (George et al. 1995). Prerequisites for establishing the CYP1A system of ectotherms as a biomarker of environmental contamination in such environments are that (*i*) the very low temperatures typical of arctic environments do not abolish the responsiveness of the enzyme system in the particular species to be used and (*ii*) the influence of temperature on the biomarker response in that species has been carefully quantified.

The anadromous Arctic char (*Salvelinus alpinus*) is the northernmost distributed salmonid fish, and the species is common and widespread in arctic and subarctic regions of Europe, North America, and Asia (Johnson 1980). The adult fish reside in seawater for 40–50 days each summer, when most of the annual feed intake and growth occur (Mathisen and Berg 1968; Jørgensen et al. 1997). The seawater residence is restricted to local coastal waters (Finstad and Heggberget 1993), where pollutants from both remote and local sources may contribute to the pollutant load. Previous investigations have shown that the CYP1A enzymes of this species respond well to PAH exposure, even at a relatively low temperature (5°C) (Wolkers et al. 1996, 1998). Thus, the Arctic char is considered to be a possible indicator species for monitoring pollutant contamination and xenobiotic-associated stress in aquatic environments in the Arctic.

In the present study, we investigated the time-dependent CYP1A response in Arctic char after contamination with benzo[*a*]pyrene (BaP) at 1 and 10°C. In order to reveal the effects of seasonal temperature acclimation on the temperature response, two experiments were conducted: one during winter with winter-acclimated Arctic char and one during autumn with summer-acclimated Arctic char.

Methods

Fish and experimental design

Two experiments were conducted: one during winter (10 January – 2 February 1996) and one during autumn (21 October – 13 November 1997). Both experiments were performed with immature Spitsbergen, Norway, Arctic char. The fish used in the winter experiment were obtained as eyed eggs from wild anadromous Arctic char caught in Spitsbergen in 1992 and hatched in 1993. The fish used in the autumn experiment were 2- to 2.5-year-old offspring from first-generation, hatchery-reared anadromous Spitsbergen Arctic char. The experiments were carried out at Kårvik Research Station, Tromsø, Norway.

During the last 6 months before the start of the winter experiment, the fish were held at natural temperature and under simulated natural light conditions, which were about 1°C and 5 h light : 19 h dark, respectively, at the start of the experiment. In the autumn experiment, the fish were held at natural temperature and under simulated natural light conditions until August, after which they were maintained at a water temperature of 10°C and continuous light until the start of the experiment. In both experiments, the fish had been individually tagged (FTF-69, Floy Tag and Manufacturing, Seattle, Wash.) at the time of sorting, 6 months before the start of the experiment. All fish had been fed to satiety with commercial pelleted fish feed (Skretting, Norway) since the start of feeding.

At the start of each experiment, 1 week before BaP administration, the fish were sorted into four groups of 20 fish per group. These were transferred to four circular tanks with a water volume of 300 L. The average weight of the fish used in the winter experiment was 558 g and in the autumn experiment was 425 g. Two groups in each experiment were maintained at the water temperature at which they were acclimated, i.e., 1 and 10°C in the winter and autumn experiments, respectively. The temperatures in the other two tanks were gradually elevated within 1 week from 1 to 10°C in the winter experiment and lowered from 10 to 1°C in the autumn experiment. Simulated natural light and continuous light conditions prevailed throughout the experimental periods in the winter and autumn experiments, respectively.

The fish in one group from each temperature regime (exposed groups, 1 and 10°C) were given one oral dosage (60 mg·kg body weight^{-1}) of BaP (obtained from Sigma, St. Louis, Mo.) by force feeding a gelatine capsule containing fish oil with 35 mg BaP·mL^{-1}. The fish in the remaining groups (control groups, 1 and 10°C) received a gelatine capsule containing fish oil only. In order to ensure proper dissolving of the capsules in the fishes' stomach, the fish were starved during the last 3 days before BaP administration.

After 2, 6, 12, and 23 days following BaP administration, five fish from each group were killed by a blow to the head and weighed. Thereafter, the liver (gallbladder carefully excised) was removed, frozen in liquid nitrogen, and stored at –70°C until analysis about 4 months later.

Preparation of microsomes, and cytochrome P450 content and microsomal enzyme activity analyses

Preparation of microsomes and measurement of hepatic CYP1A catalytic activities (ethoxyresorufine-*O*-deethylation (EROD)) were carried out according to the methods described by Wolkers et al. (1996). Briefly, about 400 µg of microsomal protein was incubated in a 0.1 M Tris buffer at 20°C with ethoxyresorufin (5 µM) for 10 min in the presence of an NADPH-regenerating system (containing 5 mM glucose-6-phospate, 1 unit glucose-6-phospate dehydrogenase·mL^{-1}, and 0.5 mM NADPH). The EROD rates were determined fluorimetrically in 24-well plates in triplicate. Measurements were performed using a Cytofluor 2300 plate reader with excitation and emission wavelengths of 530 and 590 nm, respectively.

CYP1A protein levels were measured by enzyme-linked immunosorbent assay (ELISA), as described by Nilsen et al. (1998). Unfortunately, the microsomes for ELISA analyses from the autumn experiment were accidentally lost; therefore, only data on CYP1A enzyme activity from this experiment are presented.

Statistical analyses

A one-way ANOVA was used to test for possible differences in CYP1A enzyme activities (EROD) and CYP1A levels between contaminated and control fish and between time points within and between each group, in baseline EROD activities between temperatures and seasons, and in baseline CYP1A levels between temperatures. Linear regression analyses on $\log_{10}$-transformed data were used to test for possible relationships between individual EROD activities and CYP1A levels at each of the two temperatures in the winter experiment. All statistical analyses were performed with Statistica (StatSoft Inc., Tulsa, Okla.) A probability level of less than 0.05 was considered significant.

Results

The weight range of the fish used in the present study was relatively large (190–873 g), but there were no significant

© 1999 NRC Canada

Fig. 1. Hepatic EROD activities (mean ± SD, $n = 5$) at different times after oral administration of BaP in control (●) and exposed (○) summer-acclimated Arctic char (autumn experiment) at (*a*) 1°C and (*b*) 10°C and winter-acclimated Arctic char (winter experiment) at (*c*) 1°C and (*d*) 10°C. Statistical differences in the respective EROD activity values between control and exposed fish: $*p < 0.05$; $***p < 0.001$; ns, $p > 0.05$.

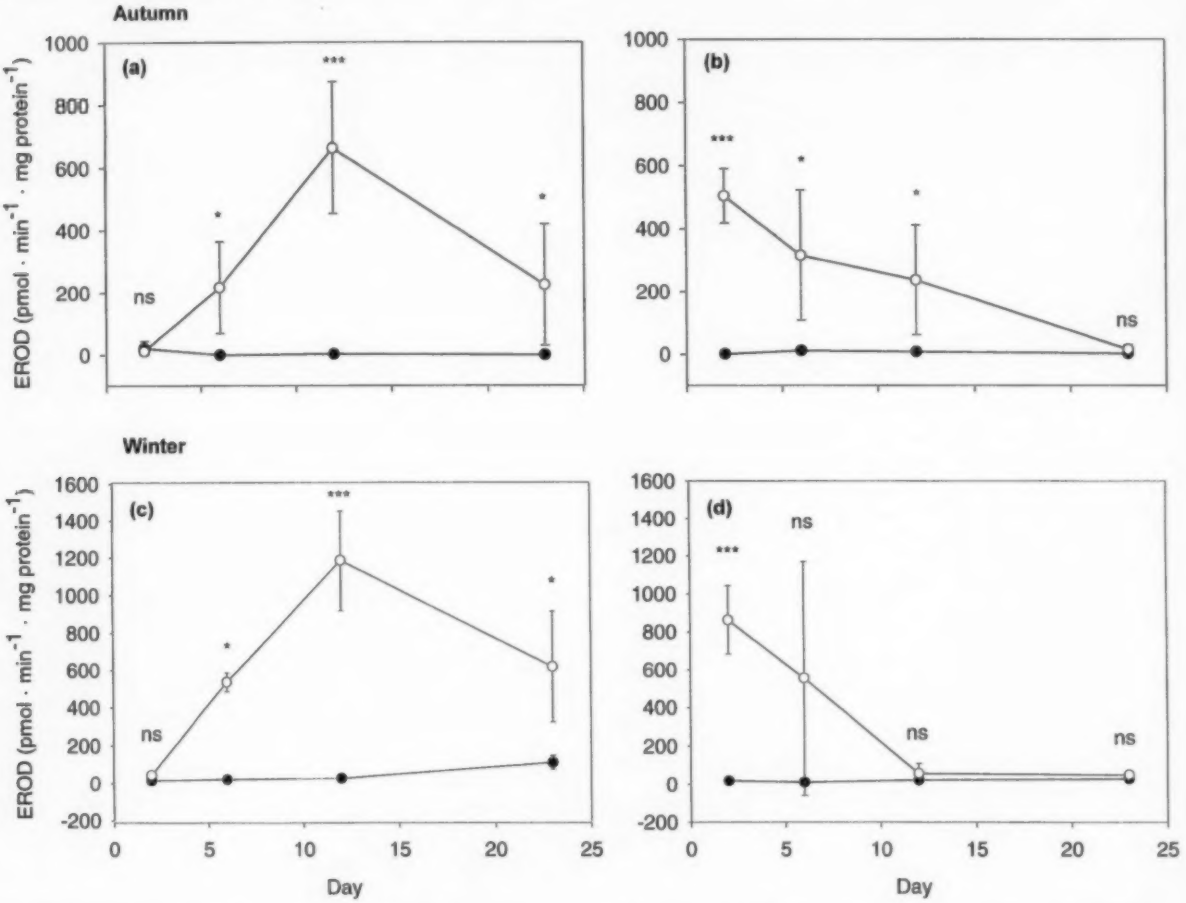

relationships between fish size and EROD activity or CYP1A level in any group ($p > 0.05$).

In the autumn experiment, the baseline EROD activities were low, and there were no significant differences in mean EROD activities between time points ($p > 0.05$) or temperatures ($p > 0.05$). At both temperatures, a strong and time-dependent induction of EROD activities after BaP exposure was observed. In the fish held at 1°C, maximum EROD induction was recorded at day 12 (Fig. 1*a*). In contrast, maximum EROD induction was already recorded 2 days after BaP exposure in the fish held at 10°C (Fig. 1*b*).

Also in the winter experiment, a significant and time-dependent EROD induction was recorded at both temperatures. The time of maximum EROD induction was the same as in the autumn experiment, i.e., at 12 and 2 days for the fish held at 1 (Fig. 1*c*) and 10°C (Fig. 1*d*), respectively. In both the winter and autumn experiments, the recorded maximum EROD activity of the BaP-exposed fish tended to be higher at 1°C (day 12) than at 10°C (day 2), but these differences were not statistically significant ($p > 0.05$)

The recorded maximum EROD activities of the exposed fish were significantly higher in the winter-acclimated than in the summer-acclimated Arctic char at both temperatures ($p < 0.01$). In contrast, the magnitude of the induction responses was higher in the summer- than in the winter-acclimated Arctic char. In the autumn experiment, maximum EROD activities were 202 and 369 times higher in the exposed than in the control fish held at 1 and 10°C, respectively, as compared with a maximum 42 times difference at both temperatures in the winter experiment. This difference was due to a significantly ($p < 0.001$) higher average baseline EROD activity in the winter experiment (mean values ± SD: 35.5 ± 38.2 ($n = 20$) and 20.5 ± 14.2 pmol·min^{-1}·mg protein^{-1} ($n = 20$) at 1 and 10°C, respectively) than in the autumn experiment (mean values ± SD: 6.0 ± 13.9 ($n = 20$) and 6.1 ± 6.7 pmol·min^{-1}·mg protein^{-1} ($n = 20$) at 1 and 10°C, respectively).

The CYP1A protein level also showed a strong and time-dependent induction after BaP exposure in the winter experiment at 1 and 10°C (Fig. 2). A maximum 5.2 times increase was observed at day 12 in the fish held at 1°C (Fig. 2*a*). In the fish held at 10°C, a maximum 2.2 times induction was

© 1999 NRC Canada

Fig. 2. Hepatic CYP1A protein levels (ELISA absorbance at 492 nm; mean ± SD, $n = 5$) in control (●) and exposed (○) winter-acclimated Arctic char at different times after oral administration of BaP at (*a*) 1°C and (*b*) 10°C. Statistical differences in the respective CYP1A levels between control and exposed fish: $^{*}p < 0.05$; $^{**}p < 0.01$; $^{***}p < 0.001$; ns, $p > 0.05$.

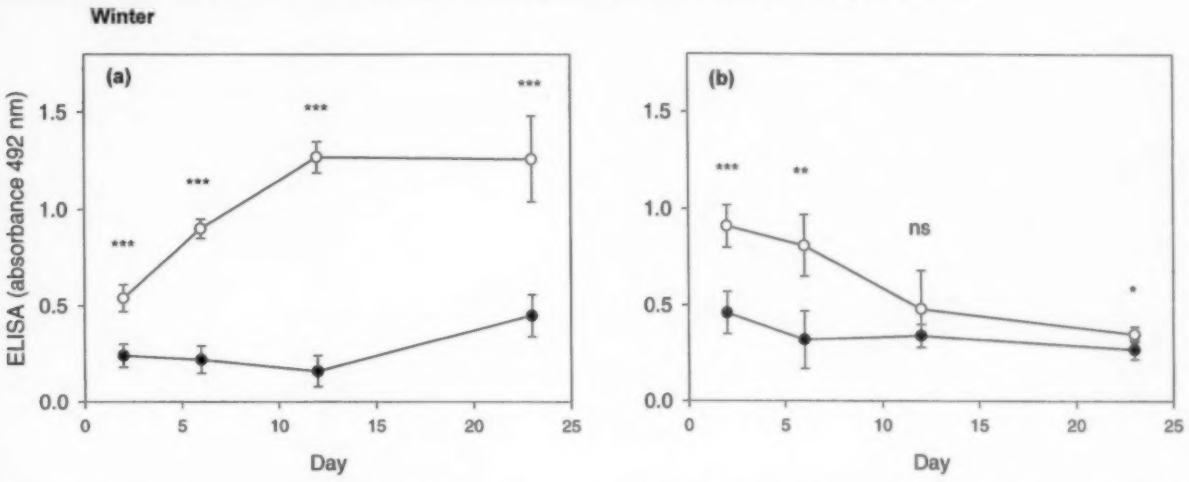

Fig. 3. Relationships between $\log_{10}$-transformed values for EROD activities and CYP1A protein levels (ELISA absorbance at 492 nm) for individual winter-acclimated Arctic char at 1°C (●) and 10°C (○). The relationships can be described by the following equations where y represents CYP1A protein levels and x represents EROD activity. For 1°C, $y = 0.35x - 0.99$, $r^2 = 0.86$, $p < 0.0001$; for 10°C, $y = 0.28x - 0.83$, $r^2 = 0.77$, $p < 0.0001$.

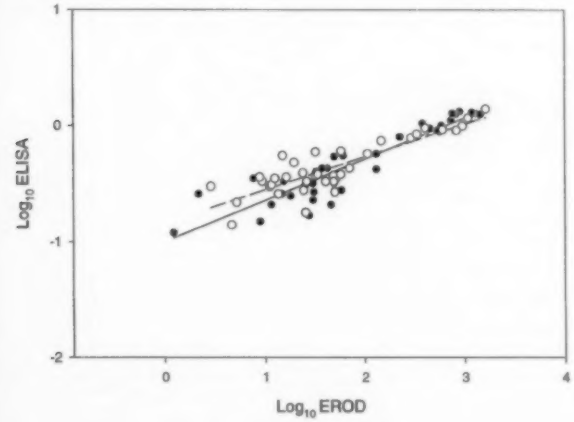

recorded at day 2 (Fig. 2*b*). There were no significant differences in the average baseline CYP1A level in the control fish between the two temperature treatments ($p > 0.05$).

The relationships between EROD activity and CYP1A protein level for individual fish at 1 and 10°C (control and exposed fish) are presented in Fig. 3. At both temperatures, a significant positive correlation was found between EROD activity and CYP1A level ($p < 0.0001$).

Discussion

The anadromous Arctic char is the northernmost distributed freshwater fish and is found as far north as 82°34′ N on the northern coast of Ellesmere Island (Johnson 1980). In the northernmost part of the distribution area, temperatures close to 0°C prevail during most of the year. Consequently, the Arctic char must be considered to be well adapted to the very low temperatures of the high Arctic. Within the arctic and subarctic distribution area of this species, temperatures may reach 10°C in midsummer; thus, the temperatures used in the present experiment are representative of the temperature range that the anadromous Arctic char experiences in the wild. In correspondence to the results obtained in previous experiments with Arctic char (Wolkers et al. 1996, 1998), a strong induction of the CYP1A enzyme activity was seen after oral exposure to BaP in the present experiment (Fig. 1).

Many enzymatic processes in ectothermic organisms show temperature compensation. This is a compensatory increase in enzymatic reaction rate functions with reduced environmental temperatures, resulting in a homeokinetic net output that is brought about by alterations in the concentration and (or) specific activity of specific enzymes (Prosser 1991). Accordingly, a compensatory increase in CYP1A levels and activities with acclimation to low temperatures has been demonstrated in a number of experiments with fish, with regard to both baseline CYP1A protein levels and activities (e.g., Kloepper-Sams and Stegeman 1992; Sleiderink et al. 1995; Lange et al. 1998) and the induction response following xenobiotic exposure (e.g., Kloepper-Sams and Stegeman 1992; Sleiderink et al. 1995; Grøsvik et al. 1997). In the high Arctic species used in the present experiment, maximum EROD activities following BaP exposure tended to be higher (but not significantly so) at 1°C than at 10°C, in both the winter- and summer-acclimated fish (Fig. 1). Although the exact maximum EROD activity of the BaP-exposed fish cannot be determined, since peak values could have occurred at times other than the sampling times that were used, there is no doubt that the present experiment has demonstrated temperature compensation in the monooxygenase system of the Arctic char. It is important in this respect to note that temperature compensation was seen even after the

© 1999 NRC Canada

very short-lasting acclimation to 1°C in the summer-acclimated Arctic char, which had been gradually transferred from 10 to 1°C within only 1 week. It is also worth noticing that the differences between 1 and 10°C in maximum EROD responses were quite similar in winter- and summer-acclimated Arctic char, indicating that neither the direction of the temperature change (from 10 to 1°C or from 1 to 10°C) nor season influenced the temperature-dependent patterns of rate functions.

On the other hand, both the average baseline EROD activities of control fish and the maximum EROD activity of BaP-exposed fish were higher in the winter than in the summer experiment at both 1 and 10°C (Fig. 1). This difference may be due to a seasonal temperature compensation associated with the long-term cold acclimation of the fish used in the winter experiment. It is known that temperature adaptation is associated with an alteration of the microsomal membrane fatty acid profile, which results in higher NADPH-cytochrome reductase activity, and hence an increased overall biotransformation rate (Blanck et al. 1989). Such alterations are probably more likely to be important after long-term cold acclimation (i.e., the winter acclimation in the present experiment).

However, other factors may also have contributed to the differences in baseline and maximum EROD activities between seasons in the present experiment. It is obvious from many studies that seasonal events such as sexual maturation and temporal variations in food intake and diet composition may strongly affect both baseline EROD activities and the magnitude of the induction response (e.g., Larsen et al. 1992; Viganò et al. 1993; Arukwe and Goksøyr 1997). In the present experiment, the significantly elevated baseline EROD activities found in winter-acclimated fish resulted in a lower magnitude of the induction response in these fish. Such seasonal differences will complicate the use of the P450 system as a biomarker of xenobiotic exposure. Due to the strong seasonality of arctic environments and the corresponding adaptive processes displayed by the animals living there, a variety of biological variables need to be investigated, and controlled, before xenobiotic-induced P450 responses can be implemented as a biomarker of xenobiotic exposure in the Arctic.

In accordance with the results in other experiments with fish (James and Bend 1980; Andersson and Koivusaari 1985; Jimenez et al. 1987), the induction response to BaP exposure in the present experiment was delayed and more long-lasting at 1°C than at 10°C in both the autumn and winter experiments (Fig. 1). The delayed and more long-lasting response at 1°C may be a result of both a slower absorption and elimination rate of BaP from the alimentary canal at this temperature (Varanasi et al. 1981) and a longer half-life of CYP1A mRNA in cold- than in warm-acclimated fish (Kloepper-Sams and Stegeman 1992). The strong and long-lasting response to acute BaP exposure at 1°C found in the present investigation must be considered advantageous for biomonitoring in the Arctic, since temperatures close to 0°C prevail for most of the year in high-latitude aquatic environments. On the other hand, the effect of temperature on the uptake and elimination rates of PAHs and the corresponding CYP1A responses to long-term contamination cannot be interpreted from the results obtained in the present study. Since long-term, low-level contamination is a more "normal" situation in high-latitude environments, investigations on the long-term responses to such contamination need to be done.

Catalytic assays (e.g., EROD activity) depend upon biologically active samples, of which sample preservation is a critical factor for quality assurance. The quantification of CYP1A protein level by ELISA methods does not depend upon biologically active samples and is consequently superior in situations in which catalytic activity may be inhibited or degraded (Goksøyr 1991). Thus, CYP1A level quantification by ELISA may be an alternative or, preferably, supplemental measurement to include in monitoring programs. In the present study, the CYP1A level measured by ELISA responded to the presence of BaP in a manner similar to the EROD activity: whereas the response to BaP was faster at 10°C than at 1°C, the magnitude of the induction seemed to be lower at 10°C than at 1°C (Fig. 2). The lower magnitude of the induction response seen at 10°C was mainly a result of a higher maximum CYP1A level in the fish exposed to BaP at 1°C, and temperature compensation was consequently also evident for the CYP1A protein level.

Previous field investigations have shown that catalytic assays (e.g., EROD activity) may be more sensitive than the immunochemical assay (ELISA) as an indicator of contaminant exposure (Collier et al. 1995), although a very good correlation between EROD activity and CYP1A level was found in all three species of flatfish sampled for analyses in that study. In the present study, statistically significant positive relationships between individual EROD activities and CYP1A levels were found at both 1 and 10°C (Fig. 3). The relationships were almost identical at the two temperatures, although the correlation was slightly better at 1°C than at 10°C. These results suggest that the induction response following BaP exposure was mainly due to increased CYP1A protein synthesis, whereas increased activity of existing CYP1A enzymes seems to represent only a minor contribution. Further, the results clearly confirm the applicability of the semiquantitative ELISA determination of CYP1A enzyme induction in the Arctic char as a biomarker in environmental monitoring.

In conclusion, the hepatic P450 system of the Arctic char responded strongly to the presence of BaP within the temperature range normally experienced by wild Arctic char. In general, there were greater differences in the magnitude of the induction response (EROD) between seasons than between temperatures, whereas temperature strongly affected the temporal aspects of the response. The results of the experiment are promising with respect to the applicability of the Arctic char for future monitoring of pollution in high-latitude aquatic environments.

Acknowledgements

The study was supported in part by funding from the Norwegian Research Council, project No. 113807/120. We thank Professor Anders Goksøyr and Kjersti Helgesen, University of Bergen, Norway, for carrying out the ELISA analyses.

© 1999 NRC Canada

References

Andersson, T., and Förlin, L. 1992. Regulation of the cytochrome P450 enzyme system in fish. Aquat. Toxicol. **24**: 1–20.

Andersson, T., and Koivusaari, U. 1985. Influence of environmental temperature on the induction of xenobiotic metabolism by β-naphthoflavone in rainbow trout, *Salmo gairdneri*. Toxicol. Appl. Pharmacol. **80**: 43–50.

Arukwe, A., and Goksøyr, A. 1997. Changes in three hepatic cytochrome P450 subfamilies during the reproductive cycle in turbot (*Scophthalmus maximus* L.). J. Exp. Zool. **277**: 313–325.

Blanck, J., Lindström-Seppä, P., Hänninen, O., Rein, H., and Ruckpaul, K. 1989. Temperature compensation of hepatic microsomal cytochrome P-450 activity in rainbow trout. I. Thermodynamic regulation during water cooling in winter. Comp. Biochem. Physiol. C. Comp. Pharmacol. **93**: 55–60.

Bucheli, T.D., and Fent, K. 1995. Induction of cytochrome P450 as a biomarker for environmental contamination in aquatic ecosystems. Crit. Rev. Environ. Sci. Technol. **25**: 201–268.

Collier, T.K., Anulaction, B.F., Stein, J.E., Goksøyr, A., and Varanasi, U. 1995. A field evaluation of cytochrome P450 1A as a biomarker of contaminant exposure in three species of flatfish. Environ. Toxicol. Chem. **14**: 143–152.

Finstad, B., and Heggberget, T.G. 1993. Migration, growth and survival of wild and hatchery-reared anadromous Arctic charr (*Salvelinus alpinus*) in Finnmark, northern Norway. J. Fish Biol. **43**: 303–312.

George, S.G., Christensen, J.S., Killie, B., and Wright, J. 1995. Dietary crude oil exposure during sexual maturation induces hepatic mixed function oxygenase (CYP1A) activity at very low environmental temperatures in polar cod *Boreogadus saida*. Mar. Ecol. Prog. Ser. **122**: 307–312.

Goksøyr, A. 1991. A semi-quantitative cytochrome P4501A1 ELISA: a simple method for studying the monooxygenase induction response in environmental monitoring and ecotoxicological testing of fish. Sci. Total Environ. **101**: 255–262.

Goksøyr, A. 1995. Use of cytochrome P450 1A (CYP1A) in fish as a biomarker of aquatic pollution. Arch. Toxicol. Suppl. **17**: 80–95.

Goksøyr, A., and Förlin, L. 1992. The cytochrome P-450 system in fish, aquatic toxicology and environmental monitoring. Aquat. Toxicol. **22**: 287–312.

Grøsvik, B.E., Larsen, H.E., and Goksøyr, A. 1997. Effects of piperonyl butoxide and β-naphtoflavone on cytochrome P4501A expression and activity in Atlantic salmon (*Salmo salar*). Environ. Toxicol. Chem. **16**: 415–423.

Holdway, D.A., Brennan, S.E., and Ahokas, J.T. 1995. Short review of selected fish biomarkers of xenobiotic exposure with an example using mixed-function oxidase. Aust. J. Ecol. **20**: 34–44.

James, M.O., and Bend, J.R. 1980. Polycyclic aromatic hydrocarbon induction of cytochrome P-450-dependent mixed-function oxidases in marine fish. Toxicol. Appl. Pharmacol. **54**: 117–133.

Jimenez, B.D., Cirmo, C.P., and McCarthy, J.F. 1987. Effects of feeding and temperature on uptake, elimination and metabolism of benzo(*a*)pyrene in the bluegill sunfish (*Lepomis macrochirus*). Aquat. Toxicol. **10**: 41–57.

Johnson, L. 1980. The Arctic charr, *Salvelinus alpinus*. *In* Charrs: salmonid fishes of the genus *Salvelinus*. *Edited by* E.K. Balon. Dr. W. Junk bv Publishers, The Hague, The Netherlands. pp. 15–98.

Jørgensen, E.H., Johansen, S.J.S., and Jobling, M. 1997. Seasonal patterns of growth, lipid deposition and lipid depletion in anadromous Arctic charr. J. Fish Biol. **51**: 312–326.

Kloepper-Sams, P.J., and Stegeman, J.J. 1992. Effects of temperature acclimation on the expression of hepatic cytochrome P4501A mRNA and protein in the fish *Fundulus heteroclitus*. Arch. Biochem. Biophys. **299**: 38–46.

Lange, U., Saborowski, R., Siebers, D., Buchholz, F., and Karbe, L. 1998. Temperature as a key factor determining the regional variability of the xenobiotic-inducible ethoxyresorufin-*O*-deethylase activity in the liver of the dab (*Limanda limanda*). Can. J. Fish. Aquat. Sci. **55**: 328–338.

Larsen, H.E., Celander, M., and Goksøyr, A. 1992. The cytochrome P450 system of Atlantic salmon (*Salmo salar*): II. Variations in hepatic catalytic activities and isozyme patterns during an annual reproductive cycle. Fish Physiol. Biochem. **10**: 291–301.

Mathisen, O.A., and Berg, M. 1968. Growth rates of the char *Salvelinus alpinus* (L.) in the Vardnes River, Troms, northern Norway. Inst. Freshwater Res. Drottningholm Rep. **48**: 177–186.

Muir, D.C.G., Wagemann, R., Hargrave, B.T., Thomas, D.J., Peakall, D.B., and Norstrom, R.J. 1992. Arctic marine ecosystem contamination. Sci. Total Environ. **122**: 75–134.

Nilsen, B., Berg, K., and Goksøyr, A. 1998. Induction of cytochrome P450 1A (CYP1A) in fish — a biomarker for environmental pollution. *In* Methods in molecular biology. Vol. 107. Cytochrome P450 protocols. *Edited by* I.R. Phillips and E.A. Shephard. Humana Press Inc., Totowa, N.J. pp. 423–438.

Prosser, C.L. 1991. Temperature. *In* Comparative animal physiology. *Edited by* C.L. Prosser. John Wiley & Sons, Inc., New York. pp. 109–165.

Selkirk, J.K. 1977. Benzo(*a*)pyrene carcinogenesis: a biochemical selection mechanism. J. Toxicol. Environ. Health, **2**: 1245–1258.

Sleiderink, H.M., Beyer, J., Scholtens, E., Goksøyr, A., Nieuwenhuize, J., Van Liere, J.M., Everaarts, J.M., and Boon, J.P. 1995. Influence of temperature and polyaromatic contaminants on CYP1A levels in North Sea dab (*Limanda limanda*). Aquat. Toxicol. **32**: 189–209.

Stegeman, J.J., and Hahn, M.E. 1994. Biochemistry and molecular biology of monooxygenases: current perspectives on forms, functions, and regulation of cytochrome P450 in aquatic species. *In* Aquatic toxicology: molecular, biochemical and cellular perspectives. *Edited by* G.K. Ostrander and D. Malins. Lewis Publishers, Boca Raton, Fla. pp. 87–206.

Varanasi, U., Gmur, D.J., and Reichert, W.L. 1981. Effect of environmental temperature on naphthalene metabolism by juvenile starry flounder. Arch. Environ. Contam. Toxicol. **10**: 203–214.

Viganò, L., Arillo, A., Bagnasco, M., Bennicelli, C., and Melodia, F. 1993. Xenobiotic metabolizing enzymes in uninduced and induced rainbow trout (*Oncorhynchus mykiss*): effects of diet and food deprivation. Comp. Biochem. Physiol. C. Comp. Pharmacol. **104**: 51–55.

Wolkers, J., Jørgensen, E.H., Nijmeijer, S.M., and Witkamp, R.F. 1996. Time-dependent induction of two distinct hepatic cytochrome P450 catalytic activities at low temperatures in Arctic charr (*Salvelinus alpinus*) after oral exposure to benzo(*a*)pyrene. Aquat. Toxicol. **35**: 127–138.

Wolkers, J., Jørgensen, E.H., Nijmeijer, S.M., and Witkamp, R.F. 1998. Dose and time dependency of cytochrome P4501A induction in liver and kidney of B(*a*)P exposed Arctic charr (*Salvelinus alpinus*). Mar. Environ. Res. **46**: 117–120.

© 1999 NRC Canada

Effect of life history strategy, environmental variability, and overexploitation on the genetic diversity of pelagic fish populations

Oscar E. Gaggiotti and Russell D. Vetter

Abstract: We study the effect of recruitment failures and variance in reproductive success on effective population size (N_e) in populations with type III survivorship curves. Special emphasis is put on determining the causes for the large differences in the genetic variability between populations of Pacific sardine (*Sardinops sagax*) and northern anchovy (*Engraulis mordax*). The results indicate that moderate differences in life history between ecologically related species can lead to substantial differences in N_e. The effect of fluctuations in vital rate parameters induced by environmental changes on N_e depends on the life history of each species. The ratio of N_e to census size is directly proportional to the total reproductive value of a population, but the sensitivity of this ratio to environmental fluctuations is inversely proportional to the generation overlap. The larger the generation overlap, the smaller the impact of environmental fluctuations on the level of genetic variability maintained by a population. The large difference in heterozygosity between Pacific sardine and northern anchovy populations is likely due to both life history differences between the two species and a recent arrival (founder event) of the Pacific sardine population to the California Current System.

Résumé : Nous étudions l'effet des failles dans le recrutement et de la variance du succès de la reproduction sur la taille pertinente de population (N_e) dans des populations dont les courbes de survie sont de type III. Nous mettons particulièrement l'accent sur la détermination des causes des importantes différences dans la variabilité génétique entre les populations de sardine du Pacifique (*Sardinops sagax*) et d'anchois du Pacifique (*Engraulis mordax*). Les résultats montrent que des différences modérées dans le cycle vital entre espèces écologiquement voisines peuvent entraîner des différences substantielles de N_e. L'effet des fluctuations des paramètres du taux démographique induites par les changements environnementaux sur N_e dépend du cycle vital de chaque espèce. Le ratio N_e/nombre d'individus recensés est directement proportionnel au potentiel reproducteur total d'une population, mais la sensibilité de ce ratio aux fluctuations environnementales est inversement proportionnelle au chevauchement entre générations. Plus ce dernier est important, moins est important l'impact des fluctuations environnementales sur le niveau de variabilité génétique maintenu par une population. La grande différence dans l'hétérozygosité entre les populations de sardines du Pacifique et d'anchois du Pacifique est probablement attribuable aux différences dans les cycles vitaux des deux espèces et à l'arrivée récente (effet du fondateur) de la population de sardines du Pacifique dans le système du courant de Californie.

[Traduit par la Rédaction]

Introduction

Genetic variation is a requisite for evolutionary adaptation to a changing environment and therefore influences the probability of long-term survival of a population (Lande and Barrowclough 1987). Finite population size results in inbreeding and loss of heterozygosity (i.e., genetic variability), and its genetic effects depend on the effective population size, N_e, rather than the actual size, N. The N_e is the size of an ideal population (i.e., with discrete generations, random mating, and constant population sizes) that would undergo the same amount of genetic drift (measured by the rate of loss of heterozygosity) as the actual population (e.g., Lande and Barrowclough 1987). The relationship between heterozygosity and N_e at equilibrium is given by

$$(1) \qquad H = \frac{4N_e\mu}{1 + 4N_e\mu}$$

where μ is the mutation rate and we assume selective neutrality (e.g., Lande and Barrowclough 1987).

Many demographic factors such as sex ratio, temporal variations in population density, mating systems, and life history schedule affect N_e. This has lead to a widespread use of N_e as a tool for studying the effect of the different demographic parameters on the level of genetic variability maintained by natural populations (for a review, see Frankham 1995). Although there are many analytical studies on N_e (see Caballero 1994 for a review), most models consider only one or two demographic factors at a time. The most illuminating analyses are those of Felsenstein (1971) and Hill

Received April 22, 1998. Accepted February 26, 1999.
J14555

O.E. Gaggiotti[1] and R.D. Vetter. Southwest Fisheries Science Center, National Marine Fisheries Service, P.O. Box 271, La Jolla, CA 92038-0271, U.S.A.

[1]Author to whom all correspondence should be addressed. Present address: Department of Zoology, University of Cambridge, Downing Street, Cambridge, CB2 3EJ, U.K. e-mail: oeg20@cam.ac.uk

© 1999 NRC Canada

(1979). Felsenstein's (1971) formulation was mainly concerned with haploid populations and clearly showed that N_e of an age-structured population is directly proportional to the total reproductive value of the population. Hill's (1979) analyses considered diploid populations and incorporated the effect of variance in reproductive success. However, illuminating as they are, these studies did not attempt to examine the effect of different life history strategies on N_e. As a consequence, the effect of life history schedule on N_e is poorly understood (see Lande and Barrowclough 1987). Recently, Nunney (1991, 1993, 1996) used Hill's (1979) model to investigate the effect of age structure and mating systems on N_e. His analysis, however, was restricted to species whose mortality schedule can be described by type I (little mortality until some age and then fairly steep mortality thereafter, e.g., most mammals) and type II survivorship curves (constant death rates with age, e.g., most birds) and ignored a large fraction of species that have type III survivorship curves (extremely steep juvenile mortality and relatively high survivorship afterward, e.g., fish, marine invertebrates, most insects).

An additional limitation of previous analyses of populations with overlapping generations is that they assumed constant population size. The dynamics of stage-structured populations in variable environments is determined, in a complicated way, by the life history schedule (e.g., see Tuljapurkar 1990), and it is not clear how the interaction between temporal environmental heterogeneity and life history schedule affects N_e. Other factors, such as variance in reproductive success, further complicate this interaction. The large number of populations, marine organisms in particular, that exhibit all these complicating factors highlights the need for more realistic models.

An important characteristic of species with age or stage structure is the so-called "storage effect" (e.g., Warner and Chesson 1985). The major element of this effect is that a strong recruitment produces a cohort of adults that survives over a number of potential reproductive periods. Thus, strong recruitments are essentially stored in the adult population and are capable of contributing to reproduction when favourable conditions return. Ellner and Hairston (1994) extended the storage effect concept to include genetic considerations. These authors showed that long-lived organisms can maintain genetic variability in heterogeneous environments due to the storage of genotypes in long-lived stages on which fluctuating selection does not act. In the present analysis, we show that it is also possible to extend this concept to consider the effect of genetic drift on the level of genetic variability.

The main objective of this study is to determine the causes for large differences in the genetic variability of two pelagic fish species that inhabit the California Current System (CCS), Pacific sardine (*Sardinops sagax*) and northern anchovy (*Engraulis mordax*) (see Hedgecock et al. 1989). In doing so, however, this study also sheds light on the effect of life history strategies, variance in reproductive success, and recruitment failures on N_e in species with type III survivorship curves. We address the effect of life history strategies and variance in reproductive success by considering a model with constant vital rates. The effect of recruitment failures is studied by introducing cyclic fluctuations in the survival of newborns. Finally, the effect of overexploitation is studied by incorporating fishing mortality into both constant and cyclic vital rate models.

Pelagic fish life histories and Leslie matrix parameters

Clupeoid populations are prone to striking increases, followed by precipitous and catastrophic declines (Blaxter and Hunter 1982). These fluctuations are caused by great natural variability in recruitment and by its interaction with fishing. The two species chosen for the present study share many similarities in life history traits and population size fluctuations but exhibit contrasting patterns of genetic variability (Hedgecock et al. 1989).

Pacific sardine and northern anchovy both spawn throughout the year, with a peak in spring (Butler 1987), and their spawning areas overlap extensively. The age-specific demographic parameters for these two species are presented in Table 1. The age of first reproduction for northern anchovy is 1 year, while that for Pacific sardine has changed from 2 years before the fishery collapse that occurred in the 1940's to 1 year of age at present (Butler et al. 1996). Mortality during the first year of life is extremely high in both species but is higher in Pacific sardine than in northern anchovy. This higher juvenile mortality is compensated by the lower adult mortality, longer life span (13 years for Pacific sardine versus 7 years for northern anchovy), and greater reproductive output of Pacific sardine (e.g., Butler et al. 1993). As in most clupeoids, the mortality pattern of the 0 age-class differs markedly form those of older age-classes. The mortality of the 0 age-class is density independent and largely determined by the availability of food. In older individuals, on the other hand, inadequate food supply translates into poor growth rates and low condition factors but does not increase mortality rate in a significant manner (Blaxter and Hunter 1982).

In both species, schooling behaviour becomes more important during the late juvenile stages (i.e., around 30 days for northern anchovy and between the first and second year for Pacific sardine), at which time the food requirements of juveniles are very similar to those of older fish (e.g., see Smith 1985). Thus, intraspecific competition involving both juveniles and adults is more likely and may lead to density-dependent regulation.

In terms of population density fluctuations, scale deposition rates in anaerobic sediments indicate that both populations have undergone similar wide cyclical fluctuations during the past 2000 years and that these fluctuations must be due to physical and biotic changes in the environment (e.g., Baumgartner et al. 1992).

An important difference between Pacific sardine and northern anchovy populations is with regard to the fisheries they support. Pacific sardine was subject to overfishing and suffered a series of population collapses during 1945–1960, while the northern anchovy fishery has been rather small.

Despite their similarities, the level of genetic variability observed in Pacific sardine is much lower than that of northern anchovy and most other clupeoids (Hedgecock et al. 1989). Of the 32 allozyme-coding loci examined by Hedgecock et al. (1989) in samples of Pacific sardine, only

© 1999 NRC Canada

Table 1. Age-specific demographic parameters of northern anchovy and Pacific sardine obtained from Butler et al. 1993 (tables 1–4).

	Northern anchovy		Pacific sardine	
Age (j)	Survival (s_j)	Fecundity (F_j)	Survival (s_j)	Fecundity (F_j)
0	3.12×10^{-5} [a]	0	2.06×10^{-6} [b]	0
1	0.40	22 000	0.47	0
2	0.46	93 000	0.67	146 000
3	0.46	194 000	0.67	388 000
4	0.46	279 000	0.67	599 000
5	0.46	327 000	0.67	849 000
6	0.46	327 000	0.67	1 167 000
7	0	327 000	0.67	1 487 000
8			0.67	1 617 000
9			0.67	1 887 000
10–12			0.67	2 156 000
13			0	2 156 000

Note: The elements of the first row of the Leslie matrix are given by $E_i = F_{i+1}s_i$, while the subdiagonal elements are given by s_j (see text). All demographic parameters are obtained from this matrix.

[a] After the carrying capacity level was achieved, this value was decreased to 7.156×10^{-6} so that $\lambda = 1$.

[b] After the carrying capacity level was achieved, this value was decreased to 1.157×10^{-6} so that $\lambda = 1$.

12% were polymorphic and the average proportion of heterozygous individuals per locus was 1.0%. These results contrast with an average of 40% polymorphic loci and 7.5% of heterozygous individuals per locus in the samples of northern anchovy analysed in the same study. Among the different possible explanations for these pronounced differences, Hedgecock et al. (1989) mentioned the collapse of the Pacific sardine fishery in the 1950's and 1960's, restrictions in population size (bottlenecks) in the more distant past, and the possibility that Pacific sardine might be a recent arrival to the CCS. They dismissed the effect of differences in life history schedule because they appeared to be rather small.

In what follows, we explore different population genetic models to determine the way in which life history strategy, temporal environmental variability, and overexploitation interact to determine the genetic variability of Pacific sardine and northern anchovy populations. This exploration will help us to explain the low level of genetic variability maintained by the Pacific sardine population.

Model

Demography

The demography is described by a Leslie matrix model in which survival of eggs to yearlings, $s_{0;t}$, fluctuates but all other age-specific rates are constant. This model was first introduced by Cohen et al. (1983) to present a Leslie matrix formulation that takes into account the fact that eggs spawned in year t are produced by the female population alive in year t. In mathematical terms, this can be expressed as follows:

$$(2a) \qquad n_{0;t} = \sum_{i=1}^{m} F_i n_{i;t}$$

where m is the maximum age considered and F_i is the average number of female eggs laid in year t per female fish aged i in that year. The postegg female population at time t consists of the survivors of the female population (including eggs) at time $t - 1$:

$$(2b) \qquad n_{i;t} = s_{i-1} n_{i-1;t-1} \qquad i = 1, 2, \ldots, m$$

where $s_i > 0$ is the fraction of female individuals (eggs or fish) aged i at $t - 1$ who survive in the population to age $i + 1$ at time t.

In conventional Leslie matrix models, this year's births (eggs) are usually attributed to last year's female population rather than to this year's, as in eq. 2*a*. To express $n_{0;t}$ in terms of the female population at time $t - 1$, we define $s_m = 0$, $F_{m+1} = 1$ (we could pick any finite value for F_{m+1}), and the effective fecundity of age-class i by $E_i = F_{i+1}s_i$. Then, upon substitution, into eq. 2*a* and since $s_m = 0$:

$$(3) \qquad n_{0;t} = \sum_{i=1}^{m} F_i s_{i-1} n_{i-1;t-1} + F_{m+1} s_m n_{m;t-1} = \sum_{j=0}^{m} E_j n_{j;t-1}.$$

Thus, changes over time in the age structure of the population can be described in the conventional way by $\mathbf{n}_t = \mathbf{L}_t \mathbf{n}_{t-1}$, where the first row of the modified Leslie matrix, $\mathbf{L}_t$, contains the effective fecundities E_i. This Leslie matrix notation should not be taken to imply that newborn individuals reproduce, since only those eggs that have reached age 1 in the following spring are able to do so (see eq. 2*a*).

The demographic parameters used in the Leslie matrix were derived from life tables and stage-specific life history parameters presented by Butler et al. (1993, tables 1–4) and are summarised in Table 1.

In the case of age-structured populations, we can define three useful demographic parameters, reproductive value, generation overlap, and mean generation time. The reproductive value of an individual of age i, v_i, is proportional to its expected average long-term contribution to the gene pool through offspring (i.e., eggs and larvae) born at or following its present age (Felsenstein 1971). Simply put, it is a measure of the expected number of offspring of an individual of a given age. The v_i's in a population at the stable age distribution are given by the left eigenvector of the Leslie matrix

© 1999 NRC Canada

corresponding to the dominant eigenvalue (e.g., Caswell 1989). This reproductive value corresponds to that defined by Fisher's (1930) original equation. We can also define the total reproductive value of a population, V, as the sum of the product of the age-specific reproductive value and the number of individuals in the corresponding age-class, N_i, $V = \Sigma_i V_i$, where $V_i = N_i v_i$ is the reproductive value of age-class i (see Felsenstein 1971).

The generation overlap, γ, is given by $\gamma = \mathbf{vPx/vx}$, where $\mathbf{v}$ is the dominant left eigenvector of the Leslie matrix whose elements give the age-specific reproductive value, $\mathbf{x}$ is the population structure (i.e., the vector whose elements x_i give the fraction of the total population in age-class i), and $\mathbf{P}$ is the survival matrix (i.e., a subdiagonal matrix with elements $p_{ij} = s_j$ for $i = j + 1$ and $p_{ij} = 0$ otherwise). In other words, the denominator is the total reproductive value of the population and the numerator is the total reproductive value of individuals that survive to the next year (see Ellner 1996). Thus, the generation overlap measures the proportion of total reproductive value that remains in the population from year to year and that is not due to newborn individuals.

The definition of mean generation time used for the constant vital rates case is the mean age of parents (e.g., see Caswell 1989) and is obtained as

$$L = \frac{\sum_i iE_i \prod_{j=1}^{i-1} s_j}{\sum_i E_i \prod_{j=1}^{i-1} s_j}$$

where E_i and s_i are the effective fecundity and survival of age-class i, respectively.

Genetics

The genetics are analysed using a haploid model appropriate for uniparentally inherited genetic markers such as mtDNA. Since the demographic model only considers the female part of the population, both models are congruent. Despite the haploid nature of this model, its results can be extrapolated to diploid markers because, under random mating and only one sex, the effective size of a haploid population with overlapping generations is exactly the same as that of the equivalent diploid population (see Felsenstein 1971).

The genetic model is based on the methodology presented by Orive (1993) who used a coalescent approach to obtain an expression for the inbreeding N_e in organisms with complex life histories. The model does not make any explicit assumption regarding the age structure of the population and is general enough to accommodate any age structure as defined by the corresponding Leslie matrix. The present analysis uses time-dependent versions of her eqs. 13–15 (see Appendix) and introduces variance in reproductive success.

Variance in reproductive success is modelled through "reproductive failures" of a fraction ρ of the population. The number of eggs at time t that were produced by individuals belonging to age-class i one time unit before is $E_i n_{i;t-1}$ (see above). Of these $n_{i;t-1}$, individuals, there is a fraction ρ that produces a small number of eggs, say Y_1, and a fraction $1-\rho$ that produces a large number of eggs, say Y_2, where $Y_1 << Y_2$. Thus, at any given time, age-class i can be divided into a less successful and a more successful group (groups 1 and 2, respectively). Reproductive success is independent of individual genotype and is solely determined by environmental conditions before and during reproduction. Assuming that the average effective fecundity of age-class i, E_i, remains constant, we write

$$(4) \qquad E_i = \rho Y_1 + (1-\rho)Y_2 \quad \text{and} \quad Y_2 = \frac{E_i - \rho Y_1}{1-\rho}.$$

To make this formulation more general, further assume that the number of eggs produced by each individual belonging to the less successful group is only a fraction f of the effective fecundity, i.e., $Y_1 = fE_k$, and thus, $Y_2 = E_k(1-\rho f)/(1-\rho)$.

Under the above assumptions, the variance in the number of offspring produced by individuals in age-class i is

$$(5) \qquad \mathrm{Var}(Y)_i = \frac{\rho E_i^2 (1-f)^2}{(1-\rho)}.$$

Note that $\mathrm{Var}(Y)_i$ is the variance in family size, which is 0 when $\rho = 0$. The fraction of fish that experience the reproductive failure increases as ρ increases. Since reproductive failure of the less successful group is greater as f approaches zero, f can be considered as a measure of how acute the reproductive failure is.

Constant vital rates

Methods

The present model is too complex to get closed-form solutions even for the simplest case of constant vital rates (see Orive 1993). Thus, the results are obtained by first iterating the Leslie matrix model in order to obtain the number of individuals in each age-class at each time interval and then inserting these values into eqs. A9 and A10 to obtain the mean coalescence time and N_e.

Note that the genetic model (see Appendix) requires that the number of individuals in any given age-class, $n_{i;t}$, never fall in the interval (0, 1) because that would lead to negative values in many parameters (see eqs. A4–A9). To avoid this problem, we used sampling whenever the number of individuals, $n_{i;t}$, in any given age-class was less than 10. The procedure used is as follows. (*i*) Given $n_{i;t}$ individuals in age-class i, generate $n_{i;t+1}$ at $t + 1$ by a binomial distribution with probability of success $s_{i;t}$ and $n_{i;t}$ trials and (*ii*) for every reproductive age-class, let E_i be the mean of a Poisson distribution, and if there are $n_{i;t}$ individuals who will reproduce, then get $n_{i;t}$ Poisson random variables (with mean E_i) and add them to get the number of offspring for age-class i.

The simulations were run for 1 000 000 iterations (years), which was enough to attain genetic steady state (the demographic steady state was achieved after 1000 iterations). For each parameter combination, we conducted 128 independent simulations (runs) starting with a single individual in the age-class with the largest reproductive value (8 years for Pacific sardine and 4 years for northern anchovy). The population was allowed to grow at a rate of 10% per year (i.e., $\lambda = 1.10$) until the number of individuals aged 1 year old or older, $N_{>0}$, reached a carrying capacity value of 50 000. Note that N_e increases linearly with $N_{>0}$, and therefore, increasing $N_{>0}$ does not change the results. After the carrying capacity level was achieved, the survival rate of the 0 age-class was adjusted so that the leading eigenvalue of the Leslie matrix

© 1999 NRC Canada

Fig. 1. Reproductive value of Pacific sardine and northern anchovy populations for the constant vital rates model. (*a*) Total reproductive value; (*b*) age-class and individual reproductive value for Pacific sardine; (*c*) age-class and individual reproductive value for northern anchovy. Note that v_0 is very small but still different from zero.

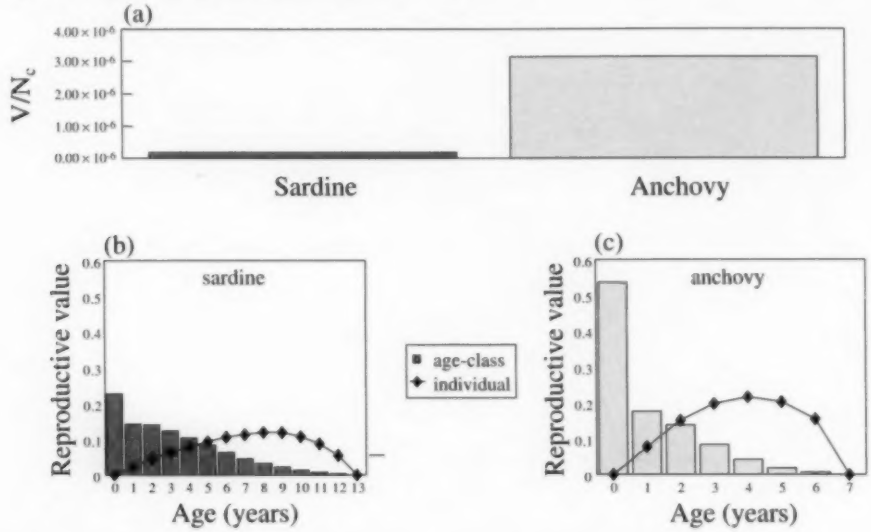

equalled unity. Note that defining the carrying capacity in terms of $N_{>0}$ implies that the reproductive population is larger in northern anchovy than in Pacific sardine, since 1 year old Pacific sardines do not reproduce. However, as mentioned above (see description of life histories), density-dependent regulation in these species is likely to be determined by the density of 1-year-old and older fish. Also, the results are presented in terms of the ratio of N_e to census size, N_c, and therefore, the results are not affected by this assumption.

Since we are interested in estimating the mean and variance of the ratio N_e/N, the numerical estimates of both demographic and genetic statistics were based on the replicates for which the population did not go extinct, usually somewhat less than 128. The code for the simulations was written in parallel FORTRAN and run on the San Diego Supercomputer Center Cray T3D benchmarked on as many as 128 nodes.

Results

Demography

Differences in survival and fecundity schedules lead to differences in reproductive value. As predicted by Fisher's (1930) equation, the individual reproductive value, v_i, first increases and then decreases with age (Fig. 1). The age-class reproductive value, however, decreases steadily. The total reproductive value of the northern anchovy population is much larger than that of the Pacific sardine population. Note, however, that the age-class contribution to the total reproductive value is more evenly distributed in Pacific sardine than in northern anchovy. As a consequence, most of the contribution to future population growth in northern anchovy is made by the 0 age-class (54%), while in Pacific sardine, most of the contribution (64%) is made by the reproductive age-classes (i = 2–13). These differences are due to the much longer life span, much lower offspring survival rate, and later maturation age of Pacific sardine, which also lead to a much larger generation time, L, and generation overlap, γ, for Pacific sardine (L = 4.62, γ = 0.34) than for northern anchovy (L = 2.33, γ = 0.09).

Total population size at equilibrium (i.e., at the stable population structure and size), N_c, was larger for Pacific sardine (1.66×10^{10}) than for northern anchovy (3.86×10^9), but their standard deviations were similar (4.75×10^8 and 5.07×10^8, respectively). Note that the standard deviations reported arise from the sampling process at small population sizes (see above). The number of individuals aged 1 year or older at equilibrium, $N_{>0}$, was somewhat less than the carrying capacity for both species (47 870 for northern anchovy and 46 210 for Pacific sardine), while its standard deviation was much larger for northern anchovy (6294.9) than for Pacific sardine (1325.3).

Genetics

Figure 2 show the results of the constant vital rates model for the case in which a fraction ρ of the population fails to reproduce (i.e., f = 0). The N_e is much smaller for Pacific sardine than for northern anchovy. This is due to the fact that the total reproductive value of the northern anchovy population is much larger than that of the Pacific sardine population, and therefore, the fraction of individuals contributing genes to future generations is larger. Note, however, that the effect of ρ on N_e is much more pronounced for northern anchovy (Fig. 2). Although the difference in N_e between Pacific sardine and northern anchovy is very large for small values of ρ, this difference almost disappears for values of ρ approaching 1, i.e., when only a very small fraction of the adult population reproduce successfully. This result is explained by Pacific sardine's longer life span and more even distribution of the age-class contribution to the total reproductive value. This demographic difference implies that a Pacific sardine that fails to reproduce in a given year is more

© 1999 NRC Canada

Fig. 2. Average N_e (constant vital rates model) for northern anchovy and Pacific sardine at the steady state for different values of ρ and for $f = 0$ (i.e., total reproductive failure). Upper and lower bounds represent 1 SD.

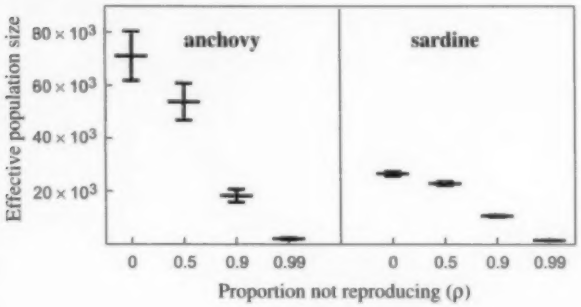

Fig. 3. Ratio of N_e to N_c (constant vital rates model) for Pacific sardine (solid symbols) and northern anchovy (open symbols) at the steady state for different values of ρ and f. Circles, ρ = 0; triangles, ρ = 0.5; squares, ρ = 0.9.

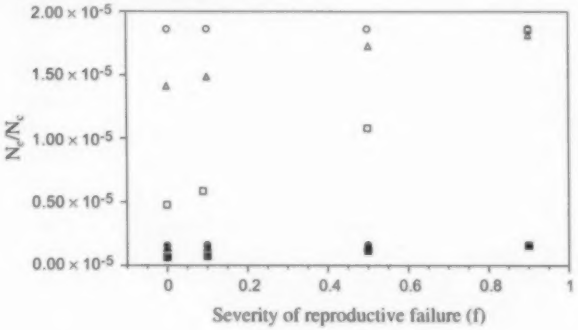

likely to reproduce in a later year than a northern anchovy in the same situation; this phenomenon is related to the storage effect concept (see Introduction). In the present situation, extensive generation overlap reduces the loss of genetic variability due to genetic drift. The larger the generation overlap, the less pronounced the loss of genetic variability.

Note that when ρ = 0, N_e of northern anchovy is larger than the number of mature individuals ($N_{>0}$; see text above and Fig. 2). This is due to the fact that when ρ = 0, the variance in family size is zero (see eq. 5), in which case, the N_e/N_a ratio can be larger than unity (see Falconer 1989). In the case of Pacific sardine, the average number of mature individuals (2-year-old and older fish) is 26 519.83 and the ratio of N_e/N_a is very close to unity but does not exceed it because of its longer generation time and much lower total reproductive value. The standard deviation of N_e is much larger for northern anchovy than for Pacific sardine due to the larger variance in adult population size observed for the northern anchovy population. Note also that the variance in N_e decreases as the proportion of individuals that fail to reproduce, ρ, increases.

The results above refer to the case of total reproductive failure ($f = 0$) for a fraction ρ of the population. More realistically, we can consider the case of partial reproductive failures ($0 < f < 1$) in which a fraction ρ produces a smaller (but positive) number of offspring than successful females. Figure 3 indicates that northern anchovy is more sensitive to reproductive failures than Pacific sardine. This again is due to the storage effect, which is greater for Pacific sardine.

The above results clearly indicate that moderate differences in life history characters between pelagic fish species might lead to large differences in N_e. Furthermore, they show that a species with a large N_e/N_c ratio can be more sensitive to reproductive failures than another species with a lower N_e/N_c ratio. Although the N_e/N_c ratio is directly proportional to the total reproductive value of the population, its sensitivity to reproductive failures is proportional to the generation overlap.

Cyclic vital rates

Methods

The methodology used for the cyclic vital rate simulations was similar to that used for the case of constant vital rates (see above). In this case, however, the survival of the 0 age-class varies as

$$s_0(t) = s + sA \cos \frac{2\pi}{T}$$

where s is the mean newborn survival, $0 < A < 1$ is the amplitude of the fluctuations, and T is the period of the oscillations measured in years. We used three values of T (5, 10, 20) and set amplitude A to 0.5. As in the previous case, we allowed the population to grow until reaching its carrying capacity and then adjusted s so that the population density oscillated around a long-term fixed average.

One of the methodological problems associated with the study of population dynamics in cyclical environments is the definition of the mean generation time, L. All the definitions in use (see Caswell 1989) are valid only for populations at the stable age distribution and therefore cannot be used in the present case. In order to avoid this problem, the results for the cyclic vital rate case are presented in terms of the mean coalescence time, $\bar{\tau}$ (see Appendix). The mean coalescence time is the time at which two genes sampled from the present population trace back to a common ancestral gene in the past. Replacing N_e with $\bar{\tau}/L$ in eq. 1, we obtain an expression for the relationship between heterozygosity and mean coalescence times:

$$H = \frac{4\bar{\tau}\mu}{L + 4\bar{\tau}\mu}.$$

This equation clearly shows that $\bar{\tau}$ is directly related to the amount of genetic variability maintained by a population. The only drawback of using $\bar{\tau}$ instead of N_e is that the former does not take into account the difference in generation time between species. Note, however, that there is no reason to believe that the introduction of cyclic recruitment failures will change the relationship between the generation times of the species studied. In other words, we expect that the generation time of northern anchovy will remain shorter than that of Pacific sardine regardless of the presence or absence of recruitment failures.

© 1999 NRC Canada

Table 2. Amplitude A of the age-class oscillations in the number of individuals for different values of T (period of the recruitment failure cycles measured in years).

	$T = 5$	$T = 10$	$T = 20$
Pacific sardine			
A_0	0.075	0.215	0.540
$A_{>0}$	0.860	0.809	0.797
A_T	0.075	0.215	0.540
Northern anchovy			
A_0	0.239	0.484	0.943
$A_{>0}$	0.711	0.717	1.027
A_T	0.239	0.484	0.943

Results

Demography

As shown by previous studies, cycles in vital rates at a frequency ω produce cycles in the age distribution at frequency ω (e.g., Tuljapurkar 1985). The results of the present simulations (Table 2) are in agreement with Tuljapurkar's (1985) analysis that showed that the response of the 0 age-class to the cycles in newborn survival rate is different from that of older age-classes. Older age-classes all exhibit the same amplification, which is larger than that observed for the 0 age-class.

In northern anchovy, the amplitude of the newborn population density cycles is much larger than in Pacific sardine for all the values of T considered (Table 2). On the other hand, the cycle amplitude of the older age-classes in Pacific sardine is slightly larger for $T = 5$, 10 but smaller for $T = 20$. Thus, the impact of fluctuations in newborn survival on the age-classes that contribute the most to future generations is much larger in northern anchovy (0 age-class) than in Pacific sardine (age-classes 2–13). This has important implications for the effect of the oscillations on N_e.

Genetics

As expected, the population cycles induced by cyclical variation in vital rates lead to cycles in $\bar{\tau}$. Figure 4 shows the effect of cyclic recruitment failures on mean coalescence time (averaged across the cycle) for different values of T and ρ. As was the case for the constant rate case, as ρ increases, mean coalescence time (i.e., genetic variability) decreases and this decrease is more pronounced for the northern anchovy population (1 order of magnitude larger). The introduction of recruitment failures decreases genetic diversity (measured in terms of mean coalescence times). This decrease is more pronounced as the period of fluctuations, T, increases because, as T increases, the amplitude of the oscillations in population size (see Table 2) also increases. Note that the decrease in $\bar{\tau}$ with increasing T is more pronounced for northern anchovy than for Pacific sardine. This is most likely due to the fact that the impact of fluctuations in newborn survival on the age-classes that contribute the most to future generations is more pronounced in northern anchovy (see above). There is an interaction between the effects of recruitment and reproductive failures (Fig. 4). The decrease in $\bar{\tau}$ with increasing T is more pronounced for smaller values of ρ. The interaction, however, is much less pronounced for Pacific sardine than for northern anchovy.

Fig. 4. Ratio of $\bar{\tau}$ to N_e for Pacific sardine (solid symbols) and northern anchovy (open symbols) for different values of ρ and T (period of the recruitment failure cycles). Squares, constant vital rates; triangles, $T = 5$; circles, $T = 10$; diamonds, $T = 20$.

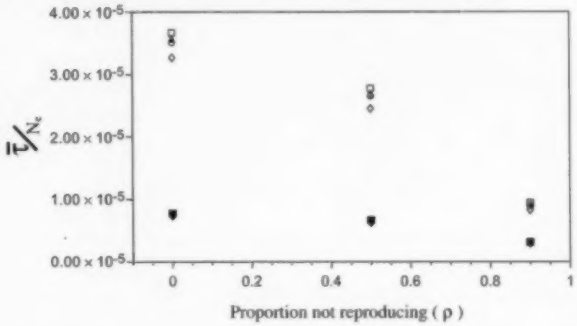

Table 3 shows the amplitude of the cycles in mean coalescence time induced by cyclical recruitment failures for different values of T and ρ. In all cases, the amplitude of the oscillations is more pronounced for northern anchovy than for Pacific sardine. As the period of the cycles in recruitment failures increases, the amplitude of the oscillations in $\bar{\tau}$ also increases; this increase is more pronounced in northern anchovy than in Pacific sardine. For any given period, the amplitude of the oscillations increases as ρ increases. Clearly, as the proportion of individuals that fail to reproduce in any given year increases, the effect of recruitment failures is more pronounced. Note that the increase in amplitude with increasing ρ is more pronounced for Pacific sardine. In fact, for values of ρ approaching unity, the difference in amplitude between Pacific sardine and northern anchovy is very small.

The above results indicate that the genetic response of the Pacific sardine population to environmentally induced changes such as reproductive (determined by ρ) or recruitment failures (determined by T) is less pronounced than that of the northern anchovy population. The longer generation time of Pacific sardine leads to a stronger storage effect and therefore to smaller temporal changes in the level of genetic variability maintained.

Effect of fishing mortality

Methods

The harvesting of Pacific sardine began in the late 1800's and became more significant in the early 1900's (Wolf 1992). The fishery rapidly increased in importance and began to inflict very high fishing mortalities by the mid-1930's. The first fishery collapse occurred in 1937 and was followed by a small recovery that lasted only a short time and was followed by a new series of collapses in the 1940's (Wolf 1992). This time, there was no real recovery, and although there were some fluctuations, the population declined steadily. By the early 1960's, the catch was insignificant, and in 1967, a moratorium was placed on fishing Pacific sardine. In 1985, the Pacific sardine population showed signs of recovery, and the moratorium was lifted (Wolf 1992). The

© 1999 NRC Canada

Table 3. Amplitude of the oscillations in the cycles of mean coalescence times for different values of ρ (the proportion of individuals that fail to reproduce) and T (period of the recruitment failure cycles measured in years).

	Pacific sardine			Northern anchovy		
T	ρ = 0	ρ = 0.5	ρ = 0.9	ρ = 0	ρ = 0.5	ρ = 0.9
5	0.31×10^{-5}	0.95×10^{-5}	6.19×10^{-5}	0.61×10^{-5}	1.18×10^{-5}	5.74×10^{-5}
10	1.19×10^{-5}	2.72×10^{-5}	16.7×10^{-5}	2.00×10^{-5}	3.10×10^{-5}	15.0×10^{-5}
20	2.23×10^{-5}	4.70×10^{-5}	27.1×10^{-5}	4.15×10^{-5}	6.59×10^{-5}	28.2×10^{-5}

samples used in Hedgecock et al.'s (1989) genetic analysis were obtained around 1985, and therefore, we will restrict our analysis of the effect of the fishery to the period extending from 1900 to 1985.

During the period of overfishing, the population of Pacific sardine underwent a number of changes in its life history. First, overfishing led to a reduction in the life span from 13 to 7 years. Also, by 1945, the age of first maturity was 1 year instead of the original 2 years (see Butler et al. 1996).

To study the effect of the fishery, we introduced fishing mortality into the simulations for the Pacific sardine population. Starting with an unexploited population that colonised the CCS T_c years ago (T_c = 10 000; 1 000 000), we introduced fishing in 1915 with an annual fishing mortality rate, F, of 0.20, a substantial but moderate value. In 1935, we increased fishing mortality to $F = 0.80$, representing overfishing. This latter value was maintained until 1967 when we completely excluded fishing mortality, i.e., we set $F = 0$.

In order to follow the changes in life history, the Leslie matrix of Pacific sardine was changed in 1940, 5 years after overfishing began, to accommodate the decreased life span and the reduction in maturation age. More precisely, we set to zero all vital rates for age-classes 8–13 and shifted the maternity function one unit to the left, i.e., $F_{i-1} = F_i$.

Results

We explored two scenarios: (*i*) we assumed that Pacific sardine colonised the CCS at the end of the Pleistocene and therefore set T_c = 10 000 (Fig. 5*a*) and (*ii*) we assumed that the population was at equilibrium and therefore set T_c = 1 000 000 (Fig. 5*b*).

Figure 5 shows the results of these simulations for the constant recruitment case and for the cyclic recruitment failures case with T = 5, 10, and 20. Population density starts to decrease right after the introduction of fishing mortality and becomes pronounced after 1935, when overfishing began. In the early 1940's, there is a small recovery due to the change in age of first maturity, but this recovery quickly fades away as overfishing continues. In the early 1970's, we see the response of the population to the moratorium on fishing, i.e., a rapid increase in abundance. This general pattern is maintained for all four cases, but in the cyclic cases, we also observe several small recoveries after the initial population crash. Since these small recoveries were also present in the time series data for the Pacific sardine fishery, the simulation results appear to be a qualitatively accurate description of the Pacific sardine fishery.

The effect of fishing on the genetic constitution of the population depends on the colonisation time of the CCS by Pacific sardine. If Pacific sardine is a recent arrival to the CCS (T_c = 10 000), we expect a steady increase in genetic variability even though the population is crashing (Fig. 5*a*). This increase lasts for at least five decades after the onset of the fisheries and is due to the fact that, after only 10 000 years, the population has yet to achieve the steady-state mean coalescence time that corresponds to its large population size. It takes several years for genetic variability to catch up with the decrease in population size. And even when it does, the decrease in $\bar{\tau}$ is rather small, at least when compared with the sharp decrease in population density. Note, however, that the decrease in $\bar{\tau}$ is more pronounced for the cases that consider cyclic recruitment failures.

If we assume that the Pacific sardine population has been present in the CCS for a long time (T_c = 1 000 000), the results are slightly different (Fig. 5*b*). In terms of population density, we observe a similar pattern, since demographic steady state is achieved in less than 1000 years. In genetic terms, however, we see that, although there is a time lag, genetic variability responds more quickly to the decrease in population density. This is simply because the population was at the genetic steady state before fishing began, and therefore, its maximum genetic variability had been realised. In this case, too, the decrease in genetic variability is more pronounced in the presence of recruitment failures.

These results indicate that the decrease in genetic variability due to fishing mortality is more pronounced in the presence of recruitment failures. In general, however, overfishing is unlikely to have had a large effect on N_e of Pacific sardine. This should not be taken to imply that overfishing cannot significantly decrease genetic variability. It can and will do so if overfishing is allowed to go on for long enough.

Discussion

The results of the present study indicate that moderate differences in life history between ecologically related species can lead to substantial differences in N_e's. Moreover, the effect of fluctuations in vital rate parameters induced by environmental changes depends on the life history of each species. Species with large N_e/N_c ratios might be more strongly affected by these changes than species with lower ratios. This is certainly the case for reproductive and recruitment failures (see above). The present simulations and previous analytical results (see Felsenstein 1971) show that the N_e/N_c ratio is directly proportional to the total reproductive value of a population. The present analysis further shows that the sensitivity of this ratio to environmental fluctuations is proportional to the generation overlap. The larger the generation overlap, the smaller the impact of environmental fluctuations on the effective size of a population. Previous studies have shown that long-lived stages provide a mechanism for the maintenance of genetic variability in the presence of tempo-

© 1999 NRC Canada

Fig. 5. Changes in N_c and $\bar{\tau}$ for an exploited population of Pacific sardine. All simulations were run assuming $\rho = 0.9$ and $f = 0$. (*a*) Results under the assumption that Pacific sardine colonised the CCS 10 000 years ago; (*b*) results under the assumption that Pacific sardine colonised the CCS such a long time ago (T_c = 1 000 000) that the population has reached the genetic steady state.

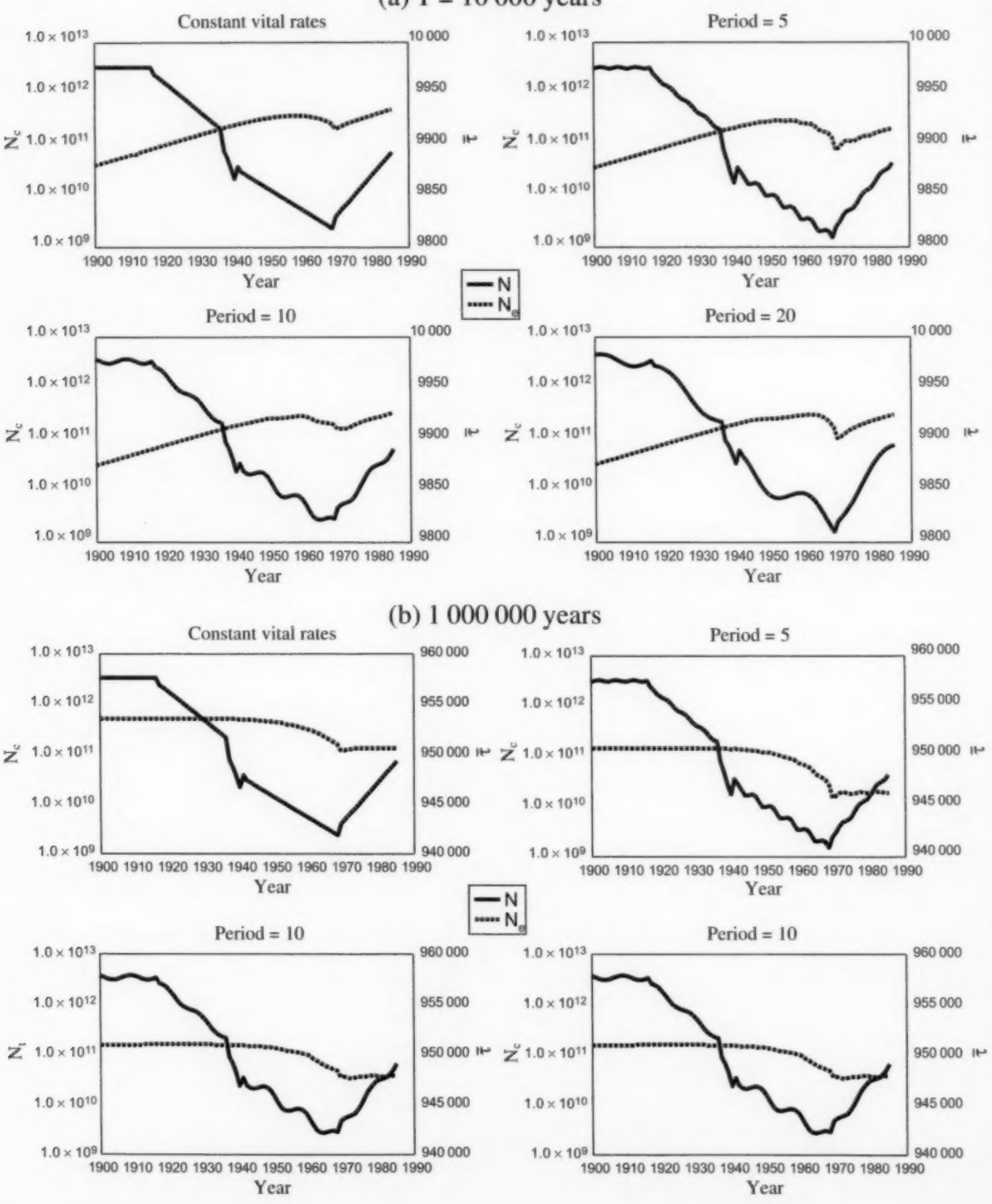

© 1999 NRC Canada

rally (Ellner and Hairston 1994) and spatially (Gaggiotti et al. 1997) fluctuating selection. The present study shows that a similar mechanism protects species with overlapping generations from the loss of genetic variability due to genetic drift. This capacity of age-structured populations to buffer the effects of diverse environmental factors that might decrease N_e can be described by the term "storage effect".

The present study represents the first detailed analysis of the genetics of pelagic fish populations, and it was achieved by relaxing many of the unrealistic assumptions made by standard population genetics models. However, some simplifying assumptions are unavoidable and their inclusion in the present model needs to be discussed. The present formulation assumes that each population was founded by a single female (see above). This assumption does not affect the final results of the model because only the steady-state results are considered. In demographic terms, starting with a larger population size would simply mean that the carrying capacity is achieved at an earlier time; the population growth rate and steady-state age structure would remain unaffected (Caswell 1989). The same happens with the genetic results; as the number of founders increases, the initial loss of heterozygosity is less pronounced but the steady-state level of heterozygosity attained is the same regardless of the number of founders (e.g., see Chackraborty and Nei 1977).

Variance in reproductive success is modelled through reproductive failures of a fraction ρ of the population. Thus, at any given time, there are two groups of individuals, a more successful group and a less successful group. Although this is a simplification of the real situation, it can be considered as an acceptable approximation. In the marine environment, reproduction is mediated by spatially and temporally varying oceanographic processes affecting gonad maturation, spawning, and fertilisation (Hedgecock 1994). Fertilisation success of externally fertilising species in the field can be drastically reduced by dilution of sperm or by low density or aggregation of spawning adults (see Hedgecock 1994 and references therein). Moreover, the particular characteristics of pelagic fish, such as their schooling behaviour and very large ranges, are likely to lead to a large variance in the physiological conditions of spawning adults. Thus, the fraction of the population that experienced unfavourable conditions prior to or during reproduction will have a low or nil reproductive output, while the fraction of the population that experienced favourable conditions will have a very large output. Our model also assumes that reproductive success is independent of genotype and is only determined by environmental conditions. In this regard, it should be noted that as compared with other vertebrates, fishes have larger phenotypic variation and lower heritabilities, i.e., they are more strongly affected by environmental fluctuations (Allendorf et al. 1987). Therefore, the assumption of fecundity being determined by environmental factors can be considered a reasonable approximation to reality.

There are many possible explanations for the low levels of genetic variability in the Pacific sardine population of the CCS (see Hedgecock et al.1989). One possibility is that the collapse of the Californian Pacific sardine fishery in the 1950's and 1960's reduced the genetic variability of Pacific sardine from levels typical of clupeoids to its current levels. The present results, however, suggest that although a fishery collapse can decrease genetic variability, this decrease is small (see Fig. 5). A second explanation is that Pacific sardine might be a recent arrival to the CCS and that its low genetic variability is attributable to a small number of founders. In this regard, it should be noted that fossil remains of *Sardinops* are absent from samples of California Pliocene and Pleistocene sediments, while evidence for *Engraulis* is present at least in some samples (e.g., Casteel 1975); this may indicate that Pacific sardine colonised the CCS some 10 000 – 100 000 years ago. Allozyme (Grant and Leslie 1996) and mtDNA (Bowen and Grant 1997) data give support to a late Pleistocene colonisation. Note that heterozygosity in northern anchovy is seven times higher than in Pacific sardine (see Introduction). Additional simulations (results not presented) indicate that this difference would be possible only if we assume that northern anchovy has been present in the CCS long enough to reach its genetic steady state and that Pacific sardine colonised the CCS 10 000 years ago or less. Moreover, the results of the model are based on the assumption that a single impregnated female colonised the CCS. This assumption is unrealistic and it is almost certain that the real number of colonisers was much larger, especially given the schooling behaviour characteristic of Pacific sardine and pelagic fish in general. Thus, the amount of genetic variability of the founding propagule must have been much larger than that assumed by the present analysis. One has to conclude, therefore, that although a recent arrival may have contributed to the lowered level of genetic variability in Pacific sardine, it cannot by itself explain the large difference in heterozygosity between Pacific sardine and northern anchovy populations.

The difference in the level of genetic variability between Pacific sardine and northern anchovy populations could also be explained by their life history differences. The level of genetic variability maintained is determined by the absolute N_e instead of the N_e/N_c ratio. Thus, we need to obtain estimates of population size for both species before being able to determine if life history differences are a good explanation. Rough estimates of population sizes can be obtained by dividing population biomass estimates by the mean weight of fish in the population (L.D. Jacobson, Southwest Fisheries Science Center, La Jolla, Calif., personal communication). Using published data, we obtained a population size estimate of 2.86×10^{10} individuals for Pacific sardine (data from Barnes et al. 1992) and 2.5×10^{10} individuals for northern anchovy (data from Jacobson et al. 1994). From these values and the N_e/N_c ratios obtained in this study (see Fig. 4), eq. 1 (with $\mu = 10^{-6}$, which is appropriate for allozyme loci) leads to heterozygosities of 0.52 for Pacific sardine and 0.91 for northern anchovy. Thus, life history differences have significantly contributed to the lowered level of genetic variability in Pacific sardine but cannot be considered the only explanation. We conclude, therefore, that both life history differences and a recent arrival to the CCS are the best explanations for the low level of genetic variability observed in the Pacific sardine population.

The present analysis also illustrates some interesting genetic characteristics of pelagic fish populations. Although these populations can exhibit large fluctuations in population numbers, the effect of these fluctuations on N_e is rather limited. This also holds true for fisheries collapses despite their

© 1999 NRC Canada

dramatic effects in terms of population numbers. For a fishery collapse to have an effect on heterozygosity similar to that of a bottleneck, the population has to reach levels that may lead to extinction due to demographic and (or) environmental stochasticity. Note, however, that the average (actual) number of alleles depends on both N_e and N, and in very large populations, a sharp decrease in N can lead to a large reduction in the number of alleles maintained (see Ryman et al. 1995).

The few existing theoretical studies on the effect of life history on N_e (e.g., Nunney 1991, 1993, 1996) have ignored the role of prereproductive individuals in the genetics of a population. Nunney's (1991) analyses, however, showed that biased sex ratios only have a measurable effect on the N_e/N_c ratio if the bias is due to differences in recruitment (i.e., newborn survival) between the two sexes. The present analysis explicitly shows that newborn survival has a large impact on the N_e/N_c ratio, suggesting that 0 age-class survival is a critical parameter in determining N_e.

The present study also provides some insight into conservation genetics issues. The fact that a population has a large N_e/N_c ratio does not necessarily mean that it is more protected from environmental fluctuations than a population with a lower ratio. A population that is insensitive to environmental changes might need only a small N_e to cope with environmental heterogeneity. On the other hand, a species with a life history that makes it prone to reductions in N_e due to changes in environmental conditions might need a larger N_e.

The present study ignores the effect of other factors that may reduce N_e because its aim is to stress the importance of life history in determining the level of genetic variability maintained by a species. The maximum level of genetic variability maintained by a population is determined by its life history traits. Whether or not this level is realised depends on other processes such as population subdivision and local extinctions and recolonisations. Our model shows that as opposed to northern anchovy, Pacific sardine populations are predetermined to have low levels of genetic variability even under the best possible environmental conditions. Other processes such as local extinction and recolonisations will decrease genetic variability even further, but, in any case, the base level of genetic variability on which these processes will operate is low.

Acknowledgements

We are particularly indebted to P.E. Smith and J.R.Hunter for sharing with us their thorough knowledge of the biology of pelagic fish. S. Tuljapurkar clarified many issues concerning the dynamics of age-structured populations in cyclic environments. W.S. Grant and P.E. Smouse critically read the manuscript and provided helpful suggestions. The comments made by two reviewers greatly improved the original manuscript. L.D. Jacobson provided data that allowed the estimation of population sizes for the species studied. R. Marciano helped with the implementation of a parallel version of the simulation program on the San Diego Supercomputer Center's Cray T3D computer. O.E.G. was funded by a National Research Council postdoctoral fellowship.

References

Allendorf, F.W., Ryman, N., and Utter, F. 1987. Genetics and fishery management: past, present, and future. *In* Population genetics and fishery management. *Edited by* N. Ryman and F.M. Utter. University of Washington Press, Seattle, Wash. pp. 1–19.

Barnes, J.T., Jacobson, L.D., MacCall, A.D., and Wolf, P. 1992. Recent population trends and abundance estimates for the Pacific sardine *Sardinops sagax*. Calif. Coop. Oceanic Fish. Invest. Rep. **33**: 60–75.

Baumgartner, T.R., Soutar, A., and Ferreira-Bartrina, V. 1992. Reconstruction of the history of Pacific sardine and northern anchovy populations over the past two millennia from sediments of the Santa Barbara basin, California. Calif. Coop. Oceanic Fish. Invest. Rep. **33**: 24–40.

Blaxter, J.H.S., and Hunter, J.R. 1982. The biology of clupeoid fish. *In* Advances in marine biology. *Edited by* J.H.S. Blaxter, F.S. Russell, and M. Yonge. Academic Press, New York. pp. 1–223.

Bowen, B.W., and Grant, W.S. 1997. Phylogeography of the sardines (*Sardinops* spp.): assessing biogeographic models and population histories in temperate upwelling zones. Evolution, **51**: 1601–1610.

Butler, J.L. 1987. Comparison of the early life history parameters of Pacific sardine and northern anchovy and implications for species interactions. Ph.D. thesis, University of California, San Diego, Scripps Institution of Oceanographic Dissertations.

Butler, J.L., Smith, P.E., and Lo, N.C.-H. 1993. The effect of natural variability of life-history parameters on anchovy and sardine population growth. Calif. Coop. Oceanic Fish. Invest. Rep. **34**: 104–111.

Butler, J.L., Granados, M.L., Barnes, J.T., Yaremko, M., and Macewics, J. 1996. Age composition, growth, and maturation of the Pacific sardine (*Sardinops sagax*) during 1994. Calif. Coop. Oceanic Fish. Invest. Rep. **37**: 152–159.

Caballero, A. 1994. Developments in the prediction of effective population size. Heredity, **73**: 657–679.

Casteel, R.W. 1975. An early post-glacial record of the Pacific sardine, *Sardinops sagax*, from Saanich Inlet, Vancouver Island, British Columbia. Copeia, **1975**: 576–579.

Caswell, H. 1989. Matrix population models: construction, analysis, and interpretation. Sinauer Associates, Inc., Sunderland, Mass.

Chackraborty, R., and Nei, M. 1977. Bottleneck effects on average heterozygosity and genetic distance with the stepwise mutation model. Evolution, **31**: 347–356.

Cohen, J.E., Christensen, S.W., and Goodyear, C.P. 1983. A stochastic age-structured population model of striped bass (*Morone saxatilis*) in the Potomac River. Can. J. Fish. Aquat. Sci. **40**: 2170–2183.

Ellner, S. 1996. Environmental fluctuations and the maintenance of genetic diversity in age or stage-structured populations. Bull. Math. Biol. **58**: 103–127.

Ellner, S., and Hairston, N.G. 1994. Role of overlapping generations in maintaining genetic variation in a fluctuating environment. Am. Nat. **143**: 403–417.

Falconer, 1989. Introduction to quantitative genetics. Longman, London, U.K.

Felsenstein, J. 1971. Inbreeding and variance effective numbers in populations with overlapping generations. Genetics, **68**: 581–597.

Fisher, R.A. 1930. The genetical theory of natural selection. Claredon Press, Oxford, U.K.

© 1999 NRC Canada

Frankham, R. 1995. Effective population size/adult population size ratios in wildlife: a review. Genet. Res. **66**: 95–107.

Gaggiotti, O.E., Lee, C.E., and Wardle, G.M. 1997. The effect of overlapping generations and population structure on gene-frequency clines. *In* Structured population models in marine, terrestrial, and freshwater systems. *Edited by* S. Tuljapurkar and H. Caswell. Chapman and Hall, New York. pp. 355–369.

Grant, W.S., and Leslie, R.W. 1996. Late Pleistocene dispersal of Indian-Pacific sardine populations in an ancient lineage of the genus *Sardinops*. Mar. Biol. **126**: 133–142.

Hedgecock, D. 1994. Does variance in reproductive success limit effective population sizes of marine organisms? *In* Genetics and evolution of aquatic organisms. *Edited by* A.R. Beaumont. Chapman and Hall, London, U.K. pp. 122–134.

Hedgecock, D., Hutchinson, E.S., Li, G., Sly, F.L., and Nelson, K. 1989. Genetic and morphometric variation in the Pacific sardine, *Sardinops sagax coerulea*: comparisons and contrasts with historical data and with variability in the northern anchovy, *Engraulis mordax* (Girard), 1966 through 1979. Fish. Bull. U.S. **87**: 653–671.

Hill, W.G. 1979. A note on effective population size with overlapping generations. Genetics, **92**: 317–322.

Jacobson, L.D., Lo, N.C.H., and Barnes, J.T. 1994. A biomass based assessment model for northern anchovy, *Engraulis mordax*. Fish. Bull. U.S. **92**: 711–724.

Lande, R., and Barrowclough, G.F. 1987. Effective population size, genetic variation, and their use in population management. *In* Viable populations for conservation. *Edited by* M.E. Soulé. Cambridge University Press, Cambridge, U.K. pp. 87–123.

Nunney, L. 1991. The influence of age structure and fecundity on effective population size. Proc. R. Soc. Lond. Ser. B, Biol. Sci. **246**: 71–76.

Nunney, L. 1993. The influence of mating system and overlapping generations on effective population size. Evolution, **47**: 1329–1341.

Nunney, L. 1996. The influence of variation in female fecundity on effective population size. Biol. J. Linn. Soc. **59**: 411–425.

Orive, M.E. 1993. Effective population size in organisms with complex life-histories. Theor. Popul. Biol. **44**: 316–340.

Ryman, N., Utter, F., and Lairke, L. 1995. Protection of intraspecific biodiversity of exploited fishes. Rev. Fish Biol. Fish. **5**: 417–446.

Smith, P.E. 1985. Year-class strength and survival of 0-group clupeoids. Can. J. Fish. Aquat. Sci. **42**: 69–82.

Tuljapurkar, S. 1985. Population dynamics in variable environments. VI. Cyclical environments. Theor. Popul. Biol. **27**: 1–17.

Tuljapurkar, S. 1990. Population dynamics in variable environments. Springer-Verlag, Hidelberg, Germany.

Warner, R.R., and Chesson, P.L. 1985. Coexistence mediated by recruitment fluctuations: a field guide to the storage effect. Am. Nat. **125**:769–787.

Wolf, P. 1992. Recovery of the Pacific sardine and the California sardine fishery. Calif. Coop. Oceanic Fish. Invest. Rep. **33**: 76–86.

Appendix. Mean coalescence times and effective population size, N_e

Orive's (1993) approach is based on the fact that in a randomly mating diploid population with nonoverlapping generations, the expected time, $\bar{\tau}$, in units of generations until a common ancestor for two alleles chosen at random is $2N_e$. Thus, the inbreeding N_e for a species with overlapping generations can be defined as $\bar{\tau}/L$, where L is the generation time and $\bar{\tau}$ is measured in years. The first step of the approach is to determine the mean coalescence time.

Orive's (1993) equilibrium formulation can be generalised to consider nonequilibrium situations if we first assume that the population was founded $\tau = t$ time units in the past by a single individual. Under this assumption, her eq. 6 can be rewritten as

$$\text{(A1)} \quad \bar{\tau}_{ij;t} = 1 + \sum_k \sum_l p_{ik;t} p_{jl;t} \alpha_{ij,kl;t} \bar{\tau}_{kl;t-1}$$

where $\tau_{ij;t}$ is the expected coalescence times for two genes sampled from stages i and j at time t, $p_{ij;t}$ is the probability at time t of an individual being in state j at time $t-1$ given that it is in state i at time t, and $\alpha_{ij,kl;t}$ is the probability at time t that two alleles randomly chosen without replacement from individuals in stages i and j do not share a common ancestral allele in the previous time unit, when they are in individuals of stages k and l.

To solve eq. A1, we need to define the entries of the p_{ij}'s and $\alpha_{ij,kl}$'s. The probability $p_{ij;t}$ is calculated from the coefficients of the Leslie matrix, $\mathbf{A}_t = \{a_{ij;t}\}$ (see Orive 1993). The probabilities $\alpha_{ij,kl}$'s are those obtained by Orive (1993) with the exception of $\alpha_{00,kk;t}$ and $\alpha_{0j,(j-1)(j-1);t}$. In a nonequilibrium population with variance in reproductive success, these probabilities are obtained as follows. The probability $\alpha_{00,kk;t}$ is the probability that two alleles chosen from newborns (eggs) with parents in the same age-class do not have the same parent (sp), i.e., $\alpha_{00,kk;t} = 1 - \Pr\{\text{sp}\}_{k;t}$. The probability at time t that two randomly sampled haploid eggs (genes), produced by individuals belonging to age-class k one time unit before, have the same parent is

$$\text{(A2)} \quad \Pr\{\text{sp}\}_{k;t} = \Pr\{\zeta_1\}_{k;t} \Pr\{\text{sp}/\zeta_1\}_{k;t} + \Pr\{\zeta_2\}_{k;t} \Pr\{\text{sp}/\zeta_2\}_{k;t}$$

where $\Pr\{\zeta_1\}$ is the probability that both eggs were produced by individuals belonging to the less successful group (i.e., those producing Y_1 eggs), $\Pr\{\zeta_2\}$ is the probability that both belong to the more successful group (i.e., those producing Y_2 eggs), and $\Pr\{\text{sp}/\zeta_i\}_{k;t}$ is the probability that both eggs come from the same parent given that they both were produced by individuals belonging to group i ($i = 1, 2$).

The probability at time t that two randomly sampled eggs were produced by the less successful individuals belonging to age-class k is

$$\text{(A3)} \quad \Pr\{\zeta_1\}_{k;t} = \frac{Y_1 \rho n_{k;t-1}}{E_k n_{k;t-1}} \frac{(Y_1 \rho n_{k;t-1} - 1)}{(E_k n_{k;t-1} - 1)} = \frac{Y_1 \rho}{E_k} \frac{(Y_1 \rho n_{k;t-1} - 1)}{(E_k n_{k;t-1} - 1)}.$$

© 1999 NRC Canada

The probability at time t that both eggs come from the same parent given that they both were produced by the less successful individuals belonging to age-class k is

$$\text{(A4)}\quad \Pr\left\{\text{sp}/\zeta_1\right\} = \frac{Y_1 - 1}{Y_1 \rho n_{k;t-1} - 1}.$$

The corresponding expressions for the case of two eggs produced by the more successful individuals are obtained by replacing subscript 1 with 2 and ρ with $(1 - \rho)$ in the expressions above. From eqs. A2–A4 and after some algebra, we have

$$\text{(A5)}\quad \Pr\left\{\text{sp}\right\}_{k;t} = \frac{Y_1 \rho (Y_1 - 1) + Y_2 (1 - \rho)(Y_2 - 1)}{E_k (E_k n_{k;t-1} - 1)}.$$

After replacing for Y_2 using eq. 2 (see "Model" section in the main text), we have

$$\text{(A6)}\quad \Pr\left\{\text{sp}\right\}_{k;t} = \frac{E_k (E_k - 1 + \rho) + \rho Y_1 (Y_1 - 2E_k)}{(1 - \rho) E_k (E_k n_{k;t-1} - 1)}.$$

From eq. A6, it follows that

$$\text{(A7)}\quad \alpha_{00,kk;t} = 1 - \frac{E_k (E_k - 1 + \rho) + \rho Y_1 (Y_1 - 2E_k)}{(1 - \rho) E_k (E_k n_{k;t-1} - 1)}.$$

The probability $\alpha_{0j,(j-1)(j-1);t}$ is the probability that, when one allele is chosen from a newborn (egg) and the other from an older individual that belonged to the same age-class as the parent of the newborn one time unit in the past, the older individual was not the parent of the newborn one time unit ago when it was aged $j - 1$, i.e., $\alpha_{0j,(j-1)(j-1);t} = 1 - \Pr\{\text{parent}\}$. Using the same arguments as before, it is easy to show that $\Pr\{\text{parent}\} = 1/n_{j-1;t-1}$, and therefore:

$$\text{(A8)}\quad \alpha_{0j,(j-1)(j-1);t} = 1 - \frac{1}{n_{j-1;t-1}}.$$

Inserting the values for $\alpha_{ij,kl;t}$ into eq. A1, we get the following system of equations:

$$\text{(A9)}\quad \begin{aligned}
\bar{\tau}_{00;t} &= 1 + \sum_k p_{0k;t}^2 \, \alpha_{00,kk;t} \, \bar{\tau}_{kk;t-1} + \sum_k \sum_{l \neq k} p_{0k;t} \, p_{0l;t} \, \bar{\tau}_{kl;t-1} \\
\bar{\tau}_{0j;t} &= 1 + \sum_{k \neq j-1} p_{0k;t} \, \bar{\tau}_{k(j-1);t-1} + p_{0(j-1);t} \, \alpha_{0j,(j-1)(j-1);t} \, \bar{\tau}_{(j-1)(j-1);t} \\
\bar{\tau}_{ij;t} &= 1 + \bar{\tau}_{(i-1)(j-1);t-1}, \quad \text{for } i, j \neq 0,
\end{aligned}$$

where $\alpha_{00,kk;t}$ and $\alpha_{0j,(j-1)(j-1);t}$ are given by eqs. A7 and A8, respectively.

In order to find N_e from the mean coalescence times, it is necessary to weight each $\bar{\tau}_{ij}$ by the probability of choosing an allele from an individual of age i and another from age j. It is also necessary to convert from arbitrary time units to generations. Defining L as the mean generation time and N_c as the total population size, we have

$$\text{(A10)}\quad N_e = \frac{\bar{\tau}}{L} = \frac{1}{L} \sum_i \frac{n_i (n_i - 1)}{N_c^2} \bar{\tau}_{ii} + \frac{1}{L} \sum_i \sum_j \frac{n_i n_j}{N_c^2} \bar{\tau}_{ij}.$$

© 1999 NRC Canada

Application of a food web bioaccumulation model for the prediction of polychlorinated biphenyl, dioxin, and furan congener concentrations in Lake Ontario aquatic biota

Heather A. Morrison, D. Michael Whittle, Chris D. Metcalfe, and Arthur J. Niimi

Abstract: A previously developed benthic/pelagic food web bioaccumulation model was parameterized to predict concentrations of nine nonmetabolized polychlorinated biphenyl (PCB) congeners in invertebrates and fish from Lake Ontario. Predicted concentrations were compared with field-measured concentrations to verify the predictability of the model. Overall, 86% of model predictions were within a factor of 2 and 100% of predictions were within a factor of 10 of field-measured concentrations. The parameterized model was used to estimate chemical metabolic rates for 15 PCB, polychlorinated dibenzo-*p*-dioxin (PCDD), and polychlorinated dibenzo-*p*-furan (PCDF) congeners that are potentially metabolized. Estimated chemical metabolic rates ranged from 7.5×10^{-3} to 1.0×10^{-7}·day^{-1} and were in general agreement with qualitative studies describing rates of metabolism of these chemicals by aquatic biota. The calibrated model was used to predict concentrations of all 24 PCB, PCDD, and PCDF congeners in invertebrates and fish commonly found in Lake Ontario but for which no field-measured data exist. These concentrations were expressed as the logarithm of the bioaccumulation factor (log BAF). The log BAF's in benthic invertebrates and salmonids ranged from 4.2 to 10.2 and from 5.1 to 11.6, respectively, and were consistent with field-measured BAF's.

Résumé : Un modèle de bioaccumulation du réseau trophique benthique et pélagique élaboré précédemment a été paramétrisé afin de prévoir la concentration de neuf congénères des polychlorobiphényles (PCB) non métabolisés chez des invertébrés et des poissons du lac Ontario. Les concentrations prévues ont été comparées aux concentrations mesurées sur le terrain pour vérifier la prévisibilité du modèle. Globalement, 86% des prévisions du modèle étaient en deçà d'un facteur de 2 et toutes les prévisions étaient en deçà d'un facteur de 10 par rapport aux concentrations mesurées sur le terrain. Le modèle paramétrisé a été utilisé pour évaluer les taux métaboliques de 15 congénères des PCB, des polychlorodibenzo-*p*-dioxines (PCDD) et des polychlorodibenzo-*p*-furanes (PCBF) qui peuvent être métabolisés. L'estimation des taux métaboliques était comprise entre $7{,}5 \times 10^{-3}$ et $1{,}0 \times 10^{-7}$·jour^{-1} et elle s'accordait en général aux études qualitatives décrivant les taux métaboliques de ces substances chimiques par le biote aquatique. Le modèle calibré a été utilisé pour prévoir les concentrations des 24 congénères des PCB, des PCDD et des PCDF chez les invertébrés et les poissons que l'on trouve couramment dans le lac Ontario, mais pour lesquels il n'existe pas de données mesurées sur le terrain. Ces concentrations ont été exprimées sous forme de logarithmes du facteur de bioaccumulation (log BAF). Les log BAF chez les invertébrés benthiques et les salmonidés étaient compris respectivement entre 4,2 et 10,2 et entre 5,1 et 11,6 et ils étaient conformes aux BAF mesurés sur le terrain.

[Traduit par la Rédaction]

Introduction

Chemical pollutants have been discharged into Lake Ontario from industries, polluted tributaries, and the atmosphere for many decades (Government of Canada 1991). Of the more than 300 identified hazardous substances detected in the ecosystem of the lake (International Joint Commission 1978), the class of chemicals known as halogenated aromatic hydrocarbons (HAH's) are considered a concern because these chemicals bioaccumulate and biomagnify in resident biota (Oliver and Niimi 1988). Some members of this class are known to be hazardous to humans and wildlife (Government of Canada 1991). Polychlorinated biphenyls (PCB's), polychlorinated dibenzodioxins (PCDD's), and polychlorinated dibenzofurans (PCDF's) are part of the suite of HAH's detected in the Lake Ontario system. These groups of chemicals contain 209, 75, and 135 individual congeners, respectively, which differ in their chemical and physical properties and their effects on biota. Because these individual congeners differ in their toxic potencies and the

Received October 14, 1998. Accepted March 17, 1999.
J14827

H.A. Morrison.[1] Aqualink, 4936 Yonge St., Suite 507, Toronto, ON M2N 4L4, Canada.
D.M. Whittle and A.J. Niimi. Department of Fisheries and Oceans, Great Lakes Laboratory for Fisheries and Aquatic Sciences, Burlington, ON L7R 4A6, Canada.
C.D. Metcalfe. Environmental and Resource Studies Program, Trent University, Peterborough, ON K9J 7B8, Canada.

[1]Author to whom all correspondence should be addressed.
e-mail: morrisonh@dfo-mpo.gc.ca

© 1999 NRC Canada

degree to which they partition among abiotic and biotic environmental compartments, it is important to assess HAH's on a congener-specific basis.

Multimedia food web bioaccumulation models are useful for understanding the processes that affect HAH transfer in food webs. Analysis of many individual toxic HAH compounds such as PCDD's and nonortho (coplanar) PCB's is technically challenging and expensive. Therefore, little information is available on the concentrations of toxic HAH's in aquatic food webs, including concentrations in aquatic invertebrates and forage fish species. When analytical data are available, they tend to describe HAH concentrations for only a few fish species rather than for the range of fish that make up the diet of anglers and aquatic biota. Multimedia food web bioaccumulation models provide a means to generate data on the concentrations of HAH's in organisms from aquatic food webs, including invertebrates and sport fish species.

Food web bioaccumulation models have been used to predict PCB congener concentrations in aquatic biota from the Great Lakes (Camphens and Mackay 1997; Morrison et al. 1997). Previous efforts to model PCB congeners in Lake Ontario indicated that the food web was at or near steady state and therefore was well described by a steady-state model (Camphens and Mackay 1997). To date, there have been few attempts to model bioaccumulation of dioxin and furan congeners in any aquatic food web. The objective of this study is to apply the steady-state food web bioaccumulation model of Morrison et al. (1997) to the Lake Ontario food web in order to estimate PCB, dioxin, and furan congener concentrations in a variety of fish species and their invertebrate forage base. To achieve this objective, the study was divided into three parts. In part 1, the ability of the food web model of Morrison et al. (1997) to predict concentrations of nonmetabolized PCB congeners in the Lake Ontario food web was verified by comparing model-predicted concentrations with field-measured concentrations. The purpose of part 1 was to determine whether or not this model accurately predicted HAH bioaccumulation in this ecosystem and to determine if the model was accurately parameterized. The objective of part 2 was to use the verified bioaccumulation model as a tool for estimating chemical metabolic rates in a variety of aquatic invertebrates and fish for potentially metabolized PCB, dioxin, and furan congeners. It was necessary to estimate these metabolic rates because, although qualitative studies suggested that some of these HAH congeners are metabolized slowly by aquatic biota, no quantitative rate constants exist at this time. In part 3, the calibrated model was used to predict metabolized and nonmetabolized HAH congener concentrations in invertebrate and fish species in Lake Ontario for which there are limited published contaminant data.

Materials and methods

Model description

The food web bioaccumulation model described by Morrison et al. (1998) was used to predict HAH congener concentrations in Lake Ontario aquatic biota. Chemical concentrations are determined at steady state using conventional chemical, biological, and environmental data. The model predicts bioaccumulation of persistent organic chemicals by phytoplankton using equilibrium partitioning between the phytoplankton's organic carbon and water. Predicted bioaccumulation of HAH's in all other species is based on the premise that the predominant routes of chemical uptake are directly from water via the respiratory surface and through consumption of contaminated food. Chemical elimination is via the gills to water, by fecal egestion, and by metabolic transformation. In addition, growth dilution, which describes the decrease in internal chemical concentration as body mass increases over time (i.e., growth), is included in the model for fish but is assumed to be negligible for invertebrates.

Field data

Biota

The model was verified and calibrated using PCB congener concentrations in *Diporeia hoyi* and *Mysis relicta* and PCDF, PCDD, and PCB congener concentrations in whole bodies of alewife (*Alosa pseudoharengus*), rainbow smelt (*Osmerus mordax*), slimy sculpin (*Cottus cognatus*), and lake trout (*Salvelinus namaycush*) collected from several offshore sites in Lake Ontario in 1992–1994. Three individual samples of lake trout ranging in ages from 1+ to 3+, six samples of lake trout of age 8+, six composite samples of rainbow smelt, six composite samples of slimy sculpin, six composite samples of alewife, four composite samples of *Mysis*, and two composite samples of *Diporeia* were collected by staff of the Great Lakes Laboratory for Fisheries and Aquatic Sciences (GLLFAS), Department of Fisheries and Oceans (DFO), at Burlington, Ont. These samples were analysed on a whole-body basis for the HAH congeners listed in Table 1 by the GLLFAS Ultratrace Analytical Laboratory according to the methods of Huestis et al. (1995), and concentrations and information on samples are reported in Niimi (1996). Furthermore, four lake trout of age 8+, two five-fish composite samples of rainbow smelt, two five-fish composite samples of alewife, two five-fish composite samples of slimy sculpin, two composite samples of *Mysis*, two composite samples of *Diporeia*, and three netplankton samples were collected by the staff at GLLFAS and analysed by the Ultratrace Analytical Laboratory according to the methods of Huestis et al. (1995) (DFO, unpublished data). In addition, six composite samples of alewife, five composite samples of slimy sculpin, three samples of *Mysis*, and six samples of *Diporeia* were collected and analysed for PCB congeners by researchers at Trent University, Peterborough, Ont., and are described in Metcalfe and Metcalfe (1997). All samples were corrected for percent recovery of HAH's.

Sediment

Five samples of the top 3 cm of bottom sediment were collected from central Lake Ontario and analysed for the HAH congeners listed in Table 1 by the GLLFAS Ultratrace Analytical Laboratory according to the methods of Huestis et al. (1995). Four samples, also comprising the top 3 cm of bottom sediment, were collected from central Lake Ontario and analysed for PCB congeners by Metcalfe and Metcalfe (1997). The mean congener concentrations in sediment from these analyses are listed in Table 1.

Water

Concentrations of PCB congeners were analysed in 13 water samples from central Lake Ontario in 1992–1993 by Metcalfe and Metcalfe (1997). After collection, samples were passed through glass fibre filters (0.3-μm pore size). Water samples were extracted by partitioning into methylene chloride. The pH of the filtered water was increased prior to extraction to increase the recovery of PCB congeners (Maguire and Tkacz 1989). A 20-L volume of water was extracted with three aliquots of methylene chloride, and the extracts were combined in 4-L amber bottles until a total extract from 160 L of water was collected. The combined extracts were

© 1999 NRC Canada

Table 1. Concentrations of PCDF, PCDD, and PCB congeners in water and sediment from Lake Ontario.

Chemical	log K_{OW}	Water used in model ($\mu g \cdot L^{-1}$)	Sediment ($\mu g \cdot kg^{-1}$)
2,3,7,8-TCDF	5.8[a]	8.0×10^{-8}[e]	0.012[g]
1,2,3,7,8-PCDF	6.79[b]	9.0×10^{-10}[e]	0.002[g]
2,3,4,7,8-PCDF	6.2[a]	1.1×10^{-8}[e]	0.003[g]
1,2,3,4,7,8-HCDF	6.6[a]	3.0×10^{-9}[e]	0.015[g]
1,2,3,6,7,8-HCDF	6.6[a]	5.0×10^{-10}[e]	0.002[g]
1,2,3,7,8,9-HCDF	7.0[c]	7.0×10^{-11}[e]	0.001[g]
2,3,4,6,7,8-HCDF	6.6[a]	7.3×10^{-10}[e]	0.003[g]
2,3,7,8-TCDD	7.0[a]	7.0×10^{-11}[e]	0.005[g]
1,2,3,7,8-PCDD	7.4[a]	5.0×10^{-11}[e]	0.002[g]
1,2,3,4,7,8-HCDD	7.8[a]	2.5×10^{-12}[e]	0.001[g]
1,2,3,6,7,8-HCDD	7.8[a]	2.5×10^{-11}[e]	0.003[g]
1,2,3,7,8,9-HCDD	7.8[c]	1.5×10^{-11}[e]	0.002[g]
PCB 31/28	5.67[d]	2.4×10^{-5}[f]	0.3[h]
PCB 52	5.84[d]	5.0×10^{-5}[c]	9.8[h]
PCB 66	6.20[d]	2.5×10^{-5}[c]	10.3[h]
PCB 90/101	6.38[d]	5.8×10^{-6}[f]	5.1[h]
PCB 118	6.74[d]	4.2×10^{-6}[f]	14.8[h]
PCB 105	6.65[d]	8.0×10^{-7}[f]	18.9[h]
PCB 153	6.92[d]	1.4×10^{-6}[f]	13.3[h]
PCB 138	6.83[d]	1.8×10^{-6}[f]	14.7[h]
PCB 180	7.36[d]	1.0×10^{-9}[c]	6.6[h]
PCB 77	6.36[d]	8.4×10^{-7}[f]	4.1[h]
PCB 126	6.89[d]	3.8×10^{-8}[f]	0.8[h]
PCB 169	7.42[d]	1.2×10^{-8}[f]	0.2[h]

[a]Endicott and Cook (1994).
[b]Sijm et al. (1989).
[c]Estimated.
[d]Hawker and Connell (1988).
[e]Estimated from measured chemical concentrations in netplankton samples comprising primarily zooplankton using eq. 1.
[f]Metcalfe and Metcalfe (1997), corrected for dissolved organic carbon.
[g]DFO, unpublished data.
[h]Average of data from DFO and Metcalfe and Metcalfe (1997).

cleaned up and fractionated on silica gel and carbon (AX-21) columns. The final extracts were analysed for PCB congeners using GC-ECD analysis (Metcalfe and Metcalfe 1997).

It was assumed that this extraction process removed particles greater than 0.3 μm in diameter from the water. Because the water column has organic carbon (OC) containing particles that are smaller than 0.45 μm in diameter, it was assumed that about 85% of the organic carbon (i.e., 0.85·OC) remained in the water sample prior to extraction. This estimate is based on the fact that particulate organic carbon concentrations (defined as particles >0.45 μm in diameter) comprise only about 8.5% of the organic carbon in the water column of Lake Ontario, and the fraction of dissolved organic carbon particles between 0.3 and 0.45 μm in diameter is estimated to be 6.5%. Consequently, the following equation was used to estimate freely dissolved concentrations in water (C_W) from measured water concentrations (C_M):

$$(1) \qquad C_W = \frac{C_M}{1 + 0.85 \cdot OC \cdot K_{OC}}$$

where K_{OC} is the organic carbon – water partition coefficient.

Concentrations of the dioxin and furan congeners in water were estimated from chemical concentrations in netplankton using the steady-state equation described by Morrison et al. (1997) because directly measured concentrations were not available. This equation was used because the netplankton samples were composed primarily of zooplankton species (Kiriluk et al. 1996) and zooplankton biomagnify hydrophobic HAH's. It was assumed that zooplankton did not metabolize any HAH congeners and that the samples were in steady state with water concentrations. To date, there is no evidence that zooplankton metabolize any of the HAH congeners used in this study. Camphens and Mackay (1997) found that plankton from Lake Ontario were in approximately equal fugacities with the water for PCB congeners. Chemical concentrations in netplankton that were below the detection limit were assigned a value of half of the minimum detection limit. Netplankton samples were used to estimate water concentrations because they were the lowest trophic level organisms for which detectable concentrations of most of the dioxin and furan congeners were available. Furthermore, plankton are more likely to reflect chemical concentrations in water compared with sediments because chemical partitions between sediment and water slowly (Baker et al. 1986) compared with plankton and water. Estimated PCDD and PCDF congener concentrations in water are listed in Table 1.

Results

Part 1: verification of model for nonmetabolized PCB congeners

Nonmetabolized PCB congeners

Nine of the 12 PCB congeners used in this study have not been observed to be metabolized to a significant extent by aquatic biota (Niimi 1996). Consequently, PCB's 31/28, 52, 66, 90/101, 118, 105, 153, 138, and 180 were used to verify the bioaccumulation model for the Lake Ontario food web.

Model parameterization

General input parameters that were used to characterize the food web were obtained from the literature and are listed in Morrison et al. (1997) and Tables 2, 3, 4, and 5. Environmental parameters that characterize the open-lake portion of Lake Ontario in 1992–1994 are mean annual water temperature of 8°C (Mackay et al. 1994), dissolved oxygen concentration of 8.6 $mg \cdot L^{-1}$ (Benson and Krause 1980, assuming 75% saturation), dissolved organic carbon concentration of 3×10^{-6} mg $C \cdot L^{-1}$ (Environment Canada STAR database, Environmental Conservation Branch, Ecosystem Health Division, Canada Centre for Inland Waters, P.O. Box 5050, Burlington, ON L7R 4A6, Canada), particulate organic carbon concentration of 2.8×10^{-7} mg $C \cdot L^{-1}$ (Environment Canada STAR database), and suspended sediment concentration of 4.0×10^{-6} mg $C \cdot L^{-1}$ (Mackay et al. 1994). Dietary compositions of benthic invertebrates and fish were determined using literature citations. These diet compositions are reported in Table 5 and, where necessary, were restricted to sediment, phytoplankton, zooplankton, invertebrate, and fish species included in this food web.

Model verification

Figure 1 illustrates the predicted versus observed concentrations of nine nonmetabolized PCB congeners in benthic invertebrates and fish from Lake Ontario. Predicted concentrations in *Mysis*, slimy sculpin, lake trout of ages 1–3+, and lake trout of age 8+ were in good agreement with observed concentrations, as indicated by geometric mean predicted versus observed ratios (C_p/C_o) that were close to unity (range 0.9–1.1). The model tended to underestimate PCB

© 1999 NRC Canada

Table 2. Ingestion rate (G_D), gill ventilation rate (G_W), growth rate (G_R), efficiency of lipid/organic carbon absorption (α), efficiency of food absorption (β), and particle scavenging efficiency (σ) of various biota from Lake Ontario.

	G_D (kg·day^{-1})	G_W (L·day^{-1})	G_R (kg·day^{-1})	α (%)	β (%)	σ (%)
Zooplankton	1.4×10^{-8}[a]	3.7×10^{-3}[a]		72[b]	90[c]	
Chironomidae	1.0×10^{-6}[d]	0.05[d]		60[c]	50[c]	
Gammarus fasciatus	1.9×10^{-6}[d]	0.05e		60[f]	50[c]	
Diporeia hoyi	1.9×10^{-7}[d]	0.05[d]		60[c]	50[c]	
Mysis relicta	2.7×10^{-7}[d]	0.07[d]		52[g]	58[c]	
Crayfish	0.0009[h]	16[d]		60[c]	50[c]	
Zebra mussels						100[i]
Fish	$0.22 \cdot M^{0.85} \exp 0.06 \cdot T$[j]	$(O_{2cons.}/[O_2] \cdot e_{ox}) \cdot 24$[k]	$0.0005 \cdot M^{0.81}$	83[m]	50–60[c]	

[a]Estimated from Peters and Downing (1984).
[b]Conover (1966).
[c]Estimated.
[d]Estimated from Morrison (1995).
[e]Estimated from *Gammarus pulex* (Rumpus and Kennedy 1974).
[f]Estimated from *Hyalella azteca* (Hargrave 1970).
[g]Lasenby and Langford (1973).
[h]Martin and Corkum (1995).
[i]Reeders et al. (1989).
[j]Weininger (1978), M = kg wet weight, T = temperature (°C).
[k]$\log O_{2cons.} = -0.76 + 0.877 \log M$ mg·h^{-1}, M = g wet weight (Thurston and Gehrke 1993); efficiency of oxygen uptake(e_{ox}) = 0.45.
[l]Thomann et al. (1992).
[m]Place (1992).

Table 3. Chemical assimilation efficiencies from food (E_D) and via the gills/respiratory surface (E_W).

Chemical	E_D	E_W[h]
2,3,7,8-TCDF	0.51[a]	0.54
1,2,3,7,8-PCDF	0.42[b]	0.45
2,3,4,7,8-PCDF	0.42[c]	0.45
1,2,3,4,7,8-HCDF	0.31[d]	0.34
1,2,3,6,7,8-HCDF	0.31[d]	0.34
1,2,3,7,8,9-HCDF	0.31[d]	0.34
2,3,4,6,7,8-HCDF	0.31[d]	0.34
2,3,7,8-TCDD	0.41[e]	0.44
1,2,3,7,8-PCDD	0.42[b]	0.45
1,2,3,4,7,8-HCDD	0.31[f]	0.34
1,2,3,6,7,8-HCDD	0.31[d]	0.34
1,2,3,7,8,9-HCDD	0.31[d]	0.34
PCB congeners	0.72[g]	0.75[i]

[a]Average from Muir et al. (1992*b*).
[b]Estimated from Muir et al. (1990).
[c]Muir et al. (1990).
[d]Estimated from Muir et al. (1986), Muir and Yarechewski (1988), and Gobas et al. (1988).
[e]Average of Hawkes and Norris (1977), Gobas et al. (1988), and Kleeman et al. (1986).
[f]Average of Muir et al. (1986), Muir and Yarechewski (1988), and Gobas et al. (1988).
[g]Average of Goerke and Ernst (1977), Klump et al. (1987), Landrum and Poore (1988), Jahan-Parwar et al. (1990), Klump et al. (1991), and Bruner et al. (1994).
[h]Estimated from E_f values.
[i]Norstrom et al. (1976).

congener concentrations in *Mysis*, alewife, and rainbow smelt (C_p/C_o = 0.8). PCB 105 was the only congener that was underestimated consistently by the model for *Mysis*, alewife, and rainbow smelt. This indicates that the concentration of this PCB congener measured in water and sediment was lower than the mean concentration experienced by these biota collected in this study. The lack of relationship between PCB congener structure and bioaccumulation agrees with the observations of Niimi (1996). Overall, 86% of model predictions were within a factor of 2 and 100% of predictions were within a factor of 10 of observed concentrations (Fig. 1). These results indicate that the steady-state model was providing realistic estimates of bioaccumulation of nonmetabolized PCB congeners by a variety of benthic invertebrate species and fish in the Lake Ontario ecosystem.

Part 2: estimation of chemical metabolic rates

It has been observed that aquatic biota are capable of metabolizing certain HAH congeners (see Niimi 1996). The ability of fish and crustaceans to metabolize PCB's 77 and 126 has been suggested by several researchers based on the lower proportions of these congeners compared with the persistent PCB 153 (Kannan et al. 1995; Metcalfe and Metcalfe 1997). PCB 169 also appeared to be nonpersistent in Lake Ontario fish, although the sample size was too small to be conclusive (Metcalfe and Metcalfe 1997). Based on the conclusions of Niimi (1996), the ability of fish and invertebrates to metabolize the other PCB congeners examined in this study appears to be very limited. Presently, no information exists on the metabolic capabilities of fish and invertebrates for the other PCDD's and PCDF's in this study. HAH metabolic rates for the coplanar PCB's 77, 126, and 169 and the PCDD and PCDF congeners had to be estimated because no published data on measured values exist. A "best-fit" approach, whereby the sum of relative squared errors (SRSE) between observed (C_o) and predicted data (C_p) (SRSE = $\Sigma((C_o - C_p)/C_o)$) was minimized, was used to estimate the metabolic rates from the observed data and the previously verified model.

Figure 2 illustrates the best fit for the seven PCDD, five PCDF, and three PCB congeners in benthic invertebrates and fish from Lake Ontario. Predicted concentrations of PCB's 77, 126, and 169 in *Diporeia* were in good agreement with observed concentrations as indicated by C_p/C_o values of 1.0. The model tended to overestimate concentrations of PCB's

© 1999 NRC Canada

Fig. 1. Observed concentrations of nonmetabolized PCB congeners (±95% confidence intervals) versus predicted congener concentrations in Lake Ontario biota. The solid line represents the ideal fit. The dotted lines represent twice the ideal fit and the dashed lines represent 10 times the ideal fit.

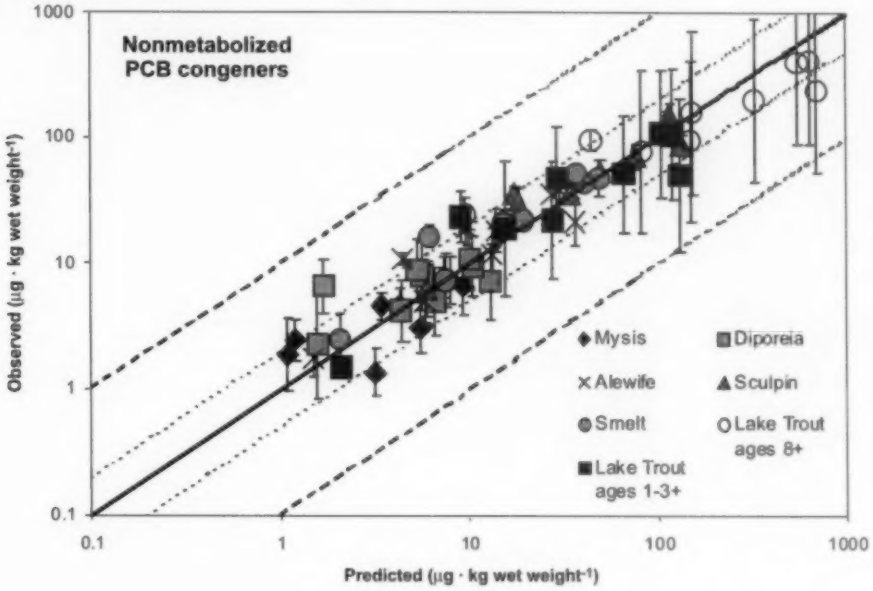

Table 4. Characteristics of Lake Ontario biota (whole animal) used in the model.

Sample	*n*	Mean no. per sample	Weight (g wet)	SD	% lipid	SD
Zooplankton	nm		11.4 µg dry wt.[a]		3.0[b]	
Gammarus	nm		0.01		2.5	
Chironomidae	nm		0.005		6.0	
Diporeia	11	—[c]	0.005		8.8	5.04
Mysis	9	—[c]	0.012		7.0	1.46
Zebra mussels	nm		0.11[d]		2.5	
Crayfish	nm		1.8[d]		2.5	
YOY fish[e]	nm		0.4		2.1	
Alewife	14	3	22.0	7.93	4.9	2.23
Rainbow smelt	10	20	14.5	4.28	6.2	1.75
Slimy sculpin	13	15	9.1	2.83	9.6	2.34
Common carp	nm		500.0		9.0	
Channel catfish	nm		500.0		4.0	
White perch	nm		679.0		7.0	
Yellow perch	nm		802.0		7.0	
Lake trout ages 1–3+	3	1	460.0	444.91	4.2	3.72
Lake trout age 8+	10	1	5430.0	1698.76	21.4	6.57
Chinook salmon	nm		4200.0		9.0	
Coho salmon (j)	nm		450.0		8.0	
Coho salmon (a)	nm		4000.0		9.0	
Rainbow trout (j)	nm		450.0		8.0	
Rainbow trout (a)	nm		4000.0		8.0	
Brown trout (j)	nm		400.0		8.0	
Brown trout (a)	nm		4000.0		8.0	

Note: j, juvenile; a, adult; nm, not measured.

[a]Estimated from Peters and Downing (1984).

[b]Estimated from lipid levels measured in netplankton from Lake Ontario that consisted primarily of zooplankton (see Kiriluk et al. (1996) for sample composition).

[c]Equivalent to 5 g wet wt.

[d]Weight without shell or exoskeleton.

[e]Primarily alewife and rainbow smelt.

© 1999 NRC Canada

Fig. 2. Observed concentrations of metabolized PCB, PCDD, and PCDF congeners (±95% confidence intervals) versus predicted congener concentrations in Lake Ontario biota. The solid line represents the ideal fit. The dotted line represent twice the ideal fit and the dashed lines represent 10 times the ideal fit.

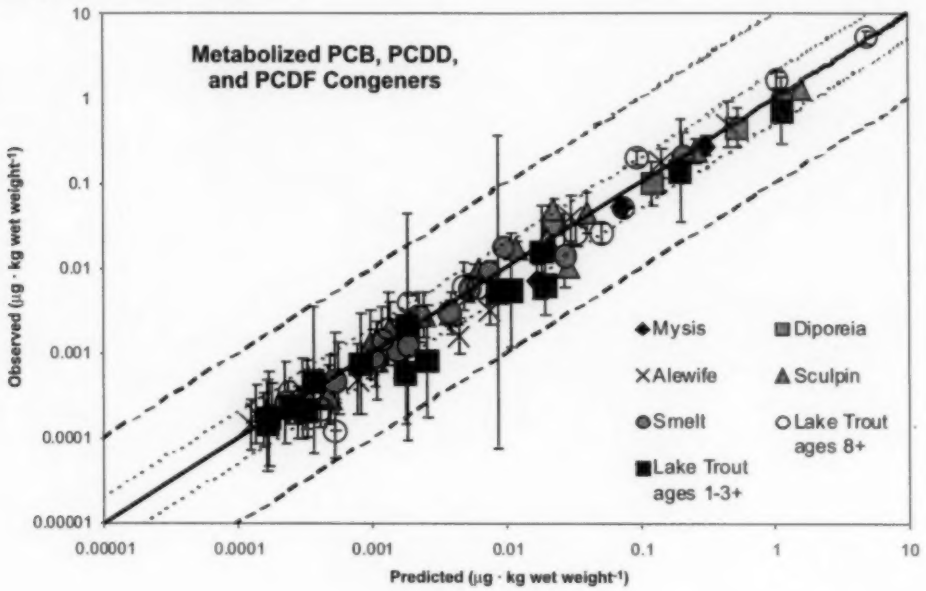

Table 5. Diet compositions (% volume) for Lake Ontario biota.

	Sed.	Phy.	Zoo.	Gam.	Chir.	Dip.	Mys.	ZM	Cray.	YOY	Ale.	Sm.	Scul.	Source[b]
Zooplankton		100												
Gammarus	20	50	30											1
Chironomidae	30	70												1
Diporeia	35	55	10											1
Mysis	20	40	15			25								2
Zebra mussels	25	60	15											3
Crayfish	15	25		10	5			45						4
YOY fish[a]			100											5
Alewife			80			15	5							6
Rainbow smelt			80		5	5	10							7
Slimy sculpin			15		20	45	20							7
Common carp	5	10		40	10	5		20	10					8
Channel catfish				10	10	10		40		20			10	8
White perch			40	10	5	5	10	10		20				8
Yellow perch			20	20	5	5	5	15		30				8
Lake trout ages 1–3+, coho salmon (450 g), rainbow trout (450 g), brown trout (400 g)				10		15	15			27	20	10	3	8
Lake trout age 8+, chinook salmon, coho salmon (4000 g), rainbow trout (4000 g), brown trout (4000 g)										35	50	10	5	8
Chinook salmon										85	7	8		8

Note: Sed., sediment/detritus; Phy., phytoplankton; Zoo., zooplankton; Gam., *Gammarus*; Chir., Chironomidae; Dip., *Diporeia*; Mys., *Mysis*; ZM, zebra mussels; Cray., crayfish; YOY, YOY fish (rimarily alewife and rainbow smelt); Ale., alewife; Sm., rainbow smelt; Scul., slimy sculpin.

[a]Primarily alewife and rainbow smelt.

[b]1, Plankton used as a surrogate for *Dreissena* pseudofaeces; 2, estimated from Johannsson et al. (1994); 3, sediment used as a surrogate for resuspended sediment; 4, estimated from Saffran (1993), MacIsaac (1994), and Martin and Corkum (1995); 5, estimated from Wu and Culver (1992); 6, estimated from Mills et al. (1995) and Rand et al. (1995); 7, estimated from DFO diet data; 8, estimated.

© 1999 NRC Canada

Table 6. Chemical metabolic rates (k_M, day^{-1}) for Lake Ontario biota used in the model.

Chemical	Crustaceans	YOY fish and rainbow smelt	Alewife	Slimy sculpin	All other fish
Furans					
2,3,7,8-TCDF	0	0	0	0	0
1,2,3,7,8-PCDF	1.0×10^{-7}	1.0×10^{-5}	5.0×10^{-4}	1.0×10^{-5}	1.0×10^{-3}
2,3,4,7,8-PCDF	0	0	0	0	0
1,2,3,4,7,8-HCDF	1.0×10^{-6}	2.0×10^{-4}	5.0×10^{-4}	2.5×10^{-5}	2.5×10^{-3}
1,2,3,6,7,8-HCDF	1.0×10^{-7}	2.5×10^{-5}	5.0×10^{-4}	2.5×10^{-5}	5.0×10^{-3}
1,2,3,7,8,9-HCDF	1.0×10^{-7}	2.5×10^{-4}	5.0×10^{-4}	2.5×10^{-4}	2.5×10^{-3}
2,3,4,6,7,8-HCDF	0	1.0×10^{-4}	5.0×10^{-4}	1.0×10^{-4}	5.0×10^{-3}
Dioxins					
2,3,7,8-TCDD	1.0×10^{-7}	1.0×10^{-7}	1.0×10^{-5}	1.0×10^{-7}	1.0×10^{-5}
1,2,3,7,8-PCDD	1.0×10^{-7}	7.5×10^{-5}	2.0×10^{-4}	2.0×10^{-4}	2.0×10^{-4}
1,2,3,4,7,8-HCDD	1.0×10^{-7}	1.0×10^{-4}	2.5×10^{-4}	2.5×10^{-4}	2.5×10^{-3}
1,2,3,6,7,8-HCDD	1.0×10^{-7}	1.0×10^{-4}	5.0×10^{-4}	2.5×10^{-4}	2.5×10^{-3}
1,2,3,7,8,9-HCDD	1.0×10^{-7}	2.5×10^{-4}	1.0×10^{-3}	5.0×10^{-4}	7.5×10^{-3}
PCB's					
31/28	0	0	0	0	0
52	0	0	0	0	0
66	0	0	0	0	0
90/101	0	0	0	0	0
118	0	0	0	0	0
105	0	0	0	0	0
153	0	0	0	0	0
138	0	0	0	0	0
180	0	0	0	0	0
77	2.5×10^{-6}	1.0×10^{-4}	2.0×10^{-4}	2.5×10^{-4}	1.0×10^{-3}
126	2.5×10^{-6}	1.0×10^{-4}	2.0×10^{-4}	5.0×10^{-4}	2.5×10^{-3}
169	5.0×10^{-6}	1.0×10^{-3}	2.0×10^{-3}	1.0×10^{-3}	7.5×10^{-3}

77, 126, and 169 in *Mysis* (C_p/C_o = 1.5). Predicted concentrations of the dioxin, furan, and three PCB congeners in alewife, rainbow smelt, slimy sculpin, and lake trout (age 8+) were in good agreement with observed concentrations with a C_p/C_o of 1.0. Predicted concentrations of the dioxin, furan, and three PCB congeners in lake trout of ages 1–3+ tended to be overestimated by the model (C_p/C_o = 1.5). There was no relationship between HAH congeners and the predictability of the model among aquatic biota. This suggests that model input parameters did not accurately describe the lake trout of ages 1–3+ sampled in this study rather than systematic differences in the partitioning properties of the congeners related to structure. Overall, the model predictions were in general agreement with observed concentrations as indicated by the fact that 89% of model predictions were within a factor of 2 and 100% of predictions were within a factor of 10 (Fig. 2).

Metabolic rates for the HAH congeners and species used in this study are listed in Table 6. As indicated by the literature review by Niimi (1996), when it has been observed at all, HAH metabolism by aquatic biota appears to be slow. The metabolic rates, estimated for "all other fish" (Table 6) in this study, were compared with overall elimination rate constants measured for PCB 77 (Coristine et al. 1996) and 2,3,7,8-TCDD (Branson et al. 1985) in rainbow trout (*Oncorhynchus mykiss*). The percentages of the overall elimination rate constants described by the metabolic rate constants were 6.8 and 0.02–0.8% for PCB 77 and 2,3,7,8-TCDD, respectively. The percentages of the overall elimination rate constants, described by the k_M for young-of-the-year (YOY) fish and rainbow smelt, for PCB's 77, 126, and 169 measured in zebrafish (*Brachydanio rerio*) (Fox et al. 1994) were 4.5, 1.0, and 13%, respectively. Branson et al. (1985) measured the elimination rate constant for 2,3,7,8-TCDD in fathead minnow (*Pimephales promelas*). The metabolic rate constant for YOY fish and rainbow smelt ranged from 8.3×10^{-4} to 7.7×10^{-4}% of these elimination rate constants. Hence, the metabolic rate constants estimated in this study described a very small percentage of total chemical elimination by Lake Ontario aquatic biota. Other important mechanisms of elimination captured by the model include elimination via respiratory surfaces and fecal egestion (Morrison et al. 1997). This observation agrees with the qualitative observations of HAH metabolism by aquatic biota, namely that rates of metabolism are slow.

Part 3: estimation of congener concentrations in other fish

The calibrated food web bioaccumulation model was used to predict metabolized and nonmetabolized HAH congener concentrations in invertebrate and fish species that are common to Lake Ontario but for which no published data on measured values exist. Table 4 lists the weights and whole-animal mass fractions of lipid of these biota, which were used to parameterize the model. Other model input parameters are listed in Tables 2–5.

Predicted chemical concentrations in these biota were expressed as the logarithm of BAF (log BAF) and were com-

© 1999 NRC Canada

Table 7. Predicted and observed (ob) logarithms of the BAF's (log BAF) for PCB, PCDF, and PCDD congeners in Lake Ontario biota.

Chemical	log K_{OW}	d (ob)	g	ch	zm	cr	lt (j) (ob)	YOY	cf	cp	wp	yp	chs	cs (j)	cs (a)	rt (j)	rt (a)	bt (j)	bt (a)	lt (a) (ob)
PCB 31/28	5.67	5.0	4.7	5.2	4.3	4.8	4.8	4.4	5.4	5.1	5.0	5.0	5.3	5.2	5.3	5.2	5.2	5.2	5.2	6.0
2,3,7,8-TCDF	5.8	5.2	4.7	5.0	4.3	4.7	4.8	4.6	5.4	5.2	5.1	5.2	5.5	5.4	5.5	5.4	5.5	5.4	5.5	5.5
PCB 52	5.84	4.9	4.8	5.2	4.4	4.8	5.7	4.7	5.5	5.3	5.3	5.3	5.7	5.5	5.6	5.5	5.6	5.5	5.6	6.3
2,3,4,7,8-PCDF	6.21	5.7	5.2	5.6	4.8	5.3	5.7	5.2	6.0	5.9	5.8	5.9	6.3	6.1	6.3	6.1	6.2	6.1	6.2	6.4
PCB 66	6.22	5.5	5.2	5.5	4.8	5.3	5.9	5.3	6.1	6.0	5.9	6.0	6.5	6.3	6.5	6.3	6.4	6.3	6.4	6.6
PCB 77	6.36	5.7	5.9	6.7	5.5	6.2	5.9	4.7	6.7	6.6	6.3	6.4	6.6	6.3	6.6	6.3	6.5	6.3	6.5	6.8
PCB 90/101	6.38	6.2	5.8	6.5	5.4	6.0	6.9	5.7	6.9	6.9	6.6	6.6	7.2	7.0	7.2	7.0	7.1	7.0	7.1	7.4
1,2,3,4,7,8-HCDF	6.61	6.4	6.0	6.9	5.8	6.4	5.8	4.5	6.3	6.4	6.0	6.1	6.3	5.8	6.3	5.8	6.3	5.8	6.3	6.5
1,2,3,6,7,8-HCDF	6.62	6.4	6.1	6.8	5.8	6.4	5.6	5.3	6.0	6.2	5.8	5.9	6.3	5.8	6.3	5.8	6.3	5.8	6.3	6.6
2,3,4,6,7,8-HCDF	6.63	6.3	6.1	6.8	5.7	6.4	5.8	4.7	6.0	6.1	5.8	5.9	6.1	5.7	6.1	5.7	6.0	5.7	6.0	6.1
PCB 105	6.65	6.9	6.1	6.8	5.8	6.3	7.4	6.3	7.3	7.4	7.1	7.2	7.8	7.6	7.8	7.6	7.7	7.5	7.7	8.0
PCB 118	6.74	6.2	6.2	6.9	5.9	6.5	7.1	6.5	7.4	7.6	7.3	7.4	8.1	7.8	8.0	7.8	7.9	7.8	7.9	7.8
1,2,3,7,8-PCDF	6.79	6.7	6.0	6.6	5.8	6.3	5.8	5.8	6.4	6.5	6.3	6.3	6.7	6.3	6.7	6.3	6.7	6.3	6.7	6.8
PCB 138	6.83	6.8	6.4	7.2	6.2	6.8	7.8	6.6	7.7	7.9	7.5	7.6	8.3	8.0	8.3	8.0	8.2	8.0	8.2	8.4
PCB 126	6.89	6.4	6.6	7.6	6.6	7.1	6.6	5.6	7.3	7.3	7.0	7.1	7.3	6.8	7.3	6.8	7.3	6.8	7.3	7.7
PCB 153	6.92	6.8	6.5	7.3	6.3	6.9	7.9	6.8	7.8	8.0	7.7	7.8	8.5	8.2	8.5	8.2	8.4	8.2	8.4	8.5
1,2,3,7,8,9-HCDF	7.01		6.7	7.5	6.5	7.0	6.5	5.0	6.9	7.0	6.7	6.8	6.8	6.6	6.8	6.6	6.7	6.5	6.7	6.2
2,3,7,8-TCDD	7.02		7.2	8.1	7.1	7.7	8.0	6.9	8.5	8.7	8.2	8.3	8.9	8.7	8.9	8.7	8.8	8.7	8.8	8.9
PCB 180	7.36	9.7	9.2	10.2	9.3	9.7	10.7	7.7	10.7	11.0	10.4	10.5	11.4	11.1	11.4	11.1	11.2	11.1	11.2	11.3
1,2,3,7,8-PCDD	7.4	7.3	7.2	7.9	7.2	7.6	7.2	6.1	8.1	8.1	7.9	7.9	7.9	7.8	7.9	7.8	7.8	7.8	7.8	8.1
PCB 169	7.42	6.5	6.7	7.5	7.0	7.3	6.1	5.5	7.0	7.0	6.9	6.9	6.8	6.2	6.8	6.2	6.8	6.2	6.8	7.2
1,2,3,4,7,8-HCDD	7.81	8.8	8.0	8.8	8.2	8.5	7.8	6.6	8.2	8.3	8.0	8.0	8.1	7.8	8.1	7.8	8.1	7.8	8.1	8.0
1,2,3,6,7,8-HCDD	7.82	7.7	7.7	8.5	7.8	8.2	7.5	6.6	7.8	7.9	7.7	7.7	7.8	7.5	7.8	7.5	7.8	7.5	7.8	8.2
1,2,3,7,8,9-HCDD	7.83	7.8	7.7	8.5	7.9	8.2	7.0	6.2	7.4	7.5	7.3	7.3	7.1	7.0	7.1	7.0	7.1	7.0	7.1	7.4

Note: d, *Diporeia*; g, *Gammarus*; ch, Chironomidae; zm, zebra mussels; cr, crayfish; lt (j), juvenile lake trout; YOY, YOY fish; cf, channel catfish; cp, common carp; wp, white perch; yp, yellow perch; chs, chinook salmon; cs (j), juvenile coho salmon; cs (a), adult coho salmon; rt (j), juvenile rainbow trout; rt (a), adult rainbow trout; bt (j), juvenile brown trout; bt (a), adult brown trout; lt (a), adult lake trout.

© 1999 NRC Canada

Table 8. Change in model output (%) due to a 10% decrease in input parameter values.

	log K_{OW}	C_W	E_W	G_W	C_D	E_D	G_D	G_R	k_M	α	β	ϕ	V_{SS}	σ
Zebra mussels														
PCB 31/28	5.67	–7.5	3.9		–3.7	–3.5				–0.7	–0.2	–10.1	–3.5	–3.5
PCB 77	6.36	–2.9	8.5		–8.5	–7.8				–3.2	–0.9	–10.1	–7.7	–7.7
1,2,3,4,7,8-HCDF	6.6	–3.6	8.2		–8.8	–7.6				–4.9	–1.4	–10.2	–7.4	–7.4
2,3,7,8-TCDD	7.0	–0.8	7.8		–10.0	–7.4				–9.9	–2.8	–10.0	–7.3	–7.3
1,2,3,6,7,8-HCDD	7.8	–2.8	3.8		–11.0	–3.9				–22.7	–10.0	–10.8	–3.2	–3.2
Gammarus														
PCB 31/28	5.67	–4.6	6.4	–5.5	–17.9	–6.1	–15.2		0.0	–13.2	–12.3	–10.1		
PCB 77	6.36	–2.1	3.2	–18.3	–26.8	–5.6	–22.4		2.4	–23.0	–21.7	–7.8		
1,2,3,4,7,8-HCDF	6.6	–3.1	2.5	–21.2	–29.1	–5.2	–24.3		2.6	–25.8	–24.5	–7.8		
2,3,7,8-TCDD	7.0	–0.9	1.6	–28.9	–36.7	–2.0	–30.6		0.3	–35.3	–33.7	–9.3		
1,2,3,6,7,8-HCDD	7.8	–3.9	1.6	–30.7	–39.8	–2.3	–32.7		0.6	–39.1	–40.5	–11.0		
Zooplankton														
PCB 31/28	5.67	–10.0	2.2	2.2	–2.1	–2.0	–2.0			–0.2	–0.7	–10.0		
PCB 77	6.36	–10.0	5.9	5.9	–5.7	–5.3	–5.3			–0.9	–3.1	–10.0		
1,2,3,4,7,8-HCDF	6.6	–10.0	6.9	6.9	–6.8	–6.3	–6.3			–1.4	–4.9	–10.0		
2,3,7,8-TCDD	7.0	–10.0	7.8	7.8	–8.5	–7.2	–7.2			–3.3	–10.7	–10.0		
1,2,3,6,7,8-HCDD	7.8	–10.0	5.2	5.2	–9.7	–5.2	–5.2			–11.0	–30.1	–10.0		
Rainbow smelt														
PCB 31/28	5.67	–7.9	9.4	10.2	–9.4	–8.7	–8.2	1.1	0.0	–5.1	–0.9	–15.2		
PCB 77	6.36	–3.5	7.7	10.5	–10.0	–13.8	–6.6	9.7	6.5	–5.3	4.3	–11.4		
1,2,3,4,7,8-HCDF	6.6	–4.6	5.4	6.1	–9.1	–14.5	–6.1	10.9	10.2	–0.9	5.3	–9.6		
2,3,7,8-TCDD	7.0	–1.4	6.2	18.5	–9.1	–10.5	0.9	16.7	0.8	–20.5	1.2	–11.4		
1,2,3,6,7,8-HCDD	7.8	–5.6	3.2	0.6	–13.3	–13.5	–6.3	8.7	10.5	–11.8	–12.7	–9.3		

pared with log BAF's measured in similar organisms from Lake Ontario. A BAF is the ratio of the wet weight concentration of chemical in the organism to the concentration of chemical dissolved in water. Of the benthic invertebrate species, Chrionomidae tended to have the highest BAF's, followed by crayfish and *Diporeia* (Table 7). Higher BAF's in these benthic invertebrates may be attributed to the high proportions of contaminated detrital material in their diet or exposure to contaminants in interstitial water (Landrum and Robbins 1990). Higher contaminant levels in crayfish are attributed to the higher trophic status of crayfish compared with the other benthic invertebrates (see Table 5). Zebra mussels (*Dreissena polymorpha*) had the lowest BAF's for 17 of 24 congeners. Filter-feeding zebra mussels are predicted to be the least contaminated benthic invertebrate due to the high proportion of phytoplankton in their diet.

The BAF's for rainbow smelt, common carp (*Cyprinus carpio*), channel catfish (*Ictalurus punctatus*), white perch (*Morone americana*), and yellow perch (*Perca flavescens*) fell between the observed BAF's for YOY fish and slimy sculpin (Table 7). The diet of YOY fish comprised zooplankton, whereas the diet of sculpin comprised primarily benthic invertebrates. The benthic invertebrate sampled in this study (*Diporeia*) was more contaminated than the zooplankton, which resulted in higher BAF's in slimy sculpin compared with YOY fish. Rainbow smelt, common carp, channel catfish, white perch, and yellow perch had diets that included different proportions of plankton, benthic invertebrates, and fish. Bioaccumulation from these exposure routes resulted in BAF's that mostly fell between those of YOY fish and slimy sculpin.

The log BAF's for 2,3,7,8-TCDD and 2,3,7,8-TCDF for the fish ranged from 6.9 to 8.7 and from 4.6 to 5.4, respectively. Field-measured log BAF's for 2,3,7,8-TCDD and 2,3,7,8-TCDF in suckers collected at a number of sites in Canada ranged from 5.3 to 7.7 and from 4.8 to 7.9 and in whitefish ranged from 6.1 to 7.9 and from 5.9 to 7.4, respectively (Muir et al. 1992*a*). The predicted BAF's in this study fell within these ranges of field-measured values.

Most of the predicted BAF's in the salmonids were between the observed BAF's of small (460 g) and large (5430 g) lake trout (Table 7). The predicted BAF's for coho salmon (*Oncorhynchus kisutch*) (450 g) and rainbow trout (450 g) and the predicted BAF's of large coho salmon (4000 g), rainbow trout (4000 g), and brown trout (*Salmo trutta*) (4000 g) were the same, respectively; hence, only the BAF's for small coho salmon (450 g), small brown trout (400 g). and large rainbow trout (4000 g) are listed (Table 7). Of the salmonid species, lake trout of age 8+ and chinook salmon (*Oncorhynchus tshawytscha*) were predicted to be the most contaminated. High contaminant levels in lake trout are attributed to their high lipid levels compared with other salmonids (21% lipid in lake trout versus 8–15% in other salmonids) and to the fact that they were the largest fish in this study (see Table 4). Higher contaminant levels in chinook salmon are attributed to their comparatively larger size in the model (see Table 4).

Discussion

A sensitivity analysis was performed on the model to identify the most important model inputs affecting the concentration of representative HAH congeners in zooplankton and a representative filter-feeding benthic invertebrate (ze-

© 1999 NRC Canada

bra mussel), detritivorous benthic invertebrate (*Gammarus*), and a fish species (rainbow smelt) (Table 8). In separate simulations, the value of each parameter was lowered by 10% and the effect of this change on model output was evaluated. Zooplankton, zebra mussels, and *Gammarus* exhibited greater sensitivity to changes in model input parameters describing chemical uptake from diet as the K_{OW} of the congener increased, whereas fish exhibited no consistent response to increasing K_{OW}. For zooplankton, the concentration of chemical in water was generally the most sensitive parameter and was equally sensitive for all congeners. The chemical concentration in the diet (C_D), the assimilation efficiency of lipid (α), and the fraction of ingested diet absorbed by the organism (β) were generally the most sensitive input parameters for *Gammarus*. The C_D and the lipid composition of the organism (ϕ) were generally the most sensitive parameters for zebra mussels. The parameters describing growth rate (G_R), chemical metabolic rate (k_M), gill ventilation rate (G_W), C_D, and ϕ were approximately equisensitive in the model for fish.

There are several assumptions and limitations with this modelling approach that may have resulted in discrepancies between predicted and observed congener concentrations. For instance, diet compositions of Lake Ontario biota were derived from literature citations and may not accurately represent the diets of the biota captured in this study. Concentrations of dioxin and furan congeners in water were estimated from netplankton concentrations and were assumed to be in steady state, although there is evidence to suggest that this assumption is not always true (Swackhamer and Skoglund 1993). These estimated concentrations may not accurately reflect average concentrations experienced by all biota. Furthermore, chemical metabolic rate constants are best-fit estimates and need to be verified with experimental measurements. This modelling approach will become more robust as more data on dioxin and furan congeners in water become available and experimental measurements of chemical metabolic rate constants become available.

Despite the assumptions, this food web bioaccumulation model provided realistic estimates of HAH congener concentrations in a variety of invertebrate and fish species from Lake Ontario. Furthermore, this modelling approach provided estimates of chemical metabolic rates for 15 HAH congeners that can be validated by experimental measurements. The calibrated model can be used to assess how changes in food web structure and chemical loadings affect chemical transfer in the Lake Ontario food web. Other uses for this model are the development of indicators of remediation success, performing biological risk assessments, and management of fisheries resources (i.e., recreational and commercial consumption advisories).

Acknowledgements

We would like to acknowledge the financial support provided by the Canadian Chlorine Coordinating Committee to C.D. Metcalfe at Trent University (Principle Investigator) and the DFO, Green Plan Toxic Chemicals Program, to D.M. Whittle. Many thanks go to M. Keir, R. Kiriluk, A. Carswell, and S. Huestis (deceased) at GLLFAS for their technical support.

References

Baker, J.E., Capel, P.D., and Eisenreich, S.J. 1986. Influence of colloids on sediment–water partition coefficients of polychlorobiphenyl congeners in natural waters. Environ. Sci. Technol. **20**: 1136–1143.

Benson, B.B., and Krause, D., Jr. 1980. The concentration and isotopic fractionation of gases dissolved in freshwater in equilibrium with the atmosphere. Oxygen. Limnol. Oceanogr. **25**: 662–671.

Branson, D.R., Takahashi, I.T., Parker, W.M., and Blau, G.E. 1985. Bioconcentration kinetics of 2,3,7,8-tetrachlorodibenzo-*p*-dioxin in rainbow trout. Environ. Toxicol. Chem. **4**: 779–788.

Bruner, K.A., Fisher, S.W., and Landrum, P.F. 1994. The role of the zebra mussel, *Dreissena polymorpha*, in contaminant cycling: II. Zebra mussel contaminant accumulation from algae and suspended particles, and transfer to the benthic invertebrate, *Gammarus fasciatus*. J. Gt. Lakes Res. **20**: 735–750.

Camphens, J., and Mackay, D. 1997. Fugacity-based model of PCB bioaccumulation in complex aquatic food webs. Environ. Sci. Technol. **31**: 577–583.

Conover, R.J. 1966. Factors affecting the assimilation of organic matter by zooplankton and the question of superfluous feeding. Limnol. Oceanogr. **11**: 346–354.

Coristine, S., Haffner, G.D., Ciborowski, J.J., Lazar, R., Nanni, M., and Metcalfe, C.D. 1996. Elimination rates of selected di-*ortho*, mono-*ortho* and non-*ortho* substituted polychlorinated biphenyls in rainbow trout (*Oncorhynchus mykiss*). Environ. Toxicol. Chem. **15**: 1382–1387.

Endicott, D.D., and Cook, P.M. 1994. Modeling the partitioning and bioaccumulation of TCDD and other hydrophobic organic chemicals in Lake Ontario. Chemosphere, **28**: 75–87.

Fox, K., Zauke, G.-P., and Butte, W. 1994. Kinetics of bioconcentration and clearance of 28 polychlorinated biphenyl congeners in zebrafish (*Brachydanio rerio*). Ecotoxicol. Environ. Saf. **28**: 99–109.

Gobas, F., Muir, D.C.G., and Mackay, D. 1988. Dynamics of dietary bioaccumulation and faecal elimination of hydrophobic organic chemicals in fish. Chemosphere, **17**: 943–962.

Goerke, H., and Ernst, W. 1977. Fate of ^{14}C-labelled di-, tri-, and pentachlorobiphenyl in the marine annelid *Nereis virens*. I. Accumulation and elimination after oral administration. Chemosphere, **9**: 551.

Government of Canada. 1991. Toxic chemicals in the Great Lakes and associated effects. Environment Canada, 25 St. Clair Ave. E, 6th Floor, Toronto, ON M4T 1M2.

Hargrave, B.T. 1970. The utilization of benthic microflora by *Hyalella azteca* (Amphipoda). J. Anim. Ecol. **39**: 427–437.

Hawker, D.W., and Connell, D.W. 1988. Octanol–water partition coefficients of polychlorinated biphenyl congeners. Environ. Sci. Technol. **22**: 382–387.

Hawkes, C.L., and Norris, L.A. 1977. Chronic oral toxicity of 2,3,7,8-tetrachlorodibenzo-*p*-dioxin (TCDD) to rainbow trout. Trans. Am. Fish. Soc. **106**: 641–645.

Huestis, S.Y., Servos, M.R., Sergeant, D.B., Leggett, M., and Dixon, D.G. 1995. Methods for the determination of organochlorine pesticides, polychlorinated biphenyl congeners and chlorinated dibenzo-*p*-dioxins and furans in fish. Can. Tech. Rep. Fish. Aquat. Sci. No. 2044.

International Joint Commission. 1978. Great Lakes Water Quality Agreement of 1978. International Joint Commission, Windsor, Ont.

Jahan-Parwar, B., Wood, L.W., and Bush, B. 1990. Assimilation of

© 1999 NRC Canada

polychlorinated biphenyls by a marine mollusc and comparison with a rat. Arch. Environ. Contam. Toxicol. **19**: 944–951.

Johannsson, O.E., Rudstam, L.G., and Lasenby, D.C. 1994. *Mysis relicta*: assessment of metalimnetic feeding and implications for competition with fish in Lakes Ontario and Michigan. Can. J. Fish. Aquat. Sci. **51**: 2591–2602.

Kannan, N., Reusch, T.B.H., Schulz-Bull, D.E., Petrick, G., and Duinker, J.C. 1995. Chlorobiphenyls: model compounds for metabolism in food chain organisms and their potential use as ecotoxicological stress indicators by application of the metabolic slope concept. Environ. Toxicol. Chem. **29**: 1851–1859.

Kiriluk, R.M., Gorrie, J.F., Carswell, A.A., Whittle, D.M., and Keir, M.J. 1996. A guide to the Great Lakes fisheries specimen bank data base (1977 to 1994). Can. Data Rep. Fish. Aquat. Sci. No. 973.

Kleeman, J.M., Olson, J.R., Chen, S.M., and Peterson, R.E. 1986. Metabolism and disposition of 2,3,7,8-tetrachlorodibenzo-*p*-dioxin in rainbow trout. Toxicol. Appl. Pharmacol. **83**: 391–401.

Klump, J.V., Krezoski, J.R., Smith, M.E., and Kaster, J.L. 1987. Dual tracer studies of the assimilation of an organic contaminant from sediments by deposit feeding oligochaetes. Can. J. Fish. Aquat. Sci. **44**: 1574–1583.

Klump, J.V., Kaster, J.L., and Sierszen, M.E. 1991. *Mysis relicta* assimilation of hexachlorobiphenyl from sediments. Can. J. Fish. Aquat. Sci. **48**: 284–289.

Landrum, P.F., and Poore, R. 1988. Toxicokinetics of selected xenobiotics in *Hexagenia limbata*. J. Gt. Lakes Res. **14**: 427–437.

Landrum, P.F., and Robbins, J.A. 1990. Bioavailability of sediment-associated contaminants to benthic invertebrates. *In* Sediments: chemistry and toxicity of in-place pollutants. Lewis Publ., Chelsea, Mich. Chap. 8. pp. 237–263.

Lasenby, D.C., and Langford, R.R. 1973. Feeding and assimilation of *Mysis relicta*. Limnol. Oceanogr. **18**: 280–285.

MacIsaac, H.J. 1994. Size-selective predation on zebra mussels (*Dreissena polymorpha*) by crayfish (*Orconectes propinquus*). J. North Am. Benthol. Soc. **13**: 206–216.

Mackay, D., Sang, S., Vlahos, P., Diamond, M., Gobas, F., and Dolan, D. 1994. A constant model of chemical dynamics in a lake ecosystem: PCBs in Lake Ontario. J. Gt. Lakes Res. **20**: 625–642.

Maguire, R.J., and Tkacz, R.J. 1989. Potential underestimation of chlorinated hydrocarbon concentrations in fresh water. Chemosphere, **19**: 1277–1287.

Martin, G.W., and Corkum, L.D. 1995. Predation of zebra mussels by crayfish. Can. J. Zool. **72**: 1867–1871.

Metcalfe, T.L., and Metcalfe, C.D. 1997. The trophodynamics of PCBs, including mono- and non-*ortho* congeners, in the food web of central Lake Ontario. Sci. Total Environ. **201**: 245–272.

Mills, E.L., O'Gorman, R., Roseman, E.F., Adams, C., and Owens, R.W. 1995. Planktivory by alewife (*Alosa pseudoharengus*) and rainbow smelt (*Osmerus mordax*) on microcrustacean zooplankton and dreissenid (Bivalvia: Dreissenidae) veligers in southern Lake Ontario. Can. J. Fish. Aquat. Sci. **52**: 925–935.

Morrison, H.A. 1995. Rates of ingestion, egestion and gill ventilation in benthic invertebrates. Can. Data Rep. Fish. Aquat. Scie. No. 955.

Morrison, H.A., Gobas, F.A.P.C., Lazar, R., Whittle, D.M., and Haffner, G.D. 1997. A foodweb bioaccumulation model for organic contaminants in western Lake Erie. Environ. Sci. Technol. **31**: 3267–3273.

Morrison, H.A., Gobas, F.A.P.C., Lazar, R., Whittle, D.M., and Haffner, G.D. 1998. Projected changes in the trophodynamics of PCBs in the western Lake Erie ecosystem attributed to the presence of zebra mussels. Environ. Sci. Technol. **32**: 3862–3867.

Muir, D.C.G., and Yarechewski, A.L. 1988. Dietary accumulation of four chlorinated dioxin congeners by rainbow trout and fathead minnows. Environ. Toxicol. Chem. **7**: 227–236.

Muir, D.C.G., Yarechewski, A.L., Knoll, A., and Webster, G.R.B. 1986. Bioconcentration and disposition of 1,3,6,8-tetrachlorodibenzo-*p*-dioxin and octachlorodibenzo-*p*-dioxin by rainbow trout and fathead minnows. Environ. Toxicol. Chem. **5**: 261–272.

Muir, D.C.G., Yarechewski, A.L., Metner, D.A., Lockhart, W.L., Webster, G.R.B., and Friesen, K.J. 1990. Dietary accumulation and sustained hepatic mixed function oxidase enzyme induction by 2,3,4,7,8-pentachlorodibenzofuran in rainbow trout. Environ. Toxicol. Chem. **9**: 1465–1474.

Muir, D.C.G., Fairchild, W.L., and Whittle, D.M. 1992*a*. Predicting bioaccumulation of chlorinated dioxins and furans in fish near Canadian bleached kraft mills. Water Pollut. Res. J. Can. **27**: 487–507.

Muir, D.C.G., Yarechewski, A.L., Metner, D.A., and Lockhart, W.L. 1992*b*. Dietary 2,3,7,8-tetrachlorodibenzofuran in rainbow trout: accumulation, disposition, and hepatic mixed-function oxidase enzyme induction. Toxicol. Appl. Pharmacol. **117**: 65–74.

Niimi, A.J. 1996. Evaluation of PCBs and PCDD/Fs retention by aquatic organisms. Sci. Total Environ. **192**: 123–150.

Norstrom, R.J., McKinnon, A.E., and deFreitas, S.W. 1976. A bioenergetics-based model for pollutant accumulation by fish. Simulation of PCB and methylmercury residue levels in Ottawa River yellow perch (*Perca flavescens*). J. Fish. Res. Board Can. **33**: 248–267.

Oliver, B.G., and Niimi, A.J. 1988. Trophodynamic analysis of polychlorinated biphenyl congeners and other chlorinated hydrocarbons in the Lake Ontario ecoystem. Environ. Sci. Technol. **22**: 388–397.

Peters, R.H., and Downing, J.A. 1984. Empirical analysis of zooplankton filtering and feeding rates. Limnol. Oceanogr. **29**: 763–784.

Place, A.R. 1992. Comparative aspects of lipid digestion and absorption: physiological correlatives of wax ester digestion. Am. J. Physiol. **263**: R464–R471.

Rand, P.S., Stewart, D.J., Lantry, B.F., Rudstam, L.G., Johannson, O.E., Goyke, A.P., Brant, S.B., O'Gorman, R., and Eck, G.W. 1995. Effect of lake-wide planktivory by the pelagic prey fish community in Lakes Michigan and Ontario. Can. J. Fish. Aquat. Sci. **52**: 1546–1563.

Reeders, H.H., Bij de Vaate, A., and Slim, F.J. 1989. The filtration rate of *Dreissena polymorpha* (Bivalvia) in three Dutch lakes with reference to biological water quality management. Freshwater Biol. **22**: 133–141.

Rumpus, A.E., and Kennedy, C.R. 1974. The effect of the acanthocephalan *Pomphorhynchus laevis* upon the respiration of its intermediate host *Gammarus pulex*. Parasitology, **68**: 271–284.

Saffran, K.A. 1993. Trophic ecology of the crayfish *Orconectes propinquus* in Colpoys Bay. M.Sc. thesis, University of Waterloo, Waterloo, Ont.

Sijm, D.T.H.M., Wever, H., de Vries, P.J., and Opperhuizen, A. 1989. Octanol/water partition coefficients of polychlorinated dibenzo-*p*-dioxins and dibenzofurans: experimental values determined with a stirring method. Chemosphere, **19**: 263–266.

Swackhamer, D.L., and Skoglund, R.S. 1993. Bioaccumulation of PCBs by algae: kinetics versus equilibrium. Environ. Toxicol. Chem. **12**: 831–838.

© 1999 NRC Canada

Thomann, R.V., Connolly, J.P., and Parkerton, T.F. 1992. An equilibrium model of organic chemical accumulation in aquatic food webs with sediment interaction. Environ. Toxicol. Chem. **11**: 615–629.

Thurston, R.V., and Gehrke, P.C. 1993. Respiratory oxygen requirements of fishes: description of OXYREF, a data file based on test results reported in the published literature. *In* Fish Physiology, Toxicology, and Water Quality Management. Proceedings of an International Symposium, Sacramento, California, U.S.A., Sept. 18–20, 1990. *Edited by* R.C. Russo and R.V. Thurston. EPA/600/R-93/157. Environmental Research Laboratory Office of Research and Development, U.S. Environmental Protection Agency, Athens, Ga. p. 95.

Weininger, D. 1978. Accumulation of PCBs by lake trout in Lake Michigan. Ph.D. thesis, University of Wisconsin, Madison, Wis.

Wu, L., and Culver, D.A. 1992. Ontogenetic diet shift in Lake Erie age-0 yellow perch (*Perca flavescens*): a size-related response to zooplankton density. Can. J. Fish. Aquat. Sci. **49**: 1932–1937.

© 1999 NRC Canada

Effects of *Gammarus lacustris* (Crustacea: Amphipoda) on plankton community structure in an alpine lake

Frank M. Wilhelm and David W. Schindler

Abstract: The amphipod *Gammarus lacustris* is generally considered as a herbivore or a detritivorous scavenger, but we and others have observed it preying on pelagic zooplankton in fishless alpine lakes of the Canadian Rockies. We tested the hypothesis that *G. lacustris* predation alters the plankton community structure of alpine lakes by manipulating *G. lacustris* density in large (2800 L) in situ enclosure experiments. Compared with control enclosures (no *Gammarus*), *Daphnia middendorffiana* abundance was reduced 49, 85, and 100% in the low, medium, and high (40, 200, and 400 individuals·m^{-2}) *Gammarus* density enclosures, respectively. *Hesperodiaptomus arcticus* density was not significantly related to *G. lacustris* density. Comparison of mesocosm results with lake data showed that *G. lacustris* predation on *D. middendorffiana* in the lake was lower, possibly because a pelagic deepwater refugium allows *Daphnia* to escape predation. The results show that *G. lacustris* predation can affect the plankton community structure in small fishless alpine lakes.

Résumé : L'amphipode *Gammarus lacustris* est généralement considéré comme un herbivore ou un détritivore, mais nous avons, avec d'autres chercheurs, observé qu'il peut se nourrir de zooplancton pélagique dans des lacs alpins des Rocheuses canadiennes dépourvus de poisson. Nous avons testé l'hypothèse que la prédation par *G. lacustris* altère la structure de la communauté planctonique des lacs alpins dans le cadre d'expériences en enclos in situ de grande taille (2 800 L) renfermant diverses densités de *G. lacustris*. Par rapport aux enclos témoins (sans *Gammarus*), l'abondance de *Daphnia middendorffiana* a chuté de 49, 85 et 100% dans les enclos renfermant des densités de *Gammarus* faible, moyenne et élevée (40, 200 et 400 individus·m^{-2}), respectivement. Il n'y avait pas de corrélation significative entre la densité de *Hesperodiaptomus arcticus* et celle de *G. lacustris*. La comparaison des résultats obtenus en mésocosme avec les données obtenues dans un lac a montré que la prédation de *D. middendorffiana* par *G. lacustris* dans le lac était plus faible, peut-être parce que *Daphnia* peut profiter d'un abri pélagique en eau profonde pour échapper à la prédation. Les résultats montrent que la prédation par *G. lacustris* peut influer sur la structure de la communauté planctonique dans les petits lacs alpins dépourvus de poisson.

[Traduit par la Rédaction]

Introduction

In this paper, we present evidence that predation by *Gammarus lacustris*, a common freshwater amphipod of northern North America, Europe, and Siberia (Segerstråle 1954; Bousfield 1958; Zhadin and Gerd 1963; Ökland 1969), can alter the plankton community structure of fishless alpine lakes. The impact of size-selective predation on zooplankton communities by vertebrate and invertebrate predators such as *Alosa*, *Chaoborus*, *Leptodora*, and some diaptomid and cyclopoid copepods is well established (Brooks and Dodson 1965; Neill 1981; Paul et al. 1995). Some benthic invertebrates, such as *Mysis relicta* and *Chaoborus* spp., also affect pelagic zooplankton communities (Neill 1981; Langeland et al. 1991; Lasenby 1991). Maly et al. (1980) reported that flatworms prey on *Daphnia*, influencing zooplankton composition and dynamics in high-elevation ponds. Investigations by Dick (1992) and Dick et al. (1993) indicated that cannibalism and mutual predation among some gammarid species are important in structuring their communities. Amphipods are conspicuous members of benthic communities in freshwaters and are generally classified as detritus feeders and (or) scavengers (Barnes 1980), not as predators. Among these, *G. lacustris* is commonly considered as a herbivorous scavenger (Bagge 1968) and detritivore (Moore 1977). However, predatory feeding by *G. lacustris* on diaptomid copepods, daphnids, and *Chaoborus* has been noted (Forbes 1893; Anderson and Raasveldt 1974 and references therein; Kortelainen 1990).

Anderson and Raasveldt (1974) and Anderson (1980) concluded that zooplankton community composition in some prairie ponds and alpine lakes was consistent with *G. lacustris* predation patterns observed by Anderson and Raasveldt (1974), suggesting that *G. lacustris* may be important in structuring zooplankton communities in fishless lakes and ponds. These conclusions, however, were based on extrapolations from *G. lacustris* predation experiments in 100-mL experimental vessels. Cautions about extrapolating

Received August 28, 1998. Accepted March 19, 1999. J14773

F.M. Wilhelm[1] **and D.W. Schindler.** Department of Biological Sciences, University of Alberta, Edmonton, AB T6G 2E9, Canada.

[1]Author to whom all correspondence should be addressed. e-mail: Frank.Wilhelm@ualberta.ca

© 1999 NRC Canada

from inappropriately scaled experimental chambers and enclosures to whole-lake ecosystems are frequent in the literature (e.g., de Lafontaine and Leggett 1987; Piercey and Maly 1998; Schindler 1998). The use of small containers usually requires higher prey densities than present in situ. As well, small containers generally yield higher predation rates compared with large containers because encounter frequency between prey and predators is enhanced and prey tend to be more active (de Lafontaine and Leggett 1987; Piercey and Maly 1998). In addition, small containers prevent spatial separation which may be important to vertically migrating species. Ideally, manipulative experiments should be executed at a scale closely reflecting field conditions. We used large (2800 L) in situ enclosures to experimentally control *G. lacustris* density to test the hypothesis that *G. lacustris* predation alters the zooplankton community structure in fishless alpine lakes.

Materials and methods

Study lake

Snowflake Lake is a small (7.13 ha, maximum depth 12.5 m) ultraoligotrophic alpine (2320 m above sea level) lake located in the Front Ranges of the Canadian Rocky Mountains in Banff National Park (51°35′N, 115°50′W), Alberta, Canada. A map and further chemical and physical descriptions are provided in Anderson (1970*a*) and McNaught et al. (1999). Ice-out usually occurs between the end of June and mid-July and the lake stratifies weakly in late summer when surface temperatures reach a maximum of 9–12°C. Freeze-up occurs between late September and early October (Anderson 1970*a*).

The biotic community of Snowflake Lake has been manipulated several times through fish and zooplankton introductions. The lake was originally fishless but was stocked with salmonids for 5 years between 1960 and 1966. The presence of fish altered the zooplankton community from one dominated by *Hesperodiaptomus arcticus* and *Daphnia middendorffiana* to one dominated by *Diacyclops* and rotifers (Anderson 1972; McNaught et al. 1999). Fish did not reproduce in the lake and declined gradually, with the last fish caught in 1984. Once the lake was devoid of fish, *G. lacustris* and *D. middendorffiana* returned (McNaught et al. 1999), but the large copepod *H. arcticus* remained absent and small cyclopoid copepod species continued to dominate the zooplankton. *Hesperodiaptomus arcticus* was reintroduced on 30 July 1992 but did not become abundant in the plankton until late in 1996. *Hesperodiaptomus arcticus* reintroduction has caused the decline in abundance or elimination of all cyclopoid copepod and rotifer species (D.W. Schindler, unpublished data).

Mesocosm sampling

We used 12 enclosures in Snowflake Lake to test *G. lacustris* predation at different densities on the zooplankton community in 1996. The enclosures were 1.0 × 1.0 × 3.0 m deep and constructed of transparent woven polyethylene. They were closed at the bottom, with a volume of 2800 L when filled. Enclosures were suspended from floating frames constructed of wood and closed-cell styrofoam anchored at a water depth of 8–10 m. They were filled on 11 July, about 1 week after ice-out, by submersing each enclosure to 6 m, opening the top, and pulling it up through the water column. After suspending all enclosures, *G. lacustris* and large zooplankton captured during filling were removed by hauling a square (0.95 × 0.95 m) 500-μm-mesh screen four times from the bottom to the top of each enclosure. We then performed four additional vertical hauls with an 64-μm-mesh, 30-cm-diameter Wisconsin plankton net to remove as much as possible of the smaller zooplankton. Each enclosure was then stocked with zooplankton collected from 11-m vertical hauls taken with the 30-cm-diameter plankton net from the deepest spot in the lake. Eight hauls, from which all *G. lacustris* were immediately removed, were used to stock each enclosure. *Gammarus lacustris* were collected with a sweep net from the east shore of the lake and added at densities of 40 (low), 200 (medium), and 400 individuals·m^{-2} (high) to triplicate enclosures on 15 July (= day 0). Three enclosures did not receive any *G. lacustris* and served as controls. Only adult *G. lacustris*, at a male to female ratio of 1:1, were stocked because this cohort dominates the diurnal migrations into the pelagic zone (F.M. Wilhelm, unpublished data).

Water samples were collected from the enclosures and the lake (near the enclosures) using a clear polyvinyl chloride tube 2.75 m in length and 0.05 m inner diameter. DeVries and Stein (1991) reported that such a tube sampler yielded zooplankton densities comparable with those from a vertical net tow and a Schindler–Patalas trap, even for highly mobile calanoids. The tube was dropped vertically into each enclosure or the lake, plugged at the top, removed, and emptied into a bucket. The procedure was repeated three times, removing about 16.2 L of water, or about 0.6% of the enclosure volume. Aliquots were removed for algal cell counts (0.25 L), chlorophyll *a* (Chl *a*) (1 L), and water chemistry (total phosphorus (TP) and total dissolved nitrogen (TDN) (0.5 L)) analyses. The remaining 14.45 L was filtered through a 10-μm-mesh net and preserved with sugared formalin for zooplankton counts. The minimum detectable limit for plankton using the tube sampler (assuming a Poisson distribution and a 95% probability of detection) was 0.2 individual·L^{-1}. To minimize depletion effects on enclosure populations, larger samples were not taken. At the end of the experiment, the contents of each enclosure were retained in a top net with 80-μm-mesh panels and a cod end. This top net was attached to close the top of each enclosure after it was loosened from the frame. After concentrating, the contents were preserved with 4% formalin. Amphipods remaining at the end of the experiments were counted to obtain a survival estimate.

Zooplankton in the lake were enumerated from five replicate 11-m hauls, preserved together, taken at the deepest spot of the lake with the 30-cm-diameter, 64-μm-mesh plankton net. We used an efficiency correction of 50% based on Anderson's (1970*b*) findings of efficiencies of up to 40% for a similar net towed in a more productive montane lake over a vertical distance exceeding 30 m. Keys from Edmondson (1959), Chengalath et al. (1971), Torke (1974), Grothe and Grothe (1977), and Czaika (1982) were used to identify zooplankton species. Zooplankton were enumerated by allowing the entire sample to settle for 24 h and then counting all individuals using both inverted and dissecting microscopes. Lake samples were subsampled (10–25 mL) from a final sample volume of 250–500 mL. Rotifer density was based on *Keratella hiemalis* abundance, as it was the dominant rotifer. Other rotifers (*Keratella cochlearis*, *Polyarthra dolichoptera*, *Notholca* spp., and *Synchaeta* spp.) were collected infrequently and contributed little to overall rotifer abundance. Chl *a*, used as an indicator of phytoplankton biomass, was determined fluorometrically with a Shimadzu model RF-1501 spectrofluorometer (Mandel Scientific, Guelph, Ont.) following the method of Welschmeyer (1994). Phytoplankton biomass, water chemistry, and zooplankton densities were compared using a repeated measures ANOVA with one between-subject factor (*Gammarus* density) and one within-subject factor (date) (Von Ende 1993). Treatment (*Gammarus* density) × time (date) interactions were also considered for each test. Only samples from days 7, 20, and 35 were included in the repeated measures analysis, as initial stocking densities (day 0) for all enclosures were estimated from two samples (4 × 11-m hauls preserved together) collected at the same time as zooplankton samples for stocking the enclosures. Results for calanoid nauplii, cyclopoid copepodites, and cyclopoid adults were not included in the analysis because densities often

© 1999 NRC Canada

Fig. 1. Mean densities of Snowflake Lake zooplankton and selected water chemistry parameters in enclosures with varying densities of the predator *G. lacustris* for 1996. Treatment *Gammarus* density: ●, control (no *Gammarus*); △, low (40 individuals·m^{-2}); ◆, medium (200 individuals·m^{-2}); ■, high (400 individuals·m^{-2}); ○, lake (200–400 individuals·m^{-2}). Error bars represent ±1 SE. Lake zooplankton samples represent a single collection and therefore do not have errors bars associated with them. Error bars less than the size of the symbol in other samples are not shown.

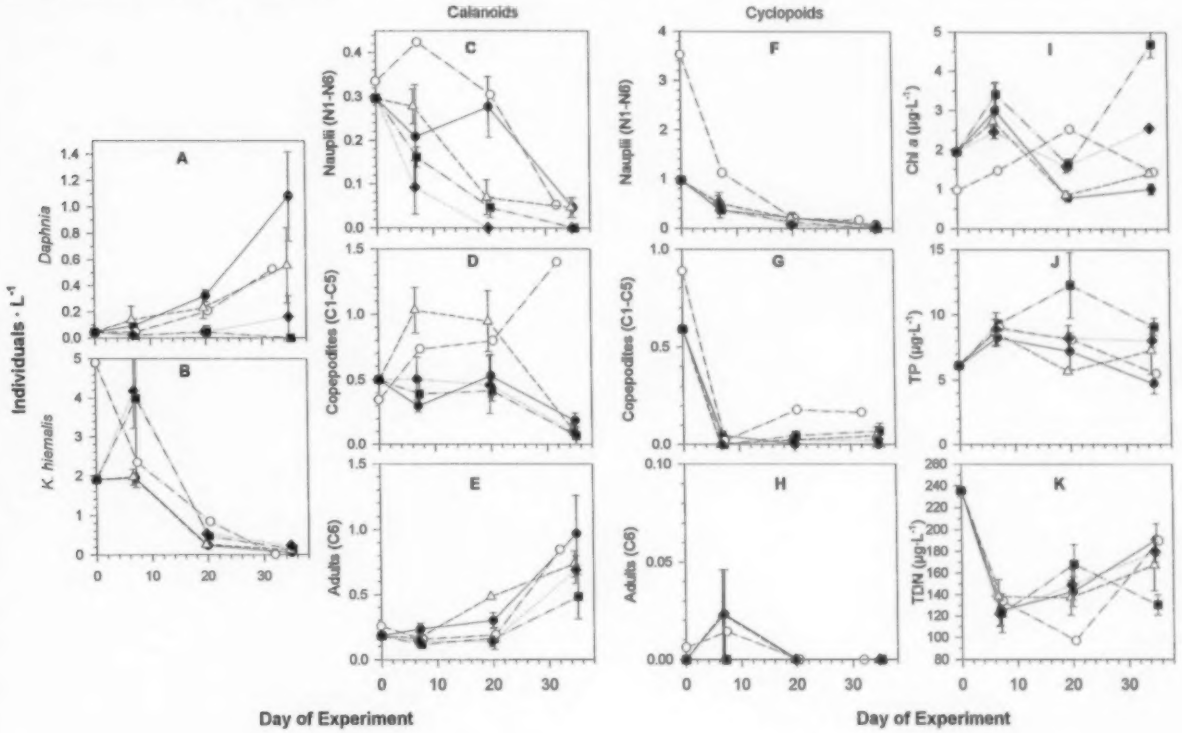

were below the detection limit of the sampler. However, we present them graphically to show the trends.

Results

Gammarus lacustris in the enclosures migrated similarly to individuals in the lake (F.M. Wilhelm, personal observation), remaining on or near the bottom of the enclosures during the day and swimming throughout the water column to within 0.1 m of the surface at night. *Gammarus lacustris* survival decreased slightly with increasing density over the course of the experiment from 93 ± 7 to 89 ± 5 to 81 ± 3% (mean ± SE) of initial densities in the low-, medium-, and high-density treatments respectively.

Daphnia middendorffiana density increased 13, 24, and 12 times in the lake, control and low density *Gammarus* enclosures, respectively, over the course of the experiment (Fig. 1A). In the medium density *Gammarus* enclosures, a small increase (3.5 times) occurred during the last sampling interval (Fig. 1A), while in the high density *Gammarus* enclosures, *D. middendorffiana* density remained constant until day 20 and then declined to zero (Fig. 1A). We examined the treatment trend on the last sampling date by regressing *Daphnia* density versus log *Gammarus* density. This showed that *D. middendorffiana* density declined strongly with increasing *G. lacustris* density (Fig. 2A; R^2 = 0.60, df = 11, p = 0.003).

Rotifer abundance declined ($p < 0.001$) in all enclosures over the course of the experiment (Table 1; Fig. 1B). The treatment effect was weak (p = 0.347; Table 1), indicating that the decline in rotifer abundance may have been related to factors other than *Gammarus* density. Although rotifer abundance was 2.5 times higher in the lake than in the enclosures on day 0, it rapidly declined to zero by August 16 (Fig. 1B).

Calanoid copepods were almost exclusively *H. arcticus*. Only two other diaptomid (*Diaptomus tyrrelli*) specimens were encountered in all samples. Nauplii declined in all enclosures and in the lake over the course of the experiment (Fig. 1C). The decline was most rapid in the medium and high density *Gammarus* enclosures, but the density was at or below our detection limit for most of the samples. Calanoid copepodite density was variable in the enclosures after stocking but declined in all enclosures by the end of the experiment (Fig. 1D). Treatment and the interaction effect were weak (p = 0.066 and 0.055, respectively; Table 1). Copepodite density in the lake, however, increased with time (Fig. 1D). *Hesperodiaptomus arcticus* adult density increased ($p < 0.001$) in all enclosures and the lake (Table 1; Fig. 1E). The treatment effect was insignificant (p = 0.120; Table 1), as was a least squares regression analysis of adult

© 1999 NRC Canada

Fig. 2. Relationships showing the effect of *G. lacustris* density on zooplankton abundance, Chl *a*, and TP concentration at the end (day 35) of the enclosure experiment. (A) *Daphnia middendorffiana* abundance versus $\log_{10}(n + 1)$ *G. lacustris* density ($Y = -0.411X + 1.12$; $R^2 = 0.60$, df = 11, $p = 0.003$); (B) *H. arcticus* abundance versus $\log_{10}(n + 1)$ *G. lacustris* density ($Y = -0.16X + 0.98$; $R^2 = 0.27$, df = 11, $p = 0.083$); (C) Chl *a* concentration versus *G. lacustris* density ($Y = 0.01X + 0.96$; $R^2 = 0.96$, df = 11, $p < 0.001$); (D) TP concentration versus $\log_{10}(n + 1)$ *G. lacustris* density ($Y = 1.58X + 4.71$; $R^2 = 0.52$, df = 11, $p = 0.008$).

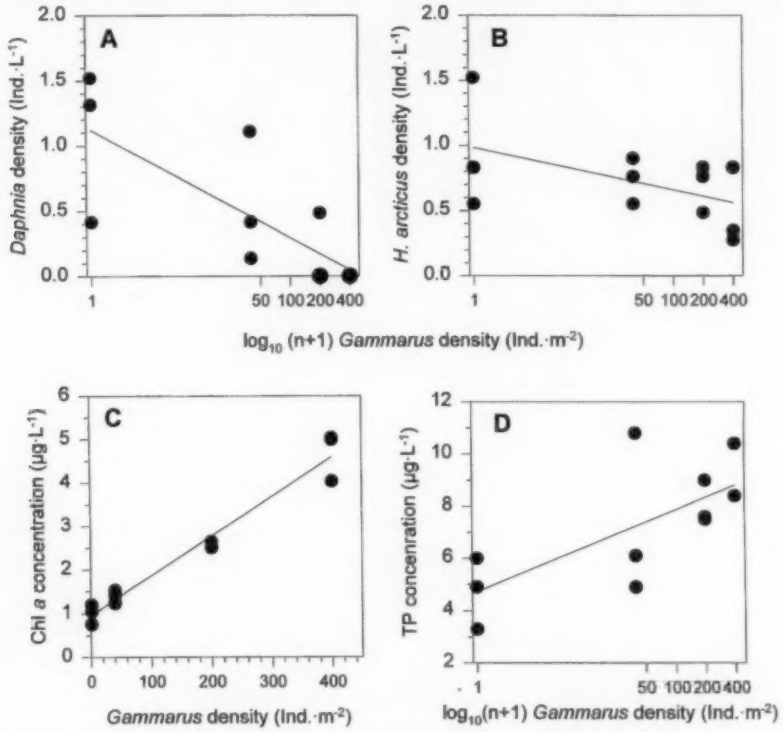

H. arcticus density versus log *Gammarus* density for the final date (Fig. 2B; $R^2 = 0.27$, df = 11, $p = 0.083$). *Hesperodiaptomus arcticus* adult density in the lake did not increase until after day 20 (Fig. 1E).

Cyclopoid nauplii density decreased ($p < 0.001$) from a high of 1 individual·L^{-1} to near zero in all enclosures without a treatment or interaction effect ($p = 0.638$ and 0.876, respectively; Table 1; Fig. 1F). Nauplii density in the lake also declined sharply over the 35-day experimental period. Although cyclopoid copepodites were present on day 0 at densities of 0.59 and 0.88 individual·L^{-1} in the enclosures and the lake, respectively, they declined to near zero by the first sampling date (19 July) and remained near undetectable levels for the remainder of the experiment (Fig. 1G). The higher nauplii density in the lake compared with the enclosures on day 0 may reflect a depletion effect of nauplii from the lake during hauls taken to stock the enclosures. Cyclopoid adults were rare in Snowflake Lake in 1996. The few that were present in the lake and the enclosures on day 0 rapidly declined to undetectable levels (Fig. 1H). Even though we used five vertical hauls to sample zooplankton in the lake on each date, cyclopoid adults were not encountered after 4 August (Fig. 1H).

Phytoplankton biomass in the enclosures was almost twice as high as in the lake on day 0 (Fig. 1I) and may be related to the selective retention of large species such as diatoms and *Dinobryon* in the net during enclosure stocking. Phytoplankton biomass increased in the lake and the enclosures until the first sampling date, after which phytoplankton biomass in the lake increased until day 20, while it declined in all enclosures (Fig. 1I). After day 20, phytoplankton biomass in the lake declined, while it increased ($p < 0.001$) in all enclosures. After day 20, phytoplankton biomass increased faster in the presence of higher amphipod densities ($p < 0.001$, treatment × date interaction; Fig. 1I). Phytoplankton biomass was also positively ($p < 0.001$) related to *Gammarus* density (Table 1). A regression analysis for the last sampling date showed that 96% of the variation in Chl *a* concentration was explained by *Gammarus* density (Fig. 2C; $R^2 = 0.96$, df = 11, $p < 0.001$).

The TP concentration increased by about 3 µg·L^{-1} in the enclosures and the lake between day 0 and the first sampling date, after which it was variable without trends with either time ($p = 0.145$) or treatment ($p = 0.069$) (Table 1; Fig. 1J). However, concentrations in the medium and high density *Gammarus* enclosures were slightly higher than in the control and low density *Gammarus* enclosures (Fig. 1J). A least squares linear regression of TP concentration versus *Gammarus* density on the final sampling date showed that TP was positively related to *Gammarus* density (Fig. 2D; $R^2 = 0.68$, df = 11, $p < 0.001$).

TDN was highest in the enclosures and the lake at the be-

© 1999 NRC Canada

Table 1. Repeated measures ANOVA for zooplankton abundance and water chemistry from Snowflake Lake mesocosms in 1996 using different densities of the predator *G. lacustris*.

Test	Source	df	MS	*p*
Daphnia				
Between subjects	Treatment	3	0.435	0.039
	Error	8	0.096	
Within subject	Date	2	0.473	0.001
	Interaction	6	0.165	0.018
	Error	16	0.045	
K. hiemalis				
Between subjects	Treatment	3	2.113	0.347
	Error	8	1.659	
Within subject	Date	2	30.883	<0.001
	Interaction	6	1.298	0.553
	Error	16	1.534	
Calanoid C1–C5				
Between subjects	Treatment	3	0.317	0.066
	Error	8	0.088	
Within subject	Date	2	0.843	<0.001
	Interaction	6	0.097	0.055
	Error	16	0.037	
Calanoid adults (C6)				
Between subjects	Treatment	3	0.120	0.120
	Error	8	0.045	
Within subject	Date	2	1.055	<0.001
	Interaction	6	0.041	0.369
	Error	16	0.035	
Cyclopoid nauplii				
Between subjects	Treatment	3	0.013	0.638
	Error	8	0.022	
Within subject	Date	2	0.547	<0.001
	Interaction	6	0.014	0.876
	Error	16	0.036	
Chl *a*				
Between subjects	Treatment	3	5.226	<0.001
	Error	8	0.085	
Within subject	Date	2	9.106	<0.001
	Interaction	6	2.061	<0.001
	Error	16	0.089	
TP				
Between subjects	Treatment	3	21.780	0.069
	Error	8	6.195	
Within subject	Date	2	7.066	0.145
	Interaction	6	6.477	0.125
	Error	16	3.229	
TDN				
Between subjects	Treatment	3	259.303	0.687
	Error	8	509.488	
Within subject	Date	2	4783.470	0.012
	Interaction	6	1250.188	0.228
	Error	16	810.668	

ginning of the experiment, after which it declined to a minimum and then increased again (Fig. 1K). The minimums in the enclosures occurred around day 7, while the lake did not reach its minimum until near day 20. This change with time is reflected in the date effect (p = 0.012; Table 1). *Gammarus* density did not (p = 0.687) influence TDN concentrations (Table 1).

Discussion

Our enclosure results show that *G. lacustris* significantly influenced the abundance of pelagic zooplankters and phytoplankton biomass. The abundance of *D. middendorffiana* was reduced in the medium and high density *Gammarus* enclosures compared with the control and low density

© 1999 NRC Canada

Gammarus enclosures (Figs. 1A and 1E). *Hesperodiaptomus arcticus* density was not reduced significantly in our experiment. Although *G. lacustris* density in Snowflake Lake was between 200 and 400 individuals·m^{-2}, as determined from night vertical plankton net and daytime bottom closing net hauls (F.M. Wilhelm, unpublished data) (corresponding to the medium- and high-density enclosures), *D. middendorffiana* density in the lake increased similar to the low *Gammarus* density enclosures (Fig. 1A), indicating a discrepancy between the enclosures and the lake. The larger vertical separation between *D. middendorffiana* and *G. lacustris* in the lake compared with the enclosures may represent a pelagic refugium where *D. middendorffiana* encounters are reduced. *Gammarus lacustris* gut content analyses show that predation on zooplankton is limited to the time that they spend in the water column at night (F.M. Wilhelm, unpublished data). Therefore, the pelagic zone over deep water may serve as a refugium for zooplankton from *G. lacustris* predation. Similarly, fish and large diaptomid copepods typically coexist in mountain lakes only if they are deeper than 16 m and larger than 16 ha (Donald et al. 1994).

The decline in rotifer abundance in all enclosures may be attributable to *H. arcticus* predation. Rotifer regulation by *H. arcticus* adults and copepodites in Snowflake Lake has been demonstrated previously (Paul et al. 1995). Our results show that the regulation of rotifers is possible at a low *H. arcticus* density. Rotifer density in all enclosures declined to less than 1 individual·L^{-1} by day 20, while *H. arcticus* density remained near 0.5 and 0.2 individual·L^{-1} for copepodites and adults, respectively (Figs. 1D and 1E). Regulation of rotifers by copepod predation in alpine lakes is possible because low food availability and cold water temperatures slow rotifer reproduction (McNaught et al. 1999). All of our enclosures had about two times higher Chl *a* concentrations than the lake at the start of the experiment, which should have ameliorated low rotifer food conditions. Either this phytoplankton was unavailable to the rotifers or, more likely, copepod predation diminished any advantages from increased food levels. Similar conclusions from fertilized mesocosms were reached by Paul et al. (1995). The simultaneous decline in rotifer abundance in the lake represents the decline and near elimination of rotifers in the lake after *H. arcticus* became the dominant zooplankter in late 1996.

The decrease in calanoid nauplii and copepodite abundance in the enclosures (Figs. 1C and 1D) over the course of the experiment is expected because of recruitment to the adult cohort. Nauplii declined from a density of 0.3 individual·L^{-1} to near zero, while copepodites declined from about 0.5 individual·L^{-1} to as low as 0.18 individual·L^{-1}. The continued copepodite increase in the lake may be related to the high nauplii density in the lake on day 7 (Fig. 1C), which indicates that peak nauplii recruitment from resting eggs deposited in lake sediment occurred after we had started the experiment. If we assume zero mortality during development, adult *H. arcticus* density should have increased by 0.62–0.82 individual·L^{-1} at the end of the experiment. Our assumption of no mortality during development is probably incorrect; however, we currently do not have any *H. arcticus* mortality rates for Snowflake Lake. Rigler et al. (1974) reported an average mortality rate of 59% for *Limnocalanus macrurus* from naupliar to adult stages in Char Lake in the high Canadian arctic. *Hesperodiaptomus arcticus* mortalities in our experiment must be less than 59% because only the mortality rate in the high-density treatment could have been that high (Fig. 1E). Lower mortalities are necessary to explain the density of adults in the other enclosures (Fig. 1E).

A longer experiment may have resulted in a significant reduction in adult *H. arcticus*. The ability of *G. lacustris* to capture and consume diaptomid copepods has been reported by Forbes (1893) and Anderson and Raasveldt (1974). In single prey feeding experiments with *H. arcticus* that we conducted in the field in 1995, *G. lacustris* also captured and consumed *H. arcticus* adults (F.M. Wilhelm, unpublished data). However, when presented with a choice of *D. middendorffiana* or *H. arcticus*, *D. middendorffiana* were always selected. This may indicate that *G. lacustris* does not switch to prey on *H. arcticus* until after *D. middendorffiana* density declines below some threshold and may have occurred in a longer experiment. However, the duration of our experiment was constrained by the open-water season and poor late-season access to Snowflake Lake. In the lake, such a switch by *G. lacustris* may not occur until late fall or after the lake is ice-covered. Predation of adult *H. arcticus* by *G. lacustris* could explain the slow reestablishment of *H. arcticus* as the dominant copepod in Snowflake Lake after its reintroduction in 1992 as well as the continued density below that characteristic of other lakes in the area (Anderson 1980; D.W. Schindler, unpublished data), for the *G. lacustris* density in Snowflake Lake is higher than in other nearby Lakes (F.M. Wilhelm, unpublished data). A seasonal examination of *G. lacustris* diet in Snowflake Lake would show if and when *H. arcticus* predation occurred.

The disappearance of cyclopoids from the enclosures was consistent with previous research showing that codominance of zooplankton by predaceous diaptomid and cyclopoid species is unlikely (Anderson 1970*c*) and that pristine mountain lakes are likely to be dominated by species of *Hesperodiaptomus* (Anderson 1980). Anderson (1970*c*) reported *H. arcticus* to consume between six and 20 cyclopoids per day, and predation experiments carried out at Snowflake Lake in 1995 showed that *H. arcticus* selectively preyed on cyclopoid nauplii and copepodites compared with its own young (A.S. McNaught, Department of Biology, Central Michigan University, Mount Pleasant, Mich., unpublished data). Although cyclopoids can prey on diaptomids and exclude them from lakes (Anderson 1970*c*), the role of predator or prey is determined by the relative size or instar of the two groups. Adult *H. arcticus*, because of their larger size compared with cyclopoid adults typically present in mountain lakes, are not vulnerable to cyclopoid predation, whereas cyclopoids remain vulnerable to predation by *H. arcticus*. The decline in cyclopoids in Snowflake Lake in 1996 (Figs. 1F–1H) marked their collapse after dominating the zooplankton assemblage for nearly 20 years while *H. arcticus* was absent from the lake.

Phytoplankton biomass at the end of the experiment was highest in the high density *Gammarus* enclosures where zooplankton abundance and hence grazing pressure was lowest (Figs. 1I and 2C). We cannot explain the decline observed in all enclosures between days 7 and 15, but it may be related to a change in algal species composition, settling of cells, or

© 1999 NRC Canada

ultraviolet effects. The increase in phytoplankton in the high density *Gammarus* enclosure was mediated directly and indirectly by *G. lacustris*. Predation by *G. lacustris* on *Daphnia* reduced grazing pressure on phytoplankton, while *G. lacustris* excretion and egestion regenerated nutrients that stimulated phytoplankton growth (Fig. 1I).

The significant positive relationship of TP with *Gammarus* density on the final sampling date (Fig. 2D) may be related to the altered plankton communities present among treatments. *Daphnia* have a high dietary P requirement and are known to sequester P relative to other zooplankton (Andersen and Hessen 1991). High *Daphnia* densities in the control and low density *Gammarus* treatments may have contained much of the TP, while in the medium and high density *Gammarus* treatments, predation on *Daphnia* by *G. lacustris* released the P, increasing the TP concentration.

Our large-enclosure experiment in Snowflake Lake supports the hypothesis that predation by *G. lacustris* influences the plankton community structure in fishless alpine lakes. *Daphnia middendorffiana* abundance decreased with increasing *G. lacustris* density. This large zooplankter would be expected to be reduced or eliminated in the presence of planktivorous fish, as seen earlier in the century when Snowflake Lake was stocked with fish (McNaught et al. 1999).

Although *G. lacustris* in the lake was present at densities similar to those in the medium- and high-density enclosures, predation in the lake was weaker, possibly because a pelagic deepwater refugium reduces predator–prey encounters. If so, the impact of *G. lacustris* on plankton community structure would be expected to be most intense in small lakes and ponds, while in large deep lakes, weaker influences on prey population dynamics and life history structure, similar to other invertebrate predators, would predominate.

Acknowledgements

This research was carried out with permission of Parks Canada and with funding from the Biodiversity Grants Program (Department of Biological Sciences, University of Alberta, and Alberta Conservation Association), a Canadian Circumpolar Institute CBAR grant to F.M. Wilhelm, and an NSERC operating grant (No. 89673) to D.W. Schindler. F.M. Wilhelm was supported by NSERC postgraduate and Izaak Walton Killam Memorial scholarships. C. Wilson and R. Whittington provided assistance in the field. A. Langeland, D. Mayhood, J. Addicott, and B. Parker provided critical reviews and helpful comments on earlier versions of the manuscript.

References

Andersen, T., and Hessen, D.O. 1991. Carbon, nitrogen, and phosphorus content of freshwater zooplankton. Limnol. Oceanogr. **36**: 807–814.

Anderson, R.S. 1970*a*. Physical and chemical limnology of two mountain lakes in Banff National Park, Alberta. J. Fish. Res. Board Can. **27**: 233–249.

Anderson, R.S. 1970*b*. Effects of rotenone on zooplankton communities and a study of their recovery patterns in two mountain lakes in Alberta. J. Fish. Res. Board Can. **27**: 1335–1356.

Anderson, R.S. 1970c. Predator–prey relationships and predation rates for crustacean zooplankters from some lakes in western Canada. Can. J. Zool. **48**: 1229–1240.

Anderson, R.S. 1972. Zooplankton composition and change in an alpine lake. Verh. Int. Ver. Limnol. **18**: 264–268.

Anderson, R.S. 1980. Relationship between trout and invertebrate species as predators and the structure of the crustacean and rotiferan plankton in mountain lakes. *In* Evolution and ecology of zooplankton communities. *Edited by* W.C. Kerfoot. University Press of New England, Hanover, N.H. pp. 635–641.

Anderson, R.S., and Raasveldt, L.G. 1974. *Gammarus* and *Chaoborus* predation and the possible effects of *Gammarus* and *Chaoborus* feeding on the zooplankton composition in some small lakes and ponds in western Canada. Can. Wildl. Serv. Occas. Pap. No. 18.

Bagge, P. 1968. Ecological studies on the fauna of subarctic waters in Finnish Lapland. Rep. Kevo Subarct. Res. Stn. **4**: 28–79.

Barnes, R.D. 1980. Invertebrate zoology. Saunders College, Philadelphia, Pa.

Bousfield, E.L. 1958. Freshwater amphipod crustaceans of glaciated North America. Can. Field-Nat. **72**: 55–113.

Brooks, J.L., and Dodson, S.I. 1965. Predation, body size, and composition of plankton. Science (Washington, D.C.), **150**: 28–35.

Chengalath, R., Fernando, C.H., and George, M.G. 1971. The planktonic Rotifera of Ontario with keys to genera and species. Biol. Ser. University of Waterloo, Waterloo, Ont.

Czaika, S.C. 1982. Identification of nauplii N1–N6 and copepodids CI–CVI of the Great Lakes calanoid and cyclopoid copepods (Calanoida, Cyclopoida, Copepoda). J. Gt. Lakes Res. **8**: 439–469.

de Lafontaine, Y., and Leggett, W.C. 1987. Effect of container size on estimates of mortality and predation rates in experiments with macrozooplankton and larval fish. Can. J. Fish. Aquat. Sci. **44**: 1534–1543.

DeVries, D.R., and Stein, R.A. 1991. Comparison of three zooplankton samplers: a taxon-specific assessment. J. Plankton Res. **13**: 53–59.

Dick, J.T.A. 1992. The nature and implications of differential predation between *Gammarus pulex* and *G. duebeni celticus* (Crustacea: Amphipoda). J. Zool. (Lond.), **227**: 171–183.

Dick, J.T.A., Montgomery, I., and Elwood, R.W. 1993. Replacement of the indigenous amphipod *Gammarus duebeni celticus* by the introduced *G. pulex*: differential cannibalism and mutual predation. J. Anim. Ecol. **62**: 79–88.

Donald, D.B., Anderson, R.S., and Mayhood, D.W. 1994. Coexistence of fish and large *Hesperodiaptomus* species (Crustacea: Calanoida) in subalpine and alpine lakes. Can. J. Zool. **72**: 259–261.

Edmondson, W.T. 1959. Freshwater biology. 2nd ed. John Wiley & Sons, New York.

Forbes, S.A. 1893. A preliminary report on the aquatic invertebrate fauna of the Yellowstone National Park, Wyoming, and the Flathead region of Montana. Bull. U.S. Fish. Comm. 1981, **11**: 207–258.

Grothe, D.W., and Grothe, D.R. 1977. An illustrated key to the planktonic rotifers of the Laurentian Great Lakes. U.S. Environmental Protection Agency, Chicago, Ill.

Kortelainen, I. 1990. *Gammarus lacustris* — herbivore or predator? Rep. Kevo Subarct. Res. Stat. **21**: 31–34.

Langeland, A., Koksvik, J.I., and Nydal, J. 1991. Impact of the introduction of *Mysis relicta* on the zooplankton and fish populations in a Norwegian lake. Am. Fish. Soc. Symp. **9**: 98–114.

Lasenby, D.C. 1991. Comments on the roles of native and introduced *Mysis relicta* in aquatic ecosystems. Am. Fish. Soc. Symp. **9**: 17–22.

Maly, E.J., Schoenholtz, S., and Arts, M.T. 1980. The influence of flatworm predation on zooplankton inhabiting small ponds. Hydrobiologia, **76**: 233–240.

© 1999 NRC Canada

McNaught, A.S., Schindler, D.W., Parker, B.R., Paul, A.J., Anderson, R.S., Donald, D.B., and Agbeti, M. 1999. Restoration of the food web of an alpine lake following fish stocking. Limnol. Oceanogr. **44**: 127–136.

Moore, J.W. 1977. Importance of algae in the diet of subarctic populations of *Gammarus lacustris* and *Pontoporeia affinis*. Can. J. Zool. **55**: 637–641.

Neill, W.E. 1981. Impact of *Chaoborus* predation upon the structure and dynamics of a crustacean zooplankton community. Oecologia (Berl.), **48**: 164–177.

Ökland, K.A. 1969. On the distribution and ecology of *Gammarus lacustris* G.O. Sars in Norway, with notes on its morphology and biology. Nytt. Mag. Zool. (Oslo), **17**: 111–152.

Paul, A.J., Leavitt, P.R., Schindler, D.W., and Hardie, A.K. 1995. Direct and indirect effects of predation by a calanoid copepod (subgenus: *Hesperodiaptomus*) and of nutrients in a fishless alpine lake. Can. J. Fish. Aquat. Sci. **52**: 2628–2638.

Piercey, D.W., and Maly, E.J. 1998. Enclosures and predation rates in aquatic zooplankton communities. Verh. Int. Ver. Limnol. **26**: 1994–1996.

Rigler, F.H., MacCallum, M.E., and Roff, J.C. 1974. Production of zooplankton in Char Lake. J. Fish. Res. Board Can. **31**: 637–646.

Schindler, D.W. 1998. Replication versus realism: the need for ecosystem-scale experiments. Ecosystems, **1**: 323–334.

Segerstråle, S.G. 1954. The freshwater amphipods *Gammarus pulex* (L.) and *Gammarus lacustris* G.O. Sars, in Denmark and Fennoscandia — a contribution to the late- and postglacial immigration history of the aquatic fauna of northern Europe. Commentat. Biol. Soc. Sci. Fenn. **15**: 1–91.

Torke, B.G. 1974. An illustrated guide to the identification of the planktonic Crustacea of Lake Michigan with notes on their ecology. Special Report 17, Centre for Great Lakes Studies, University of Wisconsin–Milwaukee, Milwaukee, Wis.

Von Ende, C.N. 1993. Repeated-measures analysis: growth and other time-dependent measures. *In* Design and analysis of ecological experiments. *Edited by* S.M. Scheiner and J. Gurevitch. Chapman and Hall, New York. pp. 113–137.

Welschmeyer, N.A. 1994. Fluorometric analysis of chlorophyll *a* in the presence of chlorophyll *b* and phaeopigments. Limnol. Oceanogr. **39**: 1985–1992.

Zhadin, V.I., and Gerd, S.V. 1963. Fauna and flora of the rivers, lakes and reservoirs of the U.S.S.R. Israel Program for Scientific Translations, Jerusalem, Israel.

© 1999 NRC Canada

Modeling data from double-tagging experiments to estimate heterogeneous rates of tag shedding in lake trout (*Salvelinus namaycush*)

Mary C. Fabrizio, James D. Nichols, James E. Hines, Bruce L. Swanson, and Stephen T. Schram

Abstract: Data from mark–recapture studies are used to estimate population rates such as exploitation, survival, and growth. Many of these applications assume negligible tag loss, so tag shedding can be a significant problem. Various tag shedding models have been developed for use with data from double-tagging experiments, including models to estimate constant instantaneous rates, time-dependent rates, and type I and II shedding rates. In this study, we used conditional (on recaptures) multinomial models implemented using the program SURVIV (G.C. White. 1983. J. Wildl. Manage. 47: 716–728) to estimate tag shedding rates of lake trout (*Salvelinus namaycush*) and explore various potential sources of variation in these rates. We applied the models to data from several long-term double-tagging experiments with Lake Superior lake trout and estimated shedding rates for anchor tags in hatchery-reared and wild fish and for various tag types applied in these experiments. Estimates of annual tag retention rates for lake trout were fairly high (80–90%), but we found evidence (among wild fish only) that retention rates may be significantly lower in the first year due to type I losses. Annual retention rates for some tag types varied between male and female fish, but there was no consistent pattern across years. Our estimates of annual tag retention rates will be used in future studies of survival rates for these fish.

Résumé : Les données tirées d'études de marquage–recapture sont utilisées pour évaluer différents taux relatifs aux populations, notamment les taux d'exploitation, de survie et de croissance. Bon nombre de ces applications supposent une perte négligeable de marques, de sorte que la perte d'étiquettes peut être un problème important. Nous avons développé différents modèles de perte de marques qui seront utilisés avec des données provenant d'expériences de double marquage, notamment des modèles pour évaluer des taux instantanés constants, des taux chronologiques et des taux de pertes de marque de type I et II. Dans le cadre de la présente étude, nous avons utilisé des modèles multinominales conditionnels (aux recaptures) mis en oeuvre à l'aide du programme SURVIV (G.C. White. 1983. J. Wildl. Manage. 47 : 716–728) pour estimer le taux de perte de marques chez le touladi (*Salvelinus namaycush*) et explorer différentes sources potentielles de variation de ces taux. Nous avons appliqué les modèle aux données de plusieurs expériences de double marquage à long terme du touladi du lac Supérieur et estimé le taux de perte de marques à ancrage chez des poissons d'élevage et des poissons sauvages et pour différents types de marques utilisées dans ces expériences. Les estimations du taux annuel de conservation des marques pour le touladi étaient assez élevés (80–90%), mais nous avons des indications (chez les poissons sauvages seulement) que le taux de conservation peut être significativement plus faible au cours de la première année en raison des pertes de type I. Pour certains types de marques, les taux annuels de conservation étaient variables chez les mâles et les femelles, mais nous n'avons observé aucun profil régulier au cours des années. Nos estimations du taux annuel de conservation des marques serviront dans des études futures du taux de survie de ces poissons.

[Traduit par la Rédaction]

Introduction

Tag retention can be a significant problem in fisheries applications that use marked or tagged fish to study exploitation, survival, growth, migration and movement, stock composition, stock size, or spawning escapement. For example, in the presence of tag loss, survival rates estimated from mark–recapture studies are negatively biased (Arnason and Mills 1981; Pollock 1981; Nichols and Hines 1993). Data for estimating tag shedding rates are provided typically by double-tagging experiments (Beverton and Holt 1957; Seber 1982).

Received October 23, 1998. Accepted March 17, 1999.
J14855

M.C. Fabrizio.[1] U.S. Geological Survey, Great Lakes Science Center, 1451 Green Road, Ann Arbor, MI 48105, U.S.A.
J.D. Nichols and J.E. Hines. U.S. Geological Survey, Patuxent Wildlife Research Center, 11510 American Holly Drive, Laurel, MD 20708-4017, U.S.A.
B.L. Swanson and S.T. Schram. Wisconsin Department of Natural Resources, P.O. Box 589, Bayfield, WI 54814, U.S.A.

[1]Author to whom all correspondence should be addressed. e-mail: mary_fabrizio@usgs.gov

© 1999 NRC Canada

Beverton and Holt (1957) described two types of tag losses in fish: type I losses, which occur immediately after tagging, and type II losses occurring subsequently. In short-term experiments and assuming constant shedding rates, type II rates can be estimated from the Chapman et al. (1965) model, whereas the Bayliff and Mobrand (1972) model is used when both type I and II shedding occurs. Under these models, probabilities of tag loss are modeled as a (linear) function of time. The slope provides an estimate of the constant type II loss rate.

In some cases, constant shedding rates are not tenable. For example, type II shedding rates have been observed to both increase with time (Baglin et al. 1980) as tags deteriorate or fail with age and decrease with time (Kirkwood 1981) as tags with higher failure rates are shed earlier in the experiment. Kirkwood (1981) proposed that for some species, particularly long-lived ones such as southern bluefin tuna (*Thunnus maccoyii*), tag shedding rates vary among tags, thus appearing time dependent. His time-dependent model of tag shedding uses exact times at liberty and requires rather large sample sizes (i.e., many recaptures). Estimates of tag shedding rates from the Kirkwood (1981) model often have low precision (Hampton and Kirkwood 1990; Lai and Culver 1991; Fabrizio et al. 1996). In general, models that use exact time at liberty for recaptures (as opposed to pooled recaptures) are not as useful for sparse data (Wetherall 1982). Additionally, inference in time-dependent models may be more difficult. In one study, for example, recapture data were fit equally well by two different models: one had a constant type II rate and included type I shedding and the other model included a decreasing type II rate with no type I shedding (Hampton and Kirkwood 1990). Model selection in this and similar situations can be problematic.

In addition to type I shedding and time dependency, tag shedding models have been parameterized to account for other sources of variation in shedding rates, such as tag age (Nichols et al. 1992), tag type (Wetherall 1982; Barrowman and Myers 1996), tagging operator (Xiao 1996), and permanence of some tags (Kirkwood 1981; Fabrizio et al. 1996). Additional complexities of double-tagging experiments have been modeled including the flexibility to use either pooled or exact times at liberty and possible tag interactions (Xiao 1996). We note, however, that among a group of similarly marked fish, tags may be retained at rates that vary with characteristics of the marked individuals such as size (Waldman et al. 1990), sex (Brewin et al. 1995), and possibly other factors.

The purpose of this study was to develop models for estimating tag retention rates of lake trout (*Salvelinus namaycush*) and investigating multiple sources of variation in these rates. The sources of variation that we considered included measurable features of the fish and aspects of the double-tagging experiment. We used a widely available program, SURVIV (White 1983), to fit various models and to compute test statistics and statistics useful in model selection. We applied the modeling approach to data from double-tagging experiments with lake trout in the Gull Island Shoal area of southwestern Lake Superior. We were able to accommodate complex experimental design features and investigate the effect of sex, tag age, and origin of fish (hatchery or wild) on tag retention rates.

Methods

Double-tagging experiments

Since the 1960's, mark–recapture experiments have been conducted with lake trout in the Gull Island Shoal area, primarily for estimation of population size and survival rates. This population is a mixture of wild and hatchery-reared fish that were stocked annually near Gull Island Shoal as part of an effort to rehabilitate this species in Lake Superior (Swanson and Swedberg 1980; Hansen et al. 1995). Lake trout were captured in gill nets set in the Gull Island Shoal area during the October spawning season from 1973 to 1992 (Fig. 1). For each fish, we determined sex by expression of milt or eggs and noted the presence of fin clips, which denoted hatchery fish. Double-tagging experiments in fisheries applications typically use fin mutilation as a permanent mark (e.g., Robson and Regier 1966; Tranquilli and Childers 1982), but we could not use fin mutilation because lake trout stocked in Lake Superior are systematically fin clipped with a variety of fin clip combinations that indicate year-class. Instead, fin clips served as a distinguishing feature of hatchery-reared fish.

Fish captured in good condition were double-tagged with anchor tags, of which at least one was imprinted with a unique identification number. We used three types of numbered anchor tags (FD-67, FD-67C, or FD-68BC) as well as an unnumbered anchor tag (FD-67F) that we refer to as a plain tag (see Fabrizio et al. (1996) for a complete description of tag types). Plain tags are actually anchor flag tags (Wydoski and Emery 1983) that we modified by removing the flattened pendant. We double-tagged 10 236 lake trout.

Different tag types used during this study represent design improvements introduced by the manufacturer (Floy Tag & Manufacturing, Inc.). The FD-67C tag was shorter than the FD-67 tag, and the plastic bead on the FD-68BC tag was introduced to prevent separation of the colored tube from the nylon anchor. In 1973 and 1974, we double-tagged lake trout with identically numbered tags (FD-67) (Table 1). Fish double-tagged in 1978, 1979, 1980, and 1982 received a numbered FD-67C tag and a plain tag; those double-tagged in 1984 and 1985 carried an FD-68BC tag and a plain tag (Table 2). Because plain tags were color-coded by year, we could determine the year of tagging for fish that retained only a plain tag.

All fish were double-tagged by B.L.S., except for the 1985 cohort of 42 fish double-tagged by S.T.S. We tested all tags for disintegration failure before insertion and used only intact tags as had been done in other studies (e.g., Mourning et al. 1994). Tags were inserted on either side of the fish, just below the dorsal fin. This placement, followed by gentle tugging and rotation of the tag, ensured that the T-bar was firmly locked between adjacent pterygiophores. Interpterygiophore distances of adult lake trout were significantly less than one half the width of the T-bar (Fabrizio et al. 1996), so variation in retention rates was not associated with fish size in this study.

Fish were recaptured annually (1974–1992) in the Gull Island Shoal area during subsequent tagging operations. We did not consider recapture information from Lake Superior commercial or tribal fishers because we could not be sure that tags would be detected and reported accurately. If fishers reported only one tag when in fact both numbered tags were actually present, tag shedding rates would be overestimated. Note also that fishers' reporting of plain-tagged fish that had shed the numbered tag was not possible because plain tags carried no reporting instructions.

Models for two numbered tags

We developed models to estimate tag retention rates by conditioning on fish that were recaptured with at least one tag. This conditioning on recaptured fish required the assumption that capture probability did not depend on whether the fish had one or two tags.

© 1999 NRC Canada

Fig. 1. Study area in Lake Superior showing three sampling sites in the Gull Island Shoal area. The solid line demarcates the Gull Island refuge, a 70 000-ha area in which commercial and sport fishing have been prohibited since 1976.

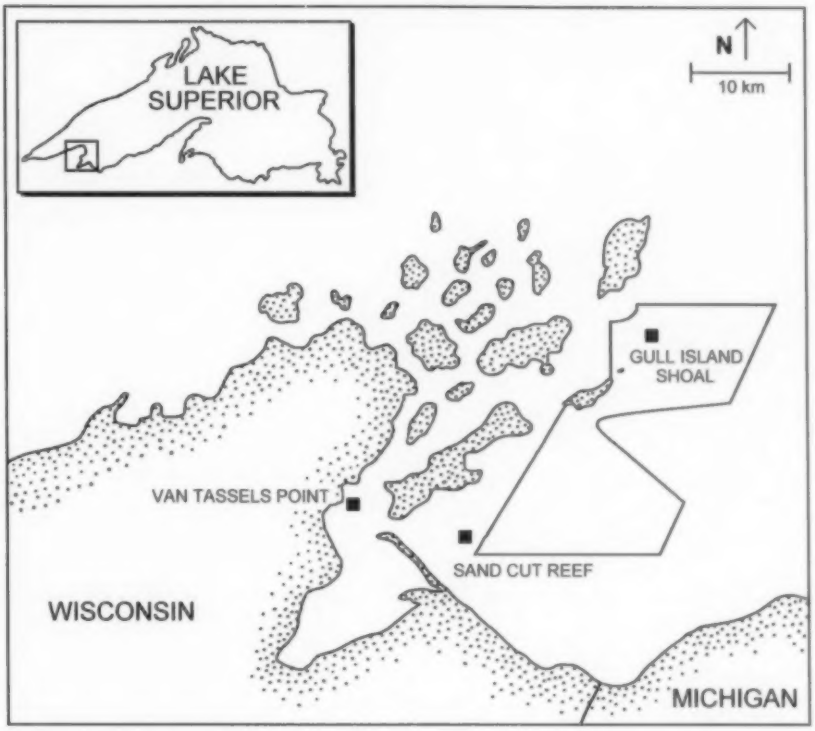

We first estimated annual tag retention rates for lake trout from double-tagging experiments conducted in 1973 and 1974 (Table 1). In both years, fish received two identical anchor tags prior to release in the Gull Island shoal area of southwestern Lake Superior.

We defined π_{ij} as the probability that a tag applied in year i is retained until year j given the fish was alive in year j. If a fish received two tags (i.e., it was not recaptured between i and j and given an additional tag), then we can observe two types of recaptures in year j: $r_{ij}^{(1)}$ is the number of fish tagged in year i and recaptured in year j with a single tag and $r_{ij}^{(2)}$ is the number of fish tagged in year i and recaptured in year j with both tags. Note that $r_{ij}^{(\bullet)} = r_{ij}^{(1)} + r_{ij}^{(2)}$ is the number of fish tagged in year i and recaptured in year j with at least one tag. Double-tagged fish that lost both tags were unobservable. We now write the expectation for the number of double-tagged fish released in year i and recaptured with both tags in year j conditional on the total number of fish double-tagged in year i and recaptured in year j as

$$(1) \qquad E(r_{ij}^{(2)} \mid r_{ij}^{(\bullet)}) = \frac{r_{ij}^{(\bullet)} P(r_{ij}^{(2)})}{P(r_{ij}^{(\bullet)})} = \frac{\pi_{ij} r_{ij}^{(\bullet)}}{2 - \pi_{ij}}$$

where $P(r_{ij}^{(2)})$ and $P(r_{ij}^{(\bullet)})$ are the respective probabilities that a fish double-tagged in year i and captured in year j has exactly two tags remaining in year j and at least one tag remaining in year j. The ratio $P(r_{ij}^{(2)})/P(r_{ij}^{(\bullet)})$ can be viewed as the expected fraction of recaptured fish with one or two tags, $r_{ij}^{(\bullet)}$, that still retains both tags.

Similarly, we can focus on double-tagged fish from release group i that are recaptured with only one tag in year j. The conditional expectation for this group of fish can be written as

$$(2) \qquad E(r_{ij}^{(1)} \mid r_{ij}^{(\bullet)}) = \frac{r_{ij}^{(\bullet)} P(r_{ij}^{(1)})}{P(r_{ij}^{(\bullet)})} = r_{ij}^{(\bullet)} \left[1 - \frac{\pi_{ij}}{(2 - \pi_{ij})} \right].$$

The ratio $P(r_{ij}^{(1)})/P(r_{ij}^{(\bullet)})$ can be viewed as the expected fraction of recaptured fish with one or two tags, $r_{ij}^{(\bullet)}$, that retains only one tag. This ratio is simply the complement of the expected fraction retaining both tags (see eq. 1). The conditional expectations 1 and 2 lead to the following conditional binomial probability model:

$$(3) \qquad P(r_{ij}^{(1)}, r_{ij}^{(2)} \mid r_{ij}^{(\bullet)}) = \frac{(r_{ij}^{(\bullet)})!}{(r_{ij}^{(1)})!(r_{ij}^{(2)})!} \times \left[\frac{\pi_{ij}}{(2 - \pi_{ij})} \right]^{r_{ij}^{(2)}} \left[1 - \frac{\pi_{ij}}{2 - \pi_{ij}} \right]^{r_{ij}^{(1)}}.$$

Some of the fish double-tagged in 1974 and subsequently recaptured with at least one tag were given a third numbered tag and rereleased following the initial and subsequent recaptures (Table 1, multiple recaptures). Some of these rereleases had both of the original 1974 tags and some had only one of the 1974 tags. When these fish marked with a year j tag (a non-1974 tag applied in the year of initial recapture) were recaptured with the year j tag intact, the number of remaining 1974 tags was also recorded.

Let $r_{j(2)k}^{(\bullet)}$ denote the number of rereleases in year j with two 1974 tags remaining at the time of release that were subsequently recaptured in year k with the year j tag intact. Let $r_{j(2)k}^{(0)}$, $r_{j(2)k}^{(1)}$, and $r_{j(2)k}^{(2)}$ denote the number of these recaptures (members of $r_{j(2)k}^{(\bullet)}$) that had zero, one, and two 1974 tags remaining, respectively. The con-

© 1999 NRC Canada

Table 1. Number of lake trout tagged with two numbered tags (FD-67) for the double-tagging experiments in 1973 (N = 77) and 1974 (N = 583).

	Hatchery		Wild		
Years at liberty	Male	Female	Male	Female	Total
		1973 releases			
Not seen again	44	24	3	1	73[a]
1	2				2
2		1			1
6		1			1
		1974 releases			
Not seen again	87	25	289	99	501[b]
1	5	1	17	3	26
2	4		5	4	13
3	3		8		11
4			4	1	5
5	1		1		2
6			1		1
7			1	2	3
8			1		1
9			1		1
10			1		1
12			1		1
18			1		1
Multiple	2		13	1	16

Note: "Multiple" refers to fish recaptured more than once, e.g., fish recaptured after 2 years at liberty, released, and rerecaptured 3 years later.

[a]Includes one hatchery fish of unknown sex.

[b]Includes one wild fish of unknown sex.

ditional expectations for these three classes of recaptures can be written as

$$(4)\quad E(r^{(0)}_{j(2)k} \mid r^{(\bullet)}_{j(2)k}) = r^{(\bullet)}_{j(2)k}(1-\pi_{jk})^2$$

$$E(r^{(1)}_{j(2)k} \mid r^{(\bullet)}_{j(2)k}) = r^{(\bullet)}_{j(2)k}(2\pi_{jk}(1-\pi_{jk}))$$

$$E(r^{(2)}_{j(2)k} \mid r^{(\bullet)}_{j(2)k}) = r^{(\bullet)}_{j(2)k}\pi^2_{jk}.$$

These expectations lead to the following conditional multinomial model:

$$(5)\quad P(r^{(0)}_{j(2)k}, r^{(1)}_{j(2)k}, r^{(2)}_{j(2)k} \mid r^{(\bullet)}_{j(2)k}) = \frac{(r^{(\bullet)}_{j(2)k})!}{(r^{(0)}_{j(2)k})!(r^{(1)}_{j(2)k})!(r^{(2)}_{j(2)k})!} \times [(1-\pi_{jk})^2]^{r^{(0)}_{j(2)k}}[2\pi_{jk}(1-\pi_{jk})]^{r^{(1)}_{j(2)k}}[\pi^2_{jk}]^{r^{(2)}_{j(2)k}}.$$

Some of the rereleases in year j had already lost one of the 1974 tags and were released in year j with one new tag from year j and one 1974 tag. Denote the number of fish from this group recaptured in year k with the year j tag intact as $r^{(\bullet)}_{j(1)k}$. Let $r^{(0)}_{j(1)k}$ and $r^{(1)}_{j(1)k}$ denote the respective number of these recaptures that had zero and one 1974 tag remaining at the time of recapture in year k. The conditional expectations for these classes of recaptures are

$$(6)\quad E(r^{(0)}_{j(1)k} \mid r^{(\bullet)}_{j(1)k}) = r^{(\bullet)}_{j(1)k}(1-\pi_{jk})$$

$$E(r^{(1)}_{j(1)k} \mid r^{(\bullet)}_{j(1)k}) = r^{(\bullet)}_{j(1)k}\pi_{jk}.$$

These expectations lead to the following binomial model:

$$(7)\quad P(r^{(0)}_{j(1)k}, r^{(1)}_{j(1)k} \mid r^{(\bullet)}_{j(1)k}) = \frac{(r^{(\bullet)}_{j(1)k})!}{(r^{(0)}_{j(1)k})!(r^{(1)}_{j(1)k})!} \times (\pi_{jk})^{r^{(1)}_{j(1)k}}(1-\pi_{jk})^{r^{(0)}_{j(1)k}}.$$

Note that models 5 and 7, which are based on rereleases, focus on tag loss parameters and statistics associated with the 1974 tags and not the tags applied at the first recapture. (None of the 1973-tagged fish were recaptured following initial recapture and rerelease.) The above models were not developed for estimating tag loss of year j tags. Also note that the use of conditional binomial and multinomial distributions requires the assumption that the loss of one tag is independent of the loss of the other.

We modeled the π_{ij} cell probabilities as functions of an initial tag retention probability, γ, and annual tag retention probabilities, θ_k. In this model, γ is the complement of the probability of type I shedding. Because all initial releases were in 1973 and 1974 (most in 1974), we defined i and j in terms of "tag age" rather than calendar year. So, θ_1 corresponds to the probability that a tag "surviving" the initial tag loss event is retained from the year of tagging (i = 0) to the time of recapture in year 1 (j = 1). We now have

$$\pi_{0j} = \gamma\prod_{k=1}^{j}\theta_k$$

$$= P(\text{tag is present } j \text{ years after initial application}) \quad \text{for } j = 1, \ldots, K$$

where K is the maximum observed tag age. Only two fish from these double-tagging experiments were recaptured with times at liberty greater than 10 years (12 and 18 years) (Table 1), so we simplified the model by assuming that the age-specific θ_k were equal after 10 years at liberty (i.e., $\theta_{10} = \theta_{11} = \theta_{12} = \ldots = \theta_{10+}$). We

© 1999 NRC Canada

Table 2. Number of double-tagged lake trout released with a plain tag (FD-67F) and a numbered anchor tag (either type FD-67C or FD-68BC) and recaptured 1 year after tagging.

		Number of tagged fish released							Number of recaptures that shed the numbered tag					Number of recaptures that retained the numbered tag				
		Hatchery			Wild				Hatchery			Wild			Hatchery			Wild		
Numbered tag type	Release year	M	F	U	M	F	U	Total	M	F	Total	M	F	Total	M	F	Total	M	F	Total
FD-67C	1978	219	121	17	1225	730	30	2342	4	1	62	47	10		12	2		112	29	
	1979	336	151	1	940	433	1	1862		1	24	22	1		11			77	10	
	1980	148	47	1	1421	300	8	1925	2	1	21	18			3	1		102	4	
	1982	288	76	7	1367	518	15	2271	3		82	71	8		9			128	19	
FD-68BC	1984	132	48	2	717	231	4	1134			3	3			5			41	4	
	1985				42			42			1	1								

Note: M, male; F, female; U, unknown sex.

modeled tag retention rates separately for males and females and for hatchery and wild fish.

Cell probabilities for captures of rereleased fish, π_{jk}, were modeled slightly differently than recaptures of initial releases. As noted in the probability models for captures of rereleased fish (eqs. 4–7), the cell probabilities correspond to the interval between rerelease (time j) and subsequent recapture (time k). If we retain the above notation of denoting the year of initial tagging as $i = 0$ and that of initial recapture as j, then j corresponds to the age of the tag, in years. Statistics for rereleases that are eventually recaptured are subscripted by j and k, denoting the ages at rerelease and subsequent recapture, respectively. The cell probabilities for recaptures of rereleases thus differ from those of new releases in not including either a θ_0 or a γ parameter. For example, consider the following two cell probabilities for recaptures of rereleases:

$$\pi_{23} = \theta_2$$

$$= P(\text{tag is present 1 year after rerelease at tag age 2})$$

$$\pi_{35} = \theta_3\theta_4$$

$$= P(\text{tag is present 2 years after rerelease at tag age 3}).$$

The annual tag retention probabilities (θ_k) are subscripted by the appropriate tag ages, and the π_{jk} do not include γ parameters because the modeling corresponds to time periods that do not include the year following initial release.

We combined the conditional probability models 3, 5, and 7 for all recaptures of all three kinds of releases ($r_{ij}^{(\bullet)}$, $r_{j(2)k}^{(\bullet)}$, and $r_{j(1)k}^{(\bullet)}$) into a product-multinomial model parameterized by the γ and θ_k tag retention parameters. We used program SURVIV (White 1983) to compute maximum likelihood estimates under this multinomial model. SURVIV also computed goodness-of-fit tests and Akaike's information criterion (AIC) to aid in model selection (e.g., see Lebreton et al. 1992; Burnham and Anderson 1998).

Models for one numbered tag

For the study with numbered and plain tags, the modeling differed, as we restricted recapture information to the year following tagging with a plain tag (Table 2). We did not extend the modeling of plain tag recapture data to years following the first because of the ambiguity associated with later recaptures. For example, recapture status the first year following tagging will not be known for a fish recaptured (with a tag) 2 years following tagging. If the fish captured in year 2 was not captured previously in year 1, then we would like to model the tag survival probability associated with the recapture event as $\theta_1\theta_2$. However, if the fish was captured in year 1, then this event will have already been modeled as θ_1, and we would model the recapture in year 2, conditional on year 1 rerelease, with just θ_2. Only recaptures occurring in the first year after tagging can be modeled with no ambiguity about previous history, and we restricted our modeling to this group for this reason. Because of this restriction, each fish contributed at most one recapture to the data set. We could not test for type I shedding, as plain tags permit estimation of tag retention probability for only the first year after release. Estimation is based on the first-year recaptures of fish retaining a plain tag in year $i + 1$. Denote these recaptures as $r_{i,i+1}^{(\bullet)}$. Some of these recaptures still had the numbered tag in year $i + 1$ (denote these as $r_{i,i+1}^{(1)}$) and some had lost the numbered tag (denote these as $r_{i,i+1}^{(0)}$). If $\pi_{i,i+1}$ is the probability that a new numbered tag in year i is retained until year $i + 1$, then we write the conditional (on $r_{i,i+1}^{(\bullet)}$) expectations as

$$(8) \qquad E(r_{i,i+1}^{(1)} \mid r_{i,i+1}^{(\bullet)}) = r_{i,i+1}^{(\bullet)}(\pi_{i,i+1})$$

$$E(r_{i,i+1}^{(0)} \mid r_{i,i+1}^{(\bullet)}) = r_{i,i+1}^{(\bullet)}(1 - \pi_{i,i+1}).$$

© 1999 NRC Canada

These expectations lead to the conditional binomial model:

$$(9)\qquad P(r_{i,i+1}^{(0)}, r_{i,i+1}^{(1)} \mid r_{i,i+1}^{(\bullet)}) = \frac{(r_{i,i+1}^{(\bullet)})!}{(r_{i,i+1}^{(0)})!(r_{i,i+1}^{(1)})!} \times [\pi_{i,i+1}]^{r_{i,i+1}^{(1)}}[1-\pi_{i,i+1}]^{r_{i,i+1}^{(0)}}.$$

Releases of fish with plain tags occurred during six different years and involved both sexes of hatchery-reared and wild fish (Table 2). Each release group for which at least one recapture occurred led to a model of the type in eq. 9, and these were combined into a product-binomial for all release groups. The $\pi_{i,i+1}$ represented the probability that a tag would be retained from the time of initial release in year i until the time of recapture in year $i + 1$. We used a single parameter, θ, for this probability, which included both type I and type II tag loss. These two types of loss could not be estimated separately under this design. As before, we used SURVIV (White 1983) to compute maximum likelihood estimates of tag retention rates, goodness-of-fit tests, likelihood ratio tests, and AIC values.

Model building and selection

For both types of double-tagging experiments (two numbered tags, numbered tag plus plain tag), we built several models by considering the effects of fish origin (hatchery versus wild), sex (male versus female), tag age (for 1973 and 1974 tags), and year of release (for plain-tagged fish). We used model building approaches described in Lebreton et al. (1992) and constrained model parameters to search for more parsimonious models. For example, with the plain tag data, we might assume no temporal variation in first-year tag retention rates and use a four-parameter model to estimate rates for hatchery male, hatchery female, wild male, and wild female fish. The four θ parameters corresponding to these four groups can be constrained to a three-parameter model by setting retention rates equal for female fish (regardless of origin). All models that we explored were nested within the general model of origin, sex, and time or tag age effects.

Our approach to estimation of retention rates and selection of models parallels that typically used for survival rates. Model selection was accomplished using AIC as described in Burnham and Anderson (1992), Lebreton et al. (1992), and Burnham et al. (1995). Models with too many parameters, while providing good fit, are characterized by estimates with low precision. Models with too few parameters may not fit the data adequately and can produce biased estimates. Model selection can be viewed as an optimization problem, where AIC is the objective function indicating which model achieves the optimal balance between fit and number of parameters (Burnham and Anderson 1992, 1998). SURVIV computes the AIC for each model; models with lower AIC's are considered better models. When the most general model did not fit the data adequately, we used a quasilikelihood approach to testing (Burnham et al. 1987) and computed QAIC following methods in Anderson et al. (1994). We also used the small-sample corrections suggested by Anderson et al. (1994) to compute AIC_c and $QAIC_c$. However, these small-sample corrections modified AIC and QAIC by small amounts and made no difference in model selection. We therefore considered AIC and QAIC values in the remainder of the study. Rather than presenting the QAIC values, we present ΔQAIC, which is the difference between the model's QAIC and the lowest QAIC among all models considered. Burnham and Anderson (1998) recommended using this approach. In some cases, we used an analysis of deviance F test to determine the significance of a particular test between tag retention models (Lebreton et al. 1992). We used the analysis of deviance approach to test specific hypotheses, not in model selection.

Results

Two numbered tags

We constructed and evaluated several models to estimate retention rates for FD-67 tags (Table 3). The model with full origin, sex, and age specificity of retention rates (model Origin–Sex–Type $I_{\text{origin-sex-tag age}}$) was the most general model that could be fit to the data. This model exhibited a significant lack of fit (goodness-of-fit test: $G = 48.28$, df = 21, $P < 0.05$), indicating structural inadequacy of the model, overdispersion in the data, or both. If the data are overdispersed, AIC cannot be used in model selection (Anderson et al. 1994). We suspected overdispersion in our data because some of the fish tagged on the same day were later recaptured together. This type of "pairing" or schooling behavior leads to a lack of independence among observations (overdispersion) and results in extrabinomial variation (Anderson et al. 1994). Although model parameter estimates are not affected by extrabinomial variation, variance estimates and related likelihood statistics (such as AIC) are biased (Anderson et al. 1994). Using a quasilikelihood approach, we adjusted for overdispersed data by estimating the variance inflation factor ($\hat{c} = G/\text{df} = 48.28/21 = 2.299$) from the general model and then using $\hat{c}$ to estimate variances and calculate QAIC values for each model (Anderson et al. 1994).

The model we selected to best describe tag retention rates in lake trout tagged with FD-67 tags was a three-parameter model that included type I retention rates for wild fish only and otherwise constant (over tag age and sex) annual retention rates for wild and hatchery fish (model Origin–Type I_W) (Table 3). Annual retention rates of FD-67 tags were somewhat higher for hatchery fish ($\theta_H = 0.94$, 95% CI = 0.85–1.0) than for wild fish (year 1, $\gamma_W\theta_W = 0.64$, 95% CI = 0.41–0.86; years 2, 3, etc., $\theta_W = 0.88$, 95% CI = 0.78–0.99) (Fig. 2). The data supported the notion that type I shedding may be occurring in wild fish, but there was insufficient evidence for type I shedding in hatchery fish. We could not reject the hypothesis that the type I retention rate for hatchery fish was 1.0 using an analysis of deviance F test of model Origin–Type I_W versus Origin–Type $I_{H,W}$ ($F = 0.483$, df = 1, 21, $P = 0.989$). Under the model Origin–Type $I_{H,W}$, the estimated type I retention rate for hatchery fish was 0.86 (95% CI = 0.66–1.0). Although we recovered about equal proportions of hatchery (4.0%) and wild fish (4.4%) 1 year after release, our inability to detect type I shedding in hatchery fish may be due to the smaller numbers of releases, and hence recaptures, of hatchery fish 1 year after tagging (eight compared with 20 wild fish recaptured) (Table 1). We also tested the null hypothesis of no difference in tag retention rates for hatchery and wild fish. We found little evidence for differences between hatchery and wild fish ($F = 3.827$, df = 1,21, $P = 0.128$).

One numbered tag

As with data from the double-tagging experiment using FD-67 tags, we constructed several models to account for variation in tag retention rates due to origin and sex. We also considered year of release and tag type as possible sources of variation, but note that these two factors are related (see Table 2). All retention rates estimated from the double-

© 1999 NRC Canada

Table 3. Tag retention models fit to the lake trout double-tagging experiments from 1973 and 1974.

Model	Notation	p	ΔQAIC
Origin–Sex–Type $I_{HM,HF,WM,WF}$–Tag Age	$(\gamma_{HM}\theta_{HM1})\theta_{HM2}\theta_{HM3}\theta_{HM4.5}\theta_{HM6.9}$ $(\gamma_{HF}\theta_{HF1})\theta_{HF2}\theta_{HF3.6}$ $(\gamma_{WM}\theta_{WM1})\theta_{WM2}\theta_{WM3}\theta_{WM4}\theta_{WM5}\theta_{WM6}\theta_{WM7}\theta_{WM8}\theta_{WM9}\theta_{WM10}$ $(\gamma_{WF}\theta_{WF1})\theta_{WF2}\theta_{WF3.4}\theta_{WF5}\theta_{WF6.7}$	23*	34.08
Origin–Sex–Type $I_{HM,HF,WM,WF}$–Tag $Age_{restricted}$	$(\gamma_{HM}\theta_{HM1})\theta_{HM2}\theta_{HM3}\theta_{HM4.9}$ $(\gamma_{HF}\theta_{HF1})\theta_{HF2.6}$ $(\gamma_{WM}\theta_{WM1})\theta_{WM2}\theta_{WM3}\theta_{WM4}\theta_{WM5}\theta_{WM6}\theta_{WM7}\theta_{WM8}\theta_{WM9}\theta_{WM10}$ $(\gamma_{WF}\theta_{WF1})\theta_{WF2}\theta_{WF3.7}$	19*	26.73
Origin–Sex–Type $I_{HM,HF,WM,WF}$	$\gamma_{HM}\theta_{HM}$ $\gamma_{HF}\theta_{HF}$ $\gamma_{WM}\theta_{WM}$ $\gamma_{WF}\theta_{WF}$	8	8.32
Origin–Sex–Type $I_{HF,WM,WF}$	θ_{HM} $\gamma_{HF}\theta_{HF}$ $\gamma_{WM}\theta_{WM}$ $\gamma_{WF}\theta_{WF}$	7	6.55
Origin–Sex–Type $I_{WM,WF}$	$\theta_{HM}\theta_{HF}$ $\gamma_{WM}\theta_{WM}$ $\gamma_{WF}\theta_{WF}$	6	4.90
Origin–Sex–Type $I_{H,W}$	$\gamma_{H}\theta_{HM}\theta_{HF}$ $\gamma_{W}\theta_{WM}\theta_{WF}$	6	4.56
Origin–Sex	$\theta_{HM}\theta_{HF}$ $\theta_{WM}\theta_{WF}$	4	5.97
Origin–Type $I_{H,W}$	$\gamma_{H}\theta_{H}$ $\gamma_{W}\theta_{W}$	4	1.52
Origin–Type I_{W}	θ_{H} $\gamma_{W}\theta_{W}$	3	0
Origin–Type I	$\gamma\theta_{H}\theta_{W}$	3	0.12
Sex	$\theta_{M}\theta_{F}$	2	4.96
Origin	$\theta_{H}\theta_{W}$	2	2.22
Simple–Type I	$\gamma\theta$	2	1.83
Simple	θ	1	3.19

Note: All lake trout were tagged with two numbered tags (type FD-67). Type I retention rates are denoted γ and type II rates are denoted θ. Subscripts refer to male (M), female (F), hatchery (H), and wild (W) fish. Other subscripts refer to tag age (1, 2, etc., in years) or to a range of tag ages (4.5, 6.9). An asterisk after the number of parameters (p) indicates that type I retention and first-year tag retention rates were not separately estimable; these rates are denoted in parentheses, e.g., $(\gamma_{HM}\theta_{HM1})$.

Fig. 2. Estimated retention rates of FD-67 tags in wild (■) and hatchery (□) lake trout from Gull Island Shoal, Lake Superior. The bars around the point estimates represent 95% CI. Tag age 10+ includes observations from fish at liberty 10 or more years.

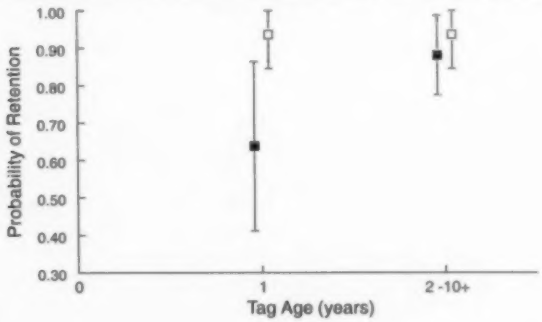

tagging experiment with plain tags are first-year retention rates, combining type I and II rates.

The most general model we fit had tag retention parameters that varied by sex, source, and year of application (model Origin–Sex–Year) (Table 4). The model was fully saturated, permitting use of AIC (rather than QAIC) in model selection.

The model with the lowest AIC (Origin–Sex–$Year_{WM}$) had nine parameters: one tag retention rate for hatchery males, one for hatchery females, six for wild males, and one for wild females (Table 4). In general, estimated tag retention rates were about 0.80 (Fig. 3) except for hatchery females, which exhibited lower retention rates (θ_{HF} = 0.50, 95% CI = 0.10–0.90). Year-specific parameters were necessary to account for variation in retention rates among wild males, and this variation did not appear to be associated with tag type for wild males (likelihood ratio test between models Origin–Sex–$Year_{WM}$ and Origin–Sex–Tag $Type_{WM}$: χ^2 = 23.825, df = 4, $P < 0.05$). The retention rate for the 1985 releases could not be estimated reliably with model Origin–Sex–

© 1999 NRC Canada

Table 4. Tag retention models fit to the lake trout double-tagging experiments from 1978, 1979, 1980, 1982, 1984, and 1985.

Model	Notation	p	ΔAIC
Origin–Sex–Year	$\theta_{HM78}\theta_{HM79}\theta_{HM80}\theta_{HM82}\theta_{HM84}$ $\theta_{HF78}\theta_{HF79}\theta_{HF80}$ $\theta_{WM78}\theta_{WM79}\theta_{WM80}\theta_{WM82}\theta_{WM84}\theta_{WM85}$ $\theta_{WF78}\theta_{WF79}\theta_{WF80}\theta_{WF82}\theta_{WF84}$	19	3.34
Origin–Sex–$\text{Year}_{WM,WF}$	$\theta_{HM}\theta_{HF}$ $\theta_{WM78}\theta_{WM79}\theta_{WM80}\theta_{WM82}\theta_{WM84}\theta_{WM85}$ $\theta_{WF78}\theta_{WF79}\theta_{WF80}\theta_{WF82}\theta_{WF84}$	13	1.59
Origin–Sex–Year_{WM}	$\theta_{HM}\theta_{HF}$ $\theta_{WM78}\theta_{WM79}\theta_{WM80}\theta_{WM82}\theta_{WM84}\theta_{WM85}$ θ_{WF}	9	0
Origin–Sex–Year_{WM}–Tag Type_{WM}	$\theta_{HM}\theta_{HF}$ $\theta_{WM78}\theta_{WM79}\theta_{WM80}\theta_{WM82}\theta_{WM(BC)}$ θ_{WF}	8	3.09
Origin–Sex–Tag $\text{Type}_{HM,WM,WF}$	$\theta_{HM(C)}\theta_{HM(BC)}\theta_{HF}$ $\theta_{WM(C)}\theta_{WM(BC)}\theta_{WF(C)}\theta_{WF(BC)}$	7	15.59
Origin–Sex–Tag $\text{Type}_{WM,WF}$	$\theta_{HM}\theta_{HF}$ $\theta_{WM(C)}\theta_{WM(BC)}\theta_{WF(C)}\theta_{WF(BC)}$	6	15.74
Origin–Sex–Year_{WM}–Tag Type_{WM}	$\theta_{HM}\theta_{HF}$ $\theta_{WM(C)}\theta_{WM(BC)}\theta_{WM80}\theta_{WF}$	6	5.00
Origin–Sex–Tag Type_{WM}	$\theta_{HM}\theta_{HF}$ $\theta_{WM(C)}\theta_{WM(BC)}$ θ_{WF}	5	15.82
Origin–Sex_{W}–Tag Type_{WM}	θ_{H} $\theta_{WM(C)}\theta_{WM(BC)}\theta_{WF}$	4	16.47
Origin–Sex_{H}–Tag Type_{W}	$\theta_{HM}\theta_{HF}$ $\theta_{W(C)}\theta_{W(BC)}$	4	13.03
Origin–Sex	$\theta_{HM}\theta_{HF}$ $\theta_{WM}\theta_{WF}$	4	22.86
Origin–Tag Type	$\theta_{H(C)}\theta_{W(C)}$ $\theta_{H(BC)}\theta_{W(BC)}$	4	13.08
Sex–Tag Type	$\theta_{M(C)}\theta_{F(C)}$ $\theta_{M(BC)}\theta_{F(BC)}$	4	13.35
Origin–Tag Type_{W}	θ_{H} $\theta_{W(C)}\theta_{W(BC)}$	3	13.68
Tag Type_{origin}	$\theta_{H(C)}\theta_{W(C)}$ $\theta_{BC)}$	3	11.88
Tag Type	$\theta_{(C)}\theta_{BC)}$	2	10.09
Origin	$\theta_{H}\theta_{W}$	2	22.06
Sex	$\theta_{M}\theta_{F}$	2	22.38
Simple	θ	1	20.46

Note: All lake trout were tagged with a plain tag and one numbered tag (either type FD-67C (denoted C in subscripts) or FD-68BC used in 1984 and 1985 (denoted BC in subscripts)). Tag retention rates, θ, apply to numbered tags only; subscripts refer to male (M), female (F), hatchery (H), and wild (W) fish; years are denoted by the last two digits; p is the number of parameters in the model.

Year_{WM} because sample size for this group of releases was very small. Both ΔAIC values and the likelihood ratio test between models Origin – Sex – Year_{WM} and Origin – Sex – Year_{WM} – Tag Type_{WM} ($\chi^2 = 5.092$, df = 1, $P < 0.05$) provided support for the model in which retention rates for FD-68BC tags in 1984 and 1985 were different. Unlike the estimated retention rate for the 1985 releases, the estimated retention rate for the 1984 releases was high ($\hat{\theta}_{1984} = 0.93$, 95% CI = 0.86–1.0).

We noted that the retention rate for wild males tagged with FD-67C tags in 1980 was higher ($\hat{\theta}_{1980} = 0.85$) than those for the three other groups of wild males tagged with FD-67C tags ($\hat{\theta}$ varied between 0.64 for 1982 releases and 0.78 for 1979 releases). We hypothesized that the higher retention rate for the 1980 release was associated with the use of different-colored FD-67C tags in that year (the only year for which numbered tags varied in color). Two sets of FD-67C tags were used in 1980: one set with grey tubing (53.6% of the tags) and another with orange (46.4%). A χ^2 test of differences in proportion of fish recaptured in 1981 with grey and orange tags provided no evidence of a difference ($\chi^2 = 0.003$, $P > 0.05$). Thus, the higher retention rate

© 1999 NRC Canada

Fig. 3. Estimated retention rates of FD-67C and FD-68BC tags in wild male (■), hatchery male (□), wild female (●), and hatchery female (○) lake trout from Gull Island Shoal, Lake Superior. These rates, shown as point estimates with 95% CI, represent tag retention after 1 year at liberty and apply to releases from 1978, 1979, 1980, 1982, and 1984. Results for the 1985 releases are not plotted because only wild males were tagged in 1985 and the resulting estimate was unreliable, being based on a single recapture.

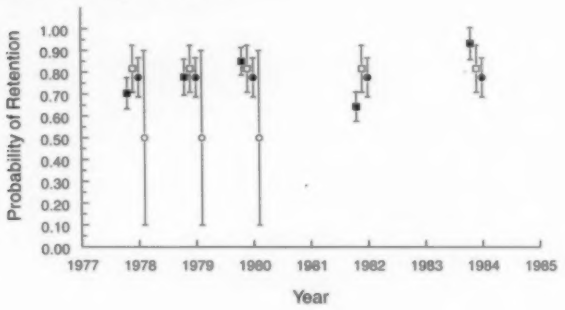

for the 1980 releases does not appear to be associated with differences in performance quality or durability of the different colors used that year. Similarly, retention rates for the 1984 releases were significantly greater than those for the 1978 and 1982 releases (Fig. 3). The greater sample sizes used to model retention rates of FD-67C tags in wild males permitted estimation of retention rates for each year. Annual fluctuations in these rates represented a source of significant variation in the data (likelihood ratio test between models Origin–Sex–$Year_{WM}$ and Origin–Sex: $\chi^2 = 32.863$, df = 5, $P < 0.05$).

Discussion

In this paper, we demonstrated that SURVIV, originally developed to model survival rates (White 1983), can be used to estimate tag retention rates for fish. This application requires specifying the conditional binomial or multinomial probabilities for each recaptured fish in the double-tagging experiment. Under the SURVIV framework, conditional binomial (and multinomial) probability models are functions of the number of fish recaptured with at least one tag and the probability of a tag being retained from year i to year j. This probability was defined as a product of the type I retention rate and the annual tag retention rate.

Data from lake trout double-tagged with two numbered tags were used to examine differences in retention rates with tag age and estimate the additional type I losses. The flexibility of our modeling approach allowed us to accommodate a unique aspect of the double-tagging experiments. Unlike most double-tagging studies, we could "observe" double-tagged fish that were recaptured with no tags. These observations were possible because some of the fish from the 1974 experiment were tagged multiple times.

Previously described methods for estimating tag retention rates have generally focused on estimation of constant rates (e.g., Chapman et al. 1965; Bayliff and Mobrand 1972; Fabrizio et al. 1996). A few models of time-dependent variation in retention rates have been described (e.g., Kirkwood 1981; Hampton and Kirkwood 1990). Our approach can be tailored to the study design and permits subsetting of the data (e.g., males versus females or by tag type), inclusion of type I rates, and variation of retention rates according to features of the tagged fish (e.g., sex, size, or origin) or aspects of the experiment. Decisions concerning the importance of factors in accounting for variation in tag retention rates are made during the model selection process using AIC or QAIC, although other objective functions could be used. In the case of nested models, the significance of factors can be tested with likelihood ratio tests or analyses of deviance (Lebreton et al. 1992).

Our estimates of annual tag retention rates for lake trout were fairly high (80–90%), but we found evidence (among wild fish only) that retention rates may be significantly lower in the first year due to type I losses. Are type I losses real? Although we were unable to detect type I losses, we suspect that they may have indeed occurred among hatchery fish. Our inability to detect lower first-year retention rates in hatchery fish may have been due to small sample sizes (too few recaptures) rather than to any biological or behavioral differences between wild and hatchery fish. One possible mechanism that may contribute to lower tag retention rates in the first year is tag disintegration. We noted that on average, 11% of the recaptured fish carried defective tags (Fabrizio et al. 1996). These fish retained the T-bar (the anchor) but not the nylon tube (the portion of the tag inscribed with a number). Although we tested for this type of tag failure before inserting the anchor tags, it remained a problem with some of the tags. However, it is not possible to unequivocally ascribe these losses to the first year because we could not determine the year of tagging for fish recaptured with defective tags.

According to our data from double-tagging experiments with FD-67C and FD-68BC tags, tag retention rates may vary between male and female lake trout. Brewin et al. (1995) found differences in shedding rates for male and female brown trout (*Salmo trutta*) tagged with Floy anchor tags. We found no evidence for annual differences in tag retention rates for wild female lake trout, although one explanation for this is that sample sizes were small. In some years, retention rates for wild males were slightly higher than for wild females, and in other years the opposite was true. Variations in tag retention rates between sexes may reflect behavioral differences of lake trout. However, if tag shedding was associated with persistent behavioral differences between male and female fish, we should have observed a consistent pattern in retention rates through time (see Fig. 3). We recommend additional double-tagging experiments with larger sample sizes, particularly for female lake trout, so that this source of variation in retention rates can be reexamined. In addition, these experiments should be conducted with two numbered tags so that type I shedding rates can be estimated as well.

Some of the data from this study were also analyzed by Fabrizio et al. (1996), who estimated constant tag shedding rates for three types of tags using nonlinear models. In general, the results presented here compare favorably with those in Fabrizio et al. (1996), although the nonlinear models describe constant tag shedding rates for all lake trout (no subsets were investigated). The results of the two studies are not

© 1999 NRC Canada

directly comparable because we examined tag shedding rates from subsets of data (e.g., male and female fish) and were also able to include data that could not be used with the nonlinear modeling approach.

Although not demonstrated here, another possible source of variation in tag retention rates is the tag operator. Hearn et al. (1991) warned against pooling recapture data from different taggers because they often display different skill levels or follow slightly different procedures. Using the approach developed in our study, tagger effects can be tested with likelihood ratio tests of nested models. Other modeling approaches permit likelihood ratio testing as well (e.g., see Barrowman and Myers 1996; Hampton 1997). It may also be desirable to determine if the skill of an individual tagger improved or deteriorated over time (years); the probability of tag retention is expected to increase as skill increases over time. Except for the lower retention of tags from the 1982 experiment, this expectation appears to be supported by results for wild males tagged with FD-67C tags (Fig. 3). (Retention rates were modeled as constants for wild females, hatchery females, and hatchery males and thus were not useful in examining this issue.) However, improvement in the tagger's skill may be offset by factors associated with the tagging operation. For example, tag placement and insertion are more accurate and effective on a stable platform, but tagging becomes difficult in rough seas.

All of our modeling and results are based on the assumption that tags on a fish are lost independently. This may not always be the case (e.g., see Diefenbach and Alt 1998). One approach to such dependence is to model the initial tag retention probability (conditional on no previous tag loss) with one parameter and the probability of loss of the second tag (conditional on loss of the first tag) with a different parameter. Such modeling would appear to require three tags, at least two individually numbered tags and a third tag (or some other mark) identifying the fish as part of the study. The modeling would then be conditional on fish captured with the third tag or mark and would model events associated with the loss of zero, one, or two numbered tags.

Considered in isolation, tag loss is fairly uninteresting from both management and ecological perspectives. One of the primary motivating factors for our study of tag retention rates was the desire to estimate survival rates for this population of lake trout in Lake Superior. In the presence of tag loss, survival rates must be adjusted to "correct" for the loss of tags, and this is typically performed using a posteriori methods. For example, $\hat{\phi}' = \hat{\phi}/\hat{\theta}$, where $\hat{\phi}'$ is the adjusted (for tag loss) survival rate for fish, $\hat{\phi}$ is the estimated survival rate for tagged fish (complement includes fish death and tag loss), and $\hat{\theta}$ is the estimated tag retention rate, assumed to be constant over time (Pollock 1981). However, when tag retention rates are less than survival rates, post hoc adjusted estimates of annual survival rates are greater than 100% (e.g., see Fabrizio et al. 1997). When survival rates are high, adjustments such as these should be avoided. In addition, variation in tag retention over time and with tag age render a posteriori "corrections" for tag loss more difficult. In cases where tag retention rates are not constant over time or for a release cohort, we believe that the most reasonable approach to survival rate estimation involves development of joint likelihoods that incorporate models of both tag retention and fish survival (e.g., Nichols et al. 1992; Nichols and Hines 1993). These models will include parameters for fish survival, tag retention, and recapture or recovery probabilities. Such models can be used in studies where all fish are double-tagged or in situations where some releases are double-tagged and others are tagged singly. These models can be tailored to reflect virtually any kind of study, as long as samples of double-tagged fish are released for the estimation of tag retention probability. A major strength of such an approach is the ability to provide not only unbiased estimates of survival rates in the face of tag loss, but also associated estimates of sampling variance that properly incorporate the sampling variance–covariance structure imposed by the double-tagging and tag loss sampling.

In summary, we estimated annual tag shedding rates for lake trout from Gull Island Shoal, Lake Superior, with software originally designed to estimate annual survival rates. The modeling approach we described affords several benefits including (*i*) availability of software, (*ii*) availability of well-established model selection procedures, (*iii*) modeling flexibility, (*iv*) ability to draw inferences about the relevance of factors associated with subsets of the data such as sex and origin, and (*v*) ability to directly incorporate tag shedding rates in survival models.

Acknowledgements

A number of dedicated people provided technical support for this study: Mary Halvorson (Wisconsin Department of Natural Resources, Bayfield, Wis.) entered and verified data, Roger Lockwood (Institute for Fisheries Research, Ann Arbor, Mich.) assisted with database translation from Apple to IBM formats, and Scott Nelson (Great Lakes Science Center, Ann Arbor, Mich.) constructed a relational database that allowed us to examine the mark–recapture data. This article is Contribution No. 1067 of the U.S. Geological Survey Great Lakes Science Center.

References

Anderson, D.R., Burnham, K.P., and White,C.C. 1994. AIC model selection in overdispersed capture–recapture data. Ecology, **75**: 1780–1793.

Arnason, A.N., and Mills, K.H. 1981. Bias and loss of precision due to tag loss in Jolly–Seber estimates for mark–recapture experiments. Can. J. Fish. Aquat. Sci. **38**: 1077–1095.

Baglin, R.E., Jr., Farber, M.I., Lenarz, W.H., and Mason, J.M., Jr. 1980. Shedding rates of plastic and metal dart tags from Atlantic bluefin tuna, *Thunnus thynnus*. Fish. Bull. U.S. **78**: 179–185.

Barrowman, N.J., and Myers, R.A. 1996. Estimating tag-shedding rates for experiments with multiple tag types. Biometrics, **52**: 1410–1416.

Bayliff, W.H., and Mobrand, L.M. 1972. Estimates of the rates of shedding of dart tags from yellowfin tuna. Inter-Am. Trop. Tuna Comm. Bull. **15**: 439–462.

Beverton, R.J.H., and Holt, S.J. 1957. On the dynamics of exploited fish populations. Chapman and Hall, New York.

Brewin, M.K., Stebbins, L.L., and Nelson, J.S. 1995. Differential losses of Floy anchor tags between male and female brown trout. N. Am. J. Fish. Manage. **15**: 881–884.

Burnham, K.P., and Anderson, D.R. 1992. Data-based selection of an appropriate biological model: the key to modern data analy-

© 1999 NRC Canada

sis. *In* Wildlife 2001: populations. *Edited by* D.R. McCullough and R.H. Barrett. Elsevier, New York. pp. 16–30.

Burnham, K.P., and Anderson, D.R. 1998. Model selection and inference: a practical information theoretic approach. Academic Press, New York.

Burnham, K.P., Anderson, D.R., White, G.C., Brownie, C., and Pollock, K.H. 1987. Design and analysis methods for fish survival experiments based on release–recapture. Am. Fish. Soc. Monogr. No. 5.

Burnham, K.P., White, G.C., and Anderson, D.R. 1995. Model selection strategy in the analysis of capture–recapture data. Biometrics, **51**: 888–898.

Chapman, D.G., Fink, B.D., and Bennett, E.B. 1965. A method for estimating the rate of shedding of tags from yellowfin tuna. Inter-Am. Trop. Tuna Comm. Bull. **10**: 333–352.

Diefenbach, D.R., and Alt, G.L. 1998. Modeling and evaluation of ear tag loss in black bears. J. Wildl. Manage. **62**: 1292–1300.

Fabrizio, M.C., Swanson, B.L., Schram, S.T., and Hoff, M.H. 1996. Comparison of three nonlinear models to describe long-term tag shedding by lake trout. Trans. Am. Fish. Soc. **125**: 261–273.

Fabrizio, M.C., Holey, M.E., McKee, P.C., and Toneys, M.L. 1997. Survival rates of adult lake trout in northwestern Lake Michigan, 1983–1993. N. Am. J. Fish. Manage. **17**: 413–428.

Hampton, J. 1997. Estimates of tag-reporting and tag-shedding rates in a large-scale tuna tagging experiment in the western tropical Pacific Ocean. Fish. Bull. U.S. **95**: 68–79.

Hampton, J., and Kirkwood, G.P. 1990. Tag shedding by southern bluefin tuna *Thunnus maccoyii*. Fish. Bull. U.S. **88**: 313–321.

Hansen, M.J., Peck, J.W., Schorfhaar, R.G., Selgeby, J.H., Schreiner, D.R., Schram, S.T., Swanson, B.L., MacCallum, W.R., Burnham-Curtis, M.K., Curtis, G.L., Heinrich, J.W., and Young, R.J. 1995. Lake trout (*Salvelinus namaycush*) populations in Lake Superior and their restoration in 1959–1993. J. Gt. Lakes Res. **21**(Suppl.1): 152–175.

Hearn, W.S., Leigh, G.M., and Beverton, R.J.H. 1991. An examination of a tag-shedding assumption, with application to southern bluefin tuna. ICES J. Mar. Sci. **48**: 41–51.

Kirkwood, G.P. 1981. Generalized models for the estimation of rates of tag shedding by southern bluefin tuna (*Thunnus maccoyii*). J. Cons. Cons. Int. Explor. Mer, **39**: 256–260.

Lai, H.-L., and Culver, B.N. 1991. Estimation of tag loss rate of black rockfish (*Sebastes melanops*) off Washington coast with a review of double tagging models. Wash. Dep. Fish. Tech. Rep. No. 113.

Lebreton, J.-D., Burnham, K.P., Clobert, J., and Anderson, D.R. 1992. Modeling survival and testing biological hypotheses using marked animals: a unified approach with case studies. Ecol. Monogr. **62**: 67–118.

Mourning, T.E., Fausch, K.D., and Gowan, C. 1994. Comparison of visible implant tags and Floy anchor tags on hatchery rainbow trout. N. Am. J. Fish. Manage. **14**: 636–642.

Nichols, J.D., and Hines, J.E. 1993. Survival rate estimation in the presence of tag loss using joint analysis of capture–recapture and resighting data. *In* Marked individuals in the study of bird population. *Edited by* J.-D. Lebreton and P.M. North. Birkhäuser Verlag, Basel, Switzerland. pp. 229–243.

Nichols, J.D., Bart, J., Limpert, R.J., Sladen, W.J.L., and Hines, J.E. 1992. Annual survival rates of adult and immature eastern population tundra swans. J. Wildl. Manage. **56**: 485–494.

Pollock, K.H. 1981. Capture–recapture models allowing for age-dependent survival and capture rates. Biometrics, **37**: 521–529.

Robson, D.S., and Regier, H.A. 1966. Estimates of tag loss from recoveries of fish tagged and permanently marked. Trans. Am. Fish. Soc. **95**: 56–59.

Seber, G.A.F. 1982. The estimation of animal abundance. Griffin, London, U.K.

Swanson, B.L., and Swedberg, D.V. 1980. Decline and recovery of the Lake Superior Gull Island reef lake trout (*Salvelinus namaycush*) population and the role of sea lamprey (*Petromyzon marinus*) predation. Can. J. Fish. Aquat. Sci. **37**: 2074–2080.

Tranquilli, J.A., and Childers, W.F. 1982. Growth and survival of largemouth bass tagged with Floy anchor tags. N. Am. J. Fish. Manage. **2**: 184–187.

Waldman, J.R., Dunning, D.J., and Mattson, M.T. 1990. A morphological explanation for size-dependent anchor tag loss from striped bass. Trans. Am. Fish. Soc. **119**: 920–923.

Wetherall, J.A. 1982. Analysis of double-tagging experiments. Fish. Bull. U.S. **80**: 687–701.

White, G.C. 1983. Numerical estimation of survival rates from band-recovery and biotelemetry data. J. Wildl. Manage. **47**: 716–728.

Wydoski, R., and Emery, L. 1983. Tagging and marking. *In* Fisheries techniques. *Edited by* L.A. Nielsen and D.L. Johnson. American Fisheries Society, Bethesda, Md. pp. 215–237.

Xiao, Y. 1996. A general model for estimating tag-specific shedding rates and tag interactions from exact or pooled times at liberty for a double tagging experiment. Can. J. Fish. Aquat. Sci. **53**: 1852–1861.

© 1999 NRC Canada

Densities of juvenile brown trout (*Salmo trutta*) in two subarctic rivers: assessing the predictive capability of habitat preference indices

Aki Mäki-Petäys, Timo Muotka, and Ari Huusko

Abstract: We examined the applicability of habitat preference indices for predicting density variations of age-0 brown trout (*Salmo trutta*) in two rivers in northern Finland. Trout densities in these rivers were monitored for 7 or 8 years. Habitat suitability for trout fry was assessed using summer and winter preference curves for water velocity, depth, and substrate. Substrate suitability indices based on summer preference curves explained 21–74% of the among-site variation in trout densities. The negative effect of high discharge on trout abundance was best predicted by the composite depth × substrate index. Sites with the highest "apparent survival" (density of age-1 trout in year t versus density of age-0 trout in year $t - 1$) produced high indices when winter substrate curves for age-0 trout were used, indicating high immigration rates to these sites. Our study shows that when preference indices are used for predictive purposes, the mechanisms underlying habitat "bottlenecks" must be known. In boreal areas, winter presents a bottleneck period for juvenile salmonids, and we stress the importance of using winter habitat curves when habitat hydraulic models are applied to areas with severe winter conditions.

Résumé : Nous avons examiné la possibilité d'utiliser des indices des préférences en matière d'habitat pour prévoir les variations dans la densité des truites brunes (*Salmo trutta*) d'âge 0 dans deux cours d'eau du nord de la Finlande. Nous y avons mesuré les densités des truites durant sept ou huit ans. Nous avons évalué la valeur de l'habitat pour les alevins de truite en utilisant des courbes de préférence estivale et hivernale en ce qui concerne la vitesse du courant, la profondeur et le substrat. Les indices de valeur du substrat fondés sur les courbes estivales de préférence ont rendu compte de 21 à 74 % de la variation des densités de truites entre les sites. L'indice composite profondeur-substrat était le meilleur pour prévoir l'effet négatif des forts débits sur l'abondance des truites. Les sites où le « taux de survie apparent » (densité des truites d'âge 1 dans l'année t versus la densité des truites d'âge 0 dans l'année $t - 1$) était le plus élevé ont montré des indices élevés quand les courbes hivernales relatives au substrat pour les truites d'âge 0 étaient utilisées, ce qui indique que les taux d'immigration vers ces sites sont élevés. Notre étude montre que quand on utilise les indices de préférence à des fins de prévision, on doit connaître les mécanismes sous-jacents aux goulots d'étranglement affectant la disponibilité des habitats. Dans les régions boréales, il y a en hiver une période où la disponibilité des habitats est réduite pour les salmonidés juvéniles, et nous soulignons l'importance d'utiliser des courbes d'habitat hivernal quand on applique des modèles hydrauliques de l'habitat à des régions où l'hiver est rigoureux.

[Traduit par la Rédaction]

Introduction

Habitat hydraulic models (e.g., physical habitat simulation system (PHABSIM) and two-dimensional models; see Leclerc et al. 1995; Bovee 1996) are frequently used to estimate the quantity of microhabitat (weighted usable area (WUA)) suitable for fish at different stream flows. In most model applications, water depth, velocity, substrate, and cover have been considered as the main flow-dependent instream variables affecting the quality of habitat for stream fish. Thus, preference curves for these variables at different life stages of a fish have an elementary role in habitat hydraulic modeling. When these curves are used for predictive purposes, fish populations are assumed to be habitat limited, resulting in a positive relationship between WUA and fish standing stock (Mathur et al. 1985). However, the use of habitat models as a management tool is biologically feasible only if the generality and predictive capability of the preference curves are rigorously assessed. Notwithstanding the increasing popularity of PHABSIM and other habitat models in stream management, these topics are rarely addressed by fisheries biologists (but see Nehring and Anderson 1993; Beecher et al. 1995; Bourgeois et al. 1996).

From a management point of view, it is imperative that the key factors underlying any "bottleneck" periods for fish

Received July 23, 1998. Accepted March 26, 1999.
J14707

A. Mäki-Petäys.[1] Finnish Game and Fisheries Research Institute, Kainuu Fisheries Research and Aquaculture, 88300 Paltamo, Finland, and Department of Biology, University of Oulu, P.O. Box 333, 90571 Oulu, Finland.
T. Muotka. Department of Biological and Environmental Science, University of Jyväskylä, P.O. Box 35, 40351 Jyväskylä, Finland.
A. Huusko. Finnish Game and Fisheries Research Institute, Kainuu Fisheries Research and Aquaculture, 88300 Paltamo, Finland.

[1]Author to whom all correspondence should be addressed.
e-mail: maki-petays@tp.rktl.fi

© 1999 NRC Canada

Fig. 1. Location of the study area and study sections used for monitoring density of age-0 brown trout in rivers Kuusinkijoki and Kitkajoki, northeastern Finland.

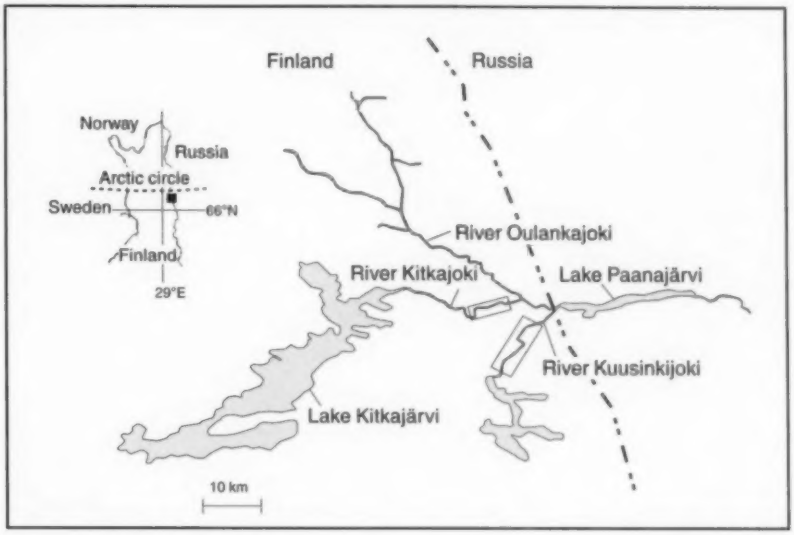

populations be accurately identified. This information is especially important if the same mechanisms limit populations in general and if the limiting factors can be affected by management. The availability of suitable habitat for overwintering of juvenile fish may play a central role in regulating populations of salmonid fishes in northern streams (Cunjak 1996; Quinn and Peterson 1996). Surprisingly few studies, however, have addressed the relationship between winter habitat availability and fish abundance, although the need for season-specific preference curves for instream flow assessments has been brought up by many authors (e.g., Irvine et al. 1987).

In this study, we evaluated the accuracy of the preference curves developed by Mäki-Petäys et al. (1997) in predicting densities of age-0 brown trout (*Salmo trutta*) in two subarctic rivers. We assigned suitability values for each study site based on the preference curves for depth, water velocity, and dominant substrate size and correlated these values with the late-summer densities of age-0 trout during the summers of 1988–1995. This procedure was repeated using both summer and winter preferences to compare the suitability of the sites as summer nursery areas versus overwintering areas for trout fry. Finally, we estimated the "apparent survival" of trout by calculating the within-site survival ratios (see Gowan and Fausch 1996) and correlated these with site-specific substrate preference indices. To our knowledge, this is the first time that survival (even if apparent) has been used as a population parameter in an assessment of habitat preference curves for any fish species.

Materials and methods

The study was conducted in Rivers Kuusinkijoki (drainage area 1006 km^2) and Kitkajoki (drainage area 1841 km^2), two third-order tributaries to River Oulankajoki, northeastern Finland. Both rivers flow through spruce and pine forests and discharge into Lake Paanajärvi on the Russian side of the border (Fig. 1). Water temperature falls below 1°C in late October, and both rivers are mainly ice covered from mid-November to late April. The flow regime of River Kuusinkijoki (mean 10 $m^3 \cdot s^{-1}$, range 1–60 $m^3 \cdot s^{-1}$, stream width 40–80 m) is characterized by wide seasonal fluctuations, whereas flow is less variable in River Kitkajoki (mean 21 $m^3 \cdot s^{-1}$, range 8–50 $m^3 \cdot s^{-1}$, stream width 30–70 m). The peak flow typically occurs after snowmelt in late May, and the lowest flows occur during winter. Both streams have constrained channels with steep banks and restricted floodplains; thus, the wetted area varies little in response to flow alterations.

Our study area covered most of River Kuusinkijoki and the lower courses of River Kitkajoki. Trout stocks in these rivers are based on natural reproduction (Huusko et al. 1990). The average (±1 SD) late-summer densities of juvenile trout were 0.48 ± 0.11 and 0.61 ± 0.16 fish·m^{-2} in Rivers Kuusinkijoki (n = 8 years) and Kitkajoki (n = 7 years), respectively. Arctic bullhead (*Cottus poecilopus*) is another dominant fish species in both rivers, with mean (±1 SD) densities of 0.96 ± 0.73 (River Kuusinkijoki) and 1.50 ± 0.90 fish·m^{-2} (River Kitkajoki). European grayling (*Thymallus thymallus*) and European minnow (*Phoxinus phoxinus*) also occur in both rivers, but generally at lower densities than trout and bullhead.

This study was based on material collected by the Finnish Game and Fisheries Research Institute to monitor the population densities of age-0 brown trout in the two rivers. Fish were sampled for 8 years (1988–1995) in River Kuusinkijoki and 7 years (1989–1995) in River Kitkajoki. Sampling was conducted in late August each year to obtain estimates of late-summer densities. Fourteen to 25 stream sites (10–20 m in length, mean (±1 SE) area 97 ± 3.1 m^2) were electrofished using the three-pass removal method, and fish densities were calculated according to Bohlin et al. (1989). Sites chosen were relatively shallow riffle areas (depth 20–50 cm), with variable flows (20–80 cm·s^{-1}) and coarse (pebble to boulder with some gravel) substrates. Stream gradient varied between 0.9 and 2.5%.

Habitat characteristics were quantified at each site immediately after electrofishing. Depth of water and dominant substrate size were determined in three transects perpendicular to the flow. The precision of habitat measurements increases with decreasing distance between transects, so we positioned our transects 2–5 m apart. Depth was measured to the nearest centimetre in the centre of six equidistant quadrats (1 m^2) per transect. Dominant substrate size was visually determined from the same quadrats and classified

© 1999 NRC Canada

according to a modified Wenthworth scale: (1) 0.07–2 mm, (2) 2.1–8 mm, (3) 8.1–16 mm, (4) 16.1–32 mm, (5) 32.1–64 mm, (6) 64.1–128 mm, (7) 128.1–256 mm, (8) > 256 mm. Surface water velocity was measured at three regularly spaced points (at 0.25, 0.50, and 0.75 of the distance along the transect) by measuring the time it took for a plastic vial (length 5 cm, diameter 3 cm) to float 4 m in the stream, and this was repeated three times at each location (see Eklöv 1996).

PHABSIM applications are ordinarily based on the calculation of WUA to estimate the amount of habitat suitable for fish in a given stream reach. The sample reach is divided into habitat cells, each of which produces a specific preference value. These values are then weighted by the area of the cell and added up to gain a WUA estimate for the whole reach (Milhous et al. 1989). We were not able to use this approach, however, because the scale of our water velocity measurements did not conform to the measurements of other habitat variables. Instead, the mean value for a habitat variable at a site was converted to a range of 0.0–1.0 (0.0, unsuitable; 1.0, optimal habitat for fish) using the preference curves of Mäki-Petäys et al. (1997); for surface water velocity, we used curves developed by A. Mäki-Petäys (unpublished). Hereafter, *P*[d], *P*[v], and *P*[s] are used for preferences for depth, velocity, and substrate, respectively. Composite preference indices (e.g., the composite index of depth and substrate *P*[ds], defined as *P*[d] × *P*[s]) are commonly used in PHABSIM applications. Therefore, we also calculated the composite indices of *P*[dv], *P*[ds], and *P*[dsv].

We used three approaches to test the applicability of the preference curves in predicting trout densities. First, we calculated correlations between late-summer densities of age-0 trout and the habitat preference values obtained from the summer preference curves of age-0 trout. This was done across all sites and separately for each year. Fausch et al. (1988) reasoned that to be biologically relevant, correlations between fish densities and suitable habitat should be based on habitat preferences of the same or a previous life stage as in the population studied. Nevertheless, since streambed structure is seasonally less variable than depth and water velocity (see Leclerc et al. 1995), we also correlated the late-summer densities of age-0 trout with the winter substrate preferences ($P[s]_w$) of overwintering fish (see the winter curves for age-0 trout in Mäki-Petäys et al. 1997). Next, we calculated the yearly means of habitat preference indices across all study sites and compared these with the yearly mean densities of trout fry and average flow conditions in August. These two approaches represent complementary spatiotemporal dimensions: the former approach emphasizes differences between sites and the latter one differences among years.

Third, we assessed the suitability of the sampling sites as overwintering areas of trout fry. To do this, we divided the density of age-1 trout at a site in year t by the density of age-0 trout at the same site in year $t - 1$. This ratio, termed apparent survival by Gowan and Fausch (1996), includes both survival and movement of fish. It may occasionally produce values >1, indicating abundant immigration to a site. For this analysis, we only accepted sites where we had data on fish densities for at least 3 successive years. Because of the commonly reported association of salmonids with substrate in winter (e.g., Heggenes et al. 1993; Mäki-Petäys et al. 1997), we focused on the relationships between apparent survival and $P[s]_w$ for age-0 trout. Nevertheless, to get a broader view of the importance of substrate to trout during their first year of life, we also calculated correlations between apparent survival and the summer preference indices ($P[s]_s$) for age-0 and age-1 trout.

We fitted linear regressions between habitat preference indices (independent variables) and trout density (dependent variable) to examine the ability of different indices to explain variation in trout densities among sampling sites. Residual plots (to examine homoscedasticity), probability plots (to examine normality), and influence measures (Cook's distance (Cook and Weisberg 1983)) were used for data diagnostics, and, if needed, dependent variables were log transformed ($\ln x + 1$) to better fit the assumptions of the regression model.

Results

Among-site predictability of age-0 trout density

In each year of the study, densities of age-0 brown trout in Rivers Kuusinkijoki and Kitkajoki were positively and significantly related to $P[s]_s$ (Fig. 2A). The proportion of variation in trout densities explained by $P[s]_s$ varied between 21 and 74% (mean 38.6%) during the 8 years of the study. Nevertheless, the mean (±1 SD) value for $P[s]_s$ was 0.33 ± 0.12, suggesting that most of the sites were only suboptimal summer nursery areas for trout fry. This was primarily caused by the dominance of coarse substrates at these sites, a habitat feature not preferred by trout fry in summer (see the substrate preference curves in Mäki-Petäys et al. 1997). In contrast, the mean (±1 SD) value for $P[s]_w$ was 0.73 ± 0.20, indicating that the same sites were highly suitable as overwintering areas for trout fry (Fig. 2B). Interestingly, winter indices were inversely related to late-summer densities of trout, illustrating the distinct seasonal changes in substrate preference by age-0 trout.

The relationship with $P[ds]_s$ was also significantly positive in all years, except for the high-flow summer of 1992. Excluding this year, $P[ds]_s$ explained 24–73% (mean 41.9%) of the density variation of trout fry. In contrast, $P[d]_s$ and $P[v]_s$, as well as composite indices other than $P[ds]_s$, were always nonsignificantly associated with trout densities.

Among-year predictability of age-0 trout density

Among-year variation in densities of age-0 trout followed closely the variation in $P[d]_s$ ($r = 0.70$, $p = 0.027$), $P[ds]_s$ ($r = 0.76$, $p = 0.014$), and $P[dsv]_s$ ($r = 0.72$, $p = 0.023$) (n = 8 years in all correlations; for indices values, see Table 1). Mean flow in August ranged between 4.0 and 17.4 $m^3 \cdot s^{-1}$ in River Kuusinkijoki and between 15.4 and 28.8 $m^3 \cdot s^{-1}$ in River Kitkajoki during the study years (Fig. 3A), resulting in considerable among-year variation in water depths and velocities. In years with high late-summer discharges, depth × substrate related preference indices produced low values, and trout densities were correspondingly low then (see Fig. 3B; Table 1). Thus, these preference indices were effective in predicting the negative impact of high flows on late-summer densities of trout fry.

Apparent survival of trout fry in relation to stream substrate

The apparent survival of trout fry was negatively correlated with $P[s]_s$ for age-0 trout and positively correlated with $P[s]_w$ for age-0 trout and $P[s]_s$ for age-1 trout (see Fig. 4). The apparent survival produced a value ≥1.0 on two of 20 occasions. At these sites, densities of age-1 trout were equal to or greater than densities of age-0 trout the previous year, due probably to a high immigration rate to these sites. According to the substrate indices, these sites were unsuitable as summer nursery areas ($P[s]_s < 0.30$; Fig. 4A) but highly suitable as overwintering areas for trout fry ($P[s]_w > 0.80$; Fig. 4B). The next summer, these same sites were again suit-

© 1999 NRC Canada

Fig. 2. Annual relationships between late-summer densities of age-0 trout and site-specific substrate preference indices based on (A) summer and (B) winter preference curves for age-0 brown trout (see Mäki-Petäys et al. 1997). Thin lines indicate 95% confidence belts for a linear regression; ns, nonsignificant regression.

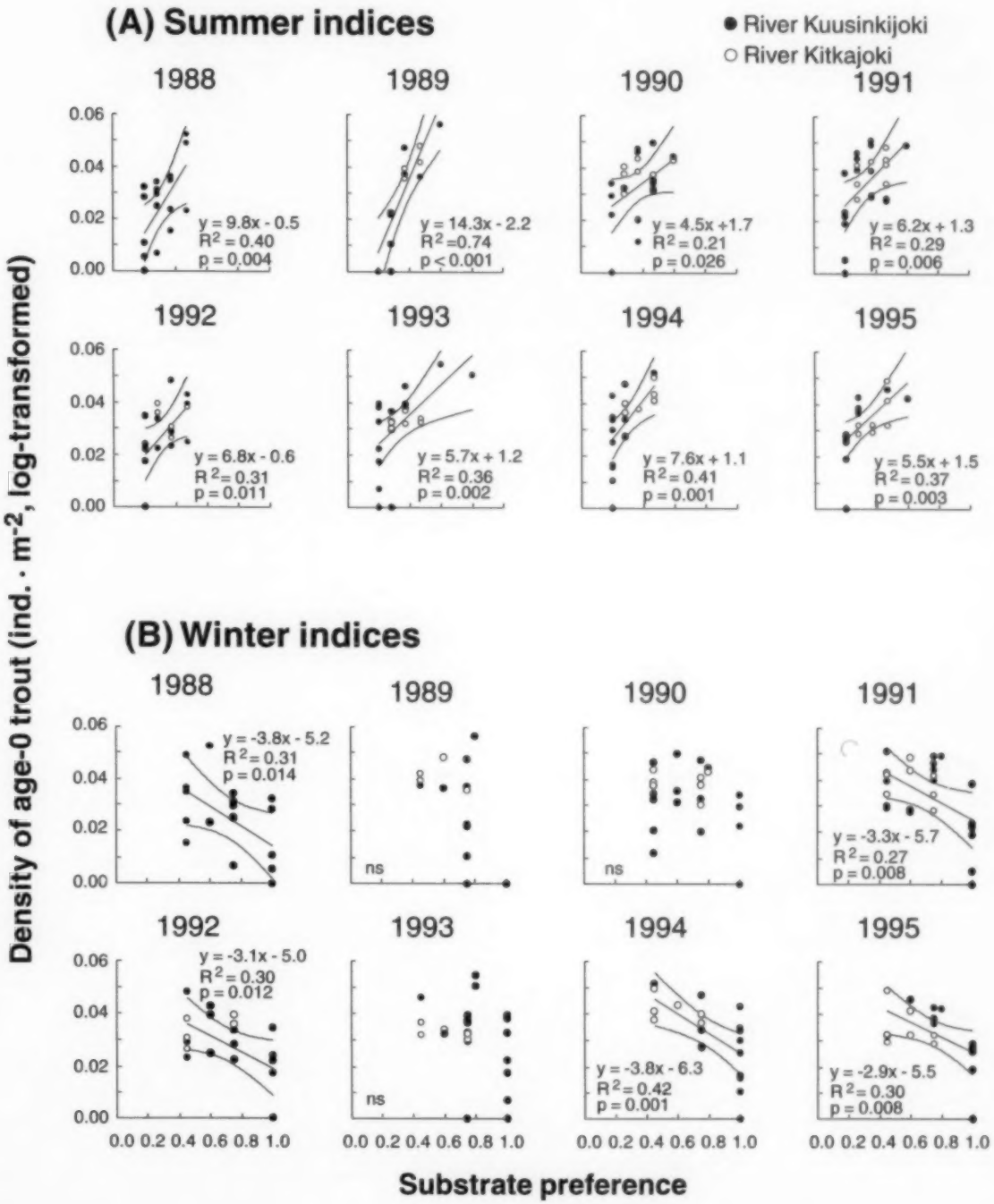

© 1999 NRC Canada

Table 1. Mean (±1 SE in parentheses) densities of age-0 brown trout and mean (±1 SE) indices values (P) for depth (d), substrate (s), and surface water velocity (v) preferences and for the composite preference indices for each study year.

Year	Density of age-0 trout (ind.·100 m^{-2})	P[d]	P[s]	P[v]	P[ds]	P[dv]	P[dsv]
1988	28.6 (11.0)	0.94 (0.03)	0.30 (0.02)	0.64 (0.04)	0.28 (0.02)	0.60 (0.03)	0.18 (0.01)
1989	57.0 (19.8)	0.97 (0.01)	0.37 (0.03)	0.67 (0.05)	0.36 (0.03)	0.65 (0.05)	0.23 (0.02)
1990	43.7 (7.6)	0.93 (0.03)	0.38 (0.02)	0.76 (0.05)	0.35 (0.03)	0.71 (0.05)	0.27 (0.03)
1991	53.3 (9.5)	0.97 (0.01)	0.34 (0.02)	0.76 (0.05)	0.33 (0.02)	0.73 (0.05)	0.25 (0.02)
1992	27.6 (6.6)	0.80 (0.05)	0.32 (0.02)	0.47 (0.05)	0.26 (0.03)	0.39 (0.06)	0.11 (0.02)
1993	44.4 (11.0)	0.93 (0.03)	0.33 (0.03)	0.87 (0.04)	0.30 (0.02)	0.82 (0.05)	0.26 (0.02)
1994	46.8 (9.5)	0.95 (0.02)	0.29 (0.02)	0.75 (0.04)	0.27 (0.02)	0.73 (0.04)	0.20 (0.02)
1995	37.9 (6.8)	0.96 (0.02)	0.32 (0.02)	0.75 (0.04)	0.30 (0.02)	0.72 (0.04)	0.22 (0.02)

Note: Data pooled across study sites.

Fig. 3. (A) Mean flow in August during the study years and (B) average annual densities of age-0 brown trout. Vertical lines indicate 1 SE of the mean. Data are pooled across the study sites. Fish were sampled in the last week of August each year.

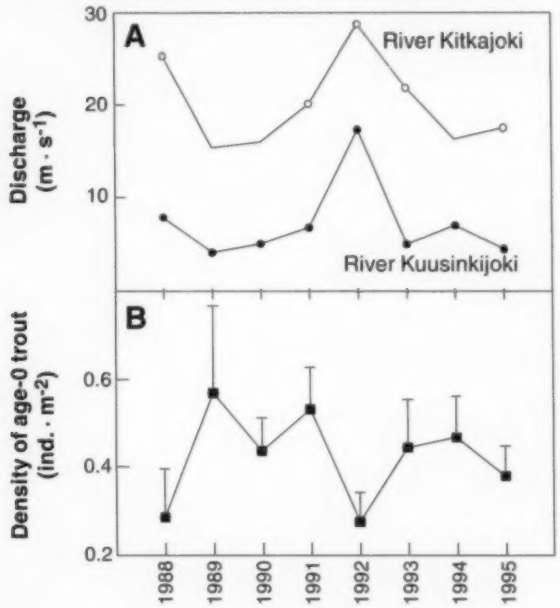

able for the summer residence of yearling trout ($P[s]_s$ > 0.70; Fig. 4C).

Discussion

The ability of the habitat preference curves to predict densities of brown trout fry varied considerably. Summer densities of age-0 trout correlated most significantly with $P[s]_s$, which explained on average 38.6% of the density variation. It must be emphasized, however, that data for Mäki-Petäys et al.'s (1997) preference curves were collected at one of the stream reaches used in this study also. Thus, our test data were not truly independent, which may have slightly increased the predictive ability of the curves. In his review, Shirvell (1989) showed that habitat models generally explained 50–96% of the variation in fish standing crop when applied to the stream that they were derived from, but only 7–30% when applied to other streams.

Densities of age-0 trout were not related to the availability of suitable water depths and velocities at the study sites. It must be emphasized, however, that the lack of relationship between fish densities and depths and water velocities was based on among-site comparisons, which may be less able to detect such relationships than are within-site comparisons. The low amount of variation in depth among the sites may have prevented us from detecting any real associations between P[d] and trout density; about 80% of the sites produced preference values near the optimum range for age-0 trout ($P[d]_s$ > 0.8). Obviously, habitat models can be expected to correlate closely with fish abundance only if a species' tolerable range for a habitat variable is exceeded (Shirvell 1989). Neither does the negligible relationship between P[v] and trout density indicate that water velocity is not an important determinant of trout distribution at a scale smaller than used in this study. Drift-feeding salmonids are known to prefer stream areas with both slow-velocity microhabitats to minimize energy costs of swimming and fast-velocity habitats to maximize availability of drifting prey (Fausch 1984; Hughes and Dill 1990). It may well be that mean water velocity measured at 0.6 × depth is not an adequate descriptor of microhabitat suitability for trout, and a more realistic habitat model should take into account velocities in adjacent cells ("feeding station analysis," Beecher 1987) or at different water depths ("vertical feeding stations").

Different preference curves were effective in predicting trout densities in among-site versus among-year comparisons. Depth and water velocity were the main components contributing to the positive association between preference indices and trout density among years, whereas they had a minor role in among-site comparisons. The $P[d]_s$ and the composite indices $P[ds]_s$ and $P[dsv]_s$ were best able to predict the negative effect of high discharge on late-summer densities of trout fry. Nehring and Anderson (1993) also found significant negative correlations between mean monthly discharge and densities of brown and rainbow trout (*Oncorhynchus mykiss*) in 11 Colorado mountain streams. In their 13-year study, however, the amount of habitat suitable (WUA) for spawning, egg incubation, and 2- to 4-week-old fry explained variations in trout density even better than the mean monthly flow, indicating that extreme flow events dur-

© 1999 NRC Canada

Fig. 4. Apparent survival of brown trout (density of age-1 trout at year t versus density of age-0 trout at year $t - 1$) during their first year of life in relation to substrate preference index based on (A) summer and (B) winter preference curves for age-0 trout and (C) summer curves for age-1 trout.

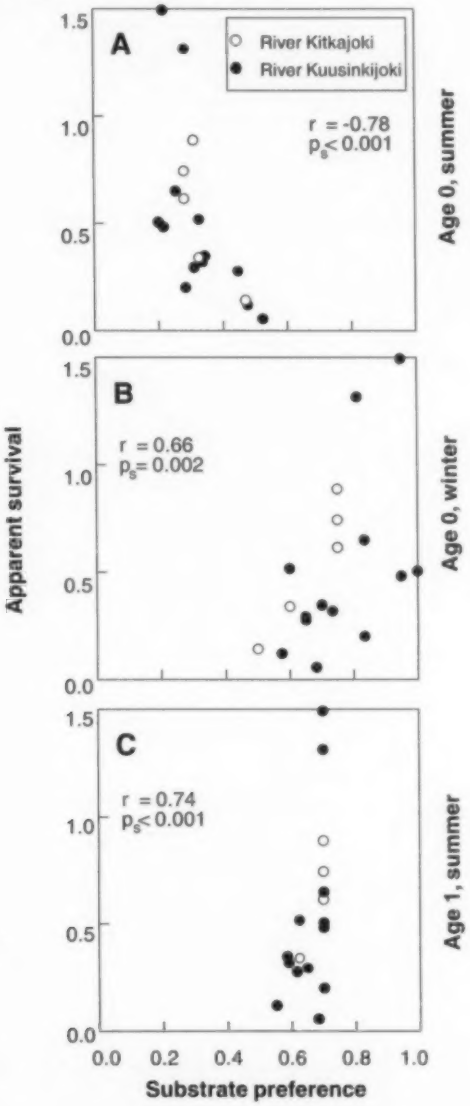

ing these vulnerable life stages may have far-reaching effects on trout population dynamics. Based on a 25-year study, Elliott (1993) concluded that population density of brown trout is primarily regulated by density-dependent survival during the early life stages. Since the territorial behaviour of trout increases markedly during the first few weeks after fry emergence (Elliott 1994), competition for flow refuges may provide the link between density-dependent survival, habitat suitability, and flow, especially during this critical period for the survival of trout fry.

Stream habitat and fish abundance will be tightly linked only if habitat availability is the prime determinant of fish density. Environmental variability, like extreme flow events, and biological factors may force fish to use less-preferred habitats, potentially masking any habitat – fish density relationships (Milner et al. 1985; Orth 1987). Nevertheless, in most PHABSIM applications, fish habitat preference is assumed to be independent of stream flow, an assumption not shared by all stream fisheries biologists. Some studies have supported this view (e.g., Heggenes 1988; Beecher et al. 1995), while others have shown that habitat preferences may change as a function of flow (Shirvell 1990; Pert and Erman 1994). This controversy may be partly explained by differential responses of dominant and subdominant fish to changing habitat conditions (Pert and Erman 1994; see also Fausch and Young 1995). In a rapidly changing environment, hierarchically subdominant "movers" may relocate to suitable microhabitats more effectively than dominant individuals that may be reluctant to abandon their territories. Thus, under variable flow conditions, only part of the microhabitats used by fish will be correctly predicted, while territorial fish would occur in microhabitats deemed unsuitable, or suboptimal, by habitat models (Pert and Erman 1994). Moreover, the effect of variable discharge on fish habitat use may be modified by flow-induced changes in predation risk (Greenberg 1991). In our study, densities of trout fry were strongly correlated with $P[ds]_s$, excluding the exceptionally high-flow summer of 1992. It thus appears that $P[s]_s$ and $P[ds]_s$ are able to predict densities of age-0 trout only in years approximating "normal" (close to long-time average) flow conditions during the first few months of a trout's life. It is thus easy to share the criticism of many previous authors (e.g., Orth 1987) that to improve their level of realism, fish habitat models should incorporate biotic factors, like differential responses of fish to varying stream flows. Obviously, manipulative experiments addressing the interactive effects of, for example, stream flow and predation risk on fish habitat use and preference are sorely needed.

Streambed provides velocity refuge, visual isolation, and overhead cover for stream salmonids, thereby linking tradeoffs among foraging, competition, and predation risk (Fausch 1993). The general importance of substrate to stream salmonids is well documented (Bohlin 1977; Moore and Gregory 1988), and the strongest dependence on suitably sized substrates is usually found during winter (e.g., Rimmer et al. 1984; Heggenes et al. 1993; Mäki-Petäys et al. 1997). In our study, sites with abundant fry in late summer often rated poorly as winter substrates, suggesting that at the onset of winter, most fry abandoned their summer habitats and moved to adjacent wintering areas affording coarser substrates. Similarly, apparent survival was highest at sites that produced high scores based on winter substrate curves but low scores when summer curves for age-0 trout were used. The negative correlation between trout density and flow suggests that either fast water dispersed fry or they avoided it. In summer, pebble to cobble substrates may provide both suitable flow refuges and visual cover from conspecifics. However, in winter when flows are reduced and severe cold is the problem, the fish are positively associated with larger substrate because it gives them space to wiggle down and possibly find water warmed by the ground. Thus,

© 1999 NRC Canada

the summer and winter correlations with substrate size are related to two different selective pressures: flow and temperature.

Many authors have documented relatively long distances (200 m or more) moved by juvenile trout in search of suitable overwintering habitats (Cunjak and Power 1986; Chisholm et al. 1987). Overall, our study indicates that when preference indices are used for predictive purposes, one must be able to identify the underlying mechanisms and timing of habitat bottlenecks. In boreal areas, winter obviously presents such a bottleneck period, and optimal overwintering areas must contain relatively coarse substrate particles (also see Huusko and Yrjänä 1998). It is equally important, however, that fish movement between summer rearing habitats and overwintering habitats be unrestricted, i.e., fish must be provided with ecological "corridors" permitting seasonal habitat shifts (see Cunjak 1996). Habitat hydraulic models will fail to identify critical habitat in areas where winter conditions limit fish unless winter curves are used. To be useful in stream fisheries management, habitat models must reflect the ecology of fish at all relevant life history stages.

Acknowledgments

We thank Olli van der Meer, Pekka Korhonen, and Vihta Raappana for collecting most of the field material for this study. We also acknowledge the two anonymous reviewers for constructive comments on a previous version of the manuscript and the staff of Kuusamo Aquaculture for logistical help during the study. This study was supported by funding from the Finnish National Graduate School on Fish Biology and Fisheries (to A.M.-P).

References

Beecher, H.A. 1987. Simulating trout feeding stations in instream flow models. *In* Regulated streams: advances in ecology. *Edited by* J.F. Craig and J.B. Kemper. Plenum Press, New York. pp. 71–82.

Beecher, H.A., Carleton, J.P., and Johnson, T.H. 1995. Utility of depth and velocity preferences for predicting steelhead parr distribution at different flows. Trans. Am. Fish. Soc. **124**: 935–938.

Bohlin, T. 1977. Habitat selection and intercohort competition of juvenile sea-trout *Salmo trutta*. Oikos, **29**: 112–117.

Bohlin, T., Hamrin, S., Heggberget, T.G., Rasmussen, G., and Saltveit, S.J. 1989. Electrofishing — theory and practice with special emphasis on salmonids. Hydrobiologia, **173**: 9–43.

Bourgeois, G., Cunjak, R.A., Caissie, D., and El-Jabi, N. 1996. A spatial and temporal evaluation of PHABSIM in relation to measured density of juvenile Atlantic salmon in a small stream. N. Am. J. Fish. Manag. **16**: 154–166.

Bovee, K.D. 1996. Perspectives on two-dimensional river habitat models: the PHABSIM experience. *In* Proceedings of the Second IAHR Symposium on Habitat Hydraulics, Ecohydraulics. *Edited by* M. Leclerc et al. Les impressions 03 inc, Quebec, Que. pp. 149–162.

Chisholm, I.M., Hubert, W.A., and Wesche, T.A. 1987. Winter stream conditions and use of habitat by brook trout in high-elevation Wyoming streams. Trans. Am. Fish. Soc. **116**: 176–184.

Cook, R.D., and Weisberg, S. 1983. Residuals and influence in regression. Chapman and Hall, London, U.K.

Cunjak, R.A. 1996. Winter habitat of selected stream fishes and potential impacts from land-use activities. Can. J. Fish. Aquat. Sci. **53**: 267–282.

Cunjak, R.A., and Power, G. 1986. Winter habitat utilization by stream resident brook trout (*Salvelinus fontinalis*) and by brown trout (*Salmo trutta*). Can. J. Fish. Aquat. Sci. **43**: 1970–1981.

Eklöv, A.G. 1996. Effects of habitat size and species richness on anadromous brown trout, *Salmo trutta* L., populations. Fish. Manag. Ecol. **3**: 97–101.

Elliott, J.M. 1993. A 25-year study of production of juvenile sea trout, *Salmo trutta*, in an English Lake District stream. Can. Spec. Publ. Fish. Aquat. Sci. No. 118. pp. 109–122.

Elliott, J.M. 1994. Quantitative ecology and the brown trout. Oxford University Press, Oxford, U.K.

Fausch, K.D. 1984. Profitable stream positions for salmonids: relating specific growth rate to net energy gain. Can. J. Zool. **62**: 441–451.

Fausch, K.D. 1993. Experimental analysis of microhabitat selection by juvenile steelhead (*Oncorhynchus mykiss*) and coho salmon (*O. kisutch*) in a British Columbia stream. Can. J. Fish. Aquat. Sci. **50**: 1198–1207.

Fausch, K.D., and Young, M.K. 1995. Evolutionary significant units and movement of resident stream fishes: a cautionary tale. Am. Fish. Soc. Symp. **17**: 360–370.

Fausch, K.D., Hawkes, C.L., and Parsons, M.G. 1988. Models that predict standing crop of stream fish from habitat variables: 1950–1985. U.S. For. Serv. Gen. Tech. Rep. PNW-213.

Gowan, C.G., and Fausch, K.D. 1996. Long-term demographic responses of trout populations to habitat manipulation in six Colorado streams. Ecol. Appl. **6**: 931–946.

Greenberg, L.A. 1991. The effect of discharge and predation on habitat use by wild and hatchery brown trout (*Salmo trutta*). Regul. Rivers Res. Manag. **7**: 205–212.

Heggenes, J. 1988. Effect of short-term flow fluctuations on displacement of, and habitat use by, brown trout in a small stream. Trans. Am. Fish. Soc. **117**: 336–344.

Heggenes, J., Krog, O.M.W., Lindås, O.R., Dokk, J.G., and Bremnes, T. 1993. Homeostatic behavioural responses in a changing environment: brown trout (*Salmo trutta*) become nocturnal during winter. J. Anim. Ecol. **62**: 295–308.

Hughes, N.F., and Dill, L.M. 1990. Position choice of drift-feeding salmonids: model and test for Arctic grayling (*Thymallus arcticus*) in subarctic mountain streams, interior Alaska. Can. J. Fish. Aquat. Sci. **47**: 2039–2048.

Huusko, A., and Yrjänä, T. 1998. Effects of instream enhancement structures on brown trout, *Salmo trutta* L., habitat availability in a channelized boreal river: a PHABSIM approach. Fish. Manag. Ecol. **4**: 453–466.

Huusko, A., van der Meer, O., and Koljonen, M.-L. 1990. Life history patterns and genetic differences in brown trout (*Salmo trutta* L.) in the Koutajoki river system. Pol. Arch. Hydrobiol. **37**: 63–77.

Irvine, J.R., Jowett, I.G., and Scott, D. 1987. A test of the Instream Flow Incremental Methodology for underyearling rainbow trout, *Salmo gairdnerii*, in experimental New Zealand streams. N.Z. J. Mar. Freshwater Res. **21**: 35–40.

Leclerc, M., Boudreault, A., Bechara, J.A., and Corfa, G. 1995. Two-dimensional hydrodynamic modeling: a neglected tool in the instream flow incremental methodology. Trans. Am. Fish. Soc. **124**: 645–662.

Mäki-Petäys, A., Muotka, T., Huusko, A., Tikkanen, P., and Kreivi, P. 1997. Seasonal changes in habitat use and preferences by juvenile brown trout, *Salmo trutta*, in a northern boreal river. Can. J. Fish. Aquat. Sci. **54**: 520–530.

© 1999 NRC Canada

Mathur, D., Bason, W.H., Purdy, E.J., and Silver, C.A. 1985. A critique of the instream flow incremental methodology. Can. J. Fish. Aquat. Sci. **42**: 825–831.

Milhous, R., Updike, M., and Snyder, D. 1989. PHABSIM system reference manual: version 2. Instream Flow Inf. Pap. 26. U.S. Fish Wildl. Serv. FWS/OBS 89/16.

Milner, N.J., Hemsworth, R.J., and Jones, B.E. 1985. Habitat evaluation as a fisheries management tool. J. Fish Biol. **27**: 85–108.

Moore, K.M., and Gregory, S.V. 1988. Response of young-of-the-year cutthroat trout to manipulation of habitat structure in a small stream. Trans. Am. Fish. Soc. **117**: 162–170.

Nehring, R.B., and Anderson, R.M. 1993. Determination of population-limiting critical salmonid habitats in Colorado streams using the Physical Habitat Simulation system. Rivers, **4**: 1–19.

Orth, D.J. 1987. Ecological consideration in the development and application of instream flow-habitat models. Regul. Rivers Res. Manag. **1**: 171–181.

Pert, E.J., and Erman, D.C. 1994. Habitat use by adult rainbow trout under moderate artificial fluctuations in flow. Trans. Am. Fish. Soc. **123**: 913–923.

Quinn, T.P., and Peterson, N.P. 1996. The influence of habitat complexity and fish size on over-winter survival and growth of individually marked juvenile coho salmon (*Oncorhyncus kisutch*) in Big Beef Creek, Washington. Can. J. Fish. Aquat. Sci. **53**: 1555–1564.

Rimmer, D.M., Paim, U., and Saunders, R.L. 1984. Changes in the selection of microhabitat by juvenile Atlantic salmon (*Salmo salar*) at the summer–autumn transition in a small river. Can. J. Fish. Aquat. Sci. **41**: 469–475.

Shirvell, C.S. 1989. Habitat models and their predictive capability to infer habitat effects on stock size. *In* Proceedings of the National Workshop on Effects of Habitat Alteration on Salmonid Stocks. *Edited by* C.D. Levings, L.B. Holtby, and M.A. Henderson. Can. Spec. Publ. Fish. Aquat. Sci. No. 105. pp. 173–179.

Shirvell, C.S. 1990. Role of instream rootwads as juvenile coho salmon (*Oncorhynchus kisutch*) and steelhead trout (*O. mykiss*) cover habitat under varying streamflows. Can. J. Fish. Aquat. Sci. **47**: 852–861.

© 1999 NRC Canada

Retinoic acid hydroxylation and teratogenesis in lake sturgeon (*Acipenser fulvescens*) from the St. Lawrence River and Abitibi region, Quebec

Christian Doyon, Réjean Fortin, and Philip A. Spear

Abstract: All-*trans*-retinoic acid (RA) is an extremely active form of vitamin A; however, excessive or insufficient concentrations elicit anomalies including those associated with limb and craniofacial development. Lake sturgeon (*Acipenser fulvescens*) from the St. Lawrence River and tributaries were estimated to have a 2.9% incidence of fin and craniofacial malformations. Among larvae raised in artificial streams, a greater incidence of fin malformations (6.3%; $p < 0.001$) occurred in St. Lawrence River sturgeon compared with larvae from the Abitibi region. To test the hypothesis that the differences in rate of malformations may be associated with metabolic imbalances of RA, cytochrome P-450 dependent conversion to 4-hydroxyretinoic acid (4-OH-RA) was investigated. Optimal assay conditions are described for in vitro 4-OH-RA production in liver microsomes. Enzyme activity tended to decrease with increasing age and gonadal development in fish collected from Abitibi, but no statistically significant effects of sex, age, length, or gonadal development were discerned. The rate of 4-OH-RA formation was 3.5-fold greater ($p < 0.0001$) in the St. Lawrence sturgeon while the concentrations of cytochrome P-450 inducing PCBs (expressed as dioxin toxic equivalents) were 20-fold greater in a composite liver sample of the St. Lawrence sturgeon. Liver retinoid concentrations were negatively correlated ($p < 0.0001$) with RA hydroxylation rate. These results are consistent with the possibility that cytochrome P-450 dependent RA metabolism increased by chemical contaminants is associated with developmental anomalies in the St. Lawrence sturgeon.

Résumé : L'acide all-*trans*-rétinoïque (RA) est une forme extrêmement active de vitamine A. Cependant, des concentrations excessives ou insuffisantes provoquent des anomalies y compris celles des membres et des structures craniofaciales. Chez l'Esturgeon jaune (*Acipenser fulvescens*) du fleuve Saint-Laurent, l'incidence de nageoire et de l'œil difformes a été estimée à 2,9 %. Parmi des larves élevées en ruisseaux artificiels, l'incidence de nageoires difformes était plus grand (6,3 %; $p < 0,001$) dans le cas des esturgeons du fleuve Saint-Laurent comparativement aux larves provenant de la région de l'Abitibi. Afin d'examiner l'hypothèse que la différence dans le taux de malformations est reliée à un déséquilibre métabolique du RA, la 4-hydroxylation dépendante du cytochrome P-450 a été évaluée. Les conditions optimales pour la conversion in vitro de RA en acide 4-hydroxyrétinoïque (4-OH-RA) dans les microsomes hépatiques de l'Esturgeon jaune ont été établies. L'activité enzymatique a eu tendance à diminuer en fonction de l'âge et du degré de développement gonadique chez les poissons de l'Abitibi, mais le sexe, l'âge, la taille et le développement gonadique n'ont affiché aucun effet statistiquement significatif. Le taux de formation de 4-OH-RA était 3,5 fois plus élevé ($p < 0,0001$) pour les esturgeons du fleuve, tandis que les concentrations des BPC inducteurs du cytochrome P-450 (exprimées en équivalents toxiques de dioxine) étaient 20 fois plus élevées dans un échantillon composé de foies provenant de plusieurs esturgeons du Saint-Laurent. Les concentrations hépatiques de rétinoïdes ont démontré des corrélations négatives ($p < 0,0001$) avec l'hydroxylation du RA. Ces résultats sont cohérents avec la possibilité que le métabolisme du RA par le cytochrome P-450, augmenté par la contamination du milieu, soit associé aux malformations chez l'Esturgeon jaune du fleuve Saint-Laurent.

Introduction

The term "retinoid" refers to biologically active molecules that have structures similar to that of retinol. Slight variations in this structure lead to remarkable differences in biological activity, all-*trans*-retinoic acid (RA) being one of the most active forms. The identification of an RA nuclear receptor (Giguère et al. 1987; Petkovich et al. 1987) structurally homologous to those of the steroid and thyroid hormones resulted in the recognition of RA's endocrine properties (Mangelsdorf et al. 1994). More recently, RA and related retinoids are known to influence genetic expression through two series of receptors (RARs, RXRs). The many possible ligands for these receptors and the numerous receptor isoforms explain pleiotropic effects (Chambon 1996), that is, diverse biological activities associated with reproduction, embryonic development, growth, and the immune system. The precise regulation of intracellular RA concen-

Received December 4, 1998. Accepted April 5, 1999.
J14337

C. Doyon, R. Fortin, and P.A. Spear.[1] Centre de recherche TOXEN and Département des sciences biologiques, Université du Québec à Montréal, C.P. 8888, Succursale Centre-Ville, Montréal, QC H3C 3P8, Canada.

[1]Author to whom all correspondence should be addressed.
e-mail: spear.philip@uqam.ca

© 1999 NRC Canada

trations, therefore, is directly related to molecular mechanisms of vitamin A activity.

In the avian and mammalian embryo, for instance, RA is a putative morphogenetic signal. The digital pattern of limbs is influenced by a shallow concentration gradient of endogenous RA across the limb bud (Thaller and Eichele 1987; Hofmann and Eichele 1994). Experimental manipulations elevating, depressing, or physically impeding the formation of the gradient result in the absence or duplication of digits. Thus, excessive or insufficient RA results in malformed limbs. Not only RA, but other retinoids are teratogenic. RAR-β receptor binding and teratogenic potential in mammalian and amphibian embryos of 4-oxoretinoic acid (4-oxo-RA), a secondary RA metabolite of cytochrome P-450 dependent metabolism, has been reported (Creech Kraft et al. 1989; Pijnappel et al. 1993). In mammals, this metabolite is known to be produced from one of the primary RA oxidative metabolites, 4-hydroxyretinoic acid (4-OH-RA) (Roberts et al. 1979). In vitro RA hydroxylation has been described in a teleost, rainbow trout (*Oncorhynchus mykiss*) (Gilbert et al. 1995), but not in a chondrostean fish. The constitutive, uninduced hydroxylation rate in trout liver microsomes (1 pmol·mg^{-1}·h^{-1} at 12°C; Gilbert et al. 1995) is 17-fold less than that of rats (0.28 pmol·mg^{-1}·h^{-1} at 37°C; Spear et al. 1988).

Our laboratory has observed a high incidence of unusual terata in juvenile and adult lake sturgeon (*Acipenser fulvescens*) collected from the St. Lawrence River, or its tributaries, in the vicinity of Montreal (Drapeau 1990). Many lake sturgeon and white sucker (*Catostomus commersoni*) were missing fins or had duplicate or triplicate fins reminiscent of RA-related anomalies in the limb bud. In addition, bifurcated rostra (i.e., anterior lateral separation along the midline giving the appearance of "horns") were occasionally observed in juvenile and adult sturgeon caught near Montreal. When embryos of white sucker were raised in artificial streams, the incidences of several types of malformations, including those associated with fins, were significantly greater in embryos from the Montreal area compared with those from a site in the Abitibi region (Branchaud et al. 1995). These casual observations led to the hypothesis that malformations in sturgeon may be related to imbalances in RA metabolism or homeostasis.

In the present study, therefore, the incidence of malformations was estimated in juvenile and adult sturgeon captured from the St. Lawrence River and its tributaries over an 8-year period. In addition, the gametes of adult lake sturgeon were collected near spawning sites in the Abitibi region and in the area of Montreal.[2] Embryos were raised in artificial streams under controlled conditions to evaluate teratogenesis. As part of measures for the conservation of sturgeon populations, the sample numbers of breeding adults were minimal and were insufficient for the biochemical studies. Therefore, RA hydroxylation was examined in appropriate samples of smaller fish, presumed a priori to be juveniles or sub-adults, which were collected away from the spawning sites in the Abitibi region and near Montreal. These specimens were obtained in collaboration with commercial fishing activities: no fish were euthanized exclusively for the RA metabolism study. The presence of NADPH-dependent RA hydroxylation activity was demonstrated in sturgeon liver microsomes and assay conditions were optimized. Possible sources of variation of RA hydroxylation were examined (i.e., sample site, sex, age, length, and stage of gonadal development).

We have reported extremely low retinoid stores in fish from the St. Lawrence River (Spear et al. 1992; Branchaud et al. 1995; Ndayibagira et al. 1995; Doyon et al. 1998), possibly associated with retinoid metabolic imbalances. Therefore, liver retinoid stores were analyzed in the same liver samples and correlations with the RA hydroxylation were assessed.

Because RA hydroxylation was increased in rainbow trout after exposure to a coplanar PCB, 3,3′,4,4′-tetrachlorobiphenyl (Gilbert et al. 1995), composite liver samples from the two sites were analyzed for total PCBs, specific mono-*ortho* congeners, and three non-*ortho* coplanar congeners.

Materials and methods

Fish sampling of specimens for RA hydroxylation

Field studies were conducted within a limited time period to minimize the influences of environmental variables (e.g., water temperature, seasonal fluctuations in benthic communities). In August 1995, 61 lake sturgeon were captured using 9-inch (228.6 mm) gill nets at Lac Berthelot in the Abitibi region (48°55′ N lat. × 76°12′ W long.). In September 1995, 67 sturgeon were caught using 8-inch (203.2 mm) gill nets in the southwestern part of Lac Saint-Louis, near Montreal. The fish comprised subsamples of commercial catches obtained by working directly with local fishermen. Immediately following euthanasia by decapitation, an anterior portion of the liver, approximately 5 g, was frozen by submersion in liquid nitrogen. Liver samples were transported on dry ice and then conserved for 11–13 months at –80°C for later analysis of RA hydroxylation. Individual data were compiled for body length, sex, gonadal development (females; method modified from Guénette et al. 1992), and age using annuli of the first ray of the pectoral fin (Cuerrier 1951; Goyette et al. 1988).

Chemicals

Standards of 4-hydroxyretinoic acid and 4-oxoretinoic acid were gifts from Dr. Peter Sorter of Hoffman-LaRoche (Nutley, N.J., U.S.A.). All solvents were high-performance liquid chromatography (HPLC) grade obtained from Fisher Scientific (Montreal, Que., Canada). NADPH was purchased from Boehringer-Mannheim (Laval, Que., Canada). All-*trans*-retinoic acid and all other chemicals were purchased from Sigma (Oakville, Ont., Canada). All authentic PCB standards and isotopic PCB standards were purchased from Cambridge Isotope Laboratory (Cambridge, Mass., U.S.A.).

Microsome preparation and reaction conditions

All steps of microsome preparation were performed at 0–4°C. Sturgeon liver was homogenized in four volumes of 50 mM Tris–HCl buffer containing 0.15 M KCl, pH 7.4, at 4°C. Homogenates were centrifuged at 10 000 × *g* for 20 min, and the supernatants were centrifuged at 100 000 × *g* for 60 min. The microsomal pellet was washed and resuspended in Tris–KCl buffer containing 0.25 M sucrose. Microsomes were immediately frozen in liquid nitrogen and kept at –80°C until analysis. Microsomal protein content, as-

[2] A detailed account of sturgeon teratogenesis in relation to organochlorine contamination of eggs will be published separately.

© 1999 NRC Canada

sayed according to Lowry et al. (1951) with bovine serum albumin as standard, varied within the range 0.7 to 1.0 mg/mL.

The reaction conditions and HPLC analysis of metabolites was modified from existing methods (Roberts et al. 1979; Leo et al. 1984; Gilbert et al. 1995). The incubation was carried out at 15°C in a shaking water bath. The reaction mixture (1 mL) contained 0.025 mM RA, 5 mM $MgCl_2$, 1 mM EDTA, 50 mM Tris and 0.15 M KCl at pH 7.4, 150 µL microsome preparation, with or without 1.5 mM NADPH. After a 7.5-min preincubation, the reaction was started with the addition of the cofactor. Blanks contained the complete system without the cofactor. After a 75-min incubation, the reaction was stopped by adding 2 mL ethyl acetate containing 50 µg/mL of butylated hydroxytoluene and then rapid freezing in dry ice – acetone. After 2 min of mixing and 5 min of centrifugation at 2000 × *g*, the organic phase was collected. The extraction procedure was performed twice. After evaporation under nitrogen, the samples were resuspended in 75 µL of methanol for HPLC analysis. Preliminary tests established that the reaction rate was constant up to 80 min incubation time and 1.3 mg/mL microsomal protein. In heat-killed microsomes, the metabolite peak was not greater than in blanks, and the complete reaction system at 0°C yielded a peak slightly greater than that of blanks at 15°C.

High-performance liquid chromatography (HPLC)

The HPLC system consisted of model 126 pump, model 210A injector equipped with a 100-µL loop, model 168 diode-array absorbance detector, and an Ultrasphere ODS analytical column (4.6 × 150 mm; 5-µm particle size) (all Beckman Scientific Instruments, Montreal, Que., Canada). The ultraviolet (UV) absorbance detector was set at 350 nm, which corresponds to the maximum light absorbance of all-*trans*-RA (Barua 1990). The use of UV detection, as opposed to radioactivity, has been confirmed previously in fish liver microsomes and permits greater metabolite peak resolution under these HPLC conditions (Gilbert et al. 1995). The mobile phase was programmed with a gradient from 100% mobile phase A to 100% mobile phase B in 12 min and continued for 3 min more at a flow rate of 1.5 mL/min. The mobile phase A was acetonitrile – water – acetic acid (50:49.75:0.25), and the mobile phase B was acetonitrile – water – acetic acid (90:9.96:0.04), both containing 10 mM ammonium acetate. Allowing for column-solvent equilibration, samples could be injected every 20–21 min. The metabolites were identified by comparing their retention times and spectral properties with those of authentic standards. Additional verifications are described in Gilbert et al. (1995). The quantitation of the metabolite 4-OH-RA was based on an external standard curve for RA multiplied by the correction factor 0.93, which corresponds to the ratio of extinction coefficients for all-*trans*-RA, $E^{1\%}_{1\,cm}$ = 1480 (Barua 1990), and 4-OH-RA, $E^{1\%}_{1\,cm}$ = 1590 (A.B. Barua, Iowa State University, Ames, Iowa, personal communication). The enzyme activity was based on the specific rate of formation of 4-OH-RA by subtracting the peak area obtained in the presence of NADPH with that obtained in blanks without NADPH.

Retinoid stores in liver

Partially frozen tissue was dehydrated with Na_2SO_4, extracted in hexane, and analyzed by reverse-phase HPLC as described in Doyon et al. (1998).

Teratology

In the spring of 1991 and 1992, adult lake sturgeon were captured near their spawning sites on the upper reaches of the Ottawa River in the Abitibi region of Quebec and in the Rivière des Prairies, confluent with the St. Lawrence River near Montreal. Fish were held in riverside enclosures and injected with carp pituitary extract to induce the final stages of gamete maturation. The eggs of 4 females from Abitibi and 3 females from Montreal were fertilized and the embryos were raised in artificial streams as described previously (Branchaud et al. 1995). External malformations of 1966 "swim-up" stage larvae were evaluated using a dissecting microscope according to standard criteria (Sharpe 1991).

Juvenile sturgeon were collected with gill nets from various sites on the St. Lawrence River downstream from Montreal between 1991 and 1993. Juveniles were also collected from the Rivière des Prairies and Rivière l'Assomption, tributaries of the St. Lawrence River north of Montreal, between 1991 and 1993. Sexually mature sturgeon were captured with gill nets near their spawning site on the Rivière des Prairies between 1995 and 1998. External morphology was examined in detail, individuals were tagged or a segment of the pectoral fin was obtained for age determination, and the sturgeon were liberated.

PCB analyses

Two composite liver samples were prepared by pooling 1.0 g of liver from each of 10 fish collected from the same site. Chemical analyses were conducted under contract to the Service des analyses, Ministère de l'environnement et de la faune, Québec. A total of 43 PCB congeners were quantified by the method of Brochu et al. (1995). Briefly, the composite liver samples (5–8 g) were dried with sodium sulfate (40 g), blended to a fine powder, and spiked prior to extraction with a mixture of three $^{13}C_{12}$ non-*ortho*, coplanar PCBs (i.e., congeners 77, 126, and 169) and seven $^{13}C_{12}$ *ortho*-substituted PCBs (i.e., congeners 28, 52, 105, 118, 153, 180, and 194). The extraction was performed in a Soxhlet extractor with toluene for 24 h. Cleanup and fractionation (total PCBs / coplanar PCBs) consisted of eluting the extract successively through a multilayer silica column and an alumina column. Total PCBs and coplanar PCBs were analyzed by HRGC/HRMS on a Hewlett-Packard 5890 GC interfaced to a VG AutospecQ mass spectrometer. A DB-5 capillary column (0.25 mm i.d.) with 0.25-mm film thickness was used along with 1-µL injection. The HRMS was operated in selected ion monitoring mode at a static resolution of 10 000. All the results were corrected for the recovery rates of the $^{13}C_{12}$ surrogates and quantified with authentic external standards of each of the 43 congeners. Total PCB concentration was calculated from the homologue distribution pattern of each sample in comparison with that of Aroclor standards. The sum of PCBs was calculated by the addition of concentrations of 43 congeners analyzed individually.

Statistical analyses

All statistical analyses were performed using the SAS software package for personal computers (SAS Institute, Cary, N.C., U.S.A.). The influence of sex and gonadal development on the rate of RA hydroxylation was examined by one-way analysis of variance (ANOVA) and the influence of age and length was examined by regression analysis. The Bonferroni correction for Pearson coefficients was not used because we were interested in identifying all variables that could possibly influence the metabolism of RA. The difference in the rate of RA hydroxylation between the two populations was examined by one-way ANOVA. Finally, regression analysis was used to examine the relationship between the rate of RA hydroxylation and liver retinoid status within each population. To respect the assumptions of these analyses, variables were transformed to natural logarithms and a maximum of 6 values (among 127) were removed to achieve normality in the regression analyses (Table 2); however, doing so did not change the overall statistical conclusions. The homoscedasticity was verified by residual plots and the normality was verified using the test of Wilk–Shapiro. Teratogenic incidence was expressed as a percentage of individuals having a particular deformity in relation to the total number of individuals observed at each site. In the artificial stream experiments, only larvae surviving to the end of the experiment were examined.

© 1999 NRC Canada

Fig. 1. Chromatogram of metabolites formed in sturgeon liver microsomal preparations with (reaction) or without (blank) NADPH. The UV absorbance detector was set at 350 nm.

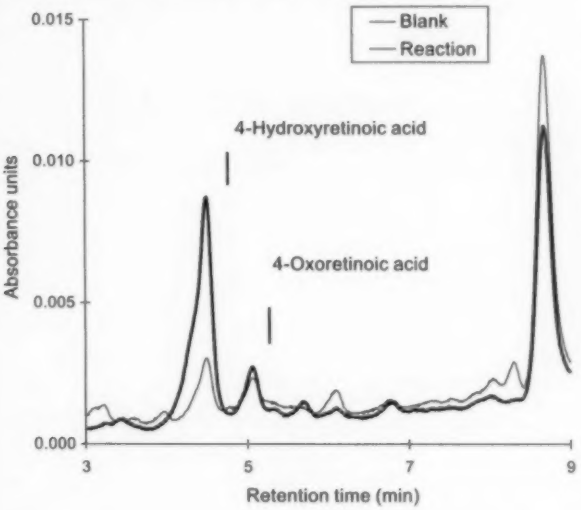

The incidence of malformations was compared by calculating a 2 × 2 (sites × deformed/normal) contingency table and using a χ^2 test.

Results

Retinoic acid metabolism

The HPLC chromatograms show peaks at 4.5 and 5.1 min corresponding to authentic standards of 4-OH-RA and 4-oxo-RA (Fig. 1). The identities of these peaks were confirmed by comparing their spectral properties with those of authentic standards and by the addition of standards to sample extracts. The peak at 4.5 min and the standard of 4-OH-RA both had a maximum light absorbance at 351 nm. Similarly, the maximum light absorbance of the peak at 5.1 min and the standard of 4-oxo-RA was 358 nm. A small peak of 4-OH-RA was typically present in the blanks (i.e., blanks did not contain the co-enzyme NADPH). To quantify the enzyme activity as the specific rate of formation of the 4-hydroxy metabolite, the blank peak area was subtracted from that obtained in reaction tubes when the co-enzyme was present.

The biological parameters of the subsamples of commercially caught lake sturgeon are presented in Table 1. Although statistical analyses did not reveal any influence of age, length, sex, or degree of gonadal development on the rate of RA hydroxylation, there was a tendency for reduced rate of hydroxylation with increasing age and gonadal development. The influence of gonadal development could not be verified for females of Lac Saint-Louis (St. Lawrence River population) because none was at the caviar stage (i.e., stage 5 in Guénette et al. 1992; Table 1).

There was a highly significant ($p < 0.0001$) difference in the rate of RA hydroxylation between the two populations. The rate of in vitro formation of 4-OH-RA in the Lac Saint-Louis sturgeon (26 ± 12 pmol·mg protein^{-1}·h^{-1}; mean ± SD) was 3.5-fold greater than that of sturgeon captured in the Abitibi region (7 ± 5 pmol·mg protein^{-1}·h^{-1}; mean ± SD). The RA hydroxylation rate for individual fish was compared with the hepatic concentrations of major retinoids (Table 2). When the two study sites were analyzed independently, there was no relationship between the rate of RA hydroxylation and liver retinoid stores, except for dehydroretinol at Lac Berthelot; however, the linear model explained only a small part of the variability ($R^2 = 0.09$).

Teratology

Gametes were collected from adult sturgeon near their spawning sites and the embryos were raised to the larval stage in artificial streams. Craniofacial deformities, principally associated with opercula, eyes, mouth, barbels. and rostrum, occurred in approximately 1.5% of larvae (N = 1966) and were not significantly different between the Abitibi and Montreal groups. Fin deformities were more often identified in the pectoral fins than the pelvic fins and were classified as absence, asymmetry, or other abnormalities. The total fin deformities were present in 6.3% (42 of 676 larvae) of the St. Lawrence River embryos and 1.7% (22 of 1290 larvae) of the Abitibi embryos, a highly significant difference ($p < 0.001$).

Teratology data for juvenile and adult lake sturgeon (N = 5477) captured from the St. Lawrence River and its tributaries near Montreal are summarized in Table 3. Fin deformities were estimated to occur in approximately 2.3% of the sturgeon, the incidence varying slightly between years. The fin anomalies were classified as supernumerary fins, absence, undersized, and other abnormalities (e.g., often atypical curvature). An example of supernumerary fin structure is the anal fin triplication shown in Fig. 2. Craniofacial malformations averaged 0.6% but were subject to greater temporal variation. The overall deformity incidence was calculated to be 2.9%.

PCB analyses

The total PCB concentration in the pooled liver sample from the St. Lawrence River sturgeon was 760 ng·g wet weight^{-1}, 18-fold greater than that of the Abitibi sturgeon (Table 4). Among the 43 PCB congeners specifically detected, the non-*ortho* coplanar and the mono-*ortho* congeners are presented because these were considered to be the most relevant to cytochrome P-450 activity in fish. Applying toxic equivalency factors established for fish, two coplanar biphenyls, PCBs 77 and 126, were estimated to be major contributors to cytochrome P-450 activity. TCDD-EQs were 20-fold greater in the composite sample of sturgeon liver from Lac Saint-Louis.

Discussion

The RA hydroxylation rate was greater ($p < 0.0001$) in sturgeon from Lac Saint-Louis (St. Lawrence River) compared with fish from Lac Berthelot (Abitibi region). This finding is significant in at least three contexts: (*i*) the metabolism of a morphogenetic signalling molecule in fish populations with different teratogenic prevalences, (*ii*) RA metabolism in relation to hepatic vitamin A stores, and

© 1999 NRC Canada

Table 1. Biological parameters of subsamples of commercial catches of lake sturgeon.

Population	*N*	Length (cm)	Age	% male/female	% caviar
Lac Berthelot	61	102.2 (80–117)	33.3 (21–42)	45.9 / 54.1	54.5
Lac Saint-Louis	67	103.1 (85–123)	18.3 (11–28)	53.7 / 46.3	0

Note: % caviar = % of females at stage 5 of gonadal development (see Guénette et al. 1992). Minimum and maximum length and age are given in parentheses below the average for the population.

Table 2. Relationship between retinoid liver stores and the rate of retinoic acid hydroxylation for two populations of lake sturgeon.

	Lac Berthelot			Lac Saint-Louis		
Retinoid	Intercept	Slope	R^2	Intercept	Slope	R^2
ROH	0.5359 (0.148)	0.1096 (–0.204)	0.04	0.0001 (–2.499)	0.1294 (0.183)	0.04
RPO	0.0001 (4.237)	0.5435 (–0.081)	0.01	0.0897 (1.884)	0.3109 (–0.352)	0.02
DR	0.0001 (2.567)	0.0221 (–0.328)	0.09	0.2341 (–0.724)	0.6069 (0.098)	0.00
DRPO	0.0001 (6.237)	0.2566 (–0.102)	0.02	0.0073 (2.992)	0.9537 (0.020)	0.00
DRLM	0.0001 (4.585)	0.3691 (–0.082)	0.01	0.6190 (0.563)	0.9769 (0.010)	0.00
DRS	0.0001 (4.885)	0.2269 (–0.120)	0.03	0.1821 (1.274)	0.7908 (0.078)	0.00

Note: ROH, retinol; RPO, retinyl palmitate/oleate; DR, dehydroretinol; DRPO, dehydroretinyl palmitate/oleate; DRLM, dehydroretinyl linoleate/myristate; DRS, dehydroretinyl stearate. Data were transformed to natural logarithms to meet the assumptions of regression analysis. Values under column headings of intercept and slope are the statistical probabilities. Values given in parentheses for intercept and slope were obtained from regression equations of the form: $\ln(\text{retinoid}) = a + b\ (\ln(\text{4-OH}))$, where 4-OH is the rate of formation of 4-hydroxyretinoic acid. Sample numbers varied from $N = 60$ to 61 for Lac Berthelot and from $N = 61$ to 66 for Lac Saint-Louis.

Table 3. Summary of malformations observed in lake sturgeon in the St. Lawrence River and its tributaries near Montreal.

Year	Number of fish observed	Fin deformities[c] (%)	Craniofacial deformities[d] (%)	Total deformities (%)
1991–1993[a]	1076	2.2	1.1	3.3
1995[b]	1410	3.0	0.1	3.1
1996[b]	1311	1.4	0.5	1.8
1997[b]	676	2.2	0.9	3.1
1998[b]	1004	2.9	0.5	3.3

[a]Juvenile sturgeon collected from four sites on the St. Lawrence River and two tributaries (Rivière des Prairies and Rivière l'Assomption). Data from Mellado (1996).

[b]Sexually mature adult sturgeon captured on spawning site in Rivière des Prairies, a tributary of the St. Lawrence River. Data from S. Thibodeau, Department of Biological Sciences, Université du Québec à Montréal, personal communication.

[c]Fin deformities include supernumerary fins, absence, undersized, and unusual structure.

[d]Craniofacial deformities associated with the rostrum, mouth, barbels, nares, and opercula.

(*iii*) the possible implication of cytochrome P-450 inducing contaminants such as PCBs.

The formation of 4-OH-RA in mammals and fish occurs in liver microsomes under conditions necessary for cytochrome P-450 activity, including the presence of NADPH (Roberts et al. 1979, 1992; Gilbert et al. 1995). Although produced under the same conditions, 4-oxo-RA requires NAD or NADP and is considered to be a subsequent step in RA metabolism independent of the cytochrome P-450 system (Roberts et al. 1979; Frolik et al. 1979). Therefore, the lack of NADPH enhancement of 4-oxo-RA in sturgeon liver microsomes (Fig. 1) is not unexpected and is similar to results obtained with rainbow trout liver microsomes (Gilbert et al. 1995). However, we have found the 4-oxo-RA metabolite to be considerably more stable in biological media (S. Boileau and P.A. Spear, Centre de recherche TOXEN, Université du Québec à Montréal, unpublished results). Intracellularly, this would mean that greater cytochrome P-450 activity could decrease the concentration of RA while increasing the concentration of 4-oxo-RA. The retinoid sig-

© 1999 NRC Canada

Fig. 2. Supernumerary anal fins (triplication with partial fusion of fins A, B, and C) of a juvenile lake sturgeon.

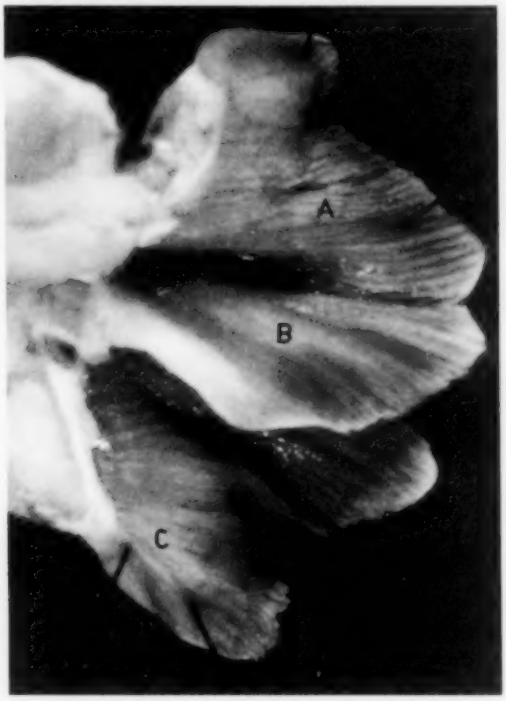

nalling pathway would be affected because both RA and 4-oxo-RA are ligands for RAR nuclear receptors (Pijnappel et al. 1993; Chambon 1996).

Elevated 4-oxo-RA concentrations are extremely teratogenic (Creech Kraft et al. 1989; Pijnappel et al. 1993) and insufficient RA also results in abnormal development and embryo mortality (Thompson et al. 1969). The results for RA metabolism are consistent with the observation that the incidence of fin and craniofacial deformities is 2.9% among juvenile and adult sturgeon captured in the Montreal area (Table 3), that is, 1 deformed fish in 35.

When raised under the same optimal conditions, larvae of St. Lawrence River sturgeon had significantly more fin deformities than the larvae of Abitibi fish. The use of artificial streams in the present study eliminates extrinsic environmental variables (e.g., fluctuations in water temperature, waterborne pathogens) as teratogenic factors. The difference in teratogenesis may be ascribed to intrinsic factors such as genetic and biochemical differences. Imbalances of retinoid metabolism are among the possible biochemical differences.

The implication of cytochrome P-450 inducing chemicals is supported by the PCB analyses (Table 4). The 3.5-fold greater RA hydroxylation rate measured in the St. Lawrence sturgeon is consistent with the results of laboratory experiments. In rainbow trout microsomal preparations, a 5.9-fold increase in the rate of RA hydroxylation was observed 56 days after a single injection of the coplanar PCB congener 77. Similarly, a single exposure to another coplanar biphenyl, 3,3′,4,4′,5,5′-hexabromobiphenyl, caused a 2.3-fold increase in the rate of RA hydroxylation in rat (Spear et al. 1988). Fiorella et al. (1995) examined the effect of TCDD in various organs of rat and found that RA hydroxylation was induced in liver, kidney, and lung.

The PCB analyses conducted in the present study were restricted to one composite sample from each site and cannot be interpreted as a definitive indication of environmental contamination at the two sites. Nonetheless, the data are interesting in that TEQs determined from toxic equivalency factors (TEFs) based in in vitro cytochrome P-450 (CYP450) induction potencies in fish liver cells gave estimates of dioxin equivalents (TCDD-EQs) that were 20-fold greater in the liver of Lac Saint-Louis sturgeon (Table 4). This result is consistent with a relationship between the concentrations of PCB congeners with potent CYP450-inducing chemicals and the rates of hydroxylation in the livers of sturgeon from the two sites. The concentrations of congeners 77 and 126 analyzed in the liver of white sturgeon (*Acipenser transmontanus*) from the upper Fraser River, British Columbia, were intermediate between those of the Lac Berthelot and the Lac Saint-Louis samples (MacDonald et al. 1997). The total PCB concentrations were nondetectable (i.e., <0.5 mg/kg) in filets of adult sturgeon from the Abitibi region, but 1750 ng/g in St. Lawrence River sturgeon filets (Paul and Laliberté 1988).

Lake sturgeon caught from the St Lawrence River had elevated EROD (ethoxyresorufin-*O*-deethylase) activity compared with that of sturgeon from the Abitibi region (Rousseaux et al. 1995), suggesting induction of cytochrome P-4501A1/2. Coplanar PCBs, such as congeners 77 and 126, are potent CYP1A inducers, whereas most other PCBs primarily induce CYP2 and CYP3 families (Goksoyr and Förlin 1992). In studies with mammals unrelated to PCB induction, many purified cytochromes P-450 catalyzed RA 4-hydroxylation, including P-4501A1 and P-4501A2 (Leo et al. 1989; Roberts et al. 1992; Martini and Murray 1993; Muindi and Young 1993). P-450RAI was recently cloned from regenerating fin epithelia of zebrafish, *Brachydanio rerio*, and found to catalyse 4-hydroxylation of RA (White et al. 1996). PCB 77 induces CYP1A1 expression in various fish cell types (Monosson and Stegeman 1991; Clemons et al. 1996; Zabel et al. 1996). It is interesting to note that EROD and RA hydroxylation activities did not coincide temporally when rainbow trout were exposed to PCB congener 77 (Gilbert et al. 1995), suggesting RA hydroxylation activity of a P-450 isozyme other than P-4501A1 or short-term saturation of the enzyme by the PCB. Alternatively, CYP1A2 is induced by 3-methylcholanthrene in rainbow trout (Berndtson and Chen 1994) and may have contributed to RA hydroxylation in the present study.

Another explanation relates to nutritional factors; specifically, a higher dietary intake of vitamin A in the Lac Saint-Louis sturgeon could account for the greater 4-OH-RA rate. In humans, consumption of a meal with high vitamin A value results in increased plasma levels of RA metabolites (Arnhold et al. 1996). This suggests a vitamin A induced RA metabolism. Conversely, low dietary vitamin A is predicted to decrease RA metabolism (Napoli 1996). The Lac Saint-Louis sturgeon, however, have significantly lower hepatic concentrations of all major retinoids (Doyon et al. 1998), which would not be expected in the case of higher vitamin A intake.

© 1999 NRC Canada

Table 4. Hepatic PCB concentrations in two populations of lake sturgeon.

			Lac Berthelot		Lac Saint-Louis	
PCB congeners	IUPAC	TEFs	Conc. (LDM)	TCDD-EQs	Conc. (LDM)	TCDD-EQs
Non-*ortho*						
3,3′,4,4′-tetraCB	77	0.0034	13 (0.1)	0.044	360 (0.1)	1.224
3,3′,4,4′,5-pentaCB	126	0.023	1.7 (0.3)	0.039	32 (0.5)	0.736
3,3′,4,4′,5,5′-hexaCB	169	0.00016	ND (0.1)		ND (0.1)	
Σ non-*ortho*			14.7		392	
Mono-*ortho*						
2,4,4′-triCB	28		130 (10)		7 900 (10)	
2,4′,5-triCB	31		95 (10)		6 300 (10)	
2′,3,4-triCB *	33		DNQ (10)		280 (10)	
2,3′,4′,5-tetraCB *	70		250 (10)		9 400 (40)	
2,4,4′,5-tetraCB	74		380 (10)		13 000 (40)	
2,3,3′,4,4′-pentaCB	105	0.000049	640 (10)	0.031	10 000 (100)	0.49
2,3′,4,4′,5-pentaCB	118	0.000017	1000 (10)	0.017	18 000 (100)	0.306
2,3,3′,4,4′,5-hexaCB	156	0.000030	390 (10)	0.012	3 600 (20)	0.108
Σ mono-*ortho*			2885		68 480	
Σ TCDD-EQs				0.143		2.864
Σ PCBs			34.8		595.6	
Total PCBs			42		760	

Note: Values for individual PCB congeners, TCDD-EQs, and sum of non-*ortho* and mono-*ortho* are in pg/g wet weight. Values for sum of PCBs and total PCBs are in ng/g (ppb) wet weight. Analyses were conducted on pooled samples of liver from 10 sturgeons at each site. LDM, limit of detection of the method; ND, not detected; DNQ, detected but not quantified; *, maximum concentration possible because this congener can coelute with others; TCDD-EQs, toxic equivalents expressed as pg/g 2,3,7,8-tetrachlorodibenzo-*p*-dioxin; TEFs, toxic equivalent factors based on cytochrome P4501A1 induction in rainbow trout liver cell line RTL-W1 (Clemons et al. 1996). In addition to the non-*ortho*- and mono-*ortho*- congeners shown in the table, congener-specific data were obtained for PCBs 17, 18, 44, 49, 52, 82, 87, 95, 99, 101, 110, 128, 132, 138, 149, 151, 153, 158, 170, 171, 177, 180, 183, 187, 191, 194, 195, 199, 205, 206, 208, and 209.

In conclusion, this study demonstrates that lake sturgeon, like mammals and rainbow trout studied previously, are able to hydroxylate retinoic acid in liver microsomal preparations. Within the two study sites, the variables age, length, sex, and degree of gonadal development in males did not have a significant influence on the reaction rate. The significantly higher hydroxylation rate in the Lac Saint-Louis (St. Lawrence River) sturgeon is particularly interesting in light of the fact that RA is a morphogenetic signalling molecule and the St. Lawrence sturgeon were found to have an elevated prevalences of malformations. A possible explanation for the differences in RA hydroxylation rate include cytochrome P-450 induction by environmental contaminants such as coplanar PCBs.

Acknowledgments

Sturgeon were captured in collaboration with commercial fishermen Henri Duranseau and Gaston Racicot and by students Claire Normandeau, Andrée Gendron, Alain Branchaud, André Bilodeau, Pedro Nilo Mellado, and Stéphanie Thibodeau. Larval sturgeon morphology was assessed by Claire Normandeau. Canada Council for the Protection of Animals guidelines were followed and the research was conducted under permits issued by the Ministère de l'Environnement et de la Faune and the Université du Québec à Montréal Animal Care Committee. Age determinations were conducted with the assistance of Pedro Nilo Mellado and the technical support of the Ministère de l'Environnement et de la Faune, Gouvernement du Québec. Christian Doyon received a graduate student scholarship from the Natural Sciences and Engineering Council of Canada (NSERC). This research was supported by NSERC and Environment Canada (Centre Saint-Laurent) research grants to Drs Réjean Fortin and Philip A. Spear.

References

Arnhold, T., Tzimas, G., Wittfoht, W., Plonait, S., and Nau, H. 1996. Identification of 9-*cis*-retinoic acid, 9,13-di-*cis*-retinoic acid, and 14-hydroxy-4,14-*retro*-retinol in human plasma after liver consumption. Life Sci. **59**: PL169–PL177.

Barua, A.B. 1990. Analysis of water soluble compounds: glucuronides. Methods Enzymol. **189**: 136–145.

Berndtson, A.K., and Chen, T.T. 1994. Two unique *CYP*1 genes are expressed in response to 3-methylcholanthrene treatment in rainbow trout. Arch. Biochem. Biophys. **310**: 187–195.

Branchaud, A., Gendron, A., Fortin, R., Anderson, P.D., and Spear, P.A. 1995. Vitamin A stores, teratogenesis, and EROD activity in white sucker, *Catostomus commersoni*, from Rivière des Prairies near Montréal and a reference site. Can. J. Fish. Aquat. Sci. **52**: 1703–1713.

Brochu, C., Hamelin, G., Moore, S., Laliberté, D., and Lafontaine, Y.D. 1995. Contribution of PCDD/PCDFs, planar and ortho substituted PCB congeners to the total TCDD-equivalent concentration in fish fillet from the St. Lawrence River. Organohalogen Compounds, **26**: 293–298.

Chambon, P. 1996. A decade of molecular biology of retinoic acid receptors. J. Fed. Am. Soc. Exp. Biol. **10**: 940–954.

Clemons, J.H., Lee, L.E.J., Myers, C.R., Dixon, D.G., and Bols, N.C. 1996. Cytochrome P4501A1 induction by polychlorinated biphenyls (PCBs) in liver cell lines from rat and trout and the

© 1999 NRC Canada

derivation of toxic equivalency factors. Can. J. Fish. Aquat. Sci. **53**: 1177–1185.

Creech Kraft, J., Löfberg, B., Chahoud, I., Bochert, G., and Nau, H. 1989. Teratogenicity and placental transfer of all-*trans*-, 13-*cis*-, 4-oxo-all-*trans*-, and 4-oxo-13-*cis*-retinoic acid after administration of a low oral dose during organogenesis in mice. Toxicol. Appl. Pharmacol. **100**: 162–176.

Cuerrier, J.-P. 1951. The use of pectoral fin rays for determining age of sturgeon and other species of fish. Can. Fish Cult. **11**: 10–18.

Doyon, C., Boileau, S., Fortin, R., and Spear, P.A. 1998. Rapid HPLC analysis of retinoids and dehydroretinoids stored in fish liver: comparison of two lake sturgeon populations. J. Fish. Biol. **53**: 973–986.

Drapeau, J.-P. 1990. Des animaux malades du fleuve. Franc Nord, **7**(5): 16–20.

Fiorella, P.D., Olson, J.R., and Napoli, J.L. 1995. 2,3,7,8-tetrachlorodibenzo-*p*-dioxin induces diverse retinoic acid metabolites in multiple tissues of Sprague-Dawley rat. Toxicol. Appl. Pharmacol. **134**: 222–228.

Frolik, C.A., Roberts, A.B., Tavela, T.E., Roller, P.P., Newton, D.L., and Sporn, M.B. 1979. Isolation and identification of 4-hydroxy- and 4-oxoretinoic acid. In vitro metabolites of *all-trans*-retinoic acid in hamster trachea and liver. Biochemistry, **18**: 2092–2097.

Giguère, V., Ong, E.S., Segui, P., and Evans, R.M. 1987. Identification of a receptor for the morphogen retinoic acid. Nature (London), **330**: 624–629.

Gilbert, N.L., Cloutier, M.-J., and Spear, P.A. 1995. Retinoic acid hydroxylation in rainbow trout (*Oncorhychus mykiss*) and the effect of a coplanar PCB, 3,3′,4,4′-tetrachlorobiphenyl. Aquat. Toxicol. **32**: 177–187.

Goksoyr, A., and Förlin, L. 1992. The cytochrome P-450 system in fish, aquatic toxicology and environmental monitoring. Aquat. Toxicol. **22**: 287–312.

Goyette, D., Guénette, S., Fournier, N., Leclerc, J., Ray, G., Fortin, R., and Dumont, P. 1988. Maturité sexuelle et périodicité de la reproduction chez la femelle de l'Esturgeon jaune (*Acipenser fulvescens*) du fleuve Saint-Laurent. Ministère du Loisir, de la Chasse et de la Pêche, Direction Régionale de Montréal. Rapport de travaux 06-02.

Guénette, S., Goyette, D., and Fortin, F. 1992. La périodicité de la croissance chez la femelle de l'Esturgeon jaune (*Acipenser fulvescens*) du fleuve Saint-Laurent est-elle reliée à la périodicité de la reproduction? Can. J. Fish. Aquat. Sci. **49**: 1336–1342.

Hofmann, C., and Eichele, G. 1994. Retinoids in development. *In* The retinoids: biology, chemistry, and medicine. 2nd ed. *Edited by* M.B. Sporn, A.B. Roberts, and D.S. Goodman. Raven Press, New York. pp. 387–441.

Leo, M.A., Iida, S., and Lieber, C.S. 1984. Retinoic acid metabolism by a system reconstituted with cytochrome P-450. Arch. Biochem. Biophys. **234**: 305–312.

Leo, M.A., Lasker, J.M., Raucy, J.L., Kim, C.-I., Black, M., and Lieber, C.S. 1989. Metabolism of retinol and retinoic acid by human liver cytochrome P450IIC8. Arch. Biochem. Biophys. **269**: 305–312.

Lowry, O.H., Rosenbrough, N.J., Farr, A.L., and Randall, R.J. 1951. Protein measurement with the Folin phenol reagent. J. Biol. Chem. **193**: 265–275.

MacDonald, D.D., Ikonomou, M.G., Rantalaine, A.-L., Rogers, I.H., Sutherland, D., and Van Oostdam, J. 1997. Contaminants in white sturgeon (*Acipenser transmontanus*) from the upper Fraser River, British Columbia, Canada. Environ. Toxicol. Chem. **16**: 479–490.

Mangelsdorf, D.J., Umesono, K., and Evans, R.M. 1994. The retinoid receptors. *In* The retinoids: biology, chemistry, and medicine. 2nd ed. *Edited by* M.B. Sporn, A.B. Roberts, and D.S. Goodman. Raven Press, New York. pp. 319–349.

Martini, R., and Murray, M. 1993. Participation of 3A enzymes in rat hepatic microsomal retinoic acid 4-hydroxylation. Arch. Biochem. Biophys. **303**: 57–66.

Mellado, P.N. 1996. Force de classes d'âge, habitats et alimentation des Esturgeons jaunes (*Acipenser fulvescens*) juvéniles du système Saint-Laurent. Mémoire MSc., Université du Québec à Montréal.

Monosson, E., and Stegeman, J.J. 1991. Cytochrome P450E (P450IA) induction and inhibition in winter flounder by 3,3′,4,4′-tetrachlorobiphenyl: comparison of response in fish from Georges Bank and Narragansett Bay. Environ. Toxicol. Chem. **10**: 765–774.

Muindi, J.F., and Young, C.W. 1993. Lipid hydroperoxides greatly increase the rate of oxidative catabolism of all-*trans*-retinoic acid by human cell culture microsomes genetically enriched in specified cytochrome P-450 isoforms. Cancer Res. **53**: 1226–1229.

Napoli, J.L. 1996. Retinoic acid biosynthesis and metabolism. J. Fed. Am. Soc. Exp. Biol. **10**: 993–1001.

Ndayibagira, A., Cloutier, M-J., Anderson, P.D., and Spear, P.A. 1995. Effects of 3,3′4,4′-tetrachlorobiphenyl on the dynamics of vitamin A in brook trout (*Salvelinus fontinalis*) and intestinal retinoid concentrations in lake sturgeon (*Acipenser fulvescens*). Can. J. Fish. Aquat. Sci. **52**: 512–520.

Paul, M., and Laliberté, D. 1988. Teneurs en mercure, plomb, cadmium, BPC et pesticides organochlorés des sédiments et de la chair de poissons du fleuve Saint-Laurent et de la Rivière des Outaouais en 1985. QEN/QE-86-07. Techn. Rep. Ministère de l'Environnment du Québec, Montréal, Qué.

Petkovich, M., Brand, N.J., Krust, A., and Chambon, P. 1987. A human retinoic acid receptor which belongs to the family of nuclear receptors. Nature (London), **330**: 444–450.

Pijnappel, W.W.M., Hendriks, H.F.J., Folkers, G.E., van der Brink, C.E., Dekker, E.J., Edelenbosch, C., van der Saag, P.T., and Durston, A.J. 1993. The retinoid ligand 4-oxo-retinoic acid is a highly active modulator of positional specification. Nature (London), **366**: 340–344.

Roberts, A.B., and Frolik, C.A. 1979. Recent advances in the in vivo and in vitro metabolism of retinoic acid. Fed. Proc. **38**: 2524–2527.

Roberts, A.B., Nichols, M.D., Newton, D.L., and Sporn, M.B. 1979. *In vitro* metabolism of retinoic acid in hamster intestine and liver. J. Biol. Chem. **254**: 6296–6302.

Roberts, E.S., Vaz, A.D.N., and Coon, M.J. 1992. Role of isozymes of rabbit microsomal cytochrome P-450 in metabolism of retinoic acid, retinol, and retinal. Mol. Pharmacol. **41**: 427–433.

Rousseaux, C.G., Branchaud, A., and Spear, P.A. 1995. Evaluation of liver histopathology and EROD activity in St. Lawrence lake sturgeon (*Acipenser fulvescens*) in comparison with a reference population. Environ. Toxicol. Chem. **14**: 843–849.

Sharpe, J.R. 1991. The influence of toxicants on the teratogenic response of fishes: a guide to the literature, a glossary of terms and a pictorial atlas. Trace Subst. Environ. Health, **24**: 63–80.

Spear, P.A., Garcin, H., and Narbonne, J.-F. 1988. Increased retinoic acid metabolism following 3,3′,4,4′,5,5′-hexabromobiphenyl injection. Can. J. Physiol. Pharmacol. **66**: 1181–1186.

Spear, P.A., Bilodeau, A.Y., and Branchaud, A. 1992. Retinoids: from metabolism to environmental monitoring. Chemosphere, **25**: 1733–1788.

Thaller, C., and Eichele, G. 1987. Identification and spatial distri-

© 1999 NRC Canada

bution of retinoids in the developing chick limb bud. Nature (London), **327**: 625–628.

Thompson, J.N., Howell, J.M., Pitt, G.A.J., and McLaughlin, C.I. 1969. The biological activity of retinoic acid in the domestic fowl and the effects of vitamin A deficiency on the chick embryo. Br. J. Nutr. **23**: 471–489.

White, J.A., Guo, Y-D., Baetz, K., Beckett-Jones, B., Bonasoro, J., Hsu, K.E., Dilworth, F.J., Jones, G., and Petkovich, M. 1996. Identification of the retinoic acid inducible all-*trans*-retinoic acid 4-hydroxylase. J. Biol. Chem. **271**: 29 922 – 29 927.

Zabel, E.W., Pollenz, R., and Peterson, R.E. 1996. Relative potencies of individual polychlorinated dibenzo-*p*-dioxin, dibenzofuran, and biphenyl congeners and congener mixtures based on induction of cytochrome P4501A mRNA in a rainbow trout gonadal cell line (RTG-2). Environ. Toxicol. Chem. **15**: 2310–2318.

© 1999 NRC Canada

Large-scale spatial heterogeneity of macrozooplankton in Lake of Geneva

Bernadette Pinel-Alloul, Catherine Guay, Nadine Angeli, Pierre Legendre, Pierre Dutilleul, Gérard Balvay, Daniel Gerdeaux, and Jean Guillard

Abstract: Spatial distribution of macrozooplankton was studied during spring in Lake of Geneva to evaluate the influence of abiotic (water temperature and stability, nutrients) and biotic (bacteria, chlorophyll *a*, fish biomass) factors on macrozooplankton distribution. Mapping and spatial analyses revealed that abiotic factors, as well as crustacean abundances, were structured along a gradient in the great lake basin. Chlorophyll *a* biomass, bacteria density, cyclopoid abundance, and fish biomass showed more patchy or inshore–offshore distribution patterns. Using canonical analyses, we determined the relative contribution of the spatial and environmental factors to the distribution of macrozooplankton species and of trophic groups based on herbivory and omnivory/carnivory. The distribution of macrozooplankton can be explained by small-scale variations and lake gradients in abiotic and biotic factors, with a dominant contribution of the abiotic factors. Water temperature and stability, as well as ammonium, are the main factors related to macrozooplankton distribution in Lake of Geneva during spring. Chlorophyll *a* biomass was also related to the distribution of cyclopoids. The canonical models explained 35–72% of the variance in the distribution of total crustaceans, species, and trophic groups. However, 28–65% of the macrozooplankton variance remained unexplained, which may be due to fine-scale variations in other environmental factors.

Résumé : La distribution spatiale du macrozooplancton dans le Lac Léman (ou Lac de Genève) a été étudiée au printemps pour déterminer l'influence des facteurs abiotiques (température et stabilité de la colonne d'eau, nutriments) et biotiques (bactéries, chlorophylle *a*, biomasse des poissons) sur la distribution du macrozooplancton. La cartographie et l'analyse spatiale ont révélé que les facteurs abiotiques, ainsi que l'abondance des crustacés, étaient structurés selon un gradient dans le grand lac. La biomasse en chlorophylle *a*, la densité des bactéries, l'abondance des cyclopoïdes et les biomasses de poissons présentaient des patrons de distribution plus agrégés ou des gradients rive-large. À l'aide d'analyses canoniques, nous avons évalué l'influence relative des facteurs environnementaux et des structures spatiales dans la distribution des espèces de macrozooplancton et des groupes trophiques basés sur les catégories d'herbivores et d'omnivores/carnivores. La distribution du macrozooplancton s'explique à la fois par les variations locales à petite échelle et les gradients à grande échelle des facteurs abiotiques et biotiques, avec une contribution plus importante des facteurs abiotiques. La température et la stabilité de la masse d'eau ainsi que les concentrations en ammoniaque sont les principaux facteurs reliés à la distribution spatiale du macrozooplancton dans le grand basin du Lac de Genève. La biomasse en chlorophylle *a* est aussi reliée à la répartition des cyclopoïdes. Les modèles canoniques expliquent 35 à 72% de la variabilité dans la distribution des crustacés totaux, des espèces et des groupes trophiques. Toutefois, de 28 à 65% de la variance du macrozooplancton reste inexpliqué, ce qui pourrait être imputable aux variations à petite échelle d'autres facteurs environnementaux.

Introduction

Zooplankton patchiness occurs on a continuum of scales in both marine and freshwater environments; zooplankton spatial heterogeneity is the product of the interaction of physical and biological processes (Pinel-Alloul 1995). Despite the importance of spatial heterogeneity for ecological theory (Hastings 1990; Bell et al. 1993; Legendre 1993) and zooplankton ecology (Pinel-Alloul et al. 1995; Megard et al. 1997), studies of distribution patterns of zooplankton in large lakes, and of their plausible causes, are yet limited. Very few studies have been carried out at the whole-lake

Received August 6, 1998. Accepted February 10, 1999.
J14734

B. Pinel-Alloul,[1] **C. Guay, and P. Legendre.** GRIL, Groupe de Recherche Interuniversitaire en Limnologie et en Environnement Aquatique, Département de Sciences biologiques, Université de Montréal, C.P. 6128, Succ. Centre-ville, Montréal, QC H3C 3J7, Canada.
N. Angeli, G. Balvay, D. Gerdeaux, and J. Guillard. Station d'Hydrobiologie lacustre, INRA, B.P. 511, 74203 Thonon-les-Bains Cedex, France.
P. Dutilleul. Department of Plant Science, Faculty of Agricultural and Environmental Sciences, Macdonald Campus, McGill University, 21111 Lakeshore Road, Sainte-Anne-de-Bellevue, QC H9X 3V9, Canada.

[1]Author to whom all correspondence should be addressed. e-mail: pinelb@ere.umontreal.ca

© 1999 NRC Canada

scale in large tropical and temperate lakes (Hart 1990; Patalas and Salki 1992; Holopainen et al. 1993; Viljanen and Karjalainen 1993) and none in large alpine lakes.

Recent studies have provided evidence that many factors may be responsible for the spatial heterogeneity of lake zooplankton: wind (Jones et al. 1995) and wind-induced currents (Lacroix and Lescher-Moutoué 1995), water temperature (Betsill and van den Avyle 1994) and inshore–offshore thermic gradients (Johannsson et al. 1991; Stockwell and Sprules 1995), size of zooplankton, swimming capacity, and avoidance behaviour (Pinel-Alloul et al. 1988; Visman et al. 1994), spatial scale of the observations (Pinel-Alloul and Pont 1991; Lacroix and Lescher-Moutoué 1995), food resources (Johannsson et al. 1991; Pourriot et al. 1994), fish predation (Johannsson et al. 1991; De Meester et al. 1993; Viljanen and Karjalainen 1993), and lake morphometry (Patalas and Salki 1992), among others. It is presently recognized that abiotic factors alone are not sufficient to satisfactorily explain the spatial variability of zooplankton (Pinel-Alloul et al. 1990, 1995). This variability may also be studied under a model of biotic interactions among the planktonic compartments (McQueen et al. 1986; Northcote 1988; Vanni 1988; Carpenter and Kitchell 1993). Hence, the plankton community is a dynamic system. Understanding it requires a combination of abiotic and biotic explanatory factors in order to reach more realistic and reliable predictions about its ecology (Carpenter 1988; Mazumder et al. 1988).

Results of an extensive whole-lake sampling program, carried out in Lake of Geneva (Lac Léman in France) in mid-April 1985, were used to study the horizontal spatial heterogeneity of macrozooplankton during the spring using geostatistical and canonical methods of analysis. We chose Lake of Geneva because it is a large alpine lake with horizontal current dynamics (Lemmin 1989); thus, it should be clearly spatially structured, presenting patches and gradients in the abiotic and biotic factors and in the zooplankton community as well (Angeli et al. 1991). This is the first whole-lake study of zooplankton spatial distribution in a large alpine lake reported in the literature. Furthermore, no study has paid attention to the relationships between the horizontal distribution of macrozooplankton and environmental factors in large alpine lakes, where water movements and advective processes are important driving forces, especially during the spring, as in all large lakes.

In this study, the spatial heterogeneity in the environment and the macrozooplankton community was analysed in order to explain the horizontal distribution of macrozooplankton with respect to abiotic (water stability and temperature, nutrients) and biotic (bacteria, chlorophyll *a*, fish) environmental factors. Our contention was that spatial heterogeneity in the biotic and abiotic factors provides for different modes of functioning of the zooplankton community, generating spatial heterogeneity in zooplankton distribution. This conceptual scheme allowed us to focus on the following specific objectives and hypotheses: (*i*) to verify that the crustacean planktonic community in Lake of Geneva presents horizontal patterns of distribution, during the spring, at the whole-lake scale, (*ii*) to confirm that both the dependent (macrozooplankton) and independent (environmental) variables were spatially structured, (*iii*) to analyse the degree of correlation among the environmental variables and between the environmental and macrozooplankton variables, (*iv*) to measure the relative importance of the effects of the biotic and abiotic variables on the horizontal distribution of macrozooplankton, and (*v*) to check whether the abiotic factors are the main factors explaining the distribution of macrozooplankton during the spring. Given the dominant role of zooplankton in the transfer of energy to roach, perch, and whitefish in alpine lakes (Angeli et al. 1995) during the spring, it is important to clearly understand and resolve how the interaction among temperature, nutrients, food, and fish predation may translate into spatial patterns of macrozooplankton distribution. Finally, we will attempt to untangle the effects of the abiotic and biotic variables on the macrozooplankton distribution in Lake of Geneva during the spring as a model for large European alpine lakes.

Materials and methods

Study site and sampling

Lake of Geneva (46°27′N; 6°32′E) is located partly in France (40%) and partly in Switzerland (60%) (Fig. 1). Its watershed covers 7975 km^2. The Rhône, Dranse, Venoge, Veveyse, and Aubonne rivers are its major tributaries (Zahner 1984). The lake is 72 km long and 13–14 km wide. With a surface area of 582 km^2, a mean depth of 153 m (maximum depth 309 m), and a volume of 89 km^3, Lake of Geneva is the largest subalpine lake in western Europe. Water retention time varies from 5 years for the surface layer to 20 years for deeper layers, with an average of 12 years (Pelletier and Blanc 1991). The lake consists of two basins: the "small lake" (the shallower and elongated western part near Geneva: mean depth 41 m) and the "great lake" (the larger and deeper eastern part). The great lake, in turn, consists of three regions: the "upper lake" (easternmost part) at the Rhone inflow, the "middle lake" in front of Lausanne, and the "lower lake" (westernmost part) near Thonon. Lake of Geneva is a warm monomictic lake, which changed rapidly from being oligotrophic to mesotrophic during the 1960's and 1970's due to anthropogenic eutrophication (Pelletier and Blanc 1991).

Sampling took place during daytime on 17–19 April 1985 during the spring, a period of the year with strong northeasterly winds (Fig. 1). Short-term sampling over 3 days enabled us to minimize the temporal variation in zooplankton distribution. Zooplankton was sampled at 33 sites over the whole lake (Fig. 1). Distances between sites were almost regular, varying from 3 to 5 km. Zooplankton samples were taken at each site by vertical filtration of 1900 L of water over the 0- to 50-m water column, using a 55-cm-wide, 175-μm-mesh biconical closing net (Asptein's type; Tranter 1968). The choice of the 0- to 50-m depth range for zooplankton sampling enabled us to avoid bias due to the vertical migrations of zooplankton, since most of the zooplankton is distributed only across the 0- to 50-m water layer during the diel cycle (Angeli et al. 1995). Water samples for chlorophyll *a*, bacteria, phosphate (PO_4), nitrate (NO_3), and ammonium (NH_4) measurements were integrated over the 0- to 10-m water column at each site using a patented integration bell that is based on Mariot's law; a previous study showed that peaks of chorophyll *a* always occurred between 3 and 7 m, and maximal primary production was situated in surface waters (2–5 m) (Balvay et al. 1985). A mean temperature was calculated for the 5- to 25-m water layer that covers the thermic vertical gradient during the sampling period (Fig. 1). The surface layer (0–5 m) was excluded from the calculation of mean values of water temperature to avoid problems of daily variation (Angeli et al. 1991).

© 1999 NRC Canada

Fig. 1. Bathymetric map of Lake of Geneva with its main affluents, different basins, and sampling stations (upper map), modified from Zahner (1984), wind speed recorded at each meteorological station (A, B, C, D) during the sampling survey (17–19 April) and the previous day (16 April) (map upper left corner), and temperature profiles at each sampling station (lower map).

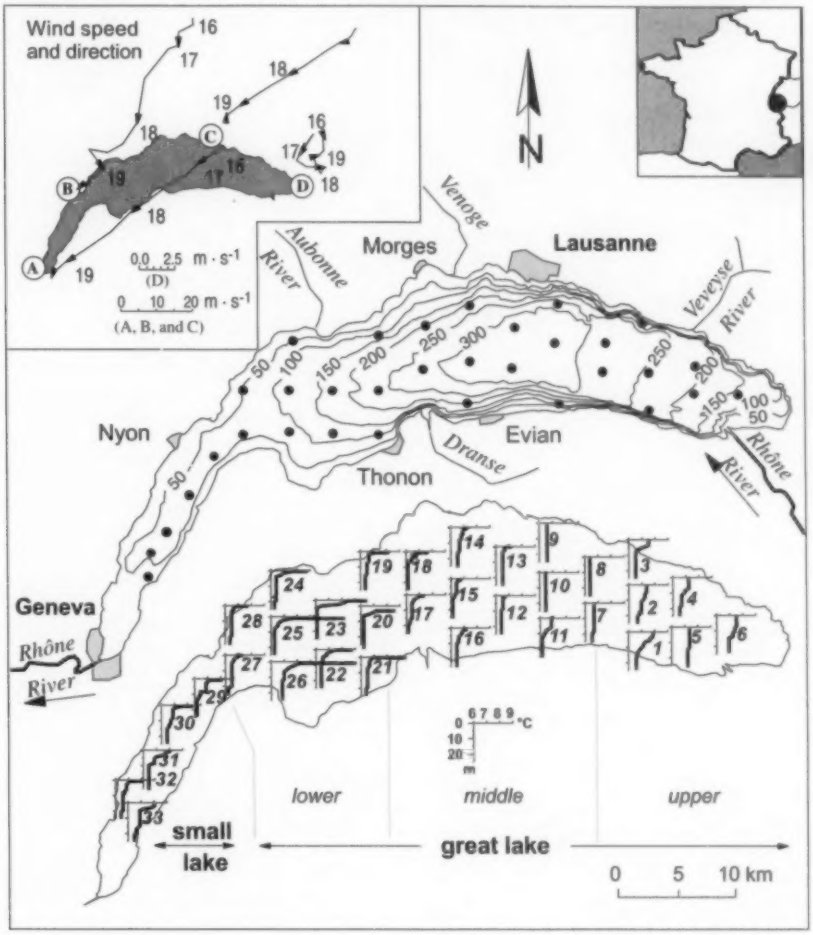

Environmental and zooplankton variables

Chlorophyll *a* concentrations were measured using a Turner™ fluorometer after acetone extraction (Yentsch and Menzel 1963) and spectrophotometric calibration. Bacterial abundances were estimated using epifluorescence microscopy (magnification 1250×) after orange acridine staining (Hobbie et al. 1977). Concentrations of NO_3 were obtained after conversion to nitrite by cadmium reduction following the method defined by the Association française de normalisation (AFNOR) and described in Gawler et al. (1986). NH_4 concentrations were measured using the indophenol blue method following the AFNOR NFT90 015 norm (Koroleff 1970). PO_4 concentrations were measured using the method of Murphy and Riley (1962).

The simplest practical method for estimating the intensity of mixing at each site was to characterize the vertical stability of the water column (N^2) using the density difference ($\delta\rho/\delta z$) over a given depth range (Reynolds 1984):

$$(1) \qquad N^2 = (g/\rho)(\delta\rho/\delta z)$$

where g is the acceleration due to gravity (about 9.81 $m \cdot s^{-2}$ at 46°N), ρ is the water density (in kilograms per cubic metre), z is the thickness (metres) of the layer, and $\delta\rho$ is the variation of water density across this layer. Water stability (N^2) has the dimension of a frequency (per second squared); it is known as the Brunt–Väisälä frequency and represents one of the resonance modes of metalimnetic oscillations (Lemmin 1995). Vertical stability profiles were calculated from temperature profiles over the 5- to 15-m depth range using a parabolic approximation (Imboden et al. 1979). The surface layer (0–5 m) was excluded from the calculation to avoid problems of daily variation (Angeli et al. 1991).

As an additional environmental variable, fish biomass was obtained from an echosounding survey concomitant with the synoptic zooplankton sampling program. Fish biomass was estimated by echointegration (20 log R; see MacLennan and Simmons 1992) using a 70-kHz SIMRAD sounder (model EY-M with a circular transducer, 11° total beam angle at –3dB). Echointegration transects were obtained for contiguous 10-min sequences over 800 m. At each site, fish biomass was estimated from the original echointegration survey and averaged over two sequences: the one recorded just before arriving at a sampling site and the one just after the site. Fish biomass was evaluated over the whole water column in volts squared per square metre; this is proportional to the energy reflected by fish targets. During the spring, fish community

© 1999 NRC Canada

in Lake of Geneva is dominated by planktivorous fish, mainly adults of roach (*Rutilus rutilus*) and whitefish (*Coregonus laveratus*) (Gerdeaux and Guillard 1986).

Identification of crustacean zooplankton was carried out on a subsample of each formaldehyde-fixed sample. Small representative subsamples (containing 100–300 individuals of the species and instars to be counted, as far as feasible) were prepared by dividing the original samples zero to five times using a Motoda box (Motoda 1959), depending on zooplankton density. Zooplankton crustaceans were counted according to species and ontogenic stages (nauplii and copepodites C1 of cyclopoids, nauplii of calanoids, copepodites C1–C5 of the calanoid species, copepodites C2–C5 of each cyclopoid species, adults of each cyclopoid and calanoid species, adults and juveniles of cladocerans) under a stereoscopic dissection microscope. We referred to Dussart (1967, 1969) for taxonomic identification of the copepods and to Flossner (1972) and Amoros (1984) for cladocerans. Zooplankton taxa were also categorized by trophic groups: small herbivores (nauplii, C1–C3 of *Eudiaptomus gracilis* and cyclopoids, juvenile daphnids), large herbivores (C4, C5, and adults of *E. gracilis*, adult daphnids), and omnivores/carnivores (C4, C5, and adults of cyclopoids) (Gawler et al. 1988).

Statistical methods

Illustrations of whole-lake spatial distributions were obtained by mapping zooplankton abundances and environmental variables. Circles, whose area is proportional to the values to be represented, were plotted on maps of the lake (see Figs. 2 and 3).

Earlier observations conducted on the lake revealed that the small and great lakes have distinct thermal and nutrient regimes and different plankton distributions and seasonal dynamics (e.g., Balvay et al. 1984; Monod et al. 1984*a*, 1984*b*). This is supported by our observations (Fig. 2). Because most methods of spatial analysis require the data to be stationary over space (Cressie 1991), we decided to exclude the five sites of the small lake (sites 29–33, Fig. 1) from the following analyses.

The significance of spatial autocorrelation for individual variables was assessed using the Geary's c autocorrelation statistics in spatial correlograms (Geary 1954). The variables should be normalized prior to spatial autocorrelation analysis (Sokal 1979). The Box–Cox transformation was used for normalization, using the form that also induces homogeneity of variances (Sokal and Rohlf 1995). Geary's c coefficients were assembled in a correlogram for each taxon or variable (see Figs. 2 and 3). In each correlogram, we used distance classes with equal numbers of pairs so that even high distance classes would contain enough pairs to carry out tests of significance of the autocorrelation statistics (Legendre and Vaudor 1991; Legendre and Legendre 1998). Levels of significance were corrected to take multiple testing into account; for 10 simultaneous tests, we used 0.05/10 = 0.005 as the corrected significance level (Bonferroni correction). Once the overall correlogram is significant based on the Bonferroni test, the shape of the spatial correlogram can be used to infer underlying ecological process affecting variable spatial patterning. For the ecological interpretation of spatial correlograms, see Legendre and Fortin (1989), Dutilleul and Legendre (1993), and Legendre and Legendre (1998).

To identify the spatial structures displayed by the multivariate tables of environmental variables, abundances of crustacean taxa, and trophic groups, Mantel correlograms were computed as a function of geographical distances (Oden and Sokal 1986; Legendre and Legendre 1998). Gower's coefficient of similarity was used to quantify the ressemblance among sites based on the environmental variables, while the Steinhaus coefficient was used for the zooplankton data (Legendre and Legendre 1998). A test of significance is attached to each statistic in a Mantel correlogram, just as in a Geary's c autocorrelogram. All correlograms were computed using the R package of Legendre and Vaudor (1991).

Different methods have been proposed recently to assess the significance of the correlation between spatially autocorrelated variables (Clifford et al. 1989; Haining 1990, 1991; Dutilleul 1993; Dutilleul and Pinel-Alloul 1996). To determine the degrees of freedom of the t test statistic, Clifford et al. (1989) and Dutilleul (1993) used an estimated effective sample size, which is a function of the autocorrelation (in sign and magnitude) present in both variables. In this study, we used Dutilleul's modification and the Spearman coefficient to compute the correlations among the environmental variables and between the zooplankton taxa and the environmental variables. A rank transformation was applied to all variables to avoid problems stemming from the nonnormality of their distributions and from the restricted (i.e., monotonic) nonlinearity of their relationships. Autocorrelation in Dutilleul's correction was estimated by $(1 - c)$, with c the Geary's coefficient computed from the original (not rank transformed) data.

To evaluate the relative importance of the spatial and environmental factors on the distribution of zooplankton, the total variation of the zooplankton taxa or trophic group matrices was partitioned into four components following Borcard et al. (1992) and Borcard and Legendre (1994): (*i*) the nonspatially structured environmental component (fraction a), representing the local effects of the environmental factors, (*ii*) the spatially structured component of the zooplankton variation (fraction b) that is shared by the independent environmental variables, which represents, for instance, environmental gradients, (*iii*) the spatial component of the zooplankton variation (fraction c) that is not shared by the environmental variables included in the analysis, and (*iv*) fraction d of undetermined (nonspatial) variation. The variance in the distribution of the macrocrustaceans (species vectors) and trophic groups (trophic group vectors) was partitioned using redundancy analysis (RDA) and partial RDA constrained by the spatial and environmental variables. RDA and partial RDA were computed using version 3.11 of the CANOCO program (ter Braak 1988, 1990). The matrix of independent environmental variables contained water temperature, water stability, concentrations of PO_4, NO_3, NH_4, and chlorophyll *a*, bacteria, and fish biomass. We excluded the N/P ratio, which was strongly correlated with both PO_4 and NH_4, to avoid collinearity among the environmental variables (see Table 4). A forward selection procedure was applied to the environmental variables in each analysis.

Because the spatial patterns of the zooplankton distribution may be more complex than primary linear gradients, we used a geographic polynomial of the second degree, which better reflects the complexity of regional distributional patterns than linear gradients, as suggested by Legendre (1990):

$$(2) \qquad f(X,Y) = b_0 + b_1X + b_2Y + b_3X^2 + b_4XY + b_5Y^2$$

where X and Y are Cartesian longitude and latitude coordinates of the sampling sites centred on their respective means. In each analysis, a forward selection procedure was used to select the terms of eq. 2 that contributed significantly to the total explained variation of the response variables.

Results

Macrozooplankton community and environmental variables

Whole-lake spatial variation in the abundance of macrozooplankton species was important in Lake Geneva during the spring. Abundances of the crustacean species or stages varied by more than an order of magnitude across the lake, and coefficients of variation (%CV in Table 1) were higher than 50% (Table 1). The most abundant species were the calanoid *E. gracilis* (47% of total crustacean abundance) and

© 1999 NRC Canada

Table 1. Mean, standard error of the mean, and range of abundance (10^3 ind.·m^{-2}) of the total crustacean zooplankton, main species, and copepodite stages over the whole lake.

Zooplankton species	Stage	Mean	SE	Maximum	Minimum	% CV
Crustacean zooplankton		1562	812	3469	426	52
Eudiaptomus gracilis	Adults	256	136	662	78	53
	C5	161	98	432	24	61
	C4	110	64	310	21	58
	C1–C3	216	148	778	42	68
Cyclops vicinus	Adults	184	187	667	11	102
	C5	26	22	80	2	87
	C4	26	23	99	3	88
	C2 and C3	38	37	157	4	98
Cyclops prealpinus	Adults	18	15	58	0	84
	C5	19	16	69	0	86
	C4	28	20	99	2	73
	C2 and C3	116	95	438	4	82
Copepodite cyclopoids	C1	63	38	160	12	61
Nauplii	Calanoids	127	69	331	25	54
	Cyclopoids	164	92	349	41	56
Daphnia hyalina	Adults	14	12	59	2	84
	Juveniles	12	9	40	0	74

Note: C5, copepodite 5; C4, copepodite 4; C1–C3, copepodites 1, 2, and 3 pooled; C2 and C3, copepodite, 2 and 3 pooled; C1, copepodite 1.

Table 2. Mean, standard error of the mean, and range of values of the abiotic (physical and chemical) and biotic environmental variables used as independent variables.

Environmental variable	Mean	SE	Maximum	Minimum	% CV
Abiotic					
Water temperature (°C)	6.38	0.23	7.04	5.93	4
Water stability (s^{-2})	0.2	0.36	1.7	0.0	160
PO_4 ($\mu g \cdot L^{-1}$)	65	4.1	74	57	6
NO_3 ($\mu g \cdot L^{-1}$)	544	12.6	570	520	2
NH_4 ($\mu g \cdot L^{-1}$)	7.8	7.0	32	1	90
N/P	8.5	0.5	9.4	7.5	6
Biotic					
Chlorophyll *a* ($\mu g \cdot L^{-1}$)	1.6	0.5	3.3	0.8	32
Bacteria (10^6 cells·mL^{-1})	1.1	0.4	2.7	0.1	39
Fish biomass ($V \cdot m^{-2}$)	1548	2911	10 000	0	188

two cyclopoid species: *Cyclops vicinus* (17%) and *Cyclops prealpinus* (12%). Copepodites C1 of *C. prealpinus* and *C. vicinus*, which could not be separated easily, were grouped. C1 stages represented, on average, only 4% of the total abundance of crustaceans, whereas nauplii of calanoids and cyclopoids represented about 8 and 10%, respectively, of the total abundances. Among the cladocerans, *Daphnia hyalina* was the most important species but only represented 1.6% of the total crustaceans. Individuals of other species (*Daphnia galeata*, *Daphnia longispina*, *Bosmina longirostris*, and *Acanthocyclops robustus*) were too rare to be included in the analyses. *Bythotrephes longimanus* and *Leptodora kindtii*, both of which prey on zooplankton, were rare and encountered only as eggs and embryos during this spring sampling.

Information concerning the environmental variables are assembled in Table 2. Water was cold during the study period; temperature ranged from 5.9 to 7°C. Although the temperature of surface waters was sometimes higher in the stations of the small and lower great lakes, temperature profiles (Fig. 1) generally indicated higher temperature (>7°C) over the 0- to 25-m depth range in most stations of the upper great lake. The high concentrations of PO_4 and NO_3 (on average 65 and 544 $\mu g \cdot L^{-1}$, respectively) reflected the important spring nutrient loading from the drainage basin. PO_4, NO_3, and the N/P ratio were relatively invariable, with CV's under 6%. By contrast, stability of the 5–15 m water layer, as well as NH_4 concentrations, varied greatly among sites (CV > 90%). The biotic variables were moderately heterogeneous and showed low mean values: 1.6 µg chlorophyll $a \cdot L^{-1}$ and 1.1×10^6 bacteria·mL^{-1}. In contrast, fish biomass was very heterogeneous across the lake; it had the highest CV of all explanatory variables.

Mapping and spatial horizontal patterns

Fairly consistent spatial patterns were observed in the distributions of macrozooplankton, when expressed as percentages of maximum abundances (Fig. 2). The general trend was an accumulation of crustaceans along the northeastern shore of the upper great lake. The pelagic zone, particularly in the middle and lower great lakes, as well as the southeast-

© 1999 NRC Canada

Fig. 2. Distribution patterns of the crustacean species densities (left) and their respective autocorrelograms over the great lake (right). Vertical axis: Geary's *c* autocorrelation coefficients; horizontal axis: distances expressed as ranked classes and km (mean value of the distances in the class). Solid squares are values significant at $\alpha' = 0.005$, open squares with a small solid square inside are values significant at $\alpha = 0.05$, and white circles are nonsignificant values. Values of Geary's *c* coefficients between 0 and 1 indicate positive autocorrelation; values higher than 1 indicate negative autocorrelation.

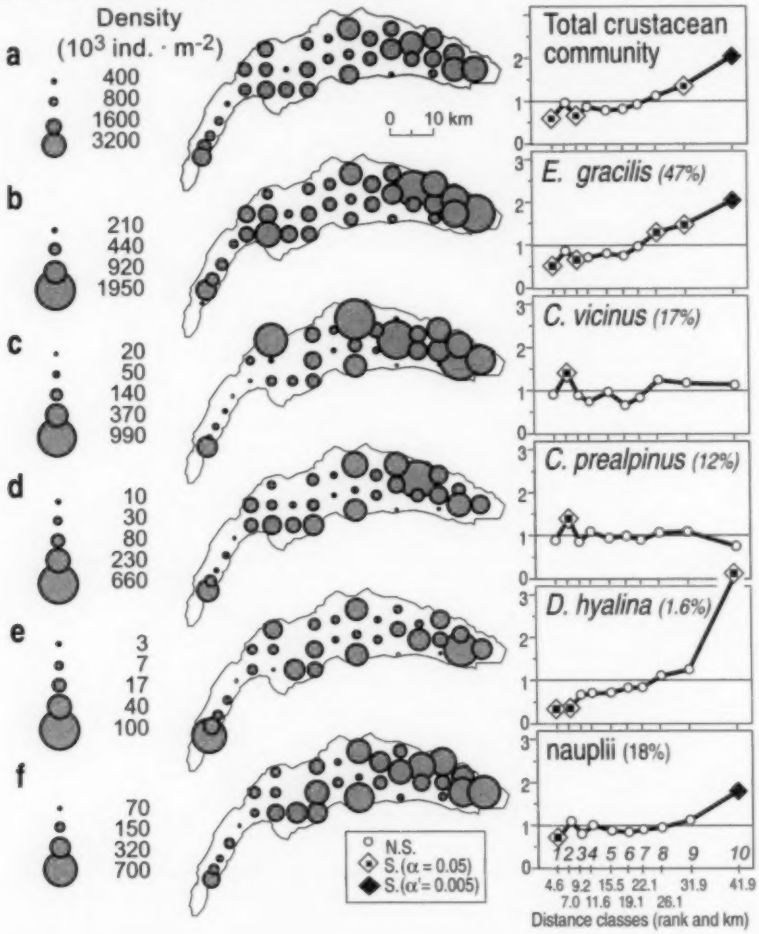

ern shore had low abundances. Abundances were low in the small lake, except at the last sampling site near Geneva.

Results of spatial autocorrelation analysis (Geary's *c* correlograms, Fig. 2) supported the impression of spatial gradients given by the maps (positive spatial autocorrelation at small distances following by negative spatial autocorrelation at large distances). Since data from the small lake were not included in the analyses, the correlograms only reflect the spatial distribution of macrozooplankton in the great lake. For total abundances of crustaceans and the abundances of *E. gracilis*, there was weak positive autocorrelation among neighbouring sites (distance classes 1–3: 4.6–9.2 km) and stronger negative autocorrelation at larger distances (classes 9 and 10: 31.9–41.9 km). Because *E. gracilis* accounted for most of the crustacean populations, the spatial distribution of *E. gracilis* in general (Fig. 2), and of its adults and C4 and C5 stages in particular (Table 3), was similar to that of the total abundance of macrozooplankton. The younger copepodite stages (C1–C3) and nauplii of calanoids also showed negative autocorrelation at large distances (Table 3). The abundances of *C. vicinus* appeared spatially independent, but the abundances of its C2 and C3 stages followed the same trend as the crustacean abundances with positive autocorrelation at intermediate (distance class 5: 15.5 km) and negative autocorrelation at large distances (distance class 10: 41.9 km) (Table 3). The correlogram of *C. prealpinus* reflected mostly the small-scale patchy distribution of its omnivorous/carnivorous older stages (adults and C4 and C5) at short distance (classes 2 and 3: 7.0 and 9.2 km) (Fig. 2; Table 3). The distribution of *D. hyalina* followed that of the crustacean community with weak small-scale and large-scale autocorrelation (Fig. 2; Table 3). The distribution of nauplii and C1 of cyclopoids followed a similar trend to that of the total crustaceans (Fig. 2; Table 3).

A glance at the maps (Fig. 3) reveals that most environmental variables presented a gradient-like distribution over

© 1999 NRC Canada

Table 3. Values of Geary's *c* statistic from autocorrelation analysis carried out on zooplankton instars and trophic groups.

Species and stages	Trophic group	Distance class									
		1	2	3	4	5	6	7	8	9	10
Eudiaptomus gracilis											
Adults and C4 and C5	Herbivores	0.51*	0.82	0.63*	0.67*	0.92	0.78	0.96	1.24*	1.54**	2.11**
Nauplii and C1–C3	Herbivores	0.67	1.01	0.81	0.79	0.71	0.63	0.91	1.28*	1.37	1.96*
Cyclops vicinus											
Adults and C4 and C5	Omnivores/ carnivores	1.03	0.92	0.72*	1.15	0.86	1.03	1.00	1.03	1.02	1.33
C2 and C3	Herbivores	0.71	0.89	0.87	0.87	0.62*	0.88	0.90	1.11	1.26	2.05*
Cyclops prealpinus											
Adults and C4 and C5	Omnivores/carnivores	0.76	1.62**	0.73*	1.13	1.15	0.86	0.91	1.11	0.81	0.87
C2 and C3	Herbivores	0.97	1.21	0.90	1.01	0.85	0.96	0.92	1.07	1.24	0.91
Cyclopoids											
Nauplii and C1	Herbivores	0.79	1.19	0.77	1.14	0.94	0.87	0.93	0.92	1.03	1.47*
Daphnia hyalina											
Adults	Herbivores	1.18	1.16	0.59*	1.01	0.98	1.02	0.94	1.04	0.95	1.23
Juveniles	Herbivores	1.08	0.83	0.61*	0.97	0.95	0.95	0.91	1.06	1.39*	1.38

Note: *Significantly different from 1 (no correction) at $\alpha = 0.05$; **significantly different from 1 at α' (Bonferroni correction) = 0.005.

the great lake. The autocorrelograms supported the hypothesis that the abiotic environmental variables were indeed distributed along a gradient in the great lake basin (for interpretation of correlograms, see Materials and methods and Legendre and Fortin 1989). The highest temperatures were observed in the upper great lake. Positive autocorrelation occurred at short distance (classes 1–3: 4.9–9.2 km) and negative autocorrelation at large distances (classes 8–10: 26.1–41.9 km). The spatial distribution of water stability values was similar to but weaker than that of temperature and NH_4 and the opposite of that of PO_4 and NO_3. The highest concentrations of NH_4 were measured in the upper great lake. The distributions of PO_4 and NO_3 concentrations formed strong inverse gradients with higher concentrations in the middle and lower great lakes (Fig. 3). These variables were positively autocorrelated at short distances (classes 1–5: 4.6–15.5 km) and negatively autocorrelated at large distances (classes 8–10: 26.1–41.9 km). The spatial distribution of the N/P ratio was inversely related to that of PO_4 and NO_3 concentrations and positively to that of NH_4 concentrations (Fig. 3).

The biotic variables have weaker spatial distributions than the abiotic variables (Fig. 3). Distribution patterns of chlorophyll *a* and bacteria show the presence of higher concentrations in the small lake and at the eastern end of the great lake. Values were positively autocorrelated at short distances (class 1: 4.6 km for chlorophyll *a*; classes 2 and 3: 7.0–9.2 km for bacteria) and negatively at large (class 9: 31.9 km for chlorophyll *a*) or intermediate distances (classes 5 and 7: 15.5 and 22.1 km for bacteria). The highest concentrations of chlorophyll *a* and bacteria were in the eastern end of the upper lake, an area that had lower concentrations of PO_4 and NO_3. The whole data set collected for fish biomass during the acoustic survey (Fig. 3, small map with black circles over the range of 0 – 20 000; modified from Gerdeaux and Guillard 1986) showed strong spatial heterogeneity with much lower fish biomass in the cooler part of the lower lake and, in most places, with very steep inshore–offshore gradients, except in a limited area of the middle lake where an opposite trend (higher fish biomass offshore than inshore) was observed. The map of the data set subsampled from the acoustic survey for the same sites as the abiotic and biotic variables (Fig. 3, small map with black circles over the range 0 – 10 000) only weakly reflects the inshore-offshore gradient of fish biomass. The values of Geary's *c*, obtained using site-specific fish biomass data, did not indicate autocorrelation (Fig. 3).

The Mantel correlograms give a composite view of the spatial heterogeneity of the environmental and macrozooplankton variables (Fig. 4). They show that the values of the environmental variables were generally positively correlated ($r > 0$) at short distance (classes 1–3: 4.6–9.2 km) and negatively correlated ($r < 0$) at larger distances (distance classes 8–10: 26.1–41.9 km). This supports the hypothesis that the environmental variables formed a smooth large-scale gradient over the great lake (50 km). By contrast, the species and trophic groups may have formed patches at short distances, but their distributions did not display significant large-scale spatial patterns (Fig. 4).

Most of the relationships suspected from mapping over the great lake were found to be statistically significant (Ta-

© 1999 NRC Canada

Fig. 3. Distribution patterns of values of the environmental variables (left) and their respective autocorrelograms over the great lake (right). See caption to Fig. 2 for a description of the correlograms. Two maps are presented for fish biomass: the small map corresponds to the whole acoustic survey and the large map shows the sites where other abiotic and biotic factors were measured.

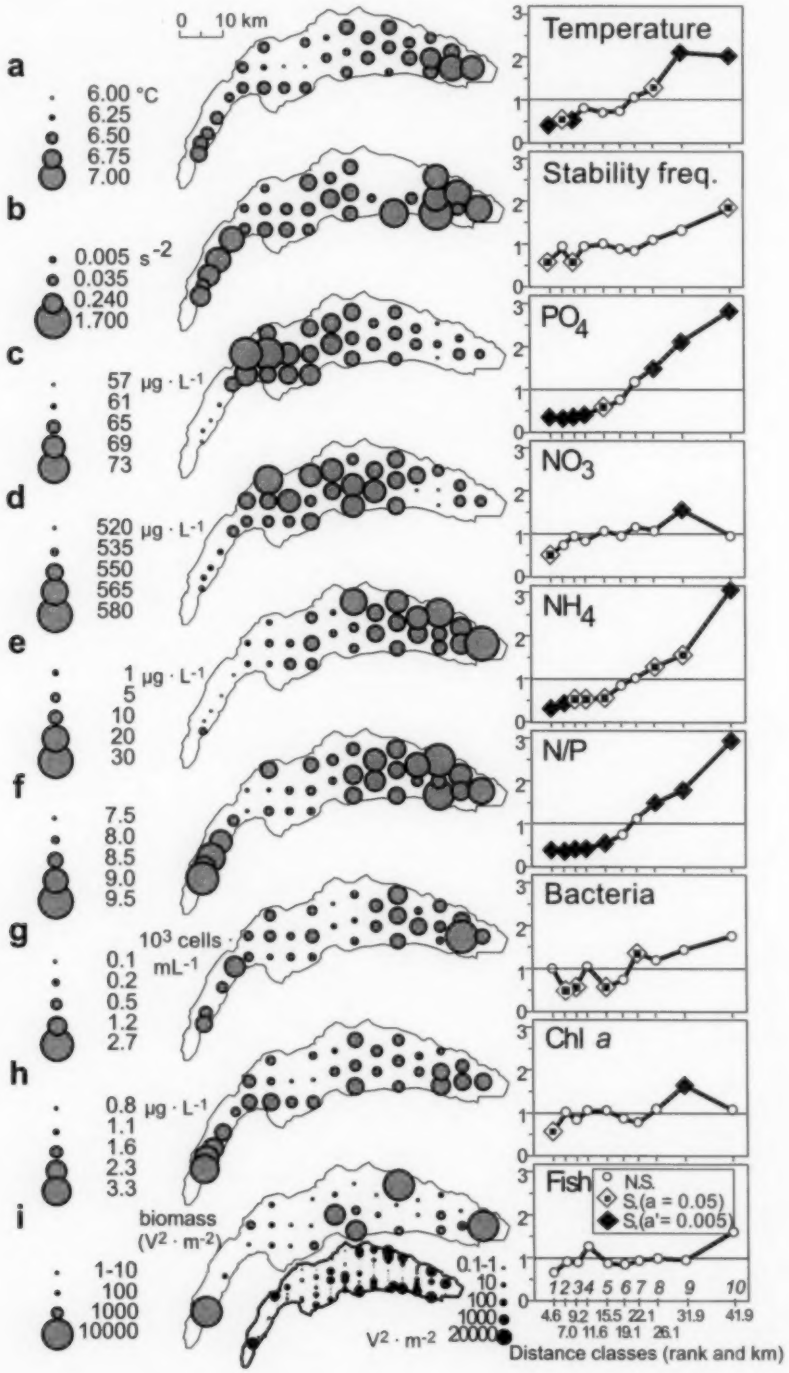

© 1999 NRC Canada

Fig. 4. Mantel correlograms for environmental variables (Env.), crustacean species (Sp.), and trophic groups (T.g.) based on their spatial distribution in the great lake. Vertical axis: values of Mantel's *r*; horizontal axis: distances expressed as ranked classes and km (mean value of the distances in the class). Solid circles circles are values significant at $\alpha' = 0.005$, open circles with a small solid circle inside are values significant at $\alpha = 0.05$, and small solid circles are nonsignificant values.

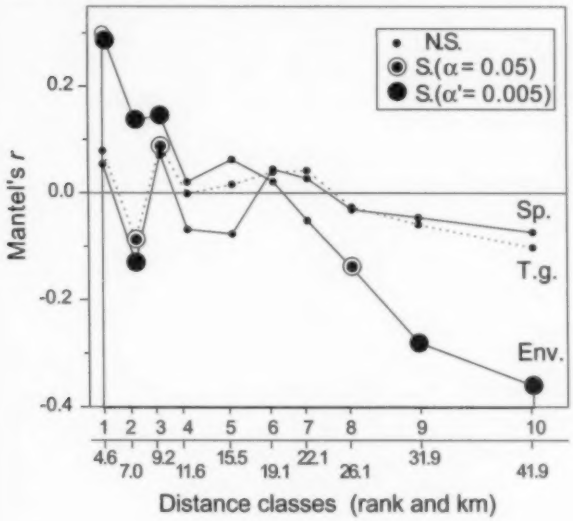

ble 4). No variable other than water temperature was linked, positively or negatively, to both the abiotic and biotic variables. Water temperature was positively correlated with NH_4 and chlorophyll *a* concentrations and negatively with PO_4 and NO_3. Water stability was inversely related to NO_3 concentrations. PO_4 showed a strong negative relationship with the N/P ratio and NH_4. Positive correlations with NH_4 were detected for water temperature, the N/P ratio, and bacteria, whereas a negative correlation occurred with PO_4. Chlorophyll *a* concentrations were positively related to water temperature and fish biomass and negatively to NO_3.

Abundances of total crustaceans, as well as most species and stages, were positively correlated with water temperature and NH_4 (Table 5). In addition, the total abundances of *C. prealpinus* and of its C2 and C3 stages were significantly correlated with chlorophyll *a* concentrations. *Cyclops vicinus* (adults, C4 and C5) were positively correlated with the N/P ratio and the abundances of bacteria. Several species (*C. vicinus*, *E. gracilis*, and *D. hyalina*) and their juvenile or copepodite stages were inversely correlated with PO_4 and (or) NO_3. No significant correlations were found between water stability or fish biomass and macrocrustaceans.

Variance partitioning

Results from RDA and partial RDA showed that local variations in the environment (fraction a: local environmental effects) and the environmental gradients (fraction b: spatially structured environment) explained 71% of the total variation in the distribution of total macrocrustacean abundances (Table 6). Together, NH_4 concentrations, water temperature, and water stability were the best explanatory variables of this distribution. Unexplained spatial effects (fraction c: space) were minor and explained less than 1% of the macrocrustacean distribution over the great lake. The relative importance of the local (fraction a) and spatially structured environmental components (fraction b) varied among species. The environmental components (fractions a and b) accounted for about 54% of the total variation in the abundances of *E. gracilis* and *C. prealpinus* and 29 and 38% of that of *C. vicinus* and *D. hyalina*, respectively (Table 6). The spatially structured environmental effects (fraction b) accounted for 60, 100, and 100% of the total explained variation (fractions a, b, and c) of *E. gracilis*, *C. prealpinus*, and *D. hyalina* abundances, respectively, while 60 and 43% of the explained variance (fractions a, b, and c) in the distribution of *C. vicinus* and nauplii abundances, respectively, could be attributable to the local environmental effects (fraction a). NH_4 was systematically selected during the forward selection of explanatory variables (in many cases, it was the only variable selected) and was responsible for 39–84% of the explained variation in any species vector. Additional environmental variables were occasionally retained: water temperature, water stability, and chlorophyll *a* concentrations. The best spatial variables retained to describe the distribution of the environmental factors were X and X^2, corresponding to a longitudinal (east–west) gradient. Relatively little spatial effects (fraction c: 0–11%) remained unexplained. The same can be said about the results for vectors of trophic groups (Table 7); the environmental components (fractions a and b) explained about 52–65% of the variation for the two herbivore vectors but only 43% of that of the omnivore/carnivore vector. Between 28 and 65% of the total variation in the distribution of species and trophic groups remained unexplained (Tables 6 and 7).

Discussion

Spatial patterns of environmental factors

The gradient-like distribution of the abiotic variables suggests the action of some underlying nonrandom process contributing to the large-scale spatial structuring of the abiotic environment in the great basin of Lake of Geneva during the spring of 1985. Although we did not study current patterns, we hypothetized that hydrodynamic processes induced by dominant northeasterly winds are prime candidates to explain the spatial heterogeneity in abiotic environmental factors during the spring in Lake of Geneva. In this lake, water circulation is complex, as it is influenced by wind-induced horizontal current, by several river inflows, and by superficial and deep currents flowing in opposite directions (Lemmin 1989). Water temperature and water stability were the highest in the upper part of the great lake (Fig. 3), an area surrounded by mountains. Wind speed patterns during the sampling survey and the previous day (Fig. 1) clearly indicated that the upper great lake was well sheltered from dominant winds. In the small lake and lower and middle great lakes, wind blew at 20 $m \cdot s^{-1}$ on the lake, whereas in the upper great lake, winds were stopped by the Jura Mountains and did not blow more than 2.5 $m \cdot s^{-1}$. Mountains in the Swiss Jura, which spread on the northeastern side of the lake, thus probably limited the mixing of the surface layer induced by the dominant northeasterly winds during the

© 1999 NRC Canada

Table 4. Values of correlation coefficients from modified *t* tests between the environmental variables used as independent variables in the canonical correlation analysis and path analysis models.

	Water stability	PO_4	NO_3	NH_4	N/P	Chlorophyll *a*	Bacteria	Fish
Water temperature	0.21	–0.65*	–0.59*	0.63**	0.50	0.71**	0.41	0.18
Water stability		–0.34	–0.45*	0.15	0.19	0.34	–0.08	0.29
PO_4			0.41	–0.74*	–0.90*	–0.30	–0.38	–0.09
NO_3				–0.42	–0.08	–0.44*	–0.27	0.09
NH_4					0.72*	0.17	0.52*	–0.03
N/P						0.20	0.29	0.14
Chlorophyll *a*							0.05	0.45**
Bacteria								–0.04

Note: Significance: *p = 0.05; **p = 0.01.

Table 5. Values of correlation coefficients from modified *t* tests between the environmental variables and the zooplanktonic variables.

	Environmental variable								
Zooplankton variable	Water temperature	Water stability	PO_4	NO_3	NH_4	N/P	Chlorophyll *a*	Bacteria	Fish
Crustacean zooplankton	0.58*	0.01	–0.41	–0.40	0.61*	0.34	0.33	0.32	–0.07
Eudiaptomus gracilis	0.64**	–0.03	–0.40	–0.50*	0.62*	0.31	0.28	0.34	–0.09
Adults and C4 and C5	0.55*	0.08	–0.40*	–0.54*	0.61*	0.29	0.23	0.30	–0.16
Nauplii and C1–C3	0.56**	–0.15	–0.31	–0.33	0.56*	0.30	0.35	0.26	–0.09
Cyclops vicinus	0.44**	0.01	–0.50*	–0.18	0.56*	0.45*	0.17	0.26	–0.14
Adults and C4 and C5	0.47**	0.07	–0.45*	–0.17	0.52*	0.39*	0.19	0.40*	–0.15
C2 and C3	0.20	–0.11	0.00	0.07	0.06	–0.02	0.19	–0.06	0.02
Cyclops prealpinus	0.55**	–0.15	–0.20	–0.29	0.50*	0.17	0.41*	0.19	0.04
Adults and C4 and C5	0.35	–0.08	–0.21	–0.26	0.34	0.12	0.15	0.15	–0.21
C2 and C3	0.55**	–0.17	–0.19	–0.31	0.51*	0.15	0.45*	0.19	0.11
Cyclopoid nauplii and C1	0.51**	–0.03	–0.38*	–0.33*	0.61**	0.33	0.29	0.33	–0.08
Total nauplii	0.52**	0.06	–0.41	–0.36*	0.63*	0.36	0.27	0.31	–0.07
Daphnia hyalina	0.41*	0.11	–0.17	–0.38*	0.30	0.03	0.31	0.25	–0.11
Adults	0.31*	0.00	–0.08	–0.34*	0.23	–0.03	0.22	0.16	–0.14
Juveniles	0.53*	0.21	–0.25	–0.38*	0.39*	0.13	0.32	0.30	–0.08

Note: Significance: *p = 0.05; **p = 0.01.

spring season (Lemmin 1989; Angeli et al. 1991). The complex patterns of water circulation, in conjunction with the presence of mountains, may also have contributed to the observed distribution patterns in the case of NH_4, chlorophyll *a*, and bacteria that also were more concentrated in the warmer and more stable waters at the northeastern end of the great lake.

Spatial distribution patterns of macrozooplankton

The distribution of crustaceans in Lake of Geneva showed considerable horizontal variability during spring. Most species and taxa formed large-scale spatial patterns, as observed in several other large lakes (Malone and McQueen 1983; Patalas and Salki 1992; Pinel-Alloul 1995; Stockwell and Sprules 1995). These large-scale patterns may be generated by a variety of vectorial and stochastic-vectorial processes such as currents and upwelling events and by physicochemical alterations caused by river inflows. In Lake of Geneva, the general spatial pattern indicated a greater accumulation of macrozooplankton along the northeastern shore and the upper-lake end of the great lake, which are inflow areas of two major rivers: the Rhône and the Veveyse. Aggregations were also localized in the vicinity of the Venoge and Aubonne inflows, on the north shore, and the Dranse inflow on the south shore (Figs. 1 and 2). The aggregation of macrozooplankton along the northeastern shore of the great lake (Fig. 2) may also be attributed to downwind accumulation due to horizontal advection in this sheltered area. During the spring season, wind speed generally varied from 7.2 $km \cdot h^{-1}$ (2 $m \cdot s^{-1}$) in sheltered areas to 54 $km \cdot h^{-1}$ (15 $m \cdot s^{-1}$) in exposed areas (Angeli et al. 1991). Variations in wind intensities between sheltered and exposed areas may have strongly influenced zooplankton distribution in Lake of Geneva. It is recognized that winds and wind-induced currents can break down the spatial structure of plankton. Horizontal advection and redistribution of plankton (Fig. 2) or a downwind accumulation of chlorophyll *a* (Fig. 3), such as observed in Lake Geneva, may then ensue (Stauffer 1982; Teraguchi et al. 1983; Jones et al. 1995; Lacroix and Lescher-Moutoué 1995).

In Lake of Geneva, despite apparent similarities in the distributions of the different zooplankton taxa (Fig. 2), re-

© 1999 NRC Canada

Table 6. Results of RDA and partial RDA on taxonomic vectors of total abundances constrained by matrices of environmental and spatial variables.

Vector	Environmental variables retained by forward selection	% of variance explained by environmental variables	Spatial variables retained by forward selection	% of variance explained by spatial variables	% of variance explained by each fraction
Crustacean zooplankton	NH_4	80**	X	60**	a: 41.7
	Water temperature	1*			b: 29.6
	Water stability	1*			c: 0.3
					d: 28.4
Eudiaptomus gracilis	NH_4	84**	X	53**	a: 14.9
			X^2	20*	b: 39.3
					c: 11.1
					d: 34.7
Cyclops vicinus	Water temperature	49**	X	52*	a: 21.0
					b: 8.2
					c: 5.8
					d: 65.0
Cyclops prealpinus	Water stability	34**	None		a: 0
	NH_4	39**			b: 54.3
	Chlorophyll *a*	19*			c: 0
					d: 45.7
Daphnia hyalina	Water temperature	69**	None		a: 0
					b: 37.6
					c: 0
					d: 62.4
Nauplii	NH_4	78**	Y	78*	a: 21.0
					b: 24.4
					c: 3.0
					d: 51.6

Note: Significance: *p = 0.05; **p = 0.01. X, longitude; Y, latitude. The percent variance explained was calculated by dividing the proportion of variance within a vector explained by each individual variable by the total variance explained by each set (either environmental or spatial) of factors. Factor: a, nonspatially structured environmental component (local effects); b, spatially structured component (gradient effects); c, residual spatial component; d, undetermined (nonspatial) variation.

Table 7. Results of RDA and partial RDA on vector of total abundances of trophic groups that were constrained by matrices of environmental and spatial variables.

Vector	Environmental variables retained by forward selection	% of variance explained by environmental variables	Spatial variables retained by forward selection	% of variance explained by spatial variables	% of variance explained by each fraction
Young herbivores[a]	NH_4	67**	X	57*	a: 45.5
	Water stability	16*			b: 20.3
	Chlorophyll *a*	15*			c: 0.1
					d: 34.1
Older herbivores[b]	NH_4	78**	X	47**	a: 12.8
			X^2	22*	b: 39.3
			Y^2	19*	c: 12.9
					d: 35.0
Omnivores/carnivores[c]	NH_4	80**	X	60**	a: 10.9
			X^2	25*	b: 32.2
					c: 2.0
					d: 54.9

Note: Significance: *p = 0.05; **p = 0.01. Abbreviations, calculations of percent variance, and factors explained in Table 6.
[a]Sum of abundances of *E. gracilis* C1–C3, nauplii, *Cyclops* spp. C1–C3, and *D. hyalina* juneviles.
[b]Sum of abundances of *E. gracilis* adults, C4, and C5 and *D. hyalina* adults.
[c]Sum of abundances of *Cyclops* spp. adults, C5, and C4.

© 1999 NRC Canada

sults from autocorrelation analyses (Table 3) suggested that spatial patterns varied among crustacean species and trophic groups, as already observed in small lakes. According to Malone and McQueen (1983), horizontal patchiness varies among zooplankton populations; diaptomids tend to form large-scale distribution patterns (type I: >1 km), whereas cyclopoids exhibit small-scale patterns (type II: 10–1000 m). In our study, the herbivorous *E. gracilis*, *D. hyalina*, and the nauplii presented a gradient-like pattern oriented southwest to northeast in the great lake. By contrast, the omnivorous/carnivorous *C. vicinus* and *C. prealpinus* presented a more patchy distribution. In Lake Créteil, a small shallow sandpit lake in France, cladocerans and calanoids also had similar lake-wide spatial distributions, which were different from the less structured distributions of cyclopoids (Lacroix and Lescher-Moutoué 1995).

Environmental control of the spatial distribution of macrozooplankton

During spring, the spatial distribution of crustacean zooplankton in Lake of Geneva was mainly driven by abiotic variables (Tables 6 and 7). The distribution of the macrozooplankton was related mostly to water temperature, water stability, and NH_4. The distribution of cyclopoids was also related to chlorophyll *a* biomass and bacteria abundances. Knowing that water temperature and NH_4 concentrations were strongly correlated (Table 4), then temperature may be a proximal control variable for macrozooplankton abundances during spring in Lake of Geneva, as suggested by Gawler et al. (1988) and Sommer (1989) for alpine lakes. The direct influence of water temperature could have been through temperature-dependent metabolism and development of zooplankton (Kersting 1978; McLaren and Corkett 1981). In large lakes, temperature and climate are thought to be the proximate factors controlling zooplankton abundances during spring and summer (Patalas 1969; Patalas and Salki 1992; Stockwell and Sprules 1995). If the overall distribution of macrozooplankton was correlated with water temperature, the distribution of each species and trophic group responded in different ways. The effect of water temperature was overall stronger on calanoids (*E. gracilis*) than on cyclopoids and daphnids (Table 5). This difference in crustacean responses to temperature may be due to the different thermal requirements of the various taxa. Munro (1974) observed that postembryonic development of *E. gracilis* was strongly temperature dependent, whereas *C. vicinus*, a cold-water species (Maier 1989), was more temperature independent and maintained high growth rates at low temperatures.

Water stability also appeared to have some influence on the distribution of crustaceans, more particularly that of *C. prealpinus* and young herbivores (Tables 6 and 7). Water stability may have kept phytoplankton in the upper warm and lighted water layers by reducing vertical mixing and enhanced the growth of phytoplankton. These different processes may explain why concentrations of PO_4 and NO_3, which are nutrients essential to phytoplankton growth, were low where values of water stability, water temperature, and chlorophyll *a* concentrations were high (Fig. 3; Table 4). The simultaneous development of the spring phytoplankton bloom and marked decreases in PO_4 and NO_3 concentrations is commonly observed in Lake of Geneva (Balvay et al. 1985). Young herbivores may have concentrated in locations where phytoplankton was abundant, whereas older herbivores may be less dependent on phytoplankton resources.

NH_4 concentrations seem to be a good indicator of macrozooplankton aggregation during spring in Lake of Geneva. The proportion of variation explained by NH_4 was always high for the different species and trophic groups (Tables 6 and 7). The high correlation values (range of significant values 0.39–0.63 in Table 5) between zooplankton abundances and NH_4 concentrations may be explained by higher excretion of NH_4 in the northeastern great lake where macrozooplankton concentrated (Esjmont-Karabin 1985). When NH_4 was excluded from the RDA for the crustacean zooplankton, *E. gracilis*, and older herbivores vectors, there were no additional explanatory variables selected, except for water temperature and (or) water stability, and the total explained variation decreased by 14–40%.

The concentration of chlorophyll *a* appeared to be positively related to the distribution of the C2 and C3 stages of *C. prealpinus* but not to that of the true herbivores *E. gracilis* and *D. hyalina* (Tables 5 and 6). It may be that the distribution of both phytoplankton and *C. prealpinus* C2 and C3 stages may have been influenced similarly, for example, by wind-induced water currents, whereas other stages were unaffected or affected differently by wind, as shown by Teraguchi et al. (1983) in a freshwater pond. Furthermore, it is unclear how the abundances of older *C. vicinus* (Table 5) and those of bacteria were linked. The relationship could have been indirect if, for example, the abundances of bacteria reflected the mineralization of fecal matter excreted by copepods, as suggested by the high positive correlation between bacterial abundances and NH_4 concentrations.

Fish planktivory is the most likely factor to explain offshore–inshore spatial patterns of zooplankton distribution in large and small lakes (Johannsson et al. 1991; Lacroix and Lescher-Moutoué 1995). In contrast, the absence of relationships between fish biomass and macrozooplankton variables in Lake of Geneva may suggest that fish predation does not affect to any great extent the spatial distribution of crustacean zooplankton during the spring in this large lake. This seems to concur with observations that, at the time of sampling, predation by *R. rutilus*, the dominant species in Lake of Geneva, was probably at its lowest because *R. rutilus* reproduces during spring and may have been less concerned with feeding than reproducing. Furthermore, in mid-April, aquatic insects (mainly Ephemeroptera) have an important contribution to the diet of planktivorous fish (Ponton and Gerdeaux 1988). Another explanation may be that fish and macrozooplankton were sampled at different scales. Macrozooplankton was sampled over a grid at 3- to 5-km intervals, whereas fish biomass was estimated by echosounding in a succession of contiguous 10-min sequences across an 800-m transect.

The unexplained spatial variation (fraction c in Tables 6 and 7) was relatively small (less than 5.8%), except for the vectors *E. gracilis* and older herbivores (less than 10%). This spatial component (Borcard and Legendre 1994; Legendre and Legendre 1998), which is due to spatially structured environmental variables or biotic factors that were not measured in this study, had little influence. Thus, we can

© 1999 NRC Canada

conclude that the large-scale longitudinal gradient of water temperature, water stability, and NH_4 and the local small-scale changes in chlorophyll *a* (fractions a and b) were the most important factors related to the macrozooplankton distribution in Lake of Geneva during the spring. However, the undetermined variation (fraction d in Tables 6 and 7) remained relatively high (28–65%) and reflects the influence of nonspatially structured (at the sampling scale) environmental factors that were not assessed during our study. For instance, small-scale spatial structures of the biotic variables at a smaller scale may also influence the distribution of zooplankton. A weaker distribution pattern was common to chlorophyll *a*, bacteria, cyclopoids, and nauplii as well as fish biomass, which indicates the existence of spatial structures at scales smaller than the scale (3- to 5-km intervals) that we considered in this study.

Acknowledgements

This research project is part of collaborative program between the GRIL and the Station d'Hydrobiologie lacustre de Thonon-les-Bains. We acknowledge the assistance of French scientist fellows, J.-P. Pelletier for sample collection and pigment analysis, Ph. Dufour for bacteria data, and P. Blanc for chemical analysis. We also are thankful to T. Niyonsenga and G. Méthot for help with the CANOCO program, D.M. Imboden for communicating the program to calculate water stability, and G. Chapuis and J. Barraud for the preparation of the zooplankton subsamples. This work was supported by the Office franco-québécois pour la jeunesse (OFQJ) (travel fund to C. Guay), the Program of France–Québec international cooperation, and NSERC and FCAR team grants to B. Pinel-Alloul.

References

Amoros, C. 1984. Crustacés cladocères. Bull. Soc. Linn. Lyon, **3**: 72–107; **4**: 120–144.

Angeli, A., Dufour, P., Gerdeaux, D., Guillard, J., and Pelletier, J.-P. 1991. Variabilité horizontale des sels nutritifs et des biomasses planctoniques dans le Léman: incidence de la bise en période de faible stabilité. *In* Hommage à F.-A. Forel: Troisième conférence internationale des limnologues d'expression française, Morges, Switzerland. *Edited by* J.-P. Vernet. Forel Institut, Morges, Switzerland. pp. 219–222.

Angeli, N., Pinel-Alloul, B., Balvay, G., and Ménard, I. 1995. Diel patterns of feeding and vertical migration in daphnids and diaptomids during the clear water phase in Lake Geneva (France). Hydrobiologia, **300/301**: 163–184.

Balvay, G., Druard, J.-C., Pelletier, J., Pongratz, E., and Revaclier, R. 1984. Plancton. *In* Le Léman: synthèse 1957–1982. Commission internationale pour la protection des eaux du Léman contre la pollution (CIPEL), Lausanne, Switzerland. pp. 261–303.

Balvay, G., Druart, J.-C., Pelletier, J.-P., and Revaclier, R. 1985. Évolution du plancton du Léman. *In* Rapports sur les études et recherches entreprises dans le bassin lémanique. Commission internationale pour la protection des eaux du Léman contre la pollution (CIPEL), Lausanne, Switzerland. pp. 49–71.

Bell, G., Lechowicz, M.J., Appenzeller, A., Chandler, M., DeBlois, E., Jackson, L., Mackensie, B., Preziosi, R., Shallenberg, M., and Tinker, N. 1993. The spatial structure of the physical environment. Oecologia, **96**: 114–121.

Betsill, R.K., and van den Avyle, M. 1994. Spatial heterogeneity of reservoir zooplankton: a matter of timing? Hydrobiologia, **277**: 63–70.

Borcard, D., and Legendre, P. 1994. Environmental control and spatial structure in ecological communities: an example using oribatid mites (Acari, Oribatei). Environ. Ecol. Stat. **1**: 37–53.

Borcard, D., Legendre, P., and Drapeau, P. 1992. Partialling out the spatial component of ecological variation. Ecology, **73**: 1045–1055.

Carpenter, S. (*Editor*). 1988. Complex interactions in lake communities. Springer-Verlag, Berlin.

Carpenter, S.R., and Kitchell, J.F. 1993. The trophic cascade in lakes. Cambridge Studies in Ecology. Cambridge University Press, Cambridge, U.K.

Clifford, P., Richardson, S., and Hémon, D. 1989. Assessing the significance of the correlation between two spatial processes. Biometrics, **45**: 123–134.

Cressie, N.A.C. 1991. Statistics for spatial data. Wiley, New York.

De Meester, L., Maas, S., Dierckens, K., and Dumont, H.J. 1993. Habitat selection and patchiness in *Scapholeberis*: horizontal distribution and migration of *S. mucronata* in a small pond. J. Plankton Res. **15**: 1129–1139.

Dussart, B. 1967. Les copépodes des eaux continentales d'Europe occidentale. Tome I: Calanoïdes et harpacticoïdes. Boubée, Paris.

Dussart, B. 1969. Les copépodes des eaux continentales d'Europe occidentale. Tome II: Cyclopoïdes et biologie. Boubée, Paris.

Dutilleul, P. 1993. Modifying the *t* test for assessing the correlation between two spatial processes. Biometrics, **49**: 305–314.

Dutilleul, P., and Legendre, P. 1993. Spatial heterogeneity against heteroscedasticity: an ecological paradigm versus a statistical concept. Oikos, **66**: 152–171.

Dutilleul, P., and Pinel-Alloul, B. 1996. A doubly multivariate model for statistical analysis of spatio-temporal environmental data. Environmetrics, **7**: 551–566.

Ejsmont-Karabin, J. 1985. Phosphorus and nitrogen excretion by lake zooplankton (rotifers and crustaceans) in relationship to individual body weights of the animals, ambient temperature and presence or absence of food. Ekol. Pol. **32**: 3–42.

Flossner, D. 1972. Krebstiere, Crustacea. Kiemen und Blattfusser, Branchiopoda, Fischlause, Branchiura. Die teirwelt Deutschlands, **60**.

Gawler, M., Blanc, P., Druart, J.-C., and Pelletier, J.-P. 1986. Dynamique de quelques populations majeures du phytoplancton printanier du lac Léman en relation avec le broutage et les sels nutritifs. Colloq. Natl. CNRS Biol. Popul., Lyon, 4–6 septembre 1986. Université Claude Bernard, Lyon, France. pp. 412–419.

Gawler, M., Balvay, G., Blanc, P., Druart, J.-C., and Pelletier, J.-P. 1988. Plankton ecology of Lake Geneva: a test of the PEG-model. Arch. Hydrobiol. **114**: 161–174.

Geary, R.C. 1954. The contiguity ratio and statistical mapping. Incorp. Stat. **5**: 115–145.

Gerdeaux, D., and Guillard, J. 1986. Approche des structures spatio-temporelles des populations de poissons du Léman. Colloq. Natl. CNRS Biol. Popul., Lyon, 4–6 septembre 1986. Université Claude Bernard, Lyon, France. pp. 420–426.

Haining, R. 1990. Spatial data analysis in the social and environmental sciences. Cambridge University Press, Cambridge, U.K.

Haining, R. 1991. Bivariate correlation with spatial data. Geogr. Anal. **23**: 210–229.

Hart, R.C. 1990. Zooplankton distribution in relation to turbidity and related environmental gradients in a large subtropical reservoir: patterns and implications. Freshwater Biol. **24**: 241–263.

Hastings, A. 1990. Spatial heterogeneity and ecological models. Ecology, **71**: 426–428.

© 1999 NRC Canada

Hobbie, J.E., Daley, R.J., and Jasper, S. 1977. Use of nuclepore filters for counting bacteria by fluorescence microscopy. Appl. Environ. Microbiol. **33**: 1225–1228.

Holopainen, A.-L., Huovinen, P., and Huffunen, P. 1993. Horizontal distribution of phytoplankton in two large lakes in eastern Finland. Verh. Int. Ver. Limnol. **25**: 557–562.

Imboden, D.M., Eid, B.S.F., Toller, T., Schurter, M., and Wetzel, J. 1979. MELIMEX, an experimental heavy metal pollution study: vertical mixing in a large limno-corral. Schweiz. Z. Hydrol. **41**: 177–183.

Johannsson, O.E., Mills, E.L., and O'Gorman, R. 1991. Changes in the nearshore and offshore zooplankton communities in Lake Ontario: 1981–88. Can. J. Fish. Aquat. Sci. **48**: 1546–1557.

Jones, R.I., Fulcher, A.S., Jayakody, J.K.U., Laybourn-Parry, J., Shine, A.J., Watson, M.C., and Young, J.M. 1995. The horizontal distribution of plankton in a deep oligotrophic lake — Loch Ness, Scotland. Freshwater Biol. **33**: 161–170.

Kersting, K. 1978. The growth efficiency of *Daphnia magna*. II. The effect of temperature. Hydrobiol. Bull. **12**: 99–106.

Koroleff, F. 1970. Direct determination of ammonia in natural waters as indophenol blue. Information on techniques and methods for seawater analysis. ICES Interlab. Rep. No. 3. pp. 19–22.

Lacroix, G., and Lescher-Moutoué, F. 1995. Spatial patterns of planktonic microcrustaceans in a small shallow lake. Hydrobiologia, **300/301**: 205–217.

Legendre, P. 1990. Quantitative methods and biogeographic analysis. *In* Evolutionary biogeography of the marine algae of the North Atlantic. *Edited by* D.J. Garbary and R.G. South. NATO ASI Series. Vol. G 22. Springer-Verlag, Berlin.

Legendre, P. 1993. Spatial autocorrelation: trouble or new paradigm? Ecology, **74**: 1659–1673.

Legendre, P., and Fortin, M.-J. 1989. Spatial pattern and ecological analysis. Vegetatio, **80**: 107–138.

Legendre, P., and Legendre, L. 1998. Numerical ecology. 2nd English ed. Elsevier Science BV, Amsterdam, The Netherlands.

Legendre, P., and Vaudor, A. 1991. The R package: multidimensional analysis, spatial analysis. Département de sciences biologiques, Université de Montréal, Montréal, Qué.

Lemmin, U. 1989. Dynamics of horizontal turbulent mixing in a nearshore zone of Lake of Geneva. Limnol. Oceanogr. **34**: 420–434.

Lemmin, U. 1995. Limnologie physique. Chap. 2. *In* Limnologie générale. Collect. Écol. 25. *Edited by* R. Pourriot and M. Meybeck. Masson, Paris. pp. 60–114.

MacLennan, D.N., and Simmons, E.J. 1992. Fisheries acoustics. Chapman and Hall, London, U.K.

Maier, G. 1989. The effect of temperature on the development times of eggs, naupliar and copepodite stages of five species of cyclopoid copepods. Hydrobiologia, **184**: 79–88.

Malone, B.J., and McQueen, D.J. 1983. Horizontal patchiness in zooplankton populations of two Ontario kettle lakes. Hydrobiologia, **99**: 101–124.

Mazumder, A., McQueen, D.J., Taylor, W.D., and Lean, D.R.S. 1988. Effects of fertilization and planktivorous fish (yellow perch) predation on size distribution of particulate phosphorus and assimilated phosphate: large enclosure experiments. Limnol. Oceanogr. **33**: 421–430.

McLaren, I.A., and Corkett, C.J. 1981. Temperature-dependent growth and production by a marine copepod. Can. J. Fish. Aquat. Sci. **38**: 77–83.

McQueen, D.J., Post, J.R., and Mills, E.L. 1986. Trophic relations in freshwater pelagic ecosystems. Can. J. Fish. Aquat. Sci. **43**: 1571–1581.

Megard, R.O., Kuns, M.M., Whiteside, M.C., and Downing, J.A. 1997. Spatial distribution of zooplankton during coastal upwelling in western Lake Superior. Limnol. Oceanogr. **42**: 827–840.

Monod, R., Blanc, P., and Corvi, C. 1984*a*. Le régime thermique du Léman. *In* Le Léman: synthèse 1957–1982. Commission internationale pour la protection des eaux du Léman contre la pollution (CIPEL), Lausanne, Switzerland. pp. 75–88.

Monod R., Blanc, P., Corvi, C., and Revaclier, R. 1984*b*. Évolution physico-chimique. *In* Le Léman: synthèse 1957–1982. Commission internationale pour la protection des eaux du Léman contre la pollution (CIPEL), Lausanne, Switzerland. pp. 89–226.

Motoda, S. 1959. Devices of simple plankton apparatus. Mem. Fac. Fish. Hokkaido Univ. **7**: 73–94.

Munro, I.G. 1974. The effect of temperature on the development of egg, naupliar and copepodite stages of two species of copepods, *Cyclops vicinus* Uljanin and *Eudiaptomus gracilis* Sars. Oecologia, **16**: 355–367.

Murphy, J., and Riley, J.P. 1962. A modified single solution method for the determination of phosphate in natural waters. Anal. Chim. Acta, **27**: 31–36.

Northcote, T.G. 1988. Fish in the structure and function of freshwater ecosystems: a "top-down" view. Can. J. Fish. Aquat. Sci. **45**: 361–379.

Oden, N.L., and Sokal, R.R. 1986. Directional autocorrelation: an extension of spatial correlograms to two dimensions. Syst. Zool. **35**: 608–617.

Patalas, K. 1969. Composition and horizontal distribution of crustacean plankton in Lake Ontario. J. Fish. Res. Board Can. **26**: 2135–2164.

Patalas, K., and Salki, A. 1992. Crustacean plankton in Lake Winnipeg: variation in space and time as a function of lake morphometry, geology, and climate. Can. J. Fish. Aquat. Sci. **49**: 1035–1059.

Pelletier, J., and Blanc, P. 1991. Sensibilité des lacs aux facteurs climatiques et anthropiques. Exemple d'un grand lac, le Léman. Océanis, **17**: 517–529.

Pinel-Alloul, B. 1995. Spatial heterogeneity as a multiscale chartacteristic of zooplankton community. Hydrobiologia, **300/301**: 17–42.

Pinel-Alloul, B., and Pont, D. 1991. Spatial distribution patterns in freshwater macrozooplankton: variation with sampling scales. Can. J. Zool. **69**: 1557–1570.

Pinel-Alloul, B., Downing, J.A., Pérusse, M., and Codin-Blumer, G. 1988. Spatial heterogeneity in freshwater zooplankton: systematic variation with body-size, depth and sampling scale. Ecology, **69**: 1393–1400.

Pinel-Alloul, B., Méthot, G., Verreault, G., and Vigneault, Y. 1990. Zooplankton species associations in Quebec lakes: variation with abiotic factors, including natural and anthropogenic acidification. Can. J. Fish. Aquat. Sci. **47**: 110–121.

Pinel-Alloul, B., Niyonsenga, T., and Legendre, P. 1995. Spatial and environmental components of freshwater zooplankton structure. Ecoscience, **2**: 1–19.

Ponton, D., and Gerdeaux, D. 1988. Quelques aspects de l'alimentation de deux poissons planctonophages du Lac Léman: le corégone (*Coregonus schinzii palea*) et le gardon (*Rutilus rutilus* L.) Bull. Fr. Piscic. **308**: 11–23.

Pourriot, R., Tifnouti, A., and Rougier, R. 1994. Répartition spatiale du zooplancton estival dans un lac de barrage: le Lalla Takerkoust (Maroc). Arch. Hydrobiol. **130**: 113–127.

Reynolds, C.S. 1984. The ecology of freshwater phytoplankton. Cambridge University Press, Cambridge, U.K.

Sokal, R.R. 1979. Ecological parameters inferred from spatial correlograms. *In* Contemporary quantitative ecology and related

© 1999 NRC Canada

ecometrics. *Edited by* G.P. Patil and M.L. Rosenzweig. Statistical Ecology Series. Vol. 12. International Co-operative Publ. House, Fairland, Md. pp. 167–196.

Sokal, R.R., and Rohlf, F.J. 1995. Biometry — the principles and practice of statistics in biological research. 3rd ed. W.H. Freeman, New York.

Sommer, U. 1989. Plankton ecology: succession in plankton communities. Brock/Springer Series in Contemporary Bioscience. Springler-Verlag, Berlin.

Stauffer, R.E. 1982. Wind stress effects on chlorophyll distribution in stratified eutrophic lakes. Limnol. Oceanogr. **27**: 66–74.

Stockwell, J.D., and Sprules, W.G. 1995. Spatial and temporal patterns of zooplankton biomass in Lake Erie. ICES J. Mar. Sci. **52**: 557–564.

Teraguchi, M., Stucke, D.E., and Noga, M.M. 1983. Spatial dynamics of *Mesocyclops edax* (S.A. Forbes), *Tropocyclops prasinus mexicanus* Kiefer, *Diaptomus pallidus* Herrick, *Ceriodaphnia lacustris* (Birge), *Bosmina longirostris* (O.F. Muller), *Daphnia parvula* (Fordyce) and nauplii in a northeastern Ohio pond. Int. Rev. Gesamten Hydrobiol. **68**: 863–883.

ter Braak, C.J.F. 1988. CANOCO — an extension of DECORANA to analyse species–environment relationships. Vegetatio, **75**: 159–160.

ter Braak, C.J.F. 1990. CANOCO release 3.11. Agricultural Mathematics Group, TNO Institute for Applied Computer Science, Wageningen, The Netherlands.

Tranter, D.J. 1968. Reviews on zooplankton sampling methods. *In* Zooplankton sampling. Monographs on Oceanographic Methodology. UNESCO, Paris.

Vanni, M.J. 1988. Freshwater zooplankton community structure: introduction of large invertebrate predators and large herbivores to a small-species community. Can. J. Fish. Aquat. Sci. **45**: 1758–1770.

Viljanen, M., and Karjalainen, J. 1993. Horizontal distribution of zooplankton in two large lakes in eastern Finland. Verh. Int. Ver. Limnol. **25**: 548–551.

Visman, V., McQueen, D.J., and Demers, E. 1994. Zooplankton spatial patterns in two lakes with contrasting fish community structure. Hydrobiologia, **284**: 177–191.

Yentsch, C., and Menzel, D. 1963. A method for the determination of phytoplankton chlorophyll and phaeophytin by fluorescence. Deep-Sea Res. **10**: 221–231.

Zahner, P. 1984. Géographie physique. *In* Le Léman: synthèse 1957–1982. Commission internationale pour la protection des eaux du Léman contre la pollution (CIPEL), Lausanne, Switzerland. pp. 35–42.

© 1999 NRC Canada

Spatial and temporal heterogeneity of an epilithic streambed community in relation to the habitat templet

Heinrich Eisenmann, Peter Burgherr, and Elisabeth I. Meyer

Abstract: The microbial community of river sediments and their relationship to environmental factors is largely unknown. In this study, the abundance of bacteria, flagellates, ciliates, and Micrometazoa was investigated for eight different sediment types. The sediment types were classified by discharge (stable versus flood period), location (upper versus lower reach), and depth (superficial versus deep sediment layer). Abundances in the lower reach were more than two times higher than in the upper reach but decreased markedly at both sites after flooding. Organism densities were similar between the two sediment layers, although deeper habitats served as potential refugia, as indicated by reduced transport of coarse particles into the deep sediment layer. The organism abundances correlated with concentration of fine organic particles. A habitat templet model was used to classify favourableness and disturbance of the sediment types. For an empirical placement of sediment types in the model, results on abundances, fine organic particles, nutrient concentrations, particle transport, and flood frequency were integrated. Local processes, mainly related to sediment transport, decreased the predicticability of the habitat templets.

Résumé : On sait peu de choses de la communauté microbienne des sédiments fluviaux et de sa relation avec les facteurs environnementaux. Dans cette étude, on a déterminé l'abondance des bactéries, des flagellés, des ciliés et des micrométazoaires chez huit types de sédiments. Les types de sédiments ont été classés en fonction du débit (période stable versus période de crue), de l'emplacement (tronçon supérieur versus tronçon inférieur) et de la profondeur (couche superficielle versus couche profonde de sédiments). Les abondances dans le tronçon inférieur étaient plus de deux fois plus élevées que celles dans le tronçon supérieur, mais elles ont chuté de façon marquée aux deux sites après la crue. Les densités des organismes dans les deux couches de sédiments étaient similaires, bien que les habitats plus profonds aient constitué des refuges potentiels vu le transport réduit des particules grossières vers la couche profonde de sédiments. Les abondances des organismes étaient corrélées avec la concentration des particules organiques fines. On a utilisé un modèle descriptif d'habitat pour établir la valeur pour les organismes et le degré de perturbation des différents types de sédiments. Pour l'intégration empirique des types de sédiments dans le modèle, on a pris en considération les résultats sur les abondances, les particules organiques fines, les concentrations de nutriants, le transport des particules et la fréquence des crues. Des processus locaux, surtout liés au transport des sédiments, ont eu pour effet de réduire la puissance prédictive des modèles descriptifs d'habitat.

[Traduit par la Rédaction]

Introduction

The vast majority of hyporheic microorganisms belong to epilithic biofilms and consist of bacteria, fungi, algae, flagellates, ciliates, and Micrometazoa (Lock et al. 1984; Eisenmann et al. 1997; Pusch et al. 1998). Although microbial activity and predatory interactions make epilithic biofilms an important factor in the metabolism of river ecosystems (Edwards et al. 1990; Schwoerbel 1994), comprehensive investigations on this community are rare (Kemp 1990; Hendricks 1993; Stanford et al. 1994). Recently, the bacterial component of river epilithon has been examined, regarding production, respiration, or substrate degradation (e.g., Fischer et al. 1996; Claret and Fontville 1997). The densities of higher trophic organisms such as flagellates, ciliates, and Micrometazoa rarely have been determined and, moreover, not simultaneously with those of bacteria (Baldock and Sleigh 1988; Bott and Kaplan 1989; Schmid-Araya 1994).

The spatiotemporal distribution of bacteria, Protozoa, and Micrometazoa in streambeds may reflect the features of hyporheic habitats. Streambed habitats vary spatially, in terms of groundwater infiltration, water temperature, organic matter content, oxygen concentration, pore structure, and sediment transport. In the temporal dimension, diel or seasonal cycles, as well as floods, can have severe effects on the hyporheic community (Baldock and Sleigh 1988; Blenkinsopp and Lock 1992; Schmid-Araya 1994). The interplay of these factors creates complex abundance patterns in stream communities. Nevertheless, several studies have discerned characteristic spatiotemporal patterns within species–

Received August 28, 1998. Accepted March 19, 1999.
J14776

H. Eisenmann.[1] National Research Center for Environment and Health, D-85764 Neuherberg, Ingolstädter Landstr. 1, Germany.
P. Burgherr. Swiss Federal Institute for Environmental Sciences and Technology, CH-8600 Dübendorf, Switzerland.
E.I. Meyer. University of Münster, Zoological Institute, D-48149 Münster, Germany.

[1]Author to whom all correspondence should be addressed.
e-mail: eisenmann@gsf.de

© 1999 NRC Canada

environment relationships for macroinvertebrate or fish communities, mainly in the longitudinal dimension of river systems (e.g., Resh et al. 1994; Maret et al. 1997; Townsend et al. 1997). Patterns of the epilithic community in relation to environmental factors such as flood effects or nutrient concentrations are less investigated.

The features of a habitat constitute a templet that structures its biocoenosis. Hildrew and Townsend (1987) adapted the two-axis templet model proposed by Greenslade (1983) to predict characteristic traits of zoobenthic communities. More recently, they called for a precise habitat characterization (Townsend and Hildrew 1994). Southwood (1977, 1988) provided an excellent overview of the habitat templet concept and asked for a quantitative definition of the templet axes. These axes can be defined in terms of spatial and temporal habitat heterogeneity, spatially as favourableness and temporally as intensity of disturbance (Southwood 1988).

In this paper, we relate the templet concept to a specific spatiotemporal structure of sampling units in river sediments. Sediment types were sampled at two sites (upstream and downstream), at two depths (0–10 and 10–34 cm), and during two different discharge periods (a low-flow period and a flood period). We discuss the spatiotemporal variability of the epilithic community with respect to nutrient concentrations and transport of sediment particles.

Methods

Study sites

The prealpine River Necker (sixth order) in Switzerland has a catchment area of 125 km^2 and was described previously by Uehlinger (1991). The long-term mean discharge is 3.4 $m^3 \cdot s^{-1}$ measured at gauging station LHG 2374 of the Swiss National Survey (23 km from source; 9°07′21″E, 47°21′56″N; Fig. 1*a*). Frequent flooding usually occurs in late spring, being typical for a nivopluvial flow regime (Weingartner and Aschwanden 1992). Porewater was previously shown to be homothermic to surface water down to 50 cm depths, indicating vertical mixing. The oxygen content was generally near saturation.

Study sites were established in the upper and lower reaches of the river basin, each about 3 m from the left river bank where water depths ranged from 10 to 20 cm during normal discharge. At the upper reach site (U, km 8; 800 m above sea level, third order), a forested gorge constrains a coarse gravel and sandy riverbed (mean width = 8.5 m) interspersed with boulders. The upper reach of the Necker receives only marginal anthropogenic influence, whereas the lower reach is about 8 km downstream of an agricultural area with sewage treatment. The study site of this lower reach (L, km 28; 565 m above sea level, sixth order) was in a 17-m-wide riffle with flat, vegetation-free gravel banks and forested slopes.

Sampling and sediment types

A detailed description of the sampling procedure is given in Eisenmann et al. (1997). We analyzed incubated substrata that consisted of presieved, combusted sediment (diameter = 4–8 mm) from the River Necker. The substratum was placed in cylindrical wire cages (diameter = 9.2 cm, volume = 393 or 197 cm^3, mesh size = 4 mm) that were arranged on a rod and separated by rubber disks. This device was incubated in a perforated stainless steel receptacle (diameter = 11.6 cm) that had been buried previously in the sediment. During incubation, the wire cages were placed at depths of 0–6, 10–24, and 28–34 cm in the sediment. We distinguished two sampling layers, a superficial layer at 0–6 cm (layer 1) and a deep layer at 10–34 cm sediment depth (layer 2). Data from simultaneously sampled cages from layer 2 were averaged. After 4–5 weeks, extraction of the sediment chambers was performed by insertion of a long perspex tube (diameter = 10.4 cm) to the bottom of the receptacle such that cages were isolated from the external environment. Subsequently, smaller plexiglass tubes were pushed over the single wire cages and sealed with the cage contents. Then, the confined chambers were retrieved by hooks. Occasionally, samples were lost because of material failures or destruction by spates. A total of 31 sediment chambers were recovered.

Samples were collected during two contrasting discharge periods between May and September 1993 (Fig. 1*b*). After a relatively long period with stable discharge, a flood period began on June 17 and continued through the end of the investigation. Each sediment chamber received at least two spates >20 $m^3 \cdot s^{-1}$ (measured at the gauging station) during that time, which was assessed as flood frequency (FF) during incubation. Sediment chambers were collected at both reaches, three times during the stable-flow period (s) and three to four times during the flood period (f).

Sediment types were grouped by three criteria: flow period (stable versus flood period), site (upper versus lower reach), and depth (superficial versus deep layer). The combination of criteria yielded eight sediment types, and each sediment type defines a certain templet. For example, the templet fU1 is represented by sediment samples that were exposed in the flood period (f), located at the upper site (U), and incubated in the superficial layer (1). We collected three samples from each sediment type, with the exception of sL1 (n = 2). Finally, averaging simultaneous samples from the deeper layer resulted in 23 samples of sediment types.

Counting procedures and measurements

In the laboratory, the sediments were gently shaken for 1 min at 100 rpm to detach lightly attached biofilm material. For the examination of nematodes, a 10-mL subsample was withdrawn with a cut-off glass pipette (data published in Eisenmann et al. 1998). Two further subsamples were taken by pooling 25 × 200 µL of porewater with a piston pipette in flasks. One was immediately fixed with formaldehyde (final concentration 4%); from the other, a dilution (1:1 to 1:8) was prepared with filtered water that allowed accurate enumeration of organisms in counting chambers. Living ciliates (CIL) and Micrometazoa (MET, <600 µm body length; rotifers, nematodes, and other Metazoa, which were not further determined) were enumerated with Nageotte counting chambers within 36 h. Seven aliquots of 100 µL were examined at 100× magnification. Thoma chambers with 0.55 µL as the unit of volume were used to count flagellates (FLG) in 10 parallels at 400× magnification. This counting procedure also was used for a crude estimate of microalgae. We found 2–11 flagellates, 4–20 ciliates, and 0–7 Micrometazoa per single counts of the samples. Average 95% confidence intervals were 32% for flagellates, 34% for ciliates, and about 79% for Micrometazoa.

To count bacteria (BAC), the fixed subsample was divided and both parts (1–2 mL) diluted with filtered water in a five-step series to 1:243 with strong shaking for 60 s after each step. After the last step, particles sedimented to the bottom of the test tube within 15 min. Excess water (about 2 mL) was transferred to another tube and stained for 10–30 min with 20 µL of 4,6-diamidino-2-phenylindole dihydrochloride (final concentration 1 $\mu g \cdot L^{-1}$; Porter and Feig 1980). Finally, 3 mL of prefiltered water was added and the sample filtered (black Nuclepore filters, pore size = 0.2 µm). Single-cell bacteria were counted with an Olympus BH2 microscope under ultraviolet excitation at an emission wavelength of 374 nm and at 1250× magnification. Twelve microscope fields, or at least 100 bacteria, were counted in each sample and resulted in average 95% confidence limits of 19%. Filamentous organisms were tallied by counting 1 µm as one cell and excluded from confidence interval calculations. Sonication and surfactants were not

© 1999 NRC Canada

Fig. 1. (*a*) Sediment types (i.e., sampling units) collected from the streambed of the River Necker at a lower reach site and an upper reach site, from superficial sediments (layer 1) and deeper sediments (layer 2), and during the stable-flow period and the flood period. (*b*) Discharge at a municipal gauging station at midreach; incubation time of sediment chambers is indicated by horizontal lines and sampling dates are marked with small vertical bars (upwards for the upper reach and downwards for the lower reach).

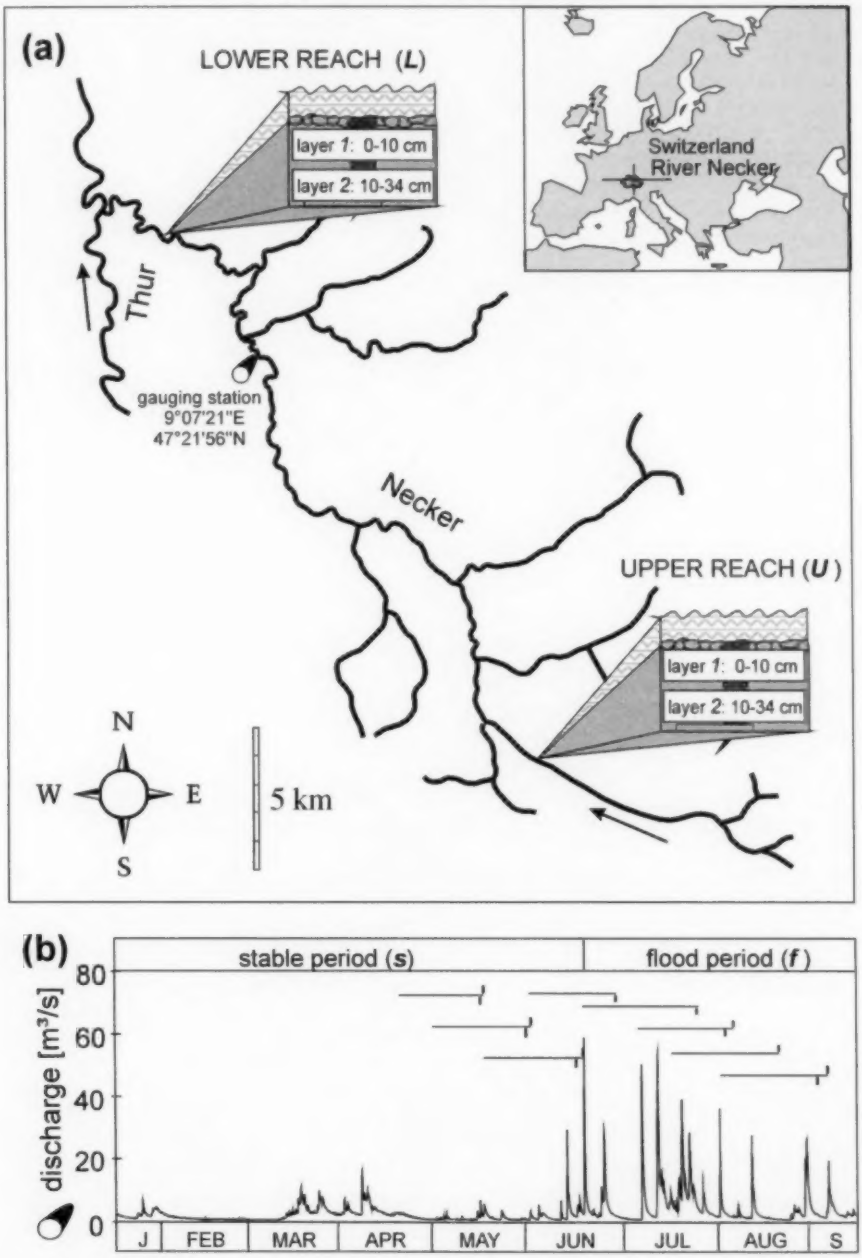

used in order to avoid potential damage to filaments, so that bacteria, which strongly adsorbed to the substrate, were not recorded.

The sediments consisted of the initially exposed matrix and of infiltrated material that had been transported into the chambers by interstitial water flow. Sediment particles were separated by wet sieving, after removal of subsamples. The effluent of original porewater was collected, and, if sufficient volume was available, nutrient concentrations (NO_3, PO_4, and dissolved organic carbon (DOC)) were determined by standard methods (DEV 1984). Very fine particles in the effluent were allowed to settle in a 1-L bottle over 2 days and subsequently treated as the other particle fractions. The dry weight of three particle size-classes was denoted as fine particulate material (FPM) (<125 µm), coarse particulate material (CPM) (>125 µm), and the initially exposed sediment matrix

© 1999 NRC Canada

Fig. 2. Sediment transport (mean values and range) into chambers that were incubated in a superficial layer (0–10 cm) and a deep layer (10–34 cm) of a streambed (River Necker). (*a*) Infiltration of FPOM (<125 µm) in the upper reach (●) and in the lower reach (■) during both the stable-flow period and the flood period. (*b*) Infiltration of CPM (>125 µm) during the stable period (○) and the flood period (□) at both study sites.

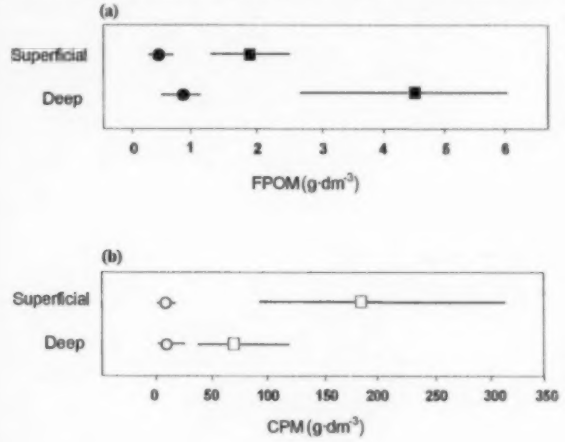

(MM) (>4 mm). The corresponding content of particulate organic matter in the sediment fractions (FPOM, CPOM, and MOM) was measured as ash-free dry mass after ignition at 520°C for 4 h. Particle loss by subsampling was found to be negligible.

Statistical tools

All statistical analyses were performed with STATISTICA for Macintosh (Statsoft 1994) or the ADE version 4 software package (Chessel and Dolédec 1996). Spearman rank correlations from all samples were used to detect statistically significant relationships among variables. Univariate tests on sediment type differences within time periods (s and f), sites (L and U), or depths (1 and 2) were made with a Kruskal–Wallis test (ANOVA by ranks). Differences between the eight sediment types were assessed by canonical discriminant analysis using a stepwise forward procedure. Missing values in the data matrix were replaced by mean values.

A habitat templet model was created with parameters that indicated either productivity or disturbance. For the productivity axis, we assessed parameters on organism densities, nutrient concentrations, and FPOM content; the disturbance axis was defined by flood frequency during chamber incubation and the input of coarse inorganic and coarse organic materials in chambers. Axes were defined by modifying the statistical approach of Townsend et al. (1997). All values were scaled between 0 and 1 following the formula of Cellot et al. (1994). Then, both data matrices were ordinated by a noncentered principal components analysis. We used the values of their first components as coordinates to define the position of each sediment type within the templet.

Results

Environmental conditions and abundances in grouped sediment types

All parameters showed high standard deviations from mean values. The coefficient of variation ranged between 19% for the initially incubated sediment matrix and 130% for the input of coarse inorganic particles. The mean concentrations of nutrients differed only minimally with depth and time period. However, inorganic nutrients were significantly higher in samples from the lower reach compared with the upper reach (Table 1). Mean concentrations were 0.08 $mg \cdot L^{-1}$ in the lower reach versus 0.02 $mg \cdot L^{-1}$ in the upper reach for PO_4 and 1.6 $mg \cdot L^{-1}$ in the lower reach versus 0.8 $mg \cdot L^{-1}$ in the upper reach for NO_3. Concentrations of DOC were similar at both sites (lower: 6.1 $mg \cdot L^{-1}$, upper: 4.9 $mg \cdot L^{-1}$).

A significant difference between the upper and lower sites was found for all organism densities (Table 2). Mean abundances were at least two times higher in the lower reach than in the upper reach. Microalgae disappeared during the spate period, although they had reached densities in the magnitude of 10^4 cells $m \cdot L^{-1}$ in the stable-flow period. The densities of flagellates, ciliates, and Micrometazoa declined to about half during the spate period, which was a significant decrease only for the Protozoa. Micrometazoa and Protozoa were more numerous in the deep sediment layer at both sites, in contrast with bacterial densities.

Similar to organism abundances, fine organic matter content was about five times higher in the lower reach site (3.3 $mg \cdot dm^{-3}$) than in the upper reach site (Fig. 2*a*). At both sites, transport was slightly greater in deeper sediments (mean = 2.8 $mg \cdot dm^{-3}$) and during the stable-flow period (mean = 2.2 $mg \cdot dm^{-3}$). The mean content of coarse organic matter (merely organic material attached to coarse mineral particles) varied only between 0.6 and 1.5 $mg \cdot dm^{-3}$ for each of the grouped sediments and did not reflect the great differences in coarse inorganic particle input. Despite biofilm detachment by shaking, most organic material was still strongly attached to the surface of the initially incubated sediment matrix (overall mean = 3.7 $mg \cdot dm^{-3}$), whereas detached material and infiltrated organic matter reached about half this value.

The transport of inorganic material differed particularly for coarse particles and in the temporal dimension. Through floods, 133 g coarse $material \cdot dm^{-3}$ was transported into the cages, but only 8 $g \cdot dm^{-3}$ infiltrated during the stable period. This infiltration was less pronounced in deeper sediment zones (Fig. 2*b*), with only 40% of the surface input (183 versus 73 $g \cdot dm^{-3}$). Fine inorganic matter showed a different transport pattern. Neither floods nor sediment depth seemed to influence its infiltration, which differed significantly between the two sites. Much more material was generally moved in the lower site relative to the upper site (57 versus 11 $g \cdot dm^{-3}$).

Correlation and discrimination analyses

Abundances of bacteria, flagellates, ciliates, and Micrometazoa showed a parallel development, as confirmed by significantly positive correlations (Table 3). Each group also was significantly correlated with fine organic and inorganic matter. Generally, organic and inorganic fractions of each size-class were closely linked. Moreover, the number of floods during incubation of the sediment chambers was highly correlated with the infiltration of coarse inorganic material.

Canonical discriminant analysis showed a separation of the sediment types by four significant discriminant functions or roots, three of which are displayed in Fig. 3. Sediment types were significantly different from each other ($P < 0.05$),

© 1999 NRC Canada

Table 1. Microbial and micrometazoan abundances and environmental parameters in sediment types from a streambed (River Necker).

Period	Site	Layer	BAC ($\times 10^6$ cells·L^{-1})	FLG ($\times 10^3$ cells·L^{-1})	CIL (cells·L^{-1})	MET (cells·L^{-1})	DOC (mg·L^{-1})	PO_4 (mg·L^{-1})	NO_3 (mg·L^{-1})
s	L	1	305 (233)	51 (42)	505 (276)	138 (139)	6.47 (0.13)	0.10 (0.03)	1.58 (0.48)
f	L	1	275 (78)	60 (24)	410 (132)	111 (60)	5.24 (1.79)	0.09 (0.12)	1.36 (0.20)
s	L	2	350 (226)	155 (11)	1137 (19)	277 (166)	7.93 (0.11)	0.07 (0.02)	2.07 (1.96)
f	L	2	170 (42)	54 (20)	325 (92)	43 (35)	3.62 (—)	0.04 (—)	1.10 (—)
s	U	1	162 (111)	41 (9)	303 (174)	33 (20)	4.84 (0.37)	0.02 (0.01)	0.66 (0.05)
f	U	1	72 (16)	8 (3)	68 (20)	16 (7)	5.00 (—)	0.02 (0.02)	0.65 (—)
s	U	2	94 (9)	52 (14)	327 (103)	49 (41)	4.55 (0.80)	0.01 (0.01)	1.02 (0.29)
f	U	2	78 (24)	27 (19)	151 (27)	27 (5)	6.27 (—)	0.03 (0.01)	0.58 (—)

Note: The sediments were grouped by sampling date (stable-flow period s or flood period f), by sampling site (lower reach L or upper reach U), and by depth (layer 1 (0–10 cm) or layer 2 (10–34 cm)). Numbers are means (standard deviations in parentheses) for $n = 2$ or $n = 3$.

Table 2. Average microbial and micrometazoan abundances (standard deviations in parentheses, $n \geq 8$) from grouped sediment types in the streambed of the River Necker.

	BAC (10^6 cells·mL^{-1})	FLG (10^3 cells·mL^{-1})	CIL (cells·mL^{-1})	MET (ind.·mL^{-1})
Lower reach	283 (160)	89 (74)	596 (380)	146 (130)
Upper reach	108 (70)	32 (20)	212 (142)	31 (24)
Superficial layer	199 (140)	37 (27)	305 (213)	69 (74)
Deep layer	193 (168)	75 (72)	479 (414)	102 (131)
Stable period	233 (179)	77 (72)	574 (399)	123 (138)
Flood period	149 (95)	39 (34)	233 (152)	52 (52)

except for three stable sediments (sL1, sU1, and sU2). Each single sample was correctly classified. Root 1 effectively discerned differences between flood and stable-flow periods (with the exception of sL2) and accounted for 68% of the total variability in sediment type discrimination. Parameters of sediment transport were the most effective discriminators for root 1. Another 25% of the variability among sediment types was explained by root 2, which primarily separated the superficial samples from the deeper ones (except sU1 from sU2). Flagellate and micrometazoan variables contributed substantially to the second discriminant function. Root 3 divided the upper reach from the lower reach samples (except fL2), although explaining only 5% of the sediment type variation. Bacterial densities were not important in the multivariate model because of insignificant power for discrimination ($P > 0.9$).

Discussion

In the present study, we compared incubated sediment chambers to assess living conditions of the epilithic community. The abundances of bacteria, flagellates, ciliates, and Micrometazoa were in a mean range comparable with those reported for other benthic habitats (Gasol 1993). They are probably representative of in situ conditions, since the chambers were very similar to the natural environment, e.g., in nutrient concentrations, particle surface, temperature, and flow velocity (Eisenmann et al. 1997). However, trap effects cannot be excluded because particle infiltration by interstitial water flow caused an inevitable alteration of the incubated sediments. This particle transport and also organism densities revealed significant differences for some grouped sediment samples (i.e., between the upper reach and the lower reach or after floods).

Temporal and spatial variability

During the stable-flow period, high organism abundance suggests a productive state of the epilithic community. In contrast, a pioneering state occurred during the spate period when densities clearly declined, but the support by nutrient concentrations and FPOM remained at the same level. Floods had removed the epibenthic algal food source and had caused a sustainable biofilm abrasion through sediment movement. Since bacteria were less reduced than higher organisms, they seem to be less susceptible to flood disturbances or recover faster than Protozoa (Blenkinsopp and Lock 1992; Schmid-Araya 1994). A fast recovery was probably supported by reduced abundances of protozoan and micrometazoan grazers and increasing temperatures through springtime.

In the lower reach, biofilms were obviously favoured by the intense transport of fine particles. Under stable conditions, the daily transport rates of fine material can be estimated as 1.7 g·dm^{-3} at the lower reach site but only 0.3 g·dm^{-3} at the upper reach site. However, these rates are underestimations, since only particle input into the chambers was considered but not the passage of particles. In addition to the extensive surface of fine inorganic material and FPOM at the lower site, organisms profited from the higher PO_4 and NO_3 concentrations. The importance of DOC concentration remains unclear because of its undefined nutrient quality (Fiebig 1995).

In the deeper sediment layers, the reduced transport of particles might be due to lower interstitial flow velocity. Low particle transport and flow velocity reduced the stress

© 1999 NRC Canada

MOM ($g \cdot dm^{-3}$)	CPOM ($g \cdot dm^{-3}$)	FPOM ($g \cdot dm^{-3}$)	MM ($g \cdot dm^{-3}$)	CPM ($g \cdot dm^{-3}$)	FPM ($g \cdot dm^{-3}$)	FF (n)
2.62 (1.90)	0.23 (0.11)	1.38 (0.07)	1384 (47)	5.3 (6.4)	16.1 (1.6)	0.5 (0.7)
3.61 (0.80)	1.94 (0.11)	2.18 (0.44)	1368 (37)	121.2 (35.4)	74.3 (20.1)	3.0 (1.0)
3.31 (2.23)	1.69 (0.55)	5.82 (0.35)	1486 (101)	13.9 (9.6)	66.7 (2.5)	0.3 (0.6)
3.68 (1.73)	1.60 (0.27)	3.17 (0.58)	1529 (120)	69.1 (27.1)	56.7 (9.0)	3.3 (1.2)
3.18 (0.83)	0.25 (0.09)	0.57 (0.20)	1291 (208)	8.4 (6.2)	7.2 (3.2)	0.3 (0.6)
3.36 (0.88)	1.65 (0.48)	0.42 (0.11)	911 (407)	244.4 (112.5)	11.2 (4.0)	2.7 (1.2)
4.03 (0.72)	0.15 (0.04)	0.85 (0.31)	1510 (14)	1.8 (0.9)	9.5 (3.6)	0.3 (0.6)
6.09 (0.54)	0.70 (0.36)	0.69 (0.26)	1522 (13)	77.6 (58.7)	17.3 (9.4)	3.0 (1.0)

Fig. 3. Sediment types (sampling units) in a streambed distinguished by three significant roots from canonical discriminant analysis of 14 parameters (see Table 1). Eigenvalues of roots are shown in the histogram. The sediment types are defined as follows: stable-flow period s (one flood per month) or flood period f (two floods per month), upper reach site U (km 8) or lower reach site L (km 28), and superficial sediment layer 1 (0–10 cm) or deep sediment layer 2 (10–34 cm). Individual sample units are indicated by circles.

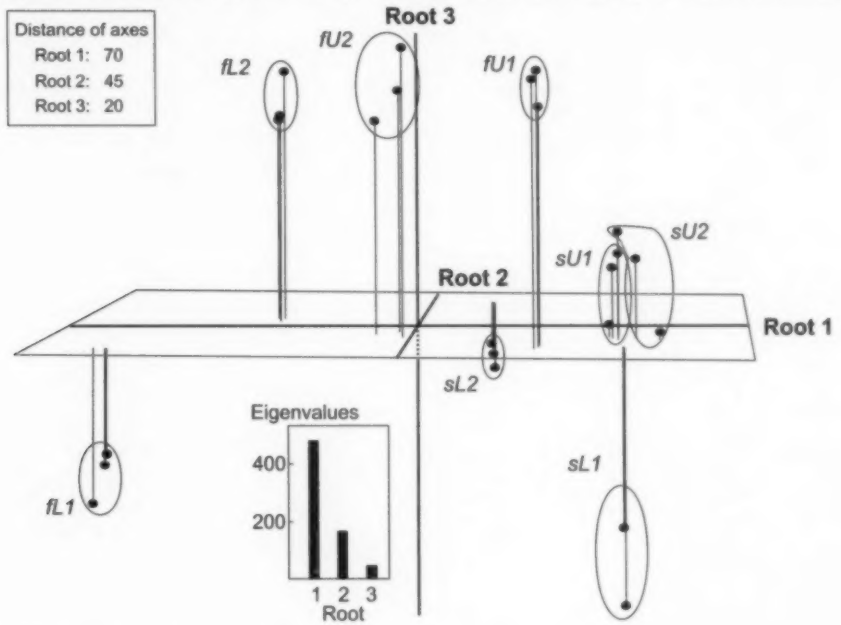

of involuntary dislocation from the epilithic surface (Patterson et al. 1989), thus explaining higher densities of Protozoa and Micrometazoa in the deeper layers. The refuge effect of the deeper sediment zone was particularly important during the spate period, when a strong sediment movement occurred at the sediment surface. During stable flow, we assume interflow of nutrient-rich groundwater (Triska et al. 1990; Fiebig 1995) and the accumulation of FPOM (Brunke and Gonser 1997) as further beneficial factors in deeper zones. Moreover, high amounts of epibenthic algae infiltrated deep into the sediment, as also found in previous studies (Borchardt and Bott 1995; Sobczak 1996), and supported the epilithic community in both layers.

A close linkage between bacteria, flagellates, ciliates, and Micrometazoa is demonstrated by strong correlation in abundances. As a major reason, we assume intense predation, since bacteria are most probably the dominant food resource for biofilm Protozoa (Korber et al. 1995). A rapid reaction of protozoan densities to the bacterial resource, which is altered through floods, is possible because of their short generation times (Müller and Geller 1993). Other reasons for the parallel development of abundances may be physical factors (e.g., mortality by floods) or strong grazing pressure from macroinvertebrates. The clear correlation of all organism groups with FPOM indicates its importance for the epilithic community, either as a substrate or as a direct product of the biofilms in the form of a polysaccharide matrix (Freeman and Lock 1995).

Templet model

The clear separation of the eight defined sediment types by canonical discriminant analysis indicates that the investi-

© 1999 NRC Canada

Table 3. Correlations of bacterial and microfaunal abundances and environmental factors in various sediment types from the streambed of the River Necker.

	BAC	FLG	CIL	MET	DOC	PO_4	NO_3	MOM	CPOM	FPOM	MM	CPM	FPM
BAC													
FLG	0.65***												
CIL	0.76***	0.81***											
MET	0.45**	0.71***	0.79***										
DOC													
PO_4					0.67***								
NO_3													
MOM													
CPOM													
FPOM	0.67***	0.68***	0.64***	0.56**					0.54***				
MM													
CPM									0.79***				
FPM	0.53*	0.48*	0.42*	0.40*					0.73***	0.87**			
FF			−0.41*						0.49**			0.79***	

Note: Significant values only: $*P < 0.05$, $**P < 0.01$, $***P < 0.005$.

Fig. 4. (*a*) Conceptual and (*b*) empirical habitat templet models for streambed sediments. The sediment types were characterized by discharge periods (stable-flow period s, flood period f), location (upper reach U, lower reach L), and depth (superficial sediment layer 1, deeper sediment layer 2). The axes of the empirical model were scaled by principal components analysis of parameters that indicate disturbance (coarse particle input and flood frequency) or productivity (organism abundances, nutrient concentrations, and FPOM content). Endpoints of lines mark the position of single sampling types; their means are indicated by centroids.

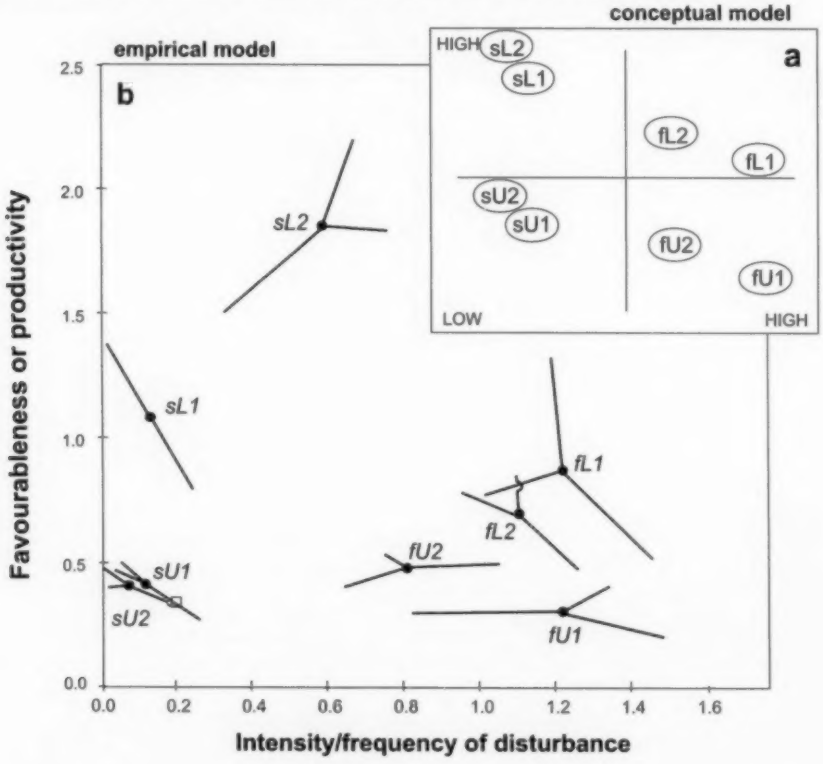

gated river sediments offered disparate conditions for the epilithic community. The difference between sites located nearly 20 km apart was almost equal to the differences between depths at a distance of 30 cm. Hence, vertical sediment heterogeneity in our sampling pattern was about four orders of magnitude stronger than longitudinal heterogeneity. Under stable conditions, separation between site locations and depths was less distinctive than after floods.

© 1999 NRC Canada

Interestingly, bacteria did not contribute significantly to the discrimination. Rather, their abundances seem to buffer differences related to sedimentological features, nutrient conditions, and predator densities. These parameters appear to be the basic categories responsible for differences between the defined sediment types.

As a distinction among sediment types was evident, it seems worthy to assess them in a habitat templet model. In the present study, we followed Hildrew and Townsend (1987), who related the spatial axis of the templet to productivity or favourableness and the temporal axis to intensity of disturbance. Our indirect quantification of disturbance was based on coarse particle transport and flood frequency. Favourableness was denoted by microfaunal densities, FPOM-content, and nutrient concentrations.

As a framework, we assigned the sediment types to a concept shown in Fig. 4*a*. Along the productivity axis, the most favourable conditions were assessed for sediment types from the lower reach because of higher nutrient levels than at the upper reach. A secondary influence was attributed to spates. Frequently flooded sediments (e.g., fL1) showed a decrease in organism densities and were therefore discerned to be less favourable than during the stable period (e.g., sL1). In particular, the more productive community in the lower reach was more strongly affected by flood disturbance than the less productive one in the upper reach. This is reflected by a greater distance of the corresponding sediment types in the templet model (compare vertical distances from sL1 to fL1 and from sL2 to fL2 with distances from sU1 to fU1 and from sU2 to fU2, respectively). Differences in depth, i.e., between the two sediment layers, can be considered of tertiary importance. Deeper sediments may be slightly more favourable than superficial ones because of their higher FPOM content and their refuge function.

Along the disturbance axis, all sediment types from the stable-flow period differed most markedly from those of the flood period. A second factor for placement along this axis was the refuge function of deeper sediments. Spates transported much more coarse material into the superficial layer than into the deep layer. Therefore, superficial layers (e.g., sU1) were classified less stable than underlying ones (e.g., sU2). Moreover, the response of superficial sediment layers to discharge was much greater under flood periods than under stable conditions. Consequently, flooded sediment layers from the same site were arranged more distant from each other than the stable sediment layers (compare horizontal distances from fU1 to fU2 and from fL1 to fL2 with distances from sU1 to sU2 and from sL1 to sL2, respectively).

Our empirical analysis of the concept showed a good correspondence (Fig. 4*b*). Deviations were found for sediment types from the deep layer at the lower study site (L2), apparently because of unexplained local processes on sediment transport that also affected microfaunal abundances. For instance, the sediment type sL2 showed a much higher productivity than predicted due to very high organism densities and effective FPOM transport during stable flow. It was also found to be more disturbed than denoted in the conceptual model because of a considerable transport of small coarse particles. Further, the location was unexpectedly unfavourable during the flood period (fL2), which may be due to an unusual decline in abundances after flood disturbances and minor transport of FPOM. In contrast with the concept, spates seemed to improve living conditions in the deep layer of the upper reach (fU2), where refuge effects were possibly strong. To conclude, more complex processes are suggested by the empirical model that were not considered in the conceptual model.

We assume that the relative positions of sediment types, as reflected by the conceptual model, are generally valid for streambed sediments of constrained rivers. However, we are aware that the discerned heterogeneity depends on the scales examined and the specific templet model employed. Thus far, only Cellot et al. (1994) integrated interstitial habitats in a templet model and found them to be more stable compared with epibenthic habitats. Productivity (for the spatial axis) and disturbance (for the temporal axis) of a templet can be defined by a variety of functional and environmental factors (Cellot et al. 1994; Townsend et al. 1997). The applied templet was the first to integrate microbial abundances. We assume that they are good indicators of environmental conditions because of their fast reaction to changing resources. A focus on species traits for Protozoa and Micrometazoa could perhaps further elucidate habitat–community relationships. For instance, small-sized Protozoa and a robust nematode species were favoured by spate periods, whereas Heliozoa and algivore ciliates profited from stable conditions (Eisenmann et al. 1998). A future challenge is to define the templet axes in such a way that predictions about sediment type positions in the templet are more objective and testable.

Acknowledgements

We thank Chris Robinson and two anonymous reviewers for critical comments on the manuscript. The project was supported by the Swiss Federal Institute for Environmental Science and Technology (EAWAG).

References

Baldock, B.M., and Sleigh, M.A. 1988. The ecology of benthic Protozoa in rivers: seasonal variation in numerical abundance in fine sediments. Arch. Hydrobiol. **111**: 409–421.

Blenkinsopp, S.A., and Lock, M.A. 1992. Impact of storm-flow on electron transport system activity in river biofilms. Freshwater Biol. **27**: 397–404.

Borchardt, M.A., and Bott, T.L. 1995. Meiofaunal grazing of bacteria and algae in a Piedmont stream. J. North Am. Benthol. Soc. **14**: 278–298.

Bott, T.L., and Kaplan, L.A. 1989. Densities of benthic Protozoa and nematodes in a Piedmont stream. J. North Am. Benthol. Soc. **8**: 187–196.

Brunke, M., and Gonser, T. 1997. The ecological significance of exchange processes between rivers and groundwater. Freshwater Biol. **37**: 1–33.

Cellot, B., Dole-Olivier, M.-J., Bornette, G., and Pautou, G. 1994. Temporal and spatial environmental variability in the Upper Rhône River and its floodplain. Freshwater Biol. **31**: 311–325.

Chessel, D., and Dolédec, S. 1996. ADE version 4: hypercard stacks and quick basic Microsoft programme library for the analysis of environmental data. User's manual. ESA CNRS 5023, Écologie des Eaux Douce et des Grands Fleuves, Université Lyon 1, France.

© 1999 NRC Canada

Claret, C., and Fontville, D. 1997. Characteristics of biofilm assemblages in two contrasted hydrodynamic and trophic contexts. Microb. Ecol. **34**: 49–57.

DEV. 1984. Deutsche Einheitsverfahren zur Wasser-, Abwasser- und Schlamm-untersuchung. 13. Lieferung, Verlag Chemie, Weinheim.

Edwards, R.T., Meyer, J.L., and Findlay, S.E.G. 1990. The relative contribution of benthic and suspended bacteria to system biomass, production, and metabolism in a low-gradient blackwater river. J. North Am. Benthol. Soc. **9**: 216–228.

Eisenmann, H., Traunspurger, W., and Meyer, E.I. 1997. A new device to extract sediment cages colonized by microfauna from coarse gravel river sediments. Arch. Hydrobiol. **139**: 547–561.

Eisenmann, H., Traunspurger, W., and Meyer, E.I. 1998. Community structure of selected micro- and meiobenthic organisms in sediment chambers from a prealpine river (Necker, Switzerland). *In* Advances in river bottom ecology. *Edited by* J. Helešic and G. Bretschko. Backhuys Publishers, Leiden, The Netherlands. pp. 155–162.

Fiebig, D.M. 1995. Groundwater discharge and its contribution of dissolved organic carbon to an upland stream. Arch. Hydrobiol. **134**: 129–155.

Fischer, H., Pusch, M., and Schwoerbel, J. 1996. Spatial distribution and respiration of bacteria in stream-bed sediments. Arch. Hydrobiol. **137**: 281–300.

Freeman, C., and Lock, M.A. 1995. The biofilm polysaccharid matrix: a buffer against changing organic substrate supply? Limnol. Oceanogr. **40**: 273–278.

Gasol, J.M. 1993. Benthic flagellates and ciliates in fine freshwater sediments: calibration of a live counting procedure and estimation of their abundances. Microb. Ecol. **25**: 247–262.

Greenslade, P.J.M. 1983. Adversity selection and the habitat templet. Am. Nat. **122**: 352–365.

Hendricks, S.P. 1993. Microbial ecology of the hyporheic zone: a perspective integrating hydrology and biology. J. North Am. Benthol. Soc. **12**: 70–78.

Hildrew, A.G., and Townsend, C.R. 1987. Organization in freshwater communities. *In* Organization of communities past and present. *Edited by* J.R.H. Gee and P.S. Giller. Blackwell Scientific Publications, Oxford, U.K. pp. 347–372.

Kemp, P.F. 1990. The fate of benthic bacterial production. Rev. Aquat. Sci. **2**: 109–124.

Korber, D.R., Lawrence, J.R., Lappin-Scott, H.M., and Costerton, J.W. 1995. Growth of microorganisms on surfaces. *In* Microbial biofilms. *Edited by* H.M. Lappin-Scott and J.W. Costerton. Cambridge University Press, Cambridge, U.K. pp. 15–45.

Lock, M.A, Wallace, R.R., Costerton, J.W., Ventullo, R.M., and Charlton S.E. 1984. River epilithon: towards a structural–functional model. Oikos, **42**: 10–22.

Maret, T.R., Robinson, C.T., and Minshall, G.W. 1997. Fish assemblages and environmental correlates in least-disturbed streams of the upper Snake River basin. Trans. Am. Fish. Soc. **126**: 200–216.

Müller, H., and Geller, W. 1993. Maximum growth rates of aquatic ciliated Protozoa: the dependence on body size and temperature reconsidered. Arch. Hydrobiol. **126**: 315–327.

Patterson, D.J., Larsen, J., and Corliss, J.O. 1989. The ecology of heterotrophic flagellates and ciliates living in marine sediments. Prog. Protistol. **3**: 185–277.

Porter, K.G., and Feig, Y.S. 1980. The use of DAPI for identifying and counting aquatic microflora. Limnol. Oceanogr. **25**: 943–948.

Pusch, M., Fiebig, D., Brettar, I., Eisenmann, H., Ellis, B.K., Kaplan, L.A., Lock, M.A., Naegeli, M.W., and Traunspurger, W. 1998. The role of micro-organisms in the ecological connectivity of running waters. Freshwater Biol. **40**: 453–495.

Resh, V.H., Hildrew, A.G., Statzner, B., and Townsend, C.R. 1994. Theoretical habitat templets, species traits, and species richness: a synthesis of long-term ecological research on the Upper Rhône River in the context of concurrently developed theory. Freshwater Biol. **31**: 539–554.

Schmid-Araya, J.M. 1994. Temporal and spatial distribution of benthic microfauna in sediments of a gravel streambed. Limnol. Oceanogr. **39**: 1813–1821.

Schwoerbel, J. 1994. Trophische Interaktionen in Fliessgewässern. Limnologica, **24**: 185–194.

Sobczak, W.V. 1996. Epilithic bacterial responses to variations in algal biomass and labile dissolved organic carbon during biofilm colonization. J. North Am. Benthol. Soc. **15**: 143–154.

Southwood, T.R.E. 1977. Habitat, the templet for ecological strategies. J. Anim. Ecol. **46**: 337–365.

Southwood, T.R.E. 1988. Tactics, strategies and templets. Oikos, **52**: 3–18.

Stanford, J.A., Ward, J.V., and Ellis, B.K. 1994. Ecology of the alluvial aquifers of the Flathead River, Montana. *In* Groundwater ecology. *Edited by* G.D.L. Danielopool and J.A. Stanford. Academic Press, San Diego, Calif. pp. 367–389.

Statsoft. 1994. STATISTICA for the Macintosh™. Vols. 1 and 2. Statsoft, Tulsa, Okla.

Townsend, C.R., and Hildrew, A.G. 1994. Species traits in relation to a habitat templet for river systems. Freshwater Biol. **31**: 265–275.

Townsend, C.R., Dolédéc, S., and Scarsbrook, M.R. 1997. Species traits in relation to temporal and spatial heterogeneity in streams: a test of habitat templet theory. Freshwater Biol. **37**: 367–387.

Triska, F.J., Duff, J.H., and Avanzino, R.J. 1990. Influence of exchange flow between the channel and hyporheic zone on nitrate production in a small mountain stream. Can. J. Fish. Aquat. Sci. **47**: 2099–2111.

Uehlinger, U. 1991. Spatial and temporal variability of the periphyton biomass in a prealpine river (Necker, Switzerland). Arch. Hydrobiol. **123**: 219–237.

Weingartner, R., and Aschwanden, H. 1992. Abflussregime als Grundlage zur Abschätzung von Mittelwerten des Abflusses. Hydrologischer Atlas der Schweiz, Landeshydrologie Bern: Kapitel 5.2.

© 1999 NRC Canada

Influence of organic acid site density on pH modeling of Swedish lakes

Stephan Köhler, Jakub Hruška, and Kevin Bishop

Abstract: A semidirect titration method was used to determine individual site densities of carboxylic acids present in natural organic matter originating from 74 Swedish lakes. The average carboxylic acid site density of natural organic matter of the studied lakes was 8.6 ± 1.6 μequiv.·mg total organic carbon^{-1}, which is more variable than the site densities observed earlier in a set of streams. These data were then used to assess the effect on modeling pH and organic anion charge contribution caused by the natural variability in site density. Air-equilibrated pH was modeled with a median error of 0.08 pH unit, equivalent to a mean error in the charge balance of 9 μmol·L^{-1}, using measured C_b–C_a and individually determined site densities. A better prediction of pH, however, was made using this average site density and the CBALK approach, which is a different method for estimating total buffering capacity. The mean error in pH prediction was decreased to 0.05 pH unit, equivalent to a mean error in the charge balance of 5 μmol·L^{-1}. These uncertainties in pH prediction are significantly smaller than reported in other studies. This implies that the existing natural variation in site density does not lead to significant effects on modeling pH or anion charge contribution in surface waters in the pH range of 4.5–8.5. Filtered samples (0.45 μm) did not show any significant change in pH, total organic carbon, or site density compared with unfiltered samples.

Résumé : On a utilisé une méthode de titration semi-directe pour déterminer à différents sites les densités des acides carboxyliques présents dans la matière organique naturelle provenant de 74 lacs suédois. La densité moyenne d'acide carboxylique dans la matière organique naturelle des divers sites des lacs étudiés était de 8,6 ± 1,6 μequiv.·mg carbone organique total^{-1}, valeur qui est plus variable que les densités observées antérieurement à d'autres sites d'un ensemble de cours d'eau. Ces données ont ensuite été utilisées pour évaluer l'effet de la variabilité naturelle de la densité observée aux divers sites sur la modélisation du pH et de la contribution de la charge anionique organique. On a modélisé le pH équilibré avec l'air avec une erreur médiane de 0,08 unité de pH, ce qui équivaut à une erreur moyenne dans l'équilibre des charges de 9 μmol·L^{-1}, en utilisant les mesures de C_b–C_a et les densités déterminées individuellement aux divers sites. On a toutefois obtenu une meilleure prévision du pH en utilisant cette densité moyenne aux divers sites et la méthode CBALK, une méthode différente pour estimer le pouvoir tampon total. On a pu ainsi réduire l'erreur moyenne dans la prévision du pH à 0,05 unité de pH, ce qui équivaut à une erreur moyenne dans l'équilibre des charges de 5 μmol·L^{-1}. Ces incertitudes dans la prévision du pH sont significativement moins importantes que celles signalées dans d'autres études. Cela signifie que la variation naturelle existante dans la densité observée aux divers sites n'a pas d'effet significatif sur la modélisation du pH ou de la contribution de la charge anionique dans les eaux de surface dont le pH se situe entre 4,5 et 8,5. La filtration (0,45 μm) n'a pas entraîné de changement significatif du pH, du carbone organique total ni de la densité des acides carboxyliques aux divers sites.

[Traduit par la Rédaction]

Introduction

The importance of natural organic matter (NOM) on pH equilibria in natural waters is well recognized (Oliver et al. 1983; Cantrell et al. 1990; Hemond 1990; Perdue 1990). Both the episodic changes in pH during hydrological events in streams and the effect of NOM on surface water acidity in lakes have been documented (Kahl 1991; Kortelainen 1992, 1993; Munson and Gherini 1993; Driscoll et al. 1994; Hruška et al. 1996). NOM also plays an important role in the ecology of lakes, as it influences the ultraviolet radiation penetration depth (Sommaruga-Wögrath et al. 1997).

All approaches to studying the effect of NOM on pH depend on the parameter selection for a value of site density, i.e., the total amount of pH-reactive sites per milligram of carbon and a set of pK_a values describing the pH-buffering areas. These characteristics of NOM might be affected by the character of the catchment and the hydrology or internal lake processes such as biological or photochemical degradation. Different organic acid analog models with different site densities and acid–base buffering characteristics have been studied in Finland (Kortelainen 1992, site density 9.2 μmol·L^{-1}) and North America (Driscoll et al. 1994, site

Received August 28, 1998. Accepted April 27, 1999.
J14766

S. Köhler.[1] Department of Forest Ecology, SLU Umeå, Sweden.
J. Hruška. Department of Forest Ecology, SLU Umeå, Sweden, Czech Geological Survey, Klarov 3, 11821 Praha, Czech Republic, and Department of Environmental Assessment, SLU Box 7050, S-750 07 Uppsala, Sweden.
K. Bishop.[2] Department of Environmental Assessment, SLU Box 7050, S-750 07 Uppsala, Sweden.

[1]Author to whom all correspondence should be addressed. e-mail: stephan.kohler@sek.slu.se
[2]Previous address: Department of Physical Geography, Umeå University, Umeå, Sweden.

© 1999 NRC Canada

Fig. 1. Sampling locations in Sweden.

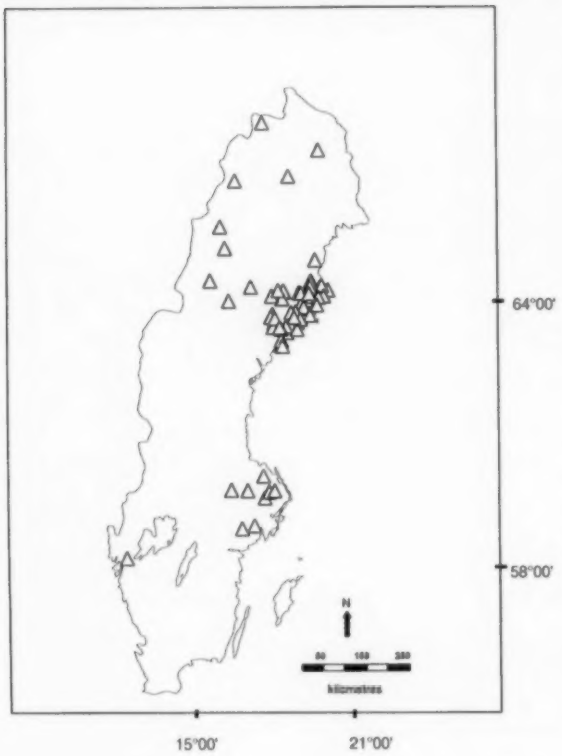

density 13.7 μmol·L^{-1}). These models are used to predict the effect of organic acidity in acidification models (Sullivan 1996) but may also be used to quantify natural acidity (Laudon et al. 1999). Site density has a profound effect on calculating pH and must be carefully calibrated. In calibrating such models, it is of special interest to validate whether the use of average values for site densities and acid strength may result in pH or acidity status predictions that are incorrect due to natural variability in the character of NOM. In the very poorly buffered pH range between pH 4.7 and 6.7, comparably small uncertainties in the charge balance caused by the varying character of NOM have been shown to cause large uncertainties in predicting pH (Schecher and Driscoll 1995). Here, very accurate pH modeling is necessary, as this is the same pH range where the solubility of inorganic Al species toxic to fish is increasing. A direct analysis of the acid–base buffering characteristics of natural surface water samples is difficult due to the low concentration of NOM, sluggish equilibria, and NOM–metal interactions (Lövgren et al. 1987). One of the two main approaches for studying NOM acid–base character consists of characterizing defined, preconcentrated fractions of NOM (e.g., Pettersson et al. 1993; Ephraim et al. 1995). This method, however, involves the risk of altering the character during the extraction procedure (Shuman 1990). The other method is the statistical evaluation of a set of samples, such as where regional surveys of lake water chemistry have been used (Driscoll et al. 1989, 1994; Wilkinson et al. 1992).

The lack of methods for direct determination has limited the direct study of site densities. Using a semidirect titration method, recently presented by Hruška (1994), it is possible to determine the site densities of individual lake samples based on the combined technique of titration and charge balance (Driscoll et al. 1989). We compare these pH modeling results with an independent but equivalent method presented by Hemond (1990) using an average site density, total organic carbon (TOC), and alkalinity titrations.

In this paper, we test the hypothesis that differences between the average site density originating from a set of samples and individual site densities may result in significant deviation between predicted and measured pH. Schecher and Driscoll (1995) demonstrated the large effect that TOC and the choice of organic acid model may have on the accuracy of the charge balance in surface waters using Monte Carlo simulations.

Despite the large variation in site density and buffering characteristics reported in the literature (Hruška et al. 1996), the original Oliver et al. (1983) equation has been successfully used in a number of studies to model anion deficit without calibration in lakes (Kortelainen 1993) and streams (LaZerte and Dillon 1984). In this study, we focus on the effect of site density on the modeling of pH and the precision of the charge balance. Here, the Oliver et al. (1983) equation is used together with the independently determined average site density to estimate organic acid deprotonation for both pH modeling approaches.

In many studies on the character and reactivity of organic acids, a distinction is made between total and dissolved components using a 0.45-μm filter (Driscoll 1984; Driscoll et al. 1994). There is increasing evidence available that this type of filtering procedure does not truly define the border between dissolved and particulate matter (Ledin 1993; Düker 1998). In this study, we analyze both filtered and unfiltered samples to test if there are differences site density, buffering capacity, and pH.

Methods

Ninety-four lakes, mostly in northern Sweden, were sampled over the course of 2 weeks during early autumn of 1997 and 1998 (Fig. 1). They were selected to encompass a large range of lake chemistry, including low ionic strength lakes from northern Sweden as well as lakes affected by seasalt and anthropogenic acidification from the southern part of the country. TOC concentrations were spread over a range of 1–36 mg·L^{-1} (average 15 mg·L^{-1}). The samples were stored in the dark and cold until further analysis within 1 week of their arrival at the laboratory. Seventy-four of the 94 samples were analyzed for site density, cations, and anions, while pH, TOC, and two-point alkalinity (Henriksen 1982) were determined on all samples. Of these 74 lakes, 13 were also filtered with a 0.45-μm filter to study the effect of filtering on site density, buffering capacity, and pH.

Inorganic constituents

The cations Ca^{2+}, Mg^{2+}, Na^+, K^+, Al^{3+}, and Fe^{3+} were determined with flame atomic absorption spectroscopy (AAS 3100, Perkin-Elmer Corp., Norwalk, Conn.) and the base cations (C_b) were calculated as

$$(1) \qquad C_b = 2[Ca^{2+}] + 2[Mg^{2+}] + [Na^+] + [K^+].$$

Concentrations of the inorganic anions SO_4^{2-}, Cl^-, and NO_3^- in the samples were determined by liquid ion chromatography (LC-

© 1999 NRC Canada

6A, Shimadzu Corp., Kyoto, Japan). The amount of strong acids (C_a) may then be calculated from these concentrations:

$$(2) \quad C_a = 2[SO_4^{2-}] + [Cl^-] + [NO_3^-].$$

Organic acid determination

The analytical procedure to estimate the organic acid concentration of natural waters has been presented by Hruška et al. (1996). To determine the organic acid concentration, an aliquot of sample was passed through a column with strongly acidic cation-exchange resin (Dowex 50 Wx12, 50/100 mesh, BDH Laboratories, Poole, England). The column used in this study was 10 mm in diameter and 65 mm high containing 4.5 mL of resin with a total volume of 5.1 mL. The exchange sites of the resin were presaturated with H^+ using 4 mol HCl·L^{-1}. After this preparation, deionized water was passed through the column to remove the remaining HCl until the effluent was free of chloride. An aliquot of the sample was then placed in a sample reservoir and passed through the column with a peristaltic pump at a flow rate of 9 mL·min^{-1}. An initial volume of effluent (about 40 mL) was discarded and 100 mL of exchanger-processed effluent was collected. Cations (except strongly complexed forms of Al and Fe) were retained in the resin, displacing H^+. Thus, the resulting effluent contained a mixture of strong mineral acids (H_2SO_4, HCl, HNO_3), organic acids, dissolved Si, and strong Al–organic and Fe–organic complexes. The sum of the mineral and organic acid concentrations was determined by potentiometric titration of the effluent immediately after the cation-exchange procedure. The effluent (25 mL) was titrated beyond the inflection point with 5 mmol NaOH·L^{-1} using an autotitrator (DL 70, Mettler, Toledo, Germany). The maximum addition in one step of the titration was 0.2 mL (40 μequiv.·L^{-1}) of 5 mmol NaOH·L^{-1}. The samples were purged continuously with nitrogen gas to remove atmospheric CO_2, and the titration was carried out at room temperature. The inflection point was detected as the maximum of the first derivative of the titration curve. The equivalence point of the ion-exchanged effluent fell within the pH interval 6.8–7.8. The total acid concentration (c_{TA}) was estimated as the amount of NaOH required to reach the equivalence point.

Among the principal functional groups present in natural organic acids, the carboxylic groups have the lowest pK_a values (Stevenson 1994), generally below 7.0. Thus, we assumed that the carboxyl groups were entirely dissociated at the equivalence point, while other weak organic acid functional groups (e.g., phenolic and amino groups) remained protonated. The total carboxylic group content ($[OA^-]_{total}$) was therefore estimated as

$$(3) \quad [OA^-]_{total} = c_{TA} - C_a.$$

Organic carbon, site density, and charge density

Organic carbon (TOC and dissolved organic carbon (DOC)) were determined using a catalyzed combustion method (TOC 5000, Shimadzu Corp.). The site density of carboxylic groups, also referred to as the "concentration of acidic groups per mg C of DOC" (Driscoll et al. 1989) or "carboxyl content" (Oliver et al. 1983), was calculated as the amount of carboxylic groups estimated from the titration ($[OA^-]_{total}$, microequivalents per litre) divided by the DOC or TOC concentration (milligrams C per litre):

$$(4) \quad \text{Site density} = [OA^-]_{total}/\text{DOC} \ (\mu\text{equiv.}\cdot\text{mg}^{-1}).$$

Charge density (eq. 6) (Wright 1989) was calculated as the organic acid anion concentration, estimated from charge discrepancy (eq. 5) of base cations (C_b), strong acid anions (C_a), and bicarbonate and hydrogen ions ($[OA^-]_{pH}$, microequivalents per litre) divided by the DOC concentration (milligrams C per litre):

$$(5) \quad [OA^-]_{pH} = C_b - C_a - [HCO_3^-] - 2[CO_3^{2-}] - [OH^-] + [H^+]$$

$$(6) \quad \text{Charge density} = [OA^-]_{pH}/\text{DOC} \ (\mu\text{equiv.}\cdot\text{mg}^{-1}).$$

Two-point alkalinity

The buffering capacity down to pH 4.5 was determined using two-point alkalinity (ALK_{twp}) (Henriksen 1985). All samples were initially spiked with a standard solution (0.025 mol K_2HPO_4–KH_2PO_4·L^{-1}, 0.5 mol L^{-1} KCl) resulting in a known concentration of phosphoric acid buffer solution (about 400 μmol·L^{-1}) and KCl (5 mmol·L^{-1}). During the titration, the samples were continuously bubbled with an artificial air mixture, as recommended by Cantrell et al. (1990), of a known CO_2 content (440 ppm CO_2). Titrations were done using an automated titrator at 24 ± 1°C. The amount of weak acids in the sample was then determined as the difference between the equivalent amount of acid used for a sample and a blank titration of deionized water spiked with the K_2HPO_4–KH_2PO_4 buffer solution. Two-point alkalinity may be measured within an error of 1–2% equal to 2–5 μequiv.·L^{-1} within the range of pH 4–8 and includes virtually all bicarbonate alkalinity (Stumm and Morgan 1996) plus all other weak acid systems including Al and organic acids that provide buffering from the original pH down to pH 4.5. The buffering capacity remaining at pH 4.5 is primarily due to dissociated strong organic acids (β × DOC, microequivalents per litre). In the charge balance calculations, the sum of the dissociated strong and weak organic acids is therefore estimated using the apparent charge density β at pH 4.5 (eq. 7) from the two-point alkalinity titration. Thus, C_b–C_a in eq. 5 may be substituted by CBALK (CBALK = ALK_{twp} + β × DOC).

This type of charge balance is defined as in Hemond (1990) with the exception that we used two-point alkalinity instead of Gran alkalinity:

$$(7) \quad [OA^-]_{pH} = \text{CBALK} - [HCO_3^-] - 2[CO_3^{2-}] - [OH^-] + [H^+] = ALK_{twp} + \beta \times \text{DOC} - [HCO_3^-] - 2[CO_3^{2-}] - [OH^-] + [H^+].$$

In a previous study (S. Köhler et al., unpublished data) using a large data set (n = 900), we were able to show that the use of CBALK decreased the error in charge balance calculations, thus significantly increasing the precision in modeled pH. The empirical charge density factor β (μequiv.·mg TOC^{-1}) was optimized using all lakes with a C_b–C_a below 250 μmol·L^{-1}, equivalent to selecting only samples below pH 7.5:

$$(8) \quad C_b - C_a = ALK_{twp} + \beta \times \text{DOC}.$$

Filtration

Thirteen lakes were filtered using a coarse (1.2-μm GFF) glass-fiber filter followed by a 0.45-μm Millipore filter. Filter papers were rinsed with deionized water and the first filtrate was discarded.

Air-equilibrated pH and pH modeling

The air-equilibrated pH was determined using an automated titrator. The samples were equilibrated with a known p_{CO_2} (440 and 240 ppm CO_2) using gas bottles of technical-grade air. The pH readings were obtained after 10–15 min of continuous stirring and bubbling of the gas using an Orion low ionic strength combination electrode (ROSS 8162C, Orion Research, Inc., Beverly, Mass.). The pH was modeled using two different charge balance approaches and a previously determined set of equilibrium constants for the dissociation of organic anions ($[OA^-]_{pH}$) using a three-pK_a model (Table 1). The constants for the bicarbonate sys-

© 1999 NRC Canada

Table 1. Site density and organic acid constants (pK_a) used for the modeling of $[OA^-]_{pH}$ and pH together with the original model parameters of the Oliver et al. (1983) model ($pK_a = a + b \times pH + c \times pH^2$).

	Parameters (Oliver et al. 1983)	pK_a values (this study)
	$a = 0.96$	$pK_{a1} = 3.6$
	$b = 0.9$	$pK_{a2} = 4.2$
	$c = -0.039$	$pK_{a3} = 5.5$
Site density ($\mu mol \cdot mg^{-1}$)	10	8.6

tem were corrected for effects of ionic strength (Stumm and Morgan 1996). All calculations were done in an Excel spreadsheet that had been cross-validated with the equilibrium programs ALCHEMI (Schecher and Driscoll 1995) and SolGasWater (Eriksson 1979).

As we do not use equilibrium constants for either Al or fluoride in our model, those two species are not taken into account in all the above definitions of charge balance. The measured concentrations of Al were very low and the average charge of Al at the endpoint of the titration is close to zero (Schecher and Driscoll 1995).

To predict the pH of a sample using the equilibrium model (parameters in Table 1), the pH of the sample was iteratively adjusted until the sum of the ions in the estimate of $[OA^-]_{pH}$ in eqs. 5 and 7 differed less than 0.1 $\mu equiv. \cdot L^{-1}$ from the estimated charge balance using either of the two described charge balance approaches (CBALK or C_b–C_a).

Note that the right-hand sides of both eqs. 5 and 7 are only dependent on the two measured parameters TOC and pCO_2.The only other unknown in the model is pH.

Results

Lake chemistry

The chemistry of the analyzed lakes spans a wide range of ionic strength (200–7000 $\mu mol \cdot L^{-1}$), TOC (1–36 $mg \cdot L^{-1}$), and pH (4.5–8.5) (Table 2). The correlation between CBALK and C_b–C_a in the range up to 400 $\mu mol \cdot L^{-1}$ is strong (C_b–C_a = 1.02 × CBALK, $r^2 = 0.94$, $n = 74$). The difference between filtered and unfiltered alkalinity is very small and changes in CBALK are mostly due to changes in measured DOC/TOC. The two lakes excluded in the site density analysis have a very high ratio between amount of strong acids and organic acids, which makes the site density very uncertain (see Appendix). There was a good correlation of Al and Fe with TOC.

Effects of filtering

The filtering procedure (0.45 µm) did not result in any major systematic changes in sample composition (Table 3). For the analysis, we excluded extreme values, e.g., all samples with C_b–C_a larger than 400 $\mu mol \cdot L^{-1}$. We then compared the average difference between unfiltered and filtered samples using a t test ($p < 0.02$).

Generally, there was a very strong correlation between the filtered and the unfiltered samples. On average, filtering removed about 2 $\mu mol\ Fe \cdot L^{-1}$, 3 $\mu mol\ Ca \cdot L^{-1}$, 5 $\mu mol\ Cl \cdot L^{-1}$, and 0.3 $mg\ TOC \cdot L^{-1}$, but none of those changes was significantly different from the unfiltered values ($p < 0.02$) (Table 3). No parameter connected to buffering, i.e., the amount of titrated organic acid ($[OA^-]_{total}$), anion deficit ($[OA^-]_{pH}$), two-point alkalinity (ALK_{twp}), or the calculated site density, showed any significant change after filtering.

Site density

After initial data treatment (see Appendix), the range of observed site densities was between 5.7 and 12.7 $\mu equiv. \cdot mg\ TOC^{-1}$. The average site density is almost normally distributed around 8.5 $\mu equiv. \cdot mg\ TOC^{-1}$ with a standard deviation of ±1.6 $\mu equiv. \cdot mg\ TOC^{-1}$ (Fig. 2). The range in site densities of this lake data set is larger than that observed for the four streams (range 6.3–9.9 $\mu equiv. \cdot mg\ TOC^{-1}$, $n = 100$). Site density was determined on both filtered and unfiltered samples from 13 of the study lakes. The average difference in site density determination was 1.1 $\mu equiv. \cdot mg\ TOC^{-1}$.

Charge density factor β

Charge density factor β in eq. 8 was optimized using the results from C_b–C_a lower than 250 $\mu mol \cdot L^{-1}$. It was changed until the slope of C_b–C_a against CBALK was not significantly different from a line of origin ($p < 0.02$). The β in eq. 8 for this data set is 7.0 $\mu mol \cdot mg\ TOC^{-1}$.

Modeling of charge balance and pH

The measured site densities were used to study how site density affects charge balance calculations and modeling of pH. As a first step, measured pH was compared with model calculations of pH using an average site density for all the lakes and the data with CBALK below 400 $\mu mol \cdot L^{-1}$. The mean error in pH prediction is 0.05 pH unit for the CBALK approach and 0.1 pH unit for C_b–C_a using a uniform site density. Using the individual site densities for the same data, the use of CBALK resulted in a mean error of prediction of 0.17 pH unit compared with 0.08 pH unit using C_b–C_a.

The precision of the two approaches for estimating $[OA^-]_{pH}$ (eqs. 5 and 7) may be compared using fixed pH calculations with the data points where C_b–C_a is lower than 400 $\mu mol \cdot L^{-1}$. In this case, no pH iteration is executed, but instead, $[OA^-]_{pH}$ is calculated from the measured pH, pCO_2, and TOC. The mean difference in charge balance using CBALK and average site density was the lowest of all possible combinations used in the charge balance calculations (Table 4).

The importance of the specific value chosen when using a uniform site density for all the study objects was further investigated by modeling pH in each lake using three different site densities (8.6, 7.0, and 10.2 $\mu equiv. \cdot mg\ TOC^{-1}$, average 8.6 ± 1.6 $\mu equiv. \cdot mg\ TOC^{-1}$) but using the same set of pK_a values (Table 2).

Discussion

To predict the influence of DOC on the pH of surface waters, one can refer to a variety of equilibrium models that specify site densities and pK_a distributions for NOM (Gamble 1970; Oliver et al. 1983; Cantrell et al. 1990; Perdue 1990; Tipping and Hurley 1992; Kortelainen 1993; Driscoll et al. 1994; Leenheer et al. 1995; Hruška et al. 1997). The range for the reported site densities lies between 5 and 20 $\mu equiv. \cdot mg\ TOC^{-1}$ (Fillion et al. 1998). There is also a large span in the published acid–base properties (pK_a values) of NOM. This may lead to a large uncertainty in the pH prediction of surface waters.

© 1999 NRC Canada

Table 2. CBALK, C_b–C_a, site density, and charge density of all analyzed lakes with measured pH below 7.0.

pH class												
4.5–5	94	116	91	160	77							
	77	85	69	139	65							
	7.7 (0.5)	5.7 (1.3)	6.6 (0.5)	7.4 (0.5)	7.7 (0.5)							
	4.8 (0.6)	4.4 (0.4)	4.6 (0.4)	5.7 (0.2)	5.4 (0.3)							
5–5.5	223	162	53	142	111	197	155	249	164			
	188	154	42	136	102	194	138	239	162			
	7.0 (0.5)	6.9 (0.5)	6.4 (0.5)	7.6 (0.5)	7.3 (0.5)	7.5 (0.5)	8.1 (0.5)	7.6 (0.5)	7.7 (0.5)			
	5.6 (0.1)	6.0 (0.1)	4.9 (0.4)	5.8 (0.1)	6.0 (0.1)	6.5 (0.1)	6.0 (0.1)	6.7 (0.0)	6.7 (0.1)			
5.5–6	212	196	116	117	245	227	94	81				
	218	193	104	126	212	225	75	93				
	7.6 (0.5)	7.6 (0.5)	7.6 (0.5)	8.5 (0.5)	6.6 (0.5)	7.6 (0.5)	6.8 (0.7)	7.9 (0.6)				
	7.5 (0.0)	7.1 (0.0)	6.4 (0.1)	8.6 (0.2)	6.5 (0.1)	8.0 (0.1)	6.5 (0.3)	8.4 (0.3)				
6–6.5	57	211	118	252								
	60	206	114	263								
	11.1 (0.7)	8.0 (0.5)	7.6 (0.7)	8.3 (0.6)								
	9.4 (0.6)	7.8 (0.1)	7.7 (0.3)	9.2 (0.3)								
6.5–7	129	158	171	128	120	149	111	266	182	183	82	151
	89	166	180	116	111	158	120	268	198	147	59	142
	6.4 (0.6)	8.7 (0.6)	9.1 (0.5)	6.7 (0.6)	6.7 (0.6)	8.6 (0.6)	9.2 (0.7)	8.7 (0.5)	10.4 (0.6)	6.6 (0.4)	7.1 (1.2)	6.7 (0.6)
	5.8 (0.4)	9.1 (0.8)	9.8 (0.9)	7.8 (1.2)	6.8 (0.7)	9.6 (1.5)	8.2 (1.3)	9.4 (0.9)	11.2 (2.1)	6.7 (0.9)	1.4 (9.0)	7.7 (1.3)

Note: The errors of site density (see Appendix) and charge density (using a pH interval of 0.1 unit) are given in parentheses. Samples were sorted into pH intervals of 0.5 pH unit.

© 1999 NRC Canada

Table 3. Statistical evaluation of the effect of filtering on different aqueous constituents.

	TOC ($mg \cdot L^{-1}$)	Al ($mg \cdot L^{-1}$)	Fe ($mg \cdot L^{-1}$)	Ca ($mg \cdot L^{-1}$)	Mg ($mg \cdot L^{-1}$)	ANC ($mol \cdot L^{-1}$)	c_A ($mol \cdot L^{-1}$)
r^2	0.977	0.985	0.851	0.983	0.952	0.999	0.999
Difference	0.39 ns	0.009 ns	0.12 ns	0.12 ns	0.015 ns	0.046 ns	–0.008 ns

Note: Data are coefficients of variance between filtered and unfiltered samples. ns, not significant at $p < 0.02$.

Fig. 2. Distribution of site density data of the studied lakes compared with the data from long-term measurements on two first-order, organic-rich streams in the Czech Republic (Czerny Potok and Filic) and site densities from two streams in northern Sweden (Svartberget catchment weirs SVA and SVG) measured through the spring flood episode of 1997 (J. Hruška, unpublished data) and a normal distribution curve (mean = 8.6 μequiv.·mg TOC^{-1}, standard deviation = ±1.6 μequiv.·mg TOC^{-1}).

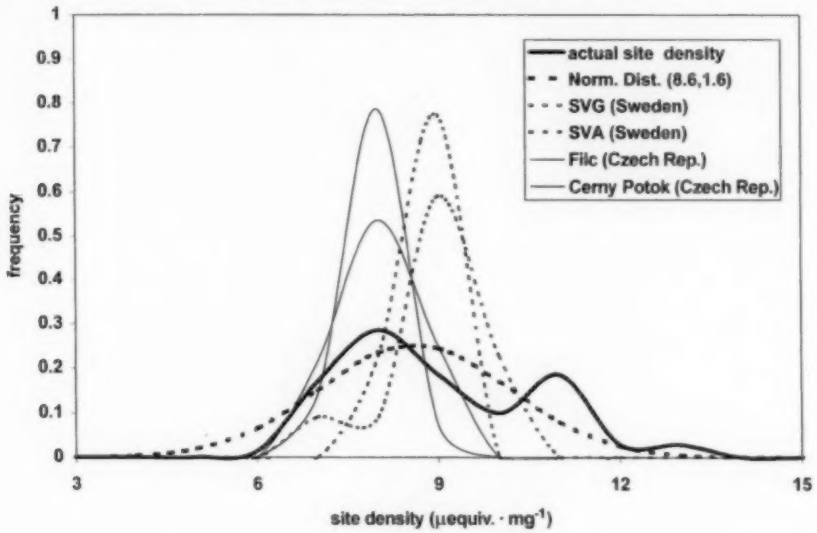

Table 4. Average error in charge balance calculations ($\mu mol \cdot L^{-1}$).

	CBALK	C_b–C_a
Individual site density	16	10
Average site density	5	12

The methodological problems when using natural samples with comparatively low concentrations of NOM and the presence of other aqueous constituents are complicated by the fact that a true equilibrium analysis is difficult to achieve above pH 6 (Lövgren et al. 1987). If the span in site density and pK_a values results largely from methodological constraints, and there is a degree of similarity in NOM properties, it may be possible to find generalized models of NOM properties. These are useful in the context of environmental monitoring programs and other such applications where it is not feasible to calibrate for each specific object being studied. This study has therefore sought to analyze the variation in site density of Swedish surface waters using an equilibrium model very similar to the original values published by Oliver et (1983), since this is probably the model that has been applied most widely.

The observed variability in site density (Fig. 2) was relatively large, 5.7–12.7 μequiv.·mg TOC^{-1}, and the observed site densities are almost normally distributed around the average value of 8.6 μequiv.·mg TOC^{-1}. This may reflect either the true range of natural variation or the random error in the analytic determination of site density. Both the data from the long-term analysis of the streams (Hruška et al. 1997) and the replicate measurements of the site densities of the filtered and unfiltered lake samples, using exactly the same analytical procedure, show standard deviations below 1 μequiv.·mg TOC^{-1}. This is an indication that the observed range of site densities is most likely due to natural variability within the sample population of lakes. The combined use of C_b–C_a and the individual site densities performed better in the charge balance calculations at fixed pH (mean error about 9 $\mu mol \cdot L^{-1}$) than when the average site densities and C_b–C_a (mean error about 12 $\mu mol \cdot L^{-1}$) or CBALK together with the individual site density were used (mean error about 16 $\mu mol \cdot L^{-1}$). Although the combined use of CBALK and the average site density (8.6 μmol·mg TOC^{-1}) did show the best performance (Table 4) in the charge balance, we conclude that the natural variation in site density is no artifact. The results obtained from the individual site densities and the determination of C_b–C_a as an estimate of buffering capacity are thus consistent.

Some samples have site densities that deviate more than two times the analytic error sigma ($\sigma_{site\ density}$, see Appendix) from the average value of 8.6. There are 11 lakes with significantly higher site density (site density > $8.6 + 2\sigma_{site\ density}$) and 16 with significantly lower site density (site density <

© 1999 NRC Canada

Fig. 3. (*a*) Modeled and measured pH using individual site densities (solid triangles) and average site densities (open diamonds). (*b*) Effect of varying site density ($[OA^-]_{pH}$·TOC $^{-1}$) on pH modeling using C_b–C_a and equilibrium constants from Table 1. Open circles, site density 10.2; open diamonds, site density 8.6; solid circles, site density 7.0.

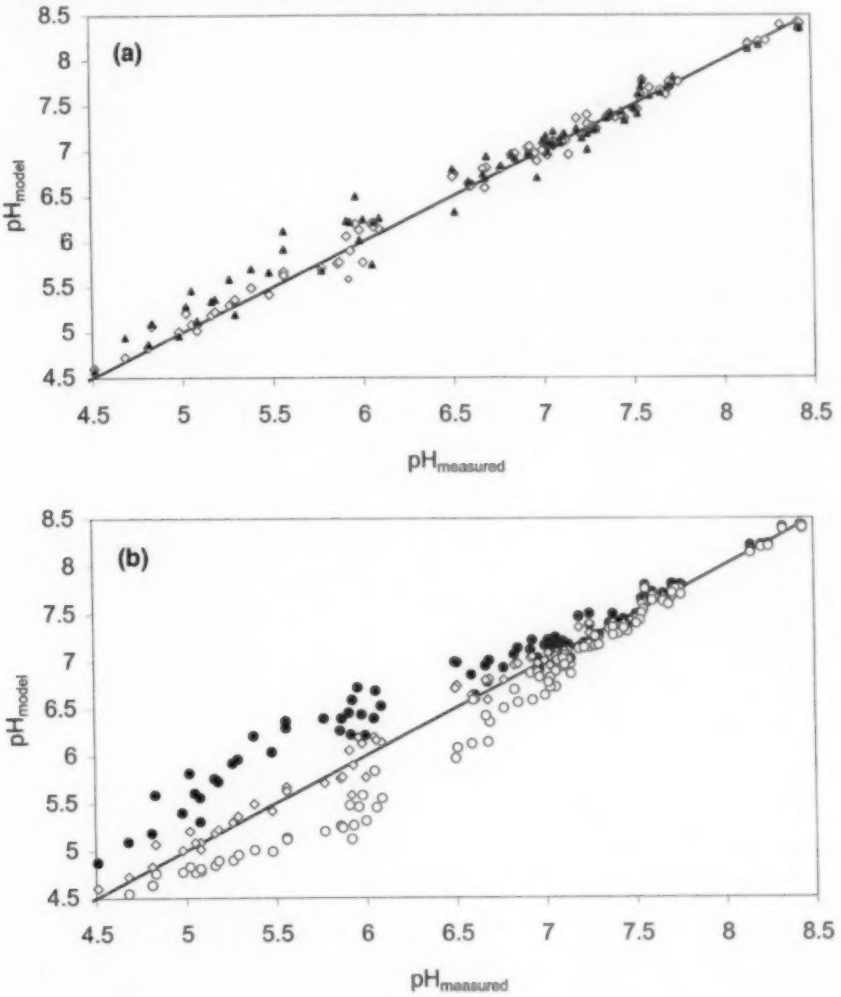

$8.6 - 2\sigma_{\text{site density}}$). Of the 11 lakes, only three lakes, all with pH below 7, have a pH deviation from the model (Table 1 using CBALK and average site density) larger than 0.1 pH unit. Site density may have a pronounced effect on modeled pH within the poorly buffered pH range of 5.0–6.5 (Fig. 3*b*). But due to the large buffering capacity of bicarbonate, site density has only a very marginal effect on the outcome of the pH modeling at pH higher than 7.0. This leads to a large uncertainty in the charge density calculation in that pH range. Thus, lakes with pH higher than 7.0 cannot be used to validate organic acid site densities. For the three lakes with a pH error of greater than 0.1 unit when using CBALK and the average site density, the individual site density with C_b–C_a did not result in a significantly (defined here as 0.1 pH unit, see below) better pH calculation.

Of the 11 lakes with a significant lower site density, only five had a pH prediction deviating more than 0.1 pH unit from the measured value. Here, the use of C_b–C_a and the individual site density did produce better pH modeling in two of the five cases. Taken together, we have no strong evidence that the use of CBALK and the average site density leads to systematic errors in pH and organic acid charge modeling; instead, this approach renders the best pH modeling performance in our data set. An uncertainty in the pH determination of 0.1 pH unit that may arise from the use of standard buffer solutions (National Bureau of Standards, error 0.05 pH unit) is too large to validate organic acid site densities.

The mean error in model prediction presented here (0.05 pH unit) gives us confidence that even the choice of pK_a values (Table 1) used in our model reproduces very well the acid–base characteristics of TOC present in Swedish surface waters. The equilibrium model used here also compares well with the one presented for Finnish lakes by Kortelainen

© 1999 NRC Canada

(1993). Her model was calibrated through the use of extracted hydrophobic and hydrophilic NOM. That both models show such large similarities suggests that the acid–base character of NOM was not changed quantitatively by the extraction procedure. A slightly lower value of organic acid site density was previously observed by Eshleman and Hemond (1985), who gave a site density of 7.5 μmol·mg TOC^{-1}, almost half of the value documented by Driscoll et al. (1994).

No pH deviation between modeled and measured pH larger than 0.23 pH unit (n = 77 lakes) was observed in the pH range below 7.5 except for one sample (0.33 pH unit). This error is much lower than the one predicted by Schecher and Driscoll (1995), who gave 0.7 pH unit (pH range between 5.4 and 6.8, average 5.8) as an 98% confidence limit for the range of pH predictions for a sample containing 15 mg TOC·L^{-1} (equivalent to about 1250 μmol C·L^{-1}). Their estimate of the 98% confidence limit for charge balance (from C_b–C_a) is larger than 40 μmol·L^{-1} and was mainly ascribed to arise from the large uncertainty in the organic equilibrium constants. Given Schecher and Driscoll's (1995) estimate of large uncertainties in pH predictions, it would be very difficult for policy makers to distinguish between natural and anthropogenically caused acidity in samples with pH below about 6.8. In our data set, 98% of the samples in the pH range of interest between 5.0 and 6.8 have an uncertainty lower than 14 μmol·L^{-1}, which gives a much lower uncertainty in pH prediction. Whether the discrepancy between our error and the one estimated by Schecher and Driscoll (1995) is due to the methodology used or to different carbon character is unclear. It is important to quantify the accuracy of acidification models, as pointed out by Schecher and Driscoll (1995). If the 98% confidence measure for charge balance (C_b–C_a) is to be adapted in environmental monitoring programs, the comparably large uncertainty in both models is of concern.

Another point of interest was to study the effect of particulate material on pH in the lake water samples. The amount of particulate material collected during sampling is dependent on the geometry of the lake and the time of sampling. Especially in larger streams and lakes under high-flow conditions, it is important to distinguish between dissolved and particulate samples when analyzing Al (Driscoll 1984). We observed no significant changes after filtering through a 0.45-μm filter. Our data suggest that filtering of lake water does not affect pH equilibria or pH modeling within the observed precision using the CBALK approach. Our modeled pH is only affected by changes in TOC and measured alkalinity, both of which did not change significantly during the filtering procedure. We suggest that not enough particulate material is removed by filtering Swedish lake water to quantitatively effect pH buffering down to pH 4.5.

Conclusions

The observed variation in site densities for the studied lakes is larger than that in the densities observed in two very different sets of streams in Sweden and the Czech Republic using exactly the same analytical procedure. This variation (5.7–12.7 μequiv.·mg TOC^{-1}) is probably due to differences in catchment character and the probable reprocessing of carbon in the lakes studied. This variability, however, does not affect pH modeling in the pH range below pH 7.5. We found that a uniform and independently estimated site density, together with a set of three acid–base equilibrium constants for TOC using measured alkalinity, is able to reproduce pH within an average error of 0.05 pH unit compared with an average error of 0.09 pH unit when using individually determined site densities (average 8.6 μequiv.·mg TOC^{-1}) and measured C_b–C_a. Filtering did not affect lake water chemistry significantly and had no effect on the modeling of pH.

Acknowledgements

The postdoctoral position of J. Hruška was financed by the Swedish Natural Science Research Council. The Ph.D. position of S. Köhler is financed through the Center for Environmental Research in Umeå. K. Bishop was financed through a grant from the Umeå University Faculty of Mathematics and Natural Sciences.

References

Cantrell, K.J., Serkiz, S.M., and Perdue, P.M. 1990. Evaluation of acid neutralization capacity data for solutions containing natural organic acids. Geochim. Cosmochim. Acta, **54**: 1247–1254.

Driscoll, C.T. 1984. A procedure for the fractionation of aqueous aluminum in dilute acidic waters. Int. J. Environ. Anal. Chem. **16**: 267–283.

Driscoll, C.T., Fuller, R.D., and Schecher, W.D. 1989. The role of organic acids in the acidification of surface waters in the eastern U.S. Water Air Soil Pollut. **43**: 21–40.

Driscoll, C.T., Lehtinen, M.D., and Sullivan, T.J. 1994. Modeling the acid–base chemistry of organic solutes in Adirondack, New York, Lakes. Water Resour. Res. **30**: 297–306.

Düker, A. 1998. Natural aquatic colloidal matter — characteristics and impact on the mobility of trace metals and organics. Ph.D. thesis, Stud. Art Sci. No. 180, University of Linköping.

Ephraim, J.E., Pettersson, C., Norden, M., and Allard, B. 1995. Potentiometric titrations of humic substances: do ionic strength effects depend on the molecular weight. Environ. Sci. Technol. **29**: 622–628.

Eriksson, G. 1979. An algorithm for the computation of aqueous multi-component, multiphase equilibria. Anal. Chim. Acta, **112**: 375–383.

Eshleman, K.N., and Hemond, H.F. 1985. The role of organic acids in the acid–base status of surface waters at Bickford Watershed, Massachusetts. Water Resour. Res. **21**: 1503–1510.

Fillion, N., Probst, A., and Probst, J.L. 1998. Natural organic matter contribution to throughfall in French forests. Environ. Internat. **24**: 547–558.

Gamble, D.S. 1970. Titration curves of fulvic acid: the analytical chemistry of a weak acid polyelectrolyte. Can. J. Chem. **48**: 2662–2669.

Hemond, H.F. 1990. Acid neutralizing capacity, alkalinity, and acid–base status of natural waters containing organic acids. Environ. Sci. Technol. **24**: 1486–1489.

Henriksen, A. 1982. Alkalinity and b acid precipitation research. Vatten, **38**: 83–85.

Hruška, J. 1994. Contribution of organic acids to total acidity of surface waters in peatland areas affected by anthropogenic acidification.. Ph.D. thesis, Czech Geological Survey, Prague, Czech Republic. (In Czech.)

© 1999 NRC Canada

Hruška, J., Johnson, C.E., and Kram, P. 1996. Role of organic solutes in the chemistry of acid-impacted bog waters of the western Czech Republic. Water Resour. Res. **32**: 2841–2851.

Hruška, J., Johnson, C.E., Kram, P., and Liao, C.Y. 1997. Organic solutes and the recovery of a bog stream from chronic acidification. Environ. Sci. Technol. **31**: 3677–3681.

Kahl, J.S., Norton, S.A., Cronan, C.S., Fernandez, I.J., Bacon, L., and Raines, T.A. 1991. Maine. *In* Acid deposition and aquatic ecosystems. *Edited by* D.F. Charles. Springer-Verlag, New York. pp. 203–225.

Kortelainen, P. 1992. Charge density of total organic carbon in Finnish lakes. Environ. Pollut. **77**: 2–3.

Kortelainen, P. 1993. Contribution of organic acids to the acidity of Finnish lakes. Ph.D. thesis, Water Environ. Res. Inst. Natl. Board Waters Environ. No. 13, Helsinki, Finland.

Laudon, H., and Bishop, K. 1999. Quantifying sources of ANC depression during spring flood episodes in northern Sweden. Environ. Pollut. **105**: 427–435.

LaZerte, B.D., and Dillon, P.J. 1984. Relative importance of anthropogenic versus natural sources of acidity in lakes and streams of central Ontario. Can. J. Fish. Aquat. Sci. **41**: 1664–1677.

Ledin, A. 1993. Colloidal carrier substances — properties and impact on trace metal distribution in natural waters. Ph.D. thesis, Stud. Art Sci. No. 91, University of Linköping.

Leenheer, J.A., Wershaw, R.L., and Reddy, M.M. 1995. Strong-acid, carboxyl-group structures in fulvic acid from the Suwannee River, Georgia. 1. Minor structures. Environ. Sci. Technol. **29**: 393–398.

Lövgren, L., Hedlund, T., Öhman, L.O., and Sjöberg, S. 1987. Equilibrium approaches to natural water systems — 6. Acid–base properties of a concentrated bog-water and its complexation reactions with aluminium(III). Water Resour. Res. **21**: 1401–1407.

Munson, R.K., and Gherini, S.A. 1993. Influence of organic acids on the pH and acid-neutralizing capacity of Adirondack lakes. Water Resour. Res. **29**: 891–899.

Oliver, B.G., Thurman, E.M., and Malcolm, R.L. 1983. The contribution of humic substances to the acidity of colored natural waters. Geochim. Cosmochim. Acta, **47**: 2031–2035.

Perdue, E.M. 1990. Modeling the acid–base chemistry of organic acids in laboratory experiments and in freshwaters. *In* Organic acids in aquatic ecosystems. Dahlem Workshop Reports in Life Sciences Research Report 48. *Edited by* E.M. Perdue and E.T.J. Gjessing. John Wiley & Sons, New York. pp. 111–126.

Pettersson, C., Håkansson, K., Karlsson, S., and Allard, B. 1993. Metal speciation in a humic surface water system polluted by acidic leachates from a mine deposit in Sweden. Water Res. **27**: 863–871.

Schecher, W.D., and Driscoll, C.T. 1995. ALCHEMI: a chemical equilibrium model to assess the acid–base chemistry and speciation of aluminum in dilute solutions. *Edited by* R. Loeppert, A.P. Schwab, and S. Goldberg. Soil Science Society of America, Inc., Madison, Wis. pp. 325–356.

Shuman, M.S. 1990. Carboxyl acidity of aquatic organic matter: possible systematic errors introduced by XAD extraction. *In* Organic acids in aquatic ecosystems. Dahlem Workshop Reports in Life Sciences Research Report 48. *Edited by* E.M. Perdue and E.T.J. Gjessing. John Wiley & Sons, New York. pp. 97–110.

Sommaruga-Wögrath, S., Koinig, K.A., Schmidt, R., Sommaruga, R., Tessadri, R., and Psenner, R. 1997. Temperature effects on the acidity of remote alpine lakes. Nature (Lond.), **387**: 64–67.

Stevenson, F.J. 1994. Humus chemistry: genesis, composition, reactions. John Wiley & Sons, New York.

Stumm, W., and Morgan, J.J. 1996. Aquatic chemistry. John Wiley & Sons, New York.

Sullivan, T.J., Cosby, B.J., Driscoll, C.T., Charles, D.F., and Hemond, H.F. 1996. Influence of organic acids on model projections of lake acidification. Water, Air and Soil Pollut. **91**: 271–282.

Tipping, E., and Hurley, M.A. 1992. A unifying model of cation binding by humic substances. Geochim. Cosmochim. Acta, **56**: 3627–3641.

Wilkinson, K.J., Jones, H.G., Campbell, P.G.C., and Lachance, M. 1992. Estimating organic-acid contributions to surface water acidity in Quebec (Canada). Water Air Soil Pollut. **61**: 57–74.

Wright, R.F. 1989. RAIN project: role of organic acids in moderating pH change following reduction in acid deposition. Water Air Soil Pollut. **46**: 251–259.

Appendix. Error analysis of site density determination

Uncertainty in the site density arises from three sources: the error in TOC analysis, the sum of the inorganic acid anions (c_A), and the standard error in the titration (c_{TA}). The standard deviation of the site density may be derived from the uncertainty in the individual analyses:

(A1) $$\sigma_{c_A} = \sqrt{\sigma_{SO_4^{2-}} + \sigma_{NO_3^-} + \sigma_{Cl^-}} \quad (\mu mol \cdot L^{-1})$$

$$\sigma_{c_{TA}} = \sqrt{\sigma_{c_A} + \sigma_{c_{TA}}} \quad (\mu mol \cdot L^{-1})$$

(A2) $$\sigma_{\text{site density}} = 0.01 \times \text{site density} \times \sqrt{(100\,\sigma_{c_{TA}}(\text{site density} \times TOC^{-1}))^2 + \sigma_{TOC}^2} \quad (\mu mol \cdot L^{-1}).$$

For this calculation, we assumed that the relative standard deviation (RSD, σ) in determination of the individual inorganic acid anions (SO_4^{2-}, Cl^-, and NO_3^-) and TOC is around 5%, while the error for the titration (c_{TA}) was assumed to be 3% (Table A1).

Table A1. Potential error in site determination arising from the uncertainties in the determination of the strong acids, TOC, and the titration.

Ratio $[OA^-] \cdot c_{TA}^{-1}$	70	60	50	40	30	20	10
Error (%)	9	10	11	13	20	35	75

© 1999 NRC Canada

Analysis of charge density and site density

Site densities for all samples ranged from 1 to 13 μequiv.·mg TOC^{-1} with an average value of 8.4 ± 2.4 μequiv.·mg TOC^{-1}. Two samples, with site densities of 0.9 and 2.1 μequiv.·mg TOC^{-1} and with an error in site density higher than 3.9 μequiv.·mg TOC^{-1}, were excluded as outliers using Dixon's Q test (Miller and Miller 1993). The modeling of pH using individual site densities can be hampered by the fact that some lakes showed charge densities (cf. eq. 5) that were larger than the total site density as determined by titration (cf. eq. 3). This should by definition not be the case. Charge densities are affected by the measured pH, and therefore, we will have to allow for an error in pH determination to check this. A lower charge density, valid at a pH value 0.1 unit below the measured pH, was calculated. This hypothetical lower charge density should be lower than the sum of measured site density and its potential error. Five of the 74 lakes did not fulfill this criterion, four of which had a potential error in site determination of larger than 2.8 μequiv.·mg TOC^{-1}. The small ratio between organic acids and strong minerogenic acids in these four lakes leads to a large uncertainty in the site density determination and therefore should be excluded from such analysis. Thus, we conclude that the apparent contradiction of a charge density larger than the analyzed site density in the vast majority of the samples may simply be a feature of the magnitude of error in the different analyses.

Appendix Reference

Miller, J.C., and Miller, J.N. 1993. Statistics for analytical chemistry. 3rd ed. Ellis Horwood, Chichester.

© 1999 NRC Canada

Bioavailability and acute toxicity of copper to rainbow trout (*Oncorhynchus mykiss*) in the presence of organic acids simulating natural dissolved organic carbon

J.C.A. Marr, J. Lipton, D. Cacela, J.A. Hansen, J.S. Meyer, and H.L. Bergman

Abstract: Copper bioavailability and toxicity to early life stage rainbow trout (*Oncorhynchus mykiss*) were evaluated by laboratory toxicity testing performed using organic acid mixtures. Geochemical modeling was used to design exposure solutions that simulate dissolved organic carbon (DOC) of a natural aquatic system and to determine the fractions of total Cu present as inorganic species (e.g., Cu^{2+}) and as individual Cu–organic complexes. Failure time modeling indicated that mortality was best predicted by a combination of total inorganic Cu and distinct Cu–organic complexes. The Cu–organic complexes that contributed to toxicity are characterized as low-affinity Cu–ligands, and our results support the hypothesis that Cu toxicity in nature is a function of the binding characteristics of individual ligands. Estimates of time-independent median lethal concentration thresholds determined at widely varying equivalent concentrations of DOC (0–16 mg/L) were constant (7.9–8.6 µg Cu/L) when modeled using the sum of inorganic Cu and Cu bound to the two low-affinity ligands as predictors of toxicity. Our results indicate that Cu bound to organic complexes may be available to fish and that acute toxicity of Cu is determined by the binding affinities of specific DOC components relative to Cu-binding affinity of fish gill.

Résumé : Nous avons évalué la biodisponibilité du cuivre et sa toxicité pour les premières phases du cycle biologique de la truite arc-en-ciel (*Oncorhynchus mykiss*) par des essais de toxicité en laboratoire à l'aide de mélanges d'acides organiques. La modélisation géochimique a servi à composer des solutions d'exposition simulant la teneur en carbone organique dissous (COD) d'un système aquatique naturel et à déterminer les fractions de Cu total présentes sous la forme d'espèces inorganiques (p.ex. Cu^{2+}) et de complexes organiques avec Cu. La modélisation de la durée jusqu'à défaillance a indiqué que la prédiction de la mortalité était optimale avec une combinaison de Cu inorganique total et de complexes organiques avec Cu. Les complexes organiques qui contribuaient à la toxicité se caractérisaient comme des ligands du cuivre à faible affinité, et nos résultats confirment que la toxicité de ce métal dans la nature est fonction des caractéristiques de liaison de chaque ligand. Les estimations des seuils médians de concentration létale indépendante de la durée, calculées pour des concentrations équivalentes très diverses de COD (0–16 mg/L) étaient constantes (7,9–8,6 µg Cu/L) lorsqu'on les modélisait avec la somme du Cu inorganique et du Cu lié aux deux ligands à faible affinité comme prédicteurs de la toxicité. Nos résultats indiquent que le Cu lié aux complexes organiques peut être biodisponible pour le poisson, et que la toxicité aiguë du Cu est déterminée par les affinités de liaison de composantes spécifiques du COD par rapport à l'affinité de liaison des branchies de poissons pour le Cu.

[Traduit par la Rédaction]

Introduction

The chemical speciation of Cu is likely to influence its toxicity to fish and therefore may have important environmental implications. The cupric ion, Cu^{2+}, is generally accepted as toxic (Howarth and Sprague 1978; Chakoumakos et al. 1979; Laurén and McDonald 1986). Other Cu–inorganic species that have been reported to contribute to toxicity include: $CuOH^+$ (Pagenkopf et al. 1974; Howarth and Sprague 1978; Chakoumakos et al. 1979), $CuCO_3^0$ (Shaw and Brown 1974), $Cu(OH)_2^0$ (Chakoumakos et al. 1979; Laurén and McDonald 1986), and $Cu_2(OH)_2^{2+}$ (Howarth and Sprague 1978; Chakoumakos et al. 1979).

A number of authors have reported that dissolved organic carbon (DOC) can reduce Cu toxicity through formation of less bioavailable Cu–organic species. Numerous ligands with differing metal complexation strengths have been used in laboratory bioassays to evaluate metal bioavailability,

Received December 19, 1997. Accepted June 2, 1998.
J14357

J.C.A. Marr[1]. Caribbean Marine Research Center, 250 Tequesta Drive, Suite 304, Tequesta, FL 33469, U.S.A.
J. Lipton and D. Cacela. Hagler Bailly Services, Inc., P.O. Drawer O, Boulder, CO 80306, U.S.A.
J.A. Hansen, J.S. Meyer, and H.L. Bergman. Department of Zoology and Physiology, University of Wyoming, Laramie, WY 82071, U.S.A.

[1]Author to whom all correspondence should be addressed. e-mail: jmarr@gate.net

© 1999 NRC Canada

including various sources of synthetic organic compounds (e.g., glycine, oxalic acid, salicylic acid, nitrilotriacetic acid, ethylenediaminetetraacetic acid), purified soil extracts, and natural waters (Winner 1985; Daly et al. 1990; Playle et al. 1993*a*; Erickson et al. 1996; Welsh et al.1996; Roy and Campbell 1997; MacRae et al. 1999*a*).

A majority of the toxicological literature supports the concepts of attenuated toxicity and bioavailability of Cu and other metals due to metal–ligand complexation. Brown et al. (1974) found that survival time for rainbow trout (*Oncorhynchus mykiss*) exposed to Cu increased linearly at humic acid concentrations of 0.9–4.5 mg DOC/L; the survival time at 4.5 mg humic acid/L increased more than twofold compared with the treatment without humic acid. Welsh et al. (1993) found that 96-h median lethal concentration thresholds (LC_{50}s) for larval fathead minnow (*Pimephales promelas*) increased in relation to concentration of naturally occurring DOC in low-pH soft water over DOC concentrations ranging from 0 to 16 mg DOC/L. Using the DOC derived from algal and daphnid blooms of a microcosm, Cu-induced mortality in *Daphnia magna* was also reduced in the presence of DOC (Meador 1991). In concept, these example studies are in agreement showing attenuation of acute Cu toxicity through the formation of Cu–organic complexes. However, certain studies have concluded that some Cu–organic complexes may be bioavailable and toxic (e.g., Guy and Kean 1980; Borgmann and Ralph 1984; Daly et al. 1990; Florence et al. 1992; Erickson et al. 1996).

Critical factors that determine Cu bioavailability in the presence of organic ligands may include the specific complexation characteristics of ligands for Cu, such as Cu-binding affinity and capacity. For instance, Cu-binding affinities determined for fish gills by Playle et al. (1993*a*, 1993*b*) and MacRae et al. (1999*a*) suggest that some forms of organically complexed Cu may be available to fish because the Cu-binding affinity of fish gills is greater than that of some organic ligands.

The ability to measure or control experimental variables (e.g., relative concentrations of free and bound metal species) and the complexation characteristics of ligands are critical to the interpretation of toxicity data and therefore important to our understanding of metal bioavailability and conclusions about metal toxicity moderation in the presence of various DOC sources. The issue of DOC mediation of metal effects is relevant to the problem of determining thresholds for metal toxicity in natural systems. For example, in the Panther Creek Basin, located in the Northern Rocky Mountain physiographic province in central Idaho, metals are released from a large inactive Cu and Co mining operation. We conducted a laboratory bioassay in which rainbow trout were exposed to Cu and a mixture of commercially available organic acids to assess Cu bioavailability and to determine remediation targets for site waters containing DOC. The mixture of organic acids was selected to simulate conditions in Panther Creek by characterizing the Cu-binding properties of site-specific DOC using the methods and rationale described by MacRae et al. (1999*b*). Further details about the geochemistry and physiography of Panther Creek are provided in the companion paper by MacRae et al. (1999*b*). We evaluated bioavailabilty of Cu with respect to acute toxicity and differences in the Cu speciation characteristics of exposure waters.

Materials and methods

The experiment was conducted at the Red Buttes Environmental Biology Laboratory, University of Wyoming, Laramie, Wyo., U.S.A.

Experimental fish

Rainbow trout eggs were obtained from Dubois Fish Hatchery, Wyoming Game and Fish Department; the fish were hatched and cultured in the laboratory using well water (hardness 220 mg/L as $CaCO_3$, alkalinity 180–210 mg/L as $CaCO_3$, pH 7.2–7.8, temperature 7°C). After hatching, rainbow trout were transferred to circular holding tanks and acclimated for >14 days to the control water used in the bioassay (hardness 25–30 mg/L as $CaCO_3$, alkalinity 22–28 mg/L as $CaCO_3$, pH 7.3–7.6, temperature 10°C). Fish condition and health were monitored daily, and fish were kept on a 12 h light : 12 h dark light cycle.

At swim-up, rainbow trout were fed frozen BioDiet® once daily at a ration in excess of 4.5% (wet weight food per wet weight body), which was a sufficient ration for growth. Fish were deprived of food 48 h before and throughout the bioassay. Fry used in the bioassay were similar in size (mean wet weight 0.36 g (SD = 0.13 g) and mean total length 35.0 mm (SD = 3.4 mm), n = 41).

Exposure water and monitoring

Exposure waters for the bioassay were formulated to simulate conditions in the Panther Creek Basin during spring runoff periods when metal concentrations are elevated. Waters were formulated by continuously mixing well water and deionized water (well water treated with sediment filtration, reverse osmosis, and separate-bed deionization) and automatically adjusted to the desired pH, as described in Marr et al. (1996). Concentrated Cu stock solutions were prepared by mixing reagent-grade chloride salt ($CuCl_2 \cdot 6H_2O$) in deionized water, stored in Mariotte bottles, and delivered to exposure aquaria via continuous-flow proportional diluters.

Organic acid (DOC) stock solutions contained malonic acid disodium salt ($C_3H_2O_4Na_2$), oxalic acid disodium salt ($Na_2C_2O_4$), and dipicolinic acid ($C_7H_5NO_4$) in deionized water mixed at constant molar ratios of 1.0:0.4:0.02, respectively, to reflect the Cu-binding characterization of natural DOC. Nominal total DOC concentrations were 0, 0.11, 0.21, 0.42, 0.84, and 1.68 mg/L, which were selected to provide Panther Creek DOC Cu-binding capacities equivalent to 0, 2, 4, 8, 16, and 32 mg/L (denoted as DOC_{eq}), respectively (MacRae et al. 1999*b*). The Cu-binding characteristics (conditional stability constants and complexation capacities) of natural DOC were determined through nonlinear regression analysis of bound versus free Cu concentraions in site waters following titration with Cu and measurement with a cupric ion selective electrode. The influence of other site-water constituents and parameters, such as competing ions, suspended particles, iron oxide particles, and storage, were evaluated and did not have an appreciable influence on Cu–DOC complexation. Furthermore, the analysis indicated that the Cu-binding characteristics of the natural DOC did not change qualitatively as shown by similarities in Cu-binding affinity and complexation capacity of site waters collected at various locations in the drainage and during low and high flows.

DOC_{eq} stock solutions for the bioassay were stored in Mariotte bottles covered with black plastic and refrigerated (4°C) to reduce bacterial growth and bio- or photo-degradation. Stock solutions were used for a maximum of 7 days. Exposure dilutions of the DOC_{eq} were achieved by metering each stock solution into the headbox of separate continuous-flow diluters so that each diluter independently maintained a constant concentration of the DOC_{eq} mixture. The average water delivery to each aquarium (8 L water

© 1999 NRC Canada

volume) was 0.2 L/min, providing a flow rate of 288 L/day (36 water volume renewals per day) and a 90% volume replacement time of <1.5 h, well within the recommendations of Sprague (1969).

Temperature and pH in headtanks were monitored and recorded continuously with a Hewlett Packard® (model 3497A) data acquisition and alarm system. Exposure and control waters were analyzed daily in water samples from randomly selected aquaria to ensure that the water quality parameters were within 10% of desired levels for hardness, alkalinity, conductivity, pH, dissolved oxygen, and temperature. Alkalinity was determined by titration using H_2SO_4 and Gran plot calculations. Hardness was determined by the EDTA titrimetric method (APHA 1992), and pH was measured using a calibrated Beckman® Omega 12 pH/ISE meter and Orion® Ross Sure Flow combination electrode with a Beckman® temperature compensation probe. Temperature was measured using a centigrade thermometer, conductivity was measured using a VWR® digital conductivity meter, and dissolved oxygen was measured using a YSI® (model 58) meter and probe.

Exposure and control waters were sampled every 3 days from randomly selected aquaria for analysis of Cu, major cations, and major anions. Water samples (25 mL) for total Cu and cations were acidified with 25 µL of 70% HNO_3 (Instra-Analyzed grade) and concentrations were determined by atomic absorption spectrophotometry using either a graphite furnace (Perkin-Elmer® model 2380 or Varian SpectrAA® model 600) or a flame (Perkin-Elmer® model 372). Water samples (25 mL) for anion analyses were stored at 4°C in the dark and analyzed using a Dionex® ion chromatograph (model 2110i). Method detection limits were as follows: Cu, 0.9 µg/L; Ca, 0.09 mg/L; K, 0.1 mg/L; Mg, 0.01 mg/L; Na, 0.06 mg/L; Cl, 0.12 mg/L; SO_4, 0.34 mg/L.

Water samples for DOC_{eq} analysis were collected in amber glass bottles, acidified with 200 µL of concentrated H_2SO_4, sealed with tinfoil under the plastic cap, and stored at 4°C in the dark until analysis. DOC was measured with a Shimadzu® TOC-5000 organic carbon analyzer. Because the DOC exposure concentrations were less than the method detection limit (2.2 mg/L), DOC concentrations were measured in the stock solutions, and the exposure concentrations were calculated based on DOC concentrations in stocks, measured stock delivery rates, and measured dilution water flow rates.

Mortality was monitored every 2 h for the first 48 h and every 6 h thereafter. Dead fish were removed upon observation and measured for length. At the end of the bioassay, all surviving fish were measured for total length and wet weight.

Exposure design

A randomized block design was used to assign exposure and control waters to aquaria. Fish were exposed to nominal Cu concentrations of 0, 5, 10, and 20 µg/L and DOC_{eq} concentrations of 0, 2, 4, 8, 16, and 32 mg/L for a total of 24 different treatments. Nominal water quality conditions were fixed as described above. Each treatment was replicated in three separate aquaria with initial density of 20 fish per aquarium. The initial loading of the fish in each aquarium was <1.5 g fish/L.

Data analysis

Calculations to determine the various inorganic and organic chemical species of Cu were performed using the geochemical speciation computer program MINEQL⁺ (Schecher and McAvoy 1991), as described in greater detail in MacRae et al. (1999*b*).

We used parametric and nonparametric methods of data analysis to evaluate relationships between Cu toxicity and DOC_{eq} and to assess Cu species in exposure waters that contributed to lethality responses. LC_{50}s were determined by maximum likelihood estimation of linear functions relating log metal concentration (as micrograms of measured total Cu and modeled Cu species per litre) to probit transformations of percent mortality (Finney 1971; McCullagh and Nelder 1989). For these analyses, a single aquarium holding 20 fish was treated as the experimental unit and time-specific percent mortality within individual aquaria were considered independent replicates. The time-independent LC_{50} estimates, or incipient lethal levels (ILLs), were determined by inspection of curves of LC_{50} values plotted versus time (Sprague 1969, 1970; Newman 1994).

Time to death (hours) of individual fish was used to estimate survivorship curves and to investigate relationships between exposure chemistry and survival. Mortality among control aquaria (0 µg Cu/L) was observed beginning at about 168 h, so statistical analyses were based on complete censoring at 168 h. Differences in survivorship between individual aquaria were statistically compared using log-rank tests for differences in Kaplan–Meier estimates of survivor functions (Kalbfleish and Prentice 1980). The geometric mean of Kaplan–Meier point estimates bounding 50% survival was determined as the median lethal time (LT_{50}). All such nonparametric analyses were conducted using nominal Cu concentration and DOC_{eq} exposure regimes as categorical strata. Preliminary analyses of this type were used to assess the efficacy of pooling fish from different aquarium replicates within a treatment for subsequent time to death analyses (Newman 1994). No significant difference ($p > 0.05$) between replicates was detectable in 23 of the 24 different treatments. This result was considered to be strong evidence for the absence of position effects, so all subsequent time to death analyses were based on pooled data.

Parametric curve fitting was used to examine the performance of different Cu species concentrations and organic acid levels as independent variables in time to death (failure time) models. The primary purpose of parametric modeling was to discern the bioavailable Cu species, which was done by identifying model(s) in which coefficients associated with DOC_{eq} were nonsignificant. Several candidate functional forms (exponential, Weibull, lognormal, and loglogistic) were compared using graphical inspection of linearizations, log likelihoods, and deviance (i.e., using goodness-of-fit criteria). These comparisons indicated that a lognormal model performed the best with the goodness-of-fit criteria, although differences in the candidate forms were minor. The lognormal failure time model asserts that the log of survival time for an individual organism is related to exposure levels. The model uses the assumption that the mean of log(survival time) can be described as a function of various stressors (e.g., Cu exposures) and that variability in specific survival times follows a normal distribution with constant variance. Mathematically, if T is a random variable representing survival times of individual organisms, then the mean of $\log(T)$ is estimated by $\hat{\mu} = \hat{\beta}\mathbf{x}$, where $\hat{\beta}$ are estimated coefficients and $\mathbf{x}$ are selected levels of modeled stressor variables (e.g. [Cu], [DOC]). The estimated survivor function $\hat{F}(t) = 1 - \hat{S}(t) = (P(T \le t)$ is given by

$$(1) \qquad \hat{F}(t) = 1 - \phi((\log(t) - \hat{\mu})/\hat{\sigma})$$

where $\hat{F}$ is frequency distribution and t is a particular nonnegative time, $\hat{\sigma}$ is the estimated standard deviation, and $\phi(\ )$ is the Gaussian distribution (Kalbfleish and Prentice 1980). The instantaneous probability of dying at t is given by the hazard function

$$(2) \qquad \hat{h}(t) = \hat{f}(t)/\hat{S}(t)$$

where $\hat{f}(t) = \exp((-\log(t) - \hat{\mu})^2/2\hat{\sigma}^2)/\hat{\sigma}t\sqrt{2\pi}$. Hence, $\hat{S}(t)$ describes the survivorship of a population of exposed organisms and $h(t)$ describes the probability that a particular organism will die at a particular time. The relative magnitude and statistical significance levels of the estimated coefficients $\hat{\beta}$ can be used, along with additional biological criteria, to assess the biological significance of the stressors of interest. Measured total Cu concentration, modeled concentrations of inorganic Cu species, Cu–organic com-

© 1999 NRC Canada

Table 1. Water chemistry conditions during the bioassay.

	pH	Alkalinity (mg/L as $CaCO_3$)	Hardness (mg/L as $CaCO_3$)	Dissolved oxygen (mg/L)	Temperature (°C)	Ca (mg/L)	K (mg/L)	Mg (mg/L)	Na (mg/L)	Cl (mg/L)	SO_4 (mg/L)
Mean	7.6	33	24.2	8.3	10	5.4	5.7	2.5	2	0.7	3.2
SD	0.08	6.6	1.9	0.3	0.3	0.62	2.99	0.22	1.22	0.12	1.32
n	69	62	77	56	69	196	196	196	196	196	193

Table 2. Mean (SD) measured Cu and geochemical species of Cu determined with the computer program MINEQL⁺.

Nominal DOC_{eq} (mg/L)[a]	Nominal Cu (µg/L)	Total Cu (µg/L)[b]	Cu_{INRG} (µg/L)	Cu^{2+} (µg/L)	Cu_{MAL} (µg/L)	Cu_{OX} (µg/L)	Cu_{DIP} (µg/L)
0	0	<0.9 (0.36)	—	—	—	—	—
0	5	4.90 (0.60)	4.9	0.79	0	0	0
0	10	9.71 (0.58)	9.72	1.58	0	0	0
0	20	18.98 (0.90)	19.01	3.09	0	0	0
2	0	<0.9 (0.35)	—	—	—	—	—
2	5	5.17 (0.56)	2.07	0.34	0.36	0.95	1.79
2	10	10.27 (0.68)	4.96	0.81	0.86	2.17	2.29
2	20	20.01 (0.85)	10.89	1.77	1.9	4.64	2.57
4	0	<0.9 (0.51)	—	—	—	—	—
4	5	5.76 (0.54)	1.28	0.2	0.44	1.15	2.88
4	10	11.23 (1.64)	3.21	0.51	1.11	2.82	4.1
4	20	20.82 (1.00)	7.27	1.16	2.49	6.21	4.87
8	0	<0.9 (0.52)	—	—	—	—	—
8	5	5.73 (0.39)	0.58	0.09	0.41	1.06	3.67
8	10	10.75 (0.59)	1.35	0.22	0.95	2.48	5.96
8	20	20.48 (0.74)	3.45	0.56	2.42	6.21	8.36
16	0	<0.9 (0.35)	—	—	—	—	—
16	5	4.59 (0.32)	0.21	0.03	0.29	0.77	3.32
16	10	9.95 (0.43)	0.53	0.08	0.73	1.91	6.84
16	20	20.97 (0.75)	1.45	0.23	2.02	5.29	12.21
32	0	<0.9 (0.37)	—	—	—	—	—
32	5	4.83 (0.39)	0.1	0.02	0.29	0.78	3.66
32	10	10.04 (0.58)	0.23	0.04	0.66	1.74	7.41
32	20	21.05 (0.79)	0.57	0.09	1.61	4.28	14.59

[a] DOC_{eq} (simulated natural DOC source) concentrations, which consisted of a combination of malonic acid, sodium oxalate, and dipicolinic acid.
[b] $9 \geq n \geq 7$.

plexes, and nominal DOC_{eq} were used as independent continuous variables in these procedures. In summary, parametric curve fitting provided a means to evaluate combinations of Cu fractions that produced nearly identical hazard function curves (i.e., see Figs. 3*e* and 3*f*) and the best fit of predicted survival to observed survival (i.e., as in Fig. 4).

All statistical calculations were performed using SAS (SAS Institute Inc. 1990) or S-PLUS (Statistical Sciences Inc. 1993).

Results

Water chemistry

Measured concentrations of water quality parameters and major cations and anions were used in all data analyses and interpretations (Table 1). In the text that follows, we use the following abbreviations for expressing the various modeled inorganic and organic Cu species: total inorganic Cu, Cu_{INRG}; ionic Cu, Cu^{2+}; Cu bound to malonic acid, oxalic acid, and dipicolinic acid, Cu_{MAL}, Cu_{OX}, and Cu_{DIP}, respectively. The measured total Cu concentrations, which fell within 92–115% of the nominal concentrations, and the calculated inorganic and organic species of Cu are shown in Table 2. All calculated values for DOC concentrations in exposure waters (based on measured concentrations in stock solutions) were between 81 and 90% of nominal. Based on the agreement between the calculated concentrations and the nominal concentrations, the nominal concentrations were deemed accurate and were used in geochemical speciation calculations and data interpretation.

© 1999 NRC Canada

Dose–response relationship

Mean survival in each of the DOC_{eq} concentrations at 0 µg/L Cu (controls) was greater than 90% at the end of the 336 h, with the exception of the 2 mg DOC_{eq}/L exposure, which had 73% survival. Control survival rates were indicative of good laboratory conditions, healthy fish, and no toxicity from the DOC_{eq} alone, but due to the possible confounding effects of starvation occurring beyond 7 days, survivorship analyses were not conducted on data collected beyond 168 h. Survival curves for controls were not significantly different ($p > 0.69$) between different DOC_{eq} exposures, except for fish exposed to 2 mg DOC_{eq}/L, which had slightly reduced survival due to unidentified causes. Results from control Cu exposures were not used in statistical modeling.

Survivorship at 168 h among fish exposed to 32 mg DOC_{eq}/L was >90% at all Cu levels, indicating that mortality response to Cu exposure was insufficiently different from controls (0 µg Cu/L). Therefore, results from exposures with 32 mg DOC_{eq}/L were not included in lethality endpoint and failure time analyses.

We observed an inverse relationship between Cu toxicity and DOC_{eq}; percent survival decreased with increasing Cu concentration and increased with increasing DOC_{eq} concentration over the range of concentrations tested (Fig. 1). In the absence of DOC_{eq} (0 mg/L), survival was exposure dependent: the 20, 10, and 5 µg Cu/L exposures reduced survival to about 0, 20, and 60%, respectively (Fig. 1). Similarly for the cells containing DOC_{eq}, survival showed a monotonically increasing dose–response relationship of mortality with Cu concentrations, with the exception of the highest DOC_{eq} level, 32 mg/L, which showed no increase in mortality (Fig. 1). Within a given Cu treatment, DOC_{eq} concentrations between 0 and 4 mg/L had no effect on survival. Survival improved as DOC was increased further (Fig. 1).

Assessment of Cu bioavailabilty

Acute lethality estimates (LC_{50}) were determined for total Cu and the modeled Cu species. LC_{50} values commonly decreased through 96 h at each DOC_{eq} level (Fig. 2). The LC_{50} curves were relatively stable for time periods beyond 96 h, with slopes approximately parallel to the time axis and minimal to no differences between 96-h estimates and 168-h estimates. This indicates that the LC_{50} values provided good predictors of ILL's, and we used the 168-h LC_{50} estimate as an ILL for comparing effects of DOC_{eq} levels within the various Cu species. When expressed as total Cu, ILL's, as well as LC_{50}'s for all time periods >48 h, increased in relation to DOC_{eq} concentration (Table 3; Fig. 2*a*). This relationship shows that total Cu overpredicted toxic Cu species over the range of DOC_{eq} concentrations tested. In contrast, Cu_{INRG}, Cu^{2+}, and $Cu_{INRG} + Cu_{MAL}$ all showed a decreasing trend in relation to DOC_{eq} concentration (Figs. 2*b*–2*d*; Table 3), showing that these Cu species underpredicted toxic Cu fractions. After 72 h, the different LC_{50} curves for DOC_{eq} concentrations began to converge towards equivalent values for both $Cu_{INRG} + Cu_{OX}$ and $Cu_{INRG} + Cu_{MAL} + Cu_{OX}$ (Figs. 2*e* and 2*f*). Consequently, ILL values determined for both $Cu_{INRG} + Cu_{OX}$ and $Cu_{INRG} + Cu_{MAL} + Cu_{OX}$ were consistent (within 2 µg/L among the DOC_{eq} levels; Table 3). These results indicate that a combination of inorganic Cu species and organic complexes (i.e., complexes with malonic acid and oxalic acid) contributed to toxicity.

Pooled survival data were used to derive failure time (parametric) models and further evaluate bioavailability of Cu species by including coefficients for DOC_{eq} and for fractions of total Cu (comprising Cu species), with both characteristics treated as continuous variables. Models were compared based on the magnitude and statistical significance of coefficient estimates (Table 4). There was a significant residual effect of DOC_{eq} on failure time in all the models considered, except in the cases with the following combination of Cu species: (*i*) $Cu_{INRG} + Cu_{OX}$ and (*ii*) $Cu_{INRG} + Cu_{OX} + Cu_{MAL}$ (Table 4). As with the ILL results, this indicates that both inorganic and organic Cu species contributed to observed toxicity.

Hazard functions corresponding to fitted models that included DOC_{eq} and various Cu fractions as parameters were distinctive for each separate DOC_{eq} concentration except for the two models containing the above Cu species (i.e., $Cu_{INRG} + Cu_{OX}$ and $Cu_{INRG} + Cu_{OX} + Cu_{MAL}$ (Fig. 3)). We tested several Cu stressor levels, and the pattern and relative density of DOC_{eq} curves within each Cu species plot were consistent regardless of Cu stressor level input in the model. Figure 3 presents comparisons of $h(t)$ at different DOC_{eq} levels for the failure time model fitted using the concentration of DOC_{eq} and alternative Cu species as predictors. In each panel of Fig. 3, $h(t)$ is shown where the concentration of Cu is set at the 96-h LC_{50} for Cu derived from the 4 mg DOC_{eq}/L treatment level. This stressor level was chosen because it is a sufficient concentration of Cu to determine $h(t)$ for each of the respective Cu species (i.e., indicative of a lethal Cu concentration within the range of DOC_{eq} tested). Results from the parametric modeling were consistent with those from the nonparametric modeling (i.e., ILL/LC_{50} comparisons) in showing those Cu species demonstrating the least amount of variability to lethality across DOC_{eq} levels. Various survivor functions, $S(t)$, were plotted using different Cu species fractions to express the lognormal failure time model in comparison with observed survival. Observed survival was reasonably well predicted by modeling survivorship as a function of $Cu_{INRG} + Cu_{OX} + Cu_{MAL}$, although predicted survival tended to exceed observed survival for treatments with low Cu and low DOC_{eq} concentrations (Fig. 4).

Timing of mortality

For treatments where ≥50% mortality occurred within 168 h, LT_{50} estimates were within a narrow range (45–75 h), with no apparent trend relating timing of mortality to DOC_{eq} level (Fig. 1). LT_{50} was estimated to be >168 h in the two lowest Cu treatments regardless of DOC_{eq} and in the Cu exposures of 10 and 20 µg/L with $DOC_{eq} > 4$ and >8 mg/L, respectively.

Discussion

Our results show that the bioavailable fraction of Cu is best predicted by considering the various inorganic and organic fractions of Cu. Analysis of both failure time models and acute toxicity endpoints (ILL/LC_{50}) consistently showed that Cu–inorganic species (i.e., Cu_{INRG}, Cu^{2+}) do not appear

© 1999 NRC Canada

Fig. 1. Cumulative survival curves (with 95% confidence intervals) estimated by the Kaplan–Meier method for each of the Cu–DOC_{eq} treatments. Curves depicted are based on censoring at 336 h.

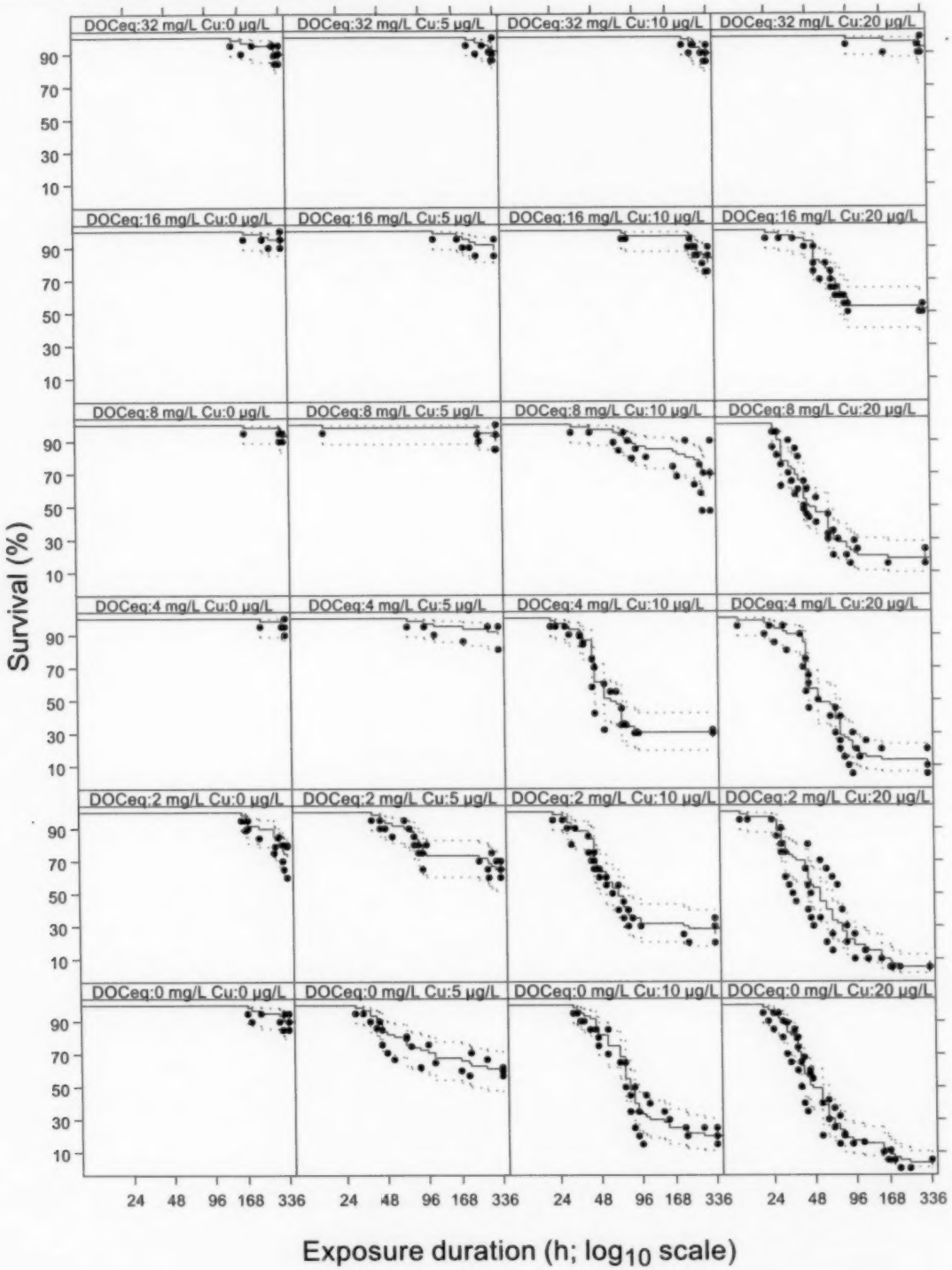

© 1999 NRC Canada

Fig. 2. Median lethal concentrations (LC_{50}) determined using (*a*) measured total Cu and (*b–f*) modeled Cu species fractions. Plotted lines are the LC_{50} values over time estimated separately for DOC_{eq} treatment levels (0–16 mg DOC_{eq}/L).

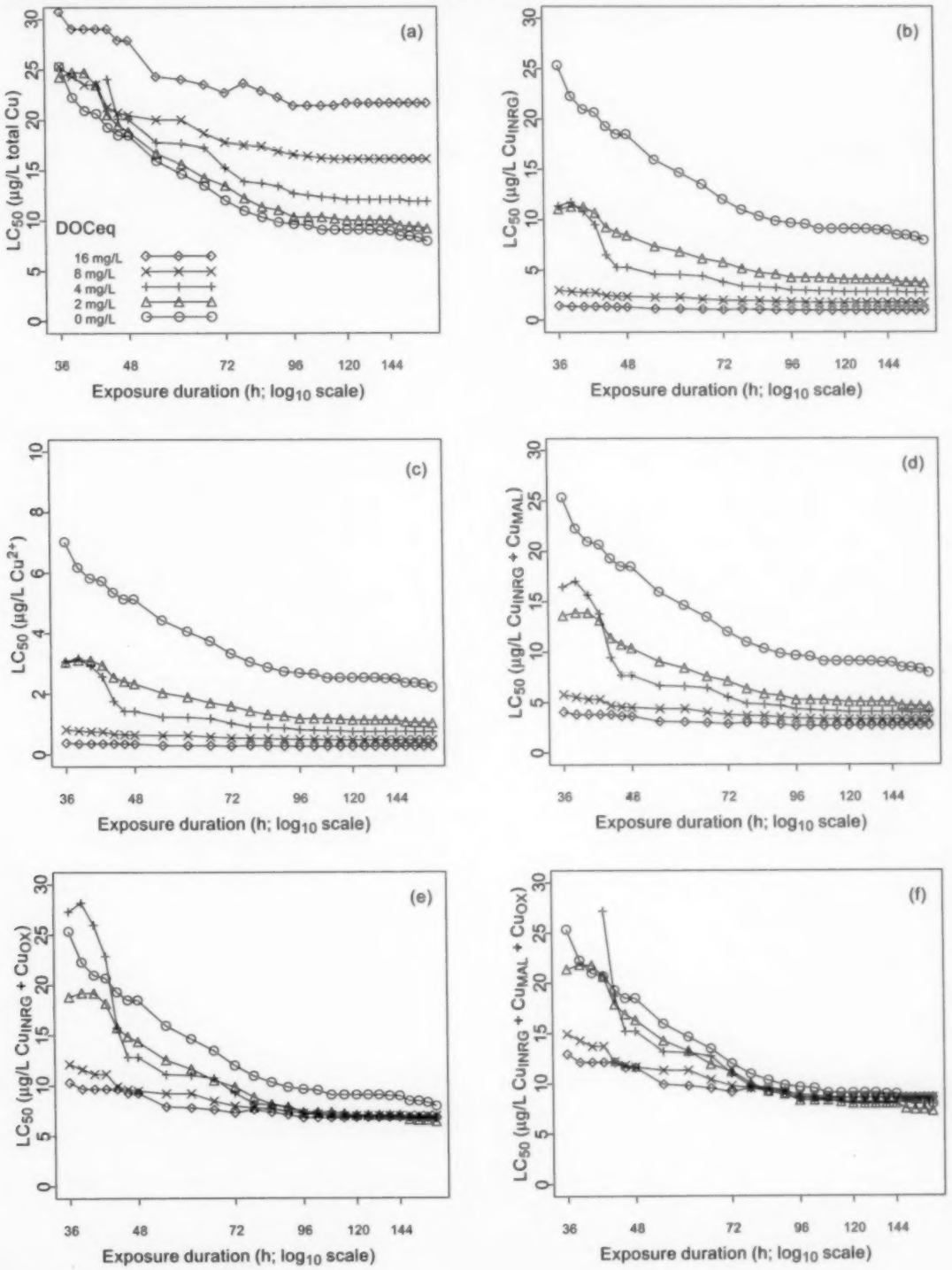

© 1999 NRC Canada

Table 3. Estimates of ILL (168-h LC_{50}) (SE) based on measured Cu and modeled Cu species.

Nominal DOC_{eq} (mg/L)	Total Cu (µg/L)	Cu_{INRG} (µg/L)	Cu^{2+} (µg/L)	Cu_{INRG} + Cu_{MAL} (µg/L)	Cu_{INRG} + Cu_{OX} (µg/L)	Cu_{INRG} + Cu_{MAL} + Cu_{OX} (µg/L)
0	7.9 (2.7)	7.9 (2.7)	2.2 (0.7)	7.9 (2.7)	7.9 (2.7)	7.9 (2.7)
2	9.2 (3.0)	3.7 (1.4)	1.0 (0.4)	4.5 (7.8)	6.4 (2.4)	7.2 (2.8)
4	11.9 (2.9)	2.7 (0.9)	0.7 (0.2)	4.0 (1.3)	6.7 (2.1)	8.0 (2.5)
8	16.1 (3.0)	1.7 (0.4)	0.5 (0.1)	3.3 (0.8)	7.0 (1.7))	8.6 (2.1)
16	21.7[a] (5.3)	1.0[a] (0.3)	0.3[a] (0.1)	2.7 (0.8)	6.9[a] (1.9)	8.6 (2.4)

[a]Value exceeds the measured or modeled exposure concentration and estimated by extrapolation.

to be the only toxic Cu fraction in the bioassay. According to the models and the comparisons of endpoints, toxicity of Cu was best explained by combinations of Cu–inorganic (Cu_{INRG}) plus the Cu bound to the two low-affinity organic ligands used in our bioassay, oxalic acid and malonic acid (Cu_{OX}, Cu_{MAL}) (see Figs. 2 and 3; Tables 3 and 4). These two organic acids had substantially lower Cu-binding affinities (log K_{Cu} = 5.58 and 6.60 for malonic acid and oxalic acid, respectively) than dipicolinic acid (log K_{cu} = 8.15) (MacRae et al. 1999*b*). The fraction of Cu bound to the high-affinity ligand (i.e., dipicolinic acid, Cu_{DIP}) did not appear to be bioavailable as indicated by both failure time models and lethality endpoints that excluded Cu_{DIP} (i.e., Cu_{INRG} combined with Cu_{OX} and Cu_{MAL}) compared with those that included Cu_{DIP} (i.e., total Cu) in the various DOC_{eq} levels. By distinguishing among combinations of inorganic and organic Cu species, we show that a portion of Cu complexed with DOC_{eq} contributed to toxicity, in addition to the toxicity caused by inorganic Cu. These general results are in agreement with Erickson et al. (1996) who concluded that organically complexed Cu was potentially available and toxic to fathead minnow and with Daly et al. (1990) who found that some portions of organically complexed Cu (Cu bound to glycine) contributed to the observed Cu toxicity in freshwater shrimp.

Our conclusions regarding the differential toxicity of Cu bound to high- versus low-affinity organic ligands may be explained by considering binding characteristics of the different organic acids relative to those of the fish gill. The Cu-binding constants determined by Playle et al. (1993*b*) and MacRae et al. (1999*a*) suggest that some forms of DOC-bound Cu may be available to fish. The conditional stability constants for the two low-affinity organic ligands in our study, malonic acid and oxalic acid, are lower than the values empirically derived for fish gill tissue (log K_{Cu} = 7.2–7.5) (Playle et al. 1993*b*; MacRae et al. 1999*a*). Thus, Cu complexed with organic ligands for which log K_{Cu} values are lower than gill tissue may be available to the organism and contribute to toxicity, whereas Cu complexed with organic ligands for which log K_{Cu} are greater than fish gill appears to be nontoxic (Table 5).

As with natural sources of DOC, gill tissue is composed of individual ligands, primarily consisting of phospholipids with amino, phospho, and carboxylate functional groups (Seimiya and Ohki 1973; Bolis et al. 1984) and an associated external mucus layer composed of polyanionic mucopolysaccharides and glycoproteins (Wold and Selset 1977; Van de Winkel et al. 1986). These functional groups each have characteristic binding affinities and capacities for metals and protons that collectively determine the complexation characteristics of gill tissue (Miller and Mackay 1982; Part and Lock 1983; Reid and McDonald 1991). Given the heterogenous and changing composition of gill epithelia and associated mucus, estimating the specific Cu binding of individual component ligands may be both difficult and physiologically inappropriate. Therefore, reasonable estimates of Cu complexation characteristics of gill tissue likely will derive from competition bioassays to determine Cu-binding constants determined for the whole gill (e.g., Playle et al. 1993*b*; MacRae et al. 1999*a*). Additional research in this arena will help determine whether this mechanistic explanation can be verified and generalized.

Our conclusions indicate that an evaluation of Cu bioavailability in the presence of DOC should consider the Cu-binding characteristics of the individual ligands comprising the DOC. The conclusion that the nature of the ligand is important in evaluating Cu bioavailability and determining Cu toxicity is supported by Azenha et al. (1995). Their study used Cu–ligands covering a broad range of stability constants and found that Cu bound to weak to moderate ligands was available and toxic to bacterial cells. In a followup study, these researchers showed that Cu bound to organic ligands is displaced by bacteria and chitin, and as expected with equilibrium theory, the nature of both the abiotic and biotic ligands was important in Cu distribution (Vasconcelos et al. 1997).

Although we were able to distinguish among Cu species that contributed to overall toxicity in the bioassay, we cannot conclude whether the Cu_{OX} and (or) Cu_{MAL} fractions contributing to toxicity were directly available through adsorption/uptake or indirectly available through dissociation/association. Research into distinctions between direct and indirect biological availability of various Cu fractions deserves greater attention. New information in this research area will continually improve assessments in bioavailability and determining underlying mechanisms that explain relative contributions to toxicity from various Cu fractions bound by DOC.

The overall protective effect of total DOCeq (the composite of individual ligands comprising DOC_{eq}) observed through increased survival was only appreciable above thresholds of ≥8 and ≥16 mg DOC_{eq}/L for the 10 and 20 µg Cu/L exposures, respectively (Fig. 1). For exposures where ≥50% mortality occurred within 168 h, LT_{50} fell within a narrow range for low-DOC_{eq} treatments (45–75 h) but was >168 h for higher DOC_{eq} levels. This effect occurred at a DOC_{eq} of >4 mg/L and at a DOC_{eq} of >8 mg/L for nominal Cu of 10 and 20 µg/L, respectively. Similarly, time-dependent protective effects of DOC were reported by Brown et al. (1974) using humic acid and Andrew et al. (1977) using pyrophosphate, where increased median sur-

© 1999 NRC Canada

Table 4. Parameter estimates for lognormal models of failure time as a function of various Cu species, determined with and without DOC_{eq} as an independent variable.

		DOC_{eq} included in model						DOC_{eq} omitted from model					
		96 h			168 h			96 h			168 h		
Cu species	Variable	Coefficient	SE	*p*	Coefficient	SE	*p*	Coefficient	SE	*p*	Coefficient	SE	*p*
Total Cu	Intercept	6.519	0.15	<0.001	7.906	0.20	<0.001	6.687	0.15	<0.001	8.234	0.22	<0.001
	log(Cu species)	–0.896	0.06	<0.001	–1.376	0.08	<0.001	–0.839	0.06	<0.001	–1.304	0.08	<0.001
	log(DOC_{eq})	0.243	0.02	<0.001	0.389	0.03	<0.001						
	Scale (σ)	0.625			0.907			0.677			1.007		
	log likelihood	–601			–778			–665			–868		
Cu_{INRG}	Intercept	6.082	0.11	<0.001	7.237	0.16	<0.001	5.183	0.06	<0.001	5.912	0.08	<0.001
	log(Cu species)	–0.855	0.05	<0.001	–1.313	0.07	<0.001	–0.477	0.03	<0.001	–0.756	0.04	<0.001
	log(DOC_{eq})	–0.382	0.04	<0.001	–0.571	0.05	<0.001						
	Scale (σ)	0.610			0.884			0.660			0.969		
	log likelihood	–590			–774			–664			–835		
Cu^{2+}	Intercept	5.366	0.08	<0.001	6.150	0.11	<0.001	4.820	0.04	<0.001	5.343	0.05	<0.001
	log(Cu species)	–1.087	0.07	<0.001	–1.683	0.10	<0.001	–0.624	0.04	<0.001	–0.997	0.06	<0.001
	log(DOC_{eq})	–0.336	0.04	<0.001	–0.500	0.06	<0.001						
	Scale (σ)	0.634			0.930			0.673			0.994		
	log likelihood	–624			–815			–663			–857		
Cu_{INRG} + Cu_{MAL}	Intercept	6.076	0.11	<0.001	7.220	0.16	<0.001	5.510	0.07	<0.001	6.405	0.10	<0.001
	log(Cu species)	–0.818	0.05	<0.001	–1.253	0.07	<0.001	–0.606	0.04	<0.001	–0.948	0.05	<0.001
	log(DOC_{eq})	–0.212	0.03	<0.001	–0.310	0.04	<0.001						
	Scale (σ)	0.610			0.880			0.633			0.920		
	log likelihood	–584			–767			–611			–796		
Cu_{INRG} + Cu_{OX}	Intercept	6.124	0.12	<0.001	7.284	0.16	<0.001	6.063	0.10	<0.001	7.225	0.14	<0.001
	log(Cu species)	–0.788	0.05	<0.001	–1.203	0.07	<0.001	–0.771	0.04	<0.001	–1.186	0.06	<0.001
	log(DOC_{eq})	–0.023	0.02	0.308	–0.022	0.03	0.486						
	Scale (σ)	0.609			0.878			0.610			0.879		
	log likelihood	–581			–763			–581			–763		
Cu_{INRG} + Cu_{MAL} + Cu_{OX}	Intercept	6.142	0.12	<0.001	7.308	0.16	0.000	6.206	0.11	<0.001	7.437	0.15	<0.001
	log(Cu species)	–0.779	0.05	<0.001	–1.187	0.07	0.000	–0.795	0.05	<0.001	–1.219	0.06	<0.001
	log(DOC_{eq})	0.027	0.02	0.223	0.053	0.03	0.082						
	Scale (σ)	0.607			0.876			0.608			0.877		
	log likelihood	–578			–761			–579			–762		

© 1999 NRC Canada

Fig. 3. Hazard functions ($h(t)$) derived from the lognormal failure time model determined using (*a*) measured total Cu and (*b–f*) modeled Cu species fractions. The Cu stressor variable used for the output depicted is the 96-h LC_{50} for each Cu species at the 4 mg DOC_{eq}/L level. Plotted lines are the probability values for each time interval that were estimated separately for DOC_{eq} treatment levels (0–16 mg DOC_{eq}/L).

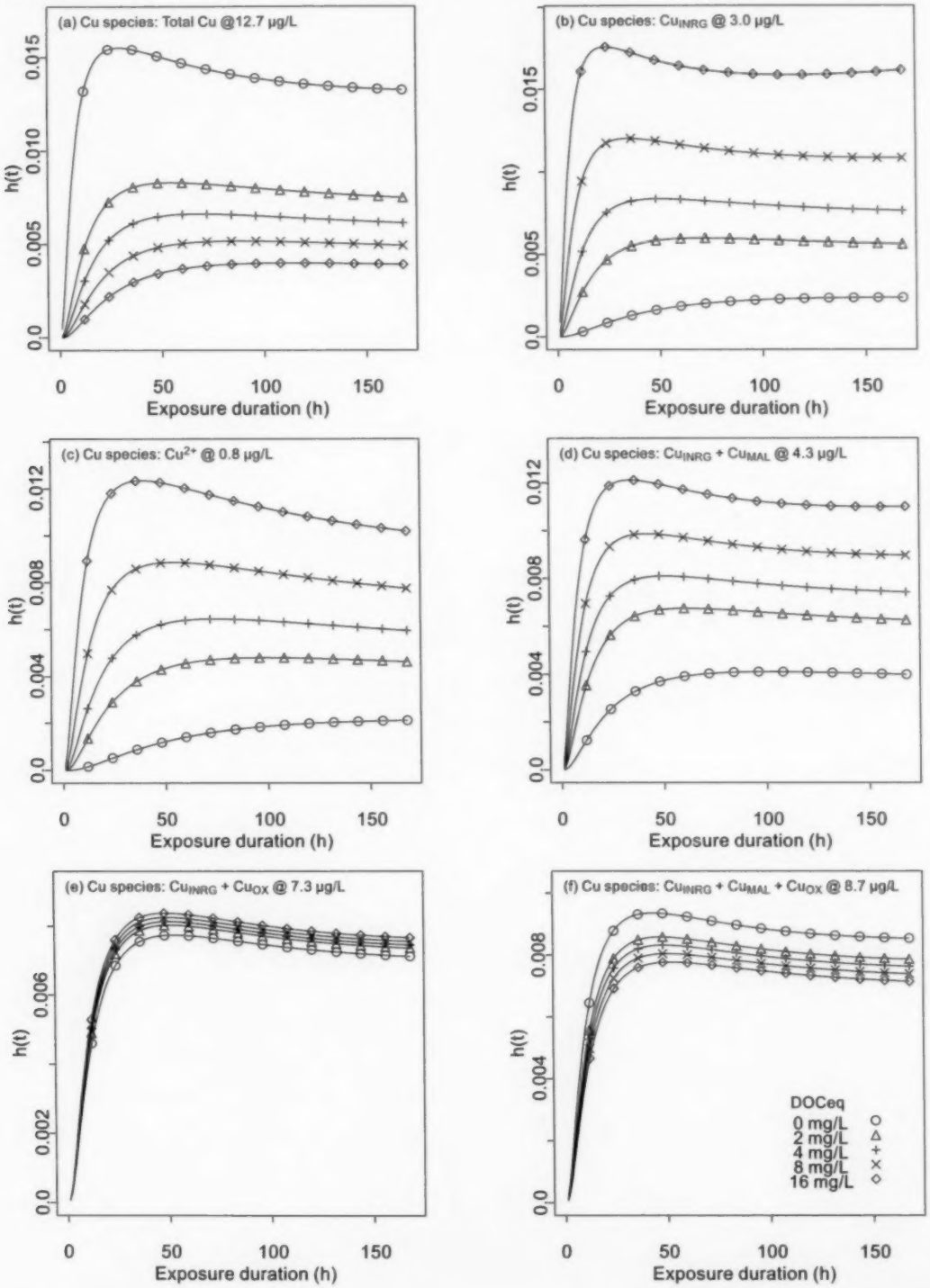
(a) Cu species: Total Cu @12.7 µg/L
(b) Cu species: Cu$_{INRG}$ @ 3.0 µg/L
(c) Cu species: Cu^{2+} @ 0.8 µg/L
(d) Cu species: Cu$_{INRG}$ + Cu$_{MAL}$ @ 4.3 µg/L
(e) Cu species: Cu$_{INRG}$ + Cu$_{OX}$ @ 7.3 µg/L
(f) Cu species: Cu$_{INRG}$ + Cu$_{MAL}$ + Cu$_{OX}$ @ 8.7 µg/L
h(t)
Exposure duration (h)
DOCeq
0 mg/L
2 mg/L
4 mg/L
8 mg/L
16 mg/L

© 1999 NRC Canada

Fig. 4. Observed survival and estimated survival functions ($S(t)$) derived from the lognormal failure time model expressed as a function of the Cu species fraction, $Cu_{INRG} + Cu_{OX} + Cu_{MAL}$.

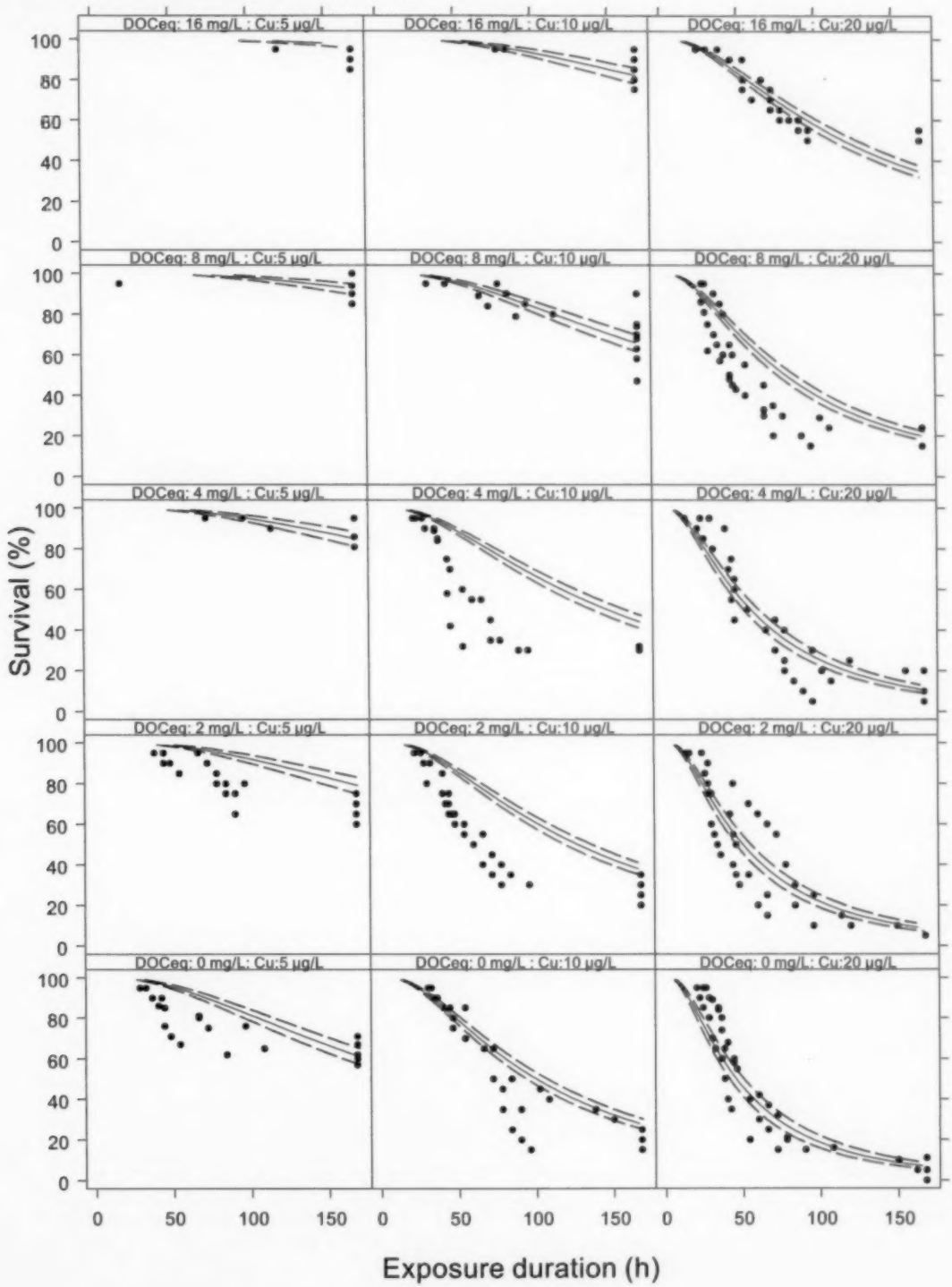

© 1999 NRC Canada

Table 5. Cu-binding affinities (K_{Cu}) of organic acids used in the bioassay and reported for fish gills.

Ligand	log K_{Cu}	Source
Malonic acid	5.58	MacRae et al. 1999*b*
Oxalic acid	6.6	MacRae et al. 1999*b*
Dipicolinic acid	8.15	MacRae et al. 1999*b*
Rainbow trout (*Oncorhynchus mykiss*) fish gill	7.5	MacRae et al. 1999*a*
Brook trout (*Salvelinus fontinalis*) fish gill	7.25	MacRae et al. 1999*a*
Fathead minnow (*Pimephales promelas*) fish gill	7.4	Playle et al. 1993*b*

vival times were directly related to the total concentration of the Cu ligand.

Conclusions

Our study demonstrates that Cu bound in low-affinity organic complexes similar to those found in nature contributes to acute toxicity in rainbow trout. These results are consistent with the hypothesized model wherein (*i*) Cu toxicity is proportional to the effective bioavailable concentration of Cu and (*ii*) a threshold for Cu bioavailability is determined by the Cu-binding affinity of the fish gill, which may be greater than or less than the affinity of particular organic ligands present in natural waters. Furthermore, the results presented show that studies to assess specific conditions of Cu toxicity should include analysis of specific Cu–ligand complexes to determine their relative concentration, bioavailability, and toxicity. This includes studies that establish water quality criteria intended to be protective of fish because toxicity thresholds cannot be accurately determined without considering site-specific geochemical characteristics that determine the bioavailability of Cu.

Acknowledgments

This research work was funded by the National Oceanic and Atmospheric Administration, the U.S. Department of Agriculture/Forest Service, and the State of Idaho. We are grateful to the entire project staff and for the assistance of D.G. Dixon, N. Iadanza, E. Little, and C. Mebane. Comments provided by two anonymous reviewers are greatly appreciated.

References

Andrew, R.W., Biesinger, K.E., and Glass, G.E. 1977. Effects of inorganic complexing on the toxicity of copper to *Daphnia magna*. Water Res. **11**: 309–315.

APHA (American Public Health Association, American Water Works Association and Water Pollution Control Federation). 1992. Standard methods for the examination of water and wastewater. 18th ed. APHA, Washington, D.C.

Azenha, M., Vasconcelos, M.T., and Cabral, J.P.S. 1995. Organic ligands reduce copper toxicity in *Pseudomonas syringae*. Environ. Toxicol. Chem. **14**: 369–373.

Bolis, C.L., Cambria, A., and Fama, M. 1984. Effects of acid stress on fish gills. *In* Toxins, drugs, and pollutants in marine animals. *Edited by* C.L. Bolis, A. Cambria, and M. Fama. Springer-Verlag, Berlin. pp. 122–129.

Borgmann, U., and Ralph, K.M. 1984. Copper complexation and toxicity to freshwater zooplankton. Arch. Environ. Contam. Toxicol. **13**: 403–409.

Brown, V.M., Shaw, T.L., and Shurben, D.G. 1974. Aspects of water quality and the toxicity of copper to rainbow trout. Water Res. **8**: 797–803.

Chakoumakos, C., Russo, R.C., and Thurston, R.V. 1979. Toxicity of copper to cutthroat trout (*Salmo clarki*) under different conditions of alkalinity, pH, and hardness. Environ. Sci. Technol. **13**: 213–219.

Daly, H.R., Campbell, I.C., and Hart, B.T. 1990. Copper toxicity to *Paratya australiensis*: I. Influence of nitrilotriacetic acid and glycine. Environ. Toxicol. Chem. **9**: 997–1006.

Erickson, R.J., Benoit, D.A., Mattson, V.R., Nelson, H.P., Jr., and Leonard, E.N. 1996. The effects of water chemistry on the toxicity of copper to fathead minnows. Environ. Toxicol. Chem. **15**: 181–193.

Finney, D.J. 1971. Probit analysis. 3rd ed. Cambridge University Press, London, U.K.

Florence, T.M., Powell, H.K.J., Stauber, J.L., and Town, R.M. 1992. Toxicity of lipid-soluble copper(II) complexes to the marine diatom *Nitzschia closterium*: amelioration by humic substances. Water Res. **26**: 1187–1193.

Guy, R.D., and Kean, A.R. 1980. Algae as a chemical speciation monitor. I. A comparison of algal growth and computer calculated speciation. Water Res. **14**: 891–899.

Howarth, R.S., and Sprague, J.B. 1978. Copper lethality to rainbow trout in waters of various hardness and pH. Water Res. **12**: 455–462.

Kalbfleish, J.D, and Prentice, R.L. 1980. The statistical analysis of failure time data. Wiley, New York.

Laurén, D.J., and McDonald, D.G. 1986. Influence of water hardness, pH, and alkalinity on the mechanisms of copper toxicity in juvenile rainbow trout, *Salmo gairdneri*. Can. J. Fish. Aquat. Sci. **43**: 1488–1496.

MacRae, R.K., Smith, D.E., Swoboda-Colberg, N., Meyer, J.S., and Bergman, H.L. 1999*a*. The copper binding affinity of rainbow trout (*Oncorhynchus mykiss*) and brook trout (*Salvelinus fontinalis*) gills: implications for assessing bioavailable metals. Environ. Toxicol. Chem. **18**: 1180–1189.

MacRae, R.K., Maest, A.S., and Meyer, J.S. 1999*b*. Selection of an organic acid analogue of dissolved organic matter for use in toxicity testing. Can. J. Fish. Aquat. Sci. **56**: 1484–1493.

Marr, J.C.A., Lipton, J., Cacela, D., Hansen, J.A., Bergman, H.L., Meyer, J.S., and Hogstrand, C. 1996. Relationship between copper exposure duration, tissue copper concentration, and rainbow trout growth. Aquat. Toxicol. (Amst.), **52**: 17–30.

McCullagh, P.M., and Nelder, J.A. 1989. Generalized linear models. 2nd ed. Chapman and Hall, New York.

Meador, J.P. 1991. The interaction of pH, dissolved organic carbon, and total copper in the determination of ionic copper and toxicity. Aquat. Toxicol. (Amst.), **19**: 13–32.

Miller, T.G., and Mackay, W.C. 1982. Relationship of secreted mucus to copper and acid toxicity in rainbow trout. Bull. Environ. Contam. Toxicol. **28**: 68–74.

Newman, M.C. 1994. Lethal and other quantal responses to stressors. *In* Quantitative methods in aquatic ecotoxicology. *Edited by* M.C. Newman. CRC Press, Inc., Boca Raton, Fla. pp. 119–176.

Pagenkopf, G.K., Russo, R.C., and Thurston, R.V. 1974. Effect of complexation on toxicity of copper to fishes. J. Fish. Res. Board Can. **31**: 462–465.

© 1999 NRC Canada

Part, P., and Lock, R.A.C. 1983. Diffusion of Ca, Cd, Hg in mucous solution from rainbow trout. Comp. Biochem. Physiol. C, Comp. Pharmacol. **76**: 259–263.

Playle, R.C., Dixon, D.G., and Burnison, K. 1993*a*. Copper and cadmium binding to fish gills: modification by dissolved organic carbon and synthetic ligands. Can. J. Fish. Aquat. Sci. **50**: 2667–2677.

Playle, R.C., Dixon, D.G., and Burnison, K. 1993*b*. Copper and cadmium binding to fish gills: estimates of metal–gill stability constants and modelling of metal accumulation. Can. J. Fish. Aquat. Sci. **50**: 2678–2687.

Reid, S.D., and McDonald, D.G. 1991. Metal binding activity of the gills of rainbow trout (*Oncorhynchus mykiss*). Can. J. Fish. Aquat. Sci. **48**: 1061–1068.

Roy, R.L., and Campbell, P.G.C. 1997. Decreased toxicity of Al to juvenile atlantic salmon (*Salmo salar*) in acidic soft water containing natural organic matter: a test of the free-ion model. Environ. Toxicol. Chem. **16**: 1962–1969.

SAS Institute Inc. 1990. SAS/STAT user's guide, version 6, edition 4. Vol. 1. SAS Institute Inc., Cary, N.C.

Schecher, W.D. and McAvoy, D.C. 1991. MINEQL$^+$: a chemical equilibrium program for personal computers. User's manual, version 2.1. The Procter and Gamble Company, Cincinnati, Ohio.

Seimiya, T., and Ohki, S. 1973. Ionic structure of phospholipid membranes, and binding of calcium ions. Biochim. Biophys. Acta, **298**: 546–561.

Shaw, T.L., and Brown, V.M. 1974. The toxicity of some forms of copper to rainbow trout. Water Res. **8**: 377–382.

Sprague, J.B. 1969. Measurement of pollutant toxicity to fish. I. Bioassay methods for acute toxicity. Water Res. **3**: 793–821.

Sprague, J.B. 1970. Measurement of pollutant toxicity to fish. II. Utilizing and applying bioassay results. Water Res. **4**: 3–32.

Statistical Sciences Inc. 1993. S-PLUS for Windows, version 3.1. Statistical Sciences Inc., Seattle, Wash.

Van de Winkel, J.G.J., van Kuppevelt, T.H.M.S.M., Janssen, H.M.J., and Lock, R.A.C. 1986. Glycosaminoglycans in the skin mucus of rainbow trout (*Salmo gairdneri*). Comp. Biochem. Physiol. B, Comp. Biochem. **85**: 473–475.

Vasconcelos, M.T.S.D., Azenha, A.O., and Cabral, J.P.S. 1997. Comparison of availability of copper(II) complexes with organic ligands to bacterial cells and to chitin. Environ. Toxicol. Chem. **16**: 2029–2039.

Welsh, P.G., Skidmore, J.F., Spry, D.J., Dixon, D.G., Hodson, P.V., Hutchinson, N.J., and Hickie, B.E. 1993. Effect of pH and dissolved organic carbon on the toxicity of copper to larval fathead minnow (*Pimephales promelas*) in natural lake waters of low alkalinity. Can. J. Fish. Aquat. Sci. **50**: 1356–1362.

Welsh, P.G., Parrott, J.L., Dixon, D.G., Hodson, P.V., Spry, D.J., and Mierle, G. 1996. Estimating acute Cu toxicity to larval fathead minnow (*Pimephales promelas*) in soft water from measurements of dissolved organic carbon, calcium, and pH. Can. J. Fish. Aquat. Sci. **53**: 1263–1271.

Winner, R.W. 1985. Bioaccumulation and toxicity of copper as affected by interactions between humic acid and water hardness. Water Res. **19**: 449–455.

Wold, J.K., and Selset, R. 1977. Glycoproteins in the skin mucus of the char (*Salmo alpinus* L.). Comp. Biochem. Physiol. B, Comp. Biochem. **56**: 215–218.

© 1999 NRC Canada

Selection of an organic acid analogue of dissolved organic matter for use in toxicity testing

Russell K. MacRae, Ann S. Maest, and Joseph S. Meyer

Abstract: Uncontaminated stream waters in the vicinity of a Co mine in Idaho were titrated with Cu to determine the Cu-binding characteristics of natural dissolved organic matter (DOM) and suspended particles. Nonlinear regressions of bound versus free Cu concentrations were consistent with a two-ligand model for DOM complexation of Cu, in which the conditional stability constants (log K) and complexation capacities (CC) were log K_1 = 7.26, CC_1 = 0.21 μmol Cu·mg dissolved organic carbon $(DOC)^{-1}$ and log K_2 = 5.13, CC_2 = 2.89 μmol Cu·mg DOC^{-1}. Copper-binding constants were similar in filtered (0.45 μm) and unfiltered water samples. Calcium, Mg, and Co did not compete appreciably with Cu for DOM complexation at concentrations present in site waters. Copper binding to amorphous iron oxide flocs also was not important at the Fe concentrations present in the stream waters. We selected a mixture of three organic acids, dipicolinic, oxalic, and malonic, to mimic the Cu-binding properties of this DOM. Geochemical models were developed to estimate Cu speciation and evaluate its bioavailability in companion fish toxicity tests using the DOM analogue (Marr et al. 1999. Can. J. Fish. Aquat. Sci. 56: 1471–1483).

Résumé : On a titré avec du Cu des eaux courantes non contaminées se trouvant au voisinage d'une mine de Co de l'Idaho pour déterminer les caractéristiques de liaison avec le Cu de la matière organique dissoute (MOD) et des particules en suspension naturelles. Les régressions non linéaires des concentrations de Cu lié en fonction des concentrations de Cu libre correspondaient à un modèle à deux ligands pour la complexation du Cu avec la MOD, dans lequel les constantes de stabilité conditionnelle (log K) et les capacités de complexation (CC) étaient log K_1 = 7,26, CC_1 = 0,21 μmol Cu·mg carbone organique dissous $(COD)^{-1}$ et log K_2 = 5,13, CC_2 = 2,89 μmol Cu·mg COD^{-1}. Les constantes de liaison avec le Cu étaient similaires dans les échantillons d'eau filtrés (0,45 μm) et non filtrés. Le Ca, le Mg et le Co ne concurrençaient pas de façon appréciable le Cu pour la complexation avec la MOD aux concentrations présentes dans les eaux du site. La liaison du Cu avec les floculats amorphes d'oxyde de fer n'était aussi pas importante aux concentrations de Fe présentes dans les eaux courantes. Nous avons choisi un mélange de trois acides organiques, dipicolinique, oxalique et malonique, pour imiter les propriétés de liaison avec le Cu de cette MOD. Nous avons développé des modèles géochimiques pour estimer la spéciation du Cu et évaluer sa biodisponibilité dans des tests connexes de toxicité à l'égard de poissons utilisant l'analogue de la MOD (Marr et al. 1999. J. can. sci. halieut. aquat. 56 : 1471–1483. Ce numéro).

[Traduit par la Rédaction]

Introduction

The purpose of this study was to determine the Cu-binding characteristics of natural dissolved organic matter (DOM) in a stream receiving acid mine drainage and create a DOM analogue with comparable Cu-complexation characteristics. This DOM analogue could be produced in large quantities, so long-term, flow-through laboratory fish toxicity studies of Cu bioavailability could be performed.

Received February 9, 1998. Accepted February 16, 1999. J14422

R.K. MacRae[1] **and J.S. Meyer.** Department of Zoology and Physiology, University of Wyoming, Laramie, WY 82071, U.S.A.
A.S. Maest. Hydrosphere, Inc., Boulder, CO 80302, U.S.A.

[1]Author to whom all correspondence should be addressed. Present address: U.S. Fish and Wildlife Service, New Mexico Ecological Services Field Office, Environmental Contaminants Division, 2105 Osuna NE, Albuquerque, NM 87113, U.S.A. e-mail: russ_macrae@fws.gov

Over the past 20 years, aquatic biologists have recognized that metal toxicity cannot be adequately explained in terms of total or dissolved metal concentrations (Borgmann 1983; Jonnalagadda and Prasada Rao 1993; Campbell 1995). Instead, aqueous metal speciation, not total metal concentration, determines the bioavailability of metals to aquatic biota. In this context, we define bioavailable metal as the fraction (or sum of fractions) of the total metal concentration that correlates with toxicity. One of the most important factors affecting metal speciation in natural waters is the presence of DOM (Sposito 1981; Saar and Weber 1982; McKnight et al. 1983). DOM often has a much higher metal-binding affinity, or strength, than do inorganic ligands. In addition, the metal-binding capacity, or amount of metal that a specified quantity of DOM can bind, often is quite high.

Metal-induced toxicity to aquatic life can be modified by the presence of DOM in surface waters. Specifically, organically complexed Cu species, such as Cu–fulvic or Cu–humic complexes, can be significantly less toxic to aquatic life than is free Cu (Pagenkopf et al. 1974; Borgmann 1983; Verweij et al. 1992; Erickson et al. 1996). These Cu–DOM com-

© 1999 NRC Canada

plexes can decrease the bioavailability of Cu and thus decrease toxicity below that predicted from measured total Cu concentrations. However, some organically bound Cu may also be bioavailable if biotic ligands, such as a fish gill or algal surfaces, have higher affinities for Cu than do abiotic ligands in the water (Playle et al. 1993*a*, 1993*b*; Gonzalez-Davila et al. 1995; MacRae et al. 1999).

Although synthetic organic ligands have been added to fish toxicity test waters (Campbell and Stokes 1985; Playle et al. 1993*a*, 1993*b*), we know of no studies in which the metal-binding characteristics, rather than simply the total concentrations, of natural DOM were matched. In our study, the conditional stability constants and concentrations of Cu–organic complexes are known, so full inorganic and organic speciation can be determined using modified geochemical models. Playle et al. (1993*a*, 1993*b*) and Erickson et al. (1996) added DOM in some toxicity tests, but the metal-binding characteristics were not measured. Consequently, the relationships between metal speciation and toxicity could not be elucidated.

In this study, we characterized the Cu-binding affinities and capacities of DOM in a stream draining a Co mine in Idaho. We then selected a mixture of commercially available organic acids to mimic the Cu-binding characteristics of that natural DOM. A companion paper (Marr et al. 1999) describes results of fish toxicity studies that used the DOM analogue. Through the use of geochemical modeling, the toxicity observed in laboratory studies can be explained in terms of metal species rather than total metal concentrations. In that way, the bioavailable portion of the total metal concentration can be determined for any well-characterized natural or laboratory water.

Methods

Study site

Panther Creek, a major tributary of the Middle Fork of the Salmon River in central Idaho, drains a 1380-km^2 montane watershed that includes the Blackbird Mine. Blackbird and Big Deer creeks drain the mine site, which contains ores rich in Co and Cu and contributes high concentrations of Co and Cu to Panther Creek. Deep and Napias creeks, the largest contributors of uncontaminated flows in the vicinity of the Blackbird Mine, enter Panther Creek downstream of Blackbird Creek and upstream of Big Deer Creek.

Field methods

Water samples for metal-binding studies were collected from three uncontaminated stream reaches: Panther Creek upstream of Blackbird Creek (PA02), the mouth of Deep Creek (DE01), and the mouth of Napias Creek (NA01). Samples were collected at each location three times (May 10–11, May 24–25, and July 20–21) during the 1994 high-flow sampling period.

Water was collected in acid-cleaned HDPE cubitainers from the stream center at each sampling location. Within 24 h of collection, approximately half of each sample was filtered through disposable 0.45-μm in-line filters (Gelman Sciences large-volume groundwater sampling capsules). Samples for the analysis of dissolved organic carbon (DOC) were filtered through disposable syringe-mounted 0.45-μm Ag filters (Gelman Sciences). Filtered and unfiltered samples were shipped to the University of Wyoming Red Buttes Environmental Biology Laboratory for metal-binding studies and determination of trace metals, major cations and anions, organic carbon, and alkalinity.

Samples for metal-binding studies were preserved at 4°C in the dark from immediately after collection until they were analyzed. Samples for determination of metals and major cations were preserved with ultrapure HNO_3 to pH < 2. Samples for total organic carbon (TOC) and DOC analysis were preserved with ulltrapure H_2SO_4 to pH < 2. Concentrations of Ca, Mg, Na, and K were measured using flame atomic absorption spectrometry (AAS) (Perkin Elmer® model 372), Co, Cu, Fe, and Mn by graphite furnace AAS (Varian® model 600), pH using an Orion® Ross Sure Flow combination electrode, alkalinity by titration with H_2SO_4 and Gran analysis (MacIntosh Analytical® Auto Titration System model MA20), TOC and DOC by combustion/nondispersive infrared analysis (Shimadzu® model TOC 5000A), and Cl^-, NO_3^-, and SO_4^{2-} by ion chromatography (Dionex® model 2110i). Analytical methods were based on the manufacturer's recommendations. Sample collection procedures and laboratory analyses of all constituents were conducted in accordance with the University of Wyoming's Laboratory Quality Assurance Project Plan, which is based on standard U.S. Environmental Protection Agency good laboratory practices methodology.

Characterization of Cu complexation

Copper titrations

A cupric ion selective electrode (Cu-ISE) (Orion® model 94-29-00 combined with an Orion® model 90-02-00 double junction reference electrode) was used to determine the Cu^{2+} concentration ($[Cu^{2+}]$) in site waters or laboratory-prepared solutions to which known amounts of Cu were added. Preparation of the Cu-ISE was based on the method described in Blaedel and Dinwiddie (1974). Prior to each titration, the electrode was (*i*) immersed in a 7.9 μM Cu solution for 5 min to condition the electrode sensing surface, (*ii*) rinsed with deionized water, (*iii*) cleaned in 0.025 M H_2SO_4 until a potential of 120 mV was reached, and (*iv*) rinsed again. The electrode's sensing surface was then polished with 3-μm aluminum oxide paper and allowed to stabilize to a millivolt value corresponding to ≤0.0157 M Cu^{2+}. If the millivolt reading would not stabilize at this value, the sample was considered contaminated and was replaced with a fresh aliquot.

Stream water samples and laboratory solutions were titrated by adding known amounts of Cu to the samples and measuring $[Cu^{2+}]$ with the Cu-ISE. Deionized water (for calibrations) or subsamples of site water (each in 100-mL light-shielded HDPE vessels) were prepared for titration by warming to 25°C, adjusting the solution's ionic strength to 0.01 M with 5 M $NaNO_3$, and adjusting the pH to 6.0 with ultrapure HNO_3 or NaOH. All titrations were conducted at pH 6.0 instead of the original site-water pH of about 7.5 because at higher pH values the Cu-ISE was apparently unable to distinguish between Cu^{2+} and copper hydroxide and copper carbonate species. Consequently, when following the experimental methodologies described above, at pH > 6.0, the Cu-ISE appeared to incorrectly detect these inorganic copper complexes as Cu^{2+} and thus underestimate Cu–DOM stability constants.

Samples were aerated with filtered compressed air and stirred at a constant rate with a magnetic stir bar during the titrations. Copper (from a 0.157 M stock solution of $CuCl_2$) was added incrementally, beginning at a concentration of about 10^{-7} M and ending at about 10^{-5} M. The pH was maintained at 6.0 ± 0.05 by addition of ultrapure HNO_3 or NaOH. For all calibrations and analyses of samples, the electrode reading was considered stable when the rate of change was 0.2 $mV \cdot min^{-1}$. The stock solution Cu concentration was verified by AAS, and pipette calibration was checked periodically to ensure accurate Cu delivery.

The electrode was calibrated daily using Cu standards ranging in concentration from 0.157 to 7.87 μM Cu (nominal values) at the

© 1999 NRC Canada

same pH (6.0) and ionic strength (0.01 M $NaNO_3$) as the prepared samples. Stock solution Cu concentrations and dilutions were known and verified, and steps were taken to check for and minimize contamination. Potential contamination due to Cu leaching from the electrode's sensing surface would have been insignificant considering the relatively high starting total Cu concentration (0.157 µM). Electrode millivolt readings in samples were recorded and converted to $[Cu^{2+}]$ by comparison with the calibration curve regression. Calibrations were linear, with regression r^2 values of ≥0.995. Because the ionic strength was the same in both the standard solutions and the sample solutions, millivolt readings in sample solutions could be directly converted to $[Cu^{2+}]$ based on the standard curves without having to account for ionic strength differences.

Evaluation of the effects of suspended particles, iron oxide particles, and competing ions on Cu complexation

Inorganic and organic particulate matter can complex metals and may contribute to Cu binding in streams that carry high sediment loads. To evaluate potential Cu binding with natural suspended matter in Panther Creek, both filtered and unfiltered PA02 samples collected on May 11 and 25 were titrated, and the Cu-binding characteristics of the two site-water samples were compared.

Copper binding by iron oxide particles and colloids was examined in more detail because these particles can also adsorb or otherwise bind Cu and thus affect the Cu-binding characteristics of site water. To evaluate potential Cu – iron oxide binding, a low-pH, 17.9 µM Fe solution was prepared using $FeCl_3 \cdot 6H_2O$ and adjusted to pH 6.0. Following agitation of the solution to create a uniform suspension of iron oxide, 20 subsamples (5 mL) were removed from the flask and added to 10-mL polypropylene centrifuge tubes; replicate tubes were then spiked with Cu to produce 10 different total Cu concentrations ($[Cu_{total}]$) ranging from 0 to 7.9 µM. Each tube was vortexed and a 2-mL subsample was removed for total Cu and Fe analysis. Tubes were vortexed again and a subsample (1 mL) of each was centrifuged at about 14 000 rpm (12 600 × *g*) for 15 min. The supernatant (containing the "free" Cu^{2+}) was pipetted away from the iron oxide pellet (containing Cu bound to the iron oxide floc) and analyzed for total Cu and Fe. Bound [Cu] was calculated by subtracting $[Cu^{2+}]$ from the initial measured $[Cu_{total}]$.

The effects of Ca, Mg, and Co on Cu binding with DOM were tested by adding known amounts of these ions to the PA02 sample collected on May 25 and comparing Cu-binding characteristics with and without the added ions. Calcium (as $CaCl_2 \cdot 2H_2O$) and Mg (as $MgCl_2 \cdot 6H_2O$) were added separately to different PA02 sample aliquots to final Ca and Mg concentrations of about 0.62 and 1.03 mM, respectively. Cobalt (as $CoCl_2 \cdot 6H_2O$) was added separately to a final Co^{2+} concentration of 8.48 µM. To compensate for any influence that the competing cations may have had on Cu-ISE performance, standard curves were generated from Cu solutions containing the competing ions.

Evaluation of candidate organic acid analogues

Two types of candidate organic acid analogues were evaluated to determine their Cu-binding characteristics relative to the Cu-binding characteristics of DOM in site water: a commercially available humic acid and mixtures of individual commercially available organic acids.

Aldrich® Chemical Company produces a humic acid that, although poorly characterized and isolated, is commercially available and could be a candidate DOM analogue for fish toxicity studies (e.g., Erickson et al. 1996). To evaluate the Cu-binding characteristics of this commercial humic acid, solutions containing Aldrich® humic acid were titrated with Cu as described above and compared with site water. In these titrations, 0.2 and 0.8 mg Aldrich® humic acid·L^{-1} was added to deionized water. Calcium and Mg (0.18 and 0.12 mM, respectively, as Cl salts) were added to mimic concentrations in Panther Creek water.

A large number of organic acids were evaluated as candidates for the DOM analogue, based on their published Cu^{2+}, Ca^{2+}, and H^+ stability constants (NIST 1995). We titrated citric, oxalic, malonic, and dipicolinic acids with Cu and the Cu-binding characteristics of the individual organic acids and various mixtures were compared with those for DOM in site water. Solutions of sodium oxalate ($Na_2C_2O_4$), malonic acid disodium salt ($CH_2(COONa)_2$), dipicolinic acid (N:C(COOH)CH:CHCH:CCOOH), and sodium citrate ($Na_3C_6H_5O_7$) were prepared from reagent-grade chemicals (Sigma-Aldrich® Chemicals).

Data presentation and analysis

We use Scatchard plots (Scatchard 1949), based on concentrations of bound and free metal in solution, to visually illustrate the Cu-binding characteristics of titrated solutions. The general equation for the Scatchard analysis of a one-ligand system is

$$(1) \qquad \frac{[CuL]}{[Cu^{2+}]} = -K[CuL] + K \cdot CC$$

where [CuL] is the concentration of the Cu–ligand complex, K is the conditional stability constant for a complex of Cu with the ligand, which is valid for a given set of geochemical conditions (pH, ionic strength, concentrations of competing ions such as Ca^{2+}, Mg^{2+}, etc.), and CC is the complexation capacity of the ligand. At pH 6.0, the pH at which all titrations were conducted, virtually all (>97%) of the inorganic Cu is present as Cu^{2+}. Therefore, at each titration increment in filtered samples, the concentration of organically bound Cu ([CuL]) was calculated as $[CuL] = [Cu_{total}] - [Cu^{2+}]$. In a Scatchard analysis, if only one ligand is present, the titration data plot as a straight line (eq. 1). For a multiligand system, the Scatchard plot will be curved, where tangents to distinct portions of the curve represent individual ligands or types of binding sites with distinct conditional stability constants and complexation capacities.

While Scatchard plots are useful for data presentation, they are not particularly useful for quantitative determination of Cu–DOM complexation characteristics. Therefore, conditional stability constants and complexation capacities of DOM in the site waters were calculated using the nonlinear regression (NLR) analysis package in the SPSS® for Windows™ statistical package (Norusis 1993). This procedure allowed a one-, two- or three-ligand model to be fit directly to titration data by solving the following general equation:

$$(2) \qquad \sum_{i=1}^{n}\{CuL_i\} = \{Cu^{2+}\}\sum_{i=1}^{n}\left(\frac{10^{\log K_i} \cdot CC_i}{1 + 10^{\log K_i} \cdot \{Cu^{2+}\}}\right)$$

where $\{CuL_i\}$ is the activity of Cu bound to organic ligand i, K_i is the conditional stability constant for the binding of organic ligand i to Cu, CC_i is the Cu complexation capacity of organic ligand i, $\{Cu^{2+}\}$ is the chemical activity of Cu^{2+}, which in these titrations at an ionic strength of 0.01 M equals $0.659[Cu^{2+}]$, and n is the number of potential ligands (≥1). This mathematical function is derived from standard geochemical equilibrium equations (Dzombak et al. 1986).

Geochemical modeling

The geochemical model MINEQL⁺ version 2.2 (Schecher and McAvoy 1991) was used to calculate concentrations of dissolved Cu species in simulated and actual Cu titrations of the DOM analogue and in laboratory waters used in the companion fish toxicity tests (Marr et al. 1999).

© 1999 NRC Canada

Table 1. Water quality data for unfiltered and filtered water samples from Panther (PA02), Deep (DE01), and Napias (NA01) creeks for May 11 and May 25, 1994.

	PA02 filtered		PA02 unfiltered		DE01 filtered		NA01 filtered	
	May 11	May 25	May 11	May 25	May 10	May 24	May 10	May 24
Field pH	7.68	7.71	7.68	7.71	7.49	7.31	7.56	7.53
Field temperature (°C)	6.6	8.5	6.6	8.5	9.5	10.8	11.9	10.7
Alkalinity (mequiv.·L^{-1})	0.64	0.64	nd	nd	0.48	0.44	0.24	0.24
Ca (mM)	0.19	0.20	0.20	0.20	0.12	0.12	0.05	0.06
Mg (mM)	0.07	0.07	0.07	0.07	0.05	0.06	0.02	0.02
Na (mM)	0.12	0.13	0.12	0.13	0.11	0.12	0.07	0.09
K (mM)	0.02	0.02	0.02	0.02	0.04	0.03	0.02	0.03
Cl (mM)	0.01	0.01	0.01	0.01	0.01	0.02	0.01	0.02
SO_4 (mM)	0.03	0.03	0.02	0.03	0.02	0.02	0.01	0.01
Fe (μM)	1.218	2.435	nd	nd	4.512	nd	1.862	nd
Cu (μM)	<0.011	<0.011	0.024	<0.011	<0.011	0.019	<0.011	0.027
Co (μM)	<0.020	<0.020	<0.020	<0.020	<0.020	<0.020	<0.020	<0.020
DOC/TOC (mg·L^{-1})	4.46	4.68	5.69	nd	4.78	4.33	5.60	3.62

Note: nd, not determined. All samples were taken in 1994.

Two types of input data are required for the modeling program: (*i*) stability constants for metal and H^+ complexes and (*ii*) concentrations of Cu and Co, major cations and anions, organic acid ligands, and other water quality parameters (e.g., pH). Inorganic stability constants were adopted from either the MINEQL$^+$ database or values reported in the literature. Stability constants for complexes of Cu, Co, H, Ca, and Mg with organic acids were (*i*) adopted from the MINEQL$^+$ database, (*ii*) added to the MINEQL$^+$ database from values reported in the literature, or (*iii*) derived empirically in our laboratory and added to the MINEQL$^+$ database.

For copper hydroxide ($Cu(OH)_x^{2-x}$) and copper carbonate ($Cu(CO_3)_x^{2-2x}$) species, the stability constants determined by Sunda and Hanson (1979) were used as inputs to the modeling program (log *K* values used were 6.48 for $CuOH^+$, 11.78 for $Cu(OH)_2$, 6.74 for $CuCO_3$, and 10.24 for $Cu(CO_3)_2^{2-}$). Their measured copper hydroxide and copper carbonate stability constants lie in the mid-range of reported stability constants (Sunda and Hanson 1979) and provide modeled estimates that are more consistent with observed relationships between Cu toxicity and pH (Welsh et al. 1993; Erickson et al. 1996).

Results and discussion

Chemical characterization

Surface waters in the Panther Creek basin that are not impacted by the Blackbird Mine are of low hardness, alkalinity, and conductivity, near neutral pH, and contain very low concentrations of major cations, anions, Cu, and Co (Table 1). Although Cu and Co mineralization is present in Deep, Napias, and upper Panther Creek drainages, dissolved Cu and Co concentrations were quite low. Dissolved metal concentrations in Panther Creek downstream of mining influences range from 0.16 to 2.20 μM Cu and from 0 to 3.56 μM Co, with the highest concentrations occurring during spring runoff (Beltman et al. 1994). Because Cu and Co concentrations were negligible, it was not necessary to remove either of those metals from the waters prior to determining the Cu affinities of the suspended and dissolved components.

Dissolved Fe and Mn concentrations in the three sampled locations were quite low, as would be expected in oxygenated surface waters. Organic carbon concentrations ranged from 3.6 to 5.7 mg·L^{-1}. DOC concentrations in streams in cool temperate climates range from 2 to 8 mg·L^{-1}, with a mean of 3 mg·L^{-1} (Thurman 1985).

Laboratory titration of site waters

Intersample and intrasample variability and storage effects

Filtered upstream Panther Creek (PA02) water was titrated on four separate days during the course of 1 week to examine the variability in Cu-binding characteristics on a single sample. The Scatchard plots from these titrations showed close agreement in Cu-binding characteristics (MacRae et al. 1995), demonstrating high reproducibility of Cu titration results from the same sample. Conditional stability constants and binding capacities of Panther Creek DOM after 3 weeks of storage appeared to be slightly lower than those measured in the fresh sample (MacRae et al. 1995). However, the differences were similar to typical variations observed between replicate titrations on the same sample over the course of 1 week. Therefore, storage at 4°C in the dark did not appear to appreciably affect Cu-binding properties of site water.

Although DOC concentrations varied somewhat among upstream Panther, Deep, and Napias Creek samples collected on May 11, the similar titration results from the filtered samples indicate that the Cu-binding characteristics of water from the three sampling locations are very similar during high-flow conditions (Table 2; Fig. 1). The similarity of the binding affinity and complexation capacity of the DOM ligands in Panther, Napias, and Deep creeks indicates that inputs of major tributaries to Panther Creek during high flow do not qualitatively change the Cu-binding characteristics of DOM in Panther Creek. Therefore, the complexation characteristics of DOM in Panther Creek upstream of Blackbird Creek (PA02) can be used to represent Cu–DOM binding in Panther Creek downstream of Blackbird Creek during high-flow conditions. Results from titrations performed on Panther Creek samples collected on later high-flow (May 25) and low-flow (July 20) dates also did not differ considerably from the May 11 results. Therefore, all subsequent titrations were conducted using Panther Creek water collected on May 11 or 25.

© 1999 NRC Canada

Table 2. Stability constants (K) and complexation capacities (CC) estimated for complexation of Cu by dissolved and particulate matter in Panther (PA02), Deep (DE01), and Napias (NA01) creeks determined using one- and two-ligand binding models (eq. 2).

Water sample	DOC/TOC ($mg \cdot L^{-1}$)	log K_1 ($L \cdot mol^{-1}$)	CC_1 ($\mu mol\ Cu \cdot mg\ DOC/TOC^{-1}$)	log K_2 ($L \cdot mol^{-1}$)	CC_2 ($\mu mol\ Cu \cdot mg\ DOC/TOC^{-1}$)
One-ligand model					
PA02 filtered (May 11, 1994)	4.50	5.87 (5.71–6.04)	1.41 (1.17–1.64)	—	—
PA02 unfiltered (May 11, 1994)	5.69	5.74 (5.53–5.95)	1.85 (1.42–2.28)	—	—
DE01 filtered (May 10, 1994)	5.54	5.78 (5.48–6.09)	1.55 (1.00–2.09)	—	—
NA01 filtered (May 10, 1994)	5.94	6.09 (5.98–6.21)	1.02 (0.91–1.13)	—	—
Two-ligand model					
PA02 filtered (May 11, 1994)	4.50	7.26 (7.09–7.43)	0.21 (0.18–0.24)	5.13 (4.97–5.29)	2.89 (2.20–3.56)
PA02 unfiltered (May 11, 1994)	5.69	7.54 (7.34–7.74)	0.23 (0.20–0.27)	5.00 (4.66–5.34)	3.94 (1.58–6.31)
DE01 filtered (May 10, 1994)	5.54	7.31 (5.88–8.74)	0.19 (0.00–0.43)	4.57 (0.00–9.20)	9.80 (0.00–104.15)
NA01 filtered (May 10, 1994)	5.94	7.00 (6.83–7.16)	0.28 (0.22–0.33)	4.83 (4.26–5.40)	3.82 (0.00–7.84)
PA02 unfiltered (May 25, 1994)	nd	7.02	1.37 μM^b	4.80	18.33 μM^b
PA02 filtered (July 20, 1994)	2.7	7.32	0.28	4.25	12.9

Note: Complexation capacities were normalized to DOC or TOC concentration. Numbers in parentheses represent the 95% asymptotic confidence interval. nd, not determined.

[b]Complexation capacities expressed as µM because TOC concentration was not determined.

Fig. 1. Scatchard plots for filtered Panther (PA02, open squares), Deep (DE01, stars), and Napias (NA01, diamonds) and unfiltered Panther Creek (PA02, solid squares) water samples collected on May 11, 1994, and titrated with Cu. $[Cu_{bound}]$ is the concentration of Cu complexed with DOM (eq. 1).

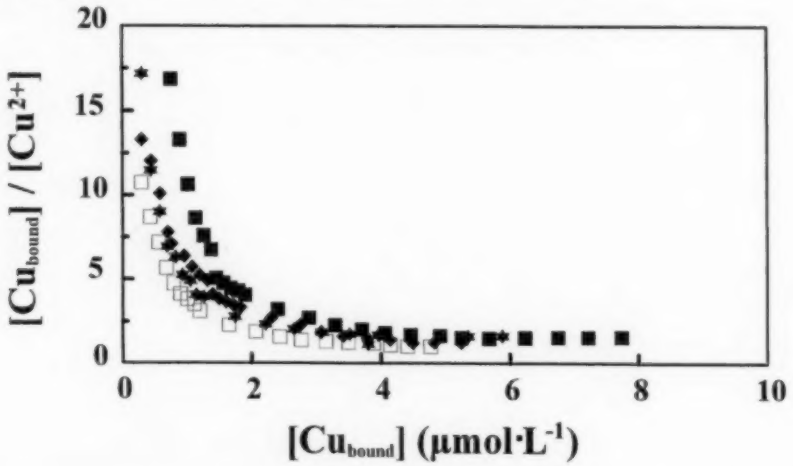

Cu–DOM complexation characteristics

Scatchard plots for all three sampling sites were nonlinear (Fig. 1), illustrating the presence of more than one type of Cu-binding site in the natural DOM. The presence of multiple ligands is typical of complex natural organics and agrees well with results from studies conducted at other locations (Sunda and Hanson 1979; McKnight et al. 1983; Cabaniss 1992). NLR analysis of titration data for Panther, Napias, and Deep Creek samples showed that the data for all three creeks were consistent with a two-ligand model (Table 2). The r^2 values for the two-ligand NLR model were typically >0.996, whereas r^2 values for the one-ligand model averaged 0.959. These two model-defined DOM ligands may not correspond exactly to binding sites actually present in Panther Creek DOM (which may have fewer or more Cu-binding sites), but the results indicate that the Cu-binding characteristics of Panther Creek DOM can be modeled using a two-ligand system. A three-ligand model overfit the data, as indicated by the following: (*i*) the program would not converge (i.e., the sum of squares was never stable), (*ii*) the estimate of standard errors for log K and CC were approximately the same order of magnitude as the values themselves, and (*iii*) log K and CC values were highly correlated between ligands. In general, the maximum number of ligands that can be justified in a multiligand model equals the number of orders of magnitude of metal concentration over which a sample is titrated (Dzombak et al. 1986).

The binding affinity and complexation capacity of the higher-affinity ligand (ligand 1) in Panther Creek waters were similar to those for Deep and Napias creeks (Table 2); however, the corresponding estimates for the lower affinity ligand (ligand 2) differed somewhat among the site waters. This difference is likely caused by an inherently higher variability in estimating the complexation capacity of the lower-affinity ligand rather than by actual differences in complexation capacities among the samples. However, be-

© 1999 NRC Canada

cause $[Cu_{dissolved}]$ in Panther Creek are <2.5 μM, the variability in CC_2 shown in Table 2 does not appreciably alter calculated values of free and bound Cu, for the range of $[Cu_{dissolved}]$ in Panther Creek.

The estimated conditional stability constant for the second, weaker ligand (log K = 4.25–5.13) agrees with several literature values for Cu – humic acid or Cu – fulvic acid conditional stability constants (Guy and Chakrabarti 1976; Sohn and Hughes 1981; Saar and Weber 1982; Finger and Klamberg 1993) and is similar to the Cu–DOM stability constant (log K = 4.90) used in the MINTEQA2 geochemical speciation modeling program (Allison et al. 1991).

The conditional stability constant measured for the higher-affinity ligand in this study (log K = 7.00–7.54) has been reported in only a few other investigations (e.g., Sunda and Hanson 1979; Giesy and Alberts 1989). Many previous investigators did not quantify the high Cu affinity ligand(s) because titrations were likely begun with relatively high total Cu concentrations. Sites with higher conditional stability constants have a high Cu affinity and a low complexation capacity, and only at low Cu titration concentrations will one see the high conditional stability constant sites filled without also seeing the lower conditional stability constant sites filled. Thus, if the high-affinity sites are filled at the beginning of the titration because the amount of Cu added greatly exceeds the number of high-affinity sites, the Scatchard plot will appear to fit a one-ligand model that describes only the low-affinity sites.

The conditional log K values for a one-ligand model fitted to titration data for Panther Creek basin waters ranged from 5.74 to 6.09 (Table 2), in closer agreement with commonly reported log K values for Cu–DOM conditional stability constants. However, the pronounced nonlinear shape of the Scatchard plots indicates that a one-ligand model with a lower conditional log K value would be a gross oversimplification of the binding characteristics of Panther, Napias, and Deep Creek waters and likely would overestimate the amount of bioavailable Cu. For instance, the Cu-binding constants of the fish gill range from 7.2 to 7.6 (Playle et al. 1993*a*; MacRae et al. 1999), a range that brackets the high-affinity, low-capacity DOM ligand (log K = ~7.3) in Panther Creek water. Consequently, Panther Creek DOM should reduce gill–Cu binding, and thus toxicity, by reducing bioavailable Cu. Likewise, dipicolinic acid, the high-affinity component of our organic acid analogue (see below), would also be expected to decrease Cu bioavailability (see MacRae et al. 1999; Marr et al. 1999). If a one-ligand DOM model is used, with a log K below that of the fish gill, most DOM-bound Cu would be mistakenly considered bioavailable.

Effect of Panther Creek suspended particles on Cu-binding characteristics

Observed differences in binding characteristics between filtered and unfiltered samples (Table 2) were attributed to association of Cu with suspended matter in the water. Although the TOC concentration in unfiltered upstream Panther Creek water was over 1 $mg \cdot L^{-1}$ higher than the DOC concentration measured in the filtered PA02 sample (Table 2), the Cu–DOM conditional stability constants for the two-ligand model were similar (log K_1 = 7.26 and 7.54 and log K_2 = 5.13 and 5.00 in filtered and unfiltered water, respectively). Therefore, particulate organic matter in the unfiltered Panther Creek sample did not substantially affect the water's overall Cu-binding ability.

Effect of competing ions on Cu–DOM complexation in site waters

Calcium, Mg, and Co do not compete appreciably with Cu for DOM binding sites at the concentrations present in site waters. NLR 95% confidence intervals for log K and CC values consistently overlapped with those of PA02 waters. These findings are in agreement with (*i*) the lower conditional stability constants for complexation of Ca, Mg, and Co with several organic acids relative to the corresponding Cu conditional stability constants (NIST 1995) and (*ii*) results of competitive binding studies in the literature (O'Shea and Mancy 1978; Sunda and Hanson 1979; Hering and Morel 1988; Cabaniss 1992; Tipping 1993). Therefore, at concentrations relevant to Panther Creek, variations in hardness (Ca and Mg) or the presence of Co do not appreciably influence the Cu–DOM conditional stability constants.

Effect of iron oxyhydroxide particles on Cu-binding characteristics

In samples collected in May, dissolved Fe concentrations were 2.43 μM in Panther Creek and 4.51 μM in Deep Creek. At measured stream pH (7.68 for PA02 and 7.49 for DE01) in oxygenated surface waters, these high Fe concentrations indicate the presence of small iron oxyhydroxide particles and (or) colloids that passed through the 0.45-μm filters. The Cu complexation capacity and conditional stability constant of iron oxyhydroxides are quite low (CC = 0.016 $\mu mol\ Cu \cdot \mu mol\ Fe^{-1}$, log K = 5.72) compared with those for the high-affinity ligand in Panther Creek water (Fig. 2). The Cu-binding affinity of the Fe floc is similar to that of the lower-affinity ligand in Panther Creek water. However, at the concentrations of Fe relative to DOC measured in site water, the Cu complexation capacity of iron oxyhydroxide is much less than the Cu complexation capacity of DOM, and any binding of Cu by iron oxyhydroxides would be minimal.

Selection of an organic acid analogue

In selecting an organic acid mixture that simulates Cu binding by DOM in natural site water, it is important that both the conditional stability constants and the complexation capacities of the natural organic acid and the DOM analogue be similar. A number of commercially available organic acids, including Aldrich® humic acid, were examined to determine if they would, either alone or in combination, meet this requirement.

Aldrich® humic acid has appreciably higher Cu conditional stability constants than the site water DOM (log K_1 = 8.14 versus ~7.2 and log K_2 = 6.15 versus ~5.0), and would cause an underestimation of the bioavailability of Cu in the range of dissolved Cu concentrations occurring in Panther Creek ($[Cu_{dissolved}]$ < 2.5 μM). Therefore, Aldrich® humic acid was unsuitable as an analogue of Panther Creek DOM for use in the companion laboratory toxicity experiments.

Cu-ISE titrations conducted on Panther Creek waters clearly showed that a single organic acid is an oversimplification of the binding characteristics of natural organic matter and underestimates the Cu-binding affinity of DOM in

© 1999 NRC Canada

Fig. 2. Scatchard plots for Cu titrations of a laboratory-prepared solution of an iron oxide (FeO(OH)) colloid (circles and solid line) and filtered Panther Creek water (PA02) (stars and broken line) collected on May 11, 1994. The log K_{Cu} of the FeO(OH) was 5.72.

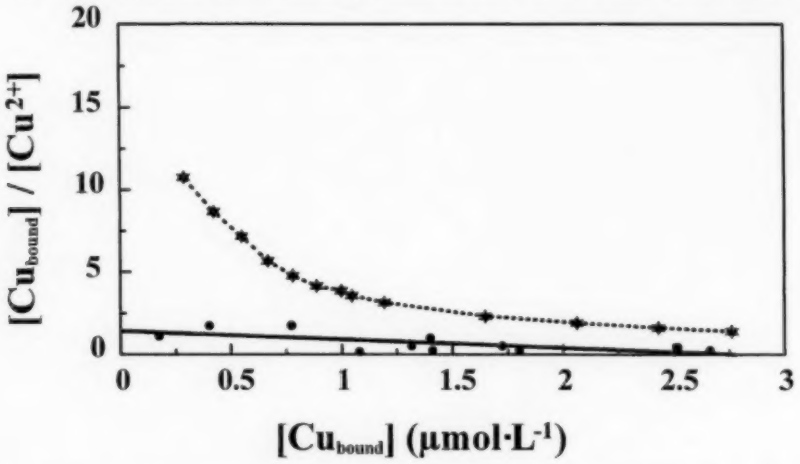

the range of dissolved Cu occurring in Panther Creek. Therefore, a more realistic simulation of Cu–DOM binding characteristics would require that two or more organic acids be selected to create an appropriate DOM analogue. Initial screening narrowed the list of candidate organic acids to four: citric, dipicolinic, malonic, and oxalic. Subsequently, we eliminated citric acid because its Ca-binding properties were quite dissimilar to natural DOM (e.g., Hering and Morel 1988).

Although NLR analysis indicated that a two-ligand system appeared to provide a better simulation of the Cu-binding characteristics of Panther Creek DOM than a three-ligand system, no combination of two commercially available organic acids was able to accurately simulate the Cu-binding properties of Panther Creek water. Therefore, we investigated combinations of three commercially available organic acids. When viewed in combination, the Scatchard plots of dipicolinic (DIP), oxalic (OX), malonic (MAL) acids each appeared to contribute to a specific portion of the Scatchard binding plot for Panther Creek samples. Various concentration ratios were then tested to determine if the three-acid combination could simulate the Cu-binding characteristics of Panther Creek DOM.

DIP has the highest conditional stability constant with Cu (log K = 8.15, in the absence of other ligands; NIST 1995). The other two selected organic acids, OX and MAL, with lower conditional stability constants (log K = 6.60 and 5.58, respectively) are straight-chain aliphatic acids containing two carboxylic acid groups. In contrast, DIP contains a nitrogen-substituted benzene ring with two carboxylic acid groups. The presence of the nitrogen atom likely enhances Cu binding. Addition of this nitrogen-containing compound to the organic acid mixture not only simulates the high-affinity ligand(s) in Panther Creek DOM, it also better simulates the heterogeneity of binding sites present in natural organic matter. Elemental analyses of natural organic matter have demonstrated that both carboxyl and nitrogenous functional groups are important metal-binding sites (Thurman 1985).

The concentrations of DIP, OX, and MAL that together simulate the Cu-binding characteristics of DOM in Panther Creek water were determined iteratively, using a combination of MINEQL$^+$ modeling and actual titrations of three-acid mixtures. Because of apparent interactions among the acids in the mixture, the conditional stability constants that provided the best fit to the titration data for the three-acid mixture differed slightly from the values listed above. The Cu–DIP, Cu–OX, and Cu–MAL stability constants (for single ligands) used in our MINEQL$^+$ model were log K = 8.50, 6.75, and 5.70, respectively. The agreement of the Scatchard plot predicted by MINEQL$^+$ with the actual Scatchard plot (Fig. 3) and the log K and CC values calculated by NLR (Table 3) indicate that the iteratively determined conditional stability constants and complexation capacities accurately predict the actual Cu-binding characteristics of the DOM analogue (MacRae et al. 1995).

The Cu-binding characteristics of Panther Creek DOM containing 4.5 mg DOC·L^{-1} were closely matched by a mixture of DIP, OX, and MAL at concentrations of 0.1, 2.0, and 5.0 µM, respectively. These complexation capacities vary linearly with DOM concentrations; thus, to mimic a DOC concentration of 9 mg·L^{-1} in Panther Creek, twice the concentration of each organic acid would be used. At pH ≥ 6.0, both ligands on each organic acid will be fully deprotonated and able to complex 1 mol Cu·mol organic acid^{-1}. Based on results of Panther Creek titrations at different DOC concentrations, Cu–DOM conditional stability constants do not change significantly at slightly higher or lower DOC concentrations (e.g., in the range of about 26 mg DOC·L^{-1}).

The fit between PA02 and the DOM analogue is quite close (Fig. 3; Table 3). Because [Cu_{total}] in fish toxicity studies typically do not exceed 2.5 µM, comparisons between the DOM analogue and the site-water DOM were not made above this Cu concentration.

Geochemical modeling of toxicity test waters

Gill–Cu binding constants determined in two studies (Playle et al. 1993*b*; MacRae et al. 1995) suggest that some forms of DOM-bound Cu may be available to fish because

© 1999 NRC Canada

Fig. 3. Scatchard plots for Cu titrations of Panther Creek water (PA02, circles), the DOM analogue (diamonds), and the MINEQL⁺ model of the analogue (solid line).

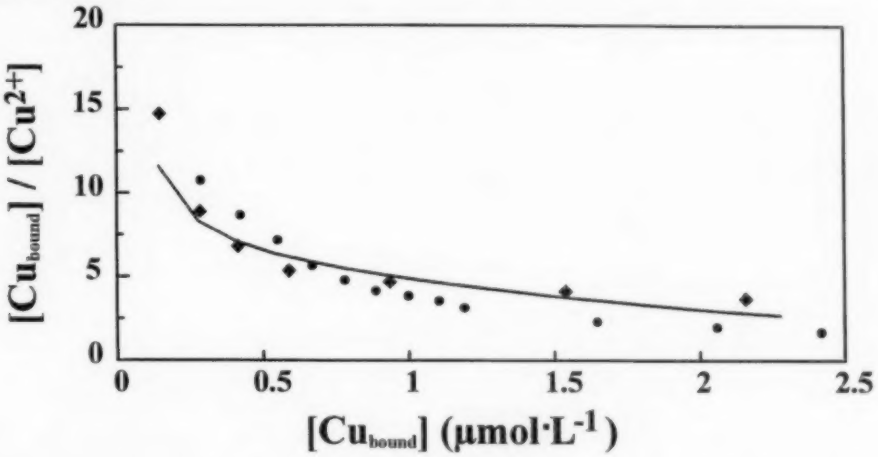

Table 3. Stability constants (K) and complexation capacities (CC) estimated for complexation of Cu by DOM in Panther Creek (PA02), the organic acid analogue, and the MINEQL⁺ model determined using two-ligand binding models (eq. 2).

Titration	log K_1 (L·mol^{-1})	CC_1 (µM)	log K_2 (L·mol^{-1})	CC_2 (µM)
PA02 filtered	7.26 (7.09–7.43)	0.945 (0.810–1.080)	5.13 (4.97–5.29)	13.01 (9.90–16.02)
DOM analogue	8.70 (6.35–11.04)	0.151 (0.045–0.256)	5.52 (5.36–5.68)	19.13 (13.70–24.55)
MINEQL⁺ model	7.80 (7.62–7.99)	0.221 (0.173–0.269)	6.25 (6.22–6.28)	4.12 (4.02–4.21)

Note: Numbers in parentheses represent the 95% asymptotic confidence interval.

Table 4. Predicted [Cu^{2+}] at varying [Cu_{total}] in the presence of Panther Creek (PA02) DOM, the organic acid analogue, and the MINEQL⁺ model.

	[Cu^{2+}] (µM)		
[Cu_{total}] (µM)	PA02	Organic acid analogue	MINEQL⁺ model
0.157	0.014	0.009	0.014
0.393	0.042	0.053	0.047
0.787	0.124	0.136	0.123
1.181	0.262	0.223	0.218
1.573	0.442	0.313	0.330

Note: [Cu^{2+}] were back-calculated using eq. 2 with the corresponding log K and CC values (Table 3).

Cu–DOM binding constants can range from 4 to 15 (log K), with average values for humic acids of 4.9–6.8 (Guy and Chakrabarti 1976; Giesy and Alberts 1989). During the toxicity tests, rainbow trout (*Oncorhynchus mykiss*) fry were exposed to Cu concentrations representative of site water (Marr et al. 1999). Fish were exposed to Cu combined with a broad range of concentrations of the organic acid analogue that was selected to mimic the Cu-binding affinity and capacity of DOM in site water. To help determine the bioavailable concentration of Cu, we calculated the concentrations and percentages of Cu in the various inorganic and organic chemical species that might have formed in the exposure waters. From these model predictions, toxicity could be correlated with specific Cu species. Close agreement between the MINEQL⁺ model-predicted Scatchard plot and an actual Cu-ISE titration of the organic acid mixture indicates that the model's Cu speciation predictive power is acceptable (Fig. 3). And based on the NLR-calculated binding constants, predicted [Cu^{2+}] (Table 4) for PA02, the organic acid analogue, and the simulated MINEQL⁺ model were within 0.01 µM of one another over the range of [Cu_{total}] examined in the companion fish toxicity studies (Marr et al. 1999).

Stability constants used in this model were based on the results of the NLR analyses discussed earlier (Table 2). Stability constants for complexes of inorganic cations associated with organic acid anions were adopted from either the MINEQL⁺ thermodynamic database or values reported in the literature or were derived empirically in our laboratory.

Limitations of the DOM analogue

The mixture of DIP, OX, and MAL that we selected to mimic the Cu-binding characteristics of site-water DOM is most appropriate for use at pH 6.0, the pH at which we performed the Cu titrations, because of limitations in detecting Cu^{2+} with a Cu-ISE at pH > 6.5. Although pH-dependent competition of Cu^{2+} and H^+ for binding to the three organic acids in our DOM analogue is automatically incorporated into the MINEQL⁺ calculations by way of the acid dissociation constants, this does not guarantee that Cu-binding sites on site-water DOM will respond to pH changes in the same manner. For example, potential pH-dependent conformational changes in the DOM might affect Cu-binding affinities and (or) capacities independent of the effect of proton

© 1999 NRC Canada

loading and unloading as pH changes. Currently, the relative importance of this effect is unclear. Sunda and Hanson (1979) reported that Cu-binding constants of DOM from a river in the southeastern United States increased by 1 log unit per unit of pH increase. Nonetheless, because of the uncertainty surrounding pH-induced conformational changes, we have not incorporated a pH dependency of the log K values for Cu–DOM complexes in our MINEQL$^+$ speciation calculations for site waters. Additional research into such phenomena will be important for predicting Cu bioavailability in the presence of natural DOM.

Conclusions

The binding of Cu by Panther Creek DOM is consistent with a two-ligand model in which Cu–DOM conditional stability constants and complexation capacities for the two-ligand model are log K_1 = 7.26, CC_1 = 0.21 μmol Cu·mg DOC^{-1} and log K_2 = 5.13, CC_2 = 2.89 μmol Cu·mg DOC^{-1}. Copper-binding characteristics of site water were not appreciably affected by date of water sample collection or storage time at 4°C or by competing cations (Ca^{2+}, Mg^{2+}, or Co^{2+}), iron oxide particles, or other suspended particulates at the concentrations present in Panther Creek.

A mixture of three commercially available organic acids (0.022 μM DIP, 0.44 μM OX, and 1.11 μM MAL) has a Cu-binding affinity and capacity equivalent to 1 mg $DOC \cdot L^{-1}$ within the range of dissolved Cu concentrations occurring in Panther Creek ($[Cu_{dissolved}] < 2.5$ μM). This mixture is a suitable analogue of DOM for use in fish toxicity studies (e.g., Marr et al. 1999).

Acknowledgments

This research was funded by the U.S. National Oceanic and Atmospheric Administration, the U.S. Forest Service, and the State of Idaho. Jamie Schardt and Candace Bath (Hagler Bailly Consulting, Inc.) assisted with sample collection and preparation, and Connie Boese and Mike Suedkamp (University of Wyoming) assisted with chemical analyses and Cu titrations.

References

Allison, J.D., Brown, D.S., and Novo-Gradac, K.J. 1991. MINTEQA2/PRODEFA2, a geochemical assessment model for environmental systems: version 3.0 user's manual. U.S. Environmental Protection Agency Report No. EPA/600/3-91/021, Environmental Research Laboratory, Athens, Ga.

Beltman, D., Cacela, D., Lipton, J., Maest, A., and Schardt, J. 1994. Surface water resource injury assesment: Blackbird Mine site NRDA. Hagler Bailly Consulting, Inc., P.O. Drawer O, Boulder, CO 80306-1906, U.S.A.

Blaedel, W.J., and Dinwiddie, D.E. 1974. Study of the behavior of copper ion-selective electrodes at submicromolar concentration levels. Anal. Chem. **46**: 873–877.

Borgmann, U. 1983. Metal speciation and toxicity of free metal ions to aquatic biota. *In* Aquatic toxicology. *Edited by* J.O. Nriagu. John Wiley & Sons, Inc., New York. pp. 47–72.

Cabaniss, S.E. 1992. Synchronous fluorescence spectra of metal – fulvic acid complexes. Environ. Sci. Technol. **26**: 1133–1138.

Campbell, P.G.C. 1995. Interactions between trace metals and aquatic organisms: a critique of the free-ion activity model. *In* Metal speciation and bioavailability in aquatic systems. *Edited by* A. Tessier and D.R. Turner. John Wiley & Sons, Inc., New York.

Campbell, P.G.C., and Stokes, P.M. 1985. Acidification and toxicity of metals to aquatic biota. Can. J. Fish. Aquat. Sci. **42**: 2034–2049.

Dzombak, D.A., Fish, W., and Morel, F.M.M. 1986. Metal–humate interactions. 1. Discrete ligand and continuous distribution models. Environ. Sci. Technol. **20**: 669–675.

Erickson, R.J., Benoit, D.A., Mattson, V.R., Nelson, H.P., Jr., and Leonard, E.N. 1996. The effects of water chemistry on the toxicity of copper to fathead minnows. Environ. Toxicol. Chem. **15**: 181–193.

Finger, W., and Klamberg, H. 1993. Interactions between soil humic substances and metal ions. III. Complex formation of soil humic acids and soil fulvic acids with metal ions. Z. Pflanzenernaehr. Bodenkd. **156**: 19–24.

Giesy, J.P., and Alberts, J.J. 1989. Conditional stability constants and binding capacities for Cu(II) by ultrafilterable material isolated from six surface waters of Wyoming, USA. Hydrobiologia, **188/189**: 659–679.

Gonzalez-Davila, M., Santana-Casiano, J.M., Perez-Pena, J., and Millero, F.J. 1995. Binding of Cu(II) to the surface and exudates of the alga *Dunaliella tertiolecta* in seawater. Environ. Sci. Technol. **29**: 289–301.

Guy, R.D., and Chakrabarti, C.L. 1976. Studies of metal–organic interactions in model systems pertaining to natural waters. Can. J. Chem. **54**: 2600–2611.

Hering, J.G., and Morel, F.M.M. 1988. Humic acid complexation of Ca and Cu. Environ. Sci. Technol. **22**: 1234–1237.

Jonnalagadda, S.B., and Prasada Rao, P.V.V. 1993. Toxicity, bioavailability and metal speciation. Comp. Biochem. Physiol. C. Comp. Pharmacol. **106**: 585–595.

MacRae, R.K., Meyer, J.S., Maest, A., Beltman, D., and Cors, C. 1995. Geochemical complexation studies. Blackbird Mine NRDA, Idaho. Hagler Bailly Consulting, Inc., P.O. Drawer O, Boulder, CO 80306-1906, U.S.A.

MacRae, R.K., Smith, D.E., Swoboda-Colberg, N., Meyer, J.S., and Bergman, H.L. 1999. The copper binding affinity of rainbow trout (*Oncorhynchus mykiss*) and brook trout (*Salvelinus fontinalis*) gills: implications for assessing bioavailable metals. Environ. Toxicol. Chem. **18**: 1180–1189.

Marr, J.C.A., Lipton, J., Cacela, D., Hansen, J.A., Meyer, J.S., and Bergman, H.L. 1999. Bioavailability and acute toxicity of copper to rainbow trout in the presence of organic acids simulating natural dissolved organic carbon. Can. J. Fish. Aquat. Sci. **56**: 1471–1483.

McKnight, D.M., Feder, G.L., Thurman, E.M., Wershaw, R.L., and Westall, J.C. 1983. Complexation of Cu by aquatic humic substances from different environments. Sci. Total Environ. **28**: 65–76.

NIST. 1995. NIST standard reference database 46: NIST critically selected stability constants of metal complexes database, version 2.0. User's guide. National Institute of Standards and Technology, Gaithersburg, Md.

Norusis, M.J. 1993. SPSS for Windows®: professional statistics, release 6.0. SPSS Inc., Chicago, Ill.

O'Shea, T.A., and Mancy, K.H. 1978. The effect of pH and hardness metal ions on the competitive interaction between trace metal ions and inorganic and organic complexing agents found in natural waters. Water Res. **12**: 703–711.

Pagenkopf, G.K., Russo, R.C., and Thurston, R.V. 1974. Effect of complexation on toxicity of copper to fishes. J. Fish. Res. Board Can. **31**: 462–465.

Playle, R.C., Dixon, D.G., and Burnison, K. 1993*a*. Copper and

© 1999 NRC Canada

cadmium binding to fish gills: modification by dissolved organic carbon and synthetic ligands. Can. J. Fish. Aquat. Sci. **50**: 2667–2677.

Playle, R.C., Dixon, D.G., and Burnison, K. 1993*b*. Copper and cadmium binding to fish gills: estimates of metal–gill stability constants and modelling of metal accumulation. Can. J. Fish. Aquat. Sci. **50**: 2678–2687.

Saar, R.A., and Weber, J.H. 1982. Fulvic acid: modifier of metal-ion chemistry. Environ. Sci. Technol. **16**: 510A–517A.

Scatchard, G. 1949. The attraction of proteins for small proteins and ions. Ann. N.Y. Acad. Sci. **51**: 660–672.

Schecher, W.D., and McAvoy, D.C. 1991. MINEQL$^+$: a chemical equilibrium program for personal computers. User's manual version 2.1. The Procter and Gamble Company, Cincinnati, Ohio.

Sohn, M.L., and Hughes, M.C. 1981. Metal ion complex formation constants of some sedimentary humic acids with Zn(II), Cu(II), and Cd(II). Geochim. Cosmochim. Acta, **45**: 2393–2399.

Sposito, G. 1981. Trace metals in contaminated waters. Environ. Sci. Technol. **15**: 396–403.

Sunda, W.G., and Hanson, P.J. 1979. Chemical speciation of Cu in river water: effect of total Cu, pH, carbonate, and dissolved organic matter. *In* Chemical modeling in aqueous systems: speciation, sorption, solubility and kinetics. ACS Symposium Series 93. *Edited by* E.A. Jenne. American Chemical Society, Washington, D.C. pp. 147–180.

Thurman, E.M. 1985. Organic geochemistry of natural waters. NIJHOFS/ JUNK, Dordrecht, The Netherlands.

Tipping, E. 1993. Modeling the competition between alkaline earth cations and trace metal species for binding by humic substances. Environ. Sci. Technol. **27**: 520–529.

Verweij, W., Glazewski, R., and DeHaan, H. 1992. Speciation of copper in relation to its bioavailability. Chem. Speciation Bioavailability, **4**: 43–51.

Welsh, P.G., Skidmore, J.F., Spry, D.J., Dixon, D.G., Hodson, P.V., Hutchinson, N.J., and Hickie, B.E. 1993. Effect of pH and dissolved organic carbon on the toxicity of copper to larval fathead minnow (*Pimephales promelas*) in natural lake waters of low alkalinity. Can. J. Fish. Aquat. Sci. **50**: 1356–1362.

© 1999 NRC Canada

Assessing the toxicity of lead in sediments to *Hyalella azteca*: the significance of bioaccumulation and dissolved metal

Uwe Borgmann and Warren P. Norwood

Abstract: The relationship between bioaccumulation and toxicity of Pb to *Hyalella* was the same for animals exposed to Pb in water alone and for those exposed to Pb-spiked sediments, provided that the animals were gut cleared before Pb analysis. The same critical body concentration (about 126 nmol·g dry mass^{-1}) can be used to predict Pb toxicity in both water-only and sediment exposures. Furthermore, Pb bioavailability in Pb-spiked sediments was due primarily to dissolved metal: animals caged above the sediments accumulated the same amount of Pb and had the same mortality as animals exposed directly to sediment. Increasing the water to sediment ratio from 4:1 to 67:1 resulted in a lower dissolved organic C and lower total dissolved Pb concentration in the water but no change in bioavailable Pb (i.e., bioavailable Pb was not proportional to total dissolved Pb). The overlying water concentration may be a useful indicator of bioavailable Pb in sediment tests, provided a large water to sediment ratio is used to reduce the effect of sediment on overlying water quality (i.e., Pb-complexing capacity). Although less reliable than body concentration measurements, this could provide a useful screening tool for possible Pb-induced toxicity because it can be measured without test animals present.

Résumé : La relation entre la bioaccumulation et la toxicité du Pb chez *Hyalella* était la même pour les animaux exposés au Pb présent dans l'eau seulement et ceux exposés à des sédiments auxquels on a ajouté du Pb, dans la mesure où les animaux étaient éviscérés avant le dosage du Pb. La même concentration corporelle critique (environ 126 nmol·g masse à sec^{-1}) peut être utilisée pour prévoir la toxicité du Pb présent dans l'eau seulement et dans les sédiments. De plus, c'est principalement sous sa forme dissoute que le Pb des sédiments plombés était biodisponible : les animaux encagés au-dessus des sédiments ont accumulé la même quantité de Pb et ont connu le même taux de mortalité que les animaux exposés directement aux sédiments. L'accroissement du ratio eau à sédiment de 4:1 à 67:1 a eu pour effet de réduire les concentrations du C organique dissous et du Pb dissous total dans l'eau, mais n'a pas fait varier le Pb biodisponible (c.-à.-d. que le Pb biodisponible n'était pas proportionnel au Pb dissous total). La concentration dans l'eau sus-jacente peut constituer un indicateur utile du Pb biodisponible dans les essais de sédiments, dans la mesure où un ratio eau/sédiments élevé est utilisé pour réduire l'effet des sédiments sur la qualité de l'eau sus-jacente (effet lié à leur capacité de complexation du Pb). Bien que moins fiable que les mesures de la concentration corporelle, cette approche peut constituer un bon moyen pour dépister la toxicité que peut induire le Pb parce qu'elle permet de réaliser des mesures sans utilisation d'animaux expérimentaux.

[Traduit par la Rédaction]

Introduction

The need for assessing and managing contaminated sediments has led to the development of chemically based sediment quality criteria (referred to variously as guidelines, assessment values, or effect concentrations). Good data and methods for predicting cause and effect relationships in toxic sediments are, however, limited. Most guidelines or sediment assessment values have been developed by comparing observed biological effects with chemical composition of the sediments (e.g., Persaud et al. 1993; Ingersoll et al. 1996; Smith et al. 1996). This is the same rationale used in the sediment quality triad approach (Chapman 1990) in which sediment chemistry, sediment bioassays, and in situ biological assessment of natural benthic communities are compared in an attempt to link potential cause (chemistry) to effect (biological response). However, sediments are rarely contaminated by one substance alone, and the concentrations of many contaminants correlate with those of others. Consequently, when a critical sediment concentration is exceeded, there is, statistically, an increased probability of a toxic effect, but it is not possible to claim that the effect is due to the presence of that specific contaminant. To complicate matters further, the bioavailability of metals in sediments is highly variable. If sediment components display a strong binding towards metal ions, or if they include metals firmly bound within the matrix of mineral or organically derived particles, then a high total metal concentration in the sediment may still be nontoxic to aquatic biota. On the other hand, another sediment with much lower total metal concentrations may contain more bioavailable metal and be toxic

Received December 8, 1998. Accepted April 8, 1999.
J14933

U. Borgmann[1] and W.P. Norwood. Environment Canada, National Water Research Institute, Aquatic Ecosystem Restoration Branch, P.O. Box 5050, 867 Lakeshore Rd., Burlington, ON L7R 4A6, Canada.

[1]Author to whom all correspondence should be addressed.
e-mail: uwe.borgmann@cciw.ca

© 1999 NRC Canada

(e.g., Borgmann and Norwood 1997*a*). This makes prediction of effects from total metal concentrations in the sediment extremely difficult. There are, therefore, two disadvantages with reliance on current sediment quality guidelines: there is no proof of cause and effect and variations in metal bioavailability are not taken into account.

Studies on metal toxicity in waterborne exposures suggest a possible solution to these drawbacks: prediction of effects from metals accumulated by the biota rather than metal concentrations in the exposure medium. Body concentrations of cadmium and Tl correlated much more closely with toxicity to the amphipod *Hyalella azteca* than concentrations in the water (Borgmann et al. 1991, 1998). Similarly, Cu accumulated by duckweed correlated much better with toxicity than either total Cu or free Cu ion concentrations in the water (Huebert et al. 1993). The lethal body concentrations of Cd to *Hyalella* exposed to Cd-spiked sediments also compared reasonably well with those obtained in water-only exposures (Borgmann et al. 1991). However, the relationship between bioaccumulation and toxicity for Cu and Zn in *Hyalella*, without gut clearance, differed between water-only and spiked-sediment exposures (Borgmann and Norwood 1997*b*). One potential problem with sediment exposures is metal present in the gut. The strong propensity of metals to bind to sediments means that ingestion of even small amounts of sediment can result in substantial increases in total body concentration for some metals (Neumann et al. 1999). Furthermore, the high exposure to sediment-bound and (or) ingested metals can result in different internal distribution patterns for metals in the bodies of invertebrates (Saouter et al. 1993). This complicates the interpretation of the biological significance of a given level of metal accumulation in sediment-exposed animals.

A recent study examining the rate of clearance of metals from the gut of *Hyalella* revealed that gut contents contributed more to the total body burden for Pb (81%) than for Cd, Cu, or Zn (Neumann et al. 1999). Incomplete gut clearance, or additional uptake of metal from ingested sediment, could, therefore, substantially affect the relationship between bioaccumulation and toxicity for Pb. Furthermore, since Pb is not an essential metal, the difference between background and lethal body concentrations in *Hyalella* is much greater than for Cu or Zn. This makes Pb a useful metal for testing whether the lethal body concentration is the same for animals exposed to metal in water and for those exposed to metal in sediment.

The objectives of this study were to address the following three questions. (*i*) Does Pb-induced toxicity to *Hyalella* occur at the same body concentration of Pb for water-only and contaminated sediment exposures and, if so, does this apply to gut-cleared or non-gut-cleared animals? (*ii*) Is toxicity due primarily to dissolved metal, or does the solid phase contribute substantially to Pb bioaccumulation and (or) toxicity? (*iii*) Does the ratio of water to sediment used in a sediment toxicity test affect bioaccumulation and (or) toxicity? Answers to these questions will tell us whether body concentrations of Pb in *Hyalella* can be used reliably to predict Pb-induced effects, whether dissolved Pb in water can be used as an indicator of bioavailable Pb, and whether body or water concentrations are better predictors of toxic effects. To do this, we conducted toxicity tests with Pb-spiked sediments using two different exposure vessels: beakers with a 4:1 water to sediment ratio and Imhoff settling cones with a 67:1 sediment to water ratio (1 L to 15 mL). Animals were exposed both directly to the sediment and in cages suspended over the sediment (i.e., preventing direct contact with the solid-phase sediment), and results were compared with previous studies conducted in water-only exposures.

Table 1. Measured Pb concentration in mixtures of Pb-spiked and unspiked sediments (μmol·g dry mass^{-1}), standard deviation of logarithmically transformed data (n = 6), and predicted Pb concentration based on the regression Pb_{sed} = 0.6032 + 1.2822·spike.

Spike (%)	Geometric mean Pb (μmol·g^{-1})	SD (log Pb)	Predicted off regression
0	0.59	0.056	0.60
3	5.3	0.132	4.45
6	7.43	0.133	8.3
10	13.3	0.094	13.4
18	22.0	0.104	23.7
32	37.7	0.139	41.6
56	79.9	0.072	72.4
100	136	0.133	129

Materials and methods

Amphipods were cultured in dechlorinated Burlington city tap water (from Lake Ontario, hardness 130 mg·L^{-1}, alkalinity 90 mg·L^{-1}, pH 7.9–8.6) as described in Borgmann et al. (1989). Young were harvested and culture water was renewed weekly, providing a continuous supply of 0- to 1-week-old amphipods for experiments. Cultures and experimental animals were kept in an incubator at 25°C with a 16 h light : 8 h dark photoperiod; the same conditions were used for the experiments.

Sediment was collected from the center of the western basin in Hamilton Harbour with a Ponar sampler and stored in polyethylene buckets at 4°C until used. This is a fine-grained sediment with about 75% moisture content, a loss on ignition of about 10%, and an organic C content of 3%. Measured metal concentrations in unspiked sediment were Co 12, Cr 119, Cu 101, Fe 45 400, Mn 1720, Ni 47, Pb 113, and Zn 1240 μg·g dry weight^{-1}. Sediment from this site is not "clean" but consistently supports high survival in 4-week chronic toxicity tests. The sediment was not sieved or treated in any other way prior to spiking with Pb. Sediment was spiked with Pb by mixing equal volumes of sediment and 50 mM $PbCl_2$ in Milli-Q deionized water in polypropylene bottles and rotating the mixture for 24 h at 4 rpm on a mechanical mixer. The sediment was then allowed to settle and the surface water was decanted. The spiking procedure was repeated three more times with additional volumes of 50 mM $PbCl_2$. Control sediment was treated in the same way but without $PbCl_2$ added to the water. Spiked sediments of lower concentration were then made by thoroughly mixing 3, 6, 10, 18, 32, or 56% metal-spiked sediment with control sediment. Sediment spiking was performed only once and a single sediment batch was produced for each Pb concentration. The same sediment batches were used throughout to minimize differences between experiments and container types. Measured Pb concentrations (micromoles per gram dry mass) in sediments were linearly related to the percentage of the Pb-spiked sediment added to each mixture, following the relationship Pb_{sed} = 0.6032 + 1.2822·spike (based on regression after log transformation, Table 1). The predicted Pb concentrations in sediment were used in all subsequent calculations instead of the mean measured Pb at each concentration

© 1999 NRC Canada

Table 2. Summary of percent survival of controls in each chronic (4-week) toxicity test conducted with Pb-spiked sediments and number (in parentheses) of replicate containers used for each treatment.

Experiment No.	Small beaker, direct exposure to sediments	Large beaker, direct exposure to sediments	Caged animals in large beaker	Cone, direct exposure to sediments	Caged animals in cone
1	—	92 (2)	92 (2)	—	—
2	80 (1)	84 (2)	88 (2)	100 (1)	—
3	95 (1)	—	—	90 (2)	46 (2)[a]

[a]Survival data from this treatment not used in calculations due to low survival of controls.

Fig. 1. Comparison of volumes and shapes of test containers used in this study. The small and large beakers contained the same sediment to water ratio (4:1) but only the large beakers could accommodate a cage. The shape of the Imhoff settling cone allows a large sediment to water ratio (67:1) while still maintaining a substantial sediment depth (2.3 cm).

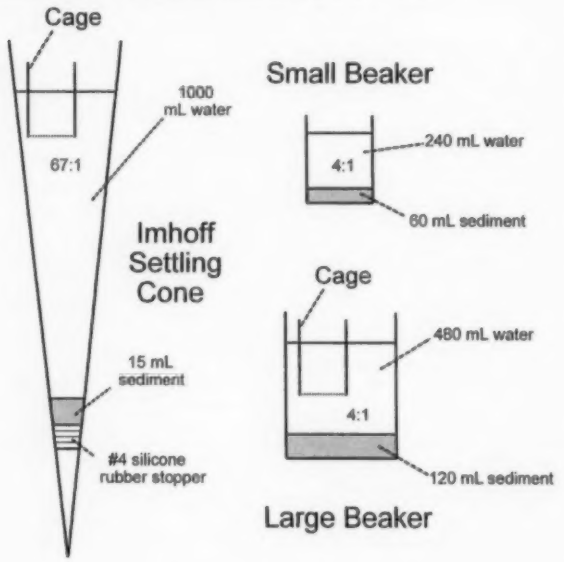

because we judged the error due to sediment mixing to be less than the error associated with measurement of Pb in sediment.

Toxicity tests were conducted as described in Borgmann and Norwood (1997*b*), except that three different experimental containers were used: small (500 mL) polyethylene beakers, large (1000 mL) beakers, and polycarbonate Imhoff settling cones plugged with a No. 4 silicone rubber stopper (Fig. 1). A volume of 60, 120, or 15 mL of sediment and 240, 480, or 1000 mL of overlying water was added to the small beakers, large beakers, and cones, respectively. This gave a water to sediment ratio of 4:1 for the beakers and 67:1 for the cones. Sediment was carefully added to containers partially filled with water using a large plastic syringe with an enlarged opening and injected onto the bottom with minimal mixing with overlying water. The containers were then filled to the desired volume with dechlorinated tap water and aerated for 1–2 weeks to equilibrate and allow oxygenation of the surface sediment before addition of animals. The sediment surface area was about 7.5, 48, and 82 cm^2 in the cones, small beakers, and large beakers, respectively. A cage, consisting of a 250-mL polypropylene specimen container with the bottom cut out and replaced with a 200-μm-mesh nylon screen, was added to the large beakers and in one of the experiments with cones. A 5 × 5 cm piece of cotton gauze was added to the cage to provide a substrate for the animals. Containers were covered with plastic lids and gently aerated throughout the experiments. Twenty 0- to 1-week-old amphipods were added to each beaker and 15 or 20 to the cones. An equivalent number of animals was added to the cages, if present. No density effects were observed when cones were inoculated with 5–30 young amphipods in preliminary experiments, and survival and growth were similar in cones and beakers. Tetra-Min® fish food flakes were added to each test container, and to the cages if present, in the following amounts: 2.5 mg at the start of week 1, 2.5 mg twice in week 2, 2.5 mg three times in week 3, and 5 mg three times in week 4. Feeding did not affect water clarity and all food added was either eaten or decomposed rapidly.

Three separate experiments were run, with varying container types (Table 2). Survival of controls ranged from 80 to 100%, except for poor survival (46%) of caged animals in the cones in experiment 3 (Table 2); survival data from this last treatment were not used in any of the analyses. After 4 weeks of incubation, the overlying water was carefully decanted (so as not to resuspend the sediments) into clean polyethylene containers and then filtered through 0.4-μm polycarbonate filters for analysis of dissolved organic C (DOC), major ions, and Pb. All equipment used for water sampling and filtering was acid cleaned and kept covered prior to use, and filters were rinsed in nitric acid and Milli-Q deionized water before use. Blanks were collected simultaneously to correct for background contamination. In addition, 1-mL water samples were collected periodically from selected containers by pipette and filter syringes for time trend analysis of total and dissolved Pb. The surviving amphipods were sorted from the sediment by sieving and rinsed in clean water. One half of the animals from each container were placed in 120-mL plastic specimen containers with 50 μM EDTA and cotton gauze for 24 h to clear their guts; the other half were processed immediately. Amphipods were weighed as a group to provide a mean mass per container for growth rate comparison and then dried at 60°C overnight.

Groups of four dried amphipods (about 0.5–3 mg total dry mass) were digested with 70% nitric acid at room temperature for 1 week, after which 30% hydrogen peroxide was added and digestion allowed to continue for another 24 h. Each sample was then made up to 0.5–2 mL with Milli-Q deionized water. Acid, peroxide, and total volumes were 25 μL, 20 μL, and 1 mL, respectively, for samples of about 1 mg dry mass. These were halved or doubled for samples weighing closer to 0.5 or 2 mg respectively, keeping the volume ratios the same. Dried sediment samples were analyzed using similar dry mass to acid to peroxide ratio and digestion times but with larger volumes (20 mg of sediments, 250 μL of nitric acid, 200 μL of peroxide, 10 mL final volume). Water, digested amphipods, and sediments were analyzed for Pb on a Varian SpectraAA 400 graphite furnace atomic absorption spectrophotometer with Zeeman background correction using a platform and ammonium phosphate modifier. All analyses were corrected using appropriate blanks with equivalent acid, peroxide, and Milli-Q deionized water but no sample. Recovery of Pb in Tort-1 lobster hepatopancreas reference material (National Research Council of Canada) was 102% in previous studies using this procedure (MacLean et al. 1996). One-way ANOVA of log[dissolved Pb in water] by group (each experiment, container type, and concentra-

© 1999 NRC Canada

Table 3. DOC ($mg \cdot L^{-1}$) and major ion concentrations ($mmol \cdot L^{-1}$) in tap water (Lake Ontario), in overlying water at the end of the incubation period in cones or beakers with unspiked sediment (0.6 μmol Pb·g^{-1}), in Pb-spiked sediment with 24 or 129 μmol Pb·g dry mass $sediment^{-1}$, and in cones or beakers with cotton gauze added as a substrate instead of sediment.

Water source	DOC	SO_4^{2-}	Cl^-	Ca^{2+}	Mg^{2+}	Na^+	K^+	HCO_3^-
Tap water	1.7	0.32	0.68	0.92	0.36	0.56	0.04	1.73
Cone, Pb 0.6	4.6	0.44	0.79	1.17	0.38	0.71	0.08	1.90
Cone, Pb 24	3.8	0.38	0.84	1.14	0.38	0.77	0.10	2.00
Cone, Pb 129	4.4	0.47	1.24	1.38	0.39	0.72	0.06	1.80
Beaker, Pb 0.6	9.6	1.93	0.98	2.47	0.50	0.94	0.08	1.65
Beaker, Pb 24	7.8	1.58	1.55	2.54	0.45	0.79	0.07	1.57
Beaker, Pb 129	10.8	1.88	5.02	4.39	0.53	0.91	0.07	1.46
Cone, gauze	5.9	0.33	0.75	0.92	0.36	0.64	0.05	1.78
Beaker, gauze	7.1	0.32	0.78	0.90	0.38	0.66	0.06	1.80

tion representing a different group) gave a mean square error (MSE) of 0.0035, equivalent to a standard deviation of 0.059 ($MSE^{0.5}$) between replicate experimental containers (±1 SD = 0.87–1.15 × mean). Total (unfiltered) Pb in water was also measured, but the results are not reported here. Total Pb matched dissolved Pb closely, except for the first 24 h when it was much higher and for the occasional erratic high value. One-way ANOVA of log[Pb in *Hyalella*] by group gave an MSE of 0.032, equivalent to a standard deviation of 0.18 between replicate experimental containers (±1 SD = 0.66–1.51 × mean) for gut-cleared animals and a slightly lower MSE (0.027) for non-gut-cleared animals. Alkalinity was measured by titration, DOC by ultraviolet digestion and infrared detection, anions by colorimetry (ferric thiocyanate for Cl^- and methylthymol blue for SO_4^{2-}), and cations by inductively coupled plasma – optical emission spectrometry by the National Laboratory for Environmental Testing, Environment Canada, Burlington, Ont.

Statistical analyses were performed using Systat 7.0. Mathematical relationships between Pb in water or *Hyalella* and Pb in sediment were obtained using the NONLIN module. Relationships between mortality rates ($m = -\ln(N \cdot N_{initial}^{-1}) \cdot time^{-1}$) and measured Pb in different media and LC50s, LC25s, and 95% Wald confidence intervals were also computed with this module. All metal concentration data, mortality rates, and amphipod body mass data were logarithmically transformed before statistical analysis to normalize the data and equalize variances. All equations used were log–log relationships, with inclusion of background (or control) values and a maximum, if appropriate. Curve fitting was performed on the combined data from all experiments to provide a best estimate of the overall relationship. In addition, metal concentrations resulting in 50% mortality (LC50) in individual experiments were estimated using the trimmed Spearman–Karber (TSK) method (Hamilton et al. 1977) to provide a measure of variation between experiments that was independent of the mathematical models used in curve fitting.

Results and discussion

Water chemistry

Major ion concentrations in the overlying water fell into one of three different patterns. First, concentrations of several ions, including Mg^{2+}, Na^+, K^+, and HCO_3^-, were negligibly affected by either the type of experimental container used or the concentration of Pb in the sediment (Table 3). The second pattern was seen for SO_4^{2-} and DOC. The concentrations of these constituents were elevated severalfold in the beakers, were lower in the cones, and were not related to the concentration of Pb in the sediment. The higher water to sediment ratio in the cones substantially reduced the effect of sediment on overlying water chemistry, especially for SO_4^{2-}. The third pattern, observed for Ca^{2+} and especially Cl^-, was a marked increase in concentration in the beaker, a small increase in the cone, and a correlation between concentration in the water and Pb in the sediment (Table 3). The increase in Cl^- probably resulted from the addition of $PbCl_2$ to the spiked sediment. The increase in Ca^{2+} probably resulted from the displacement of Ca^{2+} adsorbed to the sediment by Pb^{2+}. In both cases, however, the higher water to sediment ratio in the cones dramatically reduced the effect on overlying water chemistry.

The differences in major ion composition among beakers, cones, and initial tap water are primarily due to the presence of the sediments and not to the addition of food or animals. Major ion composition of beakers or cones with animals and food added at the same rate, but without sediments, was similar to that in the initial tap water (Table 3). The DOC concentrations in cones and beakers without sediment were, however, higher than in the tap water and in the cones with sediment but lower than in the beakers with sediment (Table 3). The presence of animals and food did, therefore, contribute some DOC to the overlying water. Microorganisms present in the sediment probably degraded some of this DOC (hence the lower DOC value in the cones with sediment than in the gauze treatment), but any such degradation was outweighed by leaching of DOC into the overlying water in the beakers with sediment.

The dissolved (0.4-μm filtered) Pb concentration in the overlying water increased in a nonlinear fashion with increasing Pb in the sediment. Furthermore, the Pb concentration in the beaker water at the higher Pb exposures was about threefold greater than in the water in the cones (Fig. 2; ANOVA, $P < 0.001$). The relationship between water and sediment Pb obtained by nonlinear regression was

$$(1) \quad Pb_{wbk} = 3.5 + 780 \cdot Pb_{sed}^{2.5} \cdot (34\,400 + Pb_{sed}^{2.5})^{-1}$$

$$(2) \quad Pb_{wcn} = 3.5 + 290 \cdot Pb_{sed}^{2.5} \cdot (49\,300 + Pb_{sed}^{2.5})^{-1}$$

where Pb_{wbk} is Pb in the beaker water (nanomoles per litre, $R^2 = 0.92$), Pb_{wcn} is Pb in the cone water (nanomoles per litre, $R^2 = 0.82$), and Pb_{sed} is Pb in the sediment (micromoles per gram). The water concentration data were variable at the lower Pb sediment concentrations and indistinguishable between cones and beakers. The background Pb in water (3.5 $nmol \cdot L^{-1}$) chosen was the median of overlying water

© 1999 NRC Canada

Fig. 2. Relationship between Pb in water filtered through a 0.4-μm filter and Pb in the sediment. The curves are given by eqs. 1 and 2 in the text. Each symbol represents the mean value from a single experiment in a different test container.

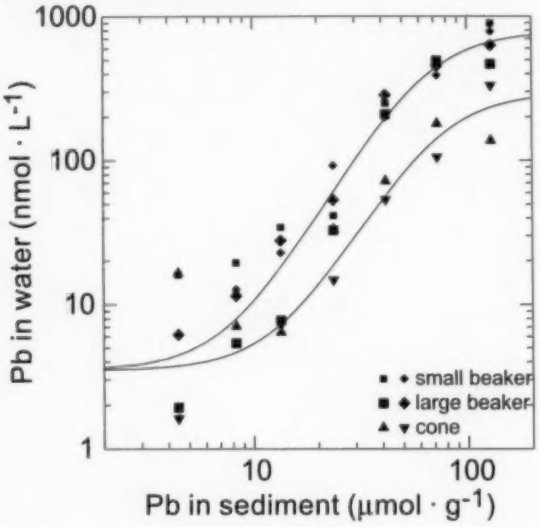

Fig. 3. Lead in filtered water as a function of incubation time for two different sediment Pb concentrations in both beakers and cones. Test animals were added on day 14. The inverse triangles on days 14 and 42 represent measurements made in a separate replicate cone on these dates only.

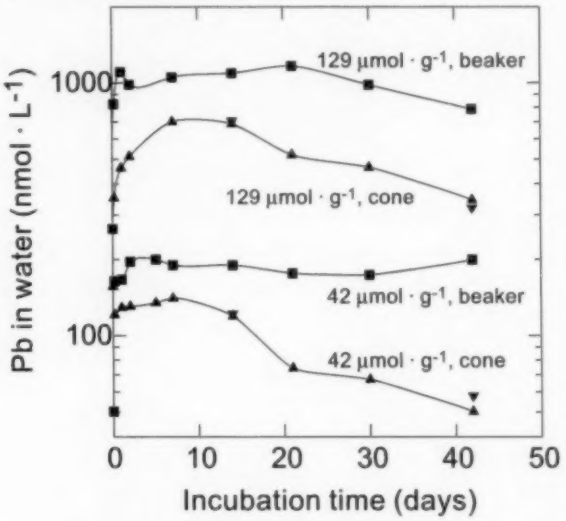

concentrations in all containers with unspiked sediment; the other parameters were fitted by regression. The curves flatten at high Pb in sediment, reaching a maximum water concentration of 780 nmol·L^{-1} (95% CI = 419–1140) in the beakers and 290 nmol·L^{-1} (95% CI = 51–528) in the cones. This probably results from a limit in Pb solubility in the overlying water. The beakers contained higher DOC concentrations than the cones, so it is probable that the higher dissolved Pb in the beakers resulted from a higher concentration of DOC-complexed Pb which increased the total dissolved Pb but not necessarily the free Pb ion. The exponent of 2.5 was fitted to the nearest 0.5 and was the same for both cones and beakers. This indicates a very rapid rise in overlying water Pb with increasing Pb in sediment, possibly resulting from a sudden increase in unbound Pb, as a limited number of binding sites in the sediment are saturated.

A time series of measurements of Pb in water was taken in order to determine if the lower Pb concentration in the overlying water in the cones was due to a limited dissolution rate combined with a larger water to sediment ratio. This would result in a slower buildup of dissolved Pb in the cones. However, maximum concentrations of Pb in water were achieved rapidly, within less than a week in both cones and beakers (Fig. 3). Concentrations declined slightly after 2 weeks, especially in the cones, but were always higher in the beakers than in the cones. Kinetic effects clearly do not account for the differences between cones and beakers. Mass balance calculations demonstrate that only a very small fraction (<0.1%) of the total Pb in any container was in solution. This means that the sediments effectively contained an almost inexhaustible supply of Pb, in terms of their ability to supply Pb to the overlying water. It is unlikely, therefore, that the large water to sediment ratio in the cones was dissolving and depleting the available Pb. It is more likely that the higher dissolved Pb in the beakers resulted from the higher concentration of DOC and greater complexing capacity of the overlying water. The gradual drop in dissolved Pb after week 2 (Fig. 3) might be due to an alteration or breakdown of some of the DOC, resulting in a reduced capacity to bind Pb.

Lead bioaccumulation by *Hyalella*

The Pb content of *Hyalella*, following a gut clearance period of 24 h, increased with increasing Pb in the sediment but was independent of container type and was indistinguishable between animals exposed directly to sediments and animals exposed in cages (Fig. 4; ANOVA, $P > 0.05$). The relationship between Pb in *Hyalella* and Pb in sediment obtained by nonlinear regression was

$$(3) \qquad Pb_{TB} = 2.6 + 233 \cdot Pb_{sed}^{2.5} \cdot (2880 + Pb_{sed}^{2.5})^{-1}$$

where Pb_{TB} is the total body Pb concentration (nanomoles per gram dry mass, $R^2 = 0.74$). The median background concentration of Pb in *Hyalella* exposed to unspiked sediments was 2.6 nmol·g^{-1}; the other parameters were fitted by regression. This relationship is similar to that obtained between Pb in overlying water and Pb in sediment. The exponent, fitted to the nearest 0.5, is the same as that obtained for eqs. 1 and 2, suggesting that Pb accumulation was proportional to Pb in water at concentrations below saturation. Lead bioaccumulation leveled off at high concentrations in the sediment (233 nmol·g^{-1}, 95% CI = 157–309), as did the water concentrations. The data in Fig. 4 indicate that almost all of the bioavailable Pb was in the dissolved fraction and not in the solid phase (comparison of caged and sediment-exposed animals). They also indicate that all of the dissolved Pb was not bioavailable because total dissolved Pb was higher in the beakers than in the cones (Fig. 2). The dissolved bioavail-

© 1999 NRC Canada

Fig. 4. Lead accumulation in *Hyalella* by the end of the 4-week exposure period as a function of Pb in the sediment. The curve is given by eq. 3 in the text. Each symbol represents the mean value from a single experiment in a different test container for animals exposed either to sediment directly (bottom) or in cages.

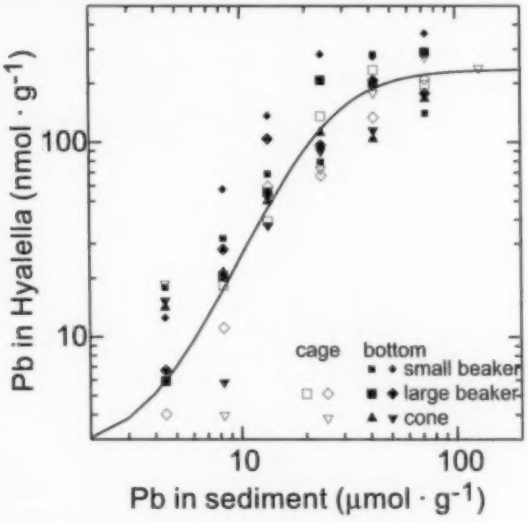

Fig. 5. Survival of *Hyalella* after 4-week exposure to Pb-spiked sediments. The curve is given by Survival (percent) = $100 \times e^{-mt}$ where m is given by eq. 4 in the text and $t = 4$. Each symbol represents the mean value from a single experiment in a different test container for animals exposed either to sediment directly (bottom) or in cages.

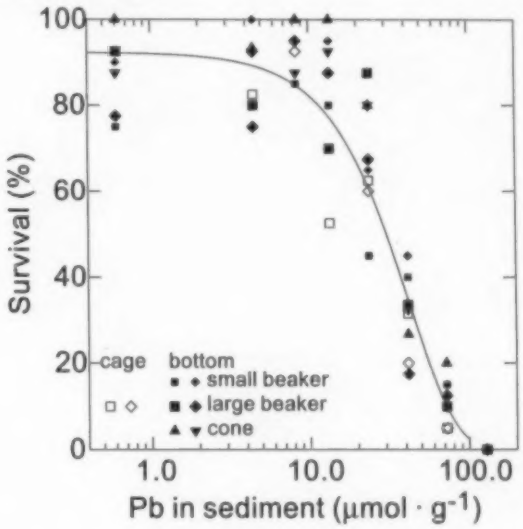

able Pb is apparently similar in both beakers and cones (Fig. 4). This further suggests that the difference in total dissolved Pb between beakers and cones was due to a difference in nonbioavailable Pb, probably DOC-complexed Pb. Complexation by DOC is generally believed to greatly reduce metal bioavailability (Borgmann et al. 1991; Welsh et al. 1993).

Lead toxicity

Survival of *Hyalella* decreased with increasing Pb in sediment but, as observed in the relationship between Pb accumulation and Pb in sediment, was independent of container type and was indistinguishable between animals exposed directly to sediments and animals exposed in cages (Fig. 5). The data for survival in the cages in the cones are not shown in Fig. 5 because survival in unspiked control sediments (46%) and the lower concentrations was unacceptably low. The survival data were transformed into mortality rates ($m = -\ln(N \cdot N_{initial}^{-1}) \cdot time^{-1}$). The mortality rates were then related to Pb concentration using the relationship

$$m = m' + a[\mathrm{Pb}]^n$$

where m' is the control mortality rate (per week) and a and n are constants. For the data in Fig. 5, the nonlinear least squares regression, using log-transformed mortality rates to equalize variances, gave

(4) $$m = 0.0200 + 0.907 \cdot \mathrm{Pb}_{sed}^{1.5} \cdot 1000^{-1}$$

($R^2 = 0.85$). The line in Fig. 5 was obtained by back-transforming the mortality rate relationship into survival. The exponent (1.5) was fit to the nearest 0.5. The data for all treatments overlap, again indicating that the majority of bioavailable Pb was in the dissolved phase (survival in cages equals survival in sediment) and that the dissolved Pb was not all bioavailable (survival in beakers equals survival in cones in spite of higher total dissolved Pb).

Mortality rates were also compared with Pb bioaccumulated in the amphipod bodies. The resultant relationship was

(5) $$m = 0.0380 + 3.18 \cdot \mathrm{Pb}_{TB}^{3.5} \cdot 10^{-9}$$

where the exponent (3.5) was fitted to the nearest 0.5 ($R^2 = 0.88$). This very steep relationship between mortality and body concentration ($n = 3.5$) was also observed previously for Pb, Cu, and Zn in toxicity tests with *Hyalella* exposed to metals in water ($n = 4$, Borgmann and Norwood 1995; MacLean et al. 1996). The equivalent relationships obtained by regressing mortality rates against Pb in water were

(6) $$m = 0.0336 + 1.31 \cdot \mathrm{Pb}_{wbk} \cdot 1000^{-1}$$

(7) $$m = 0.00162 + 4.00 \cdot \mathrm{Pb}_{wcn} \cdot 1000^{-1}.$$

In both eqs. 6 ($R^2 = 0.86$) and 7 ($R^2 = 0.94$), the best fit was obtained using an exponent of 1.0 (±0.2).

A relationship for final wet weight (milligrams) of *Hyalella* as a function of Pb in the sediment, obtained by least squares regression of the data for the same animals as shown in Fig. 5, was

(8) $$W = 1.74 \cdot (1 + 0.011 \cdot \mathrm{Pb}_{sed})^{-1}.$$

This equation explained only a small amount of the variation in weight ($R^2 = 0.12$) because growth was not strongly affected at concentrations below those causing mortality.

The Pb concentrations that resulted in a 50 or 25% mortality or growth reduction after a 4-week exposure to the spiked sediments, as calculated from eqs. 4–8, are summarized in Table 4. Survival was a more sensitive indicator of Pb toxicity than was growth. This is similar to previous ob-

© 1999 NRC Canada

Table 4. Four-week LC50s and LC25s (95% CIs in parentheses) and EC50 and EC25 for growth from nonlinear least squares regression of log(mortality rate) or log(final body mass) against log[Pb] in various media in Pb-spiked sediment experiments and comparison with published results in water-only experiments.

Medium	LC50 spiked-sediment test	LC25 spiked-sediment test	LC25 water-only test	EC50	EC25
Sediment ($\mu mol \cdot g^{-1}$)	33 (31–36)	18 (17–20)	—	91	30
Body ($nmol \cdot g^{-1}$)	162 (157–168)	126 (122–130)	73[a]–180[b]	—	—
Beaker water ($nmol \cdot L^{-1}$)	132 (115–151)	55 (48–63)	—	—	—
Cone water ($nmol \cdot L^{-1}$)	43 (36–52)	18 (15–21)	—	—	—
Flask water ($nmol \cdot L^{-1}$)	—	—	42[a]–43[b]	—	—

[a]From Borgmann et al. (1993), as reported in Borgmann et al. (1998).
[b]From MacLean et al. (1996), as reported in Borgmann et al. (1998).

servations of Pb toxicity in water-only exposures (Borgmann et al. 1993) and Zn, but not Cu, toxicity in spiked sediment exposures (Borgmann and Norwood 1997*b*). The 4-week lethal body concentration for Pb in the spiked-sediment experiments (LBC25 = 126 $nmol \cdot g^{-1}$) was similar to previous estimates obtained in water-only exposures (73–180 $nmol \cdot g^{-1}$), although these numbers should be compared with caution because a 24-h gut clearance was applied only for the sediment tests. Similarly, the Pb toxicity expressed on an overlying water concentration basis (18–55 $nmol \cdot L^{-1}$) was similar to previous estimates of Pb toxicity in Lake Ontario water-only tests (42–43 $nmol \cdot L^{-1}$) (Table 4), further supporting the conclusion that the majority of the bioavailable Pb was in the dissolved fraction. The toxicity of Pb to *Hyalella* in spiked Hamilton Harbour sediments (4-week LC25 = 18 $\mu mol \cdot g^{-1}$) (Table 4) was in the same range as that of Cu (16 $\mu mol \cdot g^{-1}$) and Zn (54 $\mu mol \cdot g^{-1}$), but toxicity on a body concentration basis (LBC25 = 126 $nmol \cdot g^{-1}$) was much greater than that of Cu (1050 $nmol \cdot g^{-1}$) or Zn (3080 $nmol \cdot g^{-1}$). Similarly, toxicity on a water concentration basis in tests using beakers (LC25 = 55 $nmol \cdot L^{-1}$) was also greater for Pb than for Cu (1360 $nmol \cdot L^{-1}$) or Zn (3290 $nmol \cdot L^{-1}$) (Borgmann and Norwood 1997*b*). Lead in spiked sediments is much less bioavailable than Cu or Zn, but the bioaccumulated Pb is much more toxic, resulting in a similar toxicity on a sediment concentration basis. The toxicity of Pb on a body concentration basis is also slightly greater than that of Cd (270 $nmol \cdot g^{-1}$), Hg (350 $nmol \cdot g^{-1}$), or Tl (290 $nmol \cdot g^{-1}$) in *Hyalella* (Borgmann et al. 1998).

Variability between experiments and gut clearance effects

The data in Table 4 provide a best estimate of the overall mean toxicity of Pb for the combined data, but they do not show the variability between experiments. Curve fitting is easier with the combined data because the data from single experiments often do not contain more than one or two data points at concentrations with partial effects (i.e., survival >0% and less than control). To obtain a true indication of variability between experiments, and to verify the conclusions obtained by the methods described above, LC50s were computed independently for each experiment and exposure type using the TSK method. In addition, log–log regressions of Pb in water and Pb in *Hyalella* against Pb in sediment were performed separately for each experiment for midrange data (10–100 $\mu mol \cdot g^{-1}$), and the Pb concentrations in water and *Hyalella* at a sediment concentration of 50 $\mu mol \cdot g^{-1}$ were calculated (Table 5). Water concentrations at 50 μmol Pb·g sediment^{-1} in the beakers were threefold higher than in the cones, but concentrations in *Hyalella* overlapped between beakers and cones and also between sediment-exposed and caged animals, in agreement with previous conclusions. The LC50s for Pb in sediment computed using the TSK method were all very similar (Table 5) and approximately equivalent to the 33 $\mu mol \cdot g^{-1}$ calculated using eq. 4. This supports the use of a single equation (eq. 4) to describe all the data in Fig. 5. The mean of the TSK LC50s for Pb in water was lower for the cones (43 $nmol \cdot L^{-1}$) than for the beakers (126 $nmol \cdot L^{-1}$) (Table 5; $P < 0.01$, ANOVA) and similar to values computed from eqs. 6 and 7 (43 and 132 $nmol \cdot L^{-1}$) (Table 4). This supports the previous conclusion that water concentrations differ between the cones and beakers (Fig. 2), even though toxicity is equivalent on a sediment concentrations basis. The LBC50s on a body concentration basis following gut clearance (mean 150 $nmol \cdot g^{-1}$) (Table 5) were also similar to those computed from eq. 5 (162 $nmol \cdot g^{-1}$) and not significantly different among cones, beakers, and cages. This would be expected if both bioaccumulation (Fig. 4) and toxicity (Fig. 5) were the same in each exposure type. However, there is some variation in the data, and it is likely that LBC50s are slightly lower in the cages (about 100 $nmol \cdot g^{-1}$) than in the sediments (150–170 $nmol \cdot g^{-1}$) (Table 5). Previous bioaccumulation studies designed to establish metals in gut contents and gut clearance times, conducted at only one concentration of spiked sediment but over a range of gut clearance times, also showed a slightly lower Pb concentration in *Hyalella* in cages (20 $nmol \cdot g^{-1}$) than for those exposed directly to sediments (28 $nmol \cdot g^{-1}$) after correction for gut contents (Neumann et al. 1999).

The LBC50s were also computed from data for amphipods that had not been allowed to clear their guts. These were from two- to nine-fold greater than the LBC50s obtained after gut clearance, demonstrating the importance of clearing the gut before measuring Pb in *Hyalella* exposed to Pb-contaminated sediments (Table 5). The much lower bioaccumulation factor (metal in *Hyalella*/metal in sediment) for Pb as compared with Cd, Cu, or Zn makes proper gut clearance much more important for Pb than for the other metals (Neumann et al. 1999). Although a gut clearance time of 6 h is adequate for *Hyalella* (Neumann et al. 1999), a 24 h gut clearance time was used in this study to avoid the need for a 14-h workday to process all the animals. A 24-h gut clearance time will result in estimates of body Pb concentrations equal to about 73% of the body concentration (exclusive of gut contents) at the time that animals are removed

© 1999 NRC Canada

Table 5. Lead in water (Pb_w) and Pb in *Hyalella* (Pb_{TB}) at a sediment Pb concentration of 50 μmol·g^{-1} computed from log–log regressions of Pb_w or Pb_{TB} against Pb in sediment separately for each experiment (Exp.) for data between 10 and 100 μmol Pb·g sediment^{-1} and individual 4-week LC50s (sediment and water) and lethal body concentrations (LBC50s) computed using the TSK method for each exposure type in each experiment along with means computed from logarithmically transformed LC50s.

Exposure type	Exp. No.	Pb_w at 50 μmol·g^{-1} (nmol·L^{-1})	Pb_{TB} at 50 μmol·g^{-1} (nmol·g^{-1})	LC50 for sediment (μmol·g^{-1})	LC50 for water (nmol·L^{-1})	LBC50, gut cleared (nmol·g^{-1})	LBC50, not gut cleared (nmol·g^{-1})
Sediment, small beaker	2	234	162	35	137	130	608
Sediment, small beaker	3	274	317	37	150	272	623
Sediment, large beaker	1	256	243	36	102	182	1099
Sediment, large beaker	2	247	169	32	121	139	609
Mean		253	223	35	126	173	709
Sediment, cone	2	94	133	33	50	104	941
Sediment, cone	3	61	175	37	37	124	403
Mean		78	154	35	43	113	616
Cone plus beaker mean		—	200	35	—	150	677
Cage, large beaker	1	—	225	(30)[a]	(63)[a]	(127)[a]	(305)[a]
Cage, large beaker	2	—	150	30	108	99	300
Cage, cone	3	—	191	nc[b]	nc[b]	nc[b]	nc[b]

[a]Calculated omitting data at 13 μmol Pb·g sediment^{-1} due to abnormally low survival.
[b]Not calculated due to high control mortality.

from the contaminated sediment because of depuration of Pb from the body (Neumann et al. 1999). Consequently, the true body concentration of Pb (corrected for gut contents) at the time that animals were removed from the test containers may have been around 173 nmol·g^{-1} at the LC25 (i.e., 126/0.73); this is still within the range estimated from water-only toxicity tests (Table 4).

General discussion

The initial purpose of our experiments was to determine if the relationship between toxicity and bioaccumulation after gut clearance was the same for *Hyalella* exposed to Pb in water and for *Hyalella* exposed to Pb-spiked sediments. If so, this would simplify the use of body concentration measurements in assessing the contribution of Pb to sediment toxicity. This is in fact the case, and separate estimates of critical body concentrations are not needed for water-only and sediment exposures. The critical body concentration resulting in chronic toxicity was similar for water-only and Pb-spiked sediments (Tables 4 and 5), and an overall average LBC25 (126 nmol·g^{-1}) (Table 4) can be used for estimating the contribution of Pb to toxicity, regardless of whether exposure is through contaminated water or contaminated sediment plus accompanying porewater and overlying water. Furthermore, our results suggest that the bioavailability and toxicity of Pb in Pb-spiked sediments are almost entirely due to dissolved Pb and not to Pb associated with the solid phase itself. Both the bioaccumulation and the toxicity of Pb were very similar between sediment-exposed and caged animals (Figs. 4 and 5).

The animals exposed directly to the sediment could have obtained the metal either from the overlying water or from the porewater in the oxygenated surface layers of the sediments where they spend most of their time. At any given moment, very few of the *Hyalella* were visible above the sediment surface. The animals in the cages, on the other hand, obviously obtained their body metal concentrations from the overlying water. Lead in the overlying water equilibrated rapidly with Pb in the sediment (Fig. 3). Consequently, Pb in the porewater in the surface oxygenated sediment layers was probably also in equilibrium with the overlying water, and measurement of bioavailable Pb in the overlying water should be indicative of bioavailable Pb in the porewater near the sediment surface.

The cones are probably better test chambers for use in sediment bioassays than beakers, if inferences about Pb bioavailability and toxicity are to be made from measurements of Pb in overlying water. The actual fraction of the dissolved metal that is bioavailable will always be less than 1, but it will be greater in the cones than in the beakers. Determination of the true bioavailable fraction will require additional research in defined media in which major ions and DOC are varied in a controlled manner and Pb speciation is calculated. This will show if only free ions are taken up or if other complexes are also bioavailable.

Several studies with other metals suggest that the importance of dissolved metals in controlling metal bioavailability to *Hyalella* is not restricted to Pb. Deaver and Rodgers (1996) found that the toxicity of Cu to *Hyalella* in Cu-spiked sediments was not constant on the basis of total Cu in the sediment. It also varied, although less so, on the basis of total dissolved Cu in the overlying water. Copper toxicity expressed as Cu in overlying water measured by anodic stripping voltammetry was, however, very similar between sediments, implying that the bioavailable Cu in the overlying water was constant for a given toxicity. This is analogous to the situation in our study in which Pb bioavailability was due to dissolved metal, and bioavailable Pb was the same in cones and beakers but total dissolved Pb was not. Warren et al. (1998) used an entirely different approach to investigate the relative importance of dissolved metal and

© 1999 NRC Canada

metal in the sediment. They placed Cd-spiked sediments in a lake with low overlying Cd in the water and plotted Cd accumulated by benthic invertebrates against Cd in the sediment. By extrapolating to the natural Cd concentration in the sediment, they were able to show that most of the Cd accumulated in the body of *Hyalella*, and several other invertebrates as well, was related to Cd in the overlying water and not Cd in the sediment. The importance of dissolved metal in controlling bioavailability and toxicity of metal-contaminated sediments may therefore be relatively common for some invertebrates.

The data in Figs. 4 and 5 lend support to the equilibrium partitioning approach to developing sediment quality criteria. This concept relies on the assumption that metal bioavailability in sediments is due to the dissolved free metal concentration which is in equilibrium with metal bound to the sediment (Shea 1988; Di Toro et al. 1991). Our results suggest that Pb bioavailability and toxicity to *Hyalella* are, in fact, due to a portion of the dissolved metal in equilibrium with the sediment. It should therefore be possible to develop sediment quality criteria for Pb if the fraction of the dissolved metal that is bioavailable can be quantified and if the concentrations and binding strengths of metal-binding components in the sediment (organic C, iron hydroxides, etc.) can be measured. It might, however, be simpler to place the sediment sample in a settling cone with bioassay water, equilibrate for several days, and measure Pb in the overlying water directly.

Comparison with sediment quality criteria and prediction of effects in the field

The LC25 for Pb toxicity in Pb-spiked sediments (33 $\mu mol \cdot g^{-1}$ = 6840 $\mu g \cdot g^{-1}$) (Table 4) is about 100-fold higher than a number of sediment quality assessment values. For example, the threshold effect level (TEL) (sediment concentrations below this are rarely associated with biological effects) was estimated at 35 $\mu g \cdot g^{-1}$ for Pb, and the probable effect level (PEL) (sediment concentrations above this are frequently associated with biological effects) was estimated at 91 $\mu g \cdot g^{-1}$ by Smith et al. (1996). There are two possible reasons for this. First, the bioavailability of metals in sediments is highly variable, and it is possible that the Pb in spiked Hamilton Harbour sediments is unusually strongly bound to the sediment and exhibits abnormally low bioavailability. While this may be partially true, Pb was added as a highly soluble salt ($PbCl_2$) and should therefore be more readily available than some other forms of the metal in sediments (Pb in mineral particles, paint chips, etc.). Another possibility is that the sediment assessment values are not indicative of Pb toxicity. These guidelines are based on associations between observed biological effects and chemical concentrations in the sediments. This means that a Pb concentration exceeding the guideline for Pb is indicative of a possible biological effect, but the effect is not necessarily due to Pb. Contaminated sediments are often contaminated by more than one substance, and the sediments used to calculate the TEL and PEL were collected from the field and contained contaminant mixtures (the TELs and PELs for all contaminants were calculated from the same data set). Consequently, a correlation between Pb in the sediment and biological effects could be due to the presence of other contaminants at concentrations that correlate with those of Pb. The TELs and PELs cannot be used to infer cause–effect relationships (Smith et al. 1996). By comparison, the EC25 for Cu toxicity to *Hyalella* in spiked Hamilton Harbour sediments was 5.2 $\mu mol \cdot g^{-1}$ (330 $\mu g \cdot g^{-1}$, Borgmann and Norwood 1997*b*), which is much closer to the PEL (197 μg $Cu \cdot g^{-1}$, Smith et al. 1996) than is the EC25 for Pb. It is possible, therefore, that Cu is more frequently the cause of sediment toxicity than is Pb. Unfortunately, this hypothesis cannot be tested directly because metal bioavailability is highly variable and sediment quality assessment values are based on total, and not bioavailable, metal.

The observations reported here suggest two ways of assessing possible Pb-induced toxicity in sediments collected from the field. These methods are likely to be much more reliable than measurement of total Pb concentrations in the sediment. First, Pb-induced toxicity can be inferred from Pb bioaccumulation by *Hyalella* in laboratory exposures to sediments, provided that the animals are allowed to clear their guts before Pb in the body is measured. The similarity in Pb accumulation and toxicity for sediment-exposed and caged animals (Figs. 4 and 5) suggests that the lethal body concentration is approximately the same for both routes of exposure (126 nmol·g dry $mass^{-1}$) (Table 4). The exposure time required is relatively short, since metal concentrations in *Hyalella* equilibrate with those in water or sediments within about 1 week (MacLean et al. 1996; Borgmann and Norwood 1997*b*). A 1-week exposure is therefore sufficient to predict Pb-induced chronic toxicity from measurements of Pb bioaccumulation. The second method of inferring Pb-induced toxicity is by measuring Pb in the overlying water because Pb bioavailability and toxicity are due to the dissolved metal. Although the dissolved Pb concentration of the overlying water is not as direct an indicator of Pb bioavailability as is Pb within the body of *Hyalella*, it has the advantage that it can be measured even without the presence of animals in the test chamber. However, the total amount of dissolved Pb overlying the sediments will be a function of the sediment to water ratio used and the amount of Pb-complexing capacity (e.g., DOC) released from the sediment. A higher sediment to water ratio will result in a lower total (but not lower bioavailable) dissolved Pb concentration. The use of a large water to sediment ratio is preferred, since this will reduce the amount of nonbioavailable metal leached into the overlying water by DOC originating from the sediment. In the present study, the LC25 for Pb in the overlying water in the cones was 18 $nmol \cdot L^{-1}$ (3.7 $\mu g \cdot L^{-1}$) (Table 4).

Acknowledgments

Richard MacLean conducted several initial toxicity and bioaccumulation experiments with Pb-spiked sediments that provided the background and methodology for much of this study.

References

Borgmann, U., and Norwood, W.P. 1995. Kinetics of excess (above background) copper and zinc in *Hyalella azteca* and their relationship to chronic toxicity. Can. J. Fish. Aquat. Sci. **52**: 864–874.

© 1999 NRC Canada

Borgmann, U., and Norwood, W.P. 1997*a*. Identification of the toxic agent in metal-contaminated sediments from Manitouwadge Lake, Ontario, using toxicity–accumulation relationships in *Hyalella azteca*. Can. J. Fish. Aquat. Sci. **54**: 1055–1063.

Borgmann, U., and Norwood, W.P. 1997*b*. Toxicity and accumulation of zinc and copper in *Hyalella azteca* exposed to metal-spiked sediments. Can. J. Fish. Aquat. Sci. **54**: 1046–1054.

Borgmann, U., Ralph, K.M., and Norwood, W.P. 1989. Toxicity test procedures for *Hyalella azteca*, and chronic toxicity of cadmium and pentachlorophenol to *H. azteca*, *Gammarus fasciatus*, and *Daphnia magna*. Arch. Environ. Contam. Toxicol. **18**: 756–764.

Borgmann, U., Norwood, W.P., and Babirad, I.M. 1991. Relationship between chronic toxicity and bioaccumulation of cadmium in *Hyalella azteca*. Can. J. Fish. Aquat. Sci. **48**: 1055–1060.

Borgmann, U., Norwood, W.P., and Clarke, C. 1993. Accumulation, regulation and toxicity of copper, zinc, lead and mercury in *Hyalella azteca*. Hydrobiologia, **259**: 79–89.

Borgmann, U., Cheam, V., Norwood, W.P., and Lechner, J. 1998. Toxicity and bioaccumulation of thallium in *Hyalella azteca*, with comparison to other metals and prediction of environmental impact. Environ. Pollut. **99**: 105–114.

Chapman, P.M. 1990. The sediment quality triad approach to determining pollution-induced degradation. Sci. Total Environ. **97/98**: 815–825.

Deaver, E., and Rodgers, J.H., Jr. 1996. Measuring bioavailable copper using anodic stripping voltammetry. Environ. Toxicol. Chem. **15**: 1925–1996.

Di Toro, D.M., Zarba, C.S., Hansen, D.J., Berry, W.J., Swartz, R.C., Cowan, C.E., Pavlou, S.P., Allen, H.E., Thomas, N.A., and Paquin, P.R. 1991. Technical basis for establishing sediment quality criteria for nonionic organic chemicals using equilibrium partitioning. Environ. Toxicol. Chem. **10**: 1541–1583.

Hamilton, M.A., Russo, R.C., and Thurston, R.V. 1977. Trimmed Spearman–Karber method for estimating median lethal concentrations in toxicity bioassays. Environ. Sci. Technol. **11**: 714–719.

Huebert, D.B., Dyck, B.S., and Shay, J.M. 1993. The effect of EDTA on the assessment of Cu toxicity in the submerged aquatic macrophyte, *Lemna trisulca* L. Aquat. Toxicol. **24**: 183–194.

Ingersoll, C.G., Haverland, P.S., Brunson, E.L., Canfield, T.J., Dwyer, F.J., Henke, C.E., Kemble, N.E., Mount, D.R., and Fox, R.G. 1996. Calculation and evaluation of sediment effect concentrations for the amphipod *Hyalella azteca* and the midge *Chironomus riparius*. J. Gt. Lakes Res. **22**: 602–623.

MacLean, R.S., Borgmann, U., and Dixon, D.G. 1996. Bioaccumulation kinetics and toxicity of lead in *Hyalella azteca* (Crustacea, Amphipoda). Can. J. Fish. Aquat. Sci. **53**: 2212–2220.

Neumann, P.T.M., Borgmann, U., and Norwood, W. 1999. Effect of gut clearance on metal body concentrations in *Hyalella azteca*. Environ. Toxicol. Chem. **18**: 976–984.

Persaud, D., Jaagumagi, R., and Hayton, A. 1993. Guidelines for the protection and management of aquatic sediment quality in Ontario. Queen's Printer for Ontario, Toronto, Ont.

Saouter, E., Hare, L., Campbell, P.G.C., Boudou, A., and Ribeyre, F. 1993. Mercury accumulation in the burrowing mayfly *Hexagenia rigida* (Ephemeroptera) exposed to CH_3HgCl or $HgCl_2$ in water and sediment. Water Res. **27**: 1041–1048.

Shea, D. 1988. Developing national sediment quality criteria. Equilibrium partitioning of contaminants as a means of evaluating sediment quality. Environ. Sci. Technol. **22**: 1256–1261.

Smith, S.L., MacDonald, D.D., Keenleyside, K.A., Ingersoll, C.G., and Field, L.J. 1996. A preliminary evaluation of sediment quality assessment values for freshwater ecosystems. J. Gt. Lakes Res. **22**: 624–638.

Warren, L.A., Tessier, A., and Hare, L. 1998. Modelling cadmium accumulation by benthic invertebrates in situ: the relative contributions of sediment and overlying water reservoirs to organism cadmium concentrations. Limnol. Oceanogr. **43**: 1442–1454.

Welsh, P.G., Skidmore, J.F., Spry, D.J., Dixon, D.G., Hodson, P.V., Hutchinson, N.J., and Hickie, B.E. 1993. Effect of pH and dissolved organic carbon on the toxicity of copper to larval fathead minnow (*Pimephales promelas*) in natural lake waters of low alkalinity. Can. J. Fish. Aquat. Sci. **50**: 1356–1362.

© 1999 NRC Canada

Combined phylogenetic analysis of ribosomal ITS1 sequences and new chromosome data supports three subgroups of Dolly Varden char (*Salvelinus malma*)

Ruth B. Phillips, Linda I. Gudex, Kathleen M. Westrich, and Alfred L. DeCicco

Abstract: A phylogenetic analysis of the subspecies of *Salvelinus malma* (Dolly Varden char) was done using DNA sequences from the first internal transcribed spacer (ITS1) of the ribosomal DNA (rDNA). Sequences were obtained from the northern *S. malma malma* from the Noatak River, Alaska, and the Kamchatka River, Russia; from the southern North American form *S. malma lordi* from the Fox River, Kenai peninsula, and Auke Bay near Juneau, Alaska; and from the southern Asian form *S. malma kraschenninnikovi* from Belaya River in Sakhalin Island, Russia. These sequences were combined with others from *Salvelinus alpinus* (Arctic char) from several locations in the North Pacific and Europe and analyzed using maximum parsimony and neighbor joining algorithms with *Salvelinus namaycush* (lake trout) as an outgroup. The resulting trees had two well-supported groups: *S. m. malma* and *S. m. kraschenninnikovi* in one group and *S. m. lordi* and various populations of *S. alpinus* in the other. *Salvelinus m. malma* and *S. m. kraschenninnikovi* were sister taxa, and *S. m. lordi* was most closely related to *S. alpinus* from Northwest Territories (*S. a. erythrinus*). New chromosome data from *S. m. malma* from northwestern Alaska supported the three named subspecies because *S. m. malma* from both Alaska and Russia have $2n = 78$ compared with $2n = 82$ for the two southern forms and the location of the nuclear organizer regions (NORs) was different in each of the three subspecies.

Résumé : On a réalisé une analyse phylogénétique des sous-espèces de *Salvelinus malma* (Dolly Varden) en utilisant des séquences d'ADN du premier espaceur transcrit interne de l'ADN ribosomique (ADNr). On a obtenu des séquences de la forme septentrionale *S. malma malma* de la Noatak (Alaska) et du fleuve Kamtchatka (Russie), de la forme méridionale nord-américaine *S. malma lordi* de la Fox (péninsule de Kenai) et de la baie Auke, près de Juneau en Alaska, ainsi que de la forme méridionale asiatique *S. malma kraschenninnikovi* de la Bélaïa (île Sakhaline, Russie). Ces séquences ont été combinées à d'autres de *Salvelinus alpinus* (omble chevalier) provenant de divers endroits du Pacifique Nord et d'Europe, et analysées au moyen de la méthode de parcimonie maximale et d'algorithmes de liaison de voisinage, *Salvelinus namaycush* (touladi) faisant office de groupe externe. Les arbres résultants montrent deux groupes bien définis : *S. m. malma* et *S. m. kraschenninnikovi*, d'une part, et *S. m. lordi* et diverses populations de *S. alpinus*, d'autre part. *Salvelinus m. malma* et *S. m. kraschenninnikovi* étaient des taxons-frères, et *S. m. lordi* était le plus étroitement apparenté à *S. alpinus* des Territoires du Nord-Ouest (*S. a. erythrinus*). De nouvelles données chromosomiques provenant de *S. m. malma* du nord-ouest de l'Alaska ont confirmé la réalité des trois sous-espèces susmentionnées, la formule chromosomique de *S. m. malma* d'Alaska et de Russie étant $2n = 78$ et celle des deux formes méridionales $2n = 82$, et les organisateurs nucléolaires se trouvant à des sites différents chez les trois sous-espèces.

[Traduit par la Rédaction]

Introduction

Salvelinus malma (Dolly Varden char) is a member of the Arctic char complex (McPhail 1961; Behnke 1980, 1984; Savvaitova 1980, 1995). *Salvelinus alpinus* (Arctic char) has a continuous circumpolar distribution in the Arctic, but *S. malma* is found only in the North Pacific, occasionally sympatrically with *S. alpinus*. Two major subspecies of *S. malma* are thought to occur in North America: the northern form, *S. malma malma*, occurs north of the Alaska Peninsula to the Mackenzie River in Canada, and the southern form, *S. malma lordi*, occurs south of the Alaskan peninsula in south central and southeastern Alaska and south to Washington (Behnke 1980, 1984; Morrow 1980). The northern form is also found in eastern Russia and is chromosomally different ($2n = 78$, Viktorovsky 1975) from the southern

Received November 17, 1998. Accepted April 15, 1999.
J14899

R.B. Phillips,[1] L.I. Gudex, and K.M. Westrich. Department of Biological Sciences, University of Wisconsin–Milwaukee, Milwaukee, WI 53211, U.S.A.
Alfred L. DeCicco. Alaska Department of Fish and Game, Fairbanks, Alaska.

[1]Author to whom all correspondence should be addressed. e-mail: rp@csd.uwm.edu

© 1999 NRC Canada

Table 1. *Salvelinus* sp. from these locations were used in this study.

Species	Location	N
S. malma krascheninnikovi	River Belaya, Sakhalin Island, Russia, 50°5′N 141°30′E	2
S. malma malma	River Kamchatka, Kamchatka, Russia, 55°44′N 161°23′E	1
S. malma malma	Noatak River, Alaska, U.S.A., 66°5′N 152°5′W	2
S. malma lordi	Fox River, Kenai Peninsula, Alaska, U.S.A., 60°5′N 152°5′W	2
S. malma lordi	Auke Creek, Juneau, Alaska, U.S.A., 58°22′N 34°35′W	2
S. alpinus sp.	Finger Lakes, Kenai, Pen., Alaska, U.S.A., 60°8′N 149°27′W	1
S. alpinus sp.	Dolly Varden Lake, Kenai Pen., Alaska, U.S.A., 60°10′N 150°14′W	1
S. alpinus erythrinus	Nauyuk Lake, N.W.T., Canada, 67°8′N 106°54′W	2
S. alpinus alpinus, Storvatn stock	Freshwater Institute, Manitoba (originally from Norway)	2
S. namaycush, Marquette stock	Iron River Fish Hatchery, Wis., U.S.A.	6

Asian form, *S. malma krascheninnikovi* ($2n = 82$) found in Hokkaido, Japan, Sakhalin Island, and the mainland of Russia south of the Amur River (Behnke 1984). The karyotype of the North American southern form, *S. m. lordi* is also $2n = 82$ (reviewed in Cavender and Kimura 1989), but prior to this study, the North American northern form, *S. m. malma*, had not been karyotyped.

There are many unanswered questions concerning the relationships of the char in the *S. alpinus* – *S. malma* complex (reviewed in Behnke 1980, 1984, 1989; Cavender 1980; Glubokowsky and Chereshnev 1981; Johnson 1980; Savvaitova 1980) to each other and to the other Asian chars. In Europe and Asia, sympatric forms of char are found in many lakes and a large number of species and subspecies have been named by different authors. There is a consensus that the sympatric forms in a given lake are usually closely related forms of either *S. malma* or *S. alpinus* that entered the lake and then diverged into different morphotypes. However, sympatric populations of *S. malma* and *S. alpinus* have been described from Kodiak Island (Delacy and Morton 1943) and from other lakes in Alaska and Kamchatka (Behnke 1984). Most authors have assumed that *S. malma* and *S. alpinus* are distinct species, but Savvaitova has suggested that these two "species" are actually morphotypes that evolved sympatrically in many localities (Savvaitova 1980, 1995). McPhail (1961) and Behnke (1984) have suggested that the northern and southern *S. malma* in North America may have been isolated by a Pleistocene glaciation, subsequent to the divergence of *S. malma* and *S. alpinus*.

A recent survey of char from east and west of the Mackenzie River system in Canada (Reist et al. 1997) in which meristic characters and enzyme loci were examined has confirmed that the riverine char from the continental north slope west of the Mackenzie River are *S. malma*, whereas the lacustrine char from this area are relictual *S. alpinus*. (Reference groups in this study were *S. m. lordi* from the Klutina River in south central Alaska and *S. alpinus erythrinus* from Cambridge Bay, Northwest Territories.) They also indicated the possibility of three forms of *S. malma* in North America and northeastern Asia.

In previous work, we examined the relationships of North Pacific chars using sequences from the first internal transcribed spacer (ITS1) of the ribosomal DNA (rDNA) (Pleyte et al. 1992; Phillips et al. 1995) and found preliminary evidence that the southern *S. m. lordi* from southeastern Alaska was more closely related to *S. alpinus* than the northern *S. m. malma*. However, we examined the sequence of only one individual from one population for each of the North American taxa and no sequences from *S. malma* from Asia. In this paper, we present an analysis of additional ITS1 sequences from representatives of the subspecies of *S. malma* from different locations in North America and Asia and include an analysis of new karyotypic data.

Materials and methods

ITS1 sequences

Tissue samples for DNA extraction from 2–4 individuals of each subspecies were obtained from *S. malma* from the following locations: *S. m. lordi* from Auke Creek near Juneau, Alaska, and from Fox River near Anchorage, Alaska; *S. m. malma* from Noatak River in northern Alaska and Kamchatka River in Kamchatka, Russia; and *S. m. krascheninnikovi* from Belaya River in Sakhalin Island, Russia. Samples from *S. alpinus* were obtained from the following sources: *S. alpinus erythrinus* from Nauyuk Lake, Northwest Territories; *S. alpinus* sp. from Dolly Varden Lake and East Finger Lake in the Kenai Peninsula, Alaska; *S. alpinus alpinus* from Storvatn, Norway; and *S. namaycush* of Marquette stock from Iron River Fish Hatchery, Iron River, Wisconsin. The locations and number sampled from each population are shown in Table 1.

DNA was isolated from liver by phenol extraction of proteins for samples obtained prior to 1992 and by the salt extraction method (Stratigene, Inc.) for samples obtained after 1992. The ITS1 from at least two individuals of each population or subspecies was amplified using primers homologous to the 3′ end of the 18S rDNA (KP2: 5′-AAAAAGCTTCCGTAGGTGAACCTGCG) and the 5′ end of the 5.8S rDNA (5.8S: 5′-AGCTTGCTGCGTTCTTCATCGA-3′)(Phillips et al. 1995). PCR reactions were of 100 µL total volume containing 2.5 units of *Taq* (Promega, Madison, Wis.), 6 µL of 25 mM $MgCl_2$, 10 µL of 10× buffer supplied by the manufacturer, 2 µL each of 1 mM dATP, dTTP, dGTP, and dCTP, 30 pmol of each primer, and 100 ng of genomic DNA. Amplifications were carried out in a Ericomp thermalcycler with an initial incubation of 3 min at 94°C followed by 35 cycles of 1 min 30 s at 94°C, 1 min at 55°C, 2 min at 72°C, and a 5-min final extension at 72°C.

Concentrations of PCR products were estimated by electrophoresis in 1% low-melting agarose gel with 1 µg/µL φX174/HaeIII Marker (Promega) and visualized by ethidium bromide staining. Approximately 30 ng PCR product was ligated with 1 µg T-tailed pGEM vector (Promega) in a 10-µL reaction. The ligation reaction was transformed with *Escherichia coli* JM109 high-efficiency cells and plated on LB amp plates along with ITPG and X-Gal according to manufacturer's instructions (Promega). Positive colonies were grown overnight in LB amp media and double-stranded DNA was extracted using Wizard Plus Minipreps DNA Purification System (Promega). Two to five clones were sequenced per individual using the vector primers and one internal primer: ITS-1 int (5′-

© 1999 NRC Canada

Fig. 1. Aligned DNA sequences of the first internal transcribed spacer (ITS1) of ribosomal DNA for subspecies of *S. malma* (Dolly Varden char) and *S. alpinus* (Arctic char). Two different sequences are given for *S. m. lordi*. The first sequence was obtained in 3 of 4 individuals. * indicates informative sites. The last three positions (570, 571, and 572) are only informative if gaps are considered as a fifth base.

```
                                                                                                                    60
S.namaycush      GGTTGCCAGC CGCCGGCATG GGGCTGTGCT CCGAAAACCA AACTCTGCTG TGGGTTGGGT
S.m.malma(AK)    .......... .......... .......... .......... ..G....... ....G.....
S.m.malma(RU)    .......... .......... .......... .......... ..G....... ....G.....
S.m.kraschen.    .......... .......... .......... .......... ..G....... ....G.....
S.m.lordi-1      .......... .......... .......... .......... ..G....... ....G.....
S.m.lordi-2      .......... .......... .......... .......... ..G....... ....G.....
S.a.sp.(AK)      .......... .......... .......... .......... ..G....... ....G.....
S.a.erythrinus   .......... .......... .......... .......... ..G....... ....G.....
S.a.alpinus      .......... .......... .......... .......... ..G....... ....G.....

                                                                  *                 120
S.namaycush      TGGGTAGGGT ATGGGGGCTC ACGCCCCCCG CCTCGCCCAT CTCTCGGCGC AGGTGTCCTC
S.m.malma(AK)    A.....---- -......... .......... ......T... .......... G.........
S.m.malma(RU)    A.....---- -......... .......... ......T... .......... G.........
S.m.kraschen.    A.....---- -......... .......... ......T... .......... G.........
S.m.lordi-1      A.....---- -......... .......... .......... .......... G.........
S.m.lordi-2      A.....---- -......... .......... .......... .......... G.........
S.a.sp.(AK)      A.....---- -......... .......... .......... .......... G.........
S.a.erythrinus   A.....---- -......... .......... .......... .......... G.........
S.a.alpinus      A.....---- -......... .......... .......... .......... G.........

                                                                                    180
S.namaycush      GGTCTTAGCC CGGTTCCCTG CTATTCCTTT TGCCT--GGG TTGCGCCC-A CCGGCTCCAT
S.m.malma(AK)    .......... ........C. .......... .....AA... ....A...G. ..........
S.m.malma(RU)    .......... ........C. .......... .....AA... ....A...G. ..........
S.m.kraschen.    .......... ........C .......... .....AA... ....A...G. ..........
S.m.lordi-1      .......... ........C. .......... .....AA... ....A...G. ..........
S.m.lordi-2      .......... ........C. .........A A....AA... ....A...G. ..........
S.a.sp.(AK)      .......... ........C. .......... .....AA... ....A...G. ..........
S.a.erythrinus   .......... ........C. .......... .....AA... ....A...G. ..........
S.a.alpinus      .......... ........C. .......... .....AA... ....A...G. ..........

                                                                                    240
S.namaycush      CCCTTTTCCC CGTTAGCCAC GGCCACATGA CGCACCTATG GGCAGGTGAG TCGGCTGCTA
S.m.malma(AK)    .......... .......... .........G .......... .......... .....C....
S.m.malma(RU)    .......... .......... .........G .......... .......... .....C....
S.m.kraschen.    .......... .......... .........G .......... .......... .....C....
S.m.lordi-1      .......... .......... .........G .......... .......... .....C....
S.m.lordi-2      .......... .......... .........G .......... .......... .....C....
S.a.sp.(AK)      .......... .......... .........G .......... .......... .....C....
S.a.erythrinus   .......... .......... .........G .......... .......... .....C....
S.a.alpinus      .......... .......... .........G .......... .......... .....C....

                                                                        *    *      300
S.namaycush      CCGAAGGGGA CTGGGGGTGT CCGGTGAACC GGGACTTCCC GAAATGGTCT CCCATGTTTA
S.m.malma(AK)    .......... .......... .......... .......... ......TAAA .....T.A..
S.m.malma(RU)    .......... .......... .......... .......... ......TAAA .....T.A..
S.m.kraschen.    .......... .......... .......... .......... ......TAAA .....T.A..
S.m.lordi-1      .......... .......... .......... .......... ....C.TAA. .....T.A..
S.m.lordi-2      .......... .......... .......... .......... ....C.TAA. .....T.A..
S.a.sp.(AK)      .......... .......... .......... .......... ....C.TAA. .....T.A..
S.a.erythrinus   .......... .......... .......... .......... ....C.TAA. .....T.A..
S.a.alpinus      .......... .......... .......... .......... ......TAA. .....T.A..
```

GTTAGCCACGGCCACATGACGCAC-3′). Sequences were determined using an ABI (model 373A) automatic DNA sequencer. Contigs were assembled and individual consensus sequences were aligned with the Sequencer computer program (Gene Codes Corp., Ann Arbor, Mich.). The sequences have the following GenBank accession numbers: AF059896-AF059905, M94901, and M94905.

Previously obtained sequences for these taxa (Phillips et al. 1995) were combined with the new sequences and aligned using Sequencer with gaps inserted to maintain the alignment. Most of the gaps were inserted to align the char sequences with the outgroup *S. namaycush* (Fig. 1). Phylogenetic analyses of aligned sequences were done using test version 4.0d64 of PAUP*, written by David L. Swofford. Maximum parsimony was used with gaps considered as a fifth base and *S. namaycush* as an outgroup. An exhaustive search was done using the branch and bound algorithm and the data were bootstrapped (1000 replicates) retaining branches occurring at least 50% of the time.

Pairwise sequence divergences were calculated directly from the aligned sequences. Genetic distances were calculated using by the Jukes and Cantor method (Table 2) and trees were constructed from the genetic distances with the neighbor-joining method (Saitou and Nei 1987) using the beta version 4.0d64 of PAUP* (Swofford 1998).

Karyotypic data

Blood samples for leucocyte cultures were obtained from four specimens of *S. m. malma* from the Noatak River and shipped to Milwaukee on ice for culturing. Leucocytes were separated from red blood cells by centrifugation and cultured in minimal essential medium (MEM, Gibco, Life Technologies Inc., Rockville, Md.) supplemented with 10% fetal bovine serum (FBS), 1.2% penicillin/streptomycin, and 2% glutamine. Lipopolysaccharide (LPS) (Sigma) was used as the mitogen. The number of active NORs in metaphase cells was determined by silver staining (Howell and Black 1980).

Results

ITS1 sequences

The aligned sequences of the ITS1 from various char populations are given in Fig. 1. Individuals from the same sub-

© 1999 NRC Canada

Fig. 1 (*concluded*).

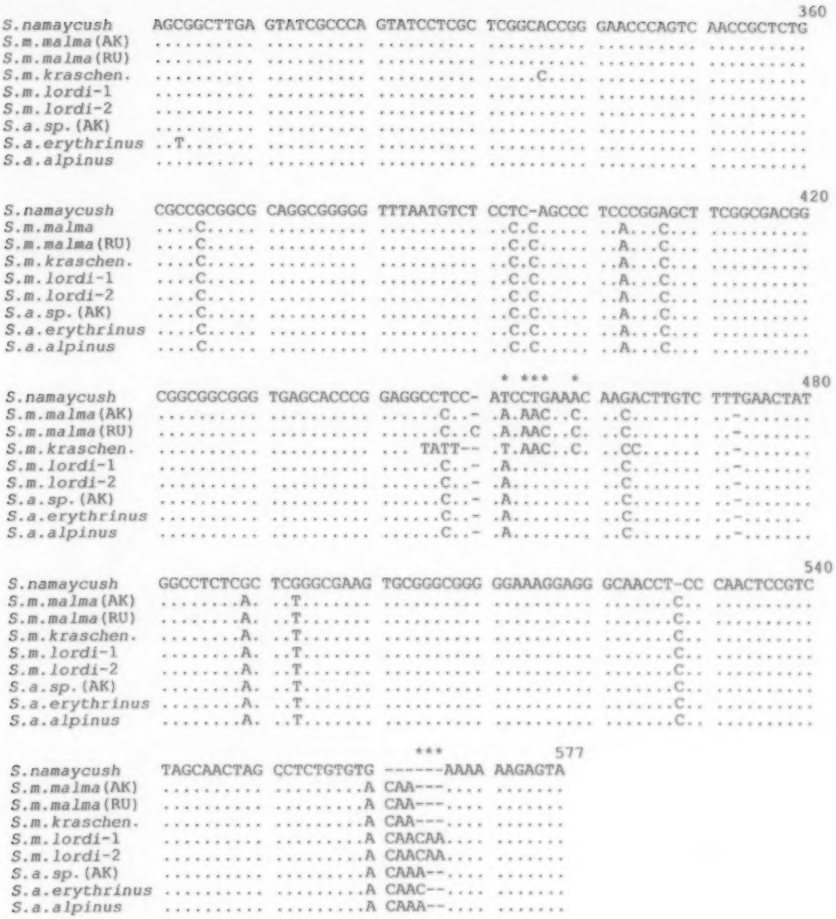

species had identical sequences with two exceptions. The sequence of the Russian *S. m. malma* differed at 1 base pair (site 450) from the Alaskan *S. m. malma*, and one *S. m. lordi* from Juneau differed at 2 base pairs (sites 150 and 151) from the other 3 sequences of this subspecies. In both cases, the nucleotides at these sites were invariant in the other taxa, so these sites were not informative for the phylogenetic analysis. Because of the relatively small number of variable sites, gaps were counted as a fifth base in the analysis.

Phylogenetic analysis of the ITS1 sequences with maximum parsimony (PAUP*, test version 4.0d64), using *S. namaycush* as an outgroup, yielded two trees. The only differences in the trees involved rearrangements of the taxa in the *S. m. malma* subgroup. The consensus bootstrapped tree is shown in Fig. 2. There are two major subgroups: one with *S. m. malma* and *S. m. krascheninnikovi* and the other with *S. m. lordi* and various populations of *S. alpinus*. The branch leading to two *S. malma* subspecies is supported by 6 shared derived characters (sites 97, 290, 454, 455, 456, and 459) or synapomorphies (90% bootstrap). The two *S. m. lordi* sequences differed from that of *S. m. krascheninnikovi* at 18–20 sites and from that of *S. m. malma* (Russia) at 10–12 sites.

Jukes and Cantor genetic distances between the taxa are shown in Table 2. The neighbor-joining tree is shown in Fig. 3. The topology of the tree is the same as one of the trees obtained from the parsimony analysis. The largest genetic distances were between the two major subgroups. The distance between *S. m. lordi* and the other *S. malma* is 0.014–0.028, whereas the distance between *S. m. lordi* and the *S. alpinus* taxa is 0.002–0.003. The distance between *S. m. krascheninnikovi* and *S. m. malma* is 0.014.

Karyotypic data

The karyotype of the northern *S. m. malma* from the Noatak River is shown in Fig. 4. The diploid number is 78 with 10 pairs of metacentrics and 29 pairs of acrocentrics. This is the same karyotype described for the Russian *S. m. malma* populations (Viktorovsky 1975; Frolov 1995). The nucleolar organizer region (NOR) was on a single pair in the two specimens examined: a medium-sized acrocentric–subtelocentric pair (third line of the karyotype on the ex-

© 1999 NRC Canada

Table 2. Jukes and Cantor genetic distances among ITS1 sequences of chars.

	1	2	3	4	5	6	7	8
1. *S. namaycush*	0.000							
2. *S. m. malma* (Alaska)	0.069	0.000						
3. *S. m. malma* (Russia)	0.070	0.002	0.000					
4. *S. m. kraschen.*	0.080	0.014	0.014	0.000				
5. *S. m. lordi**	0.061	0.014	0.016	0.028	0.000			
6. *S. a.* sp. (Kenai)	0.059	0.012	0.014	0.026	0.002	0.000		
7. *S. a. erythrinus*	0.063	0.016	0.018	0.030	0.002	0.003	0.000	
8. *S. a. alpinus*	0.058	0.010	0.012	0.025	0.003	0.005	0.005	0.000

*For *S. m. lordi*, the sequence found in 3 out of 4 individuals (2 from Kenai and 2 from Juneau) was used for the calculations. In the other cases, the sequences from different individuals of the same subspecies were identical.

Fig. 2. Consensus tree of *S. malma* and *S. alpinus* ITS1 sequences produced with PAUP* (tester version 4.0.d64) using the branch and bound option. Numbers above branches indicate bootstrap values. Gaps were considered a fifth base and 1000 replications were performed.

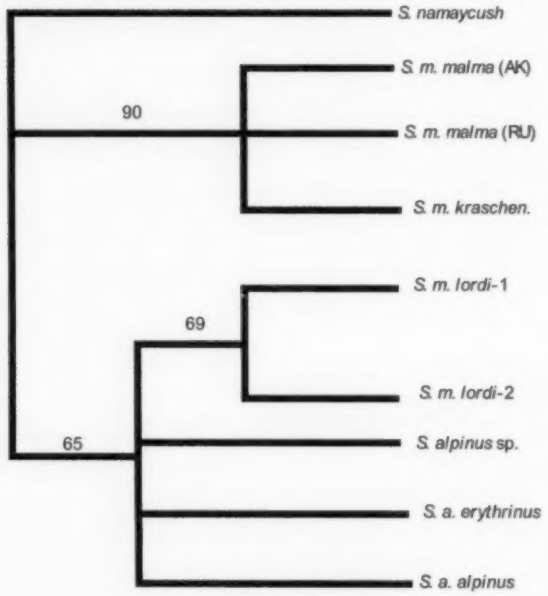

Fig. 3. Neighbor-joining tree obtained with Jukes and Cantor distances from ITS1 sequences using PAUP*, tester version 4.0.d64.

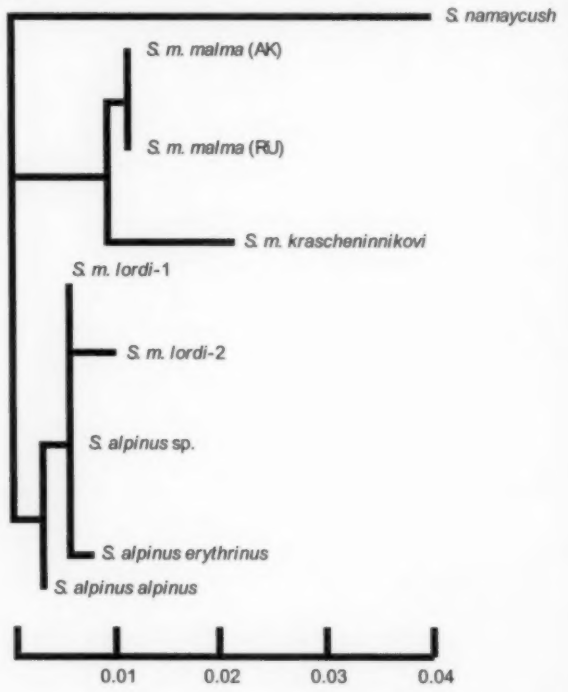

treme right). NORs have been found at multiple locations in Russian *S. m. malma* (Frolov 1995) but not in North American *S. m. lordi* (Cavender 1984; Phillips et al.1989).

Discussion

Karyotype data from the major species in the genus *Salvelinus*, including the three named subspecies of Dolly Varden char (*S. malma*), are shown in Table 3. It is generally assumed that *S. fontinalis*, *S. namaycush*, and *S. leucomaenis* are the basal taxa and that they all have $2n = 84$ with NF (number of chromosome arms) of 100 (Lee and Wright 1981; Phillips and Zajicek 1982; Ueda and Ojima 1983). Recent molecular data as well as allozyme data have shown that *S. leucomaenis* is closely related to *S. confluentus* (Phillips and Oakley 1997). Although *S. confluentus* has $2n = 78$, the NF number is also 100 (Cavender 1984). This suggests that the difference between the two karyotypes can be explained by Robertsonian translocations (Hartley 1987). All of the named subspecies of *alpinus* and *malma* have NF = 98 and a very large acrocentric chromosome pair that appears to be the result of a tandem chromosome fusion and has resulted in a reduction in the NF number. The two southern forms of *S. malma* have $2n = 82$ (Cavender 1984) and the northern form has $2n = 78$ in Asia (Viktorovsky 1975) and North America (this paper). This difference could be explained by Robertsonian fusions. Because we do not have probes for chromosome arms at this time, we cannot determine chromosome arm homologies required to determine whether the two southern forms with $2n = 82$ have the same karyotype. There is a minor difference in the structure of the single NOR chromosome in the two southern forms (Cavender and Kimura 1989) so that the two karyotypes are

© 1999 NRC Canada

Fig. 4. Karyotype of *S. m. malma* from the Noatak River, Alaska, U.S.A.

© 1999 NRC Canada

Table 3. Chromosome data for species of the genus *Salvelinus*.

Species	2*n*	NF	NORs	References
S. namaycush	84	100	Multiple locations	Phillips and Zajicek 1982; Phillips et al. 1989
S. fontinalis	84	100	Multiple locations	Lee and Wright 1981; Phillips et al. 1989
S. leucomaenis	84	100	Single acrocentric	Ueda and Ojima 1983; Cavender and Kimura 1989
S. confluentus	78	100	Single acrocentric	Cavender and Kimura 1989
S. alpinus	78	98	Multiple locations	Cavender 1984; Phillips et al. 1988
S. m. malma (Alaska)	78	98	Single acrocentric*	This paper
S. m. malma (Russia)	78	98	Multiple locations	Viktorovsky 1975; Frolov 1995
S. m. kraschennikovi	82	98	Single acrocentric	Ueda and Ojima 1983; Cavender and Kimura 1989
S. m. lordi	82	98	Single submetacentric	Cavender 1984; Cavender and Kimura 1989; Phillips et al. 1989

*Based on only 4 individuals. Intraspecific variability in the number and location of NORs has been documented in a number of species including *S. namaycush*, *S. fontinalis*, *S. alpinus*, and *S. malma*.

not identical. Intraspecific variation in number, size, and location of NORs has been documented in several species of *Salvelinus* (Phillips et al. 1988, 1989).

The DNA results also support the previous consensus that the southern and northern forms of *S. malma* in North America are distinct (Behnke 1980). The combined DNA and karyotype results support the three named subspecies of *S. malma*, but the DNA results suggest that the divergence of *S. m. lordi* from *S. alpinus* occurred much more recently than the divergence leading to *S. m. malma* and *S. m. krascheninnikovi*. Thus *S. malma* as presently understood would be paraphyletic. The ITS1 sequence of *S. m. malma* is closer to *S. a. alpinus* than to *S. a. erythrinus*, whereas the sequence of *S. m. lordi* is closer to *S. a. erythrinus*. These results suggest that *S. m. malma* may have diverged from *S. a. alpinus* first, and that at a later time, *S. m. lordi* diverged from *S. a. erythrinus* in North America and *S. m. krascheninnikovi* diverged from *S. m. malma* in Asia. These results are contrary to the accepted notion that *S. m. lordi* and *S. m. malma* evolved from a common ancestor north and south of the exposed Beringian land mass during the Wisconsin glacial period (McPhail 1961 and Behnke 1984). Although this paraphyly of *S. malma* is the scenario supported by ITS1 sequences, it must be considered only an hypothesis until additional genetic data have been obtained for these taxa.

If *S. malma* is monophyletic as suggested by morphology and mitochondrial data, then the ITS1 results might be explained if *S. m. lordi* had hybridized with one of the subspecies of *S. alpinus*, possibly *S. a. erythrinus*, and biased concerted evolution of the rDNA occurred after hybridization. Additional data from microsatellite loci, which are evolving more rapidly than rDNA or protein-coding loci, may help resolve the relationships in the North American representatives of the *S. alpinus–malma* complex.

Acknowledgements

The authors thank the following for tissue samples: Ross Horrall, University of Wisconsin–Madison; Bob Lindsay, Randy Olson, Rockwood Fish Hatchery, Winnipeg, Manitoba; Tony Gharrett, University of Alaska–Fairbanks at Juneau; Dick Wilmot, Auke Bay Laboratory, Juneau, Alaska; and Alexander Osinov, Moscow State University. This research was supported by a grant from the National Science Foundation. Additional support to LIG came from a Ronald E. McNair Postbaccalaureate Achievement Program grant, which is a Trio Program funded by the United States Department of Education.

References

Behnke, R.J. 1980. A systematic review of the genus *Salvelinus*. Chap. 14. *In* Charrs, salmonid fishes of the genus *Salvelinus*. Vol. 1. *Edited by* E.K. Balon. Junk Publishers, The Hague. pp. 441–481.

Behnke, R.J. 1984. Organizing the diversity of the Arctic char complex. *In* Biology of the Arctic charr. *Edited by* L. Johnson, McV. Clarke, and K.E. Marshall. University of Manitoba Press, Winnipeg, Manitoba.

Behnke, R.J. 1989. Interpreting the phylogeny of *Salvelinus*. Physiol. Ecol. Jap. Spec. Vol. **1**: 35–48.

Cavender, T.M. 1980. Systematics of *Salvelinus* from the North Pacific Basin. Chap. 6. *In* Charrs, salmonid fishes of the genus *Salvelinus*. Vol. 1. *Edited by* E.K. Balon. Junk Publishers, The Hague. pp. 295–322.

Cavender, T.M. 1984. Cytotaxonomy of North American *Salvelinus*. *In* Biology of the Arctic charr. *Edited by* L. Johnson and B.L. Burns. Proc. Int. Symp. on Arctic Charr, Winnipeg, Manitoba, May 1981. Manitoba Press, Winnipeg, Man. pp. 431–445.

Cavender, T.M., and Kimura, S. 1989. Cytotaxonomy and interrelationships of Pacific basin *Salvelinus*. Physiol. Ecol. Jap. Spec. Vol. **1**: 49–68.

Delacey, A.C., and Morton, W.M. 1943. Contributions to the life histories of two Alaska chars, *Salvelinus malma* and *Salvelinus alpinus*, of the Karluk drainage system. Trans. Am. Fish. Soc. **72**: 79–91.

Frolov, S.V. 1995. Comparative karyology and karyotype evolution of chars. J. Ichthylol. **35**: 14–23.

Glubokowsky, M.K., and Cheresenev, I.A. 1981. Unresolved problems concerning the phylogeny of chars (*Salvelinus*) of the Holarctic. I. Migrating chars of the East Siberian Sea Basin. Ichthyology, **21**: 1–15.

Hartley, S.E. 1987. The chromosomes of salmonid fishes. Biol. Rev. (Cambridge), **62**: 197–214.

Howell, W.M., and Black, D.A. 1980. Controlled silver-staining of nucleolus organizer regions with a protective colloidal developer: a 1 step method. Experientia, **36**: 1014–1015.

Johnson, L. 1980. The Arctic charr, *Salvelinus alpinus*. *In* Charrs: salmonid fishes of the genus *Salvelinus*. *Edited by* E.K. Balon. Junk Publishers, The Hague. pp. 15–98.

Lee, G.M., and Wright, J.E. 1981. Mitotic and meiotic analysis of brook trout *Salvelinus fontinalis*. J. Hered. **72**: 321–327.

© 1999 NRC Canada

McPhail, J.D. 1961. A systematic study of the *Salvelinus alpinus* complex in North America. J. Fish. Res. Board Can. Bull. **18**: 793–816.

Morrow, J.E. 1980. Analysis of the Dolly Varden charr, *Salvelinus malma*, of northwestern North American and northeastern Siberia. Chap. 7. *In* Charrs, salmonid fishes of the genus *Salvelinus*. *Edited by* E.K. Balon. Junk Publishers, The Hague. pp. 323–338.

Phillips, R.B., and Oakley, T.H. 1997. Evolutionary relationships among salmonid fishes inferred from nuclear and mitochondrial sequences. Chap. 10. *In* Molecular systematics of fishes. *Edited by* Thomas Kocher and Carol Stepien. Academic Press, New York.

Phillips, R.B., and Zajicek, K.D. 1982. Q-band chromosomal banding polymorphisms in lake trout (*Salvelinus namaycush*). Genetics, **101**: 222–234.

Phillips, R.B., Pleyte, K.A., and Hartley, S.E. 1988. Stock-specific differences in the number and chromosome positions of the nucleolar organizer regions in Arctic char (*Salvelinus alpinus*). Cytogenet. Cell Genet. **48**:9–12.

Phillips, R.B., Pleyte, K.A., and Ihssen, P.E. 1989. Patterns of chromosomal nucleolar organizer (NOR) variation in fishes of the genus *Salvelinus*. Copeia, 1989(1): 47–53.

Phillips, R.B., Sajdak, S.L., and Domanico, M.J. 1995. Evolutionary relationships among charrs inferred from ribosomal DNA sequences. Nordic J. Freshwater Res. **71**: 378–391.

Pleyte, K.A., Phillips, R.B., and Duncan, S. 1992. Phylogenetic analysis of the genus *Salvelinus* from the first internal transcribed spacer of the ribosomal DNA. Mol. Phylogenet. Evol. **1**: 223–230.

Reist, J.D., Johnson, J.D., and Carmichael, T.J. 1997. Variation and specific identity of char from Northwestern Arctic Canada and Alaska. Am. Fish. Soc. Symp. **19**: 250–261.

Saitou, N., and Nei, M. 1987. The neighbor-joining method: a new method for reconstructing phylogenetic trees. Mol. Biol. Evol. **4**: 406–425.

Savvaitova, K.A. 1980. Taxonomy and biogeography of charrs in the Paleoarctic. Chap. 5. *In* Charrs, salmonid fishes of the genus *Salvelinus*. *Edited by* E.K. Balon. Junk Publishers, The Hague. pp. 281–294.

Savvaitova, K.A. 1995. Patterns of diversity and processes of speciation in Arctic char. Nordic J. Freshwater Res. **71**: 81–91.

Swofford, D.L. 1998. PAUP* 4.0 beta version, phylogenetic analysis using parsimony. Sinauer Associates Inc., Sunderland, Mass.

Ueda, T., and Ojima, Y. 1983. Karytoypes with C banding patterns of two species in the genus *Salvelinus* of the family Salmonidae. Proc. Jap. Acad. Ser. B, Phys. Biol. Sci. **59**: 343–346.

Viktorovsky, R.M. 1975. Karyotypes of the kundza (*Salvelinus leucomaenis*) and the *malma* (*S. malma*) (Salmoniformes, Salmonidae). Zool. Zh. **54**: 787–789.

© 1999 NRC Canada

Chance fluctuations and the survival of small salmon stocks

Richard D. Routledge and James R. Irvine

Abstract: In this paper, we use a Markovian approach to demonstrate that stocks with modest growth potential at low abundance can be driven quite rapidly to extinction. Under relatively benign conditions, stock survival rates may be high, but even a modest increase to the amount of chance variation in recruitment can reduce survival rates dramatically. Survival rates also depend on the form of the stock–recruitment curve, including depensation that takes hold only at extremely low abundances. Fortunately, small amounts of straying among adjacent populations can push the survival rate substantially toward the value for a combined, homogeneous unit. Our analysis also suggests modifications to existing approaches of establishing minimum target levels for spawning densities and the near impossibility of reliably estimating extinction rates.

Résumé : Dans cet article, nous utilisons une approche markovienne pour démontrer que les stocks peu abondants à faible potentiel de croissance peuvent s'éteindre assez rapidement. Dans des conditions relativement bonnes, les taux de survie des stocks peuvent être élevés, mais un accroissement léger de la variation aléatoire dans le recrutement peut suffire à les faire chuter de façon marquée. Les taux de survie dépendent aussi de la forme de la courbe stock–recrutement, et notamment du phénomène dépensatoire qui se manifeste seulement quand les abondances sont extrêmement faibles. Heureusement, un faible vagabondage entre des populations adjacentes peut suffire à relever substantiellement le taux de survie pour l'apparenter à celui d'une unité combinée et homogène. Selon nos analyses, des modifications devraient être apportées aux méthodes actuellement utilisées pour établir les densités de géniteurs minimales souhaitables, et il apparaît presque impossible d'estimer avec fiabilité les taux d'extinction.

[Traduit par la Rédaction]

Introduction

The recent reports of Nehlsen et al. (1991) and Slaney et al. (1996) highlighted the depressed status of many salmon (*Oncorhynchus* spp.) stocks on the Pacific coast of North America. Most small salmon stocks are not actively managed; in many instances, they are not even monitored. Since management can proceed with little feedback on the abundance of individual stocks, declines in abundance and even extinction may well go unnoticed.

In this context, we need to be able to assess the long-term advantages of management strategies that might, for example, lower the harvest rate on these stocks or enhance fish survival. In this paper, we develop a simple model to evaluate the potential impact of chance fluctuations on the survival of small stocks. The modelling approach is based on the ideas of Gilpin (1992), Stephan and Wissel (1994), and Kokko (1996) who used Markov chains for modelling populations that can fluctuate widely between distinct time periods. In contrast, most existing models for studying extinction probabilities develop diffusion approximations, more useful in studying populations that fluctuate more slowly over time (e.g., see Lande et al. 1994, 1995; Gaston and Nicholls 1995; Saether et al. 1996), or rely on computer simulations (e.g., Ginsberg et al. 1995; Nickelson and Lawson 1998).

Many analyses of fish population dynamics are based on deterministic stock–recruitment functions. Figure 1 portrays a typical set of such curves relevant to the problem of weak stock extinction. In our example, the curves portray a stock whose habitat can support only a relatively small number of spawners. These are plotted on the horizontal axis. The vertical axis shows the number of adults in the next generation escaping to their natal stream to spawn.

The solid and long-dashed curves show the commonly used Ricker (1954) and Beverton–Holt (Beverton and Holt 1957) relationships. Where the curves cross the 45° line, the spawners in the current generation recruit the same number of adults back to the next generation. Hence, the population is forecast to be in equilibrium at this level. If the population drops below this level, the subsequent recruitment will push the population back up, and if it exceeds this level, then it will be pushed back down. Hence, the equilibrium is said to be stable.

By contrast, a curve that remains below the 45° line depicts a population that cannot replace itself at any level of abundance and is therefore destined for extinction unless recruitment somehow improves. Finally, the short-dashed

Received July 15, 1997. Accepted April 14, 1999.
J14110

R.D. Routledge.[1] Department of Mathematics and Statistics, Simon Fraser University, Burnaby, BC V5A 1S6, Canada.
J.R. Irvine. Department of Fisheries and Oceans, Pacific Biological Station, Nanaimo, BC V9R 5K6, Canada.

[1]Author to whom all correspondence should be addressed. e-mail: routledg@cs.sfu.ca

© 1999 NRC Canada

Fig. 1. Four potential spawner–recruit relationships. The solid curve is a Ricker curve and the long-dashed curve a Beverton–Holt curve. The short-dashed curves (one each for the Ricker and Beverton–Holt versions, but which are indistinguishable in the figure) portray depensation at low spawner levels. The solid straight line is the 45° line, which represents replacement of the spawners with an equal number of recruits. Formulas are given in the Appendix. For each of the recruitment curves, slope at the origin was set to 1.8, stable population size to 30, and the cutoff for depensation to 3.

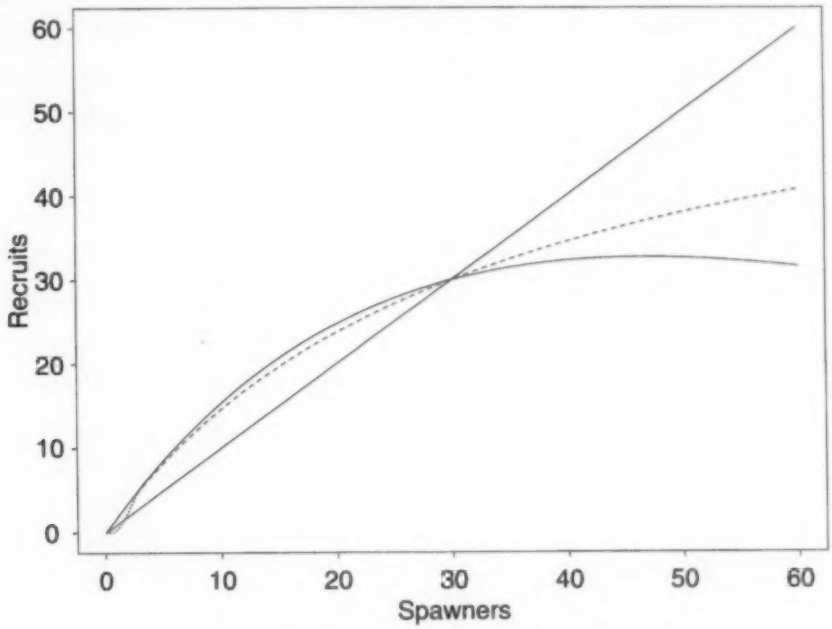

modifications to these curves depict depensatory recruitment relationships (recruitment per spawner or survival decreases as spawners become less numerous). If the number of spawners dips too low, then recruitment will fall short of replacement, and the population will go extinct.

According to a deterministic model, as long as the recruitment relationship contains sufficient growth potential at small abundance to allow the stock to increase, then the stock will not go extinct. However, actual stock–recruitment relationships are typically widely scattered about such a curve (e.g., Myers et al. 1995; Ricker 1997). Chance fluctuations are typically large, and these will increase the likelihood of extinction. For example, a stock whose mean recruitment follows the replacement line, and whose fluctuations follow the rules of a Galton–Watson branching process, will eventually become extinct with 100% probability (Harris 1963, p. 21).

In the following section, a simple stochastic model is developed that can be used to obtain rough predictions of extinction probabilities for relatively small stocks. The model is then used to explore management options for reducing these probabilities.

Model

Curves such as described above were used to model the relationship between the number of spawners in the parent generation and the mean number of spawners in the following generation. The curves are not specific to any species, although for a variety of reasons, we relied chiefly on data gathered for coho salmon (*Oncorhynchus kisutch*) in our models. Unfortunately, many stocks of coho salmon in the Pacific Northwest are declining (Nehlsen et al. 1991; Weitkamp et al. 1995; Slaney et al. 1996), and we are particularly concerned with the consequences of random fluctuations on the survival of small stocks of this important species.

Coho salmon have a relatively simple life history, which makes them relatively easy to model. In our model, which was developed to represent coho returning to streams south of northern British Columbia, we assume that all individuals return at the same age. Sandercock (1991) summarized data for British Columbia stocks indicating that between 95 and 98% of adult coho return at age 3. Furthermore, in our model, interactions between different cohorts, the nature of which remains highly uncertain (Ricker 1997 and references therein), are ignored. Because there is usually only one cohort in the same fresh and marine environments simultaneously for coho, interactions among cohorts are minimal and can therefore be ignored. Interactions with other species, which can introduce complex dynamics (Spencer 1997), have not been incorporated. It has also been assumed that stocks are genetically isolated, with no in-migration from other stocks. Support for this assumption is provided in the work of Labelle (1992), studying 14 coho stocks on Vancouver Island, who found that in the majority of cases, strays contributed less than 1% of the escapement. As well, Sandercock (1991) summarized several studies that document that coho usually exhibit very low rates of straying from home streams.

© 1999 NRC Canada

Fig. 2. Effect of increasing variance on the 100-year survival rate. All calculations were based on the Ricker curve displayed in Fig. 1 (slope at the origin = 1.8 and stable deterministic population level = 30) with recruitment modelled by the Poisson-inverse-Gaussian distribution.

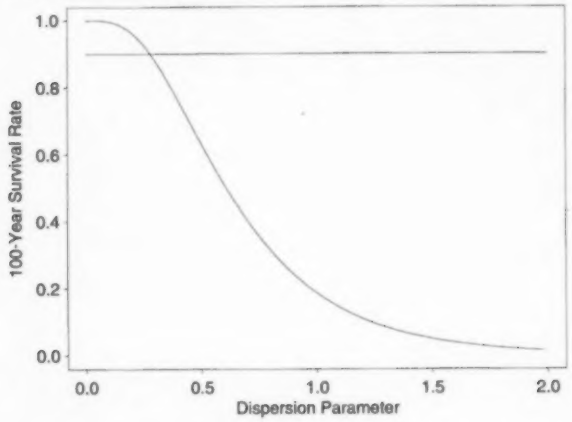

The analysis follows the fate of successive generations from a single cohort. Ricker and Beverton–Holt curves, with and without depensatory components, were used to model the mean recruitment function. The chance scatter about the recruitment curve was generated by each of two standard distributional families, the Poisson-inverse-Gaussian and negative binomial. We chose not to use the lognormal distribution, despite its attractive theoretical and empirical properties (Peterman 1981; Hilborn and Walters 1992). A discrete distribution was more appropriate for our modelling of small stocks. We chose the above two families for two reasons. First, they were computationally convenient; second, the Poisson-inverse-Gaussian is a good approximation to the Poisson–lognormal, a natural discrete version of the lognormal distribution, but involving tricky computations. (See Appendix for formulas and further justification.) Both are commonly used families that permit a flexible relationship between the mean and variance. They differ primarily in that for levels of chance recruitment variation commonly observed in fish populations, the negative binomial places a higher probability at zero (i.e., on immediate extinction).

The stock–recruitment curve was specified through three parameters, chosen so as to specify the slope at the origin, the deterministic equilibrium, and the break point, if any, where depensation set in. These collectively specified the mean for the recruitment distribution, and a fourth parameter specified the level of extra-variance (see Appendix). This extra-variance parameter permitted the inclusion of environmental variability noise (Wissel and Zaschke 1994).

This model generates a Markov process, a property shared with several recently proposed models for species extinction (see Appendix for relevant theory and references). In particular, the model predicts that, with 100% probability, any stock will eventually become extinct. However, this may take an exceedingly long time, and if it does, the abundance distribution will approach a constant. As this happens, the annual extinction probability also approaches a limit. The following analysis uses these limiting probabilities that a population will become extinct as an indicator of the health of the stock, as suggested by Allendorf et al. (1997) and others.

Analyses

Parameters for the model-based calculations were based primarily on data collected on coho from Black Creek, an unenhanced stream on Vancouver Island, B.C. At Black Creek, a counting fence is operated each fall and spring to obtain accurate estimates of spawner and smolt numbers. Because the model is designed to investigate the relationship between numbers of spawners in successive generations, data on numbers of smolts were ignored. However, coded-wire tags were placed in most migrating smolts so that we could estimate numbers of adult coho captured in the various fisheries, as described by Kuhn (1988). To isolate effects of changes to fisheries exploitation rates, data on numbers of adult (precocious males ignored) spawners versus returns (i.e., catch plus escapement) were used. For the analysis to be consistent with the extinction model, the data were analyzed in a nonstandard way. The mean number of returns was assumed to be generated by a Ricker curve. Since there is evidence of a substantial decline in marine survival over the period (e.g., Coronado and Hilborn 1998), an extra term was added to allow for a decline in the relationship over time. Furthermore, variability about this curve was assumed to be generated independently each year by a Poisson-inverse-Gaussian distribution. Finally, in keeping with the model, no adjustments were made for possible time series bias (Korman et al. 1995). The specific model, with x_i the number of spawners in year i, y_i the number of returns that they generate, and t_i the year (centered at 0 for numerical stability), was

$$y_i = ax_i \exp(-bx_i - ct_i) + \varepsilon_i$$

where ε_i is an independent Poisson-inverse-Gaussian chance error term with variance $\sigma_i^2 = \mu_i(1 + \tau\mu_i)$ with $\mu_i = ax_i \exp(-bx_i - ct_i)$.

Parameters were fit by maximum likelihood. Estimates were as follows: a = 3.84, b = 0.000289, c = 0.261, and τ (extra-variance parameter) = 0.121. Note the relatively large value of c. This appears to be driven by a dramatic decline in marine survival and suggests that the mean number of returns per spawner that could have been produced by a small number of spawners at Black Creek has declined from 12.42 through the intermediate value of 3.84 to a recent value of 1.19.

However, these estimates are subject to large uncertainty. One reason is that there is no compelling theoretical or empirical justification for the Ricker curve, the form of the time dependence, or the Poisson-inverse-Gaussian distribution. In addition, the parameter estimates, based on only 10 points, are imprecise. For example, profile likelihood tests indicate that the data are reasonably consistent with any value of τ between about 0.05 and 0.50. Furthermore, τ may well not be constant over time.

These estimates relate the number of spawners to the number of returns. The numbers of returning adults that actually spawn will be further reduced by fishing. This will introduce a further reduction to the parameter a describing

© 1999 NRC Canada

Fig. 3. Effect of the size of the equilibrium population size on the 100-year survival rate. All calculations were based on a Ricker curve (with slope at the origin = 1.8) and a Poisson-inverse-Gaussian distribution with extra-variance parameter τ set to 0.148.

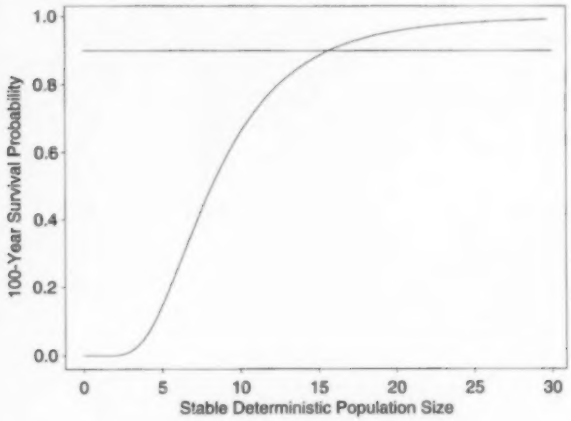

initial growth for small populations (slope at the origin). For each of the two recruitment curves (Ricker and Beverton–Holt), a was first set to 1.9. This corresponds to an approximate 50% harvest rate when $a = 3.84$. The stable population level was initially set to 30 female spawners. This value was not based on data from Black Creek. Canadian Department of Fisheries and Oceans personnel have proposed a target of three spawning female coho per kilometre as a limit reference point below which one would only occasionally want to go. To maintain optimal smolt production, in the Department of Fisheries and Oceans proposal, one would like never to go below nine females per kilometre. In our analysis, we assume three females per kilometre to represent the stable population level in the absence of chance fluctuations. The value 30 then corresponds to a 10-km stream. We have no information on the possible presence of depensation at low abundance. However, Nickelson and Lawson (1998) suggested that coho may have trouble finding a mate when spawner population size is small, especially when fish spawn over a considerable time. We arbitrarily set the depensation cutoff to 3. The extra-variance parameter was set to 0.121. The available data are sketchy, and, of course, the model is at best a rough approximation to reality. Nonetheless, this simple model can be used to illustrate the following key points.

High survival rates under benign conditions

For the recruitment curves shown in Fig. 1, and either the Poissonn-inverse-Gaussian or negative binomial distribution with extra-variance parameter set to 0.121, the model predicts that 95.1–99.3% of the stocks will survive for 100 years.

Influence of variability in recruitment

Figure 2 shows that the greater the size of the chance fluctuations (as quantified by the extra-variance parameter τ), the greater the risk that these will drive the stock to extinction. In this particular instance, the 100-year population survival rate is well below the 90% cutoff for $\tau = 0.5$, a value that is reasonably consistent with the Black Creek data. Hence, extra-variance in the recruitment distribution can have a major influence on the extinction probability. Wissel and Zaschke (1994), working with a birth and death model, reported a similarly strong influence of environmental noise on the extinction probability.

Table 1. Percentage of stocks estimated to survive for 100 years.

	No depensation		Depensation	
Recruitment curve	PIG	NB	PIG	NB
Ricker	63.3	34.9	45.0	19.3
Beverton–Holt	59.3	33.1	41.0	18.1

Note: Calculations were based on the recruitment curves shown in Fig. 1, with slope at the origin set to 1.9, extra-variance parameter 0.5, stable population size 30, and the depensation cutoff 3. The two distributions used were the Poisson-inverse-Gaussian (PIG) and the negative binomial (NB).

Imprecise predictions

It is impossible to predict survival probabilities with any reasonable reliability. Not only are the predictions sensitive to changes in imprecisely estimated parameters like τ, they are also sensitive to the form of the stock–recruitment relationship. Consider, for example, the impact of changing three features: depensation (presence versus absence), the distribution used to model the size of the next generation (Poisson-inverse-Gaussian versus negative binomial), and the shape of the recruitment curve (Ricker versus Beverton–Holt). It is unrealistic to expect a fish manager to have enough detailed information on a small stock to be confident in any of these choices. The above calculations suggest that, under benign conditions, the survival rate will be large no matter how these features are manipulated. Table 1 shows the potential impact of misspecification of these factors under less favourable conditions. For these calculations, the extra-variance parameter τ was increased to 0.5.

The estimated percentage of stocks surviving for 100 years is anywhere between 18 and 63%. Both choice of distribution and the presence versus absence of depensation have a major influence. This lack of certainty is commonly observed in extinction probability calculations. McCarthy et al. (1996) reported large uncertainty in extinction probability estimates even for a thoroughly studied species. Citing similar difficulties in bird extinction studies, Ludwig (1996) recommended a Bayesian approach for averaging over a collection of plausible models.

Size of a "stable" stock

Without chance fluctuations, a stock will settle at the point where the spawners recruit an equal number back to spawn in the next generation. The smaller these values, the lower the 100-year survival probability (Fig. 3). This result shows that so-called safe levels based on the density of spawning females per kilometre of habitat may be too simplistic. A safe density for a 10-km stream could be extremely risky in a 1-km stream. To be risk averse, one should strive for a higher minimum density in a short stream than in a longer one.

© 1999 NRC Canada

Fig. 4. Effect of a decrease in the slope at the origin on the extinction rate. All calculations were based on Ricker curves, as displayed in Fig. 1, but with the entire curve compressed in the vertical direction, as would arise from a density-independent decrease in marine survival. Recruitment was modelled by the Poisson-inverse-Gaussian distribution with extra-variance parameter τ set to 0.148. Note that the vertical axis portrays the probability of immediate extinction, not the probability of extinction some time in the next 100 years.

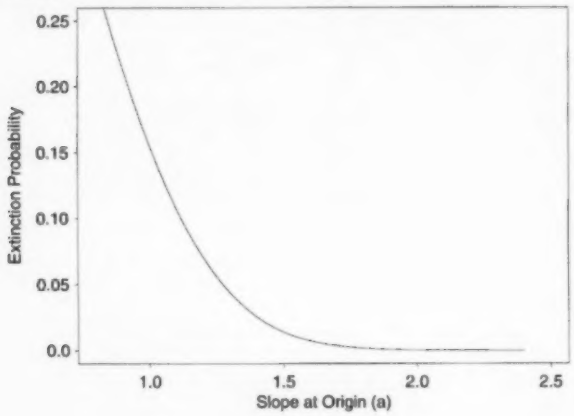

Fig. 5. Effect of straying between two identical, depressed stocks on the probability of immediate extinction. The two individual stocks were assumed to recruit according to the Ricker curve depicted in Fig. 1, but with the slope at the origin reduced to 1.1. The stray rate is the probability that an individual from either stock will stray to the other stock when it returns to spawn.

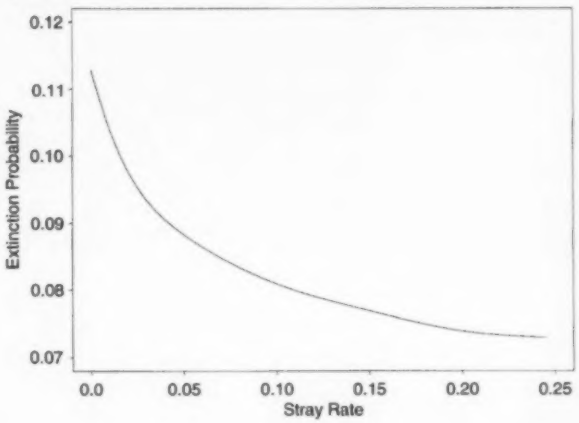

Lead time in an unforeseen downturns

Unforeseen downturns in stock productivity and survival are common. They can be local, e.g., as caused by small landslides near spawning areas, or widespread, as is the potential effect of climate change. They can be temporary, perhaps caused by autocorrelated or cyclic environmental fluctuations, or can be a more stable shift to a new regime. Autocorrelated fluctuations violate the Markov property of the model and are therefore not considered here. Downturns can quickly put a healthy stock at risk, especially if they go undetected. Consider, for example, Fig. 4, which portrays the effect of a decrease in the parameter a. An increase in fishing pressure due to bycatch in a fishery targeting on a recently enhanced stock would produce such an effect, as would a decrease in marine survival. Note that this figure portrays the probability of extinction in a single generation. If, as is thought to be the case with some coho stocks at present, the stocks are no longer able to replace themselves, over 15% of the brood lines of smaller stocks may be expected to go extinct per year. Any delay in mounting remedial action could be very costly.

Straying among spawning areas

There will be straying among adjacent stocks, although available evidence (Sandercock 1991; Labelle 1992) suggests that, for coho at least, it will be small. Recent studies confirm that there is relatively little gene flow among coho populations, indicating high reproductive isolation (Weitkamp et al. 1995; Small et al. 1998).

The Markov chain approach can theoretically be extended to model multiple stocks, among which fish can stray. However, the number of possible states of the combined stock complex is slightly larger than the product of the upper limits on each individual stock size. For two stocks, each of maximum size 50, for example, there are 51 possible states for each stock (including 0) and 2601 states for the two stocks together. Hence, the computations quickly become unwieldy.

For two small stocks, the computations are manageable. Figure 5 summarizes calculations for two severely depressed stocks whose parameter a has dropped to 1.1. Small amounts of straying noticeably reduce the extinction probability from its single-stock value of over 11%.

Summary of implications

The precise values of these extinction probability estimates should not be taken too seriously for several reasons. Our chief data set, although considered to be precise, is of relatively short duration. Mixing of returning adults from adjacent spawning areas and brood years, although likely to be small for coho (Sandercock 1991), may be higher for other species and will effectively enlarge the pool of contributing spawners and thereby reduce the extinction rate. Nonetheless, the high possible extinction rates that we calculated point to major potential losses of genetic information, which may well turn out to be invaluable (Colaninno 1996). As well, they point to the importance of depensation, environmental noise, and equilibrium stock size in controlling extinction rates. The analyses also remind us that we may lose small stocks on a regular basis, no matter how carefully we manage them. The questions to ask are not "how can we protect all our small stocks?" but "how high a local extinction rate can be accepted, and how can we keep the extinctions from exceeding this level?" These are timely concerns. For instance, in British Columbia, it has been demonstrated that coho from the Thompson River watershed (a major tributary of the Fraser River in the interior of the province) are

© 1999 NRC Canada

genetically distinct from other coho in the province (Small et al. 1998). Returns of coho to streams in the Thompson River drainage reached historic low levels in 1996 (Irvine et al. 1999).

Furthermore, it is not possible to state that a stock is safe if the density of female spawners per kilometre exceeds some target. Many other factors contribute to the extinction probability (e.g., Wainwright and Waples 1998). Stocks that spawn in small streams, or that show greater chance variation in their recruitment, or that are in streams with poor habitat (Nickelson and Lawson 1998) are at greater risk of extinction. More elaborate criteria such as those posed by Mace and Collar (1994) are needed.

Acknowledgements

This work was partially supported by a research grant from the Natural Sciences and Engineering Research Council of Canada.

References

Allendorf, F.W., Bayles, D., Bottom, D.L., Currens, K.P., Frissell, C.A., Hankin, D., Lichatowich, J.A., Nehlsen, W., Trotter, P.C., and Williams, T.H. 1997. Prioritizing Pacific salmon stocks for conservation. Conserv. Biol. **11**: 140–152.

Beverton, R.J.H., and Holt, S.J. 1957. On the dynamics of exploited fish. Fish. Invest. Ser. II Mar. Fish. G.B. Minist. Agric. Fish. Food, **19**: 1.533.

Colaninno, A. 1996. What's the big deal? Putting extinction in perspective. J. For. **94**: 60.

Coronado, C., and Hilborn, R. 1998. Spatial and temporal factors affecting survival in coho salmon (*Oncorhynchus kisutch*) in the Pacific Northwest. Can. J. Fish. Aquat. Sci. **55**: 2067–2077.

Gaston, K.J., and Nicholls, A.O. 1995. Probable times to extinction of some rare breeding bird species in the United Kingdom. Proc. R. Soc. Lond. Ser. B. Biol. Sci. **259**: 119–123.

Gilpin, M. 1992. Demographic stochasticity: a Markovian approach. J. Theor. Biol. **154**: 1–8.

Ginsberg, J.R., Mace, G.M., and Albon, S. 1995. Local extinction in a small and declining population: wild dogs in the Serengeti. Proc. R. Soc. Lond. Ser. B. Biol. Sci. **262**: 221–228.

Harris, T.E. 1963. The theory of branching processes. Springer-Verlag, Berlin.

Hilborn, R., and Walters, C.J. 1992. Quantitative fisheries stock assessment: choice, dynamics and uncertainty. Chapman and Hall, International Thomson Publishing, Toronto, Ont.

Irvine, J.R., Wilson, K., Rosenberger, B., and Cook, R. 1999. Stock assessment of Thompson River/Upper Fraser coho salmon. Can. Stock Assess. Secretariat Res. Doc. 99/28. Department of Fisheries and Oceans, Ottawa, Ont.

Kokko, H. 1996. Finding the probability of extinction: error analysis and optimal use of Markovian population models. J. Theor. Biol. **183**: 77–87.

Korman, J., Peterman, R.M., and Walters, C.J. 1995. Empirical and theoretical analyses of correction of time-series bias in stock–recruitment relationships of sockeye salmon (*Oncorhynchus nerka*). Can. J. Fish. Aquat. Sci. **52**: 2174–2189.

Kuhn, B.R. 1988. The MRP-Reporter Program: a data extraction and reporting tool for the Mark Recovery Program database. Can. Tech. Rep. Fish. Aquat. Sci. No. 1625.

Labelle, M. 1992. Straying patterns of coho salmon (*Oncorhynchus kisutch*) stocks from southeast Vancouver Island, British Columbia. Can. J. Fish. Aquat. Sci. **49**: 1843–1855.

Lande, R., Engen, S., and Saether, B-E. 1994. Optimal harvesting, economic discounting and extinction risk in fluctuating populations. Nature (Lond.), **372**: 88–90.

Lande, R., Engen, S., and Saether, B-E. 1995. Optimal harvesting of fluctuating populations with a risk of extinction. Am. Nat. **145**: 728–745.

Ludwig, D. 1996. Uncertainty and the assessment of extinction probabilities. Ecol. Appl. **6**: 1067–1076.

Mace, G.M., and Collar, N.J. 1994. Extinction risk assessment for birds through quantitative criteria. Ibis, **137**: S240–S246.

McCarthy, M.A., Burgman, M.A., and Ferson, S. 1996. Logistic sensitivity and bounds for extinction risks. Ecol. Model. **86**: 297–303.

Myers, R.A., Barrowman, N.J., Hutchings, J.A., and Rosenberg, A.A. 1995. Population dynamics of exploited fish stocks at low population levels. Science (Washington, D.C.), **269**: 1106–1108.

Nehlsen, W., Williams, J.E., and Lichatowich, J.A. 1991. Pacific salmon at the crossroads: stocks at risk from California, Oregon, Idaho, and Washington. Fisheries (Bethesda), **16**(2): 4–21.

Nickelson, T.E., and Lawson, P.W. 1998. Population viability of coho salmon, *Oncorhynchus kisutch*, in Oregon coastal basins: application of a habitat-based life cycle model. Can. J. Fish. Aquat. Sci. **55**: 2383–2392.

Peterman, R.M. 1981. Form of random variation in salmon smolt–adult relations and its influence on production estimates. Can. J. Fish. Aquat. Sci. **38**: 1113–1119.

Ricker, W.E. 1954. Stock and recruitment. J. Fish. Res. Board Can. **11**: 559–623.

Ricker, W.E. 1997. Cycles of abundance among Fraser River sockeye salmon (*Oncorhynchus nerka*). Can. J. Fish. Aquat. Sci. **54**: 950–968.

Saether, B-E., Engen, S., and Lande, R. 1996. Density-dependence and optimal harvesting of fluctuating populations. Oikos, **76**: 40–46.

Sandercock, F.K. 1991. Life history of coho salmon (*Oncorhynchus kisutch*). *In* Pacific salmon life histories. *Edited by* C. Groot and L. Margolis. University of British Columbia Press, Vancouver, B.C. pp. 397–445.

Slaney, T.L., Hyatt, K.D., Northcote, T.G., and Fielden, R.J. 1996. Status of anadromous salmon and trout in British Columbia and Yukon. Fisheries (Bethesda), **21**(10): 20–35.

Small, M.P., Beacham, T.D., Withler, R.E., and Nelson, R.J. 1998. Discriminating coho salmon (*Oncorhynchus kisutch*) populations within the Fraser River, British Columbia, using microsatellite DNA markers. Mol. Ecol. **7**: 141–155.

Spencer, P.D. 1997. Optimal harvesting of fish populations with nonlinear rates of predation and autocorrelated environmental variability. Ecol. Model. **75/76**: 193–201.

Stephan, T., and Wissel, C. 1994. Stochastic extinction models discrete in time. Ecol. Model. **75/76**: 183–192.

Wainwright, T.C., and Waples, R.S. 1998. Prioritizing Pacific salmon stocks for conservation: response to Allendorf et al. Conserv. Biol. **12**: 1144–1147.

Weitkamp, L.A., Wainwright, T.C., Bryant, G.J., Milner, G.B., Teel, D.J., Kope, R.G., and Waples, R.S. 1995. Status review of coho salmon from Washington, Oregon, and California. U.S. Dep. Commer. NOAA Tech. Memo. NMFS-NWFSC-24.

Wissel, C., and Zaschke, S-H. 1994. Stochastic birth and death processes describing minimum viable populations. Ecol. Model. **75/76**: 193–201.

© 1999 NRC Canada

Appendix

In the following standard recruitment curve formulas, a is the slope at the origin and s represents the stable population size in the absence of random fluctuations. For the Ricker (1954) curve:

$$y = axe^{-bx}, \text{ where } b = \ln(a)/s.$$

For the Beverton–Holt (Beverton and Holt 1957) curve:

$$y = ax/(1 + bx), \text{ where } b = (a - 1)/s$$

Depensation has been added by modifying these formulas at low abundance ($x \leq c$) (where c is the cutoff to depensation) by multiplying by

$$0.5[1 - \cos(\pi x/c)] \text{ for } x \leq c.$$

The numbers of returning adults were simulated according to a mixed Poisson distribution. The simplest model for generating such a distribution would be the Poisson. But this model is clearly unrealistic. It requires that individual survival be generated independently, with a constant probability. A variable environment and dependent behaviour would increase the variability. A mixed Poisson distribution will generate this extra-Poisson variation. Statisticians rarely have any firm reasons for choosing any particular model for a mixing distribution, and this application is no exception. The inverse Gaussian and gamma distributions are convenient choices in that the resultant Poisson-inverse-Gaussian and negative binomial distributions are easily calculated (Johnson et al. 1992, pp. 199 and 456). These distributions differ primarily in that the former permits a large amount of extra-Poisson variation without forcing the distribution to display a sharp peak at 0.

Each of these distributions contains two parameters (Johnson et al. 1992, pp. 199 and 455). These were specified through requiring the mean to conform to the value specified by the recruitment curve and the variance to satisfy the equation

$$\sigma^2 = \mu(1 + \mu\tau).$$

For a Poisson distribution, $\sigma^2 = \mu$. Hence, the parameter τ dictates the amount of extra-Poisson variation. In many applications, the product $\mu\tau$ is large enough that

$$\sigma^2 \approx \mu^2\tau$$

and the coefficient of variation is

$$CV = \sigma/\mu \approx \sqrt{\tau}.$$

The model generates a discrete-time Markov process on the nonnegative integers. It shares this property with several other recent models for extinction rates (Gilpin 1992; Stephan and Wissel 1994; Kokko 1996), and this paper follows their general truncation strategy. It is distinct from the Markovian models proposed by Getz and Swartzman (1981) and Overholtz et al. (1986) and discussed in Hilborn and Walters (1992, p. 263). These impose no model restrictions on the recruitment function or distribution, divide the abundance range into a few broad categories, and then estimate transition probabilities from long time series of data.

The recruitment curve and associated probability distribution effectively limit the process to a finite range. The range was truncated at the point at which there was only a small chance that the population would reach that level. This then led to a finite Markov chain whose transition probability matrix could be constructed.

Since extinction is an inescapable state, the transition matrix has the following form, with first row (1, 0, 0, 0,..., 0):

$$M = \left[\begin{array}{c|c} 1 & 0 \\ \hline R & Q \end{array}\right].$$

The dominant eigenvalue of M is 1. Furthermore, the matrix Q is positive, and hence, by the Perron contribution to the Perron–Frobenius theorem (e.g., as presented in Gantmacher 1974, p. 53), it has a dominant, positive, real eigenvalue. Since the eigenvalues of Q are identical to the subdominant eigenvalues of M, this eigenvalue must also be less than 1. Furthermore, the row eigenvectors of Q are related to the corresponding eigenvectors of M. The latter are scalar multiples of the former; however, they are augmented by the addition of a leading component. It follows that the dominant row eigenvector (p) of Q, rescaled so as to sum to 1, is the limiting conditional size distribution given that the population has not yet gone extinct and that the largest eigenvalue (λ) of this matrix is the limiting annual survival probability. Hence, $1 - \lambda$ is the asymptotic extinction probability.

The fundamental matrix (Kemeny and Snell 1976, p. 46) for the chain $(I - Q)^{-1}$ has the property that the i–jth component gives the expected number of visits to state j for a chain that starts in state i. Previous modellers have used this relationship to calculate the probability of extinction as a function of the initial population size. It can be related to p and λ as follows:

$$p(I - Q)^{-1} = p + pQ + pQ^2 + \ldots$$
$$= p[1 + \lambda + \lambda^2 + \ldots] = p/(1 - \lambda)$$

Hence, $p/(1 - \lambda)$ is the vector of expected number of times that a population with initial size distributed according to the vector p spends in each of its positive states before going extinct. Its sum, $1/(1 - \lambda)$, is the expected time to extinction for such a population.

The quantity reported in the body of the paper is $1 - \lambda$. Matrix calculations were performed with Splus functions available from the senior author. Eigenanalysis was performed with the Splus function "eigen."

Kokko (1996) proposed a strategy for assessing the error generated by the mandatory truncation. An upper limit on the extinction probability can be found by assigning all the probabilities for transitions to states beyond the truncation limit to the final state, as long as this state is more likely to lead to early extinction than the states beyond the truncation point. She obtained a lower bound by making the uppermost state absorbing.

Unfortunately, the latter strategy fails here in that although the addition of a second absorbing state decreases the extinction probability, it actually increases the asymptotic absorption probability. Hence, it does not produce a lower bound on $1 - \lambda$.

© 1999 NRC Canada

Furthermore, the side condition that larger abundances lead to lower extinction probabilities is violated for models based on the Ricker curve and also for certain parametrizations of the extra-Poisson variance. Nonetheless, it is satisfied for the Beverton–Holt-based models used here. In addition, the fact that the Beverton–Holt curve has a horizontal asymptote (and the Ricker curve has an absolute maximum) can be used to place an upper bound on the mean for the next generation. If this maximum is used to generate the last row of truncated transition probabilities, then one obtains a lower bound on $1 - \lambda$. An upper bound for models using a Ricker curve can often be obtained by making the uppermost state lead immediately to extinction with probability 1.

All single-stock calculations were based on populations truncated at 200 individuals. Where calculable, the bounds were remarkably tight. For example, in the first entry in Table 1, the bounds were 63.26 and 63.44%.

Appendix references

Beverton, R.J.H., and Holt, S.J. 1957. On the dynamics of exploited fish. Fish. Invest. Ser. II Mar. Fish. G.B. Minist. Agric. Fish. Food, **19**: 1.533.

Gantmacher, F.R. 1974. The theory of matrices. Vol. 2. Chelsea, New York.

Getz, W.M., and Swartzman, G.L. 1981. A probability transition matrix model for yield estimation in fisheries with highly variable recruitment. Can J. Fish. Aquat. Sci. **38**: 847–855.

Gilpin, M. 1992. Demographic stochasticity: a Markovian approach. J. Theor. Biol. **154**: 1–8.

Hilborn, R., and Walters, C.J. 1992. Quantitative fisheries stock assessment: choice, dynamics and uncertainty. Chapman and Hall, International Thomson Publishing, Toronto, Ont.

Johnson, N.L., Kotz, S., and Kemp A.W. 1992. Univariate discrete distributions. 2nd ed. Wiley-Interscience, New York.

Kemeny, J.G., and Snell, J.L. 1976. Finite Markov chains. Springer-Verlag, New York.

Kokko, H. 1996. Finding the probability of extinction: error analysis and optimal use of Markovian population models. J. Theor. Biol. **183**: 77–87.

Overholtz, W.J., Sissenwine, M.P., and Clark, S.H. 1986. Recruitment variability and its implications for managing and rebuilding the Georges Bank haddock stock. Can. J. Fish. Aquat. Sci. **43**: 748–753.

Ricker, W.E. 1954. Stock and recruitment. J. Fish. Res. Board Can. **11**: 559–623.

Stephan, T., and Wissel, C. 1994. Stochastic extinction models discrete in time. Ecol. Model. **75/76**: 183–192.

© 1999 NRC Canada

ASSIGNMENT OF COPYRIGHT

Ms. No. _____

To: NATIONAL RESEARCH COUNCIL OF CANADA ("NRC") Research Press

From: _____

_____

_____

_____

(name and address of author signing this form)

This refers to the manuscript entitled: _____

_____

written by myself and the following additional author(s): _____

_____

for publication in: _____

1. I declare that the list of authors fairly conforms to academic conventions about who should be listed. I declare that the manuscript, or its equivalent, has not been submitted for publication elsewhere. If it is accepted for publication by the National Research Council of Canada, I will ensure that it, or its equivalent, is not submitted for publication elsewhere.

2. I declare that I am (check ONE):

☐ (a)	the sole owner of the copyright relating to the manuscript, and →	I **assign** to NRC the entire copyright.
☐ (b)	a part owner of the copyright, in conjunction with interests held by co-authors or their employers, and →	I **assign** to NRC my entire interest in the copyright, and I expect the co-authors to also sign a form like this one.
☐ (c)	an agent of my employer with authority to assign the copyright owned by the employer, who is: _____, and →	I **assign** to NRC, on behalf of my employer, my employer's entire interest in the copyright relating to the manuscript, and I expect the co-authors to also sign a form like this one.
☐ (d)	a public servant in Canada (federal, provincial or territorial) or the United Kingdom, so that the copyright is owned by Her Majesty, and →	I have obtained the approval of my employer, according to the terms of my employment, to grant NRC **non-exclusive permission** to publish the manuscript and administer the copyright.
☐ (e)	a public servant of the United States of America, and subject to the law that creates no U.S. copyright for the manuscript, and →	I **assign** to NRC, on behalf of my employer, my employer's entire interest in any copyright that may exist outside the U.S., and I expect the co-authors to sign a form like this one.

3. I understand that my submission of this document does not guarantee publication, and that publication will not occur until **all authors** have provided a copyright transfer. If the manuscript is not published within 2 years after I sign this, the assignment is revoked.

Signed at _____ on _____

(City and Province/State) (Date)

_____

(Signature)

[Standard NRC form; alterations not acceptable.]

Comments on Copyright Transfer
(with extracts from the *Copyright Act*, Revised Statutes of Canada 1985, chapter C-42, as amended)

The publisher is not permitted to publish the manuscript without permission or an assignment of ownership of copyright. For greatest flexibility, and to be prepared to deal with future uses of the published material, the publisher requires ownership.

The owner may assign the right, but that assignment must be in writing:

13.(4) The owner of the copyright in any work may assign the right, either wholly or partially, and either generally or subject to territorial limitations, and either for the whole term of the copyright or for any other part thereof, and may grant any interest in the right by licence, but no assignment or grant is valid unless it is in writing signed by the owner of the right in respect of which the assignment or grant is made, or by his duly authorized agent.

The owner may be the author, but in many cases, the owner is the author's employer:

13.(3) Where the author of a work was in the employment of some other person under a contract of service or apprenticeship and the work was made in the course of his employment by that person, the person by whom the author was employed shall, in the absence of any agreement to the contrary, be the first owner of the copyright, but where the work is an article or other contribution to a newspaper, magazine or similar periodical, there shall, in the absence of any agreement to the contrary, be deemed to be reserved to the author a right to restrain the publication of the work, otherwise than as part of a newspaper, magazine or similar periodical.

The only exception to taking ownership arises when the manuscript is covered by Crown copyright owned by a Canadian government.

12. Without prejudice to any rights or privileges of the Crown, where any work is, or has been, prepared or published by or under the direction or control of Her Majesty or any government department, the copyright in the work shall, subject to any agreement with the author, belong to Her Majesty and in that case shall continue for the remainder of the calendar year of the first publication of the work and for a period of fifty years following the end of that calendar year.

Governments, and in particular the federal government, do not have a simple mechanism for assigning ownership of this particular type of Crown asset. Therefore, when an author is a public servant so that there is Crown copyright in the manuscript, a simple permission to use is acceptable to the publisher, if it is granted by a person with appropriate authority.

CESSION DU DROIT D'AUTEUR

Document n° _____

Au : CONSEIL NATIONAL DE RECHERCHES DU CANADA («CNRC») - Presses scientifiques

De : _____

_____

_____

_____

(nom et adresse de l'auteur qui signe le présent formulaire)

La présente cession porte sur le document intitulé : _____

_____

rédigé par moi, en collaboration avec l'auteur/les auteurs suivant(s) : _____

_____

aux fins de publication dans : _____

1. Je déclare que la liste des auteurs ci-dessus respecte les pratiques usuelles de rédaction savante quant aux personnes dont le nom doit être cité. Je déclare que le document ou son équivalent n'a pas été soumis à quelque autre organisme aux fins de publication. Si le CNRC accepte de publier le document, je m'assurerai que celui-ci ou son équivalent n'est soumis à aucun autre organisme aux fins de publication sans en obtenir la permission préalable du CNRC.

2. Je déclare être (UN SEUL choix) :

☐ (a)	le seul titulaire de droit d'auteur afférent au document,	et →	je **cède** le droit d'auteur intégral au CNRC.
☐ (b)	un titulaire partite du droit d'auteur, de concert avec des coauteurs ou leurs employeurs,	et →	je **cède** ma part du droit d'auteur au CNRC et m'attends à ce que les coauteurs signent une entente comparable.
☐ (c)	un agent de mon employeur ayant l'autorité de céder le droit d'auteur appartenant à l'employeur, nommément : _____,	et →	je **cède** au CNRC, au nom de mon employeur, la part entière du droit d'auteur afférent au document appartenant à mon employeur, et m'attends à ce que les coauteurs signent une entente comparable.
☐ (d)	un fonctionnaire du Canada (fédéral, provincial ou territorial) ou du Royaume-Uni, donc le droit d'auteur appartient à Sa Majesté,	et →	j'ai obtenu de mon employeur, en vertu de mes conditions d'emploi, l'autorisation d'accorder au CNRC la **permission non exclusive** de publier le document et de gérer le droit d'auteur.
☐ (e)	un fonctionnaire des États-Unis d'Amérique, donc sujet à la loi qui n'associe aucun droit d'auteur américain au document,	et →	je **cède** au CNRC, au nom de mon employeur, la part entière de quelque droit d'auteur en vigueur ailleurs qu'aux É.-U. appartenant à mon employeur, et m'attends à ce que les coauteurs signent une entente comparable.

3. Je comprends que la soumission du document ne garantit aucunement sa publication et que la publication ne pourra être réalisée tant que **tous les auteurs** n'auront pas signé une cession du droit d'auteur. Si le document n'est pas publié dans les deux années suivant ma signature des présentes, la cession sera automatiquement révoquée.

Signé à _____, le _____

(ville et province/état) (date)

_____

(signature)

[Formulaire normalisé du CNRC; aucune modification permise]

Commentaires sur la cession du droit d'auteur
(accompagnés d'extraits de la *Loi sur le droit d'auteur*, Lois révisées du Canada 1985, chapitre C-42 modifié)

L'éditeur ne peut publier un document sans la permission ou une cession du droit d'auteur. Pour des raisons de souplesse et en vue de l'utilisation future du document publié, l'éditeur doit devenir titulaire du droit d'auteur.

Le titulaire peut céder le droit, mais cette cession doit être faite par écrit :

13.(4) Le titulaire du droit d'auteur sur une oeuvre peut céder ce droit, en totalité ou en partie, d'une façon générale, ou avec des restrictions territoriales, pour la durée complète ou partielle de la protection; il peut également concéder, par une licence, un intérêt quelconque dans ce droit; mais la cession ou la concession n'est valable que si elle est rédigée par écrit et signée par le titulaire du droit qui en fait l'objet, ou par son agent dûment autorisé.

Le titulaire peut être l'auteur, mais dans plusieurs cas, le titulaire est l'employeur de l'auteur:

13.(3) Lorsque l'auteur est employé par une autre personne en vertu d'un contrat de louage de service ou d'apprentissage, et que l'oeuvre est exécutée dans l'exercice de cet emploi, l'employeur est, à moins de stipulation contraire, le premier titulaire du droit d'auteur; mais lorsque l'oeuvre est un article ou un autre contribution, à un journal, à une revue ou à un périodique du même genre, l'auteur, en l'absence de convention contraire, est réputé posséder le droit d'interdire la publication de cette oeuvre ailleurs que dans un journal, une revue ou un périodique semblable.

La seule exception dans la cession du droit d'auteur est lorsque le document est associé au droit d'auteur de la Couronne, qui appartient au gouvernement du Canada .

12. Sous réserve de tous les droits ou privilèges de la Couronne, le droit d'auteur sur les oeuvres préparées ou publiées par l'entremise, sous la direction ou la surveillance de Sa Majesté ou d'un ministère du gouvernement, appartient, sauf stipulation conclue avec l'auteur, à Sa Majesté et, dans ce cas, il subsiste jusqu'à la fin de la cinquantième année suivant celle de la première publication de l'oeuvre.

Les gouvernements, en particulier le gouvernement fédéral, ne disposent pas d'un mécanisme simple de cession de droit d'auteur pour ce genre de biens de la Couronne. C'est pourquoi lorsqu'un auteur est un fonctionnaire et que, par conséquent, le droit d'auteur appartient à la Couronne, une simple permission d'usage est suffisante pour l'éditeur, pour autant que celle-ci ait été octroyée par une personne jouissant de l'autorité nécessaire pour ce faire.

Guide to the Parasites of Fishes of Canada. Part IV. Trematoda

David I. Gibson

373 pages
Softcover/Édition brochée
March/mars 1996
ISBN 0-660-16403-5
ISSN 0706-6481
NRC/CNRC 40083
$42.95/42,95 $
Canadian Special Publication of Fisheries and Aquatic Sciences/ Publication spéciale canadienne des sciences halieutiques et aquatiques 124

More than 80 keys leading to the identification of more than 220 species of trematode parasites of Canadian fishes and diagnoses of more than 80 family–group taxa and 130 genera are given. Each genus is illustrated. For each species a Canadian host list, locality data, and any relevant remarks are included. Visit http://www.nrc.ca/cisti/journals/40083/133to136.html at the NRC Research Press Web to view a short chapter of this book.

On retrouve plus de 80 clefs qui permettent d'identifier quelque 220 espèces de trématodes parasites des poissons du Canada et la description de plus de 80 taxums de famille/groupe et de 130 genres. Chaque genre y est illustré. À chaque espèce sont associées des données sur l'emplacement et des remarques particulières. Visitez http://www.nrc.ca/cisti/journals/40083/f133to6.html au site Web des Presses scientifiques du CNRC pour afficher un court chapitre du livre.

To order copies of this publication/Pour commander des exemplaires de ce livre

- Telephone: (613) 993-0151
- Fax: (613) 952-7656
- Mail orders: Monograph Orders, NRC Research Press, National Research Council Canada, Ottawa, Ontario K1A 0R6, Canada
- Internet e-mail: research.journals@nrc.ca
- World Wide Web: http://www.nrc.ca/cisti/journals/formmono.html

Canadian customers please add 7% GST. Orders from Quebec add a further 6.5% QST to the total price including GST. Make cheque or money order payable to "Receiver General for Canada, credit NRC". Note that for all orders outside Canada, rates are in U.S. dollars. All sales are final.

- Téléphone : (613) 993-0151
- Télécopieur : (613) 952-7656
- Par la poste : Monographies, Presses scientifiques du CNRC, Conseil national de recherches Canada, Ottawa (Ontario) K1A 0R6, Canada
- Courrier électronique : research.journals@nrc.ca
- World Wide Web : http://www.nrc.ca/cisti/journals/formmofr.html

Les clients canadiens doivent ajouter la TPS de 7 %. Les clients du Québec doivent ajouter 6,5 % de TVQ au montant total, une fois la TPS additionnée. Libellez le chèque ou le mandat à l'ordre du «Receveur général du Canada, au crédit du CNRC». Pour les clients non canadiens, les prix sont en dollars américains. Aucun remboursement.

Please send me ____ copies of/Veuillez me faire parvenir ____ exemplaire(s) de *Guide to the Parasites of Fishes of Canada: Part IV. Trematoda.*

NRC Research Press

Monograph Program

Presses scientifiques du CNRC

Programme de monographies

NRC·CNRC

PLEASE PRINT/LETTRES MOULÉES

☐ Payment enclosed/Paiement inclus ☐ Charge to/Imputer à ☐ Visa ☐ MasterCard

Account no./ N° de compte | | | | | | | | | | | | | | | | | | Expiry date/ Date d'expiration_____

Name/Nom

Signature/Signature

Address/Adresse

City/Ville Province/Province

Postal code/Code postal Country/Pays

Telephone/Téléphone Fax/Télécopieur

e-mail/Courrier électronique Date of order/Date de la commande

CANADIAN CONFERENCE FOR FISHERIES RESEARCH: CCFFR-2000

Fredericton, New Brunswick, 6-8 January, 2000

Programme Themes and Call for Papers: (*http://www.phys.ocean.dal.ca/ccffr*)

1. Fin and shellfish culture
2. Recreational fisheries
3. Research directed at conservation of wild salmonids
4. Biotic and abiotic interactions in marine and freshwater systems
5. Joint CCFFR/SCL session (to be announced)

Papers addressing the major themes are encouraged, although submission on other themes related to fisheries and aquatic habitat biology are also welcome. We hope that session 4 will attract papers from students and postdoctoral fellows working on GLOBEC projects. GLOBEC (GLOBal ocean ECosystem dynamics) is an international research program that examines how living marine resources are affected by variability in their environment.

The **DEADLINE** for abstracts is **10 September 1999**.
CCFFR has moved to an electronic process for developing the program. See:
http://www.phys.ocean.dal.ca/ccffr

CONFERENCE CANADIENNE DE LA RECHERCHE SUR LES PECHES: CCRP-2000

Fredericton, New Brunswick, les 6-8 janvier 2000

Les Principaux Thèmes Abordés et Appel Pour Contributions: (*http://www.phys.ocean.dal.ca/ccffr*)

1. Culture des poissons, des crustacés et des mollusques
2. Pêcheries récréatives
3. Recherches dirigées vers la conservation des salmonidés sauvages
4. Interactions biotiques et abiotiques dans les systèmes marins et dulcicoles
5. Session Conjointe CCRP/SCL: (sera annoncée ultérieurement)

Des contributions reliées aux thèmes principaux sont particulièrement sollicitées, mais des contributions sur d'autres thèmes reliés aux sciences halieutiques et à la biologie des habitats aquatiques sont également bienvenues. Nous espérons que la session 4 attirera des contributions provenant d'étudiants et de stagiaires post-doctoraux oeuvrant dans des projets a GLOBEC. GLOBEC (GLOBal ocean ECosystem dynamics) est un programme de recherche international qui examine la façon avec laquelle les ressources vivantes marines sont affecttées par la variabilité de leur environnement.

La **DATE LIMITE** pour la soumission des résumés est **le 10 septembre 1999.**
La CCRP est un processus entièrement électronique pour la préparation du programme. Voir:
http://www.phys.ocean.dal.ca/ccffr

Bernadette Pinel-Alloul, Catherine Guay, Nadine Angeli, Pierre Legendre, Pierre Dutilleul, Gérard Balvay, Daniel Gerdeaux, and Jean Guillard	**1437–1451**	Large-scale spatial heterogeneity of macrozooplankton in Lake of Geneva
Heinrich Eisenmann, Peter Burgherr, and Elisabeth I. Meyer	**1452–1460**	Spatial and temporal heterogeneity of an epilithic streambed community in relation to the habitat templet
Stephan Köhler, Jakub Hruška, and Kevin Bishop	**1461–1470**	Influence of organic acid site density on pH modeling of Swedish lakes
J.C.A. Marr, J. Lipton, D. Cacela, J.A. Hansen, J.S. Meyer, and H.L. Bergman	**1471–1483**	Bioavailability and acute toxicity of copper to rainbow trout (*Oncorhynchus mykiss*) in the presence of organic acids simulating natural dissolved organic carbon
Russell K. MacRae, Ann S. Maest, and Joseph S. Meyer	**1484–1493**	Selection of an organic acid analogue of dissolved organic matter for use in toxicity testing
Uwe Borgmann and Warren P. Norwood	**1494–1503**	Assessing the toxicity of lead in sediments to *Hyalella azteca*: the significance of bioaccumulation and dissolved metal
Ruth B. Phillips, Linda I. Gudex, Kathleen M. Westrich, and Alfred DeCicco	**1504–1511**	Combined phylogenetic analysis of ribosomal ITS1 sequences and new chromosome data supports three subgroups of Dolly Varden char (*Salvelinus malma*)
Richard D. Routledge and James R. Irvine	**1512–1519**	Chance fluctuations and the survival of small salmon stocks

National Research Council Canada
Ottawa, Canada K1A 0R6

Conseil national de recherches Canada
Ottawa, Canada K1A 0R6

Postage paid at Ottawa
Publications mail
Registration No. 1240579

Port payé à Ottawa
Poste-publication
Enregistrement n° 1240579

Canadian Journal of Fisheries and Aquatic Sciences

Volume 56, Number 8, August 1999

Journal canadien des sciences halieutiques et aquatiques

Volume 56, numéro 8, août 1999

Allen H. Andrews, Kenneth H. Coale, Jocelyn L. Nowicki, Craig Lundstrom, Zenon Palacz, Erica J. Burton, and Gregor M. Cailliet 1329–1338
Application of an ion-exchange separation technique and thermal ionization mass spectrometry to ^{226}Ra determination in otoliths for radiometric age determination of long-lived fishes

Allen H. Andrews, Gregor M. Cailliet, and Kenneth H. Coale 1339–1350
Age and growth of the Pacific grenadier (*Coryphaenoides acrolepis*) with age estimate validation using an improved radiometric ageing technique

R.E.H. Smith, J.A. Furgal, M.N. Charlton, B.M. Greenberg, V. Hiriart, and C. Marwood 1351–1361
Attenuation of ultraviolet radiation in a large lake with low dissolved organic matter concentrations

Scott M. Reid, Michael G. Fox, and Thomas H. Whillans 1362–1369
Influence of turbidity on piscivory in largemouth bass (*Micropterus salmoides*)

Even H. Jørgensen and Johannes Wolkers 1370–1375
Effect of temperature on the P4501A response in winter- and summer-acclimated Arctic char (*Salvelinus alpinus*) after oral benzo[*a*]pyrene exposure

Oscar E. Gaggiotti and Russell D. Vetter 1376–1388
Effect of life history strategy, environmental variability, and overexploitation on the genetic diversity of pelagic fish populations

Heather A. Morrison, D. Michael Whittle, Chris D. Metcalfe, and Arthur J. Niimi 1389–1400
Application of a food web bioaccumulation model for the prediction of polychlorinated biphenyl, dioxin, and furan congener concentrations in Lake Ontario aquatic biota

Frank M. Wilhelm and David W. Schindler 1401–1408
Effects of *Gammarus lacustris* (Crustacea: Amphipoda) on plankton community structure in an alpine lake

Mary C. Fabrizio, James D. Nichols, James E. Hines, Bruce L. Swanson, and Stephen T. Schram 1409–1419
Modeling data from double-tagging experiments to estimate heterogeneous rates of tag shedding in lake trout (*Salvelinus namaycush*)

Aki Mäki-Petäys, Timo Muotka, and Ari Huusko 1420–1427
Densities of juvenile brown trout (*Salmo trutta*) in two subarctic rivers: assessing the predictive capability of habitat preference indices

Christian Doyon, Réjean Fortin, and Philip A. Spear 1428–1436
Retinoic acid hydroxylation and teratogenesis in lake sturgeon (*Acipenser fulvescens*) from the St. Lawrence River and Abitibi region, Quebec

Continued on inside back cover / Suite au verso

Canada

Printed in Canada by / Imprimé au Canada par
University of Toronto Press Inc.
Typesetting by / Typographie par
NRC Research Press / Presses scientifiques du CNRC

0706-652X(199908)56:8;1-H